National Research
Council Canada

Conseil national
de recherches Canada

NRC · CNRC

Canadian Journal of Fisheries and Aquatic Sciences

Journal canadien des sciences halieutiques et aquatiques

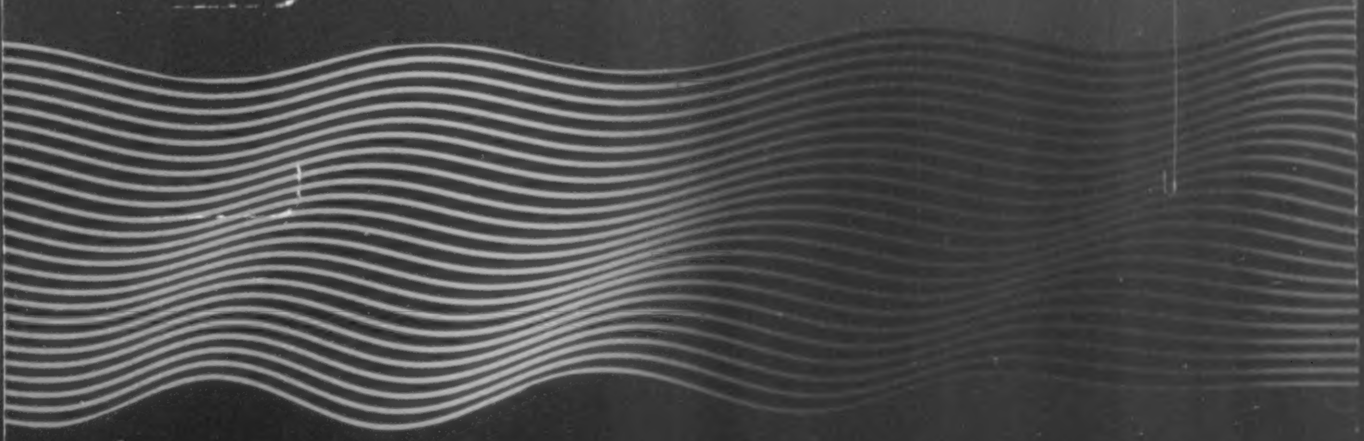

http://www.nrc.ca/cisti/journals

ISSN 0706-652X / CJFSDX 57(12) 2357–2557 (2000)

The *Canadian Journal of Fisheries and Aquatic Sciences*, previously published as *Contributions to Canadian Biology* 1901–1925, *Contributions to Canadian Biology and Fisheries* 1926–1934, *Journal of the Biological Board of Canada* 1934–1937, and *Journal of the Fisheries Research Board of Canada* 1938–1979, is issued monthly to form annual volumes of 12 numbers plus supplements.

Editorial policy: The Journal publishes original research articles, perspectives (syntheses, critiques, re-evaluations), discussions (comment and reply), and rapid communications. Manuscripts may concern cells, organisms, populations, communities, ecosystems, or processes that affect aquatic systems. They may cover a range of disciplines including biology and ecology of marine and freshwater organisms, limnology, oceanography, physiology, toxicology, genetics, economics, disease, and management. Preference will be given to manuscripts that emphasize understanding of observed phenomena and interpretation of experimental results. The Journal encourages papers that lead from clearly stated purpose or rationale and from testable hypotheses, concepts, or questions to identifiable conclusions or syntheses. Such papers may amplify, modify, question, or redirect accumulated knowledge embodied in contemporary perceptions of a particular state of aquatic sciences. The Journal discourages papers that are essentially descriptive, except in emerging disciplines; have only site-specific or local applications (a certain year, place, taxon, chemical compound, etc.); only confirm previously established principles; or apply standard techniques without breaking new methodological ground.

Manuscripts for publication should be submitted to the Editors, *Canadian Journal of Fisheries and Aquatic Sciences*, Department of Zoology, University of Guelph, Guelph, ON N1G 2W1, Canada (519-824-4120 ext. 2646; fax: 519-767-9798; e-mail: cjfas@uoguelph.ca).

Submissions in either English or French are acceptable. The information must be original, that is, not copyrighted, published, or submitted elsewhere except in abstract form or unless by written consent of the Editor. NRC accepts no responsibility for statements or opinions expressed by a contributor. Acceptance of an advertisement, announcement, or other material does not imply endorsement by either the Journal's Editors or NRC. The use of proprietary names does not imply endorsement of the product or company.

Correspondence concerning accepted manuscripts and corrected proofs should be sent to NRC Research Press, National Research Council of Canada, Ottawa, ON K1A 0R6, Canada.

Instructions to Authors are published once a year in the first issue of each volume. Copies are available from NRC Research Press or from our web site. The **Publication Policy** of NRC Research Press is also available at our web site: <http://www.nrc.ca/cisti/journals/>.

Microfilm: Issues from 1934 through the current volume can be purchased on 16- or 35-mm microfilm. Photocopies of individual articles or issues can be purchased from University Microfilms International, 330 North Zeeb Road, Ann Arbor, MI 48106, U.S.A.

U.S. periodical postage paid at Champlain, N.Y., and at additional mailing offices. Attention U.S. POSTMASTER: Send address changes to **Canadian Journal of Fisheries and Aquatic Sciences**, c/o USACAN Media Distribution Center, P.O. Box 2888, Plattsburg, NY 12901, U.S.A.

Publié sans interruption depuis 1901, le *Journal canadien des sciences halieutiques et aquatiques* a paru sous plusieurs titres : *Contributions to Canadian Biology* 1901–1925, *Contributions to Canadian Biology and Fisheries* 1926–1934, *Journal of the Biological Board of Canada* 1934–1937, et *Journal of the Fisheries Research Board of Canada* 1938–1979. Le Journal paraît tous les mois, formant ainsi un volume de 12 numéros, et offre en plus jusqu'à deux suppléments par année.

Politique éditoriale : On publie, dans le Journal, des articles rendant compte de recherche originale, des perspectives (synthèses, critiques et réévaluations), des discussions (commentaires et réponses) et des communications rapides. Les documents peuvent porter sur les cellules, organismes, populations, communautés, écosystèmes ou processus qui affectent les systèmes aquatiques. Ils peuvent relever de divers domaines y compris la biologie et l'écologie des organismes marins et d'eau douce, la limnologie, l'océanographie, la physiologie, la toxicologie, la génétique, l'économie, la pathologie et la gestion. On accorde la préséance aux articles qui contribuent à la compréhension de phénomènes observés et à l'interprétation de résultats expérimentaux. On invite les auteurs à soumettre des articles ayant des objectifs précis ou relevant d'hypothèses, de concepts ou de questions vérifiables et se terminant par de solides conclusions ou d'utiles synthèses. Ces articles enrichissent, changent, mettent en question ou réorientent les connaissances acquises sur divers aspects des sciences aquatiques. On décourage toutefois la soumission d'articles simplement descriptifs (à moins qu'il ne s'agisse de nouvelles disciplines), d'application très limitée (applicables à une seule année, une seule région ou un seul taxon, portant sur un unique composé chimique, etc.); d'articles qui ne font que reprendre les principes énoncés dans des articles précédents; et d'articles rendant compte de l'application de normes sans gain de méthodologie.

Les auteurs voudront adresser leurs **manuscrits** aux directeurs scientifiques, *Journal canadien des sciences halieutiques et aquatiques*, Department of Zoology, University of Guelph, Guelph, ON N1G 2W1, Canada (519-824-4120 poste 2646; télécopieur : 519-767-9798; courriel : cjfas@uoguelph.ca).

Les contributions peuvent être en anglais ou en français. Elles doivent être originales, c.-à.-d. qu'elles ne doivent pas avoir fait l'objet d'un copyright, avoir été publiées ou soumises ailleurs, sauf sous forme abrégée ou avec le consentement du rédacteur. Le CNRC ne se tient en aucune façon responsable des opinions exprimées par un collaborateur ou des déclarations qui pourrait faire ce dernier. La publication d'annonces publicitaires, d'avis et autres n'implique pas l'endossement de leur contenu par les directeurs du Journal ou du CNRC. L'utilisation des noms de marques de commerce ne signifie aucunement une sanction du produit en question ou de la compagnie qui le fabrique.

La correspondance ayant trait aux manuscrits acceptés et les **épreuves corrigés** doivent être envoyées aux Presses scientifiques du CNRC, Conseil national de recherches du Canada, Ottawa, ON K1A 0R6, Canada.

Recommandations aux auteurs sont publiés une fois par année dans le premier numéro de chaque volume. Des copies, ainsi que la **Politique de publication**, sont disponibles auprès des Presses scientifiques du CNRC ou au site web : <http://www.nrc.ca/cisti/journals/>.

Microfilms : On peut acheter sur microfilms de 16 ou 35 mm tous les numéros depuis 1934. Des photocopies d'articles ou de numéros individuels sont aussi en vente auprès de University Microfilms International, 330 North Zeeb Road, Ann Arbor, MI 48106, É.-U.

This journal is indexed or abstracted in / Ce journal est signalé ou résumé dans
ABSEARCH, Aquatic Sciences and Fisheries Abstracts, Biological Abstracts, Biological & Agricultural Index, CAB Abstracts, Chemical Abstracts, Current Contents, Elsevier BIOBASE, Environmental Abstracts, Environmental Periodicals Bibliography, GEOBASE, GeoRef, Life Sciences Collection, Meteorological and Geoastrophysical Abstracts, Oceanic Abstracts, PASCAL Database, and Science Citation Index.

Volume 57, Number 12, December 2000

Canadian Journal of Fisheries and Aquatic Sciences

Published by the National Research Council of Canada

Volume 57, numéro 12, décembre 2000

Journal canadien des sciences halieutiques et aquatiques

Publié par le Conseil national de recherches du Canada

Editors / directeurs scientifiques John C. Roff and Moira M. Ferguson

Assistant to the Editors / adjointe aux directeurs scientifiques **Holly Foster**

Associate Editors / directeurs scientifique associés

D. Boisclair, *Université de Montréal*
U. Borgmann, *Environment Canada, Burlington*
S.E. Campana, *DFO/MPO, Dartmouth*
R. Carignan, *Université de Montréal*
D.G. Dixon, *University of Waterloo*
A.E. Dizon, *National Marine Fisheries Service, La Jolla, Calif.*
J.J. Dodson, *Université Laval*
J.A. Downing, *Iowa State University*
K.T. Frank, *DFO/MPO, Dartmouth*
D.F. Houlihan, *University of Aberdeen, Aberdeen, Scotland*
F.A. Huntingford, *University of Glasgow*
J.A. Hutchings, *Dalhousie University*
G.S. Jamieson, *DFO/MPO, Nanaimo*
B. Jonsson, *Norwegian Institute for Nature Research, Oslo, Norway*
D.M. Mason, *NOAA-Great Lakes Environmental Research Laboratory, Ann Arbor, Mich.*
A. Mazumder, *University of Victoria*
D.L. Parrish, *Vermont Cooperative Fish and Wildlife Research Unit (USGS/BRD), University of Vermont*
P. Pepin, *DFO/MPO, St. John's*
E.E. Prepas, *University of Alberta*
T.M. Powell, *University of California, Berkeley, Calif.*
T.J. Quinn II, *University of Alaska–Fairbanks, Juneau, Alaska*
T.P. Quinn, *University of Washington*
R.D. Robarts, *Environment Canada, Saskatoon*
B. Sainte-Marie, *DFO/MPO, Mont-Joli*
D.W. Schindler, *University of Alberta*
S.J. Smith, *DFO/MPO, Dartmouth*
W.G. Sprules, *University of Toronto*
R.J. Thompson, *Memorial University of Newfoundland*
C.J. Walters, *University of British Columbia*
R.D. Ward, *CSIRO Division of Fisheries, Australia*
C.M. Wood, *McMaster University*
B. de Young, *Memorial University of Newfoundland*

NRC Research Press / Presses scientifiques du CNRC

Editor-in-chief / directeur général **Bruce P. Dancik**
Assistant Editor-in-chief / directeur général adjoint **Iain E.P. Taylor**

Journals Program / Programme des revues

(Fax / télécopieur : 613-952-7656; e-mail / courriel : research.journals@nrc.ca;
URL: http://www.nrc.ca/cisti/journals/)
Director / directrice **Aldyth Holmes**
Business Manager / gestionnaire des affaires **Paul McClymont**
Managing Editor / rédactrice administrative **Cecily M. Pearson (613-993-9099)**
Publication Officer / agente de publication **Jennifer McColl**
Advertising / annonces publicitaires **Judy Heyman (613-993-0151)**
Reprints / tirés à part **Roxanne Landriault (613-990-2254)**
Subscriptions / abonnements **Helen Goulet (613-993-9084)**

© National Research Council of Canada 2000. World rights reserved.
No part of this publication may be reproduced, stored, or transmitted in any form or by any means, without the written permission of the publisher, except as stated below.

The National Research Council of Canada grants **permission*** to individuals to make single copies of articles for personal use. Any person may reproduce short excerpts from articles in the journal for any purpose that respects the moral rights of authors, provided that the source is fully acknowledged. As a courtesy, the consent of authors of such material should be obtained directly from the author.

Authorization to reproduce items for other than personal use, as stated above, is granted by the National Research Council of Canada provided that the copyright fee of $7.00 per copy is paid directly to CANCOPY, One Yonge Street, Suite 1900, Toronto, ON M5E 1E5, Canada.

*The above permission does not extend to other kinds of copying, such as copying for general distribution, for advertising, or promotional purposes, for creating new collective works, or for resale. For such copying, arrangements must be made with the publisher, National Research Council of Canada, Ottawa, ON K1A 0R6, Canada.

© Conseil national de recherches du Canada 2000. Tous droits réservés.
Il est interdit de reproduire, de sauvegarder ou de transmettre quelque partie de la présente publication dans quelque format ou de quelque façon sans le consentement écrit de l'éditeur, à l'exception des conditions suivantes.

Le Conseil national de recherches du Canada accorde aux particuliers le droit de faire des copies individuelles pour leur usage personnel. Toute personne peut reproduire de courts extraits des articles de la Revue pour autant que les droits moraux de l'auteur soient respectés et que la mention de provenance soit clairement indiquée. Il est de convenance de demander le consentement de l'auteur avant de faire mention de son travail.

On obtiendra l'autorisation de reproduire des articles à d'autres fins que l'usage personnel (tel qu'on l'a décrit ci-dessus) auprès du Conseil national de recherches du Canada pour autant que des redevances de droits d'auteurs de 7,00 $/copie soient versées au CANCOPY, 1, rue Yonge, bureau 1900, Toronto, ON M5E 1E5, Canada.

*La permission ci-dessus ne s'applique pas à la reproduction à grande échelle, telle que la reproduction aux fins de distribution générale, publicitaire ou promotionnelle, de compilation de nouveaux ouvrages collectifs ou de revente. Dans de tels cas, il faudra ratifier une entente particulière avec l'éditeur, le Conseil national de recherches du Canada, Ottawa, ON K1A 0R6, Canada.

Subscription information

The *Canadian Journal of Fisheries and Aquatic Sciences* (ISSN 0706-652X) is published monthly by the National Research Council of Canada. 2001 annual subscription rates (second class postage) for Canada are $687CAN institutional and $208CAN personal, for US & foreign $687US institutional and $208US personal. For air mail add $150US to foreign rate. Canadian customers please include 7% GST (business no. 12149 1807 RT 0275). Subscriptions are entered for the calendar year. Remittances should be made payable to the Receiver General for Canada credit NRC. Price for regular single issues: institutional, $80.00; personal, $30.00. Supplements will be priced separately. Special rates apply to members of Canadian scientific and engineering societies if they subscribe through their respective societies.

There are no refunds on cancelled subscriptions once delivery has begun. Claims for missing issues should be made within four months (N. America) or six months (outside N. America) following the date of publication. The publisher expects to supply missing issues only when losses have occurred in transit and when the reserve stock will permit. For change of address and subscription enquiries: Subscription Office, NRC Research Press, National Research Council of Canada, Ottawa, ON K1A 0R6, Canada; tel.: 613-993-9084; fax: 613-952-7656; e-mail: research.journals@nrc.ca.

Microform backfiles are available from UMI, P.O. Box 1346, Ann Arbor, MI 48106-1346, U.S.A., and Micromedia Ltd., 20 Victoria St., Toronto, ON M5C 2N8, Canada.

All issues of the *Canadian Journal of Fisheries and Aquatic Sciences* since 1996 are available on the Web. Pricing information can be found at <http://www.nrc.ca/cisti/journals/>.

Renseignements sur l'abonnement

Journal canadien des sciences halieutiques et aquatiques (ISSN 0706-652X) est une publication mensuelle du Conseil national de recherches du Canada. Le prix de l'abonnement annuel au Canada (courrier de deuxième classe) est de 687 $CAN pour les organismes et de 208 $CAN pour les particuliers. À l'étranger (y compris les É.-U.), le prix de l'abonnement est de 687 $US pour les organismes et de 208 $US pour les particuliers. L'expédition par avion exige des frais de 150 $US en sus du prix d'abonnement à l'étranger. Les clients du Canada doivent ajouter la TPS de 7% (numéro d'entreprise 12149 1807 RT 0275). Les abonnements sont pour l'année civile. Tout paiement doit être adressé au Receveur général du Canada, crédit du CNRC. Le prix par numéro est de 80 $ pour les organismes et de 30 $ pour les particuliers. Le prix des hors-série varie. Les membres des sociétés canadiennes de sciences et de génie bénéficient de taux préférentiels en s'abonnant via leurs sociétés respectives.

Aucun remboursement ne sera accordé ni aucune annulation acceptée une fois que les livraisons auront commencé. Les réclamations de numéros manquants devront être soumises dans les quatre mois (Amérique du Nord) ou dans les six mois (à l'extérieur de l'Amérique du Nord) suivant la date de publication. L'éditeur ne fournira de numéros manquants que si le document a été perdu pendant l'expédition et que si le stock le permet. Adressez tout changement d'adresse ou toute question quant à l'abonnement au : Bureau des abonnements, Presses scientifiques du CNRC, Conseil national de recherches Canada, Ottawa, ON K1A 0R6, Canada; téléphone : 613-993-9084; télécopieur : 613-952-7656; courriel : research. journals@nrc.ca.

On peut obtenir les fichiers rétrospectifs sur **microforme** auprès de UMI, P.O. Box 1346, Ann Arbor, MI 48106-1346, É.-U., et auprès de Micromedia Ltée, 20 rue Victoria, Toronto, ON M5C 2N8, Canada.

À partir de 1996, tous les numéros de *Journal canadien des sciences halieutiques et aquatiques* sont accessibles sur le Web. On trouvera des renseignements sur les tarifs à <http://www.nrc.ca/cisti/journals>.

A fisheries management strategy robust to ignorance: rotational harvest in the presence of indirect fishing mortality

Ransom A. Myers, Susanna D. Fuller, and Daniel G. Kehler

Abstract: We develop a simple theoretical model of yield and spawning stock biomass per recruit for the American sea scallop (*Placopecten magellanicus*), which appears to have high indirect fishing mortality when harvested with dredges, i.e., mortality caused by the act of fishing that does not result in landings. The age at and degree to which individuals are affected by the indirect mortality are unknown, and it does not appear possible to develop a robust harvest strategy with yearly harvests unless indirect fishing mortality is well quantified. We show that there could be substantial benefits to a rotational harvest strategy for sessile species with high indirect fishing mortality. First, the strategy appears to be robust to ignorance about indirect fishing mortality and results in equal or better yields than a yearly harvest across a wide range of indirect fishing mortalities. Second, under most conditions, a higher spawning stock biomass is maintained. Third, rotational management is more easily enforced, as it does not require specifying a narrow range of fishing mortality in order to maximize yield.

Résumé : Nous avons développé un modèle théorique simple pour étudier le rendement et la biomasse des géniteurs par individu recruté chez le pétoncle géant (*Placopecten magellanicus*), qui semble subir une mortalité indirecte élevée due à la pêche à la drague, i.e., une mortalité causée par la pêche qui ne résulte pas en des débarquements. L'importance de cette mortalité indirecte et l'âge des individus affectés ne sont pas connus. Néanmoins, il semble qu'on ne puisse établir une solide stratégie de récolte avec pêches annuelles sans que cette mortalité indirecte ne soit bien quantifiée. Nous démontrons qu'il pourrait y avoir d'importants bénéfices à établir une stratégie de récolte par rotation chez les espèces sessiles qui ont une mortalité indirecte élevée due à la pêche. D'abord, ce type de stratégie est applicable même lorsqu'on ne connaît pas la mortalité indirecte due à la pêche et donne des résultats semblables ou meilleurs qu'une stratégie de pêche annuelle, dans un large intervalle de mortalités indirectes. En second lieu, dans la majorité des situations, il y a maintien d'une biomasse plus élevée du stock des géniteurs. Enfin, une gestion avec rotation est plus facile à appliquer, puisqu'elle n'exige pas de fixer des limites étroites à la pêche pour maximiser le rendement.

[Traduit par la Rédaction]

Introduction

Fisheries must be managed using imperfect information about the biology and state of a stock; thus, successful management strategies must be robust in light of this lack of detailed information. We examine rotational harvest of American sea scallops (*Placopecten magellanicus*) as one such robust management strategy. The scallop fishery commonly uses dredges for harvesting, which can result in a high indirect mortality. Indirect mortality caused by fishing (e.g., discarding or damage to fish not caught in fishing gear) is one of the major problems in the management of the world's fisheries (Alverson et al. 1994). Although it is now accepted that the calculations of biological reference points, such as the maximum allowed fishing mortality rate, should include indirect fishing mortality (Chen and Gordon 1997), this is rarely done in practice.

For the sea scallop, the problem of indirect fishing mortality has long been known to be a critical conservation issue (Caddy 1973). Caddy (1973) found indirect mortality rates on par with direct fishing mortality (13–17%), and a recent assessment of sea scallops (National Marine Fisheries Service 1999) estimated indirect mortality to be three times higher than the direct fishing mortality on Georges Bank. Evidence from other scallop species suggests that indirect fishing mortality may be as high as four to eight times the direct fishing mortality (Naidu 1988; McLoughlin et al. 1993).

Received August 18, 2000. Accepted December 1, 2000. Published on the NRC Research Press web site on December 20, 2000. J15928

R.A. Myers.[1] Killam Chair of Ocean Studies, Department of Biology, Dalhousie University, Halifax, NS B3H 4J1, Canada.
S.D. Fuller. Department of Biology, Dalhousie University, Halifax, NS B3H 4J1, Canada.
D.G. Kehler. Department of Mathematics and Statistics, Dalhousie University, Halifax, NS B3H 4J1, Canada.

[1] Corresponding author (e-mail: ransom.myers@dal.ca).

Fig. 1. (*a*) Yield per recruit and (*b*) percentage of the maximum spawning biomass per recruit (when $F = 0$) for sea scallops at different levels of direct fishing mortality under the assumption that (*i*) there is no indirect fishing mortality (solid line), (*ii*) there is indirect fishing mortality on prerecruits only (dotted line), and (*iii*) there is indirect fishing mortality on all ages (dashed line). Indirect fishing mortality is assumed to equal the direct fishing mortality. Note that the direct fishing mortality resulting in maximum yield per recruit is much lower when indirect fishing mortality occurs (Fig. 1*a*).

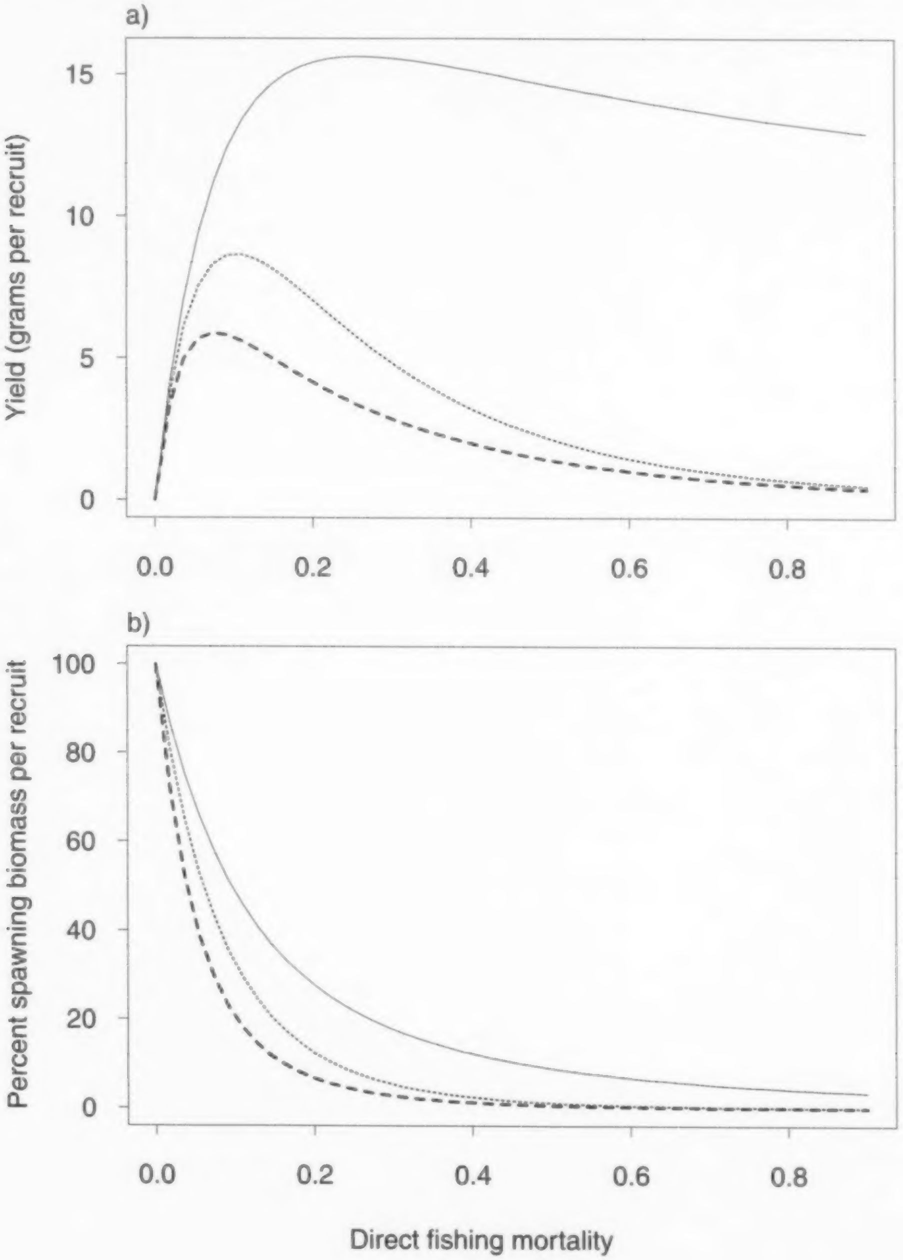

In this article, we propose rotational harvesting as an alternative strategy and investigate its robustness to different levels and types of indirect fishing mortality using deterministic models. We propose rotational harvesting as an alternative strategy and investigate its robustness to different levels and types of indirect mortality using deterministic models.

Fig. 2. (*a* and *b*) Average yield per recruit and (*c* and *d*) percentage of maximum average spawning stock biomass for sea scallops harvested over a range of direct fishing mortalities for four rotational periods: harvest every year (thick solid line), once every 3 years (dashed line), once every 6 years (dotted line), and once every 9 years years (thin solid line). Results are shown under the assumption of no indirect fishing mortality (Figs. 2*a* and 2*c*) and indirect fishing mortality equal to direct fishing mortality (Figs. 2*b* and 2*d*).

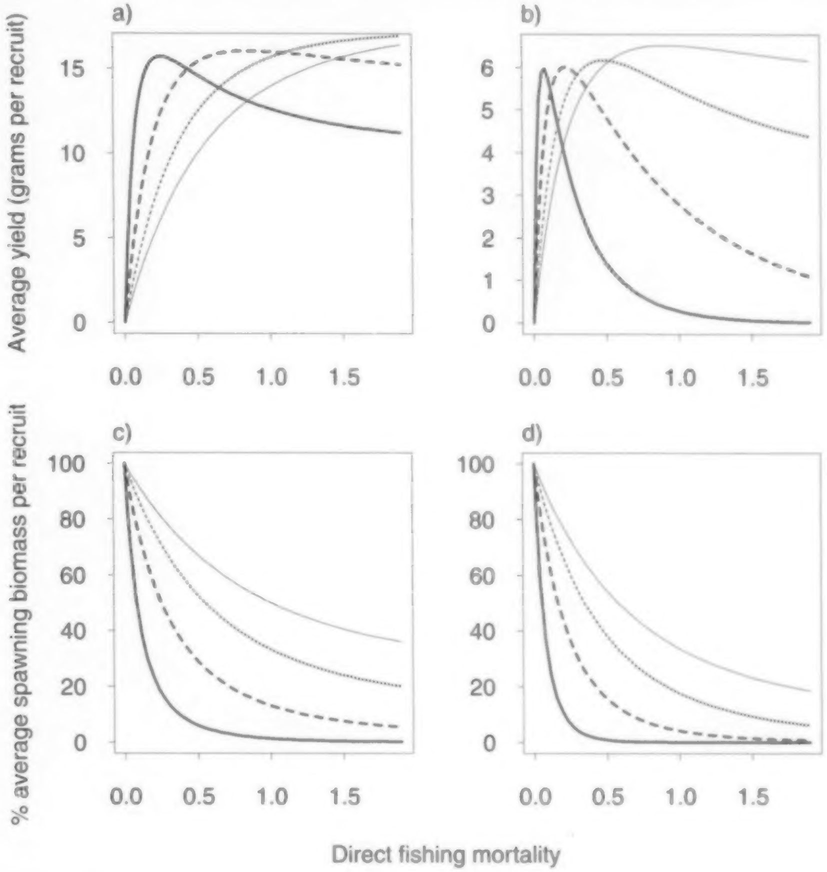

Yield per recruit analysis including indirect fishing mortality

We considered a simple discrete time population dynamics model in which fishing takes place at one time of the year and natural mortality only occurs between the periods of fishing. The discrete time model will, in general, give quantitatively, but not qualitatively, different results than the standard continuous time yield per recruit model (Beverton and Holt 1957) but can easily be extended to consider a rotational harvest. The model is more appropriate when the harvest takes place yearly, over a short period, as is proposed for the reopening of portions of the groundfish closed areas of the U.S. side of Georges Bank (New England Fisheries Management Council 2000).

In our model, we divided total fishing mortality into two components: direct and indirect mortality. Direct mortality is denoted $F_y s_a$, where s_a is the selectivity of the fishing gear to a scallop of age a and F_y is the fishing mortality in year y of the "fully selected" age or ages, i.e., where $s_a = 1$. Indirect mortality is denoted $F_y i_a$, where i_a is the age-dependent selectivity of the indirect fishing mortality. To make our analyses consistent with the National Marine Fisheries Service (1999), the year was defined to start at the midpoint of the cohort year, and thus, fishing occurs at the end of this "year."

We let $N_{y,a}$ be the number of scallops of age a at the beginning of year y and m_a be the age-specific natural mortality. We assumed that both sources of fishing mortality are operating simultaneously during the fishery. The dynamics of a cohort are given by

$$N_{y+1,a+1} = N_{y,a}\exp(-m_a - F_y(s_a + i_a))$$

and the catch in numbers from the cohort at age a is

$$C_{y,a} = N_{y,a}\exp(-m_a)(1 - \exp(-F_y(s_a + i_a)))\left(\frac{s_a}{s_a + i_a}\right).$$

In the yield per recruit analysis, it is assumed that recruitment, $N_{y,1}$ and the selectivity at age do not vary over time. This assumption is unrealistic, as recruitment will vary with

Fig. 3. Proportional loss of maximum average yield for sea scallops as a function of the ratio of indirect to direct fishing mortality under the four assumptions for fully recruited fishing mortality and the age that indirect fishing mortality occurs at four rotational harvest periods: harvest once every 1 (thick solid line), 3 (dashed line), 6 (dotted line), and 9 years (thin solid line). The assumptions for the fully recruited fishing mortality (*F*) and the indirect mortality are (*a*) $F = 0.2$ and indirect fishing mortality occurs at all ages >1 at the same rate as direct fishing mortality on ages 4, (*b*) the same as Fig. 3*a* except that $F = 0.5$, (*c*) the same as Fig. 3*a* except that $F = 1.0$, and (*d*) $F = 0.5$ and indirect fishing mortality only occurs on prerecruits but at the same rate as on fully recruited scallops.

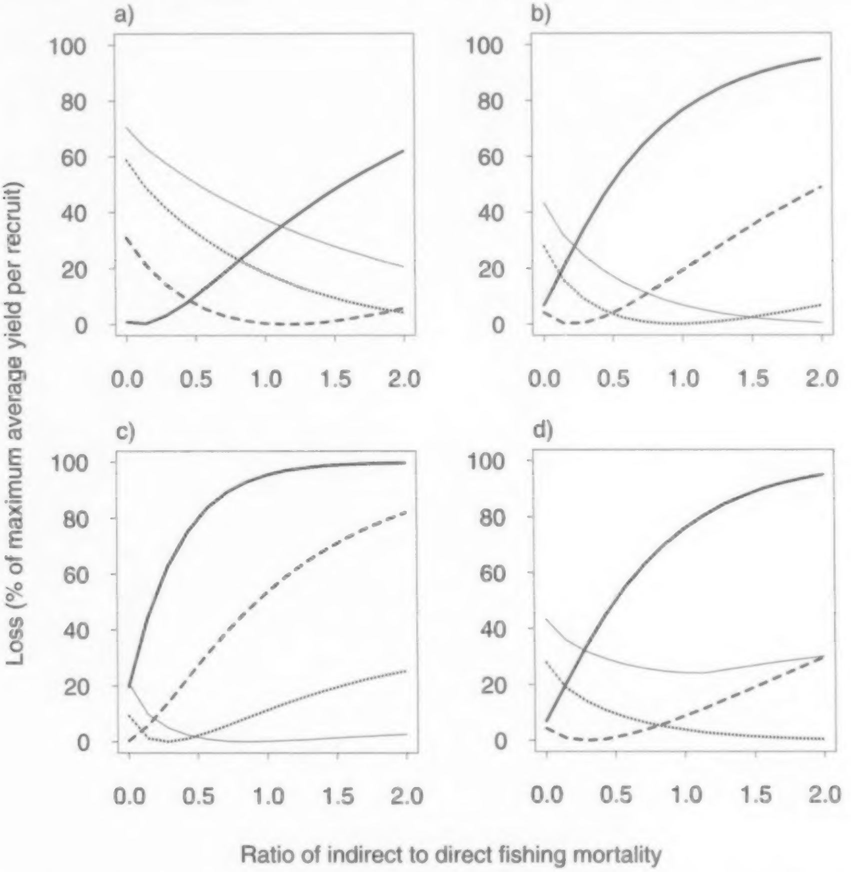

both abundance and environmental conditions, but simplifies the analysis considerably. The annual biomass yield per recruit at equilibrium, Y^*, is obtained by considering a scallop population derived from a cohort exploited over time with fishing mortality *F* and a selectivity of 1 (Clark 1990). This will be constant with time and is

$$Y^*(F) = \frac{1}{N_{y,1}} \sum_a w_a C_{y,a},$$

where w_a is the weight of the scallops at age *a* at the time of the harvest.

It is also useful to calculate the spawning stock biomass per recruit in the same manner, i.e.,

$$S(F) = \frac{1}{N_{y,1}} \sum_a N_{y,a} \phi_a w_a$$

where ϕ_a is the proportion of fish of age *a* that are mature. Again, this will not vary over time in our model.

We made the following additional assumptions in developing this model. Growth in weight (grams) was defined using the von Bertalanffy growth curve with parameters from the most recent assessments (National Marine Fisheries Service 1999):

$$w_a = 55.11(1 - \exp(-0.3374(a - 1.454)))^{3.0734}.$$

Spawning biomass was assumed to be proportional to the meat weight of the scallops. As per National Marine Fisheries Service (1999), scallops were considered mature at age 4, and natural mortality was assumed to be constant for all ages at a rate of 0.1 up to age 20. Senescence was assumed to begin at age 20, with natural mortality increasing by 0.1 every year after that age. Direct fishing selectivity of the commercial dredges was assumed to be 0 below age 3, 0.5 at age 3, and 1 for higher ages (National Marine Fisheries Service 1999), which makes the simplifying assumption that all scallops grow at the same rate. When we considered the effect of the age of recruitment to the fishery on yield, we assumed direct fishing selectivity to be 1 for scallops of age ≥4.

Two alternative patterns of indirect fishing mortality were modeled. First, indirect fishing mortality was assumed to affect all ages >1 equally and at the same rate as the fully recruited fishing mortality, i.e., $i_a = 1$ for all a, which represents an extreme situation. Second, it may only be the smaller, weaker scallops that are affected by indirect fishing mortality, and thus, we assumed that for the prerecruits ($a < 4$), $i_a = 1$, and for older scallops ($a \geq 4$), $i_a = 0$.

We began by comparing the pattern of yield given different direct fishing mortalities and age of recruitment to the fishery. The typical pattern of maximum yield at infinite mortality and a high age of recruitment (Beverton and Holt 1957) does not emerge. Instead, yield is maximized at a lower age of recruitment (≈4) and a relatively low direct fishing mortality (0.08). Ignoring indirect fishing mortality results in estimates of fishing mortality that give the maximum yield per recruit that are suboptimal (Fig. 1*a*).

The fishing mortality that results in the maximum sustainable yield is smallest when indirect fishing occurs on all ages (0.07), intermediate when indirect fishing mortality occurs only on prerecruits (0.09), and greatest with no indirect fishing mortality (0.22) (Fig. 1*a*). We also compared the spawning biomass per recruit for the three levels of indirect fishing mortality with the percentage of the spawning biomass per recruit with no fishing (Fig. 1*b*). Incorporating indirect fishing mortality results in even lower levels of spawning biomass, particularly at low levels of direct fishing mortality. We have shown using a simple model that ignoring indirect fishing mortality results in setting "optimal" fishing mortalities that are much too high.

Rotational harvest strategy

We investigated a model where fishing is rotated among p subdivisions of the fishing ground, and each subdivision is harvested every p years. The calculation of yield and spawning biomass per recruit is not straightforward for the rotational harvest, since the yield per recruit depends upon the age at which a scallop is first subjected to periodic harvesting. In other words, a scallop first harvested at age 4 and harvested every p years will have a different yield than a scallop first harvested at age 5 and harvested every subsequent p years. Thus, for a rotational harvest of p years, we need to average over the p different possible yields per recruit. Since recruitment was assumed to be constant over time, the same number of recruits will have accumulated in subdivision p over p years as in the entire fishing ground in a year. If the average yield per recruit remains the same between the rotational and nonrotational harvest schemes, then total yield (which is of greater interest) will also remain the same.

We assessed the rotational strategy in terms of average yield and spawning biomass per recruit at different fishing mortalities for four different rotational periods: 1, 3, 6, and 9 years (Fig. 2). In all cases, the rotational strategy resulted in at least as high an average yield per recruit as the nonrotational strategy, provided the fishing mortality was sufficiently high. The rotational strategy maintains a considerably larger stock biomass, thus reducing the risk of stock collapse. The larger yield per recruit obtained under rotational management results from allowing scallops to reach the ages where the ratio of somatic growth to loss by natural mortality is highest. If indirect fishing mortality only occurs on prerecruits, then there is a greater advantage in yield per recruit for a longer rotational management scheme (not shown). From a management perspective, the rotational system is appealing because it is not necessary to control fishing mortalities very precisely when $p > 5$, since near-optimal yields are achieved across a wide range of fishing mortalities. The above plots suggest that a rotational period close to 6 years, with a fishing mortality of around 0.5, would result in a close to maximum average yield per recruit and would maintain spawning biomass per recruit at acceptable levels, i.e., above 20% of the spawning stock biomass.

We examined the consequences of a nonrotational harvesting strategy by calculating the loss in yield per recruit under different assumptions about indirect fishing mortality. We defined the percent loss of fishing at a fully recruited fishing mortality of F at a rotational period p as

$$L_p(F) = 100 \times \frac{Y_p(F)}{\max\limits_{F,p}(Y_p(F))}.$$

We calculated the loss in yield per recruit for four rotational periods, 1, 3, 6, and 9 years, and three direct fishing mortalities. To determine the impact of different indirect fishing mortalities, we allowed the ratio of indirect mortality to direct fishing mortality to vary between 0 and 2 (Fig. 3).

There is a large loss under the nonrotational management regime under all assumptions of indirect mortality except when the ratio of indirect to direct fishing mortality is very small and direct fishing mortality is kept very low, around 0.2. However, the direct fishing mortality has been very much larger than 0.5 in the areas open to fishing on Georges Bank for the last 20 years (National Marine Fisheries Service 1999). If $F = 0.5$ and the rotational period is between 3 and 6 years (Figs. 3*b* and 3*d*), there is relatively little loss under most levels of indirect fishing mortality.

Discussion

Controlling the age of recruitment to the fishery has been often considered a robust approach to fishery management (Myers and Mertz 1998). In our analysis, we show that indirect fishing mortality can greatly affect the optimal fishing strategy and that a rotational harvest strategy may be a reasonable approach to use when the form and magnitude of indirect fishing mortality are uncertain. We have shown, theoretically, that the primary benefits of a rotational strategy, relative to a nonrotational strategy, are that it (*i*) provides equal or greater yield across most levels of indirect fishing mortality, (*ii*) may be more easily enforced, and (*iii*) maintains a higher spawner biomass.

In the nonrotational plan, the range of fishing mortalities resulting in maximum yield per recruit is very narrow. Fisheries managers in the past have found it very difficult to achieve such precise control. This problem has led to overfishing on Georges Bank and other regions (Walters and Maguire 1996). In contrast, the range of fishing mortality resulting in maximum yield per recruit for the rotational strategy is very broad. Enforcement of the rotational plan is simpler than that of the nonrotational plan, as it is easier to completely restrict access to an area than to enforce a fishing limit on each individual boat, particularly if all fishing vessels are required to have electronic location beacons (as scallop vessels are on the U.S. side of Georges Bank). An important conservation benefit of many rotational management strategies is the increase in spawning biomass resulting from a rotational closure. This has been noted in previous studies (e.g., Sluczanowski 1984), but the effect is much larger in fisheries with large indirect mortality, such as scallops harvested with dredges.

As the total amount of dredging can be reduced as a result of rotational harvesting, the impact of scallop dredging on other species can be reduced. However, the fishing intensity in the harvested areas may be still be quite high (0.5–1.0), and we need to insure that this does not compromise the scallop stock or other components of the ecosystem (e.g., groundfish).

There are some obvious disadvantages if very long rotational periods are used, e.g., the somatic growth of sea scallops may decrease because of crowding. As well, very long rotational periods would require the harvested area to be divided into many more areas for the rotational management, which would increase the complexity of enforcement. For these reasons, the period for rotation should probably be <7 years. Rotational management must be considered carefully in a multispecies fishery, as intense scallop fishing can have an impact on groundfish species and structure-forming epifaunal species.

Although the rotational harvest is very appealing theoretically, it remains to be seen whether it can be succesfully implemented. One of the key simplifying assumptions of our analysis is that fishing grounds, which are undoubtedly heterogeneous, can be divided into areas of relatively equal productivity. Monitoring is essential to determine if and how productivity varies over space and time.

An ideal situation for the implementation of a rotational harvest currently exists on the U.S. side of Georges Bank, as there are three sections that have been closed since 1994 to groundfish and scallop harvesting. Proposals to open these areas do not presently include a rotational plan, which is unfortunate, as such a plan could be easily implemented (New England Fisheries Management Council 2000). The implementation of a rotational strategy could also contribute to the ability of scientists to evaluate the effects of fishing through an experimental approach.

References

Alverson, D.L., Freeberg, M.H., Murawski, S.A., and Pope, J.G. 1994. A global assessment of fisheries bycatch and discards. FAO Fish. Tech. Pap. 339.

Beverton, R.J., and Holt, S.J. 1957. On the dynamics of exploited fish populations. Fish. Invest. Ser. II Mar. Fish. G.B. Minist. Agric. Fish. Food, **19**: 533.

Caddy, J.F. 1973. Underwater observations on tracks of dredges and trawls and some effects of dredging on a scallop ground. Can. J. Fish. Aquat. Sci. **30**: 173–180.

Chen, Y., and Gordon, G.N.G. 1997. Assessing discarding at sea using a length-structured yield-per-recruit model. Fish. Res. **30**: 43–55.

Clark, C.W. 1990. Mathematical bioeconomics. 2nd ed. Wiley-Interscience, New York.

McLoughlin, R., Zacharin, W., Cartwright, I., Gwyther, D., Probestl, M., and Sterling, D. 1993. New harvesters for the scallop industry in south east Australia. Aust. Fish. **52**: 12–14.

Myers, R.A., and Mertz, G. 1998. The limits of exploitation: a precautionary approach. Ecol. Appl. **8**(Suppl. 1): S165–S169.

Naidu, K.S. 1988. Estimating mortality rates in the Iceland scallop, *Chlamys islandica* (O.F. Mueller). J. Shellfish Res. **7**: 61–71.

National Marine Fisheries Service. 1999. Twenty-ninth northeast regional stock assessment workshop. NEFSC Ref. Doc. 99/14.

New England Fisheries Management Council. 2000. Framework Adjustment 13 to the Atlantic Sea Scallop Fishery Management Plan with options for the Framework Adjustment 34 to the Northeast Multispecies Fishery Management Plan. New England Fisheries Management Council, Saugus, Mass.

Sluczanowski, P.R. 1984. A management oriented model of an abalone fishery whose substocks are subject to pulse fishing. Can. J. Fish. Aquat. Sci. **41**: 1008–1014.

Walters, C., and Maguire, J.J. 1996. Lessons for stock assessment from the Northern cod collapse. Rev. Fish Biol. Fish. **6**: 125–137.

Diel variation of stomach contents of North Sea cod (*Gadus morhua*) during a 24-h fishing survey: an analysis using generalized additive models

Sara A. Adlerstein and Henny C. Welleman

Abstract: Results show that the weight of cod (*Gadus morhua*) stomach contents sampled in the North Sea varies significantly within 24 h. To determine whether feeding varied with time, over 1100 cod stomachs were collected around the clock between 7 and 18 May 1984 in two areas in the central North Sea thought to be representative for feeding studies. Here we investigate temporal feeding patterns based on the analysis of stomach-content data, using generalized additive models (GAMs). Results show significant variation of content weight and indicate morning and evening peaks. The relative peak importance differed between and within areas. We propose that differences are due to diet composition, namely, prey size and diel availability. Cod fed primarily on molluscs, mainly ocean quahog (*Cyprina islandica*), crustaceans, sandeels (*Ammodytes* spp.), haddock (*Melanogrammus aeglefinus*), herring (*Clupea harrengus*), and several flatfish species. In one area, the diet was dominated by fish, relatively large prey that perform diel vertical migration, and in the other by invertebrates, smaller prey that are digested faster. The diel pattern was more pronounced where invertebrate prey were dominant. Generalisation of results and implications for predation-mortality estimates based on data from the North Sea Stomach Content Database, used to implement multispecies models in the region, are discussed.

Résumé : La masse des contenus stomacaux de Morues franches (*Gadus morhua*) échantillonnés dans la Mer du Nord varie significativement au cours d'un cycle de 24 h. Plus de 1100 estomacs de morues récoltés jour et nuit du 7 au 18 mai 1984 dans deux régions du centre de la Mer du Nord considérées comme représentatives pour des études de nutrition ont servi à déterminer les variations de l'alimentation dans le temps. Les patterns temporels ont été générés par l'analyse des données provenant des contenus stomacaux au moyen de modèles additifs généralisés (GAM). Il y a une variation temporelle significative dans la masse des contenus stomacaux, avec des maximums le matin et le soir. L'importance relative des maximums varie à l'intérieur d'une même région et d'une région à l'autre. Nous croyons que ces différences sont dues à la composition du régime alimentaire, en particulier la taille des proies et leur disponibilité au cours du cycle journalier. La morue se nourrit surtout de mollusques, en particulier du Quahog nordique (*Cyprina islandica*), de crustacés, de lançons (*Ammodytes* spp.), d'Aiglefins (*Melanogrammus aeglefinus*), de Harengs (*Clupea harrengus*) et de plusieurs espèces de poissons plats. Dans une des régions, le régime est dominé par les poissons, des proies de taille relativement importante qui opèrent des migrations verticales journalières, dans l'autre, par des invertébrés, des proies plus petites qui se digèrent plus rapidement. Le pattern journalier est plus prononcé là où les proies invertébrées dominent. La généralisation de ces résultats fait l'objet d'une discussion; nous examinons aussi leurs répercussions sur les estimations de la mortalité par prédation basées sur la banque de données « North Sea Stomach Content Database » utilisées pour faire fonctionner des modèles multispécifiques dans la région.

[Traduit par la Rédaction]

Introduction

The study of diel patterns in feeding is relevant for multispecies assessment models that incorporate trophic interactions, since patterns affect predation estimation. Among these models is the North Sea multispecies virtual population analysis (Gislason and Helagson 1985). Data to estimate model feeding parameters in the region are available exclusively from the North Sea Stomach Content Database. Data are mainly from 1981 and 1991 stomach content sampling projects (Hislop 1997), the protocols for which did not provide for time stratification or around the clock sampling. Estimates of predation mortality based on these data can be affected, if stomach contents follow diel patterns.

To investigate whether cod feeding varies with time, a survey was conducted between 7 and 18 May 1984 on board the MS *Tridens*, in two small areas in the central North Sea (International Council for the Exploration of the Sea (ICES)

Received September 21, 2000. Accepted November 10, 2000. Published on the NRC Research Press web site on December 20, 2000.
J15986

S.A. Adlerstein.[1] Institut für Hydrobiologie und Fischereiwissenschaft, Universität Hamburg, Olbersweg 24, 22767 Hamburg, Germany.
H.C. Welleman. Netherlands Institute for Fisheries Research, P.O. Box 68, 1970 AB IJmuiden, the Netherlands.

[1] Corresponding author (e-mail: sadlerstein@uni-hamburg.de).

rectangles 40F3 and 41F3) thought to be representative for the study. The stomachs, collected in 22 hauls, provide one of the few data sets currently available for North Sea cod sampled on a 24-h basis, despite the fact that studies at fine temporal and geographical scales are essential for quantifying the effects of particular sources of variation, such as time of day. Here we report on the analysis of stomach-content weight, complemented with diet information.

The analysis of stomach-content data is the most readily available tool with which to infer fish feeding behaviour, and several approaches have been used with such data to study temporal patterns of feeding. Approaches have ranged from qualitative inference from relationships between content characteristics and time of day or light level at sunrise and sunset, as in Daan (1973), to models combining the analysis of content weight and digestion rates, as in Mergardt and Temming (1997), and dynamic models of feeding and digestion based on distribution shapes of individual stomach weights (Hall et al. 1995). We investigated temporal fluctuation through quantitative inference, using generalized additive models (GAMs) (Hastie and Tibshirani 1990), and analyzed the relationship between content weight and the time stomachs were sampled. GAMs are extensions of generalized linear models and are used to model relationships between independent variables and covariates without imposing rigid parametric forms; they were introduced by Stefánsson and Pálsson (1997) in their analysis of cod stomach contents. We regard this computational intensive approach as highly valuable, as it permits the investigation of nonlinear effects of covariates, such time of day, and the testing of significance, while incorporating appropriate description of error terms.

Materials and methods

We modelled individual stomach-content weight as a function of haul shooting time and fish length, which were introduced as nonparametric continuous variables, using routines contained in the S-Plus programming environment based on Hastie and Tibshirani (1990), with spline scatterplot smoothers, according to

$$(1) \qquad \log(\mu) = \alpha + \sum_{j=1}^{2} f_j(X_j) + \varepsilon$$

where errors ε are independent of the X_js, α is a constant, the mean μ is the expected weight Y of the stomach contents $E(Y/X_1,X_2)$, and f_j are univariate smooth functions for time X_1 and fish length X_2. Once patterns were identified, time was modelled as a factor. The gamma variance $V(\mu) = \mu^2/v$, where the parameter v determines the gamma distribution shape, and logarithmic-link $\log(\mu)$ functions were used to relate the expected weight of stomach contents to the predictors, because weights were skewed with variance proportional to the square of the mean (Hastie and Tibshirani 1990).

Data are from 844 stomachs of cod 20–60 cm in length, of which 80% were under 40 cm. The stomachs, collected in bottom hauls of 1.5-h duration at about 3-h intervals, had been sampled, individually preserved, and processed according to the ICES Stomach Sampling Program manual (Hislop 1997). Prey were identified to the lowest taxa possible, counted, measured, and weighed (molluscs without shell). The degree of digestion was determined for fish.

Results

The mean stomach weights of cod (within 10-cm length-classes and 3-h intervals) ranged from 2 to 190 g (Table 1). In area 40F3, the stomach contents of small cod were 20% heavier and of large cod were 40% lighter than comparable fish from area 41F3. Weights were higher in the early morning (around 06:00) and in the evening (18:00–21:00); however, the lowest values were observed before the morning peak in area 40F3 and before the evening peak in area 41F3. Despite these differences, weights were similar around midday.

Stepwise analysis of deviance performed by area indicates that fluctuations of mean content weight with time are significant (probability of $F < 0.05$; Table 1). The model including time and fish length reduces the null deviance for area 40F3 from 953.33 to 549.83 (with 9 df) and for area 41F3 from 547.39 to 273.42 (with 6 df). This reduction corresponds to a R^2 of about 0.5 in a normal regression. Further, the degrees of freedom for smoothers representing time, assessed within the deviance analysis by jointly increasing and decreasing them until no significant fit improvement occurred, are six for area 40F3 and three for area 41F3. Inspection of the deviance residuals indicates adequate model fits. Also, intra-haul correlation, common in studies conducted at coarser temporal and spatial resolution, was not detected. Fits to investigate interactions between covariates showed no important differences.

Fitted values for GAMs including 95% confidence bands (Fig. 1) show daily weight fluctuation. Area 40F3 values barely meet at the graph ends, since no samples were taken for 4 h at night. Here, weights increase during early morning from the lowest levels at night and continue to increase during the day, with morning and evening peaks. Extreme values in the proportion of body weight are 4 to nearly 1%. This corresponds to a 15% decrease in stomach weight within 8 h, which is in line with stomach-weight decay in the absence of feeding predicted using a gastric-evacuation model (Jones 1974 in Mergardt and Temming 1997):

$$(2) \qquad S_t = (S_0^{(1-b)} - R * (1-b) * t)^{\frac{1}{1-b}}$$

where S_t is the residual stomach content at time after digestion t and S_0 is initial weight; $b = 0.44$ for North Sea cod, $R = 0.00274$–0.0037 for prey type and size found (A. Temming, Universität Hamburg, personal communication), and temperature = 8–9°C. In area 41F3, weights increase slightly in the early morning from night levels higher than those in area 40F3 and decrease during the day; also, evening and morning peaks are not clearly separated. Difference in levels is less than in area 40F3—from 4 to slightly under 3%. However, no samples were taken between 12:15 and 18:58, when weights could have been lowest.

Time was also found to be significant when modelled as a seven-level factor for area 40F3 (probability of $F < 0.000001$) and as two-level factor for area 41F3 (06:00–20:00 and 20:00–06:00) (probability of $F = 0.02$). Model coefficients (not shown) and nonoverlapping of 95% confidence intervals (Fig. 1) between morning and evening peaks in area 41F3 and between the two time periods in area 40F3 indicate that differences are significant.

Table 1. Mean weights of stomach contents and analysis of deviance for variation in stomach-content weight with time of day.

(*a*) Mean weights (g) of stomach contents.

	Length-class (cm)									
	Area 40F3					Area 41F3				
Time	20–29	30–39	40–49	50–59	60–69	20–29	30–39	40–49	50–59	60–68
00:00–03:00	4.5	11.8	13.3	27.9	7.88	1.7	17.3	36.8	98.6	
03:00–06:00	1.9	4.6	12.4	32.0	45.1	6.9	18.9	36.8	140.4	73.5
06:00–09:00	4.9	6.9	17.1	42.1	188.8	5.5	23.4	34.5	31.8	95.6
09:00–12:00	4.6	13.7	27.9	24.5	121.0	3.2	12.4	42.1	78.5	66.1
12:00–15:00	2.7	14.2	27.2	42.1	164.5	3.5	15.0	40.5	94.7	219.7
15:00–18:00	3.8	8.9	29.1	49.9	88.2					
18:00–21:00	7.2	17.2	26.6	44.8	—	0.7	14.8	32.1	94.7	220.1
21:00–24:00	7.0	18.6	37.7	—	—	4.3	18.1	50.7	49.5	78.8

(*b*) Analysis of deviance for variation in stomach-content weight with time of day.

Term	Res. df	Res. deviance	Test	df	Deviance	F	*P* (*F*)
Area 40F3[a]							
Null model	559	953.33					
s(time,6) + *s*(length,3)	550	549.83					
s(length,3)	556	601.24	–*s*(time,6)	–6	–51.41	9.773	<0.0001
s(time,6)	553	897.95	–*s*(length,3)	–3	–348.11	132.359	0
Non-linearity	555	581.86	Time	–5	–9.93	5.663	0.0037
Area 41F3[b]							
Null model	282	547.39					
s(time,3) + *s*(length,3)	276	273.42					
s(length,3)	279	279.42	–*s*(time,3)	–3	–6.48	2.723	0.044
s(time,3)	279	526.67	–*s*(length,3)	–3	–253.24	106.313	0
Non-linearity	278	281.25	Time	–2	–7.83	3.443	0.033

Note: "Term" gives the variables in the model. "Res. df" and "Res. deviance" are the degrees of freedom and deviance of the model including the variables in Term. "Test" gives the variable excluded from the full model, with "df" and "Deviance "being the difference excluding the tested variable. "Non-linearity" of time of day is tested by comparing the full model and the model incorporating the tested variable as the linear term.

[a] Parameter v = 1.0289 (SE = 0.05423).

[b] Parameter v = 0.8292 (SE = 0.0603).

Diet in the two areas was similar, but was dominated by invertebrates in area 40F3 and fish in area 41F3 (Fig. 1). Predominant fish prey were sandeels (*Ammodytes* spp.), haddock (*Melanogrammus aeglefinus*), herring (*Clupea harengus*), and several flatfish. The most important invertebrate was ocean quahog (*Cyprina islandica*), but other molluscs, crustaceans, and polychaetes were abundant. In area 40F3, invertebrates made up over 60% of the dietary biomass of cod up to 40 cm in length, and *C. islandica* was present in one-third of the stomachs. In area 41F3, fish constituted over 50% of the biomass; sandeels dominated, being present in more than half the samples.

Changes that can be related to temporal patterns in stomach weights occurred in the diet within a 24-h period. In area 40F3, the morning peak coincides with the high contribution of invertebrates and the low proportion of stomachs containing sandeels; the further increase up to the evening maximum occurs as sandeels become more important. In area 41F3, both peaks relate to fish consumption.

The stage of digestion of fish prey gives further information about cod feeding rhythm. In both areas, sandeels (typically 1– 5 per stomach) were around 10 cm in length and, thus, similar digestion rates are to be expected. In area 40F3, undigested sandeels (out of 996) were only found in trawls that started between late morning and 15:30, further suggesting that stomach-weight increase during the daytime is related to this prey. Also, in area 41F3, the few fresh specimens found (out of 2020) were in hauls that started between early morning and past midday. Most importantly, in both areas, fresh sandeels were not found in hauls that started after sunrise or before sunset, indicating that this prey is not consumed at night. Other undigested fish were also absent in midnight hauls.

Discussion

The results presented here, indicating significant diel variation in the stomach-content weight of cod and suggesting the presence of morning and evening peaks, are in agreement with most results from similar studies. Arntz (1973) reported that cod in the Barents Sea feed between 08:00 and 20:00, varying seasonally, and that cod in the Baltic Sea take in food before sunrise and at about sunset with changes in the prey consumed between periods (i.e., *C. islandica* was present in larger quantities in evenings and fish were present in larger quantities in mornings). Rae (1967) concluded that cod in the North Sea feed at dawn and dusk, while Daan (1973) found no consistent pattern.

Although this study allowed us to identify diel feeding patterns, some aspects of the sampling could have affected

Fig. 1. Fitted mean stomach-content weights of cod as a function of time of day and accounting for fish length, derived from generalized additive models incorporating gamma variance, logarithmic-link functions, and smooth variable cod length and smooth variable time of day or time as a factor. Each plot is the contribution of time of day to the additive predictor and each line in the *x*-axis represents one observation. Dashed lines and striped bars present approximate 95% confidence bands. Fitted values are centred so that when computed for the original data they average zero. (*a*) Area 40F3 with time as a smooth. (*b*) Area 41F3 with time as a smooth. (*c*) Area 40F3 with time as a seven-level factor. (*d*) Area 41F3 with time as a two-level factor. (*e* and *f*) Diet composition in percent weight in relation to cod length (in 10-cm length-classes) in areas 40F3 (*e*) and 41F3 (*f*).

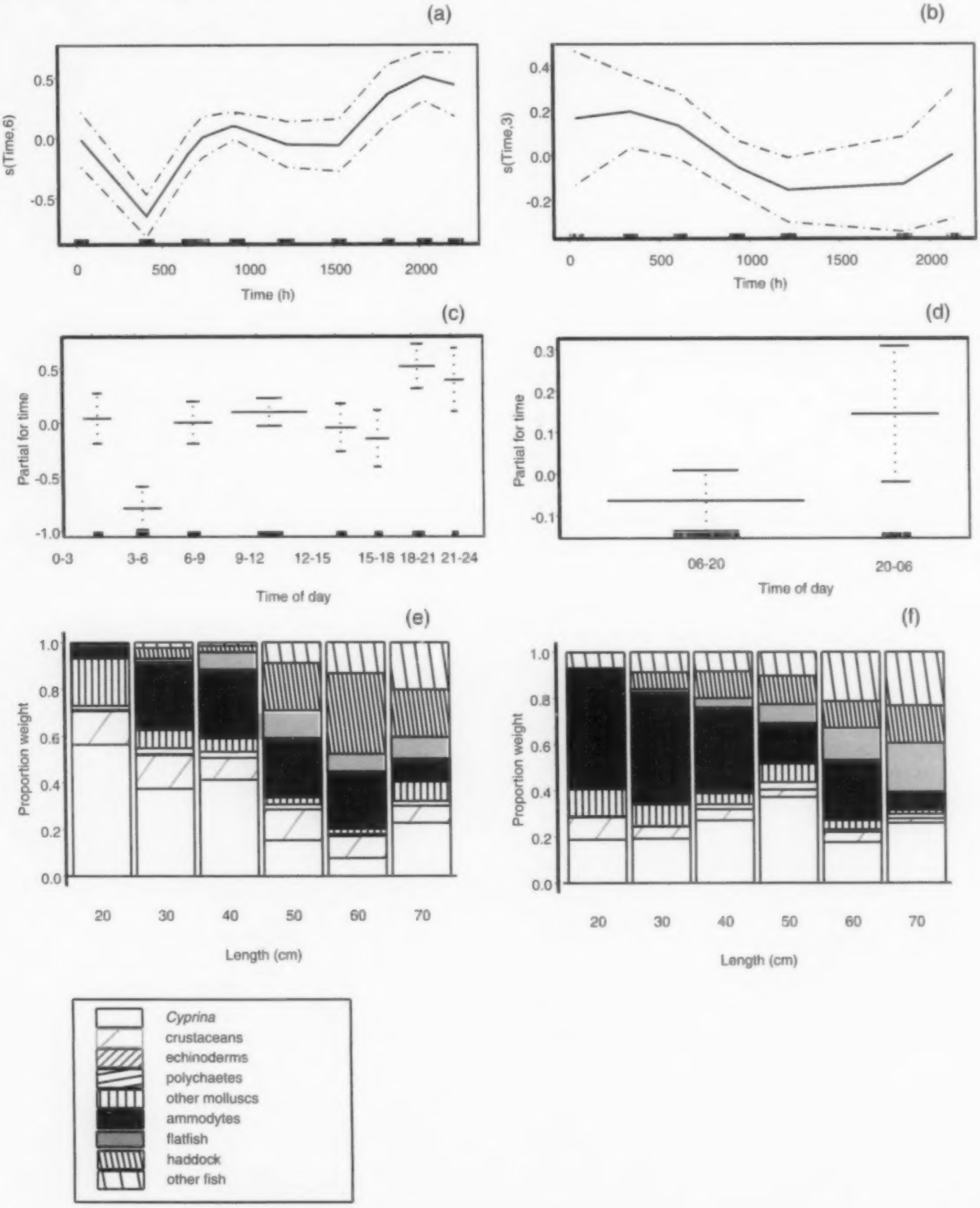

the results. First, stomachs were not actually collected at 3-h intervals. Also, it is possible that haul duration was too long, which could have caused the low percentage of fresh sandeels found in stomachs from area 41F3. Nevertheless, based on estimates from the presented gastric-evacuation model, less than 2% variation could be expected within 1.5 h under the conditions in the study.

The significant diel variation of stomach contents and the pattern found should be fairly general for the North Sea in spring and summer. This is because variations are influenced by prey type, and the diet described here is within the range of prey items reported for the North Sea (except for the high contribution of *C. islandica*) from local and regional studies (summarised by Daan (1989) and Hislop (1997)). Cod feeding within the North Sea are reported to be temporally and spatially stable in terms of stomach content weight levels and diet composition. Further, the pattern likely occurs because cod feed most intensively at sunrise and sunset, owing to changes in the availability of prey such as sandeels that are known to perform diel migration in spring and summer as they reach a length of about 4 cm. Sandeels, which bury in the sand at night, are probably vulnerable when leaving their refuge on the seabed at dawn and when returning at dusk. The absence of undigested sandeels in cod stomachs at night indicates that they are not preyed on during this period. The large contribution of *C. islandica* to the diet should not restrict generalisation of the pattern. Equivalent proportions of molluscs (such as *Acanthocardia* spp.) are characteristic of the cod diet. In addition, high proportions of *C. islandica* have often been documented in the cod diet where diel patterns have been found (Arntz 1973). What could change the diel pattern shape, we found, is a shift in the consumption of fish prey to species such as herring that have the opposite timing in vertical migration. The change in prey availability within 24 h would, nevertheless, remain. Variation would be only minor at low temperatures.

The bimodal diel pattern in stomach contents, with stronger signals occurring with an increasing proportion of small to large prey (invertebrates to fish), should also be general for the North Sea. Prey size, as well as behaviour, influences the pattern in stomach-content weight, by affecting predator satiation and digestion rates. With respect to satiation, our results show a lower value of the gamma parameter v in the model for the area where the proportion of fish prey is dominant and, thus, higher variance, indicating that cod eat more sporadically. With respect to digestion rates, the results of Mergardt and Temming (1997) from simulation scenarios of feeding provide stronger evidence for changes in stomach contents over a 24-h period when food particles are small, given that timing of food intake is the same and other conditions are equal.

The implications of these results for North Sea models that incorporate trophic interactions could be important. Diel fluctuation in stomach contents can be expected during spring and summer, but data available from the North Sea Stomach Content Database are from sampling that is not stratified by time and that occurred mostly between 06:00 and 19:00. For example, within 387 sampling stations in the third quarter of 1991, more samples were taken at 06:00 than at any other time. This could result in overestimation of predation mortality in situations such as that in area 41F3 or in underestimation in situations such as that in area 40F3. Diel feeding patterns of several North Sea predators have been documented and, thus, a potential bias in predation-mortality estimates based on this database is not exclusive to cod. An increasing interest in developing multispecies models in the region emphasizes model development and overlooks the current problems in the data used for implementation. Time stratification in future stomach sampling in the region and in other temperate ecosystems is recommended.

Acknowledgements

We thank Henk Heessen for providing us with the data. This study is a follow-up to a project on stomach-content analysis of North Sea main predators funded by European Commission Contract AIRC-CT94–2410.

References

Arntz, W. 1973. Periodicity of diel food intake of cod *Gadus morhua* in the Kiel Bay. Oikos Suppl. **15**: 138–145.

Daan, N. 1973. A quantitative analysis of the food intake of North Sea cod, *Gadus morhua*. Neth. J. Sea Res. **6**: 479–517.

Daan, N. (*Editor*). 1989. Data base report of the Stomach Sampling Project 1981. ICES (Int. Counc. Explor. Sea) Coop. Res. Rep. No. 164.

Gislason, H., and Helagson, Th. 1985. Species interactions in assessment of fish stocks with special application to the North Sea. Dana, **5**: 1–44.

Hall, S.J., Gurney, W.S., Dobby, H., Basford, D.J., Heaney, S.D., and Robertson, M.R. 1995. Inferring feeding patterns from stomach contents data. J. Anim. Ecol. **64**: 39–62.

Hastie, T., and Tibshirani, R. 1990. Generalized additive models. Chapman and Hall, London.

Hislop, J. 1997. Database report of the Stomach Sampling Project, 1991. ICES (Int. Counc. Explor. Sea) Coop. Res. Rep. No. 219.

Mergardt, N., and Temming, A. 1997. Diel pattern of food intake in whiting (*Merlangius merlangus*) investigated from the weight of partly digested food particles in the stomach and laboratory determined particle decay functions. ICES (Int. Counc. Explor. Sea) J. Mar. Sci. **54**: 226–242.

Rae, B.B. 1967. The food of cod in the North Sea and on the west Scotland grounds. Mar. Res. 1967: 1–68.

Stefánsson, G., and Pálsson, O.K. 1997. Statistical evaluation and modelling of the stomach contents of Icelandic cod (*Gadus morhua*). Can. J. Fish. Aquat. Sci. **54**: 169–181.

Effective population size of winter-run chinook salmon based on microsatellite analysis of returning spawners

Philip W. Hedrick, Vanessa K. Rashbrook, and Dennis Hedgecock

Abstract: We previously estimated the predicted effective population size for the endangered winter-run chinook salmon, *Oncorhynchus tshawytscha*, based on a number of assumptions, including random survival and return of released fish. Here we present data from actual returning spawners, identified to family by microsatellite loci, and calculate the observed effective population size. In 1994 and 1995, the observed effective population sizes were 93.6 and 78.2% of predicted values, respectively, suggesting that the numbers of returning fish were very close to random expectations in 1994 and less close to random in 1995. The ratio of the effective population size to the adult number, N_e/N, was greater than unity for 1994 and approximately 0.5 in 1995. The high ratio in 1994 reflects the success of the breeding protocol to equalize individual contributions and near random returns, while the lower number in 1995 appears to be the result of both less successful equalization and less close to random returns in that year. These findings provide an optimistic outlook for the success of this supplementation program and suggest that the overall effective population size has not been greatly reduced, since returning spawners represent a broad sample of parents and not fish from only a few families.

Résumé : Dans une étude antérieure, nous avons estimé la taille effective prédite de la population chez le Saumon quinnat à montaison hivernale, *Oncorhynchus tshawytscha*, une forme menacée d'extinction, en nous basant sur un certain nombre de suppositions, en particulier celle de la survie et du retour aléatoires des poissons libérés. Nous présentons maintenant des données obtenues sur les reproducteurs qui sont de fait revenus frayer et qui ont été identifiés à la famille à l'aide de locus microsatellites, ce qui nous a permis de calculer la taille effective observée de la population. La taille observée correspondait à 93,6% de la taille prédite en 1994 et à 78,2% de la taille prédite en 1995; le nombre de poissons qui sont revenus s'approchait donc des valeurs prédites en supposant un retour aléatoire en 1994, mais moins en 1995. Le rapport entre la taille effective de la population et le nombre d'adultes, N_e/N, était plus grand que 1 en 1994 et d'environ 0,5 en 1995. Le rapport élevé en 1994 reflète le succès du programme de reproduction qui a pu équilibrer les contributions individuelles, ainsi que le caractère aléatoire des retours; le rapport plus faible en 1995 semble être dû à une équilibration moins réussie et à des retours moins aléatoires. Ces résultats permettent d'être optimiste à l'égard de ce programme d'appoint et laissent croire que la taille effective globale de la population n'a pas diminué de façon importante, puisque les reproducteurs qui reviennent sont issus d'un large éventail de parents et pas seulement de quelques familles.

[Traduit par la Rédaction]

Introduction

Winter-run chinook salmon, *Oncorhynchus tshawytscha*, from the Sacramento River (California) drainage are listed as endangered both by the state and federally. A program to mitigate some of the factors causing endangerment has included the annual supplementation of young raised at Coleman National Fish Hatchery (CNFH) on Battle Creek, a tributary of the Sacramento River. A breeding protocol for the supplementation program was designed as an attempt to equalize the contributions from the captured spawners. Hedrick et al. (1995, 2000) evaluated the effects of this program on the effective population size (N_e) of released fish in the first 5 years of the program and found that supplementation did not appear to greatly influence the effective population size of the run, neither significantly reducing nor increasing it.

However, as discussed in Hedrick et al. (1995, 2000), these estimates of predicted effective population size made a number of assumptions, including random survival and return of individuals from the different hatchery-raised families. No actual returning individuals were identified or used in the analyses. We have now actually identified returning spawners to families by molecular markers, to directly determine whether the assumptions used in our previous analyses were true. From this information, we now calculate the

Received August 29, 2000. Accepted September 27, 2000. Published on the NRC Research Press web site on December 20, 2000.
J15946

P.W. Hedrick.[1] Department of Biology, Arizona State University, Tempe, AZ 85287, U.S.A.
V.K. Rashbrook and D. Hedgecock. Bodega Marine Laboratory, University of California—Davis, Bodega Bay, CA 94923, U.S.A.

[1] Corresponding author (e-mail: philip.hedrick@asu.edu).

observed effective population size of these returning fish, evaluate our earlier predictions, and give a direct measure of the ratio N_e/N.

Materials and methods

Collection of hatchery-origin returning spawners

Hatchery-origin winter-run chinook salmon, distinguished by clipped adipose fins and the timing of their spawning migration, were first observed passing the CNFH weir on Battle Creek in 1995. Coded-wire tags (CWTs) recovered subsequently from eight carcasses (all hatchery winter-run chinook salmon were tagged) confirmed that winter-run individuals from the CNFH 1992 year-class had indeed returned to Battle Creek and not to the Sacramento River, where they had been released as fry (U.S. Fish and Wildlife Service 1996). In contrast, no hatchery-origin fish were recovered that same year among the 85 fish live-trapped at Keswick Dam, Sacramento River, for the winter-run supplementation program, suggesting that winter-run salmon produced at the CNFH had imprinted on Battle Creek water.

Trapping operations for hatchery-origin winter-run chinook salmon began in earnest on Battle Creek in 1997. The goal was to relocate as many returning adults as possible to the winter-run spawning grounds in the Sacramento River. Returning adults trapped at the hatchery during the winter-run spawning migration were held until their run identity was determined. This was achieved by amplifying genomic DNA from a caudal fin clip and typing individuals for five microsatellite loci, *Ots-2*, *-3*, *-9*, and *-10* (Banks et al. 2000) and *One*μ*13* (Scribner et al. 1996). The odds of a given genotype being winter run were calculated as the ratio of genotypic frequencies in winter versus other runs, using frequencies for the relevant spawning populations (Banks et al. 1999) and the computer program WHICHRUN (Banks and Eichert 2000). Of the 116 fish trapped in Battle Creek in 1997, 102 had clipped adipose fins, indicating a hatchery origin. Eighteen of these returns were determined to be non-winter run, leaving 84 hatchery-origin winter-run chinook salmon available for parentage analysis. Sixteen were sacrificed to confirm family origin by examination of their CWTs, although tags were not recovered from two of these fish; the rest of the fish were released back into the Sacramento River. The trapping program in Battle Creek continued in 1998, when 117 fish were trapped. Of these, 75 were non-winter run, 32 were winter run with intact adipose fins, and only 11 were winter run with clipped adipose fins confirming their hatchery origin. Eight of these 11 were sacrificed to read their CWT (1 not recovered), owing to the possibility that fish released in 1995 were winter × spring hybrids (see Hedrick et al. 2000; D. Hedgecock, M. Banks, J. Blankenshipt, V. Rashbrook, and M. Calavetta, unpublished data).

Three other potential sources of hatchery-origin winter-run chinook salmon were exploited for this study. We examined winter-run chinook salmon carcasses with clipped adipose fins recovered by the U.S. Fish and Wildlife Service during the winter-run spawning season (May through August) from both Battle Creek (in 1996 and 1997) and the Sacramento River (in 1997 and 1998). Sixty-nine putative winter-run carcasses were recovered from Battle Creek in 1996–1997, of which 31 had either clipped adipose fins confirming hatchery origin, or CWTs allowing verification of family origin. Although 204 winter-run carcasses were collected from the Sacramento River in 1997, only four had clipped adipose fins or CWTs confirming hatchery origin. Four tagged winter-run carcasses were also recovered from the Sacramento River in 1998. We also screened 152 winter-run chinook salmon live-trapped by the U.S. Fish and Wildlife Service at the Keswick Dam in 1998, when the supplementation program resumed; only nine of these had clipped adipose fins. The low return of hatchery-origin winter-run chinook salmon to the Sacramento River, and their recovery as carcasses, is consistent with their having imprinted on Battle Creek.

Molecular genetic techniques

Hatchery-origin winter-run chinook salmon returning in 1996–1998 were most likely from the 1993, 1994, and 1995 CNFH spawns, which comprised 12, 32, and 42 different matings of wild-caught brood stock, respectively (Hedrick et al. 1995, 2000). Tissue sampled from returning adults, as well as from the parents, was stored in TEN buffer (Tris, EDTA, NaCl); genomic DNA was extracted from 1-mm^2 caudal fin clips using 5% chelex (Bio-Rad protocols) or, in the case of the degraded-carcass samples, a DNA isolation kit (Puregene, Gentra Systems, Inc.). Since the multilocus microsatellite genotypes of all the winter-run brood stock parents were known (Banks et al. 1999, 2000), we attempted to assign each returning fish to its family of origin using microsatellite markers. For each hatchery-origin fish, we determined the genotype for the five dinucleotide microsatellites listed above and for two additional tetranucleotide microsatellite markers, *Ots-104* and *-107* (Nelson and Beacham 1999), which are considerably more polymorphic (Banks et al. 2000). We used a computer program to exclude potential parents (WHICHPARENT; W. Eichert, available at http://www.bml.ucdavis.edu/salmon) and assigned a fish to family only if it was incompatible with all but one of the 86 potential matings.

Estimation of effective population size

The effective population size for the fish released in the supplementation program can be estimated using either the variance or the inbreeding effective population size, following the approaches of Crow and Denniston (1988) and Lande and Barrowclough (1987), respectively (see details in Hedrick et al. 1995, 2000). It should be noted that this actually estimates the effective number of breeders in an annual cohort (sensu Waples 1990). Because the average generation length is approximately 3 years in winter-run chinook salmon, the total effective population size is approximately three times our estimates.

To calculate the predicted effective population size and confidence intervals for the two different effective population sizes, we randomly drew 10 000 independent samples of 93 and 23 spawners for 1994 and 1995, respectively. We used this approach, because it mimics the actual return data, i.e., using only the proportions of released fish does not include the random sampling that occurs with the return of a finite number of spawners. This approach also allows the calculation of empirical confidence intervals for the estimates of effective population size. For the actual returns, we used the assignments to individual parents as determined by microsatellites to calculate the observed effective population size.

Results

Parentage determination

As expected, the examination of hatchery returns from the years 1996–1998 yielded individuals mainly from the 1994 and 1995 brood stock families. The parentage of returning fish was unambiguously assigned for two fish spawned in 1993, 93 fish spawned in 1994, and 23 fish spawned in 1995. Of these, 84 were live-trapped in Battle Creek, eight were live-trapped at Keswick Dam, and 26 were recovered as post-spawn carcasses. Four fish were assigned by CWT alone; the rest were assigned by genotype, with or without verification by CWT. Seventeen individuals were assigned to more than one family and, lacking a CWT, were excluded from calculations of effective population size.

Table 1. Sex and age at return for hatchery-origin Sacramento River winter-run chinook salmon.

	Age at return (years)			
Sex	2	3	4	Total
Male	12	27	6	45
Female	0	65	2	67
Unknown	1	16	0	17
Total	13	108	8	129[a]

[a] Total includes 118 fish assigned to a family by genetic markers or coded-wire tags, plus 11 fish assigned to two families by genetics, but with both families belonging to the same year-class, making their age, at least, unambiguous.

Twenty-seven fish that either died or were sacrificed after trapping and 14 carcasses yielded CWTs from which family or lot origin could be determined. Genetic data was not obtained for four of the carcasses but was obtained for the remaining 37 fish, allowing independent verification of genetic family assignment. In 25 cases, genetic assignment to one family agreed with the CWT reading. In nine cases, the CWT confirmed family origin for individuals whose genotypes were compatible with two or more families (often because of missing genetic data). In one case, a fish was assigned genetically to one of the families in a pooled lot of families that had been tagged with a single code. Finally, in only two cases, did the CWT and genetic family assignment disagree. One fish was matched to family 94-18J by genetic markers but was tagged as having come from the paternal half-sib family 94-14J; conceivably, this fish jumped between adjoining tanks prior to tagging. In the second case, although the CWT indicated that the fish belonged to family 94-18I, its genotype did not match any family, suggesting a mix-up in tissue samples. As a precaution, neither individual was included in the analysis.

Proportion of female and male progeny spawning

In our calculation of the variance effective population size in previous studies (Hedrick et al. 1995, 2000), we assumed that the proportions of female and male progeny spawning were 0.4 and 0.6, respectively, (Frank Fisher, California Department of Fish and Game, Red Bluff, CA 96080, unpublished data). For our application here, we now have data on returning released fish by sex and age at return (Table 1), and it appears that approximately 60% of the spawning fish are females. Therefore, in the calculations below, we assume that the proportions of female and male progeny spawning are 0.6 and 0.4, respectively, unlike our previous assumptions. In addition, from our summarized data in Table 1, 84% of the fish returned at 3 years of age. Age at return appears to be more variable in males, with 27% returning at age 2, 60% at age 3, and 13% at age 4, while 97% of females return at age 3.

Effective population size

Tables 2 and 3 give the number of progeny released from the different females and males in 1994 and 1995, respectively (for a detailed discussion see Hedrick et al. 2000). In 1994, 26 fish (16 females and 10 males) produced 43 346 released progeny. Overall, the production was fairly equal across individuals, with the proportions of progeny produced ranging from 0.032 to 0.091 (mean of 0.062) for females and from 0.029 to 0.147 (mean of 0.1) for males. In 1995, 36 fish (and six captive-reared females from Bodega Marine Laboratory) produced 51 273 released progeny. There was more variation in contribution across individuals in 1995, with the proportions of progeny produced ranging from 0.002 to 0.078 (mean of 0.037) for wild-caught females and from 0.020 to 0.113 (mean of 0.067) for males.

Table 2. The number of progeny released and the number of returning spawners from the different females and males in the 1994 brood year, and the ratio of the proportion of returns to releases for each parent.

	Releases		Returns		
	No.	Proportion	No.	Proportion	Ratio
Female					
3	3 444	0.080	10	0.108	1.35
4	3 055	0.070	5	0.054	0.77
5	2 499	0.058	7	0.075	1.29
6	2 361	0.054	6	0.065	1.20
7	2 421	0.056	3	0.032	0.57
8	2 292	0.053	2	0.022	0.42
9	2 338	0.054	5	0.054	1.00
11	2 320	0.054	7	0.075	1.39
12	2 701	0.062	3	0.032	0.52
13	3 946	0.092	8	0.086	0.93
14	1 364	0.032	2	0.022	0.69
15	3 426	0.079	10	0.108	1.37
16	2 855	0.066	10	0.108	1.64
17	2 766	0.064	7	0.075	1.17
18	3 088	0.071	4	0.043	0.61
19	2 470	0.057	4	0.043	0.75
Total	43 346		93		
Male					
B	4 433	0.102	9	0.097	0.95
C	3 152	0.073	9	0.097	1.33
D	4 360	0.107	16	0.172	1.61
E	6 013	0.139	8	0.086	0.62
F	5 223	0.120	15	0.161	1.34
G	5 098	0.128	6	0.065	0.51
H	4 432	0.102	10	0.108	1.06
I	6 353	0.147	16	0.172	1.17
J	3 012	0.070	3	0.032	0.46
K	1 270	0.029	1	0.011	0.38
Total	43 346		93		

The predicted variance and inbreeding effective population sizes for the 2 years are given in Table 4, using the release proportions from each individual. These predictions assume that there were 93 and 23 randomly returning spawners from the releases in 1994 and 1995 (the predictions in Hedrick et al. (2000) assumed replacement of parents). The variance and inbreeding effective numbers and their confidence intervals were quite close to each other for the 2 years. The predicted effective size from the releases in 1995 was smaller than that from the 1994 releases, owing partly to the greater variance in contribution across individuals in 1995. However, the predicted effective size is also dependent on the number of returning spawners and increases with the number of returns (see Discussion).

Table 3. The number of progeny released and the number of returning spawners from the different females and males in the 1995 brood year, and the ratio of the proportion of returns to releases for each parent.

	Releases		Returns		
	No.	Proportion	No.	Proportion	Ratio
Female					
4	2 219	0.043	1	0.043	1.00
5	2 086	0.041	0	0.000	0.00
6	482	0.009	0	0.000	0.00
7	2 329	0.045	1	0.043	0.96
8	3 284	0.064	6	0.261	4.08
9	1 921	0.038	1	0.043	1.13
10	687	0.013	0	0.000	0.00
11	267	0.005	1	0.043	8.60
12	1 749	0.034	0	0.000	0.00
13	3 605	0.070	1	0.043	0.61
14	2 443	0.048	0	0.000	0.00
15	3 165	0.062	0	0.000	0.00
16	3 364	0.066	0	0.000	0.00
17	102	0.002	0	0.000	0.00
18	3 225	0.063	2	0.087	1.38
19	3 987	0.078	0	0.000	0.00
20	3 468	0.068	3	0.130	1.91
21	3 732	0.073	2	0.087	1.19
22	3 469	0.068	3	0.130	1.91
23	2 930	0.057	0	0.000	0.00
24	1 622	0.032	1	0.043	1.34
1C	38	0.001	0	0.000	0.00
2C	138	0.003	0	0.000	0.00
3C	6	0.000	0	0.000	0.00
4C	23	0.000	0	0.000	0.00
5C	802	0.016	1	0.043	2.69
6C	124	0.002	0	0.000	0.00
Total	51 273		23		
Male					
D	3 253	0.064	0	0.000	0.00
E	3 341	0.065	3	0.130	2.00
F	1 869	0.036	0	0.000	0.00
G	3 429	0.067	5	0.217	3.24
H	1 007	0.020	1	0.043	2.15
I	5 493	0.107	2	0.087	0.81
J	1 691	0.033	1	0.043	1.30
K	5 476	0.107	2	0.087	0.81
L	3 310	0.065	0	0.000	0.00
M	2 848	0.056	2	0.087	1.55
N	5 498	0.107	1	0.043	0.40
O	4 889	0.095	4	0.174	1.83
P	1 533	0.030	0	0.000	0.00
Q	5 808	0.113	1	0.043	0.38
S[a]	1 822	0.036	1	0.043	1.19
Total	51 273		23		

[a] Identified as probable non-winter run. C indicates captive-reared females.

Table 4. The predicted and observed effective population sizes for 1994 and 1995.

Year	N_e estimate[a]	Predicted	Observed
1994	$N_{e(v)}$	34.8 (28.1, 41.2)	31.5
	$N_{e(i)}$	32.7 (26.5, 38.9)	30.2
1995	$N_{e(v)}$	24.5 (16.1, 34.3)	18.0
	$N_{e(i)}$	23.2 (14.8, 33.0)	18.3

Note: Values in parentheses are 95% confidence interval.

[a] $N_{e(v)}$ and $N_{e(i)}$ are the variance and inbreeding effective population sizes, respectively.

Also given in Tables 2 and 3 are the observed returning spawners in 1997 and 1998 that were assignable to families released in 1994 and 1995 using the genetic analysis described above. Every male and female parent was represented in the 93 assignable returning spawners from 1994. On the other hand, in the 23 assignable spawners returning from 1995, a number of the parents were not represented. The ratio of the proportions that were released to the proportions that returned from each individual ranged from 0.38 to 1.64 in 1994 and from 0.00 to 8.60 in 1995.

We can use the actual returns to calculate the observed effective population size (Table 4). For 1994, the observed variance and inbreeding effective population sizes were 90.5 and 92.4% of predicted values and were within the 95% confidence intervals. Using the inbreeding effective approach, we can calculate the ratio of the variance to the mean reproduction across individuals. For females and males, these ratios were 0.51 and 0.55; the values are less than unity, because of the effort to equalize contributions from each individual. Using the release data, these ratios were 0.43 and 0.45 for females and males, respectively. The slightly higher ratio of variance to mean in the observed returns compared with random returns of the releases for both sexes indicates that the observed returns were not completely at random.

In 1995, the observed variance and inbreeding effective sizes were 73.5 and 78.9% of predicted values and were within the 95% confidence intervals. Again, using the inbreeding effective approach, the ratio of the variance to the mean reproduction was 4.22 and 2.23 for females and males, respectively, much larger than unity. However, using the release data, these ratios were 3.14 and 1.62, also larger than unity but less than those observed. In this case, the 34 and 38% higher return than release ratio for females and males, respectively, explains the lower observed than predicted effective population size.

N is generally the observed or estimated number of adults and, for 1994, 29 spawners were captured and 26 of them reproduced. Because it appears that a major reason that captured spawners did not reproduce is that they were not winter run, it may be more legitimate to use the number of spawners reproducing rather than the total number of adults. Using the average observed N_e value from Table 4, the ratio N_e/N for both these values of *N* are larger than unity (Table 5). In other words, it appears that, because of the success of the breeding protocol in evening out contributions across individuals and the near random return of releases, the ratio N_e/N is very high for 1994.

For 1995, 47 spawners were captured and six captive-raised females were brought to the hatchery. Eleven of the wild-caught spawners did not reproduce, probably because most of them were not winter run, and the six captive-raised females contributed only 2.2% of the released progeny. In other words, a reasonable estimate of *N* may be 36, which is the number of wild spawners reproducing, and the resulting

Table 5. Values of the ratio N_e/N determined using the mean observed estimate (calculated from the values in Table 4) and different values of N.

	N		
Year	Source	Value	N_e/N
1994	Total no. of spawners caught	29	1.06
	No. of spawners reproducing	26	1.19
1995	Total no. of spawners caught and captive	53	0.34
	No. of wild and captive spawners reproducing	42	0.43
	No. of wild spawners reproducing	36	0.50

estimate of the ratio N_e/N is 0.50. Although this ratio is not as high as in 1994, it is still substantial, and probably reflects both the effort to equalize the contribution of individuals in the hatchery and that the return proportions were not far from random.

Discussion

Of great interest in recent years has been the effect of small population size on genetic variation and, in particular, the ratio of the effective population size to adult number (Frankham 1995; Nunney 1995). We have identified to family, using seven microsatellite loci, returning winter-run chinook spawner releases from the hatchery supplementation program. From the 1994 and 1995 releases, 93 and 23 returning spawners, respectively, were identified. The observed effective population size for these spawners was close to the value predicted when they were released, assuming random returns, and was 91.4 and 76.2% of predicted values for 1994 and 1995, respectively; the ratio N_e/N was greater than unity in 1994 and was 0.5 in 1995. It appears that returns of individuals are not very different from random and that the breeding protocol to equalize contributions of individuals has increased the N_e/N ratio.

The predicted effective population size assumes that survival and return migration of spawners is generally independent of parental origin. Using CWTs for families, two studies have examined the variation across families in salmon returns from hatcheries. Simon et al. (1986) examined returns from 5 years of releases in coho salmon (*Oncorhynchus kisutch*) from a hatchery in Oregon and found that the average variance to mean ratio across families was 2.87, with a range of 1.57–3.87. Geiger et al. (1997) examined returns from five releases of pink salmon (*Oncorhynchus gorbuscha*) from a hatchery in Alaska and found that the average variance to mean ratio across families was 2.96, with a range of 1.58–4.97. These values are similar to those observed for our 1995 year-class, however, there are several differences between these studies.

First, much of the higher variance to mean ratio in returning 1995 fish was due to a higher variance to mean ratio in the releases, even though equalization of contributions across released individuals was attempted under the breeding protocol, and was not due to large nonrandom survival and return effects of fish. In neither Simon et al. (1986) nor Geiger et al. (1997) were the returns compared with a base line predicted from the family release proportions, so some proportion of the high variance to mean ratio in returns may have been the result of a high variance to mean ratio in releases. Second, in the winter-run supplementation program, there was an effort to equalize contributions across individuals released from the hatchery, unlike the previous studies cited. The low variance to mean ratio in the release in 1994 reflects the success of this program, and the low and similar variance to mean ratio in the returns reflects both the effect of the breeding program and the near-random return of the released fish.

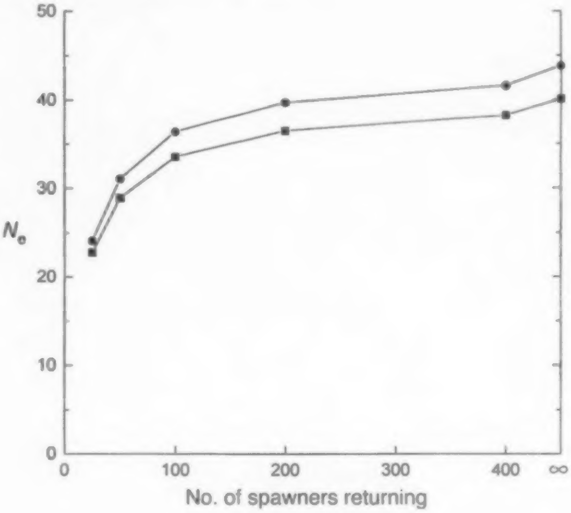

Fig. 1. The variance effective population size predicted from 10 000 samples of different numbers of randomly returning spawners, given the proportions of releases from 1994 (squares) and 1995 (circles).

Our calculation of the effective population size is a stochastic one and uses the same sample size of salmon as the number of returning salmon. If the number of salmon returning is small, then there is a large reduction in the effective population size calculated using this small number, because individual parents may not be represented as expected. For example, in 1995, a number of parents were not represented among the 23 returning progeny at all. The number of adult returns available for analysis was considerably reduced in 1998, owing to high river flow rates, which hindered both trapping operations and carcass collections. This adversely affected the number of fish assigned to families spawned in 1995, since most returning spawners are 3-year-olds. Consequently, we cannot determine the effective population size with the same degree of confidence for the1995 spawners as we can for the1994 spawners.

If the number of returning salmon is large, then the effective population size should closely reflect the proportions released from each parent. To illustrate this effect, Fig. 1 gives the predicted variance effective population sizes for 1994 and 1995, assuming different numbers of returning spawners. When there are few returning spawners, then the predicted effective population size is small for both years but, as the number of returning spawners increases, the effective population sizes increase and asymptote at the values predicted by the proportions released from different individuals. Because the number of individuals contributing is higher in

1995, in spite of a higher variance in contribution across individuals, the asymptotic value for 1995 is larger than for 1994. Interestingly, the predicted value for the 93 returns in 1994 is larger than the predicted value for the 23 returns in 1995, but this is only due to the larger number of returns in 1994.

Although there are results in the literature suggesting that effective population size may be only a small proportion of the adult number, we have found that, in samples of returning hatchery salmon spawners, the N_e/N ratio appears to be greater than unity and 0.5 in two different years. Of course, we are examining the effective population size in artificially propagated fish in which there is somewhat lower mortality before release than in a natural population. In addition, the protocol that has been used in pairing fish in the hatchery reduces the variation of progeny produced across individuals. However, because winter-run chinook salmon generally return to the Sacramento River after nearly 3 years in the Pacific Ocean, and only a small proportion actually return to spawn, there is ample opportunity for nonrandom survival and spawner return. In contrast with reports that the effective population size may be only a small proportion of the adult number (Hedgecock 1994; Frankham 1995), it appears that, overall, the effective population size is similar to values predicted on the basis of random returns (the N_e/N ratio is not low).

Acknowledgements

We appreciate the assistance of United States Fish and Wildlife Service (USFWS) employees that sent us samples. This research was conducted under a permit from the National Marine Fisheries Service and was funded by grants from the USFWS.

References

Banks, M.A., and Eichert, W. 2000. WHICHRUN (version 3.2): a computer program for population assignment of individuals based on multilocus genotype data. J. Hered. **91**: 87–89.

Banks, M.A., Blouin, M.S., Baldwin, B.A., Rashbrook, V.K., Fitzgerald, H.A., Blankenshipt, S.M., and Hedgecock, D. 1999. Isolation and inheritance of novel microsatellites in chinook salmon (*Oncorhynchus tschawytscha*). J. Hered. **90**: 281–288.

Banks, M.A., Rashbrook, V.K., Calavetta, M.J., Dean, C.A., and Hedgecock, D. 2000. Analysis of microsatellite DNA resolves genetic structure and diversity of chinook salmon (*Oncorhynchus tshawytscha*) in California's Central Valley. Can. J. Fish. Aquat. Sci. **57**: 915–927.

Crow, J.F., and Denniston, C. 1988. Inbreeding and variance effective numbers. Evolution, **42**: 482–495.

Frankham, R. 1995. Effective population size/adult population size ratios in wildlife: a review. Genet. Res. **66**: 95–107.

Geiger, H.J., Smoker, W.W., Zhivotovsky, L.A., and Gharrett, A.J. 1997. Variability of family size and marine survival in pink salmon (*Oncorhynchus gorbuscha*) has implications for conservation biology and human use. Can. J. Fish. Aquat. Sci. **54**: 2684–2690.

Hedgecock, D. 1994. Does variance in reproductive success limit effective population size of marine organisms? *In* Genetics and evolution of aquatic organisms. *Edited by* A. Beaumont. Chapman and Hall, London. pp. 122–134.

Hedrick, P.W., Hedgecock, D., and Hamelberg, S. 1995. Effective population size in winter-run chinook salmon. Conserv. Biol. **9**: 615–624.

Hedrick, P.W., Hedgecock, D., Hamelberg, S., and Croci, S.J. 2000. The impact of supplementation in winter-run chinook salmon on effective population size. J. Hered. **91**: 112–116.

Lande, R., and Barrowclough, G.F. 1987. Effective population size, genetic variation, and their use in population management. *In* Viable populations for conservation. *Edited by* M. Soule. Cambridge University Press, Cambridge, U.K. pp. 87–124.

Nelson, R.J., and Beacham, T.D. 1999. Isolation and cross species amplification of microsatellite loci useful for study of Pacific salmon. Anim. Genet. **30**: 228–229.

Nunney, L. 1995. Measuring the ratio of effective population size to adult numbers using genetic and ecological data. Evolution, **49**: 389–392.

Scribner, K.T., Gust, J.R., and Fields, R.L. 1996. Isolation and characterization of novel salmon microsatellite loci: cross-species amplification and population genetic applications. Can. J. Fish. Aquat. Sci. **53**: 833–841.

Simon, R.C., McIntyre, J.D., and Hemmingsen, A.R. 1986. Family size and effective population size in a hatchery stock of coho salmon (*Oncorhynchus kisutch*). Can. J. Fish. Aquat. Sci. **43**: 2434–2442.

U.S. Fish and Wildlife Service. 1996. Escapement of hatchery-origin winter chinook salmon (*Oncorhynchus tschawytscha*) to the Sacramento River, California in 1995, with notes on spring chinook salmon in Battle Creek. Report from the U.S. Fish and Wildlife Service, North Central Valley Fish and Wildlife Office, Red Bluff, CA 96080, U.S.A.

Waples, R.S. 1990. Conservation genetics of Pacific salmon. III. Estimating effective population size. J. Hered. **81**: 277–298.

Allometry of natural mortality as a basis for assessing optimal release size in fish-stocking programmes

Kai Lorenzen

Abstract: This study evaluates the use of general mortality–size relationships for the assessment of release size in stocked fisheries. Seven release experiments (53 stocking events) are analysed, using a survival model based on allometric mortality and linear-length growth, allowing variation between experiments in both the allometric exponent and the level of mortality at reference length or generalising in one or both of the parameters. Results support the existence of a consistent allometry that applies independently of the overall level of mortality. The best-performing model is one in which the length exponent of mortality is set to –1 a priori, while mortality at reference length is allowed to vary between experiments (ranging from 0.7 to 33 per year at 15 cm in the present study). Even though the allometry of mortality is constant, the relative survival advantage of stocking large fish increases with the level of mortality at reference length. Using the identified length exponent of mortality of –1, survival models are derived for the linear, exponential, and von Bertalanffy growth equations. The models can be used to assess alternative release sizes, given an estimate of mortality at reference length, to facilitate comparative studies and to aid in the design of release experiments.

Résumé : Le but de cette étude est d'évaluer l'utilité des relations générales entre la mortalité et la taille pour établir la taille des poissons à l'ensemencement dans les pêches qui dépendent de l'alevinage. Sept expériences d'ensemencement (53 événements) servent de base à des analyses à l'aide d'un modèle de survie basé sur une mortalité allométrique et une croissance en longueur linéaire, qui permet des variations, d'une expérience à l'autre, tant du coefficient d'allométrie que du taux de mortalité à la longueur de référence, ou alors qui autorise des généralisations de l'un ou de l'autre de ces variables. Les résultats laissent croire à l'existence d'une allométrie uniforme qui s'applique indépendamment du taux global de mortalité. Le modèle le plus performant est celui où l'exposant de la longueur dans l'estimation de la mortalité est fixé a priori à –1, alors que la mortalité à la longueur de référence peut varier d'une expérience à l'autre (allant de 0,7 à 33 par année à 15 cm dans notre étude). Bien que l'allométrie de la mortalité soit constante, l'avantage relatif pour la survie d'ensemencer avec de plus gros poissons s'accroît avec le taux de mortalité à la longueur de référence. En utilisant un exposant de la longueur de –1, j'ai pu élaborer des modèles de survie incorporant les équations de croissance linéaire, exponentielle et de von Bertalanffy. Les modèles peuvent servir à évaluer les effets des ensemencements à différentes tailles pour une estimation donnée de la mortalité à la taille de référence; ils peuvent aussi faciliter les études comparatives et contribuer à l'élaboration d'expériences d'ensemencement.

[Traduit par la Rédaction]

Introduction

Stocking is widely used in the management of freshwater and, to a lesser extent, coastal-marine fisheries (e.g., Leber and Blankenship 1995; Welcomme and Bartley 1998; Heidinger 1999). A key problem in the management of stocked fisheries is the optimisation of release size (e.g., Cowx 1994; Leber and Blankenship 1995). The optimal release size depends on the contribution that fish of a particular size will make to the catch or fishable stock and on the resources required to produce seed fish of that size. Of the data required to assess optimum size, the expected survival of seed fish of different sizes to the fishable stock (and (or) contribution to the catch) are the most difficult to obtain. Systematic assessments have been either entirely empirical (release–recapture of marked seed fish of different sizes) or based on detailed ecological studies (Wahl et al. 1995; Szendrey and Wahl 1996). However, the costs and effort involved in both approaches restrict their use to a small number of fisheries, and the results are not readily generalised. An alternative approach that implies a simple generalisation is the use of allometric mortality–size relationships (Lorenzen 1995; Lorenzen et al. 1997). Provided that natural mortality in stocked fish is subject to a consistent allometry, then an estimate of mortality for a single reference size is sufficient to predict survival for a range of different release sizes.

Theoretical and empirical studies (Peterson and Wroblewski 1984; McGurk 1986; Lorenzen 1996) point to the existence of an allometric relationship between natural mortality and body weight, in fish, of the form:

$$M_W = M_u W^b \qquad (1)$$

Received January 27, 2000. Accepted September 29, 2000. Published on the NRC Research Press web site on December 20, 2000.
J15565

K. Lorenzen. T.H. Huxley School of Environment Earth Sciences and Engineering, Imperial College of Science Technology and Medicine, Prince Consort Road, London SW7 2BP, U.K. (e-mail: k.lorenzen@ic.ac.uk).

where M_W is natural mortality at weight W, M_u is mortality at unit weight, and b is the allometric exponent. Empirical studies combining data from a large number of populations have yielded estimates for the exponent b of –0.37 for marine fish of all life stages (predictive regression; McGurk 1986) and of –0.29 for juvenile and adult freshwater and marine fish (nonparametric regression; Lorenzen 1996). The study by Lorenzen (1996) also indicates that within-population estimates of b rarely differ significantly from the overall average. Given that weight is approximately proportional to the third power of length, b values of approximately –1/3 imply that natural mortality is inversely proportional to body length. An inverse relationship between natural mortality and fish length has been assumed in a number of population-dynamics studies (e.g Logan 1985; Beyer et al. 1999) but has not been tested explicitly.

Allometric mortality–size relationships have been used in a theoretical study of the population dynamics of stocked fisheries (Lorenzen 1995) and in a practical assessment of a culture-based fishery (Lorenzen et al. 1997). However, the general applicability of such relationships to the analysis of stocking experiments has not yet been tested. In particular, it is unclear whether the mortality of stocked fish is subject to a consistent allometric relationship and, if so, whether the allometry is the same as that observed in wild fish.

The purpose of the present study is to test the applicability of survival models based on allometric mortality–size relationships to the analysis of stocking experiments, and to provide practical models for the assessment of release size based on such relationships. An equation is derived to predict the survival of stocked fish from length at release, based on linear-length growth and allometric mortality equations. Alternative models based on this survival equation, but assuming different generalisations in the mortality–size relationship, are used to analyse a set of stocking experiments. Results support the hypotheses that survival of stocked fish is governed by a consistent allometry and that the length exponent of the relationship is approximately –1 (i.e., mortality is inversely proportional to length). The dynamics of survival implied by this relationship are explored. Finally, survival models based on this relationship are presented for linear, exponential, and von Bertalanffy growth equations, and their use in practical assessments is discussed.

Materials and methods

Empirical data

Seven published stocking experiments comprising a total of 53 stocking events (cohorts stocked) were identified from the literature. Criteria for selection were the reporting of true-survival estimates (as opposed to recapture in the fishery or other measures of relative survival), the number of stocking events, and the range of release sizes. Key information on the studies selected is given in Table 1. Each study is restricted to a single species and water body, but often comprises experiments carried out over more than 1 year. The time at large between stocking and survival estimate ranged from 0.1 to 1.3 years. Because the time at large was generally short, growth was described by a linear length growth rate (see below). Average linear-growth rates, u, were estimated from data for the populations analysed, except for studies A and B, in which cases data for neighbouring populations reported in the same publication (Margenau 1992) were used. Refer to Seber (1982) for a de-

Table 1. Details of stocking experiments analysed.

Experiment	Species	Location	N	l_0	t	u	Method	Reference
A	*Esox masquinongi*	Clear Lake, Wis., U.S.A.	6	20–28	0.10–0.16	11	SMR	Margenau 1992
B	*Esox masquinongi*	Twenty-six Lake, Wis., U.S.A.	6	20–28	0.11–0.17	11	SMR	Margenau 1992
C	*Esox masquinongi*	Lake George, Ill., U.S.A.	6	11–25	0.16–0.50	20	SEMR	Szendrey and Wahl 1996
D	*Oncorhynchus mykiss*	Englishman River, B.C., Canada	9	3–8[a]	0.67–1.08	5[a]	SLD	Hume and Parkinson 1988
E	*Oncorhynchus mykiss*	Moriarty Creek, B.C., Canada	10	3–8[a]	0.67–1.08	5[a]	SLD	Hume and Parkinson 1988
F	*Stizostedion vitreum*	East Okerboji Lake, Iowa, U.S.A.	7	1–13	0.04–0.54	17	SEMR	Larscheid 1995
G	*Stizostedion vitreum*	Ridge Lake, Ill., U.S.A.	9	5–22	0.83–1.33	10	PMR	Santucci and Wahl 1993

Note: N, number of stocking events; l_0, length at release (cm); t, time at large (years); u, linear length growth rate (cm/year; eq. 4); abbreviations used for method of estimating survival: PMR, Petersen mark–recapture; SEMR, Schumacher–Eschmeyer multiple mark – recapture; SLD, Seber–Le Cren depletion sampling; SMR, Schnabel mark–recapture.

[a] Length (L) data converted from weight (W), using $L = 4.68\ W^{0.32}$.

Table 2. Parameter estimates and goodness-of-fit criteria.

	Model 1		Model 2		Model 3		Model 4		Model 5	
	M_r	c	M_r	c	M_r	c	M_r	c	M_r	c
Experiment										
A	10.8	–1.18	10.5	–1.12	9.9	–1	4.2	0.68	5.5	0.95
B	23.6	–1.79	17.1	–1.12	16.1	–1	4.2	1.58	5.5	0.95
C	135.8	–5.21	20.7	–1.12	19.8	–1	4.2	4.44	5.5	0.95
D	0.9	–0.80	0.7	–1.12	0.8	–1	4.2	0.95	5.5	0.95
E	0.9	–0.60	0.6	–1.12	0.7	–1	4.2	1.22	5.5	0.95
F	2.2	–24.58	32.3	–1.12	32.7	–1	4.2	–19.11	5.5	0.95
G	3.7	–1.74	3.1	–1.12	3.0	–1	4.2	–2.01	5.5	0.95
SSQ		0.741		0.941		0.945		1.966		6.096
n		53		53		53		53		53
m		14		8		7		7		2
$\mathrm{SSQ}(n-2m)^{-1}$		0.030		0.025		0.024		0.050		0.124

Note: M_r is the mortality at reference length l_r = 15 cm, c is the allometric length exponent of mortality, n is the number of observations, m is the number of parameters estimated, and $\mathrm{SSQ}(n-2m)^{-1}$ is the goodness-of-fit criterion.

Fig. 1. Goodness-of-fit profile (sum of squares (SSQ)) of the allometric mortality exponent, c, using model 2. The horizontal line defines the approximate 95% confidence interval for c.

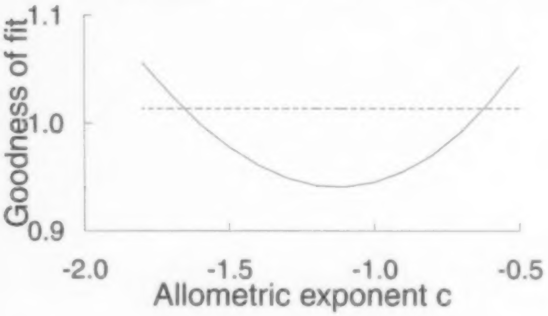

scription of the methods used to estimate post-stocking abundance and survival.

Survival model

The allometric relationship between natural mortality and body length may be described by the equation

$$(2) \qquad M_l = M_r\left(\frac{l}{l_r}\right)^c$$

where M_l is the mortality rate at length l, M_r is the instantaneous mortality rate at reference length l_r, and c is the allometric exponent of the mortality–length relationship.

If this relationship governs mortality in the stocked population, then the decline in numbers, N, of a stocked cohort (organisms of the same age and size) is described by the differential equation

$$(3) \qquad \frac{\mathrm{d}N_t}{\mathrm{d}t} = -N_t M_r\left(\frac{l_t}{l_r}\right)^c$$

where l_t is length at time t. This differential equation may be solved explicitly if a growth model is substituted for l_t. A linear length growth model is used in the empirical analysis, because time at large is short and the size of the fish is small relative to the reported maximum sizes in all stocking experiments analysed (Table 1). A model of the form

$$(4) \qquad l_t = l_0 + ut$$

is used, where l_0 is the length at stocking, t is the time since stocking, and u is the linear length growth rate. Substitution of eq. 4 into eq. 3, integration, and division by N_0 on both sides gives the following equation to predict survival, S_t (proportion of stocked fish surviving), from the time of stocking to time t:

$$(5) \qquad S_t = \frac{N_t}{N_0} = \begin{cases} \left(\dfrac{l_0}{l_0+ut}\right)^{\frac{M_r l_r}{u}} & (\text{for } c = -1) \\ \mathrm{e}^{-\frac{M_r\left(l_0\left(-\frac{l_0}{l_r}\right)^c + (l_0+ut)\left(\frac{l_0+ut}{l_r}\right)^c\right)}{(1+c)u}} & (\text{for } c \neq -1) \end{cases}$$

Analysis

To test whether the observed patterns in survival are consistent with the hypothesis of a single underlying allometry, five different models are fitted to the full data set:

$$(6) \qquad \begin{aligned} &\text{Model 1: } S = f\,(l_r, l_{0i}, t_i, u_j \mid M_j, c_j) \\ &\text{Model 2: } S = f\,(l_r, l_{0i}, t_i, u_j \mid M_j, c) \\ &\text{Model 3: } S = f\,(l_r, l_{0i}, t_i, u_j \mid M_j, -1) \\ &\text{Model 4: } S = f\,(l_r, l_{0i}, t_i, u_j \mid M, c_j) \\ &\text{Model 5: } S = f\,(l_r, l_{0i}, t_i, u_j \mid M, c) \end{aligned}$$

where the index i denotes individual stocking events (i = 1 to 53), and j denotes the experiment (j = A–G). While in model 1, both M_r and c are estimated separately for each experiment, the other models generalise across experiments by estimating a single value for either or both of the parameters. In model 3, c is not estimated but is fixed at –1 a priori, reflecting the assumption that mortality is inversely proportional to length.

Because the survival estimates have been obtained using a variety of different methods, they do not have a coherent error structure, making the application of maximum-likelihood methods difficult. Hence, the models are fitted by the method of least squares, applying an arcsine square-root transformation to observed and predicted survival, to stabilise the variance. The sum of squares (SSQ) is thus defined as

Fig. 2. Observed (■) and predicted (●) (model 3) survival in the seven stocking experiments analysed. Letters refer to the experiment codes in Table 1. Confidence limits (95%) are indicated when available from the original publication.

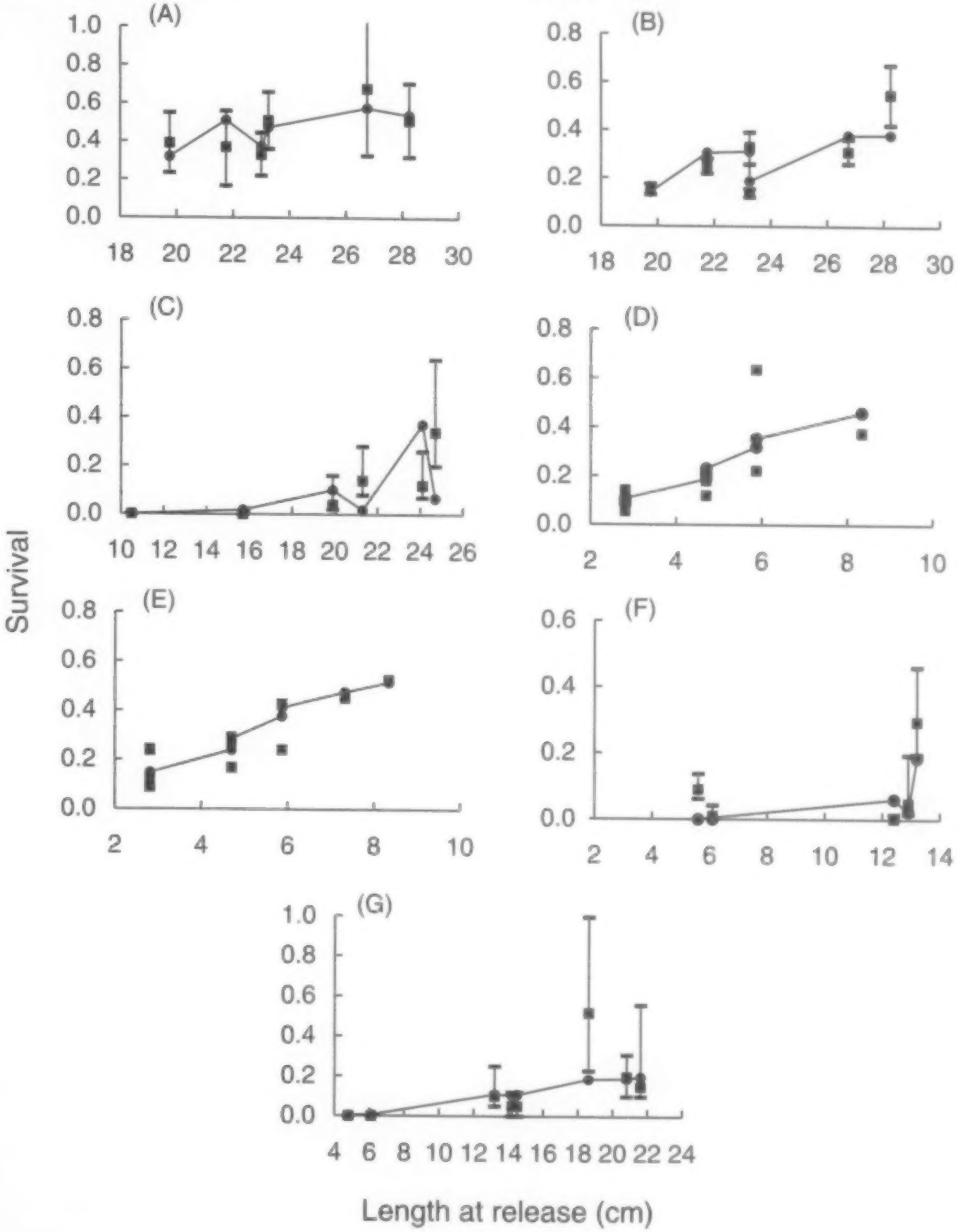

Fig. 3. Diagnostic plots of model 3 ($c = -1$) residuals against predicted survival (*a*), length at release (*b*), period at large (*c*), and growth rate (*d*).

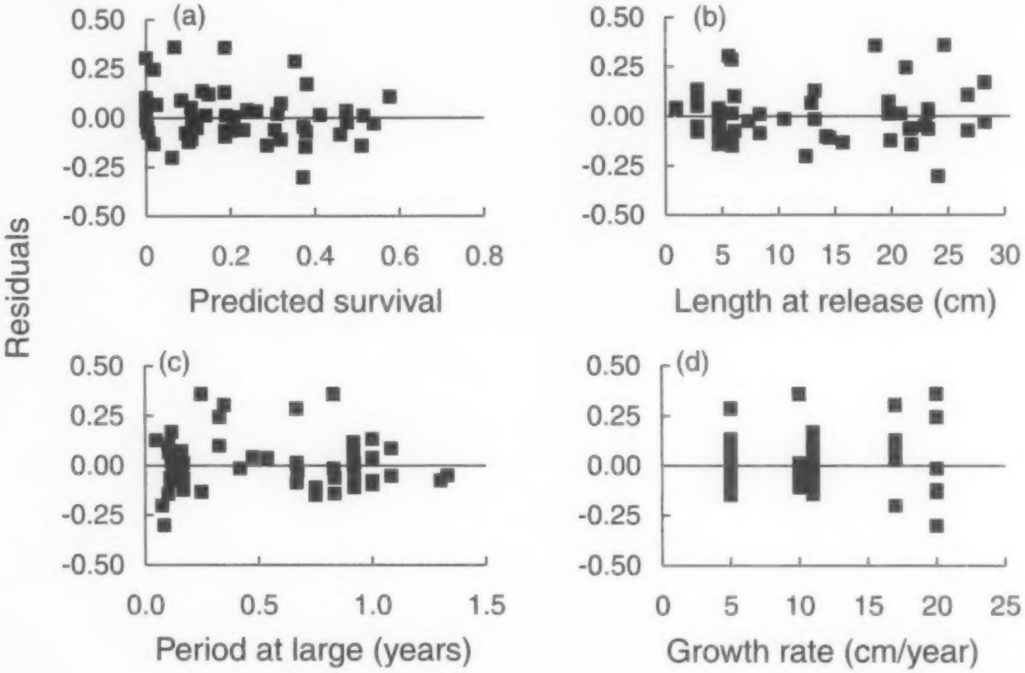

$$\text{(7)} \qquad \mathrm{SSQ} = \sum_{i=1}^{n}\left(\arcsin\sqrt{S_{i,\mathrm{o}}} - \arcsin\sqrt{S_{i,\mathrm{p}}}\right)^2$$

with $S_{i,\mathrm{o}}$ the observed survival and $S_{i,\mathrm{p}}$ the survival predicted from eq. 5. To compare the alternative models, the criterion

$$\text{(8)} \qquad \frac{\mathrm{SSQ}}{n-2m}$$

is used, where n is the number of observations and m is the number of parameters estimated (Hilborn and Mangel 1997). The model with the lowest value of the criterion is selected as the best model.

A goodness-of-fit (SSQ) profile was generated for the allometric exponent c (Hilborn and Mangel 1997). Approximate confidence bounds for c were determined from the profile as the values of c that satisfy

$$\text{(9)} \qquad \mathrm{SSQ}(c) = \mathrm{SSQ}(\hat{c})\left(1 + \frac{1}{n-1}F(1, n\text{-}1, 1\text{-}\alpha)\right)$$

where $\mathrm{SSQ}(\hat{c})$ is minimum SSQ, F is the F distribution, and $1-\alpha$ is the confidence level (Draper and Smith 1981).

Results

Parameter estimates and goodness-of-fit criteria for the alternative models (eq. 6) are given in Table 2. Models 2 and 3, based on a generalised allometry with variable M_r provide the best fit. The estimate of c in model 2 is –1.12, close to the value of –1 assumed a priori in model 3. Model 3 provides the best fit overall, with the reduction in the number of parameters to be estimated outweighing the slight increase in SSQ compared with model 2. Models 4 and 5, assuming constant M_r and variable or constant allometric exponent c, perform far worse than the others. Overall, these results indicate that, while the allometric exponent c can be generalised across experiments, M_r is too variable to be generalised.

A goodness-of-fit profile for the allometric exponent c is shown in Fig. 1. The approximate 95% confidence interval for c is (–1.66 to –0.62) and the profile is fairly flat between –1.3 and –1.0.

Model 3, with $c = -1$, is therefore selected as the best-performing model. A comparison of observed survival and model 3 predictions for the seven studies is shown in Fig. 2. Note that, because periods at large, t, vary between stocking events, data and model predictions do not form a smooth curve. In most studies, there is close correspondence between observed and predicted patterns. Relatively large deviations in experiments C and F reflect strong interannual variation in survival.

In Fig. 3, residuals of model 3 are plotted against predicted survival and the independent variables. No systematic patterns are apparent, apart from a small cluster of mainly positive residuals for periods at large between 0.2 and 0.6 years in Fig. 3*c*.

Discussion

Results from the present analysis show that stocking experiments with fish of different release sizes can be analysed and interpreted on the basis of allometric mortality–size relationships, with a constant allometric scaling and population-specific mortality at reference size. This result lends further support to the existence of a fundamental allometry of

Fig. 4. Relationships between release size and survival for different mortalities at reference length (M_r; solid line, M_r = 0/year; dashed line, M_r = 1/year; dotted line, M_r = 2/year) (*a*) and different growth rates (u; solid line, u = 0 cm/year; dashed line, u = 10 cm/year; dotted line, u = 20 cm/year) (*b*). All predictions are based on model 3 ($c = -1$), with u = 10 cm/year in *a* and M_r = 1/year in *b*. The dashed line is identical in the two graphs.

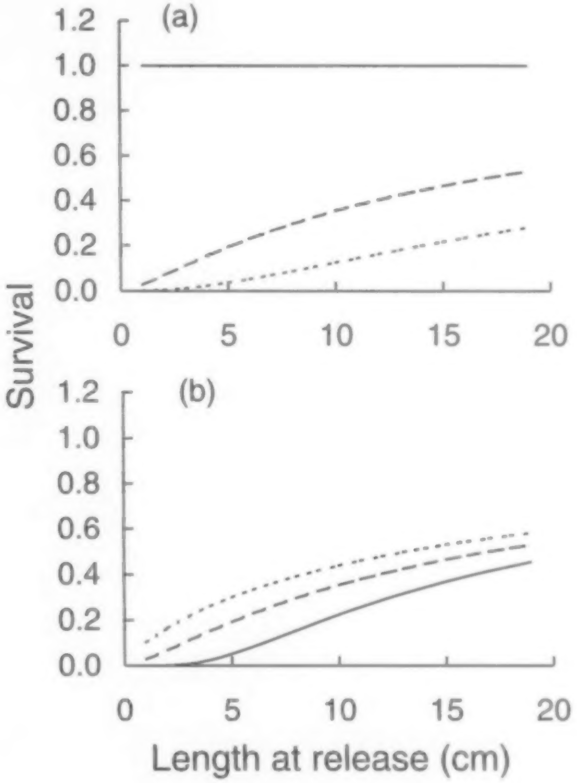

mortality that applies to stocked as well as wild fish in natural ecosystems. The allometric exponent is far more stable between populations than the overall level of mortality. Moreover, the simple assumption that mortality is inversely related to fish length, corresponding to a weight exponent of –1/3, was found to be adequate for the analysis of release size. This relationship is mathematically convenient, because it leads to relatively simple survival equations for stocked fish.

The dynamics of survival in relation to release size implied by model 3 ($c = -1$) with different levels of M_r is illustrated in Fig. 4. Figure 4*a* shows the effect on survival of different M_r (0, 1, and 2/year) at a constant growth rate, u, of 10 cm/year. Note that the relative size dependence of survival increases with M_r, i.e., constant allometry of mortality does not imply constant relative survival at different release sizes. The higher the overall level of mortality (M_r), the greater the relative survival advantage of large release sizes, a prediction consistent with the observation that high levels of predation require large seed fish for stocking (e.g., Heidinger 1999). Figure 4*b* shows the effect on survival of different linear-growth rates, u (0, 10, and 20 cm/year), for constant M_r (1/year). Survival increases with increasing growth rate, but the effect is far less pronounced than that of differences in M_r (Fig. 4*a*). Note that, in the seven studies analysed, estimates of M_r ranged from 0.7 to 33/year (a range far wider than the 0–2/year plotted in Fig. 4*a*), while estimates of the average growth rate, u, ranged from 5 to 20 cm/year (less than the range of 0–20 cm/year plotted in Fig. 4*b*). Hence, variation in the overall level of mortality (measured by M_r) is likely to play a more important role in determining optimal stocking size and the viability of enhancements than variation in growth.

Results of the present study indicate that survival models based on allometric mortality–length relationships with $c = -1$ and population-specific M_r provide practical tools for assessing optimal release size in stocking programmes. A linear length growth model was used in the analysis, because periods at large were short and fish were small relative to the asymptotic sizes reported for the respective species. However, when using allometric mortality models to predict survival over longer time periods, linear-growth models may no longer be adequate. Exponential and von Bertalanffy growth models may be substituted into eq. 3 and, in the case of c = 1, integration leads to the fairly simple survival equations given in Table 3. The application of these survival models to the analysis and prediction of stocking outcomes requires an estimate of M_r in the population in question (as well as the growth parameters). Estimation of M_r requires data on the absolute post-stocking abundance of the stocked fish; an indicator of relative survival such as the recapture rate, which reflects a combination of survival and harvesting effort, is not sufficient. If absolute-survival data are available from stocking with a particular release size, the use of the equations in Table 3 to assess the survival of alternative sizes is straightforward.

If only recapture (rather than absolute survival) has been estimated, there is a range of possible responses in recapture to changes in release size, which is dependent on the underlying true survival. To illustrate this in a simple example, assume that the recapture rate from a brief fishing event at time t after release is available. Recapture R_t is then the product of survival to time t and the proportional harvest rate H:

$$(10) \qquad R_t = S_t H$$

For a given R_t, absolute survival S_t must be between 1 (no natural mortality, $R_t = H$) and R_t (complete harvesting, $R_t = S_t$). These extremes define the range of possible responses to changes in release size, from size-independent survival at $S_t = 1$ (and therefore $M_r = 0$) to the most strongly size-dependent survival at $S_t = R_t$. This is illustrated in an example (Fig. 5) for a known recapture of $R_t = 0.125$ for 10-cm seed fish (t = 1 year, u = 10 cm/year). The range of possible responses is bounded by the extreme cases of $S = 1$ and $S = 0.125$. Although the exact response cannot be predicted without knowledge of M_r, even a bounded range of possibilities may aid management decision making and the design of experiments to resolve the remaining uncertainty. Moreover, it may often be possible to identify a likely range for the harvest rates in a fishery and, therefore, narrow down the range of possibilities. However, in practice, the analysis of

Table 3. Equations to predict the survival of stocked fish to time t after release (S_t) for c = −1 (mortality inversely proportional to length), and linear, exponential, and von Bertalanffy growth models.

Growth model	Growth equation	Survival equation
Linear	$l_t = l_0 + ut$	$S_t = \left(\frac{l_0}{l_0 + ut}\right)^{\frac{M_r l_r}{u}}$
Exponential	$l_t = l_0 e^{Gt}$	$S_t = e^{\frac{M_r l_r (e^{Gt} - 1)}{l_0 G}}$
von Bertalanffy	$l_t = l_\infty - (l_\infty - l_0)e^{-kt}$	$S_t = \left(\frac{l_0}{l_0 + l_\infty(e^{kt} - 1)}\right)^{\frac{M_r l_r}{l_\infty k}}$

Note: l_t, length at time t; l_0, length at stocking; u, linear-length growth rate; G, exponential-length growth rate; l_∞, asymptotic length; k, von Bertalanffy growth rate; M_r, mortality rate at reference length l_r.

Fig. 5. Possible responses in recapture (R) to changes in release size, when recapture is known for a single release size but absolute survival is not known. The extreme cases of $S = 1$ (thick solid line) and $S = R$ (thick dashed line) define the boundaries of possible relationships, with examples of intermediate relationships shown as thin solid lines. In this example, $R = 0.125$ for l_0 (release size) = 10 cm and u = 10 cm/year, and the extreme values of mortality are M_r = 0/year (solid line, $S = 1$) and M_r = 2/year (dashed line, $S = 0.125$).

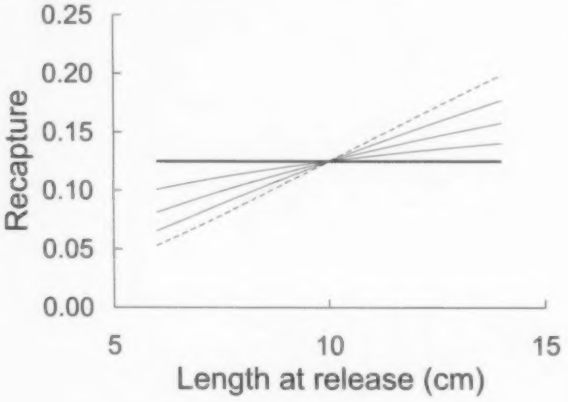

recaptures for a range of release sizes may also be complicated further by differences in harvest rates (related to, for example, differential size and habitat use at the time of harvesting). Differences in harvest rates are implicitly accounted for when absolute-abundance estimates are used, but may be difficult to separate from true differences in survival when only recapture data are available.

Although the studies analysed are unlikely to be representative of stocking programmes, and the levels of mortality should not be taken as indicative of the survival of stocked fish in general, it is interesting to compare the M_r estimates with values measured in natural populations. Based on length–weight relationships given in Carlander (1953, 1969), the approximate weight at a length of 15 cm is 15 g for *Esox masquinongi* and 35 g for *Oncorhynchus mykiss* and *Stizostedion vitreum*. Substituting these value into the empirical natural mortality – weight relationship for natural fish populations, $M = 3W^{-0.29}$ (Lorenzen 1996), gives expected values of M_r (at 15 cm) of 1.4 and 1.1 for natural populations of *E. masquinongi* and of *O. mykiss* and *S. vitreum*, respectively. Hence the estimated M_r values for stocked fish are 3 to 30 times higher than expected for natural populations in the experiments using *E. masquinongi* and *S. vitreum*, but slightly lower than expected for wild fish in the *O. mykiss* experiments. These values indicate that the mortality of stocked fish is highly variable and can be substantially higher, as well as lower, than expected for natural fish populations.

In the survival models developed in the present study, mortality is a continuous function of body size. Detailed ecological studies suggest that distinct threshold sizes for mortality may exist in some populations, for example, when fish outgrow predation by key piscivores and shift habitat use (Mittelbach and Chesson 1987). The consistency of empirical mortality – body size relationships across ecosystems and levels of organisation (McGurk 1986; Lorenzen 1996; this study) suggests that such thresholds do not in general lead to significant departures from the allometric mortality relationship. Nonetheless, departures from the continuous power relationship may occur at certain points in the ontogeny of stocked fish and, where this is the case, the detection of thresholds through experimental studies may allow further improvements in stocking regimes.

Detailed ecological studies (e.g., Wahl et al. 1995; Szendrey and Wahl 1996) are required to improve understanding of the mechanisms underlying differences in M_r and to identify measures to reduce M_r in stocked fishes. The allometric survival models derived in the present study can aid in assessing release size under a given mortality regime and, thereby, contribute to improved management of stocked fisheries. Furthermore, the allometric relationship provides a basis for the comparison of mortalities between stocking experiments. Widespread use of this approach may lead to a substantial data base that would provide much information for appraisal and evaluation of stocking programmes.

Acknowledgements

I thank Marc Mangel for a useful discussion in the course of this work and Marcel Frechette and two anonymous reviewers for constructive comments on the manuscript. This work was supported by the Department for International Development of the United Kingdom, Fisheries Management Science Programme.

References

Beyer, J.E., Kirchner, C.H., and Holtzhausen, J.A. 1999. A method to determine size-specific natural mortality applied to westcoast steenbras (*Lithognathus aureti*) in Namibia. Fish. Res. (Amst.), **41**: 133–153.

Carlander, K.D. 1953. First supplement to the handbook of freshwater fishery biology. W.C. Brown Co., Dubuque, Iowa.

Carlander, K.D. 1969. Handbook of freshwater fishery biology. 2nd ed. W.C. Brown Co., Dubuque, Iowa.

Cowx, I.G. 1994. Stocking strategies. Fish. Manag. Ecol. **1**: 15–31.

Draper, N.R., and Smith, H. 1981. Applied regression analysis. Wiley, New York.

Heidinger, R.C. 1999. Stocking for sport fisheries enhancement. *In* Inland fisheries management in North America. 2nd ed. *Edited by* C.C. Kohler and W.A. Hubert. American Fisheries Society, Bethesda, Md. pp. 375–401.

Hilborn, R., and Mangel, M. 1997. The ecological detective: confronting models with data. Princeton University Press, Princeton, N.J.

Hume, J.M.B., and Parkinson, E.A. 1988. Effects of size at and time of release on the survival and growth of steelhead fry stocked in streams. N. Am. J. Fish. Manag. **8**: 50–57.

Larscheid, J.G. 1995. Development of an optimal stocking strategy for walleyes in East Okerboji Lake, Iowa. Am. Fish. Soc. Symp. **15**: 472–483.

Leber, K.M., and Blankenship, H.L. 1995. A responsible approach to marine stock enhancement. Am. Fish. Soc. Symp. **15**: 167–175.

Logan, D.T. 1985. Environmental variation and striped bass population dynamics: a size-dependent mortality model. Estuaries, **8**: 28–38.

Lorenzen, K. 1995. Population dynamics and management of culture-based fisheries. Fish. Manag. Ecol. **2**: 61–73.

Lorenzen, K. 1996. The relationship between body weight and natural mortality in fish: a comparison of natural ecosystems and aquaculture. J. Fish Biol. **49**: 627–647.

Lorenzen, K., Xu, G., Cao, F., Ye, J., and Hu, T. 1997. Analysing extensive fish culture systems by transparent population modelling: bighead carp, *Aristichthys nobilis* (Richardson 1845), culture in a Chinese reservoir. Aquacult. Res. **28**: 867–880.

Margenau, T.L. 1992. Survival and cost-effectiveness of stocked fall fingerling and spring yearling muskellunge in Wisconsin. N. Am. J. Fish. Manag. **12**: 484–493.

McGurk, M.D. 1986. Natural mortality of marine pelagic fish eggs and larvae: role of spatial patchiness. Mar. Ecol. Prog. Ser. **34**: 227–242.

Mittelbach, G.G., and Chesson, P.L. 1987. Predation risk: indirect effects on fish populations. *In* Predation: direct and indirect impacts on aquatic communities. *Edited by* W.C. Kerfoot and A. Sih. University Press of New England, Hanover, N.H. pp. 315–332.

Peterson, I., and Wroblewski, J.S. 1984. Mortality rate of fishes in the pelagic ecosystem. Can. J. Fish. Aquat. Sci. **41**: 1117–1120.

Santucci, V.J., and Wahl, D.H. 1993. Factors influencing survival and growth of stocked walleye (*Stizostedion vitreum*) in a centrarchid-dominated impoundment. Can. J. Fish. Aquat. Sci. **50**: 1548–1558.

Seber, G.A.F. 1982. The estimation of animal abundance and related parameters. Griffin, London.

Szendrey, T.A., and Wahl, D.H. 1996. Size-specifc survival and growth of stocked muskellunge: effects of predation and prey availability. N. Am. J. Fish. Manag. **16**: 395–402.

Wahl, D.H., Stein, R.A., and DeVries, D.R. 1995. An ecological framework for evaluating the success and effects of stocked fishes. Am. Fish. Soc. Symp. **15**: 176–189.

Welcomme, R.L., and Bartley, D.M. 1998. Current approaches to the enhancement of fisheries. Fish. Manag. Ecol. **5**: 351–382.

Impact of elevated temperature on the growth, survival, and trophic dynamics of winter flounder larvae: a mesocosm study

Aimee A. Keller and Grace Klein-MacPhee

Abstract: Winter flounder (*Pseudopleuronectes americanus*) is a dominant commercial fish in Narragansett Bay, Rhode Island, and yet factors controlling its recruitment remain unclear. An experiment was conducted with six 13-m^3 land-based mesocosms (5 m deep) from February to April 1997 to address the impact of increased temperature (+3°C) on growth, survival, and trophic dynamics of winter flounder larvae. Objectives were to determine if warmer winter temperatures result in lower survival of winter flounder as a result of increased predator activity or if temperature-induced alterations in the food web result in greater food availability, perhaps leading to increased survival. Analyses of variance revealed significant ($P < 0.05$) or near-significant ($P < 0.10$) differences in phytoplankton and zooplankton abundance and biomass between warm and cool mesocosms. Winter flounder egg survival, percent hatch, time to hatch, and initial size were significantly greater in cool systems ($P < 0.05$). Mortality rates were lower in cool systems and significantly related to the abundance of active predators ($P < 0.05$). The cumulative impact of decreased survival of eggs and larvae in warm systems may partially explain the decline of winter flounder in Narragansett Bay, which has experienced elevated winter water temperatures in recent years.

Résumé : Bien que la Plie rouge (*Pseudopleuronectes americanus*) soit un poisson d'importance halieutique dans la baie de Narragansett au Rhode Island, les facteurs qui régissent son recrutement restent imprécis. Une expérience menée dans six mésocosmes de 13 m^3 (5 m de profondeur), installés sur le sol, de février à avril 1997, a permis d'étudier l'effet d'une augmentation de température (+3°C) sur la croissance, la survie et la dynamique trophique des larves de la Plie rouge. Il s'agissait de savoir si une augmentation de température en hiver réduirait la survie de la plie à cause d'un surcroît de prédation ou si alors la température modifierait le réseau alimentaire et augmenterait la disponibilité de la nourriture, permettant peut-être ainsi une survie plus grande. Des analyses de variance révèlent des différences significatives ($P < 0{,}05$) ou presque significatives ($P < 0{,}10$) dans les densités et les biomasses du phytoplancton et du zooplancton entre les mésocosmes chauds et frais. La survie des oeufs de la Plie rouge, leur pourcentage d'éclosion, la durée de l'incubation et la taille initiale sont plus élevés dans les mésocosmes frais ($P < 0{,}05$). Les taux de mortalité sont plus bas dans les mésocosmes frais et ils sont en corrélation avec la densité de prédateurs actifs ($P < 0{,}05$). L'effet cumulé de la réduction de la survie des oeufs et des larves dans les mésocosmes chauds peut expliquer, au moins en partie, le déclin des populations de la Plie rouge dans la baie de Narragansett qui a connu des températures d'eau élevées en hiver depuis quelques années.

[Traduit par la Rédaction]

Introduction

Determining the causes of fluctuations in recruitment success of marine fishes remains a critical problem in fisheries biology. Evidence suggests that much of the variation in year-class strength is related to mortality of early life history stages (Houde 1987). The principal forces controlling recruitment success in larval fish are variations in food availability, particularly during the onset of first feeding, predation by other organisms, and oceanographic conditions (Cowan and Houde 1990). The situation is further complicated by the potential interaction between any and all of these factors. Carbon dioxide production by our global industrial society has altered the earth's climate, with increased warming occurring in most regions of the Northern Hemisphere over the past century (Schuurmans 1995). In Narragansett Bay, Rhode Island, winter water temperatures significantly increased from 1959 to1994 (Oviatt 1994). In a prior study, we determined that elevated winter temperature impacts the magnitude and fate of the winter–spring diatom bloom and thus may influence food availability to higher trophic levels (Keller et al. 1999*a*). Here, we extend our prior analysis to examine impacts on ichthyoplankton during a postbloom period. In addition to alteration in food availability, elevated water temperatures may lead to increased metabolic activity of potential predators followed by increased predation rates. This may be particularly important, since previous research examining the impact of nutrient enrichment on larval winter flounder (*Pseudopleuronectes*

Received January 21, 2000. Accepted September 29, 2000. Published on the NRC Research Press web site on December 20, 2000.
J15543

A.A. Keller[1,2] and G. Klein-MacPhee. Graduate School of Oceanography, University of Rhode Island, South Ferry Road, Narragansett, RI 02882, U.S.A.

[1] Corresponding author.

[2] Present address: P.O. Box 2009, Kingston, WA 98346, U.S.A. (e-mail: aimee@gsosunl.gso.uri.edu).

americanus) suggested a link between predation and survival (Klein-MacPhee et al. 1993). Here, we examine if elevated winter water temperature, due to global climate change, influences interactions between food availability and predation and leads to variation in survival of ichthyoplankton.

The life history and ecological niche of winter flounder are unique among the demersal fishes inhabiting east coast waters (Jeffries et al. 1989). Spawning generally occurs in shallow estuaries in winter and early spring at cold temperatures ranging from 1 to 10°C, with peak spawning at about 2–5°C (Pearcy 1962). The eggs are adhesive and demersal, with incubation lasting 5–31 days (Rogers 1976). Following hatching, the pelagic larvae are about 3 mm long but increase in size to about 7–9 mm over a 6- to 8-week period, at which time metamorphosis occurs (Laurence et al. 1979). Spawning at low temperatures appears to be a mechanism to "escape in time" from warm-water predators (Jeffries et al. 1989). Winter flounder success may thus be particularly sensitive to variation in temperature of the magnitude already observed in Narragansett Bay.

Historically, winter flounder has been the most abundant demersal fish in Rhode Island, contributing the bulk of the commercial and recreational bottom fishery ($>2 \times 10^6$ kg) in Narragansett Bay (Jeffries and Johnson 1974; Gibson 1998). Populations have tended to be somewhat cyclical throughout historical assessments, with adults known to fluctuate sevenfold within a decade (Jeffries and Terceiro 1985). Concerns are currently being expressed, since the population has dropped precipitously since 1979 and has remained low for the past 14 years (Gibson 1998). Inverse relationships between winter temperature and recruitment have been noted for winter flounder (Jeffries and Johnson 1974; Jeffries and Terceiro 1985; Northeast Utilities 1999). Jeffries and Terceiro (1985) have implicated climate warming and predator control as factors governing recruitment.

We hypothesized that warmer winter temperatures could result in elevated mortality of flounder larvae due to higher metabolic rate and increased activity of predators. In this paper, we test the hypothesized direct link between warmer temperatures and the growth and survival of winter flounder larvae and examine the relationship between temperature and the trophic components leading to larval fish. We describe the impact of increasing water temperature by 3°C relative to control systems. Control systems were maintained at a temperature 2°C less than the long-term (1977–1989) average for the parent system, Narragansett Bay. The study was conducted in six enclosed mesocosms of the Marine Ecosystem Research Laboratory (MERL) over a diatom-dominated post-winter–spring bloom period. We examined the effects of altered temperature on food availability (photosynthetic algae and zooplankton), abundance of active predators, and the growth and survival of winter flounder larvae.

Materials and methods

The MERL mesocosms used for the experiment are 13-m^3 cylindrical enclosures with a 5-m water column scaled to the natural system, Narragansett Bay, in terms of physical, chemical, and biological characteristics. For this experiment, the six mesocosms were established as well-mixed systems with no exchange of seawater with Narragansett Bay after the start of the experiment. To induce natural levels of turbulence, mixing was applied via horizontal paddles located at 1-m depth intervals rotating with a rate of 4 rpm. The mixing schedule consisted of 2 h of mixing followed by 4 h of nonmixing, a scheme designed to simulate the semidiurnal tidal currents in the Bay. Each mesocosm contained a 37-cm-deep sediment tray that was filled with lower Narragansett Bay sediment containing an intact (unmixed) benthic community. Sediments were collected with a 0.25-m^2 USNEL box core and remained undisturbed for 12 months prior to the start of the experiment. No attempt was made to manipulate the abundance of benthic organisms, which was intended to represent the range of natural variation seen at the sediment collection site. Previous studies have established that the mesocosms mimic the biological and chemical characteristics of the natural systems, including pelagic and benthic species composition, primary productivity, pelagic and benthic respiration, and nutrient concentrations and fluxes (see Sullivan and McManus 1986 and references therein).

The experimental design consisted of two treatments using six outdoor mesocosms with three warm systems targeted for a temperature increase of +3°C relative to controls (also referred to below as cool). A time series based on the average monthly temperature in lower Narragansett Bay from 1977 through 1989 was used to set the temperature differential between warm and cool treatments (Fig. 1). Warm systems were heated 1°C relative to the long-term (1977–1989) Bay average, while controls were cooled 2°C below the average. Warm systems simulated the potential increase in winter water temperature expected to occur in the future, while cool systems represented typical winter temperature values experienced in the past (or current cold winters). Temperatures were controlled using polypropylene immersion type heat exchangers hung 2 m below the surface in each mesocosm. Triplicate treatments were established with natural plankton communities by filling the mesocosms with water from the adjacent Narragansett Bay. The experiment commenced on 5 February and ended on 4 April 1997.

Because winter flounder spawning tends to occur in the upper nutrient-enriched regions of Narragansett Bay, inorganic nutrients (NH_4Cl, KH_2PO_4, and Na_2SiO_3) were added daily to the six mesocosms. An N:P:Si molar ratio of 12.80:1.00:0.91 was used to mimic the ratio of nutrients in sewage effluents discharged into the Providence River (Oviatt et al. 1986). The loading level for nitrogen (2.31 $mmol \cdot m^{-3} \cdot day^{-1}$), phosphate (0.18 $mmol \cdot m^{-3} \cdot day^{-1}$), and silicate (0.165 $mmol \cdot m^{-3} \cdot day^{-1}$) was four times the average annual loading (on an areal basis) to Narragansett Bay. The four times loading is within the range (two to eight times) occurring in the upper regions of the Bay where winter flounder larvae are most abundant (Oviatt et al. 1986; Keller et al. 1999*b*).

Temperature, chlorophyll *a* (Chl *a*), phytoplankton abundance, zooplankton abundance, and ichthyoplankton characteristics were measured in each of the six mesocosms. Water temperature (degrees Celsius) 10 cm below the surface was recorded daily. Replicate Chl *a* (micrograms per litre) was measured weekly from 10-mL aliquots of water subsampled from amber polyethylene bottles containing 2 L of water collected 1 m below the surface in each mesocosm during the morning mixing cycle. Samples were filtered through 25-mm Whatman GF/F glassfiber filters at 125-mmHg maximal vacuum. Two drops of 1% magnesium carbonate were added to each sample prior to filtration. Samples were extracted overnight in the freezer using 90% acetone and analyzed within 24 h on a Turner Designs model 10 field fluorometer (Lorenzen 1966).

Phytoplankton abundance (cells per millilitre) was measured weekly in each mesocosm from the amber bottles using standard techniques (Sournia 1978). Samples were preserved in Lugol's iodine solution and counted on an inverted microscope. Depending on phytoplankton density, either concentrated (10:1) or un-

Fig. 1. Ambient temperature model (solid line) used to set weekly temperature values for the study and the observed mean temperatures for cool treatments (open circles), warm treatments (solid circles), and Narragansett Bay (open triangles) over the experimental period (5 February – 4 April 1997). The ambient model was based on the mean monthly temperatures in Narragansett Bay in the lower West Passage from 1977 through 1989. Warm tanks were targeted for a +1°C (upper broken line) increase above ambient and cool tanks for a –2°C (lower broken line) decrease below the model as shown in the figure.

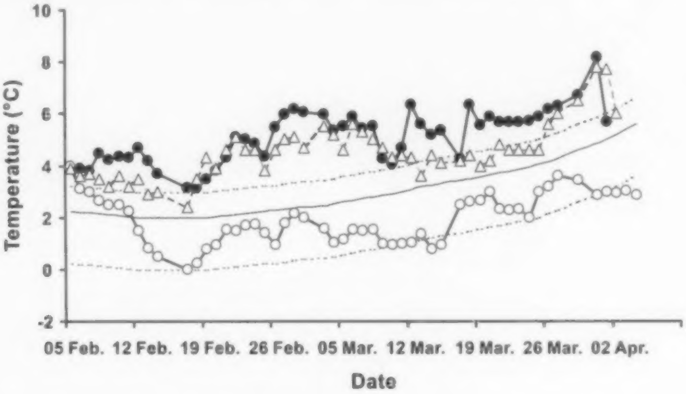

concentrated samples were counted by pipetting a 2-mL subsample into a 5-mL settling chamber and adding 3 mL of artificial seawater. Samples were settled for 20 h and a known area of the chamber counted (one to two diameters, half chamber, whole chamber) until at least 1000 cells were counted.

Zooplankton samples were collected weekly by pumping 50–100 L of water at a constant rate from each of five depth intervals (0.1, 0.5, 1.0, 2.5, and 4.5 m). Pumped samples were integrated over each depth interval (e.g., 1.0 m represents 0.5–1 m) by raising the sample hose at a constant rate. Zooplankton larger than 44 µm were filtered from the water samples, preserved in 10% formalin, staged, identified, and enumerated. Zooplankton were identified to species or genus level for adult and copepodite stages and to order or class for nauplii or other invertebrate larvae.

Winter flounder eggs and larvae were obtained from broodstock collected in Narragansett Bay primarily by otter trawl in early December 1996. Adult fish were sorted by sex and maintained in separate outdoor tanks supplied with running seawater at ambient temperature and salinity until ripe. Fertilized eggs were obtained by mechanically stripping two ripe females and three ripe males using the methods of Klein-MacPhee et al. (1982). Approximately equal numbers of newly spawned eggs (~5000) were placed in replicate egg baskets suspended at 1 m depth in each mesocosm at the start of the experiment (5 February) at temperatures of 3.9–4.0°C. Temperatures were gradually raised in the warm treatments and lowered in the cool treatments to achieve the desired 3°C temperature differential within the first week of the experiment. The cylindrical egg baskets (500 mL volume, 10 cm in diameter) were constructed of plastic with mesh (250 µm) caps and bottoms. Baskets were designed to allow incubation with good water circulation at experimental temperatures. Eggs were suspended at 1 m depth, since winter flounder eggs are demersal and occur naturally at this depth (Crawford 1990). Egg density in the baskets was set by estimating the total number of eggs required for weekly sampling (prior to hatching) plus the number of larvae needed to stock the mesocosms (after accounting for egg mortality). Egg density has not been estimated in the field, but winter flounder produce approximately 500 000 demersal eggs at spawning. Weekly subsamples of about 200 eggs were removed via pipetting (5 February – 7 March) from each egg basket and examined microscopically to determine the number of live versus dead eggs. Percent egg mortality was calculated directly from the ratio of dead to total eggs counted.

To determine percent hatch, a subsample of 100 eggs was counted and placed in replicate 4-L plastic containers with a 150-µm-mesh bottom in each mesocosm on 5 February. Eggs in these containers were incubated at depths of 0.2 m, which is shallower than the norm but allowed a rapid visually determination of when hatching occurred. Upon hatching, contents of each container were retrieved and the number of larvae counted. Percent hatch for each mesocosm was determined directly as the ratio of live larvae to eggs incubated.

After hatching, the egg baskets in each mesocosm were retrieved and newly hatched larvae were used to stock the system in which they were suspended. Larvae from replicate egg baskets were counted as they were gently poured into 4-L polycarbonate containers, combined in a 1:1 ratio, and released into the mesocosm in which they hatched. A total of 2000 larvae were added to each mesocosm. Stocking density for each mesocosm was ~150 larvae·m^{-3}, at the upper range of densities (100–150·m^{-3}) for winter flounder larvae occurring naturally (Pearcy 1962). Because winter flounder are currently at low population levels, stocking density was based on older larval density data, which are more in line with the carrying capacity of the system. Additionally, density of newly hatched larvae in the field is rarely reported since these small larvae tend to be undersampled using standard-mesh (505 µm) ichthyoplankton nets (Northeast Utilities 1999). A subsample of 30 larvae from each mesocosm was measured at hatching. Initial lengths (standard length, millimetres) were obtained by anesthetizing larvae with tricane methanesulfonate (MS 222) (to prevent curling) and measuring them alive under a dissecting microscope.

Fish larvae were collected weekly in two replicate samples using a 0.5-m-diameter, 202-µm-mesh plankton net equipped with a TSK flowmeter. Replicate tows were made with the mixers off by lowering the net to the bottom of the mesocosm and pulling it steadily to the surface. Flowmeter readings were recorded before and after each tow. Water and organisms were briefly stored in a cold room in 4-L plastic containers until the larval fish could be removed, anesthetized as above, and measured alive. The number of larvae caught per tow was used to estimate larval abundance in the mesocosm over the course of the experiment.

When the experiment was terminated, a circular (1.75-m-diameter) 333-µm-mesh net was lowered to the bottom of each mesocosm. The water column in each mesocosms was then drained through a 202-µm-mesh plankton net via a valve located 0.5 m from the bottom. Any larvae remaining in the mesocosm after draining were collected by raising the circular net through the 0.5 m of water still in the mesocosm. The total number of larvae surviving at the end of the experiment in each mesocosm was obtained directly by counting the larvae collected in both the overflow net and the bottom net. The total count of larvae obtained when the mesocosm was completely drained at the end of the experiment was then compared with the final net tow estimate (just prior to draining) to determine capture efficiency. Data were not corrected where the capture efficiency were low because capture efficiency varies with age (Klein-MacPhee et al. 1993).

Larval daily instantaneous growth rates (assuming exponential growth) were calculated via regression using the equation

$$(1)\qquad G = (\log_e \mathrm{SL}_t - \log_e \mathrm{SL}_0)/t$$

with G the daily growth rate, SL_t the larval standard length (millimetres) at time t, SL_0 the larval standard length at $t = 0$, and t the time interval (days).

Average daily instantaneous mortality rates were calculated as

$$(2)\qquad Z = (\log_e N_0 - \log_e N_t)/t$$

with Z the mortality coefficient (per day), N_t the number of winter flounder surviving at time t, N_0 the number stocked at the beginning of the study (time $t = 0$), and t the time (days). Following Laurence (1974), N_t was corrected for potential survivors removed by sampling using the formula

$$(3)\qquad N_{t'} = N_t + R\sum_{K=1}^{w-1} \mathrm{e}^{-7KZ}$$

with R the number of individuals removed each week by sampling, w the number of weeks of sampling, 7 the number of days in 1 week (adjusted if sample intervals were unequal), and Z the average daily instantaneous mortality coefficient. The initial Z value in eq. 3 is the maximum mortality rate from eq. 2 based on no survivors from samples taken and was used to calculate iteratively $N_{t'}$. The $N_{t'}$ was then substituted for N_t in eq. 2 to calculate an unbiased estimate of Z.

On 21 March 1997, the egg basket in a cool system (tank 5) was spilled, releasing an unknown number of eggs and larvae into the mesocosm. Yolk-sac larvae were collected on sampling. No yolk-sac larvae were observed on the date prior to the spill. Growth and mortality rates for this system were calculated from data collected up to the time of the spill.

The abundance of benthic predators was censused by diver survey prior to the start and near the end of the study. Numbers were confirmed following draining of the mesocosms when the experiment was terminated. Pelagic predators were determined from the net samples (ring net and overflow net) collected when the entire system was drained at the completion of the study.

We statistically assessed the effect of elevated temperature on variables measured over time throughout the entire experimental period. We used a nested analysis of variance (ANOVA), which is equivalent to a repeated-measures analysis (Winer 1971). For this design, replicate mesocosms were nested within treatments and considered random. In testing for main effects (treatments controlled as part of experimental design), sample date was considered a repeated factor and the degrees of freedom of error terms were not artificially inflated by frequent sampling. In those cases where there was a significant time-by-treatment interaction, we used a nested ANOVA on each sample date where replicate mesocosms were again considered random. Abundance data were transformed ($\ln(x + 1)$) to reduce heterogeneity of variance prior to statistical analysis, and t tests were used to determine significant differences between larval winter flounder growth and mortality rates between treatments.

Fig. 2. Increase in temperature during the peak winter flounder larval period (February–April) in Narragansett Bay from 1959 to 1998. Data were collected at hourly intervals using a buoy moored in the East Passage of the Bay by the National Oceanic and Atmospheric Administration. Winter temperature was calculated as the mean of the monthly temperatures. The regression equation ($Y = 0.053X - 100$) indicates an average increase of 0.053°C·year^{-1} for a total increase of 2.1°C over the 40-year period.

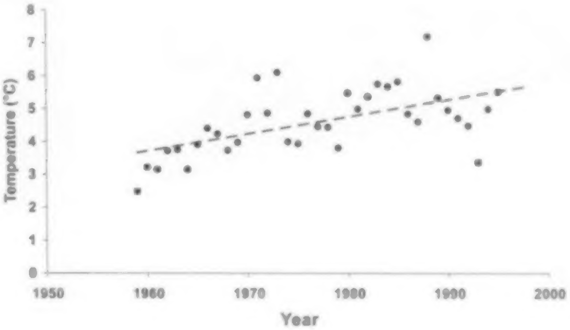

Results

Water temperature in Narragansett Bay during the winter flounder larval period (February–April) has increased significantly ($P < 0.05$) over the past 40 years (+0.053°C·year^{-1}) (Fig. 2). For the current experiment, water temperature in the warm treatments ranged from a low of 2.9°C in February to a high of 8.3°C in late March, with an average of 5.11°C (±0.14 SE) over the experimental period (Fig. 1). The cool systems increased from –0.1 to 3.7°C over the same period, with a mean temperature of 1.86°C (±0.13 SE). Since temperature did not vary significantly within treatments ($P > 0.05$), daily means are shown by treatment (Fig. 1). These values are plotted relative to the weekly model temperatures: warm (+1°C), mean, and cool (–2°C). The actual temperature difference between treatments was 3.25°C, close to the targeted differential of 3°C. Water temperature in Narragansett Bay over the same period (Fig. 1) was warm relative to long-term data, with an average temperature of 4.4°C, but on average 0.7°C cooler than the warm treatments.

Both phytoplankton abundance (~10 000 cells·mL^{-1}) and biomass as Chl *a* (~15 μg·L^{-1}) were relatively high at the start of the experiment, suggesting a minor bloom in the Bay at the time of the fill (Fig. 3). Abundance (Fig. 3A) and biomass (Fig. 3B) increased gradually in both treatments over the first 3 weeks of the experiment, with both measurements being somewhat higher in cool mesocosms. From late February through late March, total cell counts were generally higher in the warm treatments (ANOVA, $F = 1.9$, $P < 0.09$, near significance), while biomass was significantly greater in these systems (ANOVA, $F = 4.5$, $P < 0.001$) (Table 1). At the end of the experimental period, abundance and biomass were significantly greater in the cool tanks.

In general, *Detonula confervacea* was the dominant diatom in both warm (Fig. 3C) and cool (Fig. 3D) systems during the initial bloom period and was not significantly different between treatments (Table 1). Following the initial

Fig. 3. (A) Total phytoplankton cell counts and (B) Chl *a* shown as the mean (±1 SE) by treatment from 6 February to 4 April 1997. Warm tanks are represented by solid circles and cool tanks by open circles. Phytoplankton abundance for the dominant species is shown for (C) a representative warm system and (D) a representative cool system from 6 February to 4 April 1997.

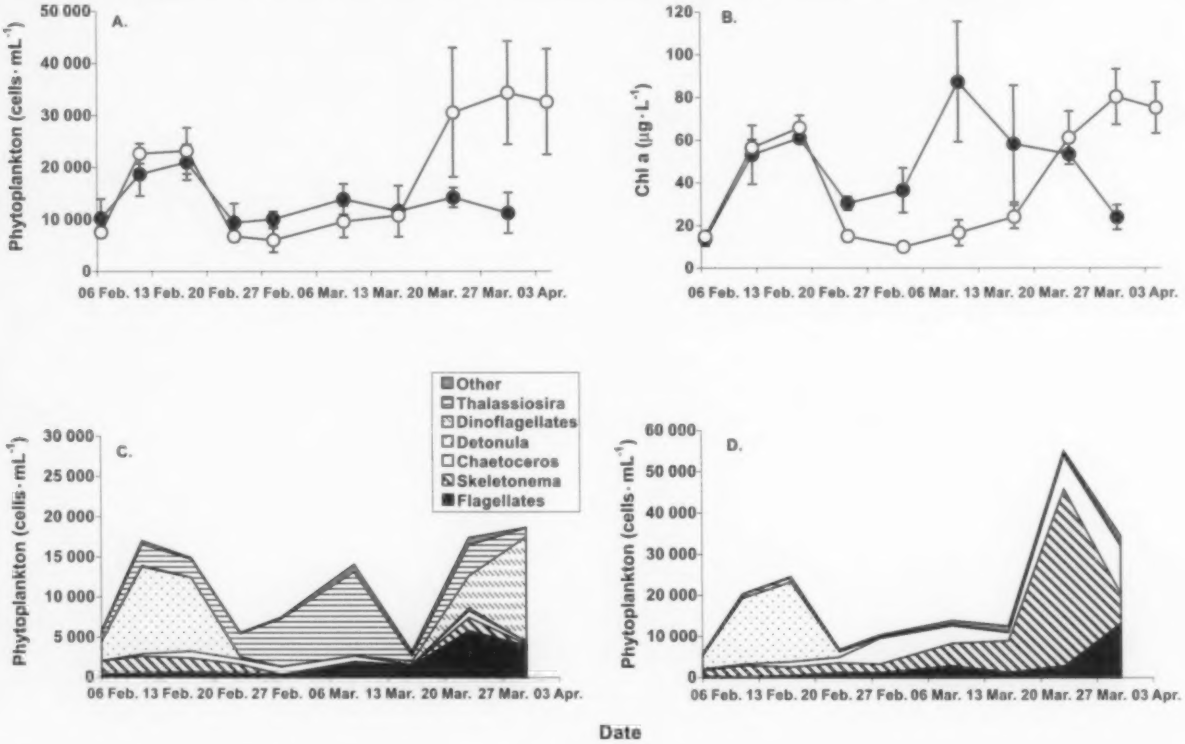

Table 1. Results of nested ANOVAs (equivalent to repeated measures analyses) showing main effects and time-by-treatment interactions of experimental manipulations (warm versus cool mesocosms) on phytoplankton and zooplankton.

	Treatment effects		Time-by-treatment interactions	
Variable	*F*	*P*	*F*	*P*
Phytoplankton (cells·mL^{-1})				
Skeletonema	23.4	0.008	4.2	0.002
Chaetoceros	21.8	0.009	6.3	0.0001
Thalassiosira	22.1	0.009	2.1	0.05
Detonula	0.72	0.45	0.4	ns
Flagellates	0.02	0.91	3.3	0.007
Dinoflagellates	0.01	0.95	2.4	0.04
Total	2.6	0.18	1.9	0.09
Chl *a* (µg·L^{-1})	5.8	0.07	2.4	0.04
Zooplankton (number·m^{-3})				
Nauplii	4.8	0.09	6.5	0.0001
Copepodites	7.2	0.05	5.4	0.0004
Adults	6.9	0.06	2.6	0.03
Total	5.7	0.07	2.9	0.02

Note: Abundance data were natural logarithmically transformed prior to analysis ($n = 52$). ns, not significant.

3-week period, the species composition between treatments began to diverge. The warm systems (Fig. 3C) were characterized by a significant increase in *Thalassiosira* spp. that did not occur in the cool systems (Fig. 3D). *Skeletonema costatum* and *Chaetoceros* spp. were the dominant species present in the cool systems during this period (Fig. 3D). *Skeletonema* and *Chaetoceros* spp. continued to dominate the cool systems during the final weeks of the study. While *Skeletonema* was present in warm systems during these last few weeks, the phytoplankton population was primarily composed of flagellates, dinoflagellates, and *Thalassiosira* spp. Flagellates increased in abundance in both treatments towards the end of the study (Figs. 3C and 3D).

Significant ($P < 0.05$) and near-significant ($P < 0.10$) treatment effects were noted for biomass as Chl *a*, total phytoplankton abundance, and abundance of *S. costatum*, *Chaetoceros* spp., and *Thalassiosira* spp. over the experimental period (Table 1). Phytoplankton biomass and cell counts were elevated in the warm treatment relative to the cool until the final week of the study. *Skeletonema* and *Chaetoceros* spp. were more abundant in cool systems, while *Thalassiosira* spp. were more abundant in warm systems. The levels of dinoflagellates and flagellates were not significantly different throughout the experimental period but exhibited significant time-by-treatment interactions (Table 1). ANOVA by sample date indicated significantly more dinoflagellates and flagellates in warm systems from late February

Fig. 4. Copepod abundance shown as the treatment means (±1 SE) by stage, (A) nauplii, (B) copepodite, and (C) adult, from 6 February to 4 April 1997. Warm tanks are represented by solid circles and cool tanks by open circles.

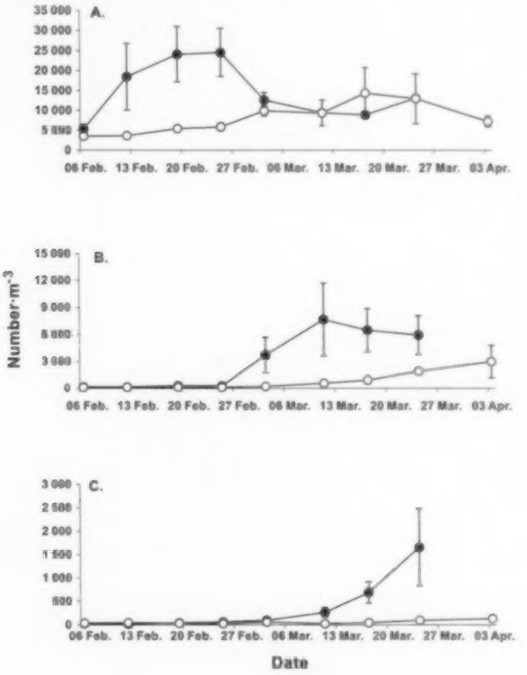

through March. The levels of *D. confervacea* were not significantly different between treatments throughout the study (Table 1).

Mean abundance (±SE) of copepods (by stage) for the triplicate control and treatment mesocosms over the experimental period is displayed in Fig. 4. Mean abundance of nauplii ($<5000 \cdot m^{-3}$) at the start of the experiment was low, reflecting the abundance of nauplii in Narragansett Bay at the time of the fill, but increased substantially in warm systems ($\sim 23\,000 \cdot m^{-3}$) relative to controls ($\sim 10\,000 \cdot m^{-3}$) during February. From 3 March 1997 through the remainder of the experiment, the abundance of copepod nauplii was similar in both treatments. At the start of the experiment, the abundance of copepodites and adult copepods was also low in all mesocosms ($<150 \cdot m^{-3}$). Copepodite numbers increased somewhat earlier (5 March) and to a greater extent in the warm systems relative to cool systems (Fig. 4). A similar pattern was observed for adult copepods. In the warm systems, abundance of adults increased markedly from 11 March through the end of the study. In the cool systems, very slight increases were observed from 11 March to 3 April 1997.

Copepod nauplii, copepodites, adult copepods, and total zooplankton levels were significantly (ANOVA, $P < 0.05$) or close to significantly (ANOVA, $P < 0.10$) greater in the warm versus the cool treatments over the experimental period (Table 1). When differences were not significant over the entire period, there were significant time-by-treatment interactions that, when examined by sample date, indicated significant differences in copepod nauplii and total zooplankton during the initial experimental period (12–25 February 1997). Abundance of copepodites varied significantly between treatments from 25 February – 24 March, while adult values were significantly greater in warm systems from 17 March to the end of the study (Table 1). The copepod community (adults and copepodites) was dominated (58–84%) by *Acartia hudsonica* in all systems. Both *A. hudsonica* and *Centropages hamatus* were significantly more abundant in the warm treatments (ANOVA, $P < 0.05$). The remainder of the zooplankton community, composed primarily of *Temora longicornis*, *Eurytemora affinis*, *Oithona* spp., harpacticoid copepods, barnacle nauplii, and polychaete larvae, showed no significant differences between treatments (ANOVA, $P > 0.05$).

Both phytoplankton (as Chl *a*, micrograms per litre) and zooplankton are important food sources for larval winter flounder (Laurence 1977; Klein-MacPhee et al. 1993). In addition to diatoms and dinoflagellates, winter flounder larvae feed primarily on copepod nauplii, calanoid and harpacticoid copepods, polychaete larvae, and invertebrate eggs. Total food availability (both phytoplankton (Fig. 3) and zooplankton (Fig. 4)) was generally higher in the warm systems relative to the cool over most of the experimental period. Mean zooplankton abundance (number per cubic metre) increased with mean phytoplankton biomass (Chl *a*, micrograms per litre) in the warm and the cool systems and was positively related (ANOVA, $F = 4.0$, $P = 0.1$, near significance) to temperature (Fig. 5). Our results indicate that food availability was not a primary factor controlling larval mortality, since mortality was higher in the warm systems (see below) where more food was present.

Hatching of winter flounder eggs in the warm systems occurred on 25 February after a 20-day incubation period at an average temperature of 4.1°C (±0.1 SE). Hatching in cool systems occurred on 7 March following a 30-day incubation period at an average temperature of 1.6°C (±0.2 SE). Egg mortality (percent) was not significantly different between treatments during the first week of the study but increased significantly (ANOVA, $F = 7.62$, $P < 0.05$) in the warm systems by 19 February and remained higher until hatching (Fig. 6). Percent hatch for the warm treatments ranged from 64.6 to 81.8%, while the range in cool systems was 91.3–94% (Fig. 7). Percent hatch in the cool systems was significantly greater than in the warm (t test, $P < 0.05$).

The size at hatching (mean standard length ± SE) in the cool systems (3.2 ± 0.01 mm) was significantly larger (t test, $P < 0.05$) than the size at hatching in warm mesocosms (3.0 ± 0.01 mm). The mean and range in larval standard length gradually increased over the experimental period in each mesocosm (Fig. 8). In general, the exponential model for growth (eq. 1) gave a good fit to growth in standard length of larval winter flounder over time as indicated by low standard errors for the estimated growth rates (Table 2). Instantaneous growth rates in the warm systems ranged from 0.016 to $0.018 \cdot day^{-1}$ and were higher than values in the cool systems (range $0.011–0.013 \cdot day^{-1}$) (Table 2). Growth rates were compared with analysis of covariance (ANCOVA) and tested for heterogeneity of slopes (since growth rates are the slopes of regression equations) between treatments. Instantaneous daily growth rates of winter flounder larvae were

Fig. 5. Empirical relationship ($Y = 609.3X - 8389$, $r^2 = 0.50$) between mean zooplankton abundance and mean phytoplankton biomass (Chl *a*) in the warm (W) and cool (C) treatments.

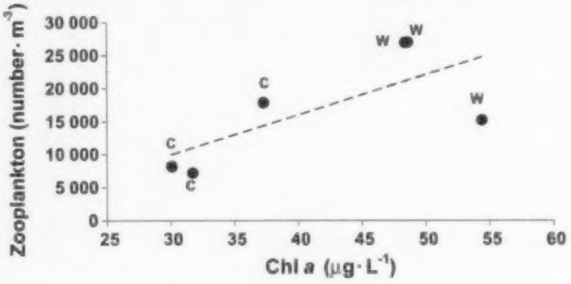

Fig. 6. Percent mortality (±1 SE) for winter flounder eggs over the incubation period for warm (solid circles) and cool treatments (open circles).

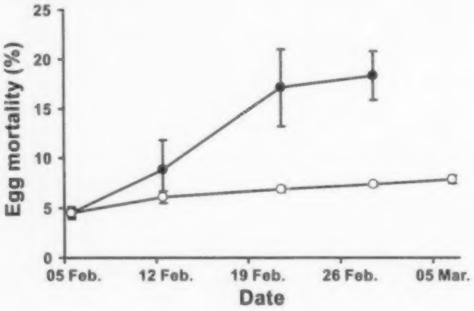

Fig. 7. Percent hatch (±1 SE) for winter flounder eggs in the three warm and three cool treatments based on replicate samples of 100 eggs placed in 4-L plastic containers and floated at the surface of each mesocosm.

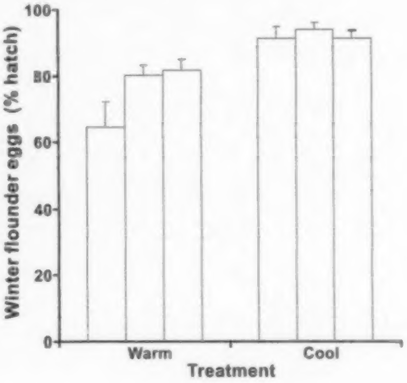

significantly greater in the warm versus the cool systems (ANCOVA, $F = 14.54$, $P = 0.0001$). Although initially smaller, the larvae in the warm systems grew more rapidly and reached a larger size than larvae in the cool systems by the end of the experiment.

Following stocking, winter flounder populations in both treatments were characterized by an initial period of rapid decline followed by a period of decreasing mortality (Fig. 9). Recall that with the exception of the final sample, abundance in each mesocosm was estimated by sampling with a plankton net. When the tanks were drained at the end of the experiment and the entire population censused in each system, the capture efficiency for the plankton nets was 55–98%. The final abundance estimate for calculating mortality rate in each mesocosm was based on the total population count rather than the co-occurring final estimate from sampling with the plankton net. Instantaneous daily mortality rates of winter flounder larvae (eq. 2) were higher in the warm enclosures (Table 3). ANCOVA indicated that differences in mortality rates were near significance (ANCOVA, $P < 0.07$) in the warm versus the cool systems.

Two potentially important benthic predators on winter flounder larvae were present in the mesocosms throughout the study (Table 4), the sand shrimp (*Crangon septemspinosa*) and the mud anemone (*Cerianthiopsis americana*) (Holohan 1993; Thornton-Whitehouse 1994). Although *Crangon* were present in the cool tanks, they were inactive and buried in the sediment. In the warm systems, *Crangon* were observed actively swimming in the water column throughout the experiment and appeared active in the benthos during the diver survey. Although less abundant, *Cerianthiopsis* were observed with their tentacles extended and considered active in all systems. Benthic organisms are not prey items for larval flounder and the abundance of benthic predators was the same prior to the start and at the end of the study. In addition to the benthic predators, chaetognaths and *Sarsia tubulosa* medusae, known or suspected pelagic predators on larval fish (Khulmann 1977; Northeast Utilities 1999), were also present in some mesocosms (Table 4). No pelagic predators were collected in plankton or pumped samples throughout the experiment but were present in the ring and overflow nets when the tanks were drained at the end of the study. The relationship between daily instantaneous larval mortality rates and the abundance of predators (benthic plus pelagic) is highly significant, with high mortality rates correlated with abundant active predators (Fig. 10).

Discussion

Winter flounder has historically been a dominant demersal fish species collected in Narragansett Bay (Jeffries and Terceiro 1985). Commercial catch and recreational catch have declined severely since 1979 (Gibson 1998). In 1990, our Narragansett Bay ichthyoplankton survey indicated that winter flounder larvae were significantly less abundant in all regions of the Bay compared with an earlier survey in 1972–1973 (Keller et al. 1999*b*). Because of concerns over drastic decreases in abundance, the Rhode Island Department of Environmental Management banned fishing for winter flounder in Narragansett Bay and its adjacent salt ponds in 1991. A limited fishery was reopened in 1995, with very little improvement in catch. Although winter flounder have tended to be somewhat cyclical throughout historical assessments, each peak and trough is now lower than preceding values and troughs are extending over longer time periods (Gibson 1998).

Although overfishing plays a role in the population decline, other factors are important in controlling recruitment

Fig. 8. Mean (± range) winter flounder larval standard length for each sample period over the experimental period in the individual mesocosm. (A–C) Warm tanks; (D–F) cool tanks.

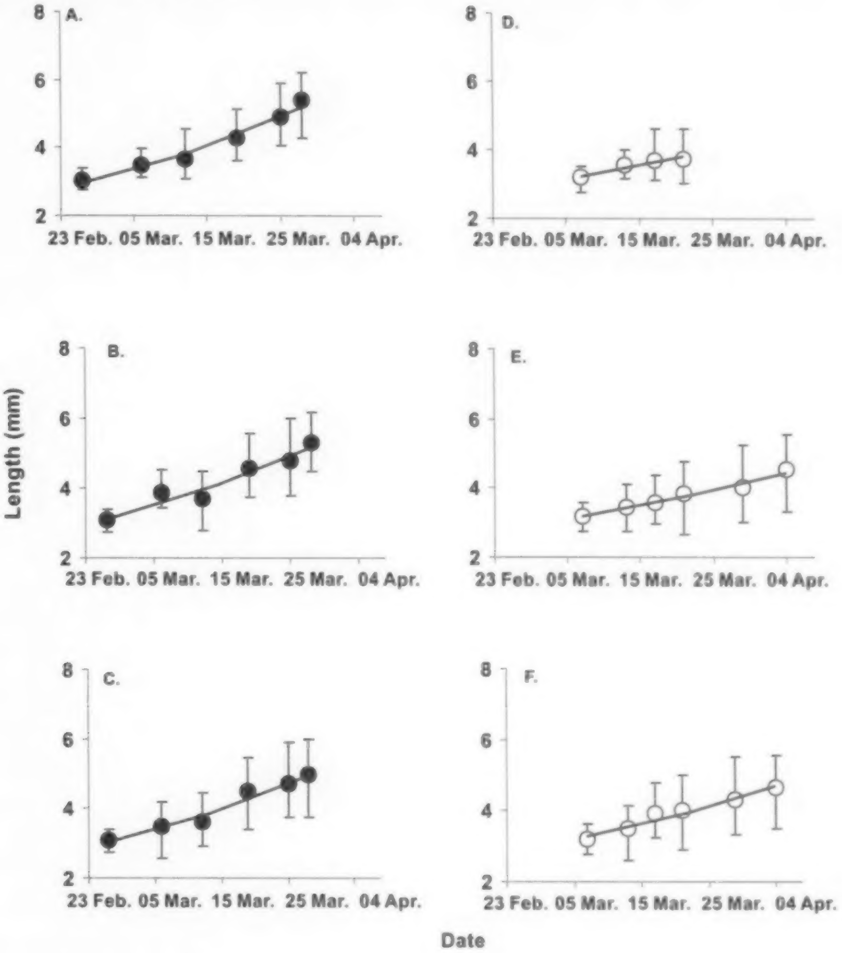

Table 2. Average daily instantaneous growth rates (G) and associated statistics for winter flounder larvae in each mesocosm from eq. 1.

Treatment	G (±SE) (day^{-1})	n	r^2	P	Δt (days)
Warm, 3	0.018 (0.001)	125	0.88	0.0001	31
Warm, 7	0.018 (0.001)	80	0.92	0.0001	31
Warm, 9	0.016 (0.001)	161	0.75	0.0001	31
Cool, 5[a]	0.011 (0.001)	49	0.61	0.0001	16
Cool, 9	0.013 (0.001)	105	0.85	0.0001	26
Cool, 13	0.012 (0.001)	146	0.78	0.0001	26

Note: Mesocosm number is shown next to the treatment. Values in parentheses are standard errors for the estimated parameters. Treatments are defined in the text.

[a] Data collection ceased in this mesocosm following the spill of egg basket on 21 March.

of winter flounder. Annual abundance, when appropriately lagged (most flounder take 1–2 years to enter the catch), is negatively correlated with winter temperature, indicating that warmer temperatures during spawning result in fewer fish (Jeffries and Johnson 1974; Jeffries and Terceiro 1985; Northeast Utilities 1999). Buckley et al. (1990) noted that cold winters favored good survival by facilitating production of large larvae in good condition (high RNA and protein content). Jeffries et al. (1989) presented the hypothesis that temperature controls flounder abundance through predation. Earlier mesocosm studies designed to assess the importance of eutrophication on growth and survival of winter flounder larvae instead suggested that benthic predators or competitors play an important role in mortality of winter flounder larvae (Klein-MacPhee et al. 1993). Since winter water temperatures in Narragansett Bay have increased significantly over the past 40 years, understanding the impact of elevated temperature on winter flounder recruitment is crucial. The current experiment was designed to test the hypothesis that experimentally increasing temperature would produce a detectable change in the survival of winter flounder larvae to metamorphosis. We hypothesized that the observed decline in winter flounder abundance was a result of the interaction

Fig. 9. Mean abundance (±1 SE) of winter flounder larvae in (A) the warm treatments and (B) the cool systems over the experimental period.

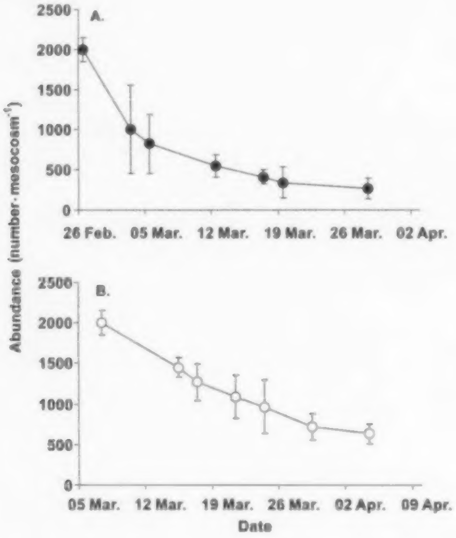

Table 3. Average daily instantaneous mortality rates (*Z*) and associated statistics for winter flounder larvae in each mesocosm from eq. 2.

Treatment	Z (±SE) (day^{-1})	n	r^2	P
Warm, 3	0.058 (0.019)	7	0.60	0.04
Warm, 7	0.093 (0.031)	7	0.63	0.03
Warm, 13	0.068 (0.008)	7	0.93	0.0004
Cool, 5[a]	0.037 (0.019)	5	0.93	0.007
Cool, 9	0.040 (0.008)	7	0.81	0.006
Cool, 15	0.041 (0.006)	7	0.89	0.0004

Note: Mesocosm number is shown next to the treatment. Values in parentheses are standard errors for the estimated parameters. Treatments are defined in the text.

[a] Data collection ceased in this mesocosm following spill of egg basket on 21 March.

between temperature and either food availability or predation, the primary factors affecting larval fish recruitment (Cowan and Houde 1990). The above results indicated that temperature differences at the experimental level impacted winter flounder larval growth and survival. Our results demonstrated that warmer winter water temperature influences the food web leading to winter flounder as well as egg mortality, percent hatch, size at hatch, growth rate, and larval mortality. It is important to note when interpreting the experimental results that although water temperature was increased 3.25°C relative to controls, the actual increase relative to the Bay temperature over the same period was 0.7°C. In essence, the experiment is comparing current and future increases in winter temperatures resulting from global climate change with temperatures more typical of cooler winters in the past.

Table 4. Abundance (number·mesocosm^{-1}) of benthic and pelagic predators in each mesocosm throughout the experiment.

Treatment	*Crangon* sp.	*Cerianthiopsis* sp.	Chaetognaths	*Sarsia* sp.
Warm, 3	4	5	0	1
Warm, 7	18	2	1	2
Warm, 13	5	9	1	0
Cool, 5	3	5	0	2
Cool, 9	0	4	0	0
Cool, 15	2	3	0	0

Note: Mesocosm number is shown next to the treatment. Although present in the cool systems, *C. septemspinosa* were inactive and not included in the total predator abundance utilized in the analysis of mortality rates.

Fig. 10. Empirical relationship ($Y = 0.003X + 0.028$, $r^2 = 0.93$) between larval winter flounder daily instantaneous mortality rate (Z) and the abundance of active predators in the warm (W) and cool (C) treatments.

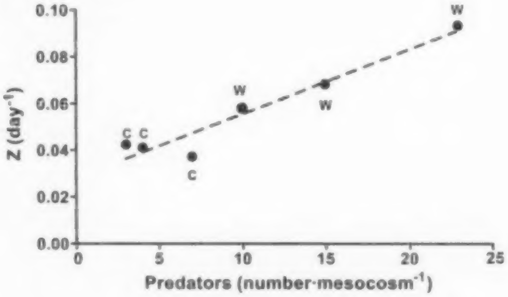

Long-term data indicate a significant increase in water temperature in Narragansett Bay during February–April over the past 40 years. Temperatures in the warm mesocosms were similar to those observed in Narragansett Bay during much of the experiment and typical of late winter temperatures generally observed in recent years. Temperatures in the cool systems were closer to those observed during recent cold winters (e.g., 1996) and more typically in the past. Both warm and cool systems demonstrated the gradual temperature increase over time that occurs from February through early April and were within the range of temperatures (–1.8 to 15°C) at which winter flounder larvae are know to occur (Williams 1975; Rogers 1976).

In an earlier temperature experiment that did not include ichthyoplankton (Keller et al. 1999*a*), we observed that the characteristic winter–spring bloom failed to occur in warm systems, similar to its failure to appear in the Bay in recent years. In the present study, when the mesocosms were filled during a period with moderate Chl *a* levels in the Bay (~15 μg·L^{-1}), blooms developed in both warm and cool systems. These results suggest that the moderate Chl *a* levels present in the tanks at the time of the fill were sufficient to prevent grazers from initially controlling bloom development. Towards the end of the study, we observed an increase in phytoplankton in the cool systems similar to our earlier results (Keller et al. 1999*a*). The dominant phytoplankton species present during the experiment (*Thalassiosira* spp., *Chaetoceros* spp., and *S. costatum*) are those typically observed during the winter–spring bloom period in the parent system, Narragansett Bay (Smayda 1973). The phytoplankton abundance and biomass levels are typical of the levels occurring in the upper regions of Narragansett Bay where winter flounder larvae are most abundant (Durbin and Durbin 1981; Keller et al. 1999*b*).

Copepod abundance increased in the warm systems compared with cool systems, again similar to results observed in our prior temperature experiment when flounder larvae were not present (Keller et al. 1999*a*). The rapid increase in copepod nauplii in the warm systems reflects the temperature-mediated hatching rate of *A. hudsonica* resting eggs combined with an egg production rate of up to 42 eggs·female^{-1}·day^{-1} (Sullivan and McManus 1986). The dominant copepod species present were those typically observed in Narragansett Bay in February and March and at levels comparable with those occurring in the upper Bay (Durbin and Durbin 1981). Winter flounder larvae feed primarily on diatoms, dinoflagellates, copepod nauplii, and copepodites (calanoid and harpacticoid) (Laurence 1977; Klein-MacPhee et al. 1993). The net result of the changes in phytoplankton and copepod abundance in the warm systems relative to the cool was that more food was available for winter flounder larvae in the warm systems. Our highest survivals during the present study occurred in the systems with the lowest food supply. There was no relationship between survival and food abundance in the current study or in our studies conducted during 1988–1991 (Klein-MacPhee et al. 1993). Laurence (1977) found that winter flounder larvae failed to survive beyond 2 weeks at prey densities between 10 and 100 nauplii·L^{-1} in laboratory studies. During the present study, copepod nauplii abundance in cool systems ranged from 2 to 27·L^{-1}, while in warm systems, nauplii were more abundant, 3–35·L^{-1}. Despite the fact that these values fall within the range associated with 100% mortality at 2 weeks in Laurence's (1977) study, we observed relatively high survival in all systems. Research in other mesocosms has also demonstrated that fish larvae grow and survive with food levels lower than laboratory estimates of required amounts (Øiestad 1985; Cowan and Houde 1990). Although food availability was not a primary factor affecting mortality in the current study, the potential for variability in food quality between warm and cool systems does exist. Recall that *Skeletonema* and *Chaetoceros* spp. were more abundant in cool systems, while *Thalassiosira* spp. were more abundant in warm systems. The dominant copepod was the same species (*A. hudsonica*) in both treatments. The nutritional value of *Skeletonema* and *Chaetoceros* versus *Thalassiosira* is unknown. Although temperature had a significant impact on the food web leading to winter flounder, this does not appear to be the dominant factor influencing larval mortality during the study.

Temperature had a direct impact on the incubation period in the current study, with cooler temperature resulting in a longer incubation. Previous research on winter flounder from Narragansett Bay has also indicated that incubation time of eggs varies inversely with temperature (Rogers 1976). Rogers (1976) noted that time to hatching was approximately 4 weeks at 3°C and 2 weeks at 8°C. Our values for the warm systems fall between these, with hatching occurring at about 3 weeks at 4.1°C. In the cool systems with average incubation temperatures of 1.6°C, the incubation period was slightly longer than the 4-week period described by Rogers (1976) at 3°C.

Winter flounder larvae hatched at a larger size in the cool mesocosms relative to the warm. Buckley et al. (1990) similarly noted that larvae were larger when incubated at 2°C compared with larvae incubated at warmer temperatures (7°C). Although smaller at hatching, the larvae in the warm mesocosms grew more rapidly. The difference in growth rates between treatments may be interpreted as a density-dependent effect, since the higher mortality in warm systems resulted in a lower abundance of fish there. Daily instantaneous growth and mortality rates were significantly and inversely related ($r^2 = 0.70$). The daily instantaneous growth rates observed in the warm systems (0.016–0.018·day^{-1}) were not significantly different from the rates observed in an earlier unrelated study (0.019–0.022·day^{-1}) at somewhat warmer temperatures (7.8°C) (Klein-MacPhee et al. 1993), while those from the cool systems (0.011–0.013·day^{-1}) were significantly lower.

Capture efficiency was unrelated to treatment and within the range expected for larval winter flounder (Pearcy 1962) and observed in prior mesocosm studies (G. Klein-MacPhee, unpublished data). Mortality rates in cool systems (0.037–0.041·day^{-1}) fell within the range of values previously observed in mesocosms operated without a benthos (0.002–0.045·day^{-1}) (Klein-MacPhee et al. 1993). These values approximate rates more common for laboratory studies where there is no predation. The higher and more variable rates observed in the warm systems (0.058–0.093·day^{-1}) tended to be somewhat lower than rates previously observed in our experiments with a benthos present (0.100–0.193·day^{-1}). Even in warm systems, the abundance of predators was relatively low during the temperature experiment. The maximum density of *Crangon* in the experiment was ~5·m^{-2} and well below the maximum winter density observed by Thornton-Whitehouse (1994) in Narragansett Bay (80·m^{-2}). *Ceriantheopsis* density was also low in the mesocosms relative to densities observed in the field (Holohan 1993). The variability in mortality rates was linearly correlated with the abundance of predators. A linear relationship between mortality rate and abundance of predators was unexpected and may be a result of the low numbers of predators present.

The cumulative impact of warmer temperatures on the early life history of winter flounder from hatching through the late larval stage resulted in 10–16% fewer larvae surviving to metamorphosis (~6 weeks). These results together with the potential for increased egg predation and post-settlement predation, most notably by *Crangon* (van der Veer and Bergman 1987; Whitting 1993), as a result of elevated winter water temperature suggest that temperature and its impact on predation rate may play a major role in regulating winter flounder abundance. Now that we know that this temperature-mediated predation effect exists, regional managers should attempt to incorporate the potential impact of warm winters in their management plans. One such approach would be to reduce fishing pressure following periods of successive warm winters. Currently, chronic overexploitaion is associated with a long-term decline in winter flounder stock abundance despite periodic production of good year-classes (Gibson 1998), suggesting that even with the higher recruitment associated with cooler winters, overfishing is a problem in Narragansett Bay.

Acknowledgments

We thank Candace Oviatt, Perry Jeffries, Eric Klos, Laura Reed, Donna VanKeuren, Edwin Requintina, Jaiping Zhang, Hal Walker, Galo Escanero, Don Webb, Jamie Hawk, and Paul Hargraves for help with sampling, nutrient analyses, field collections, phytoplankton identifications, mesocosm maintenance, and data interpretation. This work was funded under a U.S. Environmental Protection Agency Cooperative Agreement with the National Research Council, National Academy of Sciences. The contents of the manuscript do not necessarily reflect the views and policies of the U.S. Environmental Protection Agency.

References

Buckley, L.J., Smigielski, A.S., Halavik, T.A., and Laurence, G.C. 1990. Effects of water temperature on size and biochemical composition of winter flounder *Pseudopleuronectes americanus* at hatching and feeding initiation. Fish. Bull. U.S. **88**: 419–428.

Cowan, J.H., and Houde, E.D. 1990. Growth and survival of bay anchovy *Anchoa mitchilli* larvae in mesocosm enclosures. Mar. Ecol. Prog. Ser. **68**: 47–57.

Crawford, R. 1990. Winter flounder in Rhode Island coastal ponds. National Seagrant Depository Publication RIU-G-90-001, Narragansett, R.I.

Durbin, A.G., and Durbin, E.G. 1981. Standing stock and estimated production rates of phytoplankton and zooplankton in Narragansett Bay, Rhode Island. Estuaries, **4**: 24–41.

Gibson, M.R. 1998. Recent trends in abundance, recruitment, and fishing mortality for winter flounder in Narragansett Bay and Rhode Island coastal waters. Report to the Rhode Island Marine Fisheries Council. Res. Ref. Doc. 98, Rhode Island Division of Fish and Wildlife, Wickford, R.I.

Holohan, B.A. 1993. Population density and grazing of *Cerianthiopsis americanus* in Narragansett Bay. M.S. thesis, University of Rhode Island, Kingston, R.I.

Houde, E.D. 1987. Fish early life dynamics and recruitment variability. Am. Fish. Soc. Symp. **2**: 17–29.

Jeffries, H.P., and Johnson, W.C. 1974. Seasonal distribution of bottom fishes in the Narragansett Bay area: seven-year variations in the abundance of winter flounder (*Pseudopleuronectes americanus*). J. Fish. Res. Board Can. **31**: 1057–1066.

Jeffries, H.P., and Terceiro, M. 1985. Cycle of changing abundances in the fishes of the Narragansett Bay area. Mar. Ecol. Prog. Ser. **25**: 239–244.

Jeffries, H.P., Keller, A.A., and Hale, S. 1989. Predicting winter flounder (*Pseudopleuronectes americanus*) catches by time series analysis. Can. J. Fish. Aquat. Sci. **46**: 650–659.

Keller, A.A., Oviatt, C.A., Walker, H.A., and Hawk, J.D. 1999*a*. Predicted impact of elevated temperature on the magnitude of the winter–spring phytoplankton bloom in temperate coastal waters: a mesocosm study. Limnol. Oceanogr. **44**: 344–356.

Keller, A.A., Klein-MacPhee, G., and St. Onge-Burns, J. 1999*b*. Abundance and distribution of ichthyoplankton in Narragansett Bay, Rhode Island, 1989–1990. Estuaries, **22**: 149–163.

Khulmann, D. 1977. Laboratory studies on the feeding behavior of the chaetognaths *Sagitta setosa* J. Muller and *S. elegans* Verril with special reference to fish eggs and larvae as food organisms. Ber. Dtsch. Wiss. Komm. Meeresforsch. **25**: 163–171.

Klein-MacPhee, G., Howell, W.H., and Beck, A.D. 1982. Comparison of a reference strain and four geographic strains of *Artemia* as food for winter flounder, *Pseudopleuronectes americanus*, larvae. Aquaculture, **29**: 279–284.

Klein-MacPhee, G., Sullivan, B.K., and Keller, A.A. 1993. Using mesocosms to assess the influence of food resources and toxic material on larval fish growth and survival. Am. Fish. Soc. Symp. **14**: 105–116.

Laurence, G.C. 1974. Growth and survival of haddock (*Melanogrammus aeglefinus*) larvae in relation to planktonic prey concentration. J. Fish. Res. Board Can. **31**: 1415–1419.

Laurence, G.C. 1977. A bioenergetic model for the analysis of feeding and survival potential of winter flounder, *Pseudopleuronectes americanus*, larvae during the period from hatching to metamorphosis. Fish. Bull. U.S. **75**: 529–546.

Laurence, G.C., Halavik, T.A., Burns, B., and Smigielski, A.S. 1979. An environmental chamber for monitoring 'in situ' growth and survival of larval fishes. Trans. Am. Fish. Soc. **108**: 197–203.

Lorenzen, C.J. 1966. A method for continuous measurement of *in vivo* chlorophyll concentration. Deep-Sea Res. **13**: 223–227.

Northeast Utilities. 1999. Monitoring the marine environment of Long Island Sound at the Millstone Nuclear Power Station, Waterford, CT. Northeast Utilities, Environmental Laboratory, Waterford, Conn.

Øiestad, V. 1985. Predation on fish larvae as a regulatory force, illustrated in mesocosm studies with large groups of larvae. NAFO Sci. Counc. Stud. **8**: 25–32.

Oviatt, C.A. 1994. Biological considerations in marine enclosure experiments: challenges and revelations. Oceanography, **7**: 45–51.

Oviatt, C.A., Keller, A.A., Sampou, P.A., and Beatty, L.L. 1986. Patterns of productivity during eutrophication: a mesocosm experiment. Mar. Ecol. Prog. Ser. **28**: 69–80.

Pearcy, W.G. 1962. Ecology of young winter flounder in an estuary. Bull. Bingham Oceanogr. Collect. Yale Univ. **18**: 1–78.

Rogers, C.A. 1976. Effects of temperature and salinity on the survival of winter flounder embryos. Fish. Bull. U.S. **74**: 52–58.

Schuurmans, C.J.E. 1995. The world heat budget: expected changes. *In* Climate change: impact on coastal habitation. *Edited by* D. Eisma. Lewis Publishers, CRC Press, Boca Raton, Fla. pp. 1–16.

Smayda, T.J. 1973. The growth of *Skeletonema costatum* during a winter–spring bloom in Narragansett Bay, Rhode Island. Norw. J. Bot. **20**: 219–247.

Sournia, A. (*Editor*). 1978. Phytoplankton manual. UNESCO, Paris.

Sullivan, B.K., and McManus, L.T. 1986. Factors controlling seasonal succession of the copepods *Acartia hudsonica* and *A. tonsa* in Narragansett Bay, Rhode Island: temperature and resting egg production. Mar. Ecol. Prog. Ser. **28**: 121–128.

Thornton-Whitehouse, S. 1994. The abundance and distribution of *Crangon septemspinosa* in Narragansett Bay. Ph.D. thesis, University of Rhode Island, Kingston, R.I.

van der Veer, H.W., and Bergman, M.J.N. 1987. Predation by crustaceans on a newly settled 0-group plaice *Pleuronectes platessa* population in the western Wadden Sea. Mar. Ecol. Prog. Ser. **35**: 203–215.

Whitting, D.A. 1993. Effects of body size on probability of predation for juvenile summer and winter flounder based on laboratory experiments. Fish. Bull. U.S. **91**: 577–581.

Williams, G.C. 1975. Viable embryogenesis of the winter flounder *Pseudopleuronectes americanus* from –1.8° to 15°C. Mar. Biol. **33**: 71–74.

Winer, B.J. 1971. Statistical principles in experimental design. 2nd ed. McGraw-Hill, New York.

Depth-dependent vertebral number of Atlantic cod (*Gadus morhua*) on the Magdalen Shallows and Scotian Shelf: stock mixing or microgeographic trends within populations?

D.P. Swain and K.T. Frank

Abstract: We examined spatial variation in the vertebral number of Atlantic cod (*Gadus morhua*) during the summer feeding season in the southern Gulf of St. Lawrence and on the Scotian Shelf. Mean vertebral number increased significantly with depth in the southern Gulf and on the northeastern Scotian Shelf but not on the southwestern Scotian Shelf. In the southern Gulf, where sampling was most extensive, mean vertebral number increased steadily as depth increased from 25 m to over 175 m. Mean vertebral number was also strongly related to relative length within age-classes, with the larger fish at age having more vertebrae. However, the association between vertebral number and depth could not be attributed to confounding between depth and size at age. These results indicate either unexpected mixing between neighbouring cod populations or unexpected structure at fine spatial scales within cod populations.

Résumé : Nous avons examiné la variation géographique du nombre de vertèbres chez la morue franche (*Gadus morhua*) durant la saison estivale d'alimentation dans la partie sud du golfe du Saint-Laurent et sur la plate-forme néo-écossaise. Le nombre moyen de vertèbres augmente avec la profondeur de la mer dans le sud du golfe et sur la partie nord-est de la plate-forme, mais pas sur la partie sud-ouest. Dans le sud du golfe, où l'échantillonnage a été plus important, le nombre moyen de vertèbres augmente régulièrement entre les profondeurs de 25 m à plus de 175 m. Le nombre de vertèbres est aussi en forte corrélation avec la longueur relative des poissons dans chacune des classes d'âge et ce sont les poissons les plus gros d'un âge donné qui comptent le plus grand nombre de vertèbres. Cependant, l'augmentation du nombre de vertèbres avec la profondeur de la mer ne peut être attribuée à l'effet combiné de la profondeur et de la taille à un âge donné. Il s'agirait plutôt de l'effet d'un mélange de populations voisines de morues ou alors de l'existence d'une structure inattendue à petite échelle spatiale dans ces populations.

[Traduit par la Rédaction]

Introduction

Widespread patterns in vertebral number occur among populations of related fishes. Mean vertebral number tends to be higher in populations at higher latitudes or in colder waters (Jordan's rule; Jordan 1892) and in populations with greater maximum body lengths (pleomerism; Lindsey 1975). The number of vertebrae formed in developing embryos can be strongly influenced by their environment, particularly its temperature (Lindsey 1988). However, despite this lability to early environmental influences, common garden experiments have revealed a genetic basis to these trends among populations (Lindsey 1975, 1988; in particular, see Billerbeck et al. 1997). These widespread trends and their genetic basis suggest that variation in vertebral number among populations reflects local adaptation. Experiments demonstrating selective predation for vertebral number in larval fish (Swain and Lindsey 1984; Swain 1988) provide direct evidence of a link between vertebral number and fitness, with the optimal phenotype depending on larval size (Swain 1992*b*). Effects of vertebral phenotype on burst swimming performance of larvae suggest a functional basis for this link with fitness (Swain 1992*a*). While most adaptive explanations for the trends in vertebral number among populations of fishes have focussed on selection on larval fishes (Lindsey 1975; Swain 1988, 1992*a*), selection on vertebral number of juvenile and adult fish has also been suggested to be important (Reimchen and Nelson 1987; Billerbeck et al. 1997).

Vertebral number also varies within populations of fish. While patterns in vertebral number among populations have been widely studied, microgeographic variation in vertebral number within populations has received scant attention. Reimchen and Nelson (1987) described spatial variation in vertebral number within a population of threespine stickleback (*Gasterosteus aculeatus*) inhabiting a small lake. They were able to attribute most of the horizontal (lake centre to shoreline) variation to differences in distribution between the sexes and between size-classes (which differed in mean vertebral count), but differences in vertebral number between

Received April 18, 2000. Accepted September 27, 2000. Published on the NRC Research Press web site on December 20, 2000.
J15728

D.P. Swain.[1] Department of Fisheries and Oceans, Gulf Fisheries Centre, P.O. Box 5030, Moncton, NB E1C 9B6, Canada.
K.T. Frank. Department of Fisheries and Oceans, Bedford Institute of Oceanography, P.O. Box 1006, Dartmouth, NS B2Y 4A2, Canada.

[1] Corresponding author (e-mail: swaind@dfo-mpo.gc.ca).

Fig. 1. Map of the southern Gulf of St. Lawrence and Scotian Shelf (eastern Canada) showing NAFO divisions.

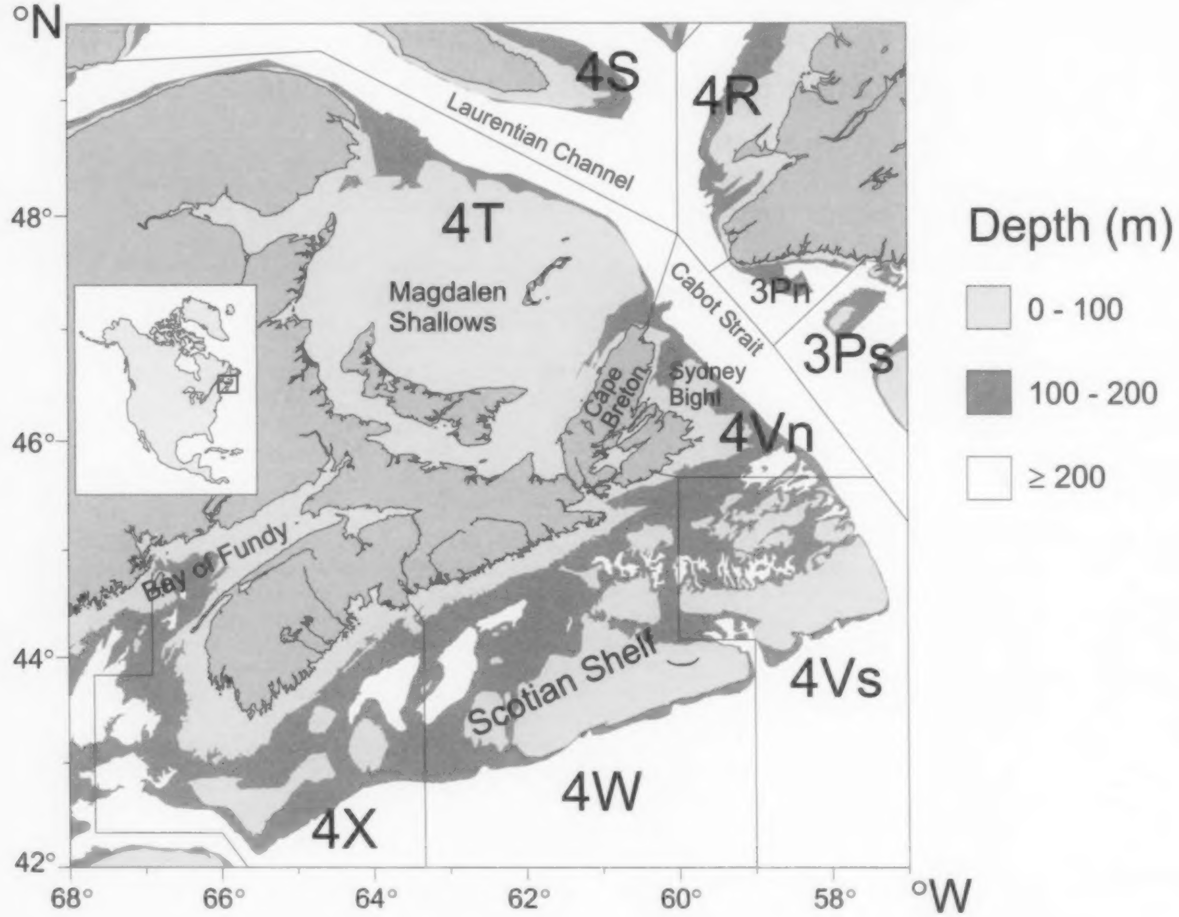

depth zones (surface versus bottom) persisted after accounting for these sources of variation.

In this study, we describe spatial variation in vertebral number within populations of Atlantic cod (*Gadus morhua*). Atlantic cod are widely distributed over the continental shelf in the Canadian Atlantic region. Several stocks or stock complexes are distinguished in this area, each named after the Northwest Atlantic Fisheries Organization (NAFO) divisions that they occupy. We examined vertebral number in populations inhabiting the Gulf of St. Lawrence and the Scotian Shelf (Fig. 1). Two large migratory populations occur in the Gulf of St. Lawrence, the southern Gulf or 4T–4Vn (December–April) stock (referred to here as the 4T stock) and the northern Gulf or 3Pn4RS stock. Tagging studies indicate little exchange between these two populations (e.g., Martin and Jean 1964; Gascon et al. 1990). For this study, we examined vertebral number in only one of these populations, the 4T stock. We also examined spatial variation in vertebral number in three stocks occupying the Scotian Shelf, the 4Vn, 4VsW, and 4X stocks.

Recent studies have compared most of these cod stocks in terms of vertebral number (Swain et al. 2001), the elemental composition of otoliths (Campana et al. 2000), and microsatellite DNA (Ruzzante et al. 2000). In addition to the stocks mentioned above, these comparisons included the 3Ps stock off southern Newfoundland. Although Ruzzante et al. (2000) found no significant differences in microsatellite DNA between cod in the northern (4R) and southern Gulf (4T), cod in both regions of the Gulf differed from those in each of the stock areas in the approaches to the Gulf. Significant differences in microsatellite DNA were also found between all the stock areas in the approaches to the Gulf as well as between samples within the 3Ps area (Ruzzante et al. 2000). The 4T, 3Pn4RS, 4Vs, and 3Ps stocks could all be distinguished from each other based on the elemental composition of their otoliths (Campana et al. 2000). Mean vertebral number was significantly lower in the 4T stock than in each of the other stocks, but no other significant differences in vertebral number occurred between these stocks (Swain et al. 2001) (Table 1).

We report here a strong association between habitat (i.e., depth) and vertebral number of cod in the southern Gulf of

Table 1. Mean vertebral counts in Atlantic cod stocks in the Gulf of St. Lawrence and its approaches.

Stock	Year	*N*	Mean	SE
3Ps	1996	79	53.975	0.144
	1997	53	53.925	0.176
3Pn4RS	1996	143	53.818	0.075
	1997	128	53.891	0.085
4T	1995	843	53.445	0.030
	1996	179	53.430	0.069
	1997	196	53.541	0.064
4Vn	1994	140	53.871	0.089
	1997	41	53.854	0.202
4Vs	1994	157	53.883	0.076
	1996	98	53.684	0.080
	1997	148	53.784	0.075

Note: Data are from Swain et al. (2001).

St. Lawrence and on the eastern Scotian Shelf. These patterns, observed during the summer feeding season when the stocks are separated, occur within areas that have been assumed to contain single populations or subpopulations of cod. While we report that vertebral number is also strongly related to size at age within these areas (with larger fish at a given age having more vertebrae), we find that these microgeographic patterns in vertebral number cannot be attributed to confounding between depth and size at age. These results suggest either unexpected mixing between neighbouring cod populations or unexpected structure at fine spatial scales within cod populations.

Material and methods

Study populations

Atlantic cod in the southern Gulf or 4T population overwinter in deep water along the southern slope of the Laurentian Channel in the Cabot Strait area (Fig. 1). They migrate into the southern Gulf in spring, spawn, and then disperse throughout the Magdalen Shallows to feed during the summer and early fall, migrating back out of the Gulf to their overwintering grounds in November. We describe depth-dependent patterns in vertebral number of 4T cod in September, during their feeding season on the Magdalen Shallows, when they are believed to be geographically separated from other cod stocks.

We also describe relationships between depth and vertebral number of cod in the three stock complexes on the Scotian Shelf. Cod in these populations do not undertake the extensive seasonal migrations exhibited by the Gulf of St. Lawrence stocks. A small population, the 4Vn stock, is resident throughout the year in the Sydney Bight area off the northeast coast of Cape Breton. A second stock complex occupies the offshore banks of the eastern Scotian Shelf in Divisions 4Vs and 4W. Tagging studies suggest that mixing of adult cod between the 4Vs and 4W areas is limited (Martin and Jean 1964), although mixing has been considered sufficient to consider the complex as a unit for stock assessment purposes (e.g., Halliday 1972). We analyse data separately for these two areas, although similar conclusions are reached grouping data over the entire 4VsW area. A third stock complex occurs on the western Scotian Shelf in Division 4X. Again, cod in this area are considered to comprise partially separate subcomponents (Clark and Brown 1996), one in the Bay of Fundy (referred to here as $4X_{bf}$) and one on the offshore banks (referred to here as $4X_{off}$). We treat data from the two areas separately, although again the same conclusions regarding effects on vertebral number are reached grouping over the area.

Study area

The southern Gulf of St. Lawrence consists of a shallow shelf, the Magdalen Shallows, with depths mostly under 100 m, bordered on the north by a 500-m trench, the Laurentian Channel (Fig. 1). Bathymetry of the Scotian Shelf area is more complex, consisting of shallow areas nearshore and on offshore banks, where depths are under 100 m, separated by deep channels and basins with depths ranging from 150 to 250 m or more.

Sample collection and processing

Samples were obtained from bottom-trawl surveys conducted during the feeding season in summer or early fall (Fig. 2). Samples from the Scotian Shelf and Bay of Fundy were obtained from a survey conducted in July 1994; those from the southern Gulf were obtained from a survey in September 1995. Random samples of cod were retained for vertebral counts. Samples were retained in order to obtain a wide spatial distribution and were not necessarily taken in proportion to cod catches (e.g., see fig. 2*a* in Swain et al. 2001). Sampling depth was estimated for each location by averaging the depths at the start and the end of each trawl tow in the case of the September 1995 survey or by averaging the minimum and maximum tow depths in the case of the July 1994 survey. Otoliths were extracted for age determination and individual length, weight, sex, and maturity recorded. We calculated a measure of relative length within age-classes by subtracting the stratified mean length at age from individual lengths. Mean lengths were calculated separately for each stock or stock component. Vertebral columns were exposed by removing all tissue from the skeleton by boiling. Counts were of centra including the urostylar half vertebra. Samples from the Scotian Shelf were assigned to stocks or stock components based on survey stratum (Fig. 2; stratum and subdivision boundaries do not always coincide exactly).

Statistical analysis

Although vertebral number is a meristic character, the level of discreteness (sensu Swain 1987) was not extreme in our samples, with a fairly wide range of values occuring within samples. Vertebral number was also clearly normally distributed within our samples (see fig. 4*a* in Swain et al. 2001). Thus, we elected to use linear regression and analysis of variance for most statistical analyses. We used randomization tests to confirm that these procedures yielded appropriate significance levels when applied to our data (see Swain et al. 2001). Effects of stock, age (or year-class), depth, length, and relative ("standardized") length were tested. Stock and age were treated as factors and depth, length, and relative length as continuous covariates. Simple parametric models (i.e., linear or quadratic regression models) did not adequately describe the effect of fish length on mean vertebral number. We used generalized additive models (GAMs; Hastie 1992) to account for this effect. These models were fit with the GAM function of S-Plus (MathSoft 1999) using the local regression smoother LOESS to fit the nonparametric term. Some models included both parametric and nonparametric terms. To control for any confounding with fish length in tests of the effect of depth on vertebral number, we used a model with a linear depth term and a nonparametric length term.

Results

Mean vertebral number of Atlantic cod was strongly related to depth in the southern Gulf of St. Lawrence, increasing steadily as depth increased from about 25 m to over 175 m (Fig. 3*a*). On the Scotian Shelf, the relationship between vertebral number and depth differed significantly ($P = 0.0012$)

Fig. 2. Spatial distribution of Atlantic cod samples collected for vertebral number and their stock or substock designation. Circles show samples collected during the September 1995 bottom-trawl survey of the southern Gulf of St. Lawrence. Squares show samples collected during the July 1994 survey of the Scotian Shelf. Symbol size is proportional to sample size. Shading indicates depth.

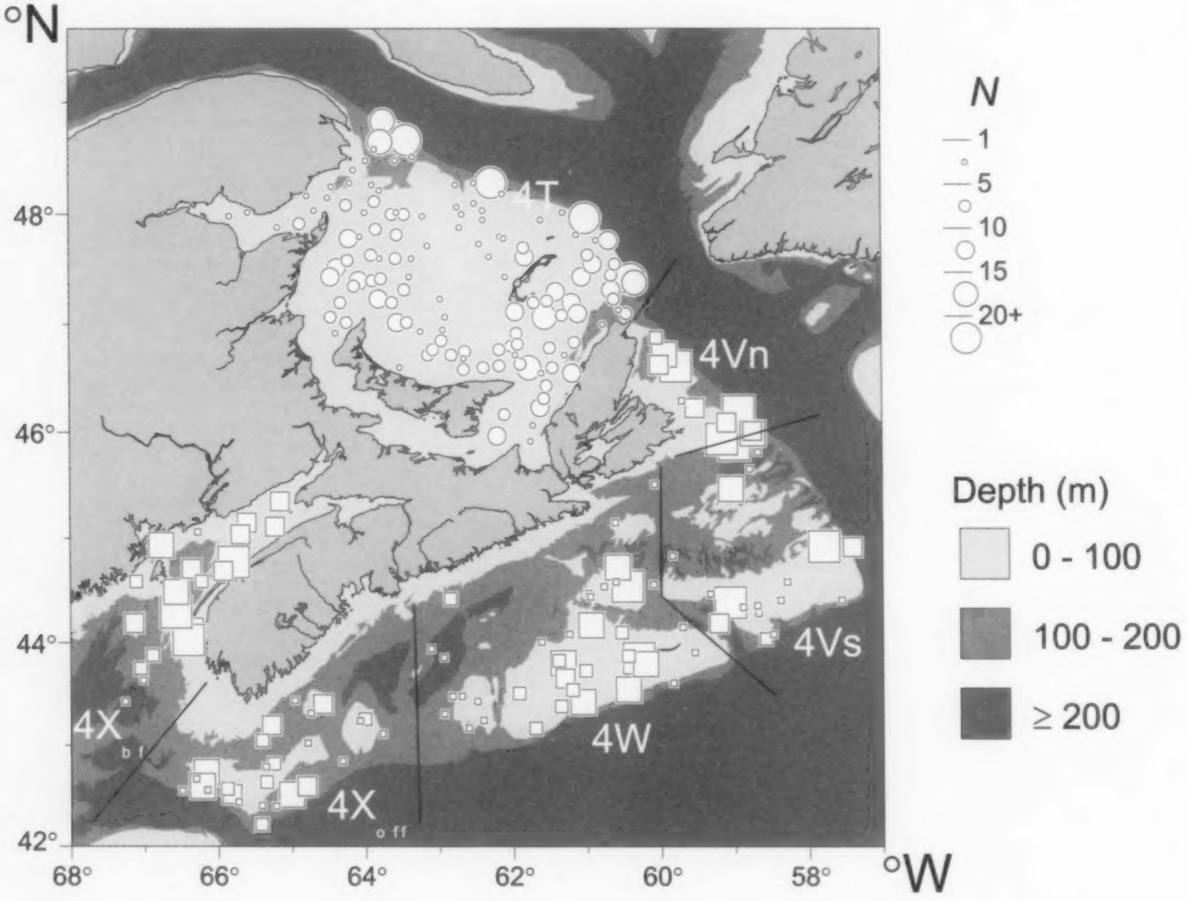

between stocks or stock components (Figs. 3*b*–3*f*). Relationships were highly significant in stock components occupying northeastern regions of the Shelf (4Vn and 4Vs) but not in those occupying the remainder of the Shelf. In the areas with significant relationships, the effect was in the same direction as in the southern Gulf, with vertebral number increasing with depth. The increase in mean vertebral number with depth on the Scotian Shelf was steepest and most significant in 4Vn cod, followed by 4Vs cod. Results were similar grouping over the entire 4VsW and 4X stocks. Vertebral number increased significantly ($P = 0.0002$) with depth over the entire 4VsW area, although mean counts departed from the regression line at depths between 75 and 100 m, reflecting the low counts at these depths in the 4W area. As in the separate analyses within the offshore and Bay of Fundy regions of 4X, vertebral number was unrelated to depth over the entire 4X area ($P = 0.3$).

These relationships between vertebral number and depth cannot be attributed to differences in depth distribution between age-classes of cod. In the southern Gulf, vertebral number did not differ between ages or year-classes ($P = 0.49$) (also see analyses in Swain et al. 2001), and the effect of depth on vertebral number remained positive and highly significant ($b = 0.00489$, SE = 0.00077, $P < 0.0001$) when age was included as a factor in the analysis. Vertebral number differed ($P = 0.0002$) among year-classes on the Scotian Shelf, but the effect of depth and its interaction with stock remained significant ($P = 0.01$ in both cases) when year-class was included as a factor in the analysis. The differences between stocks were unchanged when year-class was included in the analysis, with the strongest increase in vertebral number with depth in the 4Vn stock, followed by the 4Vs stock component.

Mean vertebral number tended to be lowest at intermediate fish lengths (near 35 cm) in the 4T stock (Fig. 4*a*). This effect was weak, only approaching significance ($P = 0.078$) for the GAM fit shown in Fig. 4*a*. The strong tendency for mean vertebral number to increase with depth in the southern Gulf could not be attributed to confounding between fish length and depth. The effect of depth remained highly signif-

Fig. 3. Relationships between vertebral number and depth in Atlantic cod collected from (*a*) the southern Gulf of St. Lawrence and (*b–f*) various regions of the Scotian Shelf. Circles show data grouped by depth. Circle size is proportional to sample size (maximum = 233, same scale for all panels). Vertical lines show ±1 SE. Regression lines are for the ungrouped data. Regions, sample sizes, and significance levels: (*a*) 4T, $N = 843$, $P < 0.0001$; (*b*) 4Vn, $N = 138$, $P = 0.0013$; (*c*) 4Vs, $N = 154$, $P = 0.018$; (*d*) 4W, $N = 228$, $P = 0.32$; (*e*) $4X_{off}$, $N = 146$, $P = 0.41$; (*f*) $4X_{bf}$, $N = 243$, $P = 0.17$.

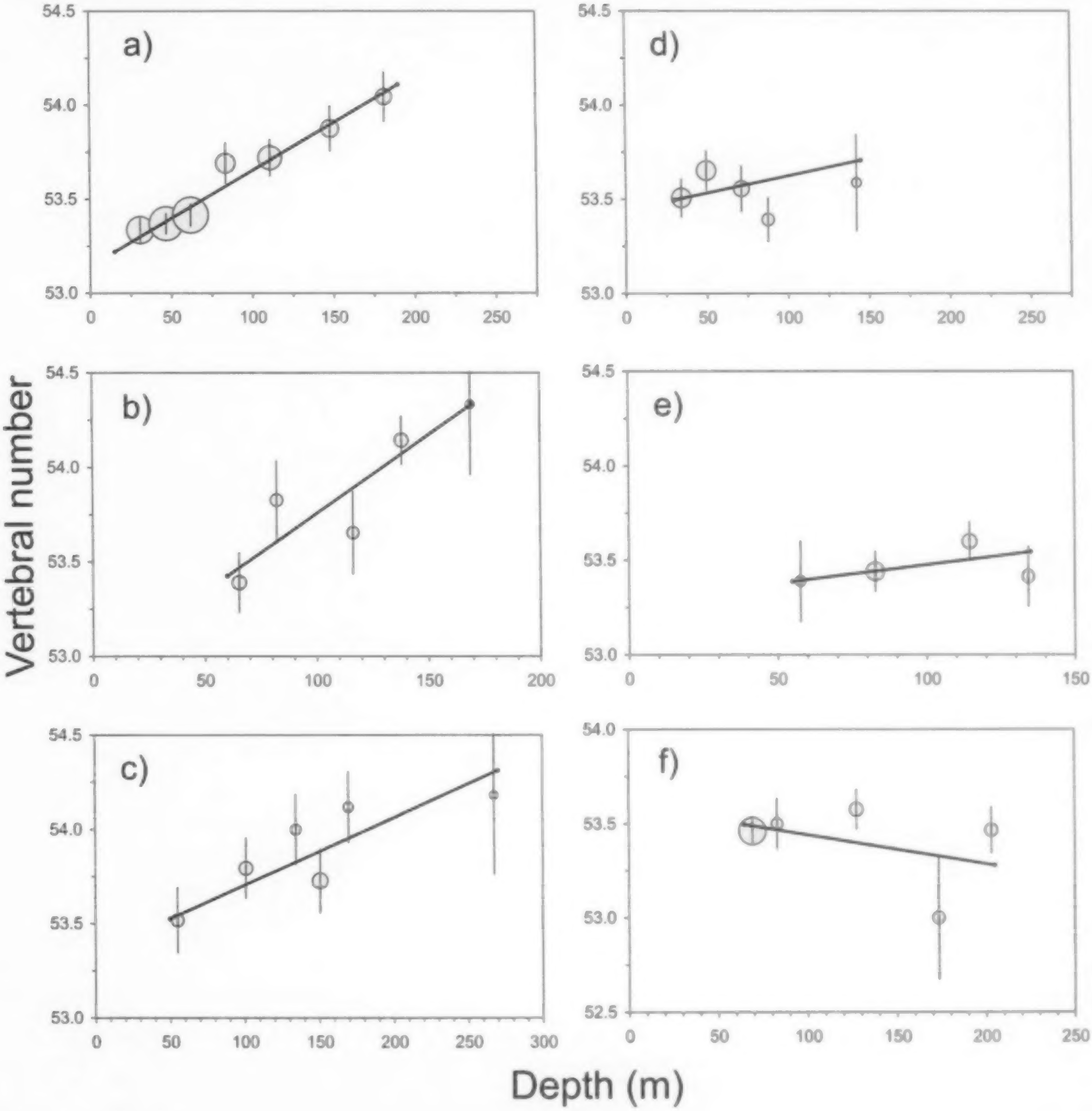

icant ($b = 0.00505$, $P < 0.0001$) in the GAM that included a nonparametric term accounting for the nonlinear relationship between vertebral number and fish length.

In contrast with the weak relationship with fish length, vertebral number was strongly related to relative or "standardized" length within age-classes in the 4T stock, with the larger fish at age having higher vertebral counts ($P < 0.0001$) (Fig. 4*b*). Neither the slope nor the intercept of this relationship differed between age-classes ($P = 0.17$ and $P = 0.59$, respectively). Fish occupying the greatest depths in 4T tended to be large for their age, although length at age also tended to be large at the shallowest depths (Fig. 5). The increase in mean vertebral number with depth could not be attributed to confounding between depth and size at age. Both

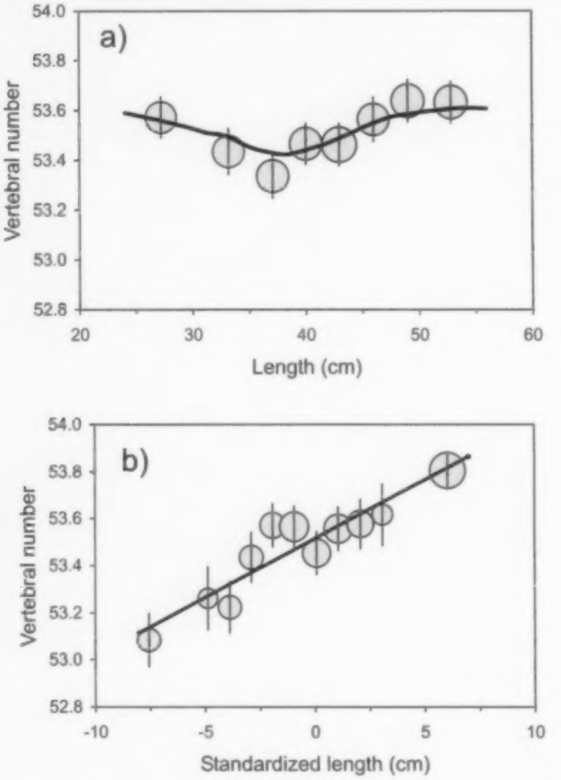

Fig. 4. Relationship between vertebral number and (*a*) length or (*b*) standardized length of Atlantic cod in the southern Gulf of St. Lawrence. Standardized length is the length of a fish of age *i* minus the stratified mean length at age *i*. Circles show data grouped by length or standardized length. Circle size is proportional to sample size (maximum = 139). Vertical lines show ±1 SE. Regression lines are for the ungrouped data: LOESS smooth (Fig. 4*a*) and linear regression (Fig. 4*b*).

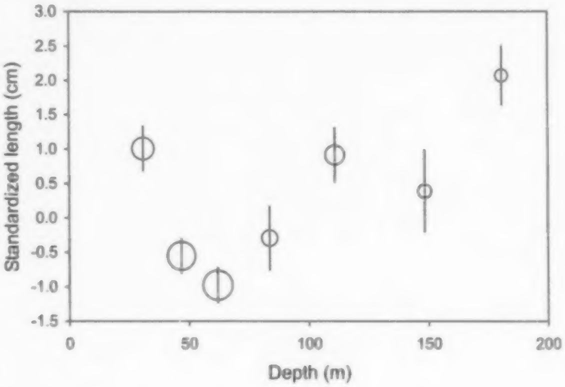

Fig. 5. Relationship between standardized length of Atlantic cod and depth in the southern Gulf of St. Lawrence. Standardized length is the length of a fish of age *i* minus the stratified mean length at age *i*. Circles show data grouped by depth. Circle size is proportional to sample size (maximum = 229). Vertical lines show ±1 SE.

the effects of depth and size at age remained positive and highly significant ($P < 0.0001$) in multiple regression models including both explanatory variables (depth: $b = 0.00436$, SE = 0.00076; standardized length: $b = 0.0475$, SE = 0.0082).

Vertebral number also tended to be lowest at intermediate lengths in the Scotian Shelf stocks ($P = 0.02$). Again, the relationship between vertebral number and depth could not be attributed to confounding with length. The effect of depth and its interaction with stock remained highly significant ($P = 0.013$ and $P = 0.0021$, respectively) in models that included a smooth (LOESS) term for length. Again, mean vertebral number increased most strongly with depth in the 4Vn stock ($b = 0.0138$, $P = 0.005$), followed by the 4Vs stock ($b = 0.00617$, $P = 0.029$).

Vertebral number also tended to increase with standardized length (i.e., relative length within age-classes) in the Scotian Shelf stocks ($P < 0.01$). The slope of this relationship did not differ among age-classes ($P = 0.17$) but did differ at a marginal level of significance among stocks ($P = 0.06$). We tested whether the effect of depth on vertebral number could be attributed to confounding between depth and standardized length in the Scotian Shelf stocks using a model with stock and age as class variables and depth and standardized length as covariates, allowing for heterogeneous slopes among stocks for both of the covariates. Effects of both covariates remained significant (depth: $P = 0.023$; standardized length: $P = 0.0025$). The slope of the depth effect again differed among stocks ($P = 0.046$), with the effect mostly strongly positive in the 4Vn stock.

Discussion

Vertebral number of Atlantic cod was strongly associated with their depth of capture during the summer feeding season on the Magdalen Shallows and northeastern Scotian Shelf but not on the southwestern Scotian Shelf. On the Magdalen Shallows, where sampling was the most extensive, mean vertebral number increased steadily as depth increased from 25 m to over 175 m. How can this striking pattern be explained?

The possibility that this pattern reflects environmentally induced variation seems unlikely. Vertebral number is fixed early in ontogeny, near or before hatching in most fishes (Lindsey 1988). Thus, direct environmental influences on vertebral number of cod will occur during the pelagic egg and larval stages. The pattern reported here could be environmentally induced if adult cod occupying different depth zones were produced from eggs and larvae developing in those different zones (and predictable differences in temperature or some other environmental factor occurred between those zones). However, this does not appear to be the case. Adults occupying a particular region of the summer feeding grounds are not derived from eggs and larvae that developed in that region. Instead, early life history stages are usually concentrated in restricted nursery areas, with adult distributions spreading out from these areas. For example, in the southern Gulf population, the distribution of 1-year-old juvenile cod is restricted to shallow inshore areas (Chouinard et al. 1991). At the older ages sampled in this study (2–13 years of age, 94% 3 years and older), distribution spreads out from these shallow nursery areas into deeper waters of the Magdalen Shallows (e.g., Swain 1993). These distributions are reestablished each year on the summer feeding grounds, after adult cod return to the southern Gulf in spring from their overwintering grounds in the Cabot Strait area. Thus, the differences in vertebral number between adult cod occupying different depth zones on the Magdalen Shallows in September cannot result from an effect of environmental differences between those depth zones on the development of eggs or larvae. These differences could be environmentally induced only if the depth preferences of adult cod were somehow related to the environmental conditions that they had experienced elsewhere as eggs and larvae.

Løken et al. (1994) also reported depth-dependent patterns in the vertebral number of cod off Norway. Recently settled (0 group) juveniles caught in shallow water had fewer vertebrae than those caught in deeper water. Similarly, mean vertebral number of older 1+ cod increased with depth in some areas off Norway. They attributed these patterns to differences in vertebral number between coastal cod stocks and the Northeast Arctic cod stock. Coastal cod, derived from juveniles settling in shallow water, have lower mean vertebral counts than Northeast Arctic cod, derived from juveniles settling in deep water. Common garden experiments revealed a genetic basis to this difference in vertebral number between coastal and Northeast Arctic cod (Løken and Pedersen 1996).

Can the clines in vertebral number with depth observed in this study be likewise attributed to mixing between stocks having different mean vertebral numbers? Mean vertebral number is higher in the northern Gulf of St. Lawrence cod stock than in the southern Gulf stock (Table 1). Cod in the northern Gulf stock also appear to occupy deeper water during the summer feeding season than do cod in the southern Gulf stock (Swain et al. 1998; Castonguay et al. 1999). Perhaps the cline in vertebral number with depth on the Magdalen Shallows reflects mixing between these two stocks, with southern Gulf cod dominating aggregations in shallow water and northern Gulf cod dominating those in deeper water. However, the close similarity between the mean vertebral number of cod on the Magdalen Shallows in September 1995 (53.45) and that of spawning aggregations of southern Gulf cod in the spring of 1996 (53.43; for details, see Swain et al. 2001) argues against the presence of substantial numbers of northern Gulf cod on the Magdalen Shallows in September 1995. On the other hand, because 85% of the cod on the Magdalen Shallows in September 1995 occurred at depths under 75 m, this explanation would require only that 10–15% of the cod on the Magdalen Shallows were of northern Gulf origin. It would also imply that northern Gulf cod penetrate surprisingly deeply onto the Magdalen Shallows in summer, some occurring at depths of 50 m and less. A difficulty with this explanation is that the extremes of the cline in vertebral number with depth are beyond the mean counts in each of the two populations. The mean vertebral number in the deepest waters is greater than the mean in the northern Gulf population (53.82 in spring 1996), while that in the shallowest waters is lower than the mean in the southern Gulf population (53.43). This would imply clines in vertebral number with depth within the two populations even if they mix in depth-dependent proportions on the Magdalen Shallows.

It is also difficult to explain the cline in vertebral number with depth in the 4Vn area in terms of stock mixing. Most of the neighbouring stocks have high mean vertebral numbers, similar to the mean for the resident 4Vn stock (Table 1). The exception is the 4T stock. Low mean vertebral counts in the fall and early spring (53.46–53.55) suggest the presence of 4T fish in the 4Vn area at these times of year (Swain et al. 2001). However, the high mean vertebral counts of spawning aggregations in the 4Vn area later in the spring (53.85) and in July (53.87) suggest that few 4T fish are present in the area at these times. Finally, the extreme vertebral counts in the shallowest and deepest waters, more extreme than the means in the spring-spawning aggregations of either the 4Vn or 4T population, again make it difficult to account for the cline in vertebral number with depth in terms of stock mixing.

Otolith chemical composition differs between northern and southern Gulf cod (Campana et al. 2000). Cod caught in deep water along the southern slope of the Laurentian Channel in September 1995 appeared to be predominantly northern Gulf cod based on the chemical composition of their otoliths (Campana et al. 2000). This interpretation supports the idea that depth-dependent mixing between the northern and southern Gulf cod stocks contributes to the cline in vertebral number with depth on the Magdalen Shallows. However, otolith elemental composition is an environmentally induced trait. The trace elements incorporated into otoliths reflect the physical and chemical characteristics of the water occupied by the fish. An alternative interpretation of these results is that cod occupying the deep water along the southern slope of the Laurentian Channel belong to the southern Gulf stock but, because of their atypical depth distribution, have an otolith elemental "fingerprint" more like that of the northern Gulf stock (which also tends to be distributed in deep water during the summer feeding season) than like that of the bulk of the southern Gulf stock (which is distributed in shallower water during the feeding season).

The alternative to stock mixing is that these patterns reflect an association between depth and vertebral number within populations. One possibility is that these patterns result from selection, with different vertebral numbers favoured at different depths. Most evidence for selection acting directly on the vertebral phenotype of fish is for the larval stage. During a narrow window of larval lengths, burst swimming performance of larvae and their susceptability to predation are strongly related to vertebral phenotype in *G. aculeatus* and peamouth (*Mylocheilus caurinus*) (Swain and Lindsey 1984; Swain 1988, 1992*a*, 1992*b*). While survival of larvae appears to be unrelated to vertebral phenotype outside of this window of larval lengths, it is possible that selection again acts on vertebral number during later life history stages. For example, Billerbeck et al. (1997) reported selection for vertebral number in adult Atlantic silverside (*Menidia menidia*), although in this case, selection appeared to be indirect, reflecting size-selective mortality. Likewise, Reimchen and Nelson (1987) reported length-dependent changes in vertebral number in juvenile and adult *G. aculeatus* that could result from selection. Based on hydrodynamic considerations, Spouge and Larkin (1979) suggested

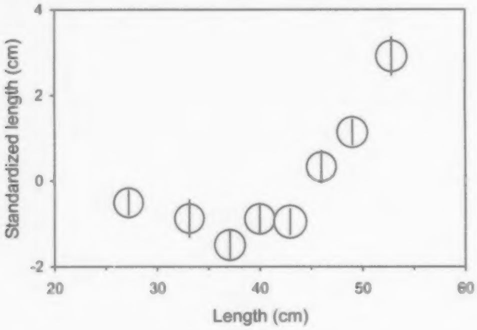

Fig. 6. Relationship between length and standardized length of Atlantic cod in the southern Gulf of St. Lawrence. Standardized length is the length of a fish of age *i* minus the stratified mean length at age *i*. Circles show data grouped by length (same grouping as in Fig. 4*a*). Circle size is proportional to sample size (maximum = 118). Vertical lines show ±1 SE.

an effect of vertebral number on swimming performance of fish over a wide range of lengths that included adult sizes. Properties such as water density and viscosity entered their model, and many of the variables in their model were temperature dependent, suggesting that the optimum number of vertebrae may depend on environmental conditions. Jordan's rule also suggests a connection between temperature and the optimal number of vertebrae. Temperature and depth are closely related, but the depth-dependent patterns in vertebral number reported here cannot be attributed to an effect of temperature. Temperature and vertebral number show different relationships with depth in these areas. Mean vertebral number increased steadily with depth, whereas temperature shows a nonmonotonic relationship with depth, with the coldest temperatures at intermediate depths (about 50–100 m; see fig. 7 in Swain 1993). Similarly, these patterns cannot be attributed to an effect of water viscosity on the optimal vertebral number. The effect of pressure on viscosity is negligible (Defant 1961), and changes in water viscosity over our study area would follow the gradients in temperature, not depth. Thus, while we cannot exclude the possibility of depth-dependent selection for vertebral number, we are unable to suggest why selection would favour different vertebral numbers at different depths.

Another possibility is that there is a link between vertebral number and habitat selection within populations. Associations between morphological and behavioural characters, including habitat selection, have been demonstrated in other cases. For example, behavoural differences related to vulnerability to predation have been reported between lateral plate phenotypes of *G. aculeatus* (Moodie et al. 1973) and pelvic phenotypes of brook stickleback (*Culaea inconstans*) (Reist 1980). Reimchen (1980) reported an association between pelvic spine phenotype and habitat selection in a population of *G. aculeatus*. He found that juveniles with pelvic spines were more common in limnetic habitats, while those without spines were more common in littoral regions, and suggested that this pattern reflected differential movement of the phenotypes after hatching. In this case, the association between morphology and habitat selection appeared to be adaptive, since spines appeared to be advantageous in avoiding the vertebrate predation prevalent in limnetic areas but disadvantageous in avoiding the invertebrate predation prevalent in littoral areas. In our case, the adaptive significance of greater vertebral number at greater depths is as yet obscure.

Pleomerism, the widespread tendency for mean vertebral number to be greater in populations with greater maximum body length, suggests a functional connection between body length and the optimal number of vertebrae (Lindsey 1975). As a consequence of this connection, mean vertebral number in a cohort would be expected to decline with length until the mean number functionally matches the body size and then increase with further increases in length as selection favours progressively higher vertebral numbers to match the increasing body size. This pattern between mean vertebral number and length has been reported in *M. caurinus* fry (Swain 1988) and in *G. aculeatus* at both the larval (Swain 1992*a*) and older stages (Reimchen and Nelson 1987). We observed a similar (although weak) tendency for mean vertebral number to decline to a minimum at intermediate lengths of juvenile and adult cod. Length-dependent effects of vertebral phenotype on burst swimming performance and ability to escape predators provide an explanation for the pattern between vertebral number and length observed at the larval stages (Swain 1988, 1992*a*, 1992*b*). The factors causing this pattern in juveniles and adults remain unclear. In this study, this pattern can be attributed to confounding between length and standardized length rather than to a functional connection between vertebral number and length at these older life history stages. Mean vertebral number tended to be low in fish with a small standardized length (i.e., fish that were small for their age), and standardized length was lowest at intermediate body lengths in our samples (Fig. 6).

The relationship between vertebral number and standardized length within age-classes was much stronger than the relationship with actual body length. Vertebral number showed a strong tendency to be greater in cod that were large for their age, irrespective of their actual length. That is, vertebral number tended to be relatively high in a 35-cm cod that was 3 years old and large for its age but relatively low in a 35-cm cod that was 5 years old and small for its age. This type of relationship could not be produced by length-dependent selection at juvenile and adult lengths. However, it might be attributed to length-dependent selection at earlier larval stages, like that reported in other larval fishes. Selection at these larval sizes could result in a positive correlation between vertebral number and growth rate, since larvae with faster growth would grow more quickly through the smaller sizes when low vertebral numbers were favoured by selection. Another possibility is that this relationship reflects an association between size at age and environmentally induced variation in vertebral number. For example, individuals produced earlier in the spawning season might be expected to achieve larger sizes by the end of their first growing season than those produced later in the spawning season. A positive correlation between vertebral number and size at age would then occur if temperatures early in the spawning season produced more vertebrae in developing embryos than the temperatures later in the season. These explanations for the positive correlation between vertebral number and length at age in our study would imply that differences in growth rate or size at age established at the larval or early juvenile stage persist throughout life. An alternative explanation for this correlation is that growth rate and vertebral number are genetically correlated in these populations of cod.

In conclusion, vertebral number and habitat selection are closely linked in cod on the Magdalen Shallows and northeastern Scotian Shelf. This could reflect a correlation between vertebral number and habitat preferences between cod populations. In this case, stock mixing is unexpectedly extensive in these areas during the summer feeding season. A correlation between vertebral number and habitat preference within populations is an alternative explanation for this pattern. This correlation could be either environmental or genetic. The latter would indicate unexpected genetic diversity within populations and a high degree of spatial structure to this diversity during the feeding season.

Acknowledgements

We thank Gary Maillet who processed the samples used in this study and made the vertebral counts reported here, Jim Simon who helped in sample collection, and Joel Chassé for discussion. Chris Foote, Don Kramer, and two anonymous reviewers provided helpful comments on the manuscript.

References

Billerbeck, J.M., Ortí, G., and Conover, D.O. 1997. Latitudinal variation in vertebral number has a genetic basis in the Atlantic silverside, *Menidia menidia*. Can. J. Fish. Aquat. Sci. **54**: 1796–1801.

Campana, S.E., Chouinard, G.A., Hanson, J.M., Fréchet, A., and Brattey, J. 2000. Otolith elemental fingerprints as biological tracers of fish stocks. Fish. Res. **46**: 343–357.

Castonguay, M., Rollet, C., Fréchet, A., Gagnon, P., Gilbert, D., and Brêthes, J.-C. 1999. Distribution changes of Atlantic cod (*Gadus morhua*) in the northern Gulf of St. Lawrence in relation to an oceanic cooling. ICES J. Mar. Sci. **56**: 333–344.

Chouinard, G.A., Hanson, J.M., and Nielsen, G.A. 1991. Definition of juvenile areas for the 4T–Vn (January–April) cod stock. CAFSAC Res. Doc. 91/6.

Clark, D.S., and Brown, L.L. 1996. Assessment of cod in Division 4X in 1996. DFO Atl. Fish. Res. Doc. 96/101.

Defant, A. 1961. Physical oceanography. Vol. I. Pergamon, New York.

Gascon, D., Aparicio, M., and Mercille, B. 1990. Estimations du mélange entre les stocks de morue du Nord du Golfe du Saint Laurent (Divisions 3Pn4RS) et les stocks adjacents (2J3KL, 3Ps, et 4TVn [Janvier–Avril]) à partir de résultats de marquage. CAFSAC Res. Doc. 90/61.

Halliday, R.G. 1972. A yield assessment of the eastern Scotian Shelf cod stock complex. Int. Comm. Northwest Atl. Fish. Res. Bull. **9**: 117–124.

Jordan, D.S. 1892. Relations of temperature to vertebrae among fishes. Proc. U.S. Natl. Mus. **14**: 107–120.

Lindsey, C.C. 1975. Pleomerism, the widespread tendency among related fish species for vertebral number to be correlated with maximum body length. J. Fish. Res. Board Can. **32**: 2453–2469.

Lindsey, C.C. 1988. Factors controlling meristic variation. *In* Fish physiology. *Edited by* W.S. Hoar and D.J. Randall. Academic Press, New York. pp. 197–274.

Løken, S., and Pedersen, T. 1996. Effect of parent type and temperature on vertebrae number in juvenile cod, *Gadus morhua* (L.). Sarsia, **80**: 293–298.

Løken, S., Pedersen, T., and Berg, E. 1994. Vertebrae numbers as an indicator for the recruitment mechanism of coastal cod of northern Norway. ICES Mar. Sci. Symp. **198**: 510–519.

Martin, W.R., and Jean, Y. 1964. Winter cod taggings off Cape Breton and on offshore Nova Scotia banks, 1959–62. J. Fish. Res. Board Can. **21**: 215–237.

MathSoft. 1999. S-Plus 2000: guide to statistics. Vol. 1. MathSoft, Inc., Seattle, Wash.

Moodie, G.E.E., McPhail, J.D., and Hagen, D.W. 1973. Experimental demonstration of selective predation on *Gasterosteus aculeatus*. Behaviour, **47**: 95–105.

Reimchen, T.E. 1980. Spine deficiency and polymorphism in a population of *Gasterosteus aculeatus*: an adaptation to predators? Can. J. Zool. **58**: 1232–1244.

Reimchen, T.E., and Nelson, J.S. 1987. Habitat and morphological correlates to vertebral number as shown in a teleost, *Gasterosteus aculeatus*. Copeia, **1987**: 868–874.

Reist, J.D. 1980. Predation upon pelvic phenotypes of brook stickleback, *Culaea inconstans*, by selected invertebrates. Can. J. Zool. **58**: 1253–1258.

Ruzzante, D.E., Taggart, C.T., Lang, S., and Cook, D. 2000. Mixed-stock analysis of Atlantic cod near the Gulf of St. Lawrence based on microsatellite DNA. Ecol. Appl. **10**: 1090–1109.

Spouge, J.L., and Larkin, P.A. 1979. A reason for pleomerism. J. Fish. Res. Board Can. **36**: 255–269.

Swain, D.P. 1987. A problem with the use of meristic characters to estimate developmental stability. Am. Nat. **129**: 761–768.

Swain, D.P. 1988. Evidence for selection of vertebral number of fry in peamouth, *Mylocheilus caurinus*. Can. J. Fish. Aquat. Sci. **45**: 1279–1290.

Swain, D.P. 1992*a*. The functional basis of natural selection for vertebral traits of larvae in the stickleback *Gasterosteus aculeatus*. Evolution, **46**: 987–997.

Swain, D.P. 1992*b*. Selective predation for vertebral phenotype in *Gasterosteus aculeatus*: reversal in the direction of selection at different larval sizes. Evolution, **46**: 998–1013.

Swain, D.P. 1993. Age- and density-dependent bathymetric pattern of Atlantic cod (*Gadus morhua*) in the southern Gulf of St. Lawrence. Can. J. Fish. Aquat. Sci. **50**: 1255–1264.

Swain, D.P., and Lindsey, C.C. 1984. Selective predation for vertebral number of young sticklebacks, *Gasterosteus aculeatus*. Can. J. Fish. Aquat. Sci. **41**: 1231–1233.

Swain, D.P., Chouinard, G.A., Morin, R., and Drinkwater, K.F. 1998. Seasonal variation in the habitat associations of Atlantic cod (*Gadus morhua*) and American plaice (*Hippoglossoides platessoides*) from the southern Gulf of St. Lawrence. Can. J. Fish. Aquat. Sci. **55**: 2548–2561.

Swain, D.P., Frank, K.T., and Maillet, G. 2001. Delineating stocks of Atlantic cod (*Gadus morhua*) in the Gulf of St. Lawrence and Cabot Strait areas using vertebral number. ICES J. Mar. Sci. In press.

The influence of stock structure and environmental conditions on the recruitment process of Baltic cod estimated using a generalized additive model

M. Cardinale and F. Arrhenius

Abstract: The recruitment process and its underlying mechanisms are among the most studied phenomena in fisheries ecology. Traditional models estimate fish recruitment assuming a direct relationship with spawning stock size. However, highly variable environmental conditions, feeding conditions, and other factors can influence and complicate the results of a simple linear regression analysis between stock and recruitment. We used generalized additive models (GAMs) to investigate the influence of environmental conditions and stock structure on the recruitment processes of Baltic cod. The interaction between abiotic factors and old spawners (>5+ years) and eggs produced by old spawners were the most significant explanatory variables. Eggs produced by young spawners have a positive impact on cod recruitment only at high levels of reproductive volume, while old spawners' eggs have the highest positive effect at low levels of reproductive volume. Here we show: (*i*) that the number of Baltic cod recruits is strictly dependent on the age structure of the population; (*ii*) that interactions between biotic and abiotic factors are crucial in explaining recruitment variability; and (*iii*) that GAMs are a powerful technique for defining and quantifying the intricate multidimensional relationship between biotic and abiotic variables involved in recruitment processes.

Résumé : Le recrutement et ses mécanismes sous-jacents sont parmi les phénomènes les plus étudiés en écologie des pêches. Les modèles traditionnels estiment le recrutement des poissons en supposant une relation directe avec le stock des reproducteurs. Cependant, les conditions très variables du milieu, les conditions alimentaires et d'autres facteurs peuvent intervenir et complexifier les résultats d'un simple analyse de régression linéaire entre le stock et le recrutement. Nous avons utilisé des modèles additifs généralisés (GAM) pour étudier les effets des conditions environnementales et de la structure du stock des reproducteurs sur le processus de recrutement chez la Morue franche de la Baltique. Les relations entre les facteurs abiotiques et les recruteurs âgés (>5+ ans) et les oeufs produits par ceux-ci se sont révélés les variables explicatives les plus significatives. Les oeufs produits par les jeunes reproducteurs n'ont d'impact positif sur le recrutement que lorsque le volume de reproduction est élevé; en revanche, les oeufs provenant des reproducteurs plus âgés ont une influence positive maximale lorsque le volume de reproduction est limité. Il est donc démontré (*i*) que le nombre de recrues dans cette population de morues dépend de la structure en âges de la population, (*ii*) que les interactions entre les facteurs biotiques et abiotiques jouent un rôle crucial dans la variation du recrutement et (*iii*) que les GAM sont une technique puissante pour définir et quantifier les relations complexes et multidimensionnelles entre les variables biotiques et abiotiques impliquées dans les processus de recrutement.

[Traduit par la Rédaction]

Introduction

An important stage in the assessment of fish resources and their management is the relationship between stock and recruitment (SRR). Different models have been used to describe the relationship between parental-stock size (fecundity, biomass, or abundance) and relative recruitment output (for a review see Hilborn and Walters 1992). Although these models (i.e., Beverton and Holt, Ricker function) provide important insights into SRR dynamics, they may not include key factors or account for specific situations (e.g., Fogarty 1993). Specific factors, such as age–size structure and maternal effects, may contribute significantly to explaining the observed recruitment variability in fish stocks (Trippel et al. 1997; Marshall et al. 1998; Cardinale and Arrhenius 2000). Nevertheless, SRR is often also complicated by highly variable environmental conditions (i.e., salinity, temperature, oxygen level, and others), feeding conditions, or other factors that can influence and mislead the results of a simple-regression analysis between stock abundance and recruitment (Sparholt 1996; Daskalov 1999). Therefore, it is considered crucial in fisheries ecology to isolate those factors behind spawning biomass that could explain the observed variability in the SRR and to understand the dynamics of the interaction between biotic and abiotic factors and their effects on recruitment.

Owing to recruitment failures in recent years, the SRR relationship in Baltic cod (*Gadus morhua*) is currently the

Received April 13, 2000. Accepted October 19, 2000. Published on the NRC Research Press web site on December 20, 2000. J15715

M. Cardinale[1] and F. Arrhenius. Institute of Marine Research, National Board of Fisheries, P.O. Box 4, SE-453 21 Lysekil, Sweden.

[1] Corresponding author (e-mail: Massimiliano.Cardinale@fisheriverket.se).

object of much attention (Vallin et al. 1999; Vallin and Nissling 2000). Generalized linear (Sparholt 1996) and nonlinear models (Solari et al. 1997) have been used previously to describe the recruitment process, assuming that the spawning biomass is proportional to the reproductive potential of the stock. However, different authors have recently challenged this paradigm (Marshall et al. 1998; Marteinsdottir and Thorarinsson 1998; Cardinale and Arrhenius 2000). The recent overexploitation of marine fish populations typically results in the loss of the large members of the stocks (Trippel et al. 1997). Depletion of these large individuals may not only affect the quantitative reproductive potential of the population but, if younger fish exhibit poorer gamete quality than older fish, the qualitative reproductive output of the stock may also be seriously depleted (Trippel et al. 1997). Moreover, the importance of environmental factors (e.g., salinity, temperature, and oxygen) in explaining the recruitment variability of fish stocks has recently been recognised (e.g., Daskalov 1999). Recruitment success in Baltic cod is also affected by fluctuations in salinity, temperature, and oxygen at depths where cod eggs are deposited (Vallin et al. 1999). These abiotic factors (temperature, salinity, and oxygen) have been included in a generalized linear model (GLM) with logarithmically transformed data to estimate Baltic cod recruitment (Sparholt 1996). In addition, stock structure (i.e., age–length) has recently been shown to influence cod-stock recruitment, through a positive relationship between female age and egg and larva viability (e.g., Cardinale and Arrhenius 2000).

Relationships between a dependent variable and two or more factors are often nonlinear. Generally, the response to environmental factors is unlikely to be monotonic, linear, or parametric (Maravelias 1997; Maravelias and Reid 1997). Therefore, traditional linear models are often inadequate for detecting and quantifying any environmental effects and their complex interaction with biological factors (Maravelias 1999). Generalized additive models (GAMs) offer an attractive possibility for overcoming statistical problems linked to the normality and linearity assumptions of GLMs (Hastie and Tibshirani 1990; Swartzman et al. 1992). GAMs extend the power of any conventional regression technique by fitting nonparametric functions to estimate relationships between the response and the predictors. Therefore, GAMs are not tied to any particular functional relationship (i.e., linearity) or to any statistical distribution of the data (i.e., normality). The underlying probability distribution for the data can be any distribution from the exponential family, including the normal, Poisson, and binomial distributions (Swartzman et al. 1992). In GAMs, dependent variables are assumed to be affected by the predictors through additive unspecified smooth functions.

In this study, we used GAMs to estimate and quantify the effect of age structure and environmental conditions on the recruitment processes of Baltic cod. Does the age structure of the population constitute a key factor in explaining the recruitment variability of Baltic cod? Is the interaction between the age structure of the population and spawning conditions also important in explaining the variability in Baltic cod recruitment? The aim of this study was to test these hypotheses and to discuss the results in the broader context of the SRR.

Materials and methods

Time series

We analysed fishery-dependent and independent data from the Baltic cod (*Gadus morhua*) stock (Fig. 1) from the ICES (International Council on the Exploration of the Sea) annual stock assessment database calculated with a virtual population analysis (VPA) (Anonymous 1998). Catch-at-age data from commercial landings were tuned with a survey index of abundance estimated from trawl surveys. Natural mortality was set at 0.2 for all age-classes. For more details on the mathematical calculations of a VPA-type model, see Hilborn and Walters (1992). Numbers of cod are given for each age-class using the VPA (Anonymous 1998). Cod recruitment is considered to be the number of 2-year cod at the beginning of the year (Anonymous 1998).

To assess the contribution to Baltic cod recruitment of different age-classes, we calculated the potential egg production for each age-class. The total egg production was based on stock numbers, proportion of mature individuals, sex ratios, and weight at age in the stock (Anonymous 1998). For proportion of mature individuals and sex ratios, the ICES Working Group assumed that the values estimated during 1980–1984 were applicable to all previous years, and thus these values were used in this study (Anonymous 1998). Relative fecundity estimates (number of eggs × weight of fish (g)) were available from Kraus et al. (2000). The value used in this study (630 $\text{eggs}\cdot\text{g}^{-1}$) was the mean of the different yearly estimations relative to the period between 1978 and 1996.

The time series of reproductive volume (RV) are from MacKenzie et al. (2000). RV is the volume of water suitable for the successful development of the early life stages of Baltic cod. It is defined by threshold levels in temperature (>1.5°C), salinity (>11‰), and oxygen (>2 $\text{mL}\cdot\text{L}^{-1}$). Below these thresholds, development of cod eggs ceases before hatch (Nissling and Westin 1991). The hydrographic data set consists of measurements from 36 different standard stations. The survey data were used to calculate the thickness of the Baltic cod spawning layer, i.e., the vertical extension of the water body considered suitable for successful egg and larval development (as defined below). Horizontal fields of the thickness of the reproductive layer were constructed by objective analysis, which was based on a standard statistical approach, the Gauss–Markov theorem, that gives an expression for the last square error linear estimate of the variables. Thus, at every single point, an estimate can be given that depends, linearly, on the total number of measurements, i.e., a weighted sum of all observations. Therefore, the reproductive volume is calculated by a simple integration between two horizontal planes, whereby the upper plane is usually given by the 11‰ isohaline and the lower one by the bottom of the layer below which the oxygen content declines to 2 $\text{mL}\cdot\text{L}^{-1}$. Data are available for February, March, April, May, August, and October for each of the deep basins in the Baltic Sea, except the central Gotland Basin, for which estimates are available as the mean for the periods February–May, May, and August (MacKenzie et al. 2000). As a delay in cod peak spawning time was observed in the Bornholm Basin during recent years, RV was adjusted to account for these changes. Therefore, mean values for April–June (1967–1989), May–July (1990–1992), and June–August (1993–1998) were used. RV is the adjusted reproductive volume in cubic kilometres calculated for the entire Baltic Sea. For further details on RV calculation, see MacKenzie et al. (2000). The data series used are presented in Table 1.

Data analysis

A nonparametric GAM was used to examine the effect of different variables on Baltic cod recruitment. In GAMs, scatterplot smooths replace least squares fits used in regression analysis (Hastie and Tibshirani 1990). In this study, we used the gamma distribution, in which the data variance is proportional to the square of the mean.

Fig. 1. Map showing the sampling stations (●) for cod (*Gadus morhua*) in the Baltic Sea.

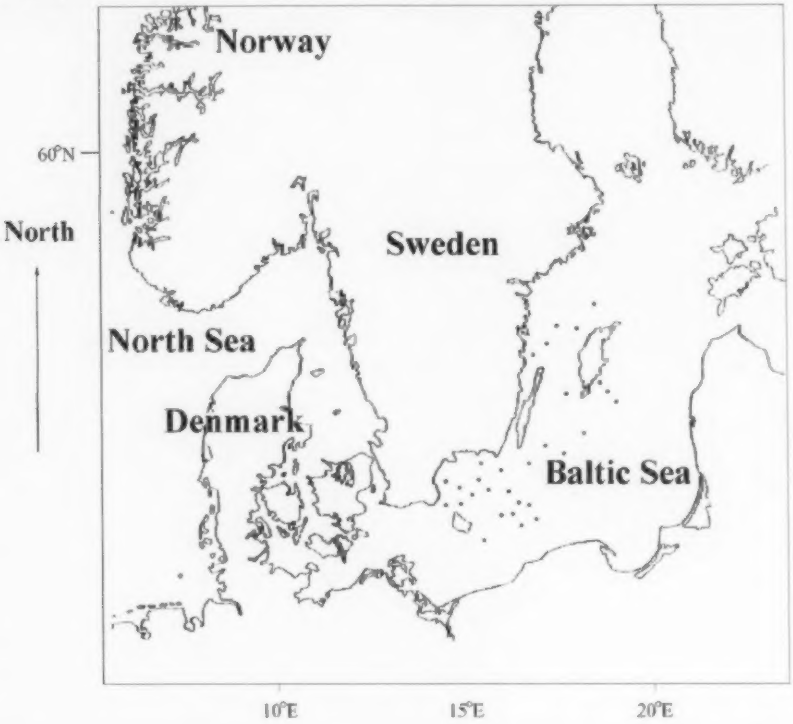

The gamma distribution was chosen, because when testing different distributions, we found that the gamma distribution gave a better fit with the data with the minimum residual deviance in the models. Kolmogorov–Smirnov and χ^2 tests (with degrees of freedom adjusted) were used to test for different distributions of cod recruitment showing that the gamma distribution was appropriate (Kolmogorov–Smirnov test: $d_{\max} = 0.078$, $p > 0.05$; $\chi^2 = 3$, $p > 0.05$; Fig. 2).

Baltic cod recruitment (dependent variable) was expressed as a sum of the smooth functions of the predictors. The hypothesised predictors were number of eggs produced by age-classes 2, 3, and 4 (young spawners (YS)), number of eggs produced by age-class 5+ (old spawners (OS)), RV, and their first-order interactions. These classification categories were based strictly on age, as in Cardinale and Arrhenius (2000). Individuals of Baltic cod older than 5 years are usually assumed to have spawned at least for a second time (Vallin and Nissling 2000). We used cubic B splines (s) to estimate the smoother (Hastie and Tibshirani 1990). The following two-step procedure was applied in analysing the data. First, the functional relationship between the response was explored using nonparametric GAM. In this way, the form of the function was found empirically, according to data without prior assumptions. The backward stepwise elimination was used to select significant predictors in the analysis. Second, model fit and parsimony were evaluated through analysis of deviance, using Akaike information criteria (AIC; Chambers and Hastie 1992). The AIC statistic accounts simultaneously for the degrees of freedom used and the goodness of the fit, whereas more parsimonious models have a lower AIC statistic. Confidence intervals and significance levels for the predictors were estimated using permutation tests and bootstrap resampling (1000 samples; percentile method) (the techniques are described in detail in Swartzman et al. 1992). Residuals were analysed to test for departure from the model assumptions or other anomalies in the data or in the model fit, using both analytical (Kitanidis 1997) and graphical (Cleveland 1993) methods. The Q_1 statistic was used to verify the general unbiased conditions of the model. Q_1 is defined as:

$$Q_1 = \frac{1}{n-1}\sum^{n}\varepsilon_k$$

where ε_k is the orthonormal residual and n is the number of observations. The null hypothesis is that Q_1 is normally distributed with mean 0 and variance $1/(n - 1)$. Therefore, we reject the model, if

$$|Q_1| > \frac{2}{\sqrt{n-1}}$$

Further, we tested whether the residuals were normally distributed using the Shapiro–Wilk test and that the residuals were not autocorrelated using the Durbin–Watson test. Residuals were also plotted against the predicted values, to test for their homogeneity. Statistical analyses were performed with the S-PLUS software (version 2000; 1999 Statistical Sciences, Seattle, Wash.). The level of significance was set at 95% for the statistical tests used in this study.

Results

Results of the significance values of all the predictors initially included in the model are presented in Table 2. The final GAM included the following variables:

$$\text{recruitment} = s(\text{RV}) + s(\text{OS}) + s(\text{YS}\cdot\text{RV}) + s(\text{OS}\cdot\text{RV})$$

Table 1. Data series used in this study.

Year	Recruitment (10^6 individuals)	Reproductive volume (km^3)	Young spawners (10^{12} eggs)	Old spawners (10^{12} eggs)
1968	320	440	22.26	37.42
1969	272	85	28.82	52.18
1970	217	525	23.55	60.69
1971	242	325	22.99	57.93
1972	292	260	18.48	56.24
1973	401	100	15.51	55.06
1974	473	540	17.94	55.26
1975	281	580	21.08	55.72
1976	283	280	30.03	63.63
1977	465	125	35.14	88.00
1978	788	400	20.70	115.60
1979	570	61	22.73	104.71
1980	403	82	38.10	102.93
1981	654	230	58.95	159.17
1982	651	162	40.85	233.68
1983	433	170	31.69	219.75
1984	280	100	50.60	197.61
1985	228	99	55.33	188.99
1986	244	100	35.60	201.56
1987	330	80	23.45	182.39
1988	203	90	18.16	149.24
1989	118	180	21.95	77.90
1990	116	158	31.23	94.01
1991	79	235	19.60	95.74
1992	130	440	13.01	67.24
1993	176	116	10.93	44.66
1994	129	154	10.33	28.41
1995	151	200	15.42	32.21
1996	154	250	18.63	45.57

Fig. 2. Frequency distribution of the variable recruitment. The line indicates the expected gamma distribution.

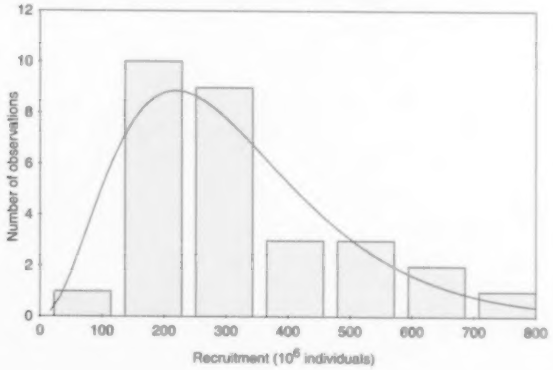

Table 2. Significance values (p levels) for the generalized additive model predictors.

Predictor	p	Variance explained (%)
Young spawners (YS)	>0.05	
Old spawners (OS)	0.01	29
Reproductive volume (RV)	0.04	12
YS–RV interaction	0.03	19
OS–RV interaction	0.01	40
YS–OS interaction	>0.05	

Note: The level of significance was set at 0.05.

The effect of the significant predictors and their interactions on recruitment is shown on the y-axis for different values of the predictor (x-axis) (Figs. 3 and 5). The 0 line indicates mean recruitment estimated by the model, while the y-axis is a relative scale where the effect of different values of the predictors on the response variable (i.e., recruitment) is shown. Thus, negative values on the y-axis indicate that, at the levels of the predictor (x-axis), the model estimates recruitment that is lower than the mean, while the opposite holds for positive values on the y-axis. The interaction between OS and RV and OS are the most significant explanatory variables (Figs. 3 and 4), explaining 40 and 29% of the variance, respectively. The effect of YS and of the interaction between YS and OS on recruitment (10^6 individuals) is not significant (Table 2) and, therefore, was excluded from the final model. Importantly, when the reproductive contribution from OS is at the lowest level, recruitment is strongly depleted, while recruitment was greatest at the highest OS levels (Fig. 4). Concerning the interaction between OS and RV, the greatest effect occurs for low values of RV (<100 km^3) for OS. At larger abundances of both OS and

Fig. 3. Generalized additive model derived effects of the interaction term between the number of potential eggs produced by old spawners (OS) and reproductive volume (RV) on the recruitment (10^6 individuals) of Baltic cod.

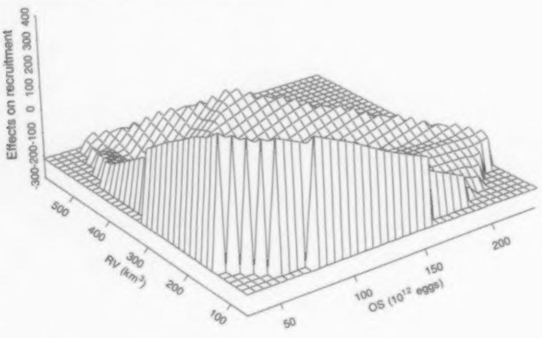

Fig. 4. Generalized additive model derived effects of the number of potential eggs produced by old spawners (OS) on the recruitment (10^6 individuals) of Baltic cod. The broken line and open circles denote mean values; the solid lines denote the 95% confidence intervals.

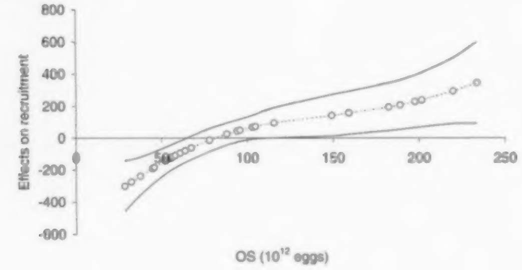

Fig. 5. Generalized additive model derived effects of the interaction between the number of potential eggs produced by young spawners (YS) and the reproductive volume (RV) on the recruitment (10^6 individuals) of Baltic cod.

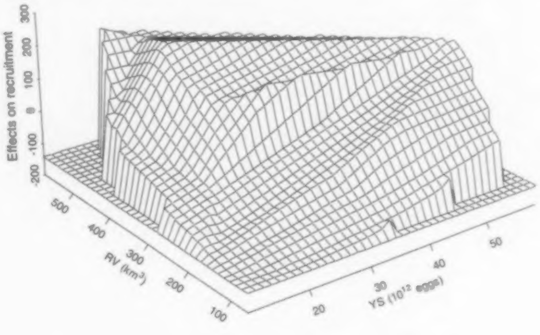

Fig. 6. Generalized additive model derived effects of the reproductive volume (RV) on the recruitment (10^6 individuals) of Baltic cod. The broken line and open circles denote mean values; the solid lines denote the 95% confidence intervals.

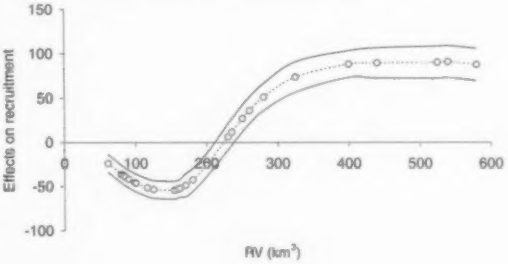

RV, the effect on recruitment is also positive but to a lesser extent. The contributions from the interaction between YS and RV and from RV are also important to Baltic cod recruitment, explaining 19 and 12% of the explained model variance, respectively, (Figs. 5 and 6). In contrast, with regard to the interaction between YS and RV, the effect on recruitment is positive only at values of RV larger than 300 km^3, irrespective of YS values (Fig. 5). An increase in the variation at larger values of both OS (Fig. 4) and RV (Fig. 6) was probably due to sparse data.

The final model showed good accuracy in predicting recruitment of Baltic cod (Fig. 7), and the successive analysis of the residuals confirmed the validity of the model. Q_1 values were not significantly different from 0 ($Q_1 = 0.00035$; $n = 30$; $p < 0.001$). The Shapiro–Wilk ($n = 30$; $p = 0.21$) and Durbin–Watson ($n = 30$; $p = 0.34$) tests were not significant. The residuals plot did not show evidence of strong violation of the model assumptions (Fig. 8).

Discussion

Recent studies have shown strong evidence of a maternal effect on the quality of offspring in fish (e.g., Kjesbu et al. 1996; Marshall et al. 1998; Marteinsdottir and Thorarinsson 1998). The age of a parental fish not only influences the size of eggs and larvae, but also has important effects on the chemical composition of ovaries and eggs, egg metabolism and fertilisation, and embryonic, larval, and juvenile survival (for a review see Kamler 1992). That larvae derived from larger eggs are larger than larvae derived from smaller eggs is a well-known phenomenon (Kamler 1992) and many recent studies have supported this theory (e.g., Kjesbu et al. 1996; Trippel 1998). Predation, which is recognised as one of the major causes of larval mortality in fish (Mills 1982), operates in a size-dependent way, with smaller larvae suffering higher levels of mortality than larger larvae (Miller et al. 1988). In addition, the adaptive significance of larval size in Atlantic cod is also related to the broader feeding spectra of larger larvae compared with smaller individuals (e.g., Knutsen and Tilseth 1985). It has also been argued that, in general, larger fish larvae may survive better than small larvae, owing to their higher growth rates (Moodie et al. 1989) and larger energy reserves (Blaxter and Hempel 1963). In contrast, many authors found no effect of egg size on viability of the progeny of different fish species (Kamler 1992). Egg size was not found to be related to female body size in North Sea cod (Oosthuizen and Daan 1974), but an effect of body size on egg size can often result from parental age (Kamler 1992). However, recently, in Baltic cod, it was shown that egg size does not affect hatching success (Nissling et al. 1999) but that larval viability and egg size are positively

Fig. 7. The observed against the predicted numbers of recruits of Baltic cod, estimated by the final generalized additive model: recruitment = *s*(reproductive volume) + *s*(old spawners) + *s*(young spawners × reproductive volume) + *s*(old spawners × reproductive volume).

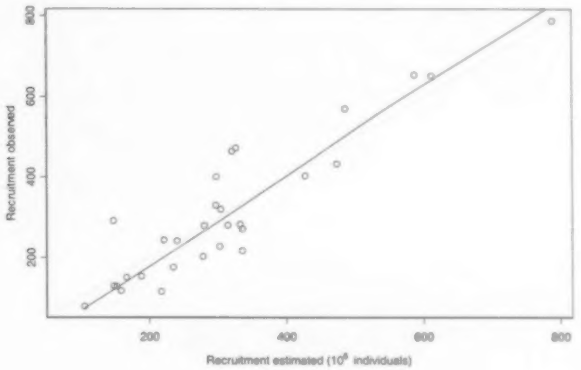

Fig. 8. Residual deviance of the generalized additive model plotted against the predicted recruitment.

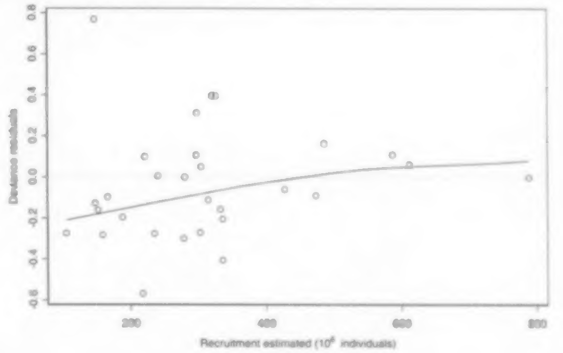

related to female size and (or) age (Vallin and Nissling 2000). These results are in agreement with experimental studies of Kjesbu et al. (1996) and Trippel (1998) showing that, in Atlantic cod, there is a positive correlation between egg size and female size and that viability of eggs and larvae is greater for repeat than for recruit spawners. First-time spawners perform poorly compared with second-time spawners. They breed for a shorter period, produce fewer egg batches, and exhibit lower fecundity (Trippel 1998).

Nevertheless, the maternal effect on recruitment and its interaction with environmental conditions are probably multidimensional and nonlinear. Therefore, results derived from experimental studies on egg and larval survival or viability are not necessarily applicable to the complex dynamics of recruitment. However, results from our study have shown the importance of stock structure for the recruitment of Baltic cod, stressing the presence of maternal effect on recruitment (e.g., Marshall et al. 1998; Scott et al. 1999; Cardinale et al. 2000). Moreover, the survival probability of cod eggs in the Baltic is dependent on (among other factors such as predation, food, etc.) the buoyancy of eggs (Nissling and Vallin 1996). Egg buoyancy is affected by salinity levels and is regarded as a major limiting factor in the successful spawning of Baltic cod, since maintenance of low specific gravity is crucial in avoiding stressful oxygen conditions in the deep layers (Nissling and Vallin 1996). Vallin and Nissling (2000) have recently shown that egg buoyancy is directly related to female age and (or) size. Data from our study strongly support this hypothesis. We found that eggs from OS have a strong positive effect at very low levels of RV (<100 km^3). Levels of RV lower than 100 km^3 correspond to a year of extremely low inflow from the North Sea (MacKenzie et al. 2000). In the absence of such inflow, oxygen concentrations below the halocline progressively decrease to <2 mL·L^{-1}, concentrations at which no Baltic cod eggs will develop and hatch successfully (Nissling and Vallin 1996). Data from this study suggest that, under such unfavourable environmental conditions, highly buoyant eggs from older individuals, having lower mortality rates than eggs from younger individuals, make the largest contribution to recruitment. In contrast, when levels of salinity, temperature, and oxygen are adequate in most of the reproductive areas of the Baltic, differences in survival are probably minor, and larger numbers of eggs derived from YS are most likely to survive. As a consequence, low values of RV had a negative effect on cod recruitment, while, when RV increased and conditions were favourable for the survival of cod eggs and larvae, the effect was positive, although the effect does not increase at RV values larger than 300 km^3.

Another important point emerging from this study is the usefulness of GAMs for analysing complex interactions between environmental factors and biological variables (Swartzman et al. 1995; Daskalov 1999; Maravelias et al. 2000). The use of GAMs is a relatively new approach in fisheries (e.g., Swartzman et al. 1995; Daskalov 1999; Cardinale and Arrhenius 2000)—an approach that can identify functional relationships suggested by the data alone in cases where linear techniques have previously failed (Daskalov 1999). However, the price of the greater flexibility is the restricted possibility of statistical inference typical for nonparametric techniques and the large number of degrees of freedom used by smoothing terms (Daskalov 1999).

Vallin and Nissling (2000) have also recently indicated the positive effect of abundance of OS on Baltic cod recruitment. They showed a positive relationship between the amount of eggs produced by females age 5+ and recruitment that explained between 28 and 48% of the variance of Baltic cod recruitment (Vallin and Nissling 2000). However, one of the major problems in the analyses was that the relationship was modelled using linear estimations, therefore neglecting the importance of nonlinear interactions between biotic and abiotic factors. In contrast, the use of a GAM allowed identification of the quantitative effect of both biotic and abiotic factors and their nonlinear interactions on the intensity of Baltic cod recruitment. The results of this study indicates that the impact of stock structure on Baltic cod recruitment is even larger under certain unfavourable environmental conditions. These abiotic factors and, mostly, their interaction with biotic variables should be carefully considered in future estimations of Baltic cod recruitment and its management.

However, the results of this study also have a general importance in understanding the recruitment variability of fish populations and, therefore, for fisheries management. As stated below, a crucial assumption in fisheries science is that spawning biomass is proportional to the reproductive potential of the stock, implying that the survival rates of offspring do not substantially change with the age or size of the spawners (Trippel et al. 1997). However, the commercial extinction of many marine fisheries worldwide (Myers et al. 1997) has raised concerns about the management of renewable resources (Pitcher et al. 1998), and even the proportionality assumption has been challenged (Gilbert 1997). In our study, we showed that the influence of parental age on Baltic cod recruitment is highly substantial. Our results confirm what has been hypothesised by different authors (Kjesbu et al. 1996; Trippel 1998; Marshall et al. 1998) and recently shown for different cod stocks (Scott et al. 1999; Cardinale and Arrhenius 2000). The presence in the spawning population of a rich variety of age-classes increases the probability of successful recruitment (e.g., Marshall et al. 1998; Marteinsdottir and Thorarinsson 1998). The positive effect of older and larger individuals on cod recruitment is likely due to the production of larger larvae with higher rates of survival, in combination with more batches being produced over a longer spawning period (Kjesbu et al. 1996; Trippel 1998). Nevertheless, abiotic factors may also influence recruitment (Daskalov 1999). Temperature, oxygen, and salinity (as it affects egg buoyancy and survival), or food availability, contribute significantly to recruitment variability in Baltic cod stocks (Vallin and Nissling 2000; this study). The implications for stock assessment and management are important. Conventional approaches overestimate the reproductive potential of the age-truncated populations, assuming proportionality between spawning biomass and recruitment (Trippel 1998). Therefore, current stock assessment increases the risk of commercial extinction, when populations are truncated by fishing mortality and the number of high-quality OS is below a certain limit (Trippel et al. 1997; Cardinale and Arrhenius 2000; this study). A certain minimum number of repeat spawners must, therefore, be present in the population, to ensure a large number of surviving offspring. In the case of the present data set, the impact of OS on recruitment was even larger where environmental conditions strongly affected the survival of eggs and larvae. This important effect of population structure (Marshall et al. 1998; Trippel 1998; Cardinale and Arrhenius 2000), as well as the influence of environmental conditions on recruitment (Sparholt 1996; Daskalov 1999; this study), should be taken carefully into account in the management of exploited fish populations in the future.

Acknowledgements

We are deeply indebted to Christos Maravelias for his support and for suggestions about the use of GAM models. We are grateful to two anonymous reviewers for their useful suggestions.

References

Anonymous. 1998. Report of the Baltic Fisheries Assessment Working Group. Advisory Committee on Fishery Management Report No. ICES CM 1998/ACFM: 16. International Council for Exploration of the Sea, Copenhagen, Denmark.

Blaxter, J.H.S., and Hempel, G. 1963. The influence of egg size on herring larvae (*Clupea harengus*). J. Cons. Cons. Perm. Int. Explor. Mer, **28**: 211–240.

Cardinale, M., and Arrhenius, F. 2000. The relationship between stock and recruitment: are the assumptions valid? Mar. Ecol. Prog. Ser. **196**: 305–309.

Chambers, J.M., and Hastie, T.J. (*Editors*). 1992. Statistical models. S. Wadsworth & Brooks/Cole Advanced Books and Software, Pacific Grove, Calif.

Cleveland, W.S. 1993. Visualizing data. Hobart Press, Summit, N.J.

Daskalov, G. 1999. Relating fish recruitment to stock biomass and physical environment in the Black Sea using generalized additive models. Fish. Res. (Amst.), **41**: 1–23.

Fogarty, M. 1993. Recruitment in randomly varying environments. ICES (Int. Counc. Explor. Sea) J. Mar. Sci. **50**: 247–260.

Gilbert, D.J. 1997. Towards a new recruitment paradigm for fish stocks. Can. J. Fish. Aquat. Sci. **54**: 969–977.

Hastie, T., and Tibshirani, R. 1990. Generalized additive models. Chapman and Hall, London.

Hilborn, R., and Walters, C.J. 1992. Quantitative fisheries stock assessment: choice, dynamics and uncertainty. Chapman and Hall, New York.

Kamler, E. 1992. Early life history of fish. An energetic approach. Fish Fish. Ser. **4**.

Kitanidis, P.K. 1997. Introduction to geostatistics. Applications in hydrogeology. Cambridge University Press, New York.

Kjesbu, O.S., Solemdal, P., Bratlan, P., and Fonn, M. 1996. Variation in annual egg production in individual captive Atlantic cod (*Gadus morhua*). Can. J. Fish. Aquat. Sci. **53**: 610–620.

Knutsen, G.M., and Tilseth, S. 1985. Growth, development, and feeding success of Atlantic cod larvae *Gadus morhua* related to egg size. Trans. Am. Fish. Soc. **114**: 507–511.

Kraus, G., Muller, A., Trella, K., and Köster, F.W. 2000. Fecundity of Baltic cod: temporal and spatial variation. J. Fish Biol. **56**: 1327–1341.

MacKenzie, B.R., Hinrichsen, H.H., Plikshs, M., and Zezera, A.S. 2000. Quantifying environmental heterogeneity: estimating the size of habitat for successful cod egg development in the Baltic Sea. Mar. Ecol. Prog. Ser. **193**: 143–156.

Maravelias, C.D. 1997. Trends in abundance and geographic distribution of North Sea herring in relation to environmental factors. Mar. Ecol. Prog. Ser. **158**: 151–164.

Maravelias, C.D. 1999. Habitat selection and clustering of a pelagic species: effects of topography and bathymetry on species dynamics. Can. J. Fish. Aquat. Sci. **56**: 437–450.

Maravelias, C.D., and Reid, D.G. 1997. Identifying the effects of oceanographic features and zooplankton on pre-spawning herring abundance using generalized additive models. Mar. Ecol. Prog. Ser. **147**: 1–9.

Maravelias, C.D., Reid, D.G., and Swartzman, G. 2000. Modelling spatio-temporal effects of environment on Atlantic herring using GAMs. Environ. Biol. Fishes, **58**(2): 157–172.

Marshall, T., Kjesbu, O.S., Yaragina, N.A., Solemdal, P., and Ulltang, Ø. 1998. Is spawner biomass a sensitive measure of the reproductive and recruitment potential of Northeast Arctic cod? Can. J. Fish. Aquat. Sci. **55**: 1766–1783.

Marteinsdottir, G., and Thorarinsson, K. 1998. Improving the stock–recruitment relationship in Icelandic cod (*Gadus morhua* L.) by including age diversity of spawners. Can. J. Fish. Aquat. Sci. **55**: 1372–1377.

Miller, T.J., Crowder, L.B., Rice, J.A., and Marshall, E.A. 1988. Larval size and recruitment mechanisms in fishes: towards a conceptual framework. Can. J. Fish. Aquat. Sci. **45**: 1657–1670.

Mills, C.A. 1982. Factors affecting the survival of dace, *Leuciscus leuciscus* (L.), in the early post-hatching period. J. Fish Biol. **20**: 645–655.

Moodie, G.E.E., Loadman, N.L., Wiegand, M.D., and Mathias, J.A. 1989. Influence of egg characteristics on survival, growth and feeding in larval walleye, (*Stizotedion vitreum*). Can. J. Fish. Aquat. Sci. **46**: 521–526.

Myers, R.A., Hutchings, J.A., and Barrowman, N.J. 1997. Why do fish stocks collapse: the example of cod in Atlantic Canada. Ecol. Appl. **7**: 91–106.

Nissling, A, and Vallin, L. 1996. The ability of Baltic cod eggs to maintain neutral buoyancy and the opportunity for survival in fluctuating conditions in the Baltic Sea. J. Fish Biol. **48**: 217–227.

Nissling, A., and Westin, L. 1991. Egg buoyancy of Baltic cod (*Gadus morhua*) and its implications for cod stock fluctuations in the Baltic. Mar. Biol. (Berlin), **111**: 33–35.

Nissling, A., Larsson, R., Vallin, L., and Frohlund, K. 1999. Assessment of egg and larval viability in cod, *Gadus morhua*—methods and result from an experimental study. Fish. Res. (Amst.), **38**: 169–186.

Oosthuizen, E., and Daan, N. 1974. Egg fecundity and maturity of North Sea cod, *Gadus morhua*. Neth. J. Sea Res. **8**: 378–397.

Pitcher, T.J., Hart, P.J.B., and Pauly, D. 1998. Reinventing fisheries management. Kluwer Academic Publishers, Dordrecht.

Scott, B., Marteinsdottir, G., and Wright, P. 1999. Potential effects of maternal factors on spawning stock – recruitment relationships under varying fishing pressure. Can. J. Fish. Aquat. Sci. **56**: 1882–1890.

Solari, A.P., Martin-González, J.M., and Bas, C. 1997. Stock and recruitment in Baltic cod (*Gadus morhua*): a new non-linear approach. ICES (Int. Counc. Explor. Sea) J. Mar. Sci. **54**: 427–443.

Sparholt, H. 1996. Causal correlation between recruitment and spawning stock size of central Baltic cod? ICES (Int. Counc. Explor. Sea) J. Mar. Sci. **53**: 771–779.

Swartzman, G., Huang, C.P., and Kaluzny, S.P. 1992. Spatial analysis of Bering Sea groundfish survey data using generalized additive models. Can. J. Fish. Aquat. Sci. **49**: 1366–1378.

Swartzman, G., Silverman, E., and Williamson, N. 1995. Relating trends in walleye pollock (*Theragra chalcogramma*) abundance in the Bering Sea to environmental factors. Can. J. Fish. Aquat. Sci. **52**: 369–380.

Trippel, E.A. 1998. Egg size and viability and seasonal offspring production of young Atlantic cod. Trans. Am. Fish. Soc. **127**: 339–359.

Trippel, E.A., Kjesbu, O.S., and Solemdal, P. 1997. Effects of adult age and size structure on reproductive output in marine fishes. *In* Early life history and recruitment in fish populations. *Edited by* R.C. Chambers and E.A. Trippel. Chapman and Hall, London. pp. 31–62.

Vallin, L., and Nissling, A. 2000. Maternal effects on egg size and egg buoyancy of Baltic cod, *Gadus morhua*—implications for stock structure effects on recruitment. Fish. Res. (Amst.), **49**: 21–37.

Vallin, L., Nissling, A., and Westin, L. 1999. Potential factors influencing reproductive success of Baltic cod, *Gadus morhua*: a review. Ambio, **28**: 92–99.

Associations between flatfish abundance and surficial sediments in the eastern Bering Sea

Robert A. McConnaughey and Keith R. Smith

Abstract: Spatially explicit relationships between pleuronectid flatfish abundance and surficial sediments in the eastern Bering Sea were investigated using published sediment descriptions and trawl survey data (1982–1994). Flatfish food habits were also examined because sediment properties are known to affect the distribution and abundance of benthic prey. For six species, we compared sediment textures in areas of highest and lowest abundance (kilograms per hectare). Sand predominated in areas of high yellowfin sole (*Pleuronectes asper*) (YFS) ($p << 0.001$) and rock sole (*Lepidopsetta* spp.) (RS) ($p << 0.001$) abundance, while mixed sand and mud was most common in areas of lowest abundance. In contrast, mixed sand and mud predominated in areas preferred by flathead sole (*Hippoglossoides elassodon*) (FHS) ($p << 0.001$), Alaska plaice (*Pleuronectes quadrituberculatus*) (AP) ($p = 0.002$), and arrowtooth flounder (*Atheresthes stomias*) (ATF) ($p = 0.004$), with more diverse substrates in low-density areas. Areas of high and low Greenland turbot (*Reinhardtius hippoglossoides*) (GT) ($p = 0.845$) abundance had similar sediment textures (primarily mixed sand and mud). Species with highly restricted diets (AP) or piscivores with weak sediment associations (GT, ATF) had relatively inflexible food habits, whereas YFS, RS, and FHS food habits varied considerably with sediment type. Our findings suggest that benthic-feeding pleuronectids prefer certain sediment textures because of adaptive differences in prey availability.

Résumé : Des résultats d'analyses de sédiments tirés de la littérature et des inventaires de poissons au chalut de 1982 à 1994 dans la région est de la mer de Bering ont servi à caractériser les relations spatiales entre la densité des poissons plats pleuronectidés et les sédiments de surface. Les habitudes alimentaires des poissons plats ont été examinées aussi, parce que les caractéristiques des sédiments affectent la distribution et l'abondance des proies benthiques. La texture des sédiments a été définie dans les zones de densités (kilogrammes par hectare) maximale et minimale de six des espèces. C'est le sable qui prédomine dans les zones de forte densité de la Limande à nageoires jaunes (*Pleuronectes asper*) (YFS) ($p << 0{,}001$) et de la Sole du Pacifique (*Lepidopsetta* spp.) (RS) ($p << 0{,}001$), alors qu'un mélange de sable et de boue caractérise le plus souvent les zones de faible densité. En revanche, la Plie à tête plate (*Hippoglossoides elassodon*) (FHS) ($p << 0{,}001$), la Plie de l'Alaska (*Pleuronectes quadrituberculatus*) (AP) ($p = 0{,}002$) et la Plie à grande bouche (*Atheresthes stomias*) (ATF) ($p = 0{,}004$) préfèrent les substrats dominés par un mélange de sable et de boue; leurs densités sont faibles sur les substrats plus diversifiés. Les zones de fortes et de faibles densités du Flétan du Groenland (*Reinhardtius hippoglossoides*) (GT) ($p = 0{,}845$) ont toutes des sédiments semblables, généralement des substrats mixtes de sable et de boue. Les espèces qui possèdent une alimentation peu diversifiée (AP) ou les espèces piscivores à faible affinité pour des sédiments particuliers (GT, ATF) ont des habitudes alimentaires rigides, alors que les régimes alimentaires des autres (YFS, RS et FHS) varient considérablement selon les types de sédiments. Nos données laissent croire que les poissons pleuronectidés benthophages préfèrent certaines textures de sédiments à cause des différences de disponibilité des proies qui s'y sont développées par sélection naturelle.

[Traduit par la Rédaction]

Introduction

Spatial distributions of fish reflect variability in the surrounding environment, and those areas normally occupied by a species constitute its habitat. Generally speaking, individual species are not ubiquitous, suggesting that habitat is restrictive. Moreover, an uneven distribution of organisms within the area of occurrence indicates that there may be important differences in habitat quality. It is commonly assumed that a species will select resources that are best able to satisfy its fundamental needs and that high-quality resources will be selected over low-quality ones (Manly et al. 1993). The process of selection is thought to be based on individual preference–avoidance responses affecting locomotor activity as well as specific physiological tolerances (Scherer 1991; Davenport and Sayer 1993). When all individuals in a population are capable of choosing the most suitable habitat and are free to occupy it, the result is an "ideal free distribution" (Fretwell and Lucas 1970). At low levels of abundance, individuals will occupy the most suitable habitat but will move into increasingly marginal/less suitable habitat as a population grows and crowding effects increase (MacCall 1990; McConnaughey 1995). If overall abundance decreases at some later time, these populations will contract in space and retreat toward the most suitable

Received February 9, 2000. Accepted September 29, 2000. Published on the NRC Research Press web site on December 20, 2000. J15608

R.A. McConnaughey[1] and K.R. Smith. National Marine Fisheries Service, Alaska Fisheries Science Center, 7600 Sand Point Way NE, Seattle, WA 98115-0070, U.S.A.

[1] Corresponding author (e-mail: bob.mcconnaughey@noaa.gov).

habitat that is available. This could be the same area occupied during the period of lowest abundance or may be an entirely new location when habitat is defined by a temporally variable feature like temperature. Thus, regardless of population size, areas occupied at the highest densities may represent the highest quality habitat and conditions there should be indicative of the species' requirements. Although direct measures of habitat quantity are possible, assessments of habitat quality are typically made by inference (Gibson 1994).

Conservation of living marine resources now generally includes elements of habitat protection. Management of essential habitat begins with consideration of factors directly affecting growth, reproduction, and mortality at critical life history stages (Langton et al. 1996), followed by synoptic habitat mapping to identify critical areas for regulatory protection. In many cases, however, fundamental knowledge of habitat associations is lacking and it has been argued that broad management for habitat complexity is the most prudent and precautionary approach (Peters and Cross 1991). Although problematic for some stocks, it has also been suggested that habitats should be defined in geographic terms to facilitate management and enforcement actions. Preliminary designations of critical habitat have been proposed, based on general patterns of abundance in research and commercial catches (e.g., Fritz et al. 1998). Ultimately, a more mechanistic understanding of habitat associations is required to balance protection with other societal benefits.

Exogenous factors such as temperature, depth, oxygen tension, salinity, and pH are known to limit the spatial distribution of fish, and numerous correlative relationships have been demonstrated (Davenport and Sayer 1993; Wootton and Thorpe 1993; Gibson 1994). Sediment properties may directly influence survival of demersal fish through effects on burial and predator avoidance (Gibson and Robb 1992). It has also been reported that maturity and growth schedules, as well as sex ratios, in English sole (*Pleuronectes vetulus*) are related to sediment type (Becker 1988; Sampson and Al-Jufaily 1999). There may also be important differences in the availability and quality of infaunal and epifaunal prey associated with different substrates (Gray 1974).

The eastern Bering Sea (EBS) is a semienclosed extension of the North Pacific and supports some of the world's most productive fisheries (National Research Council 1996). It is a dynamic environment with considerable variation in its physical properties (National Research Council 1996; Smith and McConnaughey 1999). Distributions of pleuronectid flatfish also vary spatially, suggesting the existence of functional habitat associations (Goddard and Walters 1998). Density-dependent relationships between population size and total area occupied may explain some of the spatial variability (McConnaughey 1995). However, a fundamental understanding of preferred habitat characteristics is lacking. To address this need, we first compare surficial sediments in areas of high and low pleuronectid abundance to infer preferences. Subsequently, we compare food habits in the different substrates to examine functional responses and thus gain insight into the mechanism of association. If changes in diet accompany changes in sediment type, in a manner that is consistent with habitat requirements of the prey, it would suggest that the sediment association is related to prey availability. Furthermore, food habits in areas occupied at relatively high densities should constitute the highest quality prey overall and be most adaptive for that particular species.

Methods

Flatfish distribution and abundance

Bottom trawl surveys are conducted annually in the EBS by the U.S. National Marine Fisheries Service's Alaska Fisheries Science Center (NMFS) (Goddard and Walters 1998). These surveys provide data for stock assessments and management of the fishery resources. Each June–August, the EBS shelf (approximately 463 400 km^2) is systematically surveyed at depths ranging from 20 to 200 m. An 83-112 eastern otter trawl is deployed from chartered vessels at 356 standard stations in a sampling grid with 20 × 20 nautical mile cells (Fig. 1). Each sample consists of a 30-min tow at 3 kn. The catch is processed to determine total weight and numbers by species and sex, and a variety of biological measurements and samples are collected from individual specimens.

For this study, area swept by the trawl was used to calculate population (number per hectare) and biomass (kilograms per hectare) densities of six pleuronectid species: arrowtooth flounder (*Atheresthes stomias*) (ATF), Greenland turbot (*Reinhardtius hippoglossoides*) (GT), yellowfin sole (*Pleuronectes asper*) (YFS), rock sole (*Lepidopsetta* spp. (Orr and Matarese 2000)) (RS), Alaska plaice (*Pleuronectes quadrituberculatus*) (AP), and flathead sole (*Hippoglossoides elassodon*) (FHS). In keeping with standard survey practices, ATF combines ATF and Kamchatka flounder (*Atheresthes evermanni*), while FHS includes both FHS and Bering flounder (*Hippoglossoides robustus*). Juveniles were purposely excluded from the analysis because of categorical differences in spatial distribution (McConnaughey 1995; Nichol 1997) (Table 1). Total catch weights were adjusted accordingly, using empirical length–weight relationships for each species. Densities at each station were averaged for the years 1982–1994, a period of standard gear and methods, in order to provide some measure of control for potentially important and temporally variable environmental factors not included in the analysis.

Surficial sediments

The seabed may be characterized by sediment texture, a descriptive label based on the relative distribution of grain sizes. Texture data used in this study were obtained from records of grab, core, and dredge samples collected and analyzed by others (1934–1983; subsequently expanded by Smith and McConnaughey 1999). Core subsamples were from the upper stratum of homogeneous sediment, as judged by the original investigator; 80% of these samples were from positions ≤10 cm below the sea floor. The original descriptions, based either on laboratory methods or on visual/tactile observations in the field, were standardized using a mud–sand–gravel classification scheme that we developed from a standard ternary diagram (Folk 1954) (Fig. 2). For this study, seven textural classes were defined: sand; mud; gravel; mixed sand and mud; mixed gravel and mud; mixed gravel and sand; and mixed gravel, sand, and mud. Some of Folk's textural classes were merged in order to include all available data and thus maximize sample sizes. Ultimately, classifications such as "mixed sand and mud" were used because samples described in the field frequently did not specify predominance of the components. Also, since it is likely that very small fractions of a size-class would escape detection with field methods, we eliminated trace level classes in Folk's diagram (i.e., ≤5% by weight) and reclassified the samples according to the nontrace constituents (e.g., "slightly gravelly muddy sand" became "mixed sand and mud"). An eighth classification was added for descriptive samples ($n = 9$) containing the words "rock" or "rocky"; these terms have been used in the literature to refer either to material larger than gravel or to surface bedrock.

Fig. 1. Sampling area for the annual NMFS groundfish survey in the EBS. Bottom-trawl samples are collected at the center of each 20 × 20 nautical mile grid cell. Standard methods and gear were used during the 1982–1994 study period.

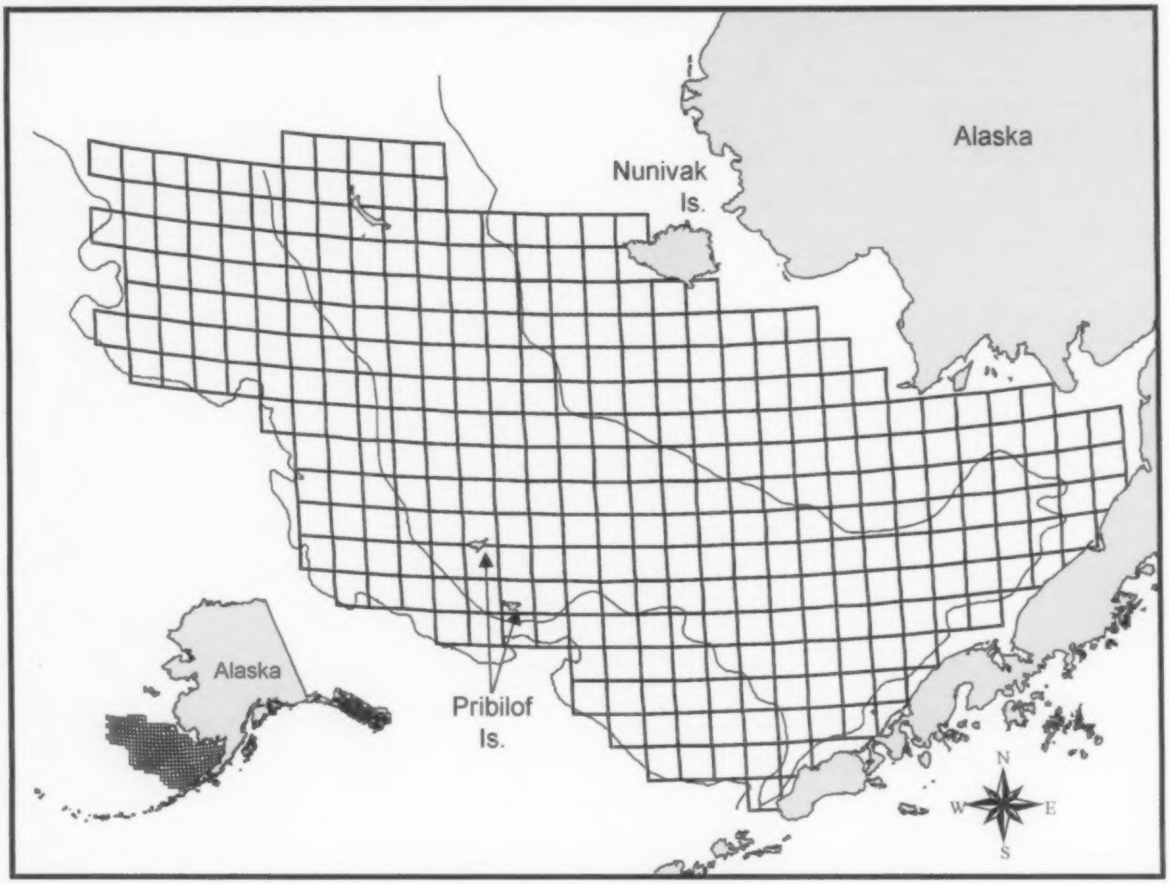

Table 1. Size limits used to exclude juvenile flatfish from density (kg·ha^{-1}) calculations and food habits descriptions.

Species	Minimum fork length (mm)
ATF	161
GT	141
FHS	121
YFS	141
RS	111
AP	211

We assume that textural classes assigned to samples analyzed in a laboratory are consistent with those assigned in the field. Strictly speaking, this probably is not the case, given the continuous nature of the grain size variable and the relative imprecision and subjectivity of field methods. However, we do not consider this a significant source of error. The ternary diagram that we used to describe the texture of laboratory samples was a culmination of efforts by Folk (1954) and others to create a standard classification system that was consistent with de facto practical limits and definitions used in the field, thus minimizing any discrepancies between the two methods of description.

Flatfish food habits

Fish stomachs collected during the NMFS research trawl surveys or by NMFS fishery observers were used to evaluate the effect of sediment texture on flatfish food habits (Table 2). Detailed information about food habits methodology is found elsewhere (Lang et al. 1995). Briefly, fish were randomly selected and stomachs were removed from specimens that showed no signs of net feeding or regurgitation and were preserved at sea. Information about the source predator and point of collection was also recorded. In the laboratory, prey items from individual stomachs were counted, weighed, and identified to the lowest practical taxon. Prey were then assigned to eight larger taxonomic groups and summarized by percent total prey weight (Table 3). Groups were defined so as to minimize the miscellaneous category, which in this case includes diverse invertebrates, unidentified organic matter, and fishery discards. Juvenile predators were excluded from consideration, as before (Table 1). Sample sizes vary according to species and area, according to the original sampling plans.

Flatfish–sediment analysis and food habits summaries

Flatfish abundance (grid) and surficial sediment (point) data were spatially joined with a geographic information system (GIS). The relationship between two classes of fish density and seven sediment classes was evaluated using a two-tailed Fisher's exact test conditioned on marginal totals. For each species, identification of

Fig. 2. Ternary diagram used to standardize historical sediment data for this study. A mud–sand–gravel ternary diagram represents the percent composition by weight along axes originating at the vertices (100%) and decreasing along a line perpendicular to the opposite side of the triangle (0%).

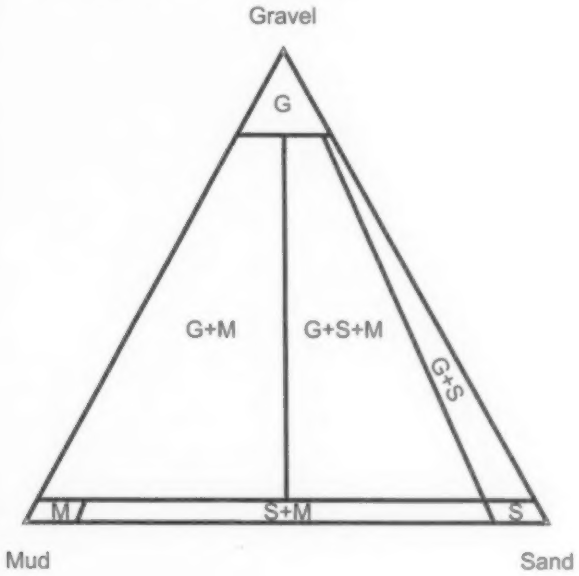

Table 2. Numbers of stomachs and prey items used to compare flatfish food habits in high- and low-density areas.

Month (1982–1994)	Stomachs	Prey items
June	2082	68 542
July	2196	75 138
August	220	20 696
Total	4498	164 376

Note: June, July, and August 1982–1994 correspond to trawl survey data used to evaluate flatfish associations with surficial sediment textures.

"preferred" sediment types was based on comparisons of sediment class frequencies in areas of high and low fish density. As explained in the introductory text, this rationale is consistent with principles of habitat utilization in an ideal free distribution.

Various (cutpoint) methods were evaluated for converting continuous fish abundance data to a nominal scale for analysis. Two of these emphasized the high versus low density contrast while, at the same time, providing comparable sample sizes for analysis: (*i*) an equal area method with 20% of the sampled area in each of five nonzero density classifications and (*ii*) a scheme with geometrically increasing data ranges in each of five nonzero classifications. In this study, "high density" refers to the highest nonzero bin, while "low density" refers to the lowest nonzero bin. Preliminary analyses indicated that the statistical results were insensitive to the cutpoint method and the density measure used, so, for simplicity, only the biomass (kilograms per hectare) and equal area results are reported.

This analysis assumes that textural properties on the EBS shelf are persistent and have not changed significantly since the original samples were collected. In keeping with the time scale of sedimentary processes, average deposition rates for recent surface strata on the east-central Bering Sea shelf (8–70 cm per millennium) are small relative to the surface interval represented in most of the sample descriptions (≥10 cm) (details in Smith and McConnaughey 1999). Secondly, we assume that fish densities at stations near the center of each survey cell are representative of conditions throughout that cell (Fig. 1). Although this is a basic premise of the NMFS trawl survey in the EBS, its validity is untested. However, our reliance on sediment class frequencies, rather than grain size averages, requires no such extrapolation and fully accounts for sediment patchiness in each cell.

Table 3. Eight aggregate prey groups used to compare food habits in areas occupied at high and low density.

Prey group	Constituent taxa
Polychaetes	Polychaete annelid worms
Clams	Bivalve molluscs
Gammarids	Gammarid amphipods
Decapods	Decapod crustaceans
Marine worms	Echiurids, priapulids, sipunculids
Echinoderms	Sand dollars, brittle stars, sea cucumbers
Fish	Teleost fish
Miscellaneous	All other prey types, including unidentified items and fishery discards

Note: Prior to grouping, prey items were identified in the laboratory to the lowest practical taxon.

The food habits and flatfish abundance data were also joined using a GIS, thus matching the trawl survey grid with stomach collection points. Statistical analyses were not performed in this case because our intention was to investigate functional responses to different sediment types rather than demonstrate summary differences in high- and low-density area diets. Such responses would be particularly relevant if major shifts within and among prey categories were consistent with known sediment preferences of the prey.

Results

Flatfish distribution and abundance

As a group, the six flatfish species occurred throughout the study area, although there were significant differences in distribution and abundance of individual species (Fig. 3). YFS and RS were most prevalent over the inner shelf and were the most abundant species overall. Their overall distributions were quite similar, except for differences in the location of high-density areas (i.e., the "preferred habitat"). Preferred RS habitat was generally southeast of the YFS area, with a second area of concentration near the Pribilof Islands (Fig. 3). On average, YFS were absent from the outer shelf and were less abundant in adjacent areas of the middle shelf, particularly in the north. RS, on the other hand, were ubiquitous on the EBS shelf, except for localized voids, especially in the southeast corner of the outer shelf. Lowest densities of RS were generally in the northwest region. FHS were distributed throughout the middle and outer shelf and were generally absent in the northeast and central regions of the inner shelf. Highest densities occurred in a relatively narrow band along the shelf break at 200 m, with a conspicuous expansion into middle shelf waters in the south. Lowest densities, on average, were on the landward edge of the general distribution, particularly north of the Pribilof Islands. AP occurred in a broad band centered on the middle shelf and were generally absent from outer shelf waters and the most eastern corner of the study area. Lowest nonzero

Fig. 3. Abundance (1982–1994 average, kg·ha^{-1}) of YFS, RS, FHS, AP, ATF, and GT in the EBS. The outlined study area is defined by the NMFS trawl survey boundary. Higher densities are represented by denser shade patterns. Each of the five nonzero classifications includes approximately 20% of the sampled area. Also shown are the 50-, 100-, and 200-m isobaths, which commonly define the inner, middle, and outer shelf areas.

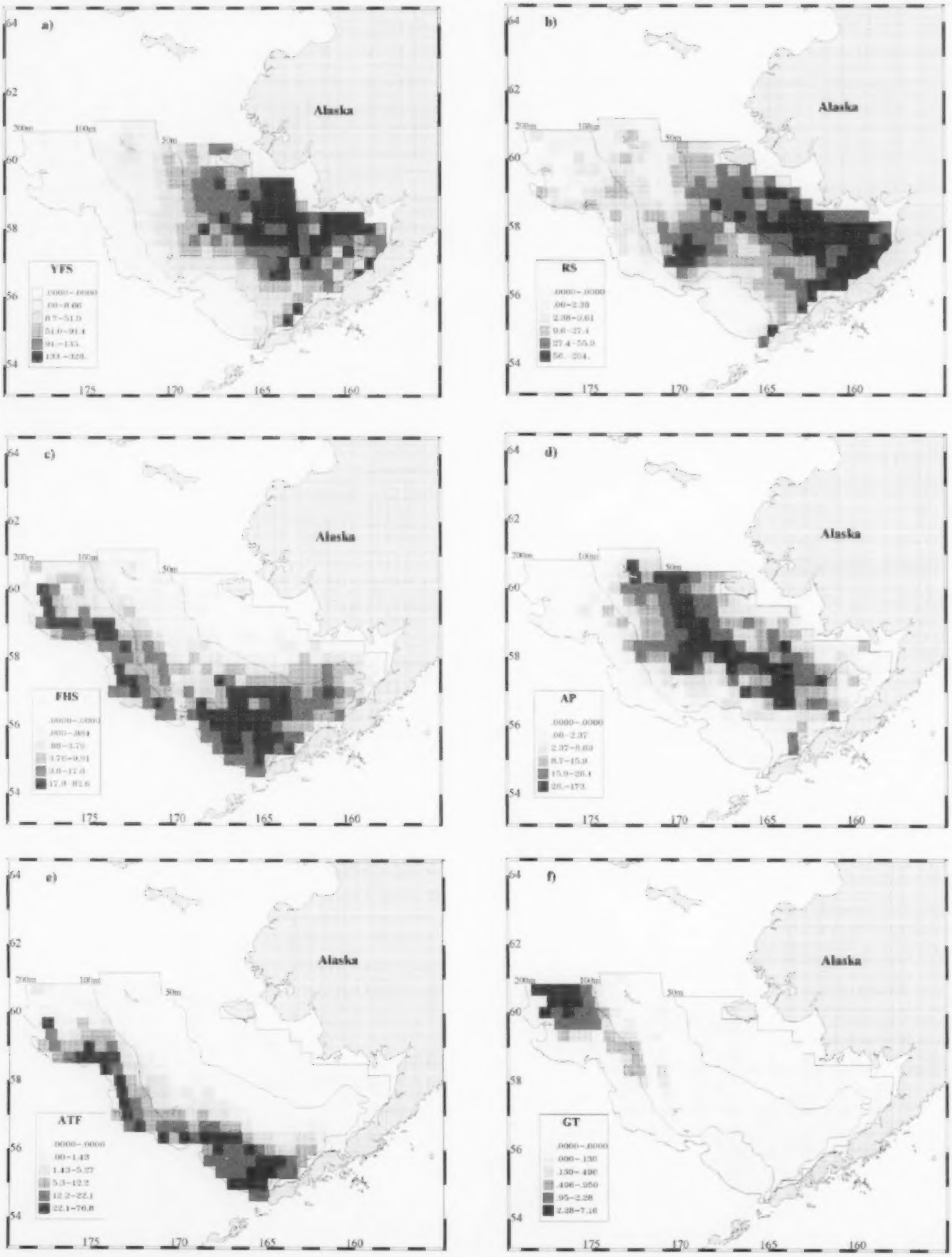
a)
b)
c)
d)
e)
f)
Alaska
200m
100m
50m
64
62
60
58
56
54
175
170
165
160
YFS
.0000–.0000
.00–8.66
8.7–51.0
51.0–91.4
91.–133.
133.–328.
RS
.0000–.0000
.00–2.38
2.38–9.61
9.6–27.4
27.4–55.9
56.–204.
FHS
.0000–.0000
.000–.884
.88–3.70
3.70–9.81
9.8–17.9
17.9–82.6
AP
.0000–.0000
.00–2.37
2.37–8.69
8.7–15.9
15.9–26.1
26.–173.
ATF
.0000–.0000
.00–1.43
1.43–5.27
5.3–12.2
12.2–22.1
22.1–76.8
GT
.0000–.0000
.000–.130
.130–.496
.496–.950
.95–2.28
2.28–7.16

Fig. 4. Distribution of sediment textures in the EBS. The 50-, 100-, and 200-m isobaths define the inner, middle, and outer shelf areas.

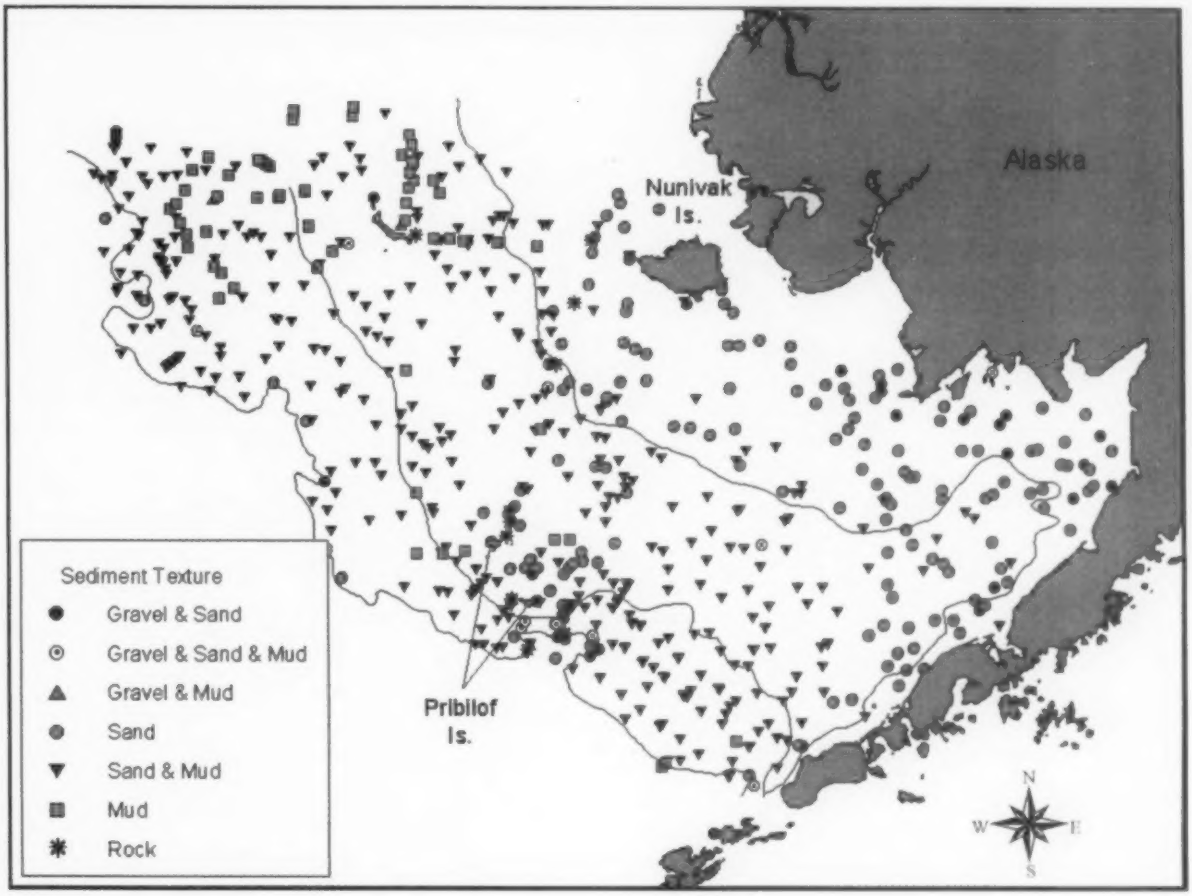

densities straddled the central band of high abundance. ATF and GT were restricted to the outer shelf. Highest densities of ATF occurred along the shelf break with some eastward extension in the south. Highest abundance of GT, on the other hand, was limited to the very northwest corner of the study area. Densities of ATF and GT declined rapidly to very low levels outside their preferred areas.

Surficial sediments

Surficial sediment samples were uniformly distributed over the EBS shelf ($n = 678$) (Fig. 4), and seven of eight possible textural classes were represented in the data ("pure" gravel did not occur). The resulting distribution of textures is consistent with published accounts, although fine-scale patchiness is represented in our case (reviewed by Smith and McConnaughey 1999). In general, the EBS continental shelf is a relatively shallow and level basin, with an average depth of 60 m and an average slope $<0.3\ \mathrm{m \cdot km^{-1}}$. Mean grain size generally decreases with distance from shore and (or) increasing water depth. Sand predominates overall, with very little gravel and a conspicuous lack of mud over the inner and middle shelf. The inner shelf has mixed gravel and sand nearshore changing to sand on the midshelf and mixed sand and mud farther offshore. The middle shelf is largely mixed sand and mud extending in a broad band from southeast to northwest and generally following the bathymetry. This pattern is disrupted by a rather continuous swath of sand along a line extending from the Pribilof Islands to the western tip of Nunivak Island, with rocky material along its northwestern edge. Surficial sediments of the outer shelf are, again, largely mixed sand and mud, with mixed gravel and sand along the outer margin southeast of the Pribilof Islands. Mud is common near the northwest corner of the outer shelf and also occurs west and northwest of the Pribilof Islands. Isolated patches of sand are found along the outer margin of the EBS shelf.

Flatfish associations with surficial sediments

Surficial sediments in areas of high and low flatfish abundance were different, with species-specific differences in the degree and nature of the response (Table 4). Sand (71% of sediment samples) predominated in areas of high YFS abundance, with finer sediments (68% mixed sand and mud, 15% mud) in areas of lowest abundance ($p << 0.001$). A strikingly similar pattern was observed for RS ($p << 0.001$); sand (72%) was most common in high-density areas, with

Table 4. Sediment textures (R, rocky; G, gravel; S, sand; M, mud) in areas of high and low flatfish abundance, with results of Fisher's exact test comparison (*n* = sample size).

		Occurrence of textural classes (%)								
Species	Density	R	G+S	G+S+M	G+M	S	S+M	M	*n*	*p*
YFS	High	0.0	8.9	0.0	0.0	71.4	19.6	0.0	56	<<0.001
	Low	0.9	6.4	2.7	0.0	7.3	68.2	14.6	110	
RS	High	2.2	7.5	0.0	0.0	72.0	15.1	3.2	93	<<0.001
	Low	0.0	2.7	1.8	0.9	4.6	68.2	21.8	110	
FHS	High	0.0	0.9	1.8	0.0	1.8	95.5	0.0	112	<<0.001
	Low	3.9	2.9	1.9	1.0	21.4	54.4	14.6	103	
AP	High	2.9	0.0	2.9	1.5	17.7	66.2	8.8	68	0.002
	Low	2.5	12.7	1.3	0.0	31.7	41.8	10.1	79	
ATF	High	0.0	4.5	4.5	0.0	4.5	82.1	4.5	67	0.004
	Low	3.6	0.0	1.8	0.0	17.9	62.5	14.3	56	
GT	High	0.0	0.0	0.0	4.0	0.0	60.0	36.0	25	0.845
	Low	0.0	0.0	0.0	0.0	0.0	68.8	31.3	16	
n		9	30	13	3	157	406	60	678	

Note: Pure gravel did not occur.

Table 5. Flatfish food habit summaries for areas of high and low density (1982–1994; detailed summaries available from the authors).

		Stomachs	Prey group (% total weight)								
Species	Density	(*n*)	Poly	Clam	Gamm	Decap	Worm	Echino	Fish	Misc	Sediment texture
YFS	High	3903	19.0	30.6	7.3	6.4	12.6	5.0	2.9	16.2	S
	Low	711	18.0	7.3	4.4	10.5	43.6	3.1	3.1	9.9	S+M
RS	High	621	40.4	7.4	6.2	2.8	20.5	1.9	17.2	3.7	S
	Low	323	54.1	3.0	9.9	2.3	26.7	1.9	1.1	1.0	S+M
FHS	High	1702	4.3	4.8	1.0	10.9	2.1	58.6	6.9	11.5	S+M
	Low	554	1.9	5.1	3.7	17.2	1.8	1.5	59.6	9.1	S
AP	High	374	52.8	8.5	9.8	1.1	23.7	3.1	0.0	1.0	S+M
	Low	120	59.0	10.6	2.5	0.2	24.1	2.4	0.0	1.2	S+M
ATF	High	1232	0.1	0.0	0.0	1.8	0.0	0.0	82.6	15.5	S+M
	Low	220	0.0	0.0	0.0	0.6	0.0	0.0	93.5	5.8	S+M
GT	High	184	0.0	0.0	0.0	0.3	0.0	0.0	99.6	0.2	S+M
	Low	15	0.0	0.0	0.0	0.0	0.0	0.0	97.0	3.0	S+M

Note: Individual prey items were grouped as polychaetes (Poly), bivalve molluscs (Clam), gammarid amphipods (Gamm), decapod crustaceans (Decap), unsegmented coelomate worms (Worm), echinoderms (Echino), and teleost fish (Fish) and all others as miscellaneous (Misc). Sediment texture is the primary type found in the area (S, sand; M, mud).

decreased incidence of sand (5%) and corresponding increases in mixed sand and mud (68%) and mud (22%) in the low-density areas. In contrast with YFS and RS, mixed sand and mud predominated in areas preferred by FHS (96%), AP (66%), and ATF (82%), while sediments in the low-density areas were more diverse ($p << 0.001$, $p = 0.002$, $p = 0.004$). While mixed sand and mud was still most common in the low-density areas, incidence of pure sand and pure mud increased for FHS and ATF, and mixed gravel and sand increased for AP. Areas of high and low GT abundance had similar surficial sediments ($p = 0.85$) consisting of mixed sand and mud (60%, 69%) and mud (36%, 31%).

Flatfish food habits

Food habits of EBS flatfish were different in areas of high and low flatfish abundance and, once again, the degree and nature of the difference varied by species (Table 5). The primary prey of YFS in high-density areas were clams (31% by weight), which were replaced by marine worms (44%) in the low-density areas. Based on raw data summarized in Table 3, *Spisula* spp. were the most important clams, while the echiurids, most notably *Echiurus echiurus*, predominated in the low-density areas. Polychaetes were the second most important prey in the high- (19%) and low-density areas (18%). All eight prey classes were consumed in both low- and high-density areas.

The RS diet was similar in the high- and low-density habitats. In both areas, the first and second most abundant prey were polychaetes and marine worms, although utilization of these prey was higher in the low-density areas (54 and 27% as compared with 40 and 21%). Among the taxonomically differentiated polychaetes, ophelids were most important in the high-density areas, while sabellids contributed the most in low-density areas. The most prevalent marine worms in the high-density areas were echiurids, shifting to sipunculids and priapulids in the low-density areas. Increased utilization of polychaetes and marine worms in the low-density areas was offset by an overall reduction in teleost fish (from 17 to

1%; primarily Pacific sand lance (*Ammodytes hexapterus*), −14%) relative to the high-density areas. Similar to YFS, RS consumed all eight prey classes in each habitat type.

The food habits response by FHS was comparatively large for the pleuronectids that we considered. A predominately echinoderm diet (59%; largely ophiuroids) in the high-density areas was replaced by a fish diet (60%; primarily walleye pollock (*Theragra chalcogramma*)) in the low-density areas. Overall, FHS consumed a very diverse group of decapods, with increased importance in the low-density areas (from 11 to 17%). The miscellaneous category was the second most common prey group in the high-density areas, composed largely of fishery discards (5%) and euphausids (3%).

The food habits of AP were quite similar in the high- and low-density areas, mostly consisting of polychaetes (53 and 59%) and marine worms (24% for both; mostly echiurids). Among the differentiated polychaetes, nephtyids and ampharetids contributed most in the high-density habitat, while ampharetids and terebellids prevailed in the low-density areas. Relatively minor changes in the gammarid amphipod (−7%) and clam (+2%) contributions were observed in the low-density areas.

In both high- and low-density habitats, the diet of ATF was almost exclusively teleost fish. The combined total of fish and fishery discards in the high-density areas was 85% by weight and exceeded 97% in the low-density areas. Walleye pollock were the primary prey in both areas. The diet in the high-density areas also included decapod shrimp (2%; consisting primarily of pandalids and crangonids).

GT food habits in high- and low-density areas were essentially identical, with 97–99% of the total weight consisting of fish (primarily walleye pollock). However, because the number of stomachs sampled in the low-density area was relatively small ($n = 15$), the results should be interpreted with caution.

Discussion

Observation and ecological theory tell us that organisms are restricted to areas, or habitats, with suitable environmental conditions. Moreover, an uneven distribution within the area of occurrence indicates that there may be important differences in habitat quality. In general, areas with a high density of individuals are indicative of preferred/optimum conditions, while conditions in areas of low density should be considered less favorable. An earlier study used generalized additive models to investigate preferred depth and temperature ranges for AP, FHS, GT, RS, and YFS in the EBS (Swartzman et al. 1992). Although they suggested that depth is the primary factor determining abundance of EBS flatfish, because of a relatively consistent effect, they concluded that investigation of other factors influencing flatfish distribution is needed (R^2 values for depth, temperature, and year models were only 0.41, 0.42, 0.59, 0.48, and 0.54). We consider depth to be a composite habitat factor that includes elements of temperature, pressure, and sediment composition. As such, biological responses to depth are expected to be complicated and perhaps inconsistent when one of the components shows temporal variability (e.g., temperature). To address this shortcoming, we assembled a comprehensive set of sediment data for the EBS (Smith and McConnaughey 1999) and directly tested its importance as a habitat factor. Our findings indicate that the distribution and abundance of benthic-feeding pleuronectids (YFS, RS, FHS, AP) are strongly associated with surficial sediment texture. Moreover, since our time-averaged approach controls for temporally variable factors, we conclude that texture is a primary factor affecting habitat quality for this group. Based on the highly significant nature of the sediment associations, we conclude that habitat factors such as temperature and depth are likely to be of secondary importance to these species (cf. Scott 1982). As such, these factors would modify the primary response to sediments (cf. RS in the EBS; Swartzman et al. 1992). For piscivorous species, with relatively weak sediment associations (e.g., GT), the significance of temperature may be relatively high. It is interesting to note that trawl surveys in the Gulf of Alaska (GOA), including those by NMFS, indicate that juvenile pleuronectids also concentrate in rather limited areas, and laboratory studies indicate that sediment texture is an important habitat factor for them as well (Moles and Norcross 1995; Norcross et al. 1999). Both juvenile and adult RS apparently prefer sand, while FHS and ATF prefer muddier areas. However, contrary to our findings for adults, juvenile YFS in the GOA do not demonstrate a strong preference for one type of sediment over another.

Behavioral mechanisms and survival-related benefits have been proposed to explain groundfish associations with bottom sediments. Most flatfish bury themselves in sediments (Walsh 1996). This behavior, which is dependent on grain size and size of the fish, presumably reduces exposure to predators, reduces physical displacement, and conserves energy (Gibson and Robb 1992). As reported for gadids (Lough et al. 1989), reduced exposure to predators may result from mottled coloration which is particularly cryptic against certain sediment backdrops (unpublished underwater video from the EBS and GOA). Although numerous studies have shown that prey organisms such as juvenile fish trade-off foraging benefits for increased safety (reviewed by Gotceitas et al. 1995), substrate-related concealment may be doubly advantageous for species that stalk or ambush their prey. Substrate specificity in flatfish and other groundfish results in habitat segregation by species, size, and sex, with apparent effects on recruitment, growth, and maturity (Scott 1982; Becker 1988; Sampson and Al-Jufaily 1999). Additional benefits may be conferred by microhabitat features that are confined to specific substrate types and hydrographic regimes (e.g., Tupper and Boutilier 1995). Because impediments to burial are unlikely for the sediment grain and fish sizes considered here, we suspect that other survival-related benefits explain the associations that we have observed.

Uneven spatial distributions, strong sediment preferences, and substrate-mediated food habits suggest that benthic-feeding species prefer certain sediment types because of adaptive differences in the availability and quality of benthic prey. Similarly, Burke (1995) concluded that spatial segregation of two estuarine flounder species was based on differences in prey distribution and food habits, which he attributed to adaptive behaviors and specific morphological differences (cf. Scott 1982; Gibson and Robb 1992; Walsh 1996). It is well known that distribution and abundance of benthic invertebrates in Alaskan waters are strongly correlated with surficial sediment properties (e.g., Stoker 1981;

Grebmeier et al. 1989). For example, deposit-feeding infauna in the Bering Sea are common in offshore areas with fine sediments and high deposition rates, while filter-/suspension-feeding groups are most common in the more turbulent coastal areas characterized by coarser sediments (Stoker 1981; Grebmeier et al. 1989). In the Chukchi Sea, epifaunal species are more common where sandy–gravelly substrates prevail and overall benthic diversity is directly related to sediment heterogeneity, or sorting (reviewed by Feder et al. 1994). Other studies confirm our findings that YFS, RS, AP, and FHS primarily consume benthic invertebrates, while ATF and GT are primarily piscivores (Yang and Livingston 1988; Pacunski 1990; Lang et al. 1995). However, these studies were not able to evaluate substrate-mediated feeding. In our case, we demonstrate that food habits of YFS, RS, and FHS vary according to sediment type, in keeping with the sediment affinities and, thus, presumed availability of their prey (e.g., Stoker 1981; Eschmeyer et al. 1983). For example, consumption of echiurids (YFS) and ophiuroids (FHS) was considerably greater in mixed sand and mud habitats, while *Spisula* clams (YFS) and Pacific sand lance (RS, YFS) were more important in sand habitats. As expected, only minor differences were observed in AP, because of its highly restricted diet (Lang et al. 1995), and in the piscivorous species with relatively weak sediment associations (ATF, GT; feeding primarily on semipelagic walleye pollock). For benthic-feeding species, habitat quality may ultimately be determined by differences in energetic costs and benefits associated with locating, capturing, and assimilating available prey. For example, FHS may prefer mixed mud and sand substrates and an energy-poor ophiuroid diet ($1.0\ \mathrm{kcal \cdot g\ dry\ weight^{-1}}$; Wacasey and Atkinson 1987), as opposed to sand areas and a walleye pollock diet ($4.0\ \mathrm{kcal \cdot g\ dry\ weight^{-1}}$; Anthony et al. 1998), because of disproportionately low foraging costs and high catchability. However, proximate composition (i.e., protein, oil, ash, and moisture content) of the prey and its seasonal variation should, among other factors, be considered in addition to raw energy density. Admittedly, our findings are only suggestive and a carefully controlled experiment is required to test the prey quality hypothesis. It is interesting to note that ophiuroids are also preferred by juvenile American plaice (*Hippoglossoides platessoides*) in the Barents Sea (Walsh 1996).

Once feature-based characterizations of habitat have been achieved, synoptic mapping can be used to establish long-term areal closures designed to protect high-quality habitats from disturbance and degradation (Fogarty and Murawski 1998; McConnaughey et al. 2000). Although prey availability is likely to be influencing flatfish distributions in the EBS, rather than surficial sediments per se, it is clearly more cost-effective to map surficial sediments as a proxy. This is because benthic fauna have inherently high spatial and temporal variability, not to mention considerable sample processing costs. However, because of the need for dedicated ship time and laboratory processing of samples, even traditional methods of collecting sediment data can be rather costly and inefficient. Moreover, broadscale mapping of sediment properties based on a limited number of samples may obscure spatial variability at biologically relevant scales. Compilations of historical data represent one option, if sufficient data are available and compatible methodologies have been used (Smith and McConnaughey 1999). More synoptic imaging with sidescan and multibeam sonars may also be appropriate, although groundtruthing with traditional methods is required and interpretation of the sonograms includes a subjective component. Another class of acoustic tool developed expressly for seabed classification operates in the background using a vessel's single-beam echosounder and statistical classification methods (e.g., Collins et al. 1996). Regardless of the seabed sampling protocol, other environmental factors such as temperature should be monitored because secondary responses may superimpose high-frequency variability on the otherwise more stable habitat associations.

Acknowledgements

The authors gratefully acknowledge G. Lang and P. Livingston for their assistance with food habits data and S. Syrjala for statistical advice. Comments by peer reviewers substantially improved the contribution.

References

Anthony, J.A., Roby, D.D., and Turco, K.R. 1998. Lipid content and energy density of forage fishes from the northern Gulf of Alaska. J. Exp. Mar. Biol. Ecol. **248**: 53–78.

Becker, D.S. 1988. Relationship between sediment character and sex segregation in English sole, *Parophrys vetulus*. Fish. Bull. U.S. **86**: 517–524.

Burke, J.S. 1995. Role of feeding and prey distribution of summer and southern flounder in selection of nursery habitats. J. Fish Biol. **47**: 355–366.

Collins, W.T., Gregory, R., and Anderson, J. 1996. A digital approach to seabed classification. Sea Technol. **37**: 83–87.

Davenport, J., and Sayer, M.D.J. 1993. Physiological determinants of distribution in fish. J. Fish Biol. **43**(Suppl. A): 121–145.

Eschmeyer, W.N., Herald, E.S., and Hammann, H. 1983. A field guide to Pacific coast fishes of North America from the Gulf of Alaska to Baja California. Houghton Mifflin Co., Boston, Mass.

Feder, H.M., Naidu, A.S., Jewett, S.C., Hameedi, J.W., Johnson, W.R., and Whitledge, T.E. 1994. The northeastern Chukchi Sea: benthos–environment interactions. Mar. Ecol. Prog. Ser. **111**: 171–190.

Fogarty, M.J., and Murawski, S.A. 1998. Large-scale disturbance and the structure of marine systems: fishery impacts on Georges Bank. Ecol. Appl. **8**: S6–S22.

Folk, R.L. 1954. The distinction between grain size and mineral composition in sedimentary rock nomenclature. J. Geol. **62**: 344–359.

Fretwell, S., and Lucas, H. 1970. On the territorial behavior and other factors influencing habitat distribution in birds. Acta Biotheor. **19**: 16–36.

Fritz, L.W., Greig, A., and Reuter, R.F. 1998. Catch-per-unit-effort, length, and depth distributions of major groundfish and bycatch species in the Bering Sea, Aleutian Islands, and Gulf of Alaska regions based on groundfish fishery observer data. U.S. Dep. Commer. NOAA Tech. Memo. NMFS-A FSC-88.

Gibson, R.N. 1994. Impact of habitat quality and quantity on the recruitment of juvenile flatfishes. Neth. J. Sea Res. **32**: 191–206.

Gibson, R.N., and Robb, L. 1992. The relationship between body size, sediment grain size and the burying ability of juvenile plaice, *Pleuronectes platessa* L. J. Fish Biol. **40**: 771–778.

Goddard, P., and Walters, G. 1998. 1994 bottom trawl survey of the eastern Bering Sea continental shelf. U.S. Dep. Commer. AFSC Processed Rep. 98-03.

Gotceitas, V., Fraser, S., and Brown, J.A. 1995. Habitat use by juvenile Atlantic cod (*Gadus morhua*) in the presence of an actively foraging and non-foraging predator. Mar. Biol. **123**: 421–430.

Gray, J.S. 1974. Animal–sediment relationships. Oceanogr. Mar. Biol. Annu. Rev. **12**: 223–261.

Grebmeier, J.M., Feder, H.M., and McRoy, C.P. 1989. Pelagic–benthic coupling on the shelf of the northern Bering and Chukchi seas. II. Benthic community structure. Mar. Ecol. Prog. Ser. **51**: 253–268.

Lang, G., Livingston, P.A., and Miller, B.S. 1995. Food habits of three congeneric flatfishes: yellowfin sole (*Pleuronectes asper*), rock sole (*P. bilineatus*), and Alaska plaice (*P. quadrituberculatus*). *In* Proceedings of the International Symposium on North Pacific Flatfish. *Edited by* B.R. Baxter. Alaska Sea Grant Rep. No. 95-04. University of Alaska, Anchorage, Alaska. pp. 225–245.

Langton, R.W., Steneck, R.S., Gotceitas,V., Juanes, F., and Lawton, P. 1996. The interface between fisheries research and habitat management. N. Am. J. Fish. Manage. **16**: 1–7.

Lough, R.G., Valentine, P.C., Potter, D.C., Auditore, P.J., Bolz, G.R., Neilson, J.D., and Perry, R.I. 1989. Ecology and distribution of juvenile cod and haddock in relation to sediment type and bottom currents on eastern Georges Bank. Mar. Ecol. Prog. Ser. **56**: 1–12.

MacCall, A.D. 1990. Dynamic geography of marine fish populations. University of Washington Press, Seattle, Wash.

Manly, B.F.J., McDonald, L.L., and Thomas, D.L. 1993. Resource selection by animals: statistical design and analysis for field studies. Chapman and Hall, London, U.K.

McConnaughey, R.A. 1995. Changes in geographic dispersion of eastern Bering Sea flatfish associated with changes in population size. *In* Proceedings of the International Symposium on North Pacific Flatfish. *Edited by* B.R. Baxter. Alaska Sea Grant Rep. No. 95-04. University of Alaska, Anchorage, Alaska. pp. 385–405.

McConnaughey, R.A., Mier, K.L., and Dew, C.B. 2000. An examination of chronic trawling effects on soft-bottom benthos of the eastern Bering Sea. ICES J. Mar. Sci. **57**: 1377–1388.

Moles, A., and Norcross, B.L. 1995. Sediment preference in juvenile Pacific flatfish. Neth. J. Sea Res. **34**: 177–182.

National Research Council. 1996. The Bering Sea ecosystem. National Academic Press, Washington, D.C.

Nichol, D.G. 1997. Effects of geography and bathymetry on growth and maturity of yellowfin sole, *Pleuronectes asper*, in the eastern Bering Sea. Fish. Bull. U.S. **95**: 494–503.

Norcross, B.L., Blanchard, A.J., and Holladay, B.A. 1999. Comparison of models for defining nearshore flatfish nursery areas in Alaskan waters. Fish. Oceanogr. **8**: 50–67.

Orr, J.W., and Matarese, A.C. 2000. Revision of the genus *Lepidopsetta* Gill, 1862 (Teleostei: Pleuronectidae) based on larval and adult morphology, with a description of a new species from the North Pacific Ocean and Bering Sea. Fish. Bull. U.S. **98**: 539–582.

Pacunski, R.E. 1990. Food habits of flathead sole (*Hippoglossoides elassodon*) in the eastern Bering Sea. M.S. thesis, University of Washington, Seattle, Wash.

Peters, D.S., and Cross, F.A. 1991. What is coastal fish habitat? *In* Stemming the tide of coastal fish habitat loss. *Edited by* R.H. Stroud. National Coalition for Marine Conservation, Savannah, Ga. pp. 17–22.

Sampson, D.B., and Al-Jufaily, S.M. 1999. Geographic variation in the maturity and growth schedules of English sole along the U.S. west coast. J. Fish Biol. **54**: 1–17.

Scherer, E. 1991. Behavioral responses as indicators of environmental alterations: approaches, results, developments. J. Appl. Ichthyol. **8**: 122–131.

Scott, J.S. 1982. Selection of bottom type by groundfishes of the Scotian Shelf. Can. J. Fish. Aquat. Sci. **39**: 943–947.

Smith, K.R., and McConnaughey, R.A. 1999. Surficial sediments of the eastern Bering Sea continental shelf: EBSSED database documentation. U.S. Dep. Commer. NOAA Tech. Memo. NMFS-AFSC-104.

Stoker, S. 1981. Benthic invertebrate macrofauna of the eastern Bering/Chukchi continental shelf. *In* The eastern Bering Sea shelf: oceanography and resources. Vol. 2. *Edited by* D.W. Hood and J.A. Calder. U.S. Department of Commerce, NOAA, Rockville, Maryland. pp. 1069–1090.

Swartzman, G., Huang, C., and Kaluzny, S. 1992. Spatial analysis of Bering Sea groundfish survey data using generalized additive models. Can. J. Fish. Aquat. Sci. **49**: 1366–1378.

Tupper, M., and Boutilier, R.G. 1995. Effects of habitat on settlement, growth and post-settlement survival of Atlantic cod (*Gadus morhua*). Can. J. Fish. Aquat. Sci. **52**: 1834–1841.

Wacasey, J.W., and Atkinson, E.G. 1987. Energy values of marine benthic invertebrates from the Canadian arctic. Mar. Ecol. Prog. Ser. **39**: 243–250.

Walsh, S.J. 1996. Life history and ecology of long rough dab *Hippoglossoides platessoides* (F) in the Barents Sea. Neth. J. Sea Res. **36**: 285–310.

Wootton, R.J., and Thorpe, J.E. (*Editors*). 1993. Factors affecting the distribution of fish. J. Fish Biol. **43**(Suppl. A).

Yang, M.S., and Livingston, P.A. 1988. Food habits and daily ration of Greenland halibut, *Reinhardtius hippoglossoides*, in the eastern Bering Sea. Fish. Bull. U.S. **86**: 675–690.

Estimability of natural mortality and other population parameters in a length-based model: *Pandalus borealis* in Kachemak Bay, Alaska

Caihong Fu and Terrance J. Quinn II

Abstract: Because stock-assessment models have become more complex, the question of estimability of population parameters is important. We conducted simulation-estimation experiments with a length-based model of the pink shrimp (*Pandalus borealis* Krøyer) population in Kachemak Bay, Alaska, to compare the robustness of various modeling approaches to specifications of natural mortality (M), catchability (q), a survey gear selectivity parameter (L_{50}), and data imprecision. Our goal was to determine the estimability of various parameters, particularly M, q, and L_{50}. Simulation results suggest that interannual variations in M and L_{50} could be estimated, if the underlying values have a trend over time. However, parameter q should be fixed at a chosen value, even when it varies over time. Estimated M for the Kachemak Bay *P. borealis* population increased in the 1980s, perhaps owing to increased predation mortality by groundfish.

Résumé : À mesure que les modèles d'évaluation des stocks se complexifient, le problème de l'estimation des paramètres démographiques devient plus critique. Des expériences de simulation et d'estimation à l'aide d'un modèle basé sur les longueurs d'une population de Crevettes nordiques, *Pandalus borealis* Krøyer, dans la baie de Kachemak, Alaska, ont permis de comparer la robustesse de différentes approches de modélisation dans la description de la mortalité naturelle (M), de la probabilité de capture (q), de la sélectivité des engins de pêche utilisés dans l'inventaire (L_{50}) et de l'imprécision des données. Nous voulions déterminer dans quelle mesure les divers paramètres, particulièrement M, q et L_{50}, peuvent être estimés correctement. Les résultats de la simulation laissent croire que les variations annuelles de M et de L_{50} peuvent être estimées si les valeurs sous-jacentes affichent une tendance dans le temps. Cependant, le paramètre q doit être fixé à une valeur choisie, même s'il varie dans le temps. Le paramètre M estimé chez la population de *P. borealis* de la baie de Kachemak a augmenté au cours des années 1980, probablement à cause d'une mortalité plus élevée due à la prédation par les poissons démersaux.

[Traduit par la Rédaction]

Introduction

Stock-assessment models have become increasingly complex to accommodate the variety of available information (Quinn and Deriso 1999). Current models are most often age- and (or) length-based and integrate frequency data from fisheries and surveys, independent estimates of relative or absolute abundance or biomass, and catch data. Increasingly, models include additional parameters for autocorrelation and for temporal, spatial, and environmental effects, using the AD model builder (ADMB) methodology (Fournier 1996). For example, the age-based stock-assessment model for walleye pollock (*Theragra chalcogramma*) in the eastern Bering Sea contains thousands of observations and 637 parameters (Ianelli et al. 1999).

Consequently, the question of estimability or, equivalently, optimal model complexity, in these models is one that is only now receiving serious attention. Theoretically, adding parameters to a model should at first reduce bias by more correctly conforming to the true underlying model structure (Burnham and Anderson 1999). The tradeoff is that variance or uncertainty in the parameter estimates increases by attempting to obtain more estimates from the same amount of information. At some point, additional parameters and (or) model structure are either redundant or mis-specify the true structure, creating an increase in bias and uncertainty. The question of how much detail should be included in a model is difficult to answer without carrying out extensive simulations.

Monte Carlo simulation has frequently been used to determine model robustness to mis-specification in error structures (Kimura 1990; Myers and Cadigan 1995*a*). Yet, there is very little research that is devoted to examining the consequences of model mis-specification in parameter structure. For instance, no simulation study concerning mis-specification of natural mortality (M) has been published, in spite of its vital role in population dynamics. In length-based stock-assessment models, such as those of Sullivan et al. (1990),

Received January 18, 2000. Accepted October 25, 2000. Published on the NRC Research Press web site on December 20, 2000. J15529

C. Fu[1,2] and T.J. Quinn II. Juneau Center, School of Fisheries and Ocean Sciences, University of Alaska, 11 120 Glacier Highway, Juneau, AK 99801-8677, U.S.A.

[1] Corresponding author.

[2] Present address: Department of Fisheries and Oceans, Bedford Institute of Oceanography, Marine Fish Division, P.O. Box 1006, Dartmouth, NS B2Y 4A2, Canada (e-mail: fuC@mar.dfo-mpo.gc.ca).

Parma and Deriso (1990), and Quinn et al. (1998), M is assumed to be known or constant over time. It is well known that M is confounded with other parameters, such as catchability (q), fishing mortality (F), and recruitment (R) (Schnute and Richards 1995), which make its estimation difficult. However, it is commonly agreed that M varies largely over time, particularly for juveniles, forage fish, and invertebrates, owing to predation. For example, Zheng et al. (1995) found that M of the Bristol Bay (Alaska) red king crab (*Paralithodes camtschaticus*) was three to six times higher in the early 1980s than during other periods. Assessment scientists often propose that the parameter q be estimated (Quinn and Deriso 1999). A previous simulation study indicated that it was difficult to estimate q even when it was constant (Fu 2000). In addition, the selectivity of survey gear may change over time, which can induce biased parameter estimates (National Research Council 1998).

With respect to the above concerns, we focus in this paper on exploring the sensitivities of a length-based assessment model (Quinn et al. 1998) to the specification of population parameters, by doing simulation-estimation experiments. In particular, we examine the specification of M, q, and survey-gear selectivity, in conjunction with uncertainty in the data. Our goals are to determine the estimability of various population parameters, especially M, by comparing the robustness of various modeling approaches to model specifications, and to apply an optimal approach to a *Pandalus borealis* Krøyer population in Kachemak Bay, Alaska, for a better understanding of its dynamics.

Pandalus borealis, commonly called northern or pink shrimp, an important circumboreal species, occurs in both the Pacific and Atlantic oceans. Owing to the lack of age structures, great efforts have been made to interpret age, growth, and mortality from length frequency distribution data (Parsons et al. 1989; Terceiro and Idoine 1990; Fournier et al. 1991). Nevertheless, analyses of population dynamics are hindered by the lack of comprehensive knowledge of fundamental population processes, including recruitment, natural mortality, and sex change. These uncertainties have caused severe difficulties in regulating fishing effort on a scientific basis (Aschan and Godø 1999). One step to improve population assessments is to develop length-based models to incorporate these processes. The length-based model in Quinn et al. (1998) is desirable for investigating the dynamics of *P. borealis* populations, because it provides flexibility in considering specific life features in recruitment, growth, and death.

The *P. borealis* population in Kachemak Bay was harvested intermittently, with small landings in the 1950s and 1960s. Since 1971, several trawl surveys have been carried out to obtain population-biomass estimates, and the fishery was managed according to a catch quota. The catch increased to 2600 metric tons (t) in 1970 and remained near that level until the early 1980s (Davis 1982). Catch in 1983 decreased by almost an order of magnitude, owing to reduced population abundance, and the fishery was closed after 1986, owing to continued low stock size (Gustafson 1994).

Along with this *P. borealis* population, many other crustacean stocks in Alaskan waters, for example, red king crab on the shelf around Kodiak Island, were depleted around the same period (Orensanz et al. 1998). The serial depletion cannot be explained simply as a result of overfishing, because some lightly or seldom fished *P. borealis* populations experienced similar declines (Anderson 1991). A simulation study with the Kachemak Bay stock indicated that no alternative harvest strategies could have changed the population's fate of collapse (Fu et al. 1999). Rather, the simulation suggested that M was the most important factor controlling population dynamics, and high M may have resulted in the collapse of the population in the 1980s. Thus, applying a more realistic population-dynamics model with some time-varying parameters may produce better parameter estimates and give a better rationale for the population's decline.

Methods

Data and population model

Data from the Kachemak Bay *P. borealis* population were provided by the Alaska Department of Fish and Game (ADF&G). They include biomass estimates and carapace length frequency data from spring surveys from 1978 to 1991 and commercial yield from 1978 to 1986.

The length-based model of Quinn et al. (1998) follows each cohort from recruiting age r to maximum age A. Since detectable amounts of *P. borealis* in Kachemak Bay become available to trawl gear at age 1, $r = 1$. In this paper, A is specified at 6, corresponding to A for the *P. borealis* population in Kachemak Bay (Davis 1982). During the initial period of A years for which no observations are available, there are A initial-recruitment parameters (R'), and $A - 1$ initial natural mortality (M') and fishing-mortality (F') parameters. Simulation experiments indicated that M' and F' could be specified at some constant and reasonable values, but that R' had to be estimated for each of the initial years (Fu 2000). Thus, M' and F' were set at 0.4 and 0.3, respectively, for each of the initial years. Other parameters during the initial period are assumed to be identical to those in the subsequent years of the model.

Observations are made starting at time $A + 1$. Somatic growth is assumed to be time independent, with parameters including von Bertalanffy L_∞ (the asymptotic length), κ (a curvature parameter governing the speed to approach the asymptote L_∞), σ (the deviation from the growth model), and σ_r (the deviation of the length-frequency normal distribution at age r). The parameters of a logistic gear-selectivity function, γ (the shape parameter) and L_{50} (the length at which 50% of the individuals are vulnerable to fishing), are estimated in the model. Other parameter estimates include time-dependent annual recruitment (R_t), natural mortality (M_t), full recruitment fishing mortality (F_t), and mean length at recruitment ($\mu_{r,t}$). The overall estimation is improved significantly when $\mu_{r,t}$ varies over time, but for simplicity, no results on $\mu_{r,t}$ are given in this paper. A detailed description of model specifications is given in the Appendix.

Parameter estimation was accomplished using the software ADMB, which estimates parameters in a step-by-step fashion known as a multiphase procedure (Fournier 1996). Specifically, interannual variation of the logarithm of M_t was modeled as the time-series structure of a random walk: $\ln(M_{t+1}) = \ln(M_t) + \delta_t$, where δ_t is the deviation term.

Parameters were estimated using nonlinear least-squares (NLS). Kimura (1990) demonstrated, with Monte Carlo simulations, that the NLS is robust to error structure in the data, such as multinomial catch-at-age data, and could be expected to find parameter estimates much more rapidly than multinomial maximum likelihood (MML) (e.g., Fournier and Archibald 1982). Therefore, the following objective function is minimized for estimating parameters:

Table 1. Parameter values estimated from Fu et al. (1999) for constructing simulated data, including spawner-recruitment (α, β), growth (L_∞, κ, σ, σ_r), and selectivity (L_{50}, γ) parameters.

Parameter	Value
α	1.225
β	0.0015
L_∞	24.582
κ	0.370
σ	0.522
σ_r	1.124
L_{50}	16.589
γ	0.577

$$(1) \qquad f = \lambda_B \sum_t \left(\sqrt{B'_t} - \sqrt{B_t}\right)^2 + \lambda_L \sum_t \sum_l \left(\sqrt{\mathrm{LF}'_{t,l}} - \sqrt{\mathrm{LF}_{t,l}}\right)^2 + \lambda_Y \sum_t \left(\sqrt{Y'_t} - \sqrt{Y_t}\right)^2 + \lambda_M \sum_t \delta_t^2$$

Variables B'_t, $\mathrm{LF}'_{t,l}$, and Y'_t denote observed values of survey biomass, surveyed length frequency, and commercial yield, respectively, while B_t, $\mathrm{LF}_{t,l}$, and Y_t denote corresponding predicted values from the model. Square-root transformation is desirable, to reduce the contrast in the magnitude of different data sources (Quinn et al. 1998). A logarithmic transformation was also investigated, but results were quantitatively similar and so are not presented. The weighting factors λ_B, λ_L, and λ_Y for the observations were set to be proportional to the inverse of the empirical variances of transformed data sets without regard to the model deviation. A better approach is to derive the variance from the sampling (Kimura 1990), which is beyond the scope of this paper. However, previous simulation results indicated that there were only slight differences among different weightings (Fu 2000).

The term $\lambda_M \sum_t \delta_t^2$ is a penalty term controlling the degree of variability in the time series of M estimates from year to year. A large value of λ_M makes the interannual deviations of M small and vice versa. Experiments with different M trends, including constant M over time, indicated that the most appropriate λ_M value was independent of the intrinsic variations in M, but was directly related to the measurement error in biomass data (Fu 2000). One empirically optimal λ_M value is calculated as the product of the coefficient of variation (CV) for biomass data and half of the empirical variance of the transformed biomass data, while keeping λ_B to be scaled to unity.

Simulation-estimation experiments

Simulation-estimation experiments were conducted to evaluate model performance under various circumstances. Uncertainties in the process of recruitment were incorporated to generate simulated data with 14 years of survey and catch data in accord with the actual observations analyzed later. Each R was generated by imposing a log-normal error with a CV of 50% upon a Beverton–Holt spawner–recruit relationship, $R = \dfrac{\alpha S}{1 + \beta S}$. Instantaneous fishing mortality (F) for fully recruited individuals was set as constant over time, with a value of 0.3. Values of other deterministic parameters for constructing simulated data (Table 1) were taken from Fu et al. (1999).

Uncertainties in the measurement of the variables B'_t, $\mathrm{LF}'_{t,l}$, and Y'_t were incorporated in the simulated data. Because our purpose is to compare the relative robustness of modeling approaches to measurement error (ME) in different data sets, we use the same type and level of ME (log-normal error, CV = 0.4) for B'_t, $\mathrm{LF}'_{t,l}$, and Y'_t, whenever measurement is subjected to error. These values are substantially higher than those determined empirically for Kachemak Bay *P. borealis* (see below), but we use larger values to assure the robustness of the simulation results. We further assume, for simplicity, that errors are independent, but acknowledge the possibility of autocorrelated measurement errors in the discussion section.

For each scenario, 50 replicates of simulated data were generated, corresponding to 50 sets of random recruitment. The same random seed was used for each scenario and for all data sets, so that the parameter estimates are comparable when certain conditions are changed. Each generated data set was put into the parameter-estimation procedure.

Within the simulation realm with all parameters known, estimation results of various scenarios were calculated in the form of bias ratios, i.e., as the ratios of estimated to true parameter values on $\log_2$ scale. Thus, a value of 0.0 indicates unbiased estimation, while a value of 1.0 stands for twofold overestimation and a value of −1.0 for twofold underestimation (Schnute and Richards 1995). If there is a significant linear trend over time in an estimated parameter such as natural mortality, the average bias ratio is near 0 when estimated natural mortality is close to the true value in the middle of the time series. However, we wish to have a criterion that is large in this circumstance. For simplicity, we further calculated mean absolute deviations (MADs), by taking the absolute values of the bias ratios and averaging them over time. The MAD is thus a combined measure of bias and variability across time for each parameter. (For scalar parameters, MAD is simply the absolute value of the single bias ratio.) The MADs from the 50 replicates were displayed using box plots, and then graphically compared among modeling approaches and different levels of ME in B'_t, $\mathrm{LF}'_{t,l}$, and Y'_t. To test for differences between two modeling approaches, we statistically compare MADs with the nonparametric Wilcoxon's rank-sum test at the significance level $\alpha = 0.05$. This test is also appropriate for comparing the effects of ME from different data sets.

Parameter estimation for *P. borealis*

With the actual data from the *P. borealis* population, variances in square rooted biomass, length-frequency, and yield data were estimated as 269, 63, and 238, respectively; therefore, the values 1.0, 4.3, and 1.1 were assigned to the weights λ_B, λ_L, and λ_Y, respectively, proportional to the inverse of their empirical variances. The estimated CV for survey-biomass estimates averaged over the years 1977–1990 is 23% (Gustafson 1994). We approximated it as 20%, and the value of λ_M was set at 26.9, using the empirical method described earlier. The bootstrap method (Efron and Tibshirani 1993) was used to estimate standard errors (SEs) for the parameter estimates and the predicted biomass and yield. Bootstrap data were calculated as $O_t^B = \left(r_{t'}^{\mathrm{sqrt}} + \sqrt{P_t}\right)^2$, where $r_{t'}^{\mathrm{sqrt}}$ denotes sampled residuals and P_t denotes predicted values. Owing to extremely lengthy calculations, only 500 replicates were conducted, and SEs were calculated as the standard deviations of the 500 replicates. Retrospective analysis was employed to evaluate the ability of the model to estimate parameters for the terminal year. We carried out the analysis by leaving out 1 year's data at a time. Weights (λs) were obtained using the same rule described above.

Results

Simulation-estimation experiments

Natural mortality

Understanding the estimability of M is our primary goal. Two modeling approaches are compared: (1) estimating one

Fig. 1. Box plots of mean absolute deviations (MADs) of estimated parameters for two modeling approaches within each panel: (1) estimating one constant *M*; (2) estimating *M* for each year. The underlying true *M* is constant at 0.5. The columns show results from different measurement-error (ME) conditions, including no ME in all data, ME only in B'_t ($\mathrm{CV}_B = 0.4$), ME only in $\mathrm{LF}_{t,l}$ ($\mathrm{CV}_L = 0.4$), ME only in Y'_t ($\mathrm{CV}_Y = 0.4$), and ME in all data (CV = 0.4). Boxes illustrate the interquartile range (25–75% quantiles); lines outside the whiskers represent extreme individual values.

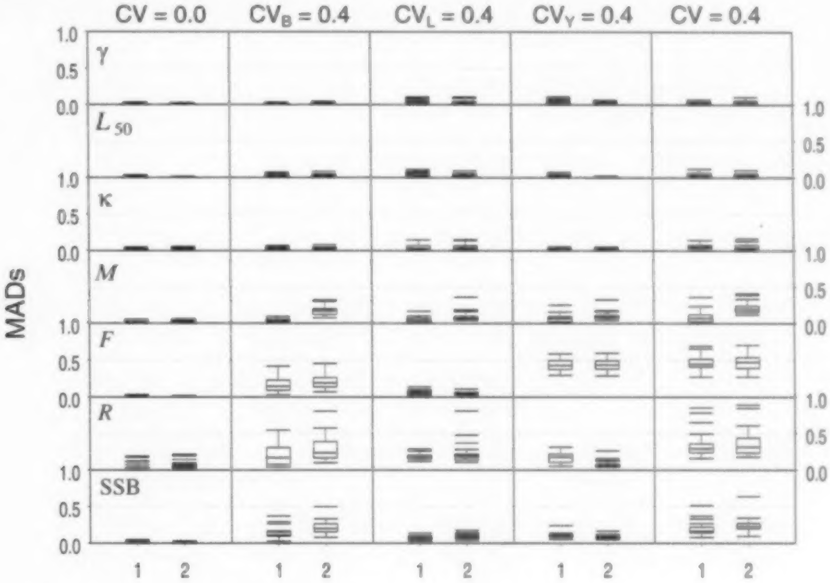

constant *M*; (2) estimating interannual variations in *M*. To determine if one approach is better than the other, they were both carried out under two situations: (1) the underlying true *M* is constant at 0.5 over time; (2) the underlying true *M* is 0.3 for years 1–3, 0.5 for years 4–7, and increases by 0.05 per year later on. The two approaches are compared under five ME conditions: (1) no ME in all data sets; (2) ME only in B'_t; (3) ME only in $\mathrm{LF}'_{t,l}$; (4) ME only in Y'_t; (5) ME in all data sets.

With the underlying *M* being constant at 0.5, the MADs from the two approaches are nearly identical when there is no ME in all data (Fig. 1). Only recruitment, which has random variability over time, has high MADs occasionally. With other levels of ME, MADs for *M* from approach 1 are significantly lower than those from approach 2. For other parameters, such as spawning-stock biomass (SSB) and *R*, the MADs are also generally smaller with approach 1. Thus, with underlying constant *M*, estimating *M* for each year should be avoided. The MADs for *F* from the two approaches are not significantly different from each other. Rather, the *F* estimates are more influenced by the ME levels, being very sensitive to the ME in Y'_t, but fairly robust to those in $\mathrm{LF}'_{t,l}$. On the other hand, the estimates of SSB and *R* are more sensitive to ME in B'_t, but relatively more robust to those in $\mathrm{LF}'_{t,l}$ and Y'_t.

When the underlying *M* varies over time, MADs are almost always significantly lower with approach 2, in which *M* was estimated for each year (Fig. 2). The only exception is for *F* when Y'_t is subject to ME, in which case the two MADs are not significantly different. Therefore, if *M* does vary over time, estimating interannual variations in *M* is desirable.

Catchability

Survey biomass is related to population biomass by the catchability (*q*) of the research gear. The parameter *q* is closely correlated with *M*. Fu (2000) demonstrated that *q* could not be estimated with sufficient accuracy along with *M* even when the underlying *q* was constant over time. Some research favors estimating *q* while assuming that *M* is known (Quinn and Deriso 1999) to accommodate the potential variability in *q*. Other research suggests estimating *M* while keeping *q* fixed at a chosen value (Zheng et al. 1995). We compared four modeling approaches in the situation with a constant *M* of 0.5 and a declining *q* over three time periods (1.0 for years 1–3, 0.8 for years 4–7, and 0.6 for the years afterwards): (1) estimating one constant *M* and fixing *q* at 1.0; (2) estimating *M* for each year and fixing *q* at 1.0; (3) estimating one constant *M* for all years and *q* for each year; (4) fixing *M* at 0.4 and estimating *q* for each year. The reason for setting *M* at an incorrect value in approach 4 is to represent the mis-specification that probably occurs when choosing a fixed value. These four approaches are compared under five conditions of ME (as in Natural mortality, above).

The most outstanding conclusion from these experiments is that approach 4 is the least favored one. The MADs for parameters SSB, *R*, and *F* are generally beyond 1.0, so we did not bother to graph them. Even with *M* fixed at the correct value, the MADs for these parameters are not substantially reduced. For the *M* estimates, the MADs from approach 1 are significantly smaller than those from approach 2 (Fig. 3), a result that is consistent with those of previous sections. Furthermore, approach 3, which estimates one constant *M* and annual *q*, resulted in even smaller MADs. Therefore, in terms of the accuracy of *M* estimates, the best approach is to

Fig. 2. Box plots of mean absolute deviations (MADs) of estimated parameters for two modeling approaches within each panel: (1) estimating one constant M; (2) estimating M for each year. The underlying true M varies over time and has an increasing trend. The columns represent results from different measurement-error (ME) conditions, including no ME in all data, ME only in B'_t ($CV_B = 0.4$), ME only in $LF_{t,l}$ ($CV_L = 0.4$), ME only in Y''_t ($CV_Y = 0.4$), and ME in all data ($CV = 0.4$).

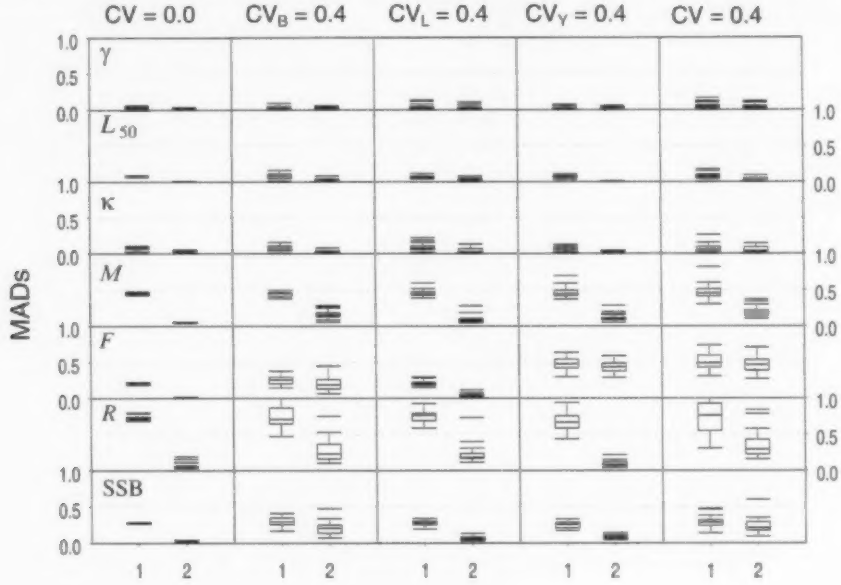

Fig. 3. Box plots of mean absolute deviations (MADs) of estimated parameters for three modeling approaches within each panel: (1) estimating one constant M and fixing q at unity; (2) estimating M for each year and fixing q at unity; (3) estimating one constant M and estimating q for each year. The underlying true M is constant at 0.5, but q decreases over three time periods.

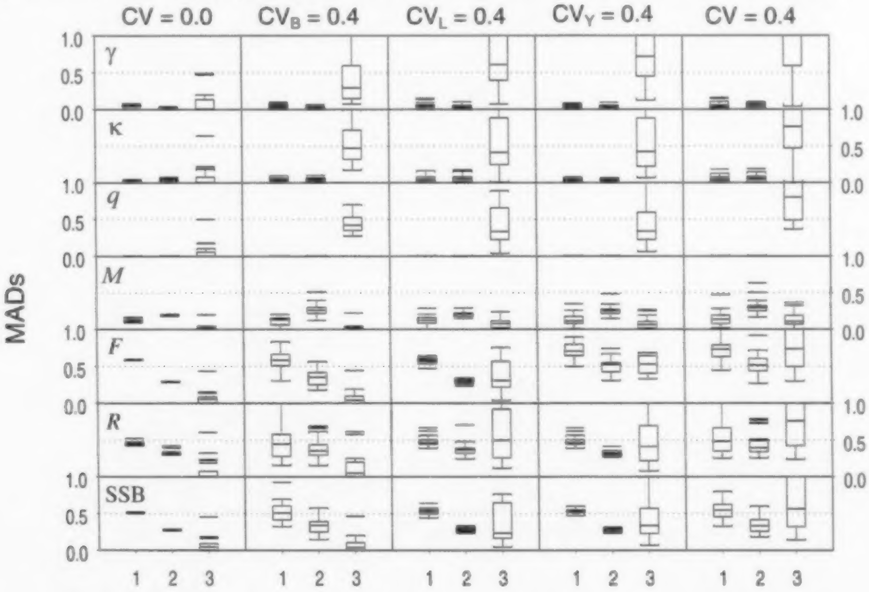

model M and q in accord with the underlying processes; that is, whether or not time variation really occurs. On the other hand, the estimates of SSB, R (except when ME exists in B'_t), and F from approach 2 have significantly smaller MADs than those from approach 1, which implies that estimating M annually can help alleviate the negative effects from q variability in parameter estimation. For further insight, the annual values of the estimated bias ratios of SSB, R, F, M, and q for each year from approach 2 under the condition of no ME are shown in column 1 of Fig. 4. Fixing q

Fig. 4. Box plots of bias ratios for the annual estimates of SSB, *R*, *F*, *M*, and *q* (first column) or L_{50} (second column). There is no measurement error (ME) in all data. The first column displays the results from the approach that estimates one constant *M* for all years but *q* for each year, with an underlying true *M* of 0.5 and *q* of varying value. The second column shows the results from the approach that estimates one constant *M* for all years but three values of L_{50} for three periods, with an underlying true *M* of 0.5 and L_{50} of varying value.

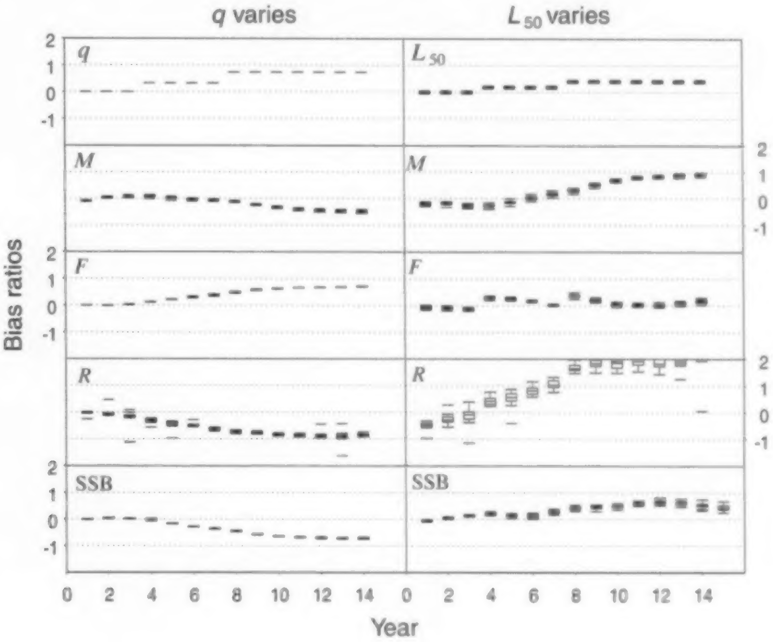

while the underlying *q* decreases to 0.6 causes underestimation of SSB, *R*, and *M*, but overestimation of *F*. The performance of approach 3, in contrast, is more affected by the ME conditions. When no ME exists in $\mathrm{LF}'_{t,l}$ and (or) Y'_t, except for a few cases, approach 3 is significantly superior to the other two in terms of the estimation of SSR, *R*, *F*, and *M*. Otherwise, approach 3 is not favored, since it produces higher MADs in the estimation of all parameters except *M*.

Gear selectivity

Changes in gear selectivity, or sometimes just the availability of younger individuals, may cause mis-specification of the selectivity parameters in stock-assessment models with constant selectivity parameters over time. To examine the consequences of different modeling approaches, we let L_{50} decrease over three time periods (16.0 mm for years 1–3, 14.0 mm for years 4–7, and 12.0 mm for the years afterwards) and set *M* at a constant value of 0.5. In addition, we also wished to see if estimating *M* could compensate the variability in L_{50} as it does that in *q*. Thus, we compared three modeling approaches: (1) estimating *M* for each year, but with one constant L_{50} for all years; (2) estimating one constant *M*, but with three levels of L_{50} for three distinct periods; (3) estimating *M* for each year, but with three level of L_{50} for three distinct periods. We also investigated the alternative of estimating L_{50} for each year. Because there is very little difference between estimating L_{50} for each year and estimating L_{50} for the three distinct periods, only results from the latter are presented here. The three approaches are compared under five ME conditions.

Even without ME in all data sets, approach 1, that of estimating *M* for each year but with only one constant L_{50} for all years, induces large bias ratios, particularly those for *R* (column 2, Fig.4). Estimating only one L_{50} for all years causes L_{50}, *M*, *R*, and SSB to be overestimated. In comparison, the estimates of *F* are the least affected by the mis-specification of L_{50}. Except for *F*, all the other parameters have significantly greater MADs using approach 1 than when using the other two approaches, regardless of ME conditions (Fig. 5). It is obvious that, when L_{50} varies over time, the best modeling approach is to explicitly model the L_{50} variability. Approach 3, that of estimating *M* for each year, resulted in generally greater MADs than approach 2, which suggests that estimating *M* annually cannot compensate for the variability in L_{50} and is not desirable when the underlying *M* is constant. Again, the *F* estimates are more affected by ME in Y'_t than by the different approaches.

Examining a more difficult situation, we let *M* increase at the same time as L_{50} decreased. Approaches 1 (estimating annual *M* for each year but with one constant L_{50} for all years) and 2 (estimating one constant *M* for all years but with L_{50} for each year) generated no significant difference in MADs for SSB, particularly when B'_t is subject to ME (Fig. 6). However, there were significant differences in the other parameters. Approach 3 (estimating *M* for each year and L_{50} for three distinct periods) greatly reduced MADs for all

Fig. 5. Box plots of mean absolute deviations (MADs) of estimated parameters for three modeling approaches within each panel: (1) estimating M for each year and one constant L_{50} for all years; (2) estimating one constant M and three levels of L_{50} for three distinct periods; (3) estimating M for each year and three levels of L_{50} for three distinct periods. The underlying true M is constant at 0.5; L_{50} decreases over three time periods.

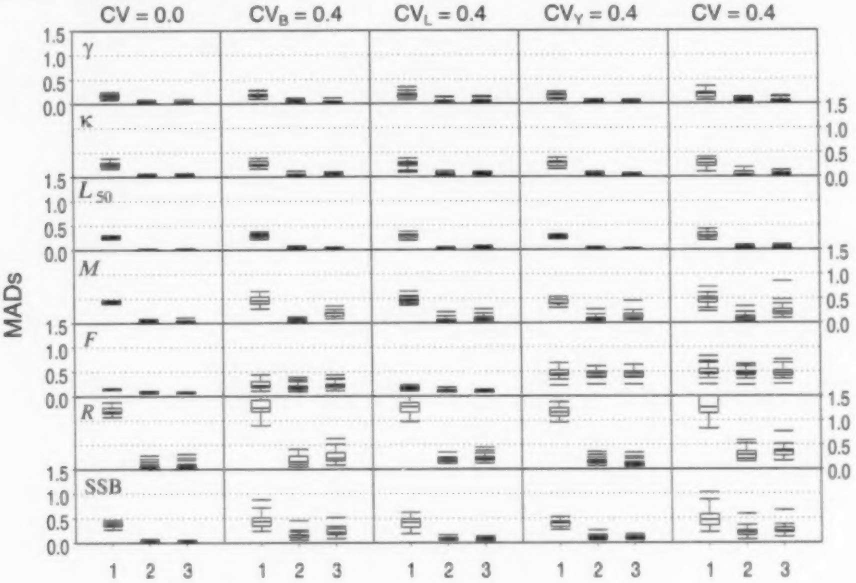

Fig. 6. Box plots of mean absolute deviations (MADs) of estimated parameters for three modeling approaches within each panel: (1) estimating M for each year and one constant L_{50} for all years; (2) estimating one constant M for all years and three levels of L_{50} for three distinct periods; (3) estimating M for each year and three levels of L_{50} for three distinct periods. The underlying true M varies over time and has an increasing trend; L_{50} decreases over three time periods.

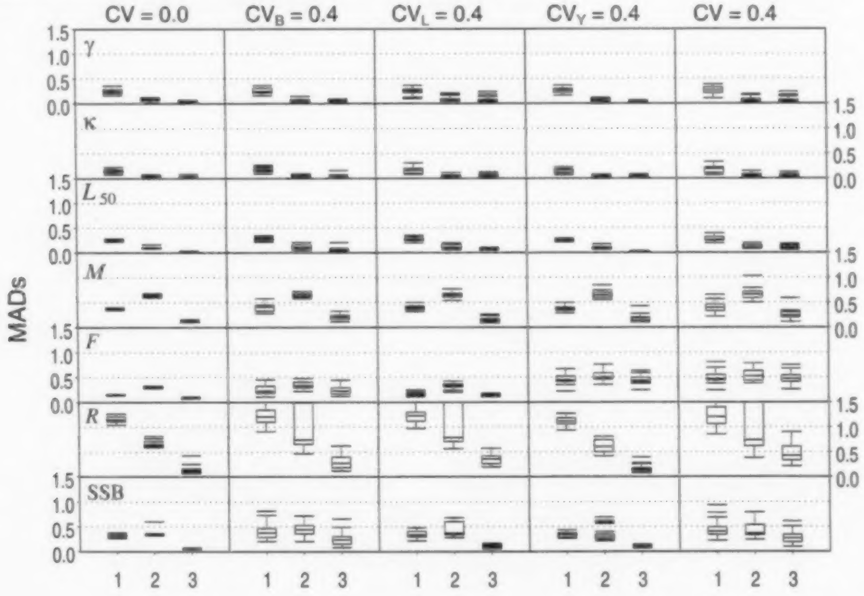

parameters. Thus, modeling M variability reduces MADs for M significantly, and further modeling the variability in L_{50} improves the M estimates even more. Again, the F estimates are more sensitive to ME in Y'_t than to other MEs, and the

Fig. 7. Plots of estimated (*a*) *M*, (*b*) *F*, and (*c*) *R* and (*d*) observed and predicted biomass (*B*; line with circles) and yield (*Y*; line with ×) (*d*). Panel *a* also shows cod-occurrence frequency in abundance (line with ×) obtained from the same spring surveys in Kachemak Bay. The bars are estimates of SEs (±1 SE).

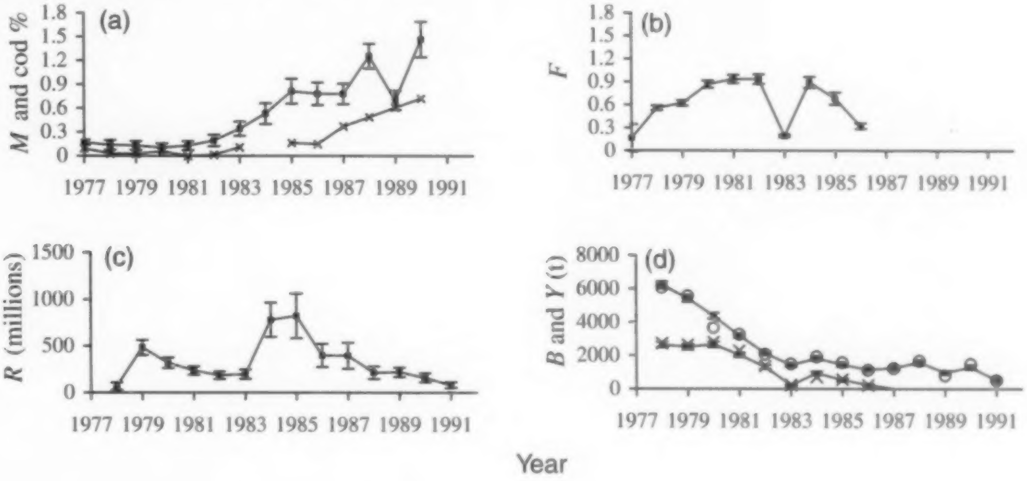

MADs from different approaches are not significantly different when ME exists in Y'_t. In contrast, *R* estimates are more affected by the modeling approaches. Specifying L_{50} correctly is important for getting good *R* estimates. The overall recommendation is that *M* and L_{50} need to be modeled correctly if they vary over time in a directional manner.

Overall, considering the most realistic situation, that of ME existing in all data sets, a good modeling approach should be one that explicitly models the time-varying processes of *M* and selectivity when they exist. However, the variability in *q* should not be modeled explicitly; instead, we recommend estimating *M* over time, while assuming some constant and conservative value of *q*.

Parameter estimation for *P. borealis*

The results from simulation experiments indicate that it is desirable to estimate interannual variations in *M* when *M* varies over time, particularly when there is a long-term trend. It is believed that *M* for *P. borealis* in Kachemak Bay started increasing in the 1980s, owing to the increasing predation by several groundfish species, including Pacific cod (*Gadus macrocephalus*; Gustafson 1994). Therefore, we estimated annual variations in *M* in the length-based population model for Kachemak Bay *P. borealis*. Because of the inability to estimate *q* when ME is present in $LF'_{t,l}$ and (or) Y'_t, we specified *q* at 1.0 to avoid possible large biases in parameter estimates. The value of 1.0 was chosen with the assumption that the trawl surveys conducted by ADF&G had 100% net efficiency (Gustafson 1994). Because this trawl survey may not be fully selective, we consider this assumption to be conservative. While the simulation study in the previous section suggests estimating selectivity parameter L_{50} for each year if this parameter varies over time, we do not have any additional information to determine whether this might have occurred (but discuss some spatial considerations below). Therefore, we still assume constant selectivity parameters in the model.

The estimates of parameters *R*, *M*, and *F* and their SEs were obtained from the bootstrap procedure (Fig. 7). Predicted length frequencies fit the observations well (Fig. 8). The estimates of growth and selectivity parameters and their SEs are given in Table 2 (the first row).

During the 1980s, the estimated *M* values show a strong increasing trend that almost parallels estimates of cod abundance obtained during the same surveys (Bechtol 1997) (Fig. 7). We suspect that the decline in *P. borealis* abundance may have resulted from intensified predation by Pacific cod and other groundfish species. The *R* estimates have a small peak in 1979 and a larger peak in the years 1984 and 1985. Field observations indicated a rebound of biomass in 1985 and 1986, mainly due to small male shrimp (Gustafson 1994). These observations agree with the estimated recruitment peaks for 1984 and 1985, given a 1-year lag from recruitment to the population at age 1 to being largely available to the fishing gear at age 2. Furthermore, despite the 2-year rebound in recruitment, the *P. borealis* population was not able to rebuild, which could be explained well by the high consumption by predators. Albers and Anderson (1985) also concluded, after studying the diet of Pacific cod in Pavlof Bay, Alaska, that the high consumption of shrimp by cod may have prevented the shrimp population in that area from rebuilding.

In general, the retrospective analysis shows that the model is able to estimate the most recent parameters well. For instance, the removal of data from 1 or 2 years (data 1990 or data 1991; see Table 2) has little effect on the estimates of *R* and *M* (Fig. 9). However, when data are available only until 1987 or 1986, the estimates of terminal *R* tend to be lower than when more data are available. The dramatic decline of *R* in 1986 may have contributed to the discrepancies in terminal *R* estimation. In contrast, the terminal estimates of *M* and *F* tend to follow the actual trend well, and so they are likely to be reliable. We can also anticipate that the estimation of terminal *R* will be reasonable, if there is no abrupt shift in recruitment 1 or 2 years before. The estimates of

Fig. 8. Comparisons of observed (symbols) and predicted (lines) length frequency distributions (LFDs) from 1978 to 1991.

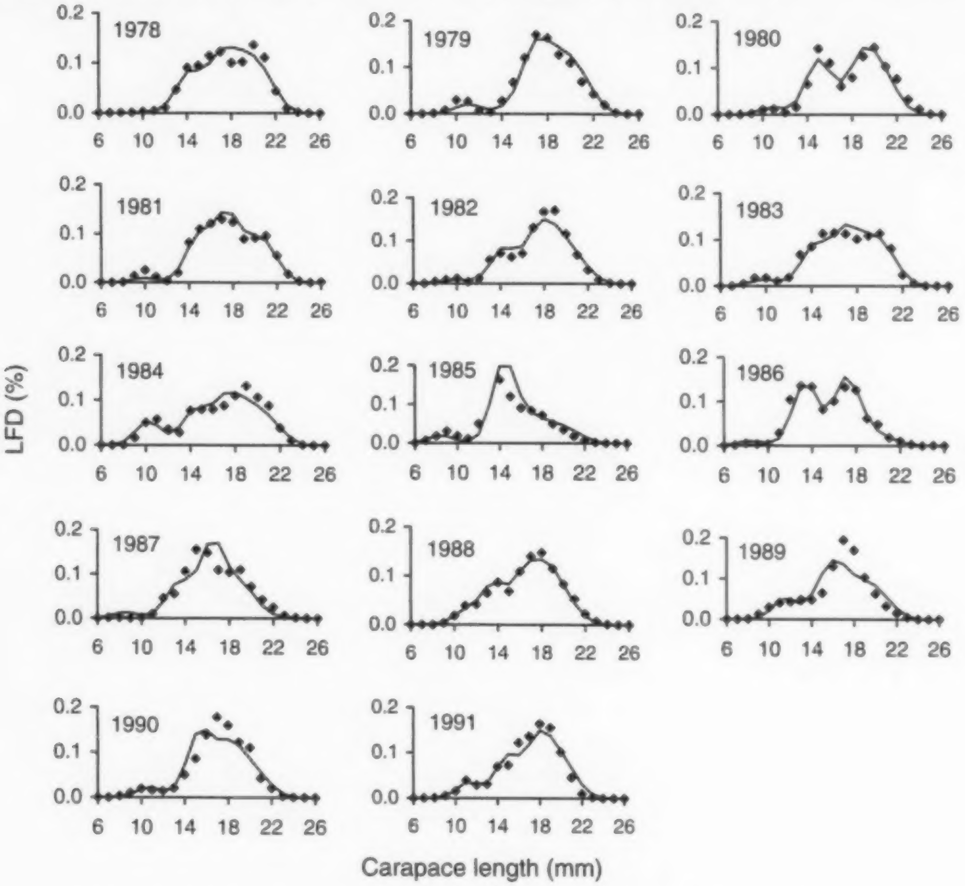

Table 2. Estimates of growth (L_∞, κ, σ, σ_r) and selectivity (L_{50}, γ) parameters from the full and reduced data sets.

	L_∞	κ	σ	σ_r	L_{50}	γ
Data 1991	23.80±0.36	0.39±0.02	0.62±0.06	1.12±0.06	15.50±0.33	0.61±0.02
Data 1990	23.98	0.38	0.60	1.12	15.50	0.61
Data 1989	24.18	0.37	0.59	1.08	15.46	0.61
Data 1988	24.22	0.36	0.61	1.01	15.27	0.61
Data 1987	24.42	0.35	0.58	1.01	15.54	0.58
Data 1986	24.56	0.35	0.55	1.02	15.84	0.57
Data 1985	24.51	0.36	0.56	1.02	15.80	0.58
Data 1984	23.95	0.40	0.63	0.98	15.97	0.55
Data 1983	24.25	0.39	0.61	0.98	16.01	0.57

Note: Data 1991 indicates the use of data for 1978–1991.

growth and selectivity parameters from the reduced data sets are also given in Table 2. The estimates show only little variation across different year ranges.

Discussion

Simulation-estimation experiments were conducted to specifically compare the performances of different modeling approaches corresponding to different underlying structures of *M*, *q*, and L_{50} and different levels of ME in various data sets. Three major conclusions or recommendations were reached. (1) This is the first stock-assessment study targeted at estimating interannual variations in *M*. We conclude that parameter *M* should be estimated each year when there is a pronounced time trend in *M*. Although estimating *M* for each year is not favored when *M* is constant over time, we agree with Schnute and Richards (1995) that realistic analyses must take account of uncertainty in *M*. (2) Interannual

Fig. 9. Comparisons of estimates of (*a*) *R* (in millions), (*b*) *M*, and (*c*) *F* from the full data sets with those from reduced data from which data for the last 1, 2,..., 8 years has been removed.

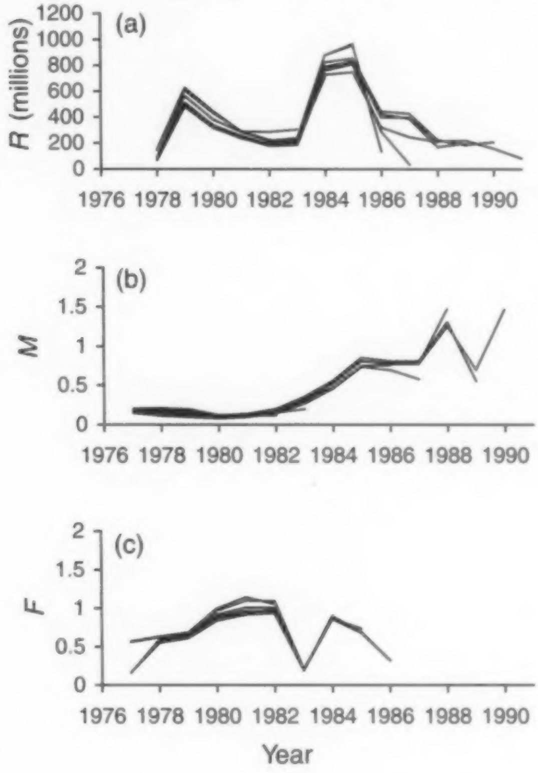

variations in *q* should not be estimated when large MEs occur in $LF'_{t,l}$ and (or) Y'_t data, even if the underlying *q* largely varies over time. Estimating *q* for each year can result in huge MADs in parameter estimates, even when *M* is correctly assumed. A better alternative for coping with time-varying *q* is to estimate *M* for each year while keeping *q* fixed at certain level. (3) The gear-selectivity parameter L_{50} should be estimated annually (or periodically), if there is underlying variability over time. Estimating *M* annually is not sufficient to compensate for the negative effects from the variability of L_{50}.

Overall, the estimation results for the Kachemak Bay *P. borealis* population are encouraging. The estimated *M* for the *P. borealis* population shows an increasing trend in the 1980s, consistent with the speculation of increased consumption by Pacific cod and other groundfish species. However, the estimated *M* values from 1977 to 1982 were below 0.2, which seems too low for a shrimp population of only six age classes. One possible interpretation for the low *M* estimates lies in the spatial distribution change after the regime shift in 1977 that caused quick warming of the water column. *Pandalus borealis* are less tolerant of warmer temperatures after becoming female (Apollonio et al. 1986). From approximately 1979 through 1981, there were high concentrations of *P. borealis*, especially of large mature females, in the offshore sampling area west of the Homer Spit. Although there are no reliable historical records of temperature in Kachemak Bay to verify the relationship between temperature and female concentrations, we suspect that the temporary redistribution of older *P. borealis* in the area west of the Homer Spit might have resulted in the overestimation of their abundance in the survey relative to young *P. borealis*. If so, this would cause low estimates of *M*. Catches west of the spit declined quickly after the period of high concentration, which is reflected in the increasing *M* estimates afterwards.

In applying the length-based model, we adopted an approach that estimates interannual variations in *M*, but assumes a constant *q* of unity, and estimates constant gear-selectivity parameters, including L_{50}. Populations of *P. borealis* or other pandalid species are well known to have large fluctuations in abundance. The large fluctuations used to be postulated as being closely related to variations in recruitment (Balsiger 1981). However, our previous research on retrospective projection concluded that *M* was a relatively more important factor than *R* in controlling *P. borealis* population dynamics (Fu et al. 1999). As a forage species, their level of *M* is undoubtedly related to predation level. The major shift in species composition from shrimp dominant to groundfish dominant in Kachemak Bay (Bechtol 1997) caused us to choose the approach of estimating annual variations in *M*. For *q*, the assumption of unity is not uncommon. Zheng et al. (1995) listed several reasons for setting *q* at unity that are also relevant to the *P. borealis* population in Kachemak Bay. However, if the actual *q* is smaller than 1.0, the result would be underestimation of SSB, *R*, and *M* and overestimation of *F*. We have no way to verify possible shifts in magnitude of the parameter estimates. Fortunately, the overall shifts are of less concern than the annual variations that the model is able to uncover. Finally, reasons for not estimating L_{50} or γ annually lie in the lack of evidence for changes in gear selectivity and the potential complexity of selectivity-curve variability. For the latter, further simulation will be helpful, to investigate appropriate modeling approaches for dealing with more complex variability in gear selectivity, such as variability in both L_{50} and γ.

With our detailed model that estimates interannual variations in *M* along with those in *R*, *F*, and mean length at recruitment, it is possible that the model may be statistically overfitting the data. This can be inferred from the small difference between the predicted and observed biomass and yield data. On the other hand, leaving out an important process in a model may introduce bias. Our simulation-estimation experiments indicate that it is necessary to estimate *M* each year when the underlying *M* has a trend, which is most likely the case for the Kachemak Bay *P. borealis* population. Therefore, we chose model realism over model parsimony in our application.

Indeed, the question of optimal model complexity is a complicated one. For estimation models with a single data source, the Akaike and Bayesian information criteria (Burnham and Anderson 1998; Quinn and Deriso 1999) offer a straightforward approach involving the likelihood of the data, the number of parameters, and the number of observations. However, in more complicated problems with several data sources, our simulation study shows that the optimal model structure depends on the true dynamic processes and the amount of ME in the data sources. An additional complication is the choice of weighting of data sources when the true variances are unknown (the usual case). It was beyond the scope of this study to consider the interaction of estimability with data weighting, but this needs to be addressed in future studies. An objective framework for data weighting using perceptions and empirical variances in a decision-making setting is given in Merritt and Quinn (2000). The use of simulation-estimation exercises, as in this paper, is probably the best means for determining optimal model complexity, until more general theoretical principles can be obtained.

One further issue pertaining to optimal model complexity and the estimability of model parameters is the error structure for the various data sources. Myers and Cadigan (1995*a*, 1995*b*) showed that correlated research survey data could lead to parameter bias and incorrect inference in a virtual population analysis (VPA) model. In particular, spurious natural mortality changes over time occurred when positive correlations in survey data within a year were ignored. In our approach, we attempt to estimate annual changes in catchability in lieu of imposing a correlated error structure. Our conclusions differ somewhat from those in Myers and Cadigan (1995*a*, 1995*b*), in that we were unable to estimate catchability differences with confidence. Given the large differences in error structure, data sources, model parameters, and assumptions between our two approaches, we suggest that further research is needed regarding the estimability of catchability in our approach or the analogous within-year correlation in the Myers and Cadigan approach.

Acknowledgements

This publication is the result of research sponsored by Alaska Sea Grant, with funds from the National Oceanic and Atmospheric Administration, Office of Sea Grant, Department of Commerce, under grant No. NA90AA-D-SG066, project numbers R/07-21 and R/31-03, and from the University of Alaska with funds appropriated by the state. We thank William R. Bechtol and Richard Gustafson (Homer Office, ADF&G), for providing data, and Gordon Kruse (ADF&G), Milo Adkison, Thomas Shirley (Juneau Center, School of Fisheries and Ocean Sciences, University of Alaska), and Ransom Myers (Dalhousie University, Canada), for their comments. In particular, we are grateful to two anonymous reviewers for their insightful comments. The U.S. Government is authorized to produce and distribute reprints for government purposes, notwithstanding any copyright notation that may appear hereon.

References

Albers, W.D., and Anderson, P.J. 1985. Diet of Pacific cod, *Gadus macrocephalus*, and predation on the northern pink shrimp, *Pandalus borealis*, in Pavlof Bay, Alaska. Fish. Bull. **83**: 601–610.

Anderson, P.J. 1991. Age, growth, and mortality of the northern shrimp *Pandalus borealis* Krøyer in Pavlof Bay, Alaska. Fish. Bull. **89**: 541–553.

Apollonio, S., Stevenson, D.K, and Dunton, E.E., Jr. 1986. Effects of temperature on the biology of the northern shrimp *Pandalus borealis*, in the Gulf of Maine. National Oceanic and Atmospheric Administration Tech. Rep. NMFS 42.

Aschan, M., and Godø, O.R. 1999. Evaluation of the shrimp (*Pandalus borealis*) stock at Flemish Cap (NAFO Div. 3M) based on an area comparison. Northwest Atl. Fish. Organ. Sci. Counc. Stud. **32**: 37–43.

Balsiger, J.W. 1981. Keynote address: a review of pandalid shrimp fisheries in the Northern Hemisphere. *In* Proceedings of the International Pandalid Shrimp Symposium. *Edited by* T. Frady. Rep. No. 81-3 of the Alaska Sea Grant College Program, University of Alaska–Fairbanks, Juneau. pp. 7–35.

Bechtol, W.R. 1997. Changes in forage fish populations in Kachemak Bay, Alaska, 1976–1995. Forage fishes in marine ecosystems. *In* Forage Fishes in Marine Ecosystems: Proceedings of the International Symposium on the Role of Forage Fishes in Marine Ecosystems. Rep. No. 97–01 of the Alaska Sea Grant College Program, University of Alaska–Fairbanks, Juneau. pp. 441–455.

Burnham, K.P., and Anderson, D.R. 1998. Model selection and inference: a practical information-theoretic approach. Springer-Verlag, New York.

Cohen, M.D., and Fishman, G.S. 1980. Modeling growth–time and weight–length relationships in a single year-class fishery with examples on North Carolina pink and brown shrimp. Can. J. Fish. Aquat. Sci. **37**: 1000–1011.

Davis, A.S. 1982. The commercial otter trawl shrimp fishery of Cook Inlet. Information Leaflet No. 205 of the Alaska Department of Fish and Game, Anchorage.

Efron, B., and Tibshirani, R.J. 1993. An introduction to the bootstrap. Chapman and Hall, New York.

Fournier, D. 1996. An introduction to AD model builder for use in nonlinear modeling and statistics. Otter Research Ltd., Nanaimo, B.C.

Fournier, D., and Archibald, C.P. 1982. A general theory for analyzing catch at age data. Can. J. Fish. Aquat. Sci. **39**: 1195–1207.

Fournier, D.A., Sibert, J.R., and Terceiro, M. 1991. Analysis of length frequency samples with relative abundance data for the Gulf of Maine northern shrimp (*Pandalus borealis*) by the MULTIFAN method. Can. J. Fish. Aquat. Sci. **48**: 591–598.

Fu, C. 2000. Length-based models and population analyses for northern shrimp *Pandalus borealis* Krøyer. Ph.D. thesis, University of Alaska–Fairbanks, Juneau.

Fu, C., Quinn, T.J., II, and Adkison, M.D. 1999. Retrospective projection using Monte Carlo simulation: an application of a length-based model to Kachemak Bay pink shrimp. *In* Ecosystem approaches for fisheries management. Rep. No. 99-01 of the Alaska Sea Grant College Program, University of Alaska–Fairbanks, Juneau. pp. 59–77.

Gustafson, R. 1994. Trawl shrimp index fishing in the southern district of the Cook Inlet management area (spring 1992 and 1993). Regiona Inf. Rep. No. 2A94-23 of the Alaska Department of Fish and Game, Anchorage.

Ianelli, J.N., Fritz, L., Honkalehto, T., Williamson, N., and Walters, G. 1999. Eastern Bering Sea walleye pollock stock assessment. *In* Stock assessment and fishery evaluation report for the groundfish resources of the BeringSea/Aleutian Islands regions. North Pacific Fishery Management Council, Anchorage, Alaska. pp. 37–150.

Kimura, D.K. 1990. Approaches to age-structured separable sequential population analysis. Can. J. Fish. Aquat. Sci. **47**: 2364–2374.

Merritt, M.F., and Quinn, T.J., II. 2000. Using perceptions of data accuracy and empirical weighting of information: assessment of a recreational fish population. Can. J. Fish. Aquat. Sci. **57**: 1459–1469.

Myers, R.A., and Cadigan, N.G. 1995*a*. Statistical analysis of catch-at-age data with correlated errors. Can. J. Fish. Aquat. Sci. **52**: 1265–1273.

Myers, R.A., and Cadigan, N.G. 1995*b*. Was an increase in natural mortality responsible for the collapse of northern cod? Can. J. Fish. Aquat. Sci. **52**: 1274–1285.

National Research Council. 1998. Improving methods for fish stock assessment. National Academies Press, Washington, D.C.

Orensanz, J.M., Armstrong, J., Armstrong, D., and Hilborn, R. 1998. Crustacean resources are vulnerable to serial depletion—the multifaceted decline of crab and shrimp fisheries in the Greater Gulf of Alaska. Rev. Fish Biol. Fish. **8**: 117–176.

Parma, A.M., and Deriso, R.B. 1990. Dynamics of age and size composition in a population subject to size-selective mortality: effects of phenotypic variability in growth. Can. J. Fish. Aquat. Sci. **47**: 274–289.

Parsons, D.G., Mercer, V.L., and Veitch, P.J. 1989. Comparison of the growth of northern shrimp (*Pandalus borealis*) from four regions of the Northwest Atlantic. J. Northwest Atl. Fish. Sci. **9**: 123–131.

Quinn, T.J., II, and Deriso, R.B. 1999. Quantitative fish dynamics. Oxford University Press, New York.

Quinn, T.J., II, Turnbull, C.T., and Fu, C. 1998. A length-based population model for hard-to-age invertebrate populations. *In* Fishery stock assessment models. *Edited by* F. Funk, T.J. Quinn II, J.N. Ianelli, J.E. Powers, J.F. Schweigert, P.J. Sullivan, and C.-I. Zhang. Rep. No. 98-01 of the Alaska Sea Grant College Program, University of Alaska–Fairbanks, Juneau. pp. 531–556.

Schnute, J.T., and Richards, L.J. 1995. The influence of error on population estimates from catch-age models. Can. J. Fish. Aquat. Sci. **52**: 2063–2077.

Sullivan, P.J., Lai, H.L., and Gallucci, V.F. 1990. A catch-at-length analysis that incorporates a stochastic model of growth. Can. J. Fish. Aquat. Sci. **47**: 184–198.

Terceiro, M., and Idoine, J.S. 1990. A practical assessment of the performance of Shepherd's length composition analysis (SRLCA): application to Gulf of Maine northern shrimp *Pandalus borealis* survey data. Fish. Bull. **88**: 761–773.

Zheng, J., Murphy, M.C., and Kruse, G.H. 1995. A length-based population model and stock-recruitment relationships for red king crab, *Paralithodes camtschaticus*, in Bristol Bay, Alaska. Can. J. Fish. Aquat. Sci. **52**: 1229–1246.

Appendix. Detailed descriptions of the length-based population model

We assumed that the length frequency of a shrimp population at recruitment is a simple discrete normal distribution (N_D). The probability density function (PDF) for the lengths x at recruiting age r and at the start of time t is

$$f_{r,t}(x) \sim N_D(\mu_{r,t}, \sigma_r^2) = \mathrm{e}^{-\frac{1}{2\sigma_r^2}(x-\mu_{r,t})^2} \Big/ \xi_{r,t}$$

where $\xi_{r,t} = \sum_x \mathrm{e}^{-\frac{1}{2\sigma_r^2}(x-\mu_{r,t})^2}$

The abundance of the newly recruited shrimp at length x is $N_{r,t}(x) = N_{r,t} \cdot f_{r,t}(x)$. To obtain abundance $N_{a+1,t+1}(x)$ at age $a + 1$ and at the start of time $t + 1$ from abundance $N_{a,t}(x)$ (starting at age r), the process of growth was accounted for first, followed by natural mortality and then fishing mortality.

The standard von Bertalanffy growth model is utilized to express the growth pattern from one age to the next, assuming that growth is constant over time:

$$L_{a+1} = L_\infty(1-\rho) + \rho L_a + \varepsilon$$

where $\rho = \mathrm{e}^{-\kappa}$ is the Brody coefficient and $\varepsilon \sim N(0, \sigma^2)$. The expected length and variance at age $a + 1$ after growth for an individual of length x at age a from Cohen and Fishman (1980) are

$$\mu_{a+1}(x) = L_\infty(1-\rho) + \rho x$$

and

$$\sigma_{a+1} = \sigma^2 \frac{1-\rho^{2(a+1-r)}}{1-\rho^2} + \rho^{2(a+1-r)}\sigma_r^2$$

After one growth increment, the relative distribution of lengths $p_{a',t'}(L)$ is

$$p_{a',t'}(L) = \sum_x f_{a,t}(x)\mathrm{e}^{-\frac{1}{2\sigma_{a+1}^2}(L-\mu_{a+1,t+1}(x))^2}$$

The absolute abundance, $N_{a+1,t+1}(x)$, at the start of time $t + 1$ after, and time-dependent natural mortality M_t and fishing mortality $F_t s_x$ during time period t is

$$N_{a+1,t+1}(x) = N_{a,t}P_{a',t'}(x)\mathrm{e}^{-(M_t+F_t s_x)}$$

The term s_x is the gear selectivity function that follows the common logistic curve:

$$s_x = \frac{1}{1+\mathrm{e}^{-\gamma(x-L_{50})}}$$

Natural mortality is assumed to be constant over length and age. Assume that a survey takes place at the start of time $t + 1$ after shrimp recruit to the population. Sum up the abundance over all ages, including recruitment $N_{r,t+1}(x)$ and $N_{a+1,t+1}(x)$, where a is less than maximum age A, to obtain the length distributions of the population at the start of time $t + 1$:

$$N_{t+1}(x) = N_{r,t+1} + \sum_{a=r}^{A-1} N_{a+1,t+1}(x)$$

Therefore, the expected survey biomass at time $t + 1$ can be calculated as:

$$B_{t+1} = \sum_x qN_{t+1}(x)s_x W_x$$

where q is a constant catchability coefficient for the survey. Weight at length is modeled as the allometric relationship

$$W_x = \alpha^* x^{\beta^*}$$

The parameters α^* (0.000549) and β^* (3.067179) were obtained independently from the survey conducted in spring 1997, the same time of a year when survey biomass indices and length–frequency distributions were collected. The expected length–frequency distributions in survey samples at time $t + 1$ are

$$\mathrm{LF}_{t+1}(x) = n_{t+1}\frac{N_{t+1}(x)s_x}{\sum_x N_{t+1}(x)s_x}$$

where n_{t+1} is the sample size for measuring length.

Commercial yield is summed over the whole time period t until the start of time $t + 1$ and is denoted as Y_{t+1} so that each yield has the same subscript as the survey data. Therefore, the estimated yield from the model at the start of time $t + 1$ is

$$Y_{t+1} = \sum_x N_{t+1}(x)(1 - e^{-F_t s_x})W_x$$

For stability and easy convergence in estimating parameters, F_t is calculated as the product of its approximation $\left(\frac{Y_{t+1}^{\text{obs}}}{B_{t+1}^{\text{obs}} + Y_{t+1}^{\text{obs}}}\right)$ and an exponential deviation term (e^{υ_t}), i.e.,

$$F_t = \frac{Y_{t+1}^{\text{obs}}}{B_{t+1}^{\text{obs}} + Y_{t+1}^{\text{obs}}} e^{\upsilon_t}$$

Reconstructing the stock–recruit relationship for Northeast Arctic cod using a bioenergetic index of reproductive potential

C. Tara Marshall, Nathalia A. Yaragina, Bjørn Ådlandsvik, and Andrey V. Dolgov

Abstract: Correlation and simulation analyses suggest that, for the Northeast Arctic (NA) cod stock, the total lipid energy (TLE (kJ)) contained in the livers of mature females is proportional to total egg production, making TLE a potential predictor of recruitment. Accordingly, the TLE of NA cod was estimated for a 51-year time period (1946–1996), using estimates of numbers at length derived from virtual population analysis, modelled values of proportion mature and weight at length, and observed values of the liver-condition index. A significant linear relationship between TLE and recruitment to age 3 was observed. The temporal trend in TLE suggests that the reproductive potential of the NA cod stock has been in decline since the mid-1970s. A multiple-regression model that included TLE, mean temperature, and mean alongshore wind stress as independent variables explained approximately 43% of the variation in recruitment. Reconstructing stock–recruit relationships using more sensitive measures of reproductive potential is the first step in resolving environmental effects on recruitment and in developing biological reference points that are more effective in stock conservation.

Résumé : Des analyses de corrélation et de simulation suggèrent que l'énergie lipidique totale (TLE (kJ)) contenue dans le foie des femelles à maturité de la population de morues du nord-est de l'Arctique (NA) est proportionnelle à la production totale d'oeufs; la TLE est donc un critère potentiel de prédiction du recrutement. C'est pourquoi nous avons calculé les TLE de la population NA de morues pour une période de 51 ans (1946–1996) en nous servant d'estimations tirées de populations virtuelles des nombres de poissons dans les différentes classes de longueurs, d'estimations par modélisation des proportions d'individus matures et des masses à chacune des longueurs et d'observations des coefficients de condition du foie. Il existe une relation linéaire statistiquement significative entre les TLE et le recrutement jusqu'à l'âge 3. L'évolution au cours des ans de la TLE laisse croire que le potentiel reproducteur de la population NA décline depuis le milieu des années 1970. Une analyse de régression multiple, qui utilise la TLE, la température moyenne et le stress éolien moyen le long des côtes comme variables indépendantes, explique environ 43% de la variation du recrutement. L'établissement de meilleures corrélations entre les stocks et le recrutement à l'aide d'indicateurs plus sensibles du potentiel reproducteur est un premier pas vers l'évaluation des effets de l'environnement sur le recrutement et vers l'établissement de repères biologiques plus efficaces pour la conservation des stocks.

[Traduit par la Rédaction]

Introduction

As in many other stocks of marine fish, the relationship between spawner biomass and recruitment for Northeast Arctic (NA) cod (*Gadus morhua*) is indeterminate. However, recent research suggests that spawner biomass is a poor proxy for total egg production for NA cod (Marshall et al. 1998, 1999) and possibly for other stocks (Lowerre-Barbieri et al. 1998; Scott et al. 1999; Kraus et al. 2000). Furthermore, variables that could influence total egg production (e.g., age diversity of the stock, condition of spawners) have shown positive associations with recruitment (Boyd et al. 1998; Marteinsdottir and Thorarinsson 1998; Marshall and Frank 1999). These convergent findings point to the need to reevaluate the stock effect on recruitment, using more accurate measures of reproductive potential (Solemdal 1997; Trippel et al. 1997; Cardinale and Arrhenius 2000).

From a bioenergetic viewpoint, the reproductive potential of individual spawners reflects the balance between food intake and energy expenditures, i.e., surplus energy. Relevant data for reconstructing the reproductive potential of a stock therefore include time series describing the quality and quantity of food and the condition of spawners. Time series of absolute abundance and demographic composition (size, sex, proportion mature) of the stock are also required, to estimate the abundance and size composition of spawning females.

The NA cod stock has a comparatively rich collection of such data. Of particular value to this study are liver-weight observations for cod in the southern Barents Sea that have been recorded monthly since 1927 by the Russian Federation (Yaragina and Marshall 2000). These data are archived as the liver-condition index (LCI), which expresses liver weight as a percentage of total body weight. Because the

Received May 16, 2000. Accepted September 27, 2000. Published on the NRC Research Press web site on December 20, 2000. J15770

C.T. Marshall[1] **and B. Ådlandsvik.** Institute of Marine Research, P.O. Box 1870 Nordnes, 5817 Bergen, Norway.
N.A. Yaragina and A.V. Dolgov. Polar Research Institute of Marine Fisheries and Oceanography, 6 Knipovich Street, Murmansk, 183763, Russia.

[1] Corresponding author (e-mail: tara@imr.no).

liver is the primary storage site of lipid energy in gadoids (Kjesbu et al. 1991), the database constitutes a highly resolved record of seasonal and interannual changes in surplus energy. Given that the lipid fraction of the liver is nonlinearly related to the LCI (Lambert and Dutil 1997*a*; Auđunsson 1999), the LCI database can also be used to estimate the energy content of cod livers (Marshall et al. 1999).

To take advantage of both the temporal scope and bioenergetic import of the LCI database, the total lipid energy (TLE (kJ)) contained in the livers of mature females was estimated annually for a 51-year time period (1946–1996). Correlation and simulation analyses have previously suggested that, for the NA cod stock, TLE is proportional to total egg production and exhibits a similar dynamic response to varying food abundance (Marshall et al. 1999). In this study, the relationship between TLE and virtual population analysis (VPA) estimates of spawner biomass was examined. A linear relationship would be expected if both variables were directly proportional to total egg production. The stock–recruit (S–R) relationship was reconstructed using TLE as a proxy for total egg production by the NA cod stock, and this relationship was compared with that of the biomass-based S–R relationship. A multivariate analysis of the recruitment variation was performed, using estimates of environmental and demographic variables representing plausible recruitment mechanisms for NA cod. The implications of the results for management are discussed, with particular reference to the biological reference points currently used for the stock.

Materials and methods

Total numbers of females by length

Previously, acoustic-survey estimates of abundance were used to quantify total egg production and TLE for NA cod (Marshall et al. 1998, 1999). Here, only VPA estimates of the number at age (ages 3–15+; ICES 2000) were used so that abundance of spawners would be consistently scaled throughout the entire time series. Thus, the assumption that the VPA numbers at age accurately describe interannual variation in stock abundance is inherent in the analysis. Because the VPA estimates of numbers at age were used to estimate both spawner biomass and TLE, differences between the two variables will result from sources other than abundance.

Because the LCI database is predominantly length based (Yaragina and Marshall 2000), the approach taken to quantify the TLE of the stock was also length based. Year-specific age–length keys were required to convert VPA estimates of numbers at age to numbers at length. Age–length keys for 1946–1979 were developed, using data from the Norwegian fishery in Lofoten (Jørgensen 1990). Each record in this database consists of age and length observations for individual cod, with corresponding information on geographic area, gear type, and sampling date. The database was subsampled by selecting the records that were sampled in the first quarter of the year and for which the otolith type was classified as being that of NA cod rather than coastal cod. Age–length keys were constructed for each year, to give the proportion of each age-class observed in 5-cm length-classes having midpoints ranging from 52.5 to 137.5 cm. Cod ages 3 and 4 were infrequently captured. When observations for these age-classes were missing, it was assumed that all cod in these age-classes were in the 52.5- and 57.5-cm length-classes, respectively. This assumption will have a negligible effect on final TLE estimates, because the proportion of mature cod in these two length-classes is very low (Fig. 6 in Marshall et al. 1998). When observations for older age-classes were missing, it was assumed that all cod in that age-class fell into a single length-class (62.5, 67.5, 97.5, 102.5, 107.5, 112.5, 117.5, and 122.5 cm for ages 5, 6, 10, 11, 12, 13, 14, and 15+, respectively). Age–length keys for 1980–1996 were constructed using data from research-vessel surveys, as well as from the commercial fishery. Otherwise, the same selection criteria were used for selecting data records.

The VPA estimates of numbers at age were multiplied by the age–length key for that year, to estimate the number at length (n_l) by year. The total number of females in each length-class was then estimated by multiplying n_l by values of the proportion "females at length" shown in Fig. 5 of Marshall et al. (1998) as a solid line. These values allow for the proportion females at length to increase with increasing length, but do not account for interannual variation in the length-specific sex ratio.

Proportion mature and weight

VPA estimates of spawner biomass use constant values for the proportion mature at age and weight at age from 1946 until either 1981 (proportion mature) or 1982 (weight). This reflects the practical difficulties of developing historical time series that are methodologically consistent. The abundance of capelin in the Barents Sea affects the growth, condition, and maturation of NA cod (Yaragina and Marshall 2000). Consequently, the approach used here was to predict the proportion mature and weight at length using statistical models that include length and capelin-stock biomass as independent variables. No attempt was made to incorporate genetic changes (e.g., selection for faster growth – earlier maturation) that have been hypothesized for NA cod.

Acoustic-survey estimates of capelin-stock biomass are available from 1973 to the present (ICES 1998). To hindcast capelin-stock biomass for the time period 1946–1972, it was assumed that the intensity of cod feeding on capelin was linearly related to capelin-stock biomass, i.e., that the availability of capelin to cod was the same as the availability of capelin to the acoustic surveys. Cod-feeding observations have been collected year-round by commercial and research vessels as part of a sampling program initiated by Russia in 1947 (Ponomarenko and Yaragina 1978). The contents of non-empty cod stomachs were classified according to the following categories of prey items observed: capelin, juvenile cod, redfish, herring, shrimp, euphausids, and other. The frequency of capelin in cod stomachs (F_{cap}) is the percentage of non-empty cod stomachs that contain capelin (Ponomarenko and Yaragina 1984). Only data for the southern Barents Sea were used here. Values of F_{cap} in year t+1 ($F_{\mathrm{cap},t+1}$) are significantly positively correlated ($n = 24$, $p < 0.001$, $r^2 = 0.63$) with the acoustic estimates of capelin-stock biomass (thousand tonnes (t)) in September–October of year t, according to the following:

$$(1) \qquad \text{capelin biomass in year } t = 159\ F_{\mathrm{cap},t+1} - 390$$

Incorporating a lag was justified as follows. The spatial overlap between the cod and capelin stocks in the Barents Sea is at its maximum in February and March. Thus, the capelin-stock biomass estimated during the September–October acoustic survey more closely approximates the biomass that will be available to cod early in the following year. Incorporating the 1-year lag between the biomass estimate and F_{cap} also gave a higher r^2 value (r^2 = 0.63, compared with 0.43 for the unlagged relationship), which was advantageous for predictive purposes. Equation 1 was then used to predict capelin-stock biomass for t equal to 1946 through to 1972. The predicted values (Fig. 1) show a sudden decline in the capelin stock in the early 1960s that is consistent with the disappearance of the 1958–1960 capelin year-classes, an event that may have been triggered by the recruitment of strong herring year-classes in 1959 and 1960 (Gjøsæter 1998).

The proportion mature at length (m_l) and weight at length (w_l (g)) were predicted for the midpoints of the 5-cm length-classes using statistical models that included capelin-stock biomass (Fig. 1) as an independent variable (Table 1). These models were developed

Fig. 1. Time series of capelin-stock biomass in the Barents Sea. Open squares and filled circles indicate observed and predicted values, respectively.

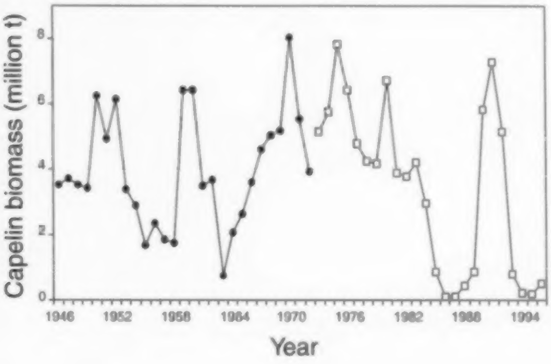

using data for females only from Norwegian surveys of both the Barents Sea and Lofoten conducted between 1985 and 1996. While this is a relatively short calibration period, it includes a dramatic signal in the growth of NA cod resulting from the collapse and recovery of the Barents Sea capelin stock (Fig. 1). Thus, the dynamic range of the data used to develop the statistical models should be sufficient to hindcast the proportion mature and weight back to 1946. Predicted values of m_l and w_l were used for the full time period (1946–1996), so that the scaling would be consistent.

Liver-condition index

Prior to 1967, only annual averages of LCI are available. From 1927 to 1950, LCI values were aggregated into three weight-classes: small (0.5–1.5 kg), medium (1.5–3.0 kg), and large (>3.0 kg). These values were assigned to the different length-classes on the basis of the predicted values of w_l. Missing values for 1951–1953 were interpolated from adjacent years. For 1954–1966, only observations for two 10-cm length-classes were available (51–60 and 61–70 cm). For these years, larger length-classes were assumed to have the same values as the 61–70 cm length-class. Since 1967, liver weights have been recorded monthly for 10-cm length-classes (51–60 to 91–100 cm). Larger length-classes were assumed to have the same values as the 91–100 cm length-class. Values for each 10-cm length-class were applied to the corresponding 5-cm length-classes.

Liver energy content

The liver energy content (LEC ($kJ{\cdot}g^{-1}$)) indicates the amount of energy (primarily lipid) contained in a known weight of liver tissue. It can be estimated from the LCI using the nonlinear regression model ($n = 407$, $p < 0.001$, $r^2 = 0.64$):

$$(2) \qquad \mathrm{LEC} = 24.77\ (1 - \exp^{-0.52(\mathrm{LCI}-0.48)})$$

Equation 2 was developed for northern Gulf of St. Lawrence cod having a LCI between approximately 1 and 8% (see Lambert and Dutil (1997*a*) for further details) and has been applied to NA cod (Marshall et al. 1999). In contrast with the equation given in Lambert and Dutil (1997*a*), eq. 2 has been reformulated using values of LCI that have total body weight as the denominator rather than somatic weight. This asymptotic equation indicates that the increase in LEC is negligible beyond a LCI value of approximately 5%, while below that value the LEC decreases rapidly.

Total lipid energy

The TLE in year t (TLE_t) was calculated as

$$(3) \qquad \mathrm{TLE}_t = \sum_{l=52.5}^{137.5} n_{l,t} \times \bar{s}_l \times m_{l,t} \times w_{l,t} \times (\mathrm{LCI}_{l,t} \times 0.01) \times \mathrm{LEC}_{l,t}$$

where l is the midpoint of 5-cm length-classes, $\bar{s}_l$ is the standard value of the proportion females at length and $\mathrm{LEC}_{l,t}$ is the value predicted from $\mathrm{LCI}_{l,t}$ using eq. 2. The factor 0.01 converts the LCI values from a percentage to a proportion of total body weight. Values of $n_{l,t}$ are time-referenced to 1 January of year t, whereas values of $\mathrm{LCI}_{l,t}$ (and hence $\mathrm{LEC}_{l,t}$) represent annual averages. Conceptually, TLE_t can be considered as an annual average of the stored energy acquired by mature cod throughout year t.

Timing considerations

In a simplified description of the seasonal cycle of energy expenditure–acquisition for NA cod, migration and spawning take place in the first 4 months of the year followed by a feeding period during which cod rebuild energy reserves for use in the next cycle of gonadal maturation that begins in the fall. Therefore, approximately two-thirds of the monthly values used to estimate $\mathrm{LCI}_{l,t}$ are from the period following spawning in year t and preceeding spawning in year t+1. Values of TLE_t were assumed to approximate the surplus energy acquired by spawners throughout year t for expenditure in spawning year t+1. Consequently, the relationship between TLE_t and spawner biomass in spawning year t+1 was examined. Likewise, the reconstructed S–R relationship was assumed to be the relationship between TLE_t and recruitment for spawning year t+1. This approach is consistent with that of Marshall and Frank (1999), who lagged recruitment by 1 year relative to an index reflecting the condition of haddock in the second half of the calendar year.

Recruitment index

The recruitment index used was the abundance of age-3 cod backshifted by 3 years to correspond to the spawning year. Estimates of recruitment were obtained from the most recent assessment (ICES 2000). Estimates in the uncoverged portion of the VPA numbers-at-age matrix were used, despite having relatively larger errors. The most recent estimate of the abundance at age 3 was for 1998, i.e., the 1995 year-class.

Environmental and demographic variables

Temperature has previously been associated with recruitment of NA cod (Ottersen and Sundby 1995). It can influence recruitment directly, via survival during egg and (or) larval stages, or indirectly, via its effects on productivity at lower trophic levels. For example, the intrusion of Atlantic water on the shelf increases the temperature and provides more prey for cod larvae. Water temperatures along the Kola hydrographic transect, located in the central part of the Barents Sea (33°30′E between 70°30′ and 72°30′N), have been monitored since 1921 (Tereshchenko 1996). Mean temperatures for the 0–200 m layer in April, May, June, and July were used here to represent temperature conditions during the pelagic stages.

Wind-induced flux of water from the Norwegian Sea into the Barents Sea may influence the growth and survival of larvae by affecting temperature and (or) the availability of zooplankton (Ottersen and Sundby 1995). It has also been suggested that interannual variation in wind speed and direction influences the horizontal dispersion of eggs and larvae of NA cod, which could, in turn, affect the location of settlement and the overwintering survival of juveniles. Monthly means of the wind-stress components τ_x (going to the east ($N{\cdot}m^{-2}$)) and τ_y (going to the north) were downloaded from the National Centers for Environmental Prediction – National Center for Atmospheric Research Global Reanalysis Project (Kalnay et al. 1996). For this analysis, the wind-stress components from a location

Table 1. Statistical models used to estimate proportion mature at length (m_l) and weight at length (w_l) for female Northeast Arctic cod.

Variable	Calibration period	Model type	Independent variables	Regression coefficient	r^2	p
m_l	1985–1996	Logistic regression	Intercept	–11.9	na	na
			Length	0.15		na
			Capelin biomass	1.2×10^{-7}		na
$\ln(w_l)$	1985–1996	Multiple regression	Intercept	–9.5	0.93	<0.0001
			ln(length)	4.07		<0.0001
			ln(capelin biomass)	0.32		<0.0001
			Interaction term	–0.07		<0.0001

Note: Length refers to the midpoint of 5-cm length-classes. Estimates of capelin biomass were obtained from annual acoustic surveys. Variables that were transformed to natural logarithms are identified as ln(variable name). The interaction term is the product of ln(length) and ln(capelin biomass). Unavailable data are indicated by na.

(13°7.5′E and 67°37′N) in the vicinity of the spawning grounds at Lofoten were selected. Monthly means were available back to 1948 only. To facilitate comparisons with the results of Ottersen and Sundby (1995), τ_x and τ_y values for April and the average of monthly τ_x and τ_y values for April through October were used to represent the wind stress at the time of spawning and from spawning through to settlement, respectively.

Both total egg production and prerecruit mortality could potentially be affected by demographic characteristics of the spawning stock. For example, maternal size influences egg quality (Solemdal et al. 1993; Marteinsdottir and Steinarsson 1998) and larval viability (Marteinsdottir and Steinarsson 1998; Nissling et al. 1998). Eggs produced by repeat spawners have a lower mortality rate than those produced by first-time spawners (Solemdal et al. 1995). To assess the influence of these demographic characteristics, the following variables were included in the multivariate analysis: (1) the mean length of spawners and (2) the percentage of repeat spawners. Both indices were calculated using females only. The percentage of repeat spawners was calculated by assuming that the percentage of repeat spawners increased with increasing length (table 8 of Marshall et al. 1998) and that these length-specific percentages were constant over time.

Statistical analysis

Multiple-regression analysis was used to develop statistical models predicting recruitment to age 3 as a function of the stock, environmental, and demographic factors described above. Stepwise variable selection was used, with the p value to enter the model and the p value to remain in the model being 0.10 and 0.05, respectively (SAS Institute Inc. 1989). The potential for collinearity among the independent variables was examined using the COLLIN and COLLINOINT options in the REG procedure in SAS. These options produce the proportion of the variance in each variable accounted for by each of the principal components of the $\mathbf{X}'\mathbf{X}$ matrix and a condition factor for each component. Collinearity is indicated when a component having a large condition value also explains a high proportion of the variance in two or more variables.

To test whether the independent variables were normally distributed, the Shapiro–Wilk's test statistic was computed for each variable using the UNIVARIATE procedure in SAS. This procedure computes a test statistic and probability for the the null hypothesis that the distribution is not normal. The null hypothesis was rejected ($p > 0.05$) for all variables included in the analysis, except for the mean length of spawners and the percentage of repeat spawners. Both had distributions that were skewed by the observation for 1982. This year had an unusually high abundance of 7-year-olds (table 3.15 in ICES 2000), which increased the mean length of spawners and the percentage of repeat spawners. The distributions of both variables were normal if this observation was deleted.

Fig. 2. The relationship between spawner biomass in spawning year t+1 and total lipid energy in year t. Lables denote the spawning year.

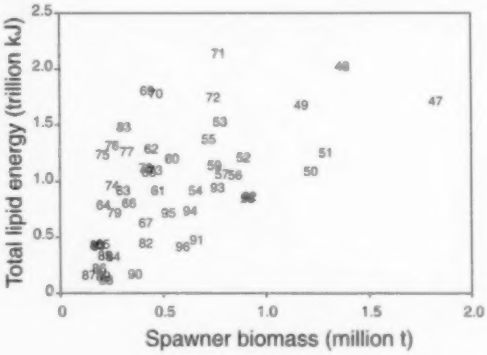

Results

If TLE and spawner biomass are both proportional to total egg production and thus to each other, then the relationship between them should be linear. This is not the case (Fig. 2). The relationship between TLE_t and spawner biomass in spawning year t+1 shows a distinct triangular pattern. Years at the beginning of the time series (1947–1951) show high values of both spawner biomass and TLE, suggesting that the cod stock in the post-war period was abundant and had a large amount of surplus energy. Spawner biomass and TLE were both low during a time period associated with a collapse of the capelin stock (1984–1989; Fig. 1). Outside of these two time periods the relationship between spawner biomass and TLE is highly variable. For example, spawner biomasses for the years 1970 and 1990 differ only by a factor of 1.3, while TLE values differ by a factor of 10.4 (Fig. 2). Thus, years having comparatively small differences in spawner biomass can have order of magnitude differences in TLE.

When the two variables are plotted as time series, other differences emerge. The TLE time series suggests that, with the exception of 1982, the reproductive potential of the stock has been below 1 trillion kJ since the mid-1970s (Fig. 3a). The high TLE value in 1982 (Fig. 3a) resulted from the large number of 7-year-olds in that year (ICES 2000). The 1983 year-class was relatively strong, which provides support for assuming that the TLE in year t will affect year-

Fig. 3. (*a*) Time series of total lipid energy. Broken horizontal line indicates a reference level of 1 trillion kJ. (*b*) Time series of spawner biomass. Broken horizontal line indicates a reference level of 500 000 t.

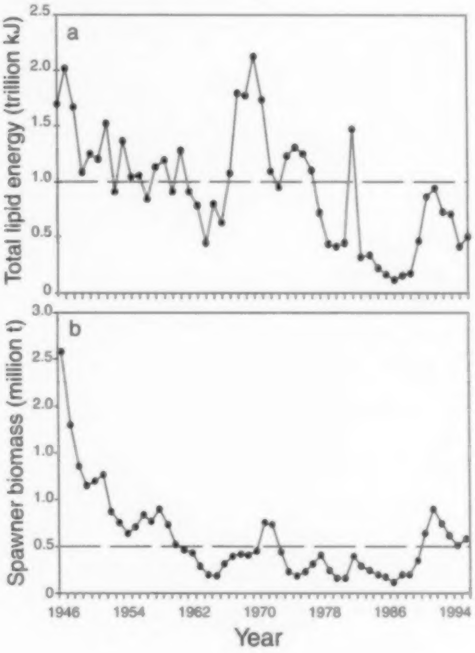

Fig. 4. (*a*) The relationship between total lipid energy in year *t* and recruitment to age 3 for spawning year *t*+1. Equation 4 is indicated as a solid line. (*b*) The relationship between spawner biomass and recruitment to age 3. The fitted Ricker curve (α = 1.81 and $\beta = 9.23 \times 10^{-7}$) is indicated by the solid line. Labels denote the spawning year.

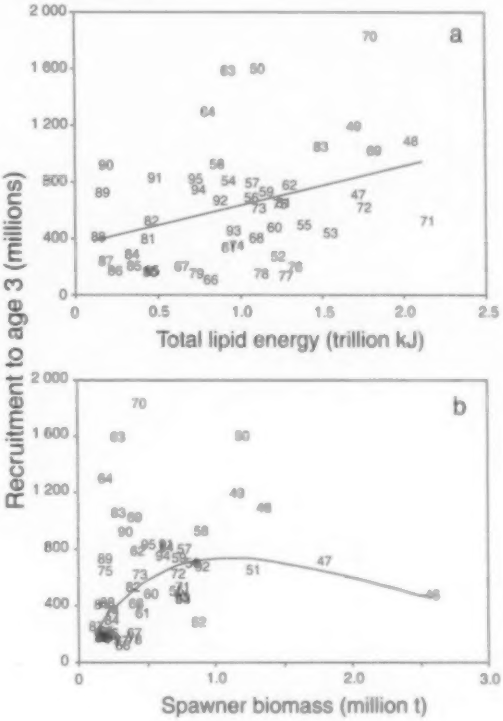

class strength in spawning year *t*+1. The TLE shows an increase in the early 1990s to a level that was approximately half that of the early 1970s (Fig. 3*a*). The temporal trend is quite different if the reproductive potential of stock is expressed as spawner biomass (Fig. 3*b*). For example, spawner biomass declined dramatically in the post-war period and thereafter fluctuated around 500 000 t. Spawner biomass in the early 1990s was comparable to biomasses observed in the early 1970s (Fig. 3*b*).

There is a significant ($n = 49$, $p = 0.013$, $r^2 = 0.12$) positive correlation between recruitment and TLE (Fig. 4*a*) that can be described by the equation:

$$\text{(4)} \qquad \text{recruitment to age } 3 = 3.5 \times 10^5 + 2.8 \times 10^{-7}\text{TLE}$$

where recruitment to age 3 is in units of thousands. By comparison, the biomass-based S–R relationship is indeterminate (Fig. 4*b*). Spawner biomasses above or below 500 000 t show no tendency to result in good or poor recruitment, respectively. When both variables are ln-transformed (e.g., Ottersen and Sundby 1995), the relationship is significant ($n = 50$, $p = 0.001$, $r^2 = 0.19$); however, the linear relationship between them is not ($n = 50$, $p = 0.09$, $r^2 = 0.06$).

The strength of the correlation between recruitment and TLE is similar in magnitude to the correlation between recruitment and Kola temperature (Table 2). None of the four wind-stress variables were significantly ($p > 0.05$) correlated with recruitment (Table 2). Both the mean length of spawning females and the percentage of repeat spawners were significantly positively correlated ($p < 0.05$; Table 2), suggesting that years having a high proportion of large fish or repeat spawners are associated with good recruitment. However, the results were affected by two anomalous observations. Bivariate plots of the relationship between recruitment and Kola temperature revealed that the observation for 1963 had higher than expected recruitment relative to temperature conditions. If the observation is deleted from the correlation analysis, then the temperature effect on recruitment becomes stronger than the effect of TLE (Table 2). Deleting the observation for 1982 normalised the distributions of both the mean length of spawners and the percentage of repeat spawners and increased the significance levels of these variables (Table 2).

Multivariate analysis

Data for the full time period yielded a multiple-regression model that included TLE and Kola temperature and that explained approximately one-quarter of the variation in recruitment (Table 3). Deleting the observation for 1963 increased the total amount of variation explained to approximately 43%. It also heightened the temperature effect, as indicated by the order in which the variables entered the model, and caused the alongshore wind stress term (τ_y April–October) to become significant. Deleting the observations for both 1963

Table 2. Correlation coefficients (*r*) for relationships between recruitment to age 3 in spawning year *t*+1 and for several stock, environmental, and demographic variables; significance levels (*p*) and number of observations (*n*) are also given.

	All years			Without 1963			Without 1963 + 1982		
Variable	*r*	*p*	*n*	*r*	*p*	*n*	*r*	*p*	*n*
Total lipid energy	0.35	0.01	49	0.38	<0.01	48	0.38	<0.01	47
Kola temperature in April–July	0.35	0.01	50	0.45	<0.01	49	0.46	<0.01	48
τ_x April	–0.02	0.88	48	–0.01	0.95	47	0.01	0.93	46
τ_y April	0.06	0.69	48	0.04	0.79	47	0.04	0.78	46
τ_x April–October	–0.10	0.50	48	–0.02	0.89	47	0.01	0.90	46
τ_y April–October	0.19	0.19	48	0.22	0.13	47	0.23	0.13	46
Mean length of spawners	0.32	0.02	50	0.33	0.02	49	0.40	<0.01	48
Repeat spawners	0.30	0.03	50	0.30	0.03	49	0.39	<0.01	48

Note: Values of total lipid energy in livers of mature females are for the year *t*. All other variables refer to values for spawning year *t*+1.

Table 3. Statistical models predicting recruitment to age 3 for spawning year *t*+1.

Model	Independent variable	Regression coefficient	*p*	r^2	*n*
All years	Intercept	–551 621	0.12	0.25	48
	TLE	2.8×10^{-7}	<0.01		
	Kola temperature	262 377	<0.01		
Without 1963	Intercept	–870 754	<0.01	0.43	47
	Kola temperature	309 186	<0.01		
	TLE	3.4×10^{-7}	<0.01		
	τ_y April–October	8.3×10^6	0.02		
Without 1963 + 1982	Intercept	–4 929 291	<0.01	0.41	46
	Kola temperature	332 915	<0.01		
	Repeat spawners	58 525	<0.01		

Note: Values of total lipid energy in livers of mature females (TLE) are for year *t*. Values for all other variables refer to spawning year *t*+1. For each model, the independent variables are listed in the order in which they entered the model. Unit for recruitment is thousands.

and 1982 caused the percentage of repeat spawners to enter the model after the Kola temperature, giving a model that explained approximately 41% of the variation in recruitment. None of the wind-stress terms were significant in this model. Collinearity was judged not to affect the models reported here, because the greatest proportion of the variance in each of the independent variables could be attributed to a single principal component. This suggests that the independent variables are approximately orthogonal to each other.

Discussion

The stock effect on recruitment

Using a bioenergetic index to represent the reproductive potential of the NA cod stock provides evidence of a stock effect on recruitment over long time scales. This suggests that the growth, condition, and abundance of spawners act in combination to affect the reproductive and recruitment potential of the stock. The reconstructed relationship differs from the biomass-based S–R relationship in that there is a statistically significant positive correlation on a linear scale. There are also differences between TLE and spawner biomass in the timing and relative magnitude of peak values. Given that the VPA estimates of numbers at age are common to both TLE and spawner biomass, differences between the two variables result from incorporating interannual variation in the LCI (to estimate both total liver biomass in the stock and the energy content of that biomass), as well as year-specific values for proportion mature and weight.

Both the mean length of spawners and the percentage of repeat spawners explained a level of recruitment variation that was comparable with TLE when the outlying observation for 1982 was deleted. This suggests that demographic characteristics affecting egg quality are important determinants of reproductive and recruitment potential. Logically, the correlation between total egg production (or its proxy) and recruitment must be stronger than correlations between indices of spawner quality and recruitment, because the effects of spawner quantity are not negligible. If this is not the case, then measurement error and (or) errors in the formulation of the proxy are introducing noise into the stock signal. There are several sources of error in estimates of TLE. Prior to 1973, the terms representing weight and maturity were predicted from values of capelin-stock biomass that were themselves predictions. The LCI for larger length-classes could be underestimated by the extrapolation scheme that was used. The age–length keys used to length-distribute the VPA estimates of the number at age could be improved so that they are more representative of the stock. These caveats illustrate the many assumptions that are required to hindcast reproductive potential on an absolute scale, using historical-data sources that are impressive relative to other stocks but still less than ideal.

The fit of the S–R relationship for the central Baltic cod stock was also improved by replacing spawner biomass with estimates of total egg production (Jarre-Teichmann et al. 2000). However, many gadoid stocks lack contemporary and (or) historical fecundity data. This necessitates the construction of proxies for reproductive potential (e.g., TLE, age diversity, condition, percentage of repeat spawners). A sensitive proxy for the reproductive potential of a stock should include terms for both the quantity and quality of spawners weighted in proportion to their effect on total egg production. The formulation of TLE differs from that of spawner biomass by incorporating spawner quality (i.e., condition) twice: once to estimate liver biomass and once to estimate liver energy content of that biomass. This amplifies the condition signal relative to the spawner-quantity signal. Many cod stocks exhibit a high degree of interannual variation in condition (e.g., Lilly 1997; Lambert and Dutil 1997*b*) that affects both the fecundity (Kjesbu et al. 1991) and egg quality (Solemdal et al. 1993; Lambert and Dutil 2000) of individual cod. Furthermore, measures of condition show positive correlation with recruitment for cod (Marshall et al. 1999), haddock (Marshall and Frank 1999), and pelagic species (Boyd et al. 1998).

In contrast to the classic non-linear S–R models, the reconstructed S–R relationship appears linear. Non-linear, density-dependent S–R models are intuitively appealing when the independent variable is an index of spawner abundance. For example, there is a highly significant, positive correlation between spawner biomass and the numerical abundance of cod age 7 and older ($n = 51$, $p < 0.001$, $r^2 = 0.77$) for NA cod. If total egg production (or its proxy) is determined by an interaction between spawner quantity and spawner quality, then fitting a density-dependent model may not be appropriate. There is no obvious mechanism for total egg production to self-regulate their numbers (in the sense of a feedback control mechanism) in the way that spawners can potentially self-regulate their numbers via density-dependent effects on terms such as proportion mature, weight, and fecundity that reflect per-capita food abundance (Cardinale and Modin 1999; Gillooly et al. 2000). Using total egg production to represent the stock effect on recruitment could mask the density effect by combining terms that may be inversely related to abundance (proportion mature, weight, fecundity) with terms that are, by definition, positively related to abundance (n_j). Density-dependent survival of prerecruit stages could also introduce non-linearity to the S–R relationship between total egg production and recruitment. Our failure to observe this could result from the estimation errors associated with TLE. Alternatively, the functional form of the S–R relationship may deviate from what is traditionally assumed.

The reconstructed S–R relationship, as well as the correlations between demographic characteristics and recuitment, represent incremental steps towards an improved S–R relationship. Estimates of total egg production have become feasible as cod fecundity data have become more readily available (Kjesbu et al. 1998; Kraus et al. 2000). Characteristics of the spawning stock that are likely to affect hatching success and larval survival could be used to estimate total viable egg production (e.g., Scott et al. 1999; Jarre-Teichmann et al. 2000).

Multivariate recruitment models

Results of the multivariate modelling show that both stock and environmental factors influence the recruitment of NA cod. This conclusion is consistent with that of Ottersen and Sundby (1995), who noted the "fruitlessness of the old simplistic discussion of whether recruitment variability is environmentally driven or driven by the spawning stock biomass." The variables that were found in this analysis to affect recruitment were qualitatively similar to those identified by the Ottersen and Sundby (1995) study. In their model, the stock and environmental effects were represented by terms for ln-transformed spawner biomass and Kola temperature, respectively. The Ottersen and Sundby (1995) study found that τ_y April–October was significantly correlated with the ln-transformed recruitment to age 3 (see Table 6 in Ottersen and Sundby (1995)); however, it was not included in the multivariate recruitment model (see model A in Table 9 in Ottersen and Sundby (1995)), owing to collinearity with temperature.

Presently, the assessment for NA cod forecasts recruitment to age 3 using a statistical model (RCT3) that includes survey estimates of abundance at the 0-group, age-1, and age-2 stages (Shepherd 1997). An alternative approach is to utilize process-oriented models, such as those developed by Ottersen and Sundby (1995) and this study, to predict recruitment. To illustrate their potential utility, the model given in Table 3 (excluding the observation for the 1963 year-class) was used to predict the recruitment to age 3 for the 1996, 1997, and 1998 year-classes. The process-oriented estimates of recruitment are consistently lower than the RCT3 estimates and are similar in magnitude to the low levels observed in the late 1960s, 1970s, and mid-1980s (Fig. 5). Thus, the short-term projections of recruitment used by the assessment are more optimistic than those based on stock and environmental conditions.

The multivariate models in Table 3 could potentially be refined by using more precise estimates of the terms that are already present or by including new variables. For example, circulation models of the Norwegian and Barents Sea (Ådlandsvik and Hansen 1998) could be used to provide a more precise description of the physical environment experienced during the pelagic stage. Variability in growth during early life-history stages was not included in our analysis. However, a multiple-regression model developed using data from ichthyoplankton surveys of the Norwegian and Barents Sea (1959–1993) predicted recruitment to age 3 from relative egg abundance, mean annual Kola temperature, and mean larval length (Mukhina 1999). Models that are hybrids of process-oriented and survey-based (e.g., RCT3) models may, in future, prove to have the greatest predictive capability.

Implications for management

Fishing mortality rates (F) for NA cod have, with the exception of a period in the early 1990s, increased to levels that are at or near historical highs (1.0 in 1997 and 0.9 in 1998; Table 3.21 in ICES 2000) and well above the precautionary reference level of $F = 0.42$. Given the strong retrospective patterns noted in recent assessments (ICES 2000),

Fig. 5. Time series of recruitment to age 3. Solid circles indicate estimates from the virtual population analysis (ICES 2000). Open triangles indicate estimates predicted by RCT3 (Table 3.7 in ICES 2000). Open squares indicate estimates predicted by the model in Table 3 that excludes the observation for 1963.

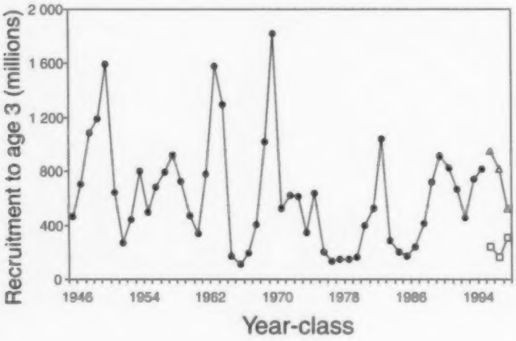

upward revisions to current F values are a distinct possibility. Developing strategies for stock rebuilding is an important task for the scientists involved in the management of NA cod. This study suggests that rebuilding strategies based on spawner biomass will be inefficient, because spawner biomass is a poor indicator of reproductive and recruitment potential. The reconstructed S–R relationship suggests that the probability of good recruitment is higher when TLE is above 1 trillion kJ. With the exception of 1982, the TLE has been below this value since the mid 1970s. Values for 1997, 1998, and 1999 were 0.49, 0.37, and 0.29 trillion kJ, respectively. Increasing recruitment would therefore require a large increase in the TLE. This can be achieved through reductions in F and (or) increases in recruitment to the spawning stock. However, if the process-oriented recruitment forecasts made here are correct, then recruitment to the spawning stock will be low over the short term. This increases the need for immediate and large reductions in F. Such management strategies have been implemented in the recent past: a large and rapid reduction in F was initiated in 1990 in response to the collapse of the Barents Sea capelin stock and low cod abundance. This protected the relatively strong 1983 year-class of NA cod as it recruited to the spawning stock. Consequently, TLE values approached 1 trillion kJ by 1992.

Incorporating reproductive potential into the standard assessment methodology for NA cod is easily achieved, particularly as many of the required elements are already in place. For example, matrices of age-specific proportion mature and weight are already used to estimate spawner biomass. The age-specific sex ratio is not used but the information required to estimate it is routinely collected. Maturity information could be partitioned by sex for species such as Atlantic cod that show differential maturation (Tomkiewicz et al. 1997; Jakobsen and Ajiad 1999). Age–length keys, which are essential for adding in length-based information (e.g., LCI or fecundity) to age-structured databases, are usually available. For many stocks, developing matrices describing temporal and size- or age-based variation in condition and (or) fecundity present the greatest immediate challenge.

Viewed objectively, traditional biomass-based S–R theory is poorly supported by empirical data (Peters 1991). This hinders the effectiveness of biological reference points that are derived from it in conserving heavily exploited species such as Atlantic cod. Our analysis has illustrated how a bioenergetic proxy for total egg production can be used to resolve the stock effect on recruitment. In essence, the proxy prorates spawner quantity by spawner quality. This approach has a precedent in fisheries science: correcting abundance indices for variation in condition has also been proposed to study the population dynamics of larval stages (Frank and McRuer 1989). The approach is also consistent with emerging insights into aquatic productivity that stress the importance of lipids in determining the reproductive potential of individuals and populations (Adams 1999; Shulman and Love 1999; Müller-Navarra et al. 2000). Viewing ecosystems as a bioenergetic continuum from primary production through to the reproduction and recruitment of vertebrates offers a useful conceptual framework for both the academic and applied branches of fisheries science.

Acknowledgements

We are grateful to staff at the Polar Research Institute of Marine Fisheries and Oceanography, who have maintained the liver-condition database from 1927 to the present. H. Gjøsæter made a suggestion that resulted in eq. 1. Assistance with databases was provided by P. Budgell, Å. Fotland, and O.R. Godø. B. Bogstad, H. Gjøsæter, O.S. Kjesbu, G. Ottersen and two anonymous reviewers commented on early versions of the manuscript. The late R.H. Peters' advocacy of empirical approaches to solving ecological problems, including the S–R relationship, was influential. Funding was provided by the European Union (QL K5-CT1999-0169).

References

Adams, S.M. 1999. Ecological role of lipids in the health and success of fish populations. *In* Lipids in freshwater ecosystems. *Edited by* M.T. Arts and B.C. Wainman. Springer-Verlag, New York. pp. 132–160.

Auðunsson, G. 1999. The effect of nutritional status of Icelandic cod (*Gadus morhua*) on macroconstituents and trace elements in the liver. Rit Fiskid. **6**: 111–129.

Boyd, A.J., Shannon, L.J., Schülein, F.H., and Taunton-Clark, J. 1998. Food, transport, and anchovy recruitment in the southern Benguela upwelling system of South Africa. *In* Global versus local changes in upwelling systems. *Edited by* M.H. Durand, P. Cury, R. Mendelssohn, C. Roy, A. Bakun, and D. Pauly. Éditions de l'Orstom, Paris. pp. 195–209.

Cardinale, M., and Arrhenius, F. 2000. The relationship between stock and recruitment: are the assumptions valid? Mar. Ecol. Prog. Ser. **196**: 305–309.

Cardinale, M., and Modin, J. 1999. Changes in size-at-maturity of Baltic cod (*Gadus morhua*) during a period of large variations in stock size and environmental conditions. Fish. Res. (Amst.), **41**: 285–295.

Frank, K.T., and McRuer, J.T. 1989. Nutritional status of field-collected haddock (*Melanogrammus aeglefinus*) larvae from southwestern Nova Scotia: an assessment based on morphometric and vertical distribution data. Can. J. Fish. Aquat. Sci. **46**(Suppl. 1): 125–133.

Gillooly, J.F., O'Keefe, T.C., Newman, S.P., and Baylis, J.R. 2000. A long-term view of density-dependent recruitment in smallmouth bass from Nebish Lake, Wisconsin. J. Fish Biol. **56**: 542–551.

Gjøsæter, H. 1998. The population biology and exploitation of capelin (*Mallotus villosus*) in the Barents Sea. Sarsia, **83**: 453–496.

ICES (International Council for the Exploration of the Sea). 1998. Report of the Northern Pelagic and Blue Whiting Working Group. ICES CM 1998/ACFM 18.

ICES (International Council for the Exploration of the Sea). 2000. Report of the Arctic Fisheries Working Group. ICES CM 2000/ACFM 3.

Jakobsen, T., and Ajiad, A. 1999. Management implications of sexual differences in maturation and spawning mortality of Northeast Arctic cod. J. Northwest Atl. Fish. Sci. **25**: 125–131.

Jarre-Teichmann, A., Wieland, K., MacKenzie, B.R., Hinrichsen, H.-H., Pliksh, M., and Aro, E. 2000. Stock–recruitment relationships for cod (*Gadus morhua callarias* L.) in the central Baltic Sea incorporating environmental variability. Arch. Fish. Mar. Res. **48**: 97–123.

Jørgensen, T. 1990. Long-term changes in age at sexual maturity of Northeast Arctic cod (*Gadus morhua* L.). ICES (Int. Counc. Explor. Sea) J. Mar. Sci. **46**: 235–248.

Kalnay, E., Kanamitsu, M., Kistler, R., Collins, W., Deaven, D., Gandin, L., Iredell, M., Saha, S., White, G., Woollen, J., Zhu, Y., Chelliah, M., Ebisuzaki, W., Higgins, W., Janowiak, J., Mo, K.C., Ropelewski, C., Wang, J., Leetmaa, A., Reynolds, R., Jenne, R., and Joseph, D. 1996. The NCEP/NCAR 40-Year Reanalysis Project. Bull. Am. Meteorol. Soc. **77**: 437–471.

Kjesbu, O.S., Klungsøyr, J., Kryvi, H., Witthames, P.R., and Walker, M.G. 1991. Fecundity, artresia, and egg size of captive Atlantic cod (*Gadus morhua*) in relation to proximate body composition. Can. J. Fish. Aquat. Sci. **48**: 2333–2343.

Kjesbu, O.S., Witthames, P.R., Solemdal, P., and Greer Walker, M. 1998. Temporal variations in the fecundity of Arcto-Norwegian cod (*Gadus morhua*) in response to natural changes in food and temperature. J. Sea Res. **40**: 303–321.

Kraus, G., Müller, A., Trella, K., and Köster, F. 2000. Fecundity of Baltic cod: temporal and spatial variation. J. Fish Biol. **56**: 1327–1341.

Lambert, Y., and Dutil, J.-D. 1997*a*. Can simple condition indices be used to monitor and quantify seasonal changes in the energy reserves of Atlantic cod (*Gadus morhua*)? Can. J. Fish. Aquat. Sci. **54**(Suppl. 1): 104–112.

Lambert, Y., and Dutil, J.-D. 1997*b*. Condition and energy reserves of Atlantic cod (*Gadus morhua*) during the collapse of the northern Gulf of St. Lawrence stock. Can. J. Fish. Aquat. Sci. **54**: 2388–2400.

Lambert, Y., and Dutil, J.-D. 2000. Energetic consequences of reproduction in Atlantic cod (*Gadus morhua*) in relation to spawning level of somatic energy reserves. Can. J. Fish. Aquat. Sci. **57**: 815–825.

Lilly, G. 1997. Size and condition of cod in Divisions 2J+3KL during 1978–1996. Northwest Atl. Fish. Organ. Sci. Counc. Res. Doc. 97/62.

Lowerre-Barbieri, S.K., Lowerre, J.M., and Barbieri, L.R. 1998. Multiple spawning and the dynamics of fish populations: inferences from an individual-based simulation model. Can. J. Fish. Aquat. Sci. **55**: 2244–2254.

Marshall, C.T., and Frank, K.T. 1999. The effect of interannual variation in growth and condition on haddock recruitment. Can. J. Fish. Aquat. Sci. **56**: 347–355.

Marshall, C.T., Kjesbu, O.S., Yaragina, N.A., Solemdal, P., and Ulltang, Ø. 1998. Is spawner biomass a sensitive measure of the reproductive and recruitment potential of Northeast Arctic cod? Can. J. Fish. Aquat. Sci. **55**: 1766–1783.

Marshall, C.T., Yaragina, N.A., Lambert, Y., and Kjesbu, O.S. 1999. Total lipid energy as a proxy for total egg production by fish stocks. Nature (London), **402**: 288–290.

Marteinsdottir, G., and Steinarsson, A. 1998. Maternal influence on the size and viability of Icelandic cod *Gadus morhua* eggs and larvae. J. Fish Biol. **52**: 1241–1258.

Marteinsdottir, G., and Thorarinsson, K. 1998. Improving the stock–recruitment relationship in Icelandic cod (*Gadus morhua* L.) by including age diversity of spawners. Can. J. Fish. Aquat. Sci. **55**: 1372–1377.

Mukhina, N.V. 1999. The use of Russian ichthyoplankton survey data in the forecasting of recruitment to Arcto-Norwegian cod stock. ICES (Int. Counc. Explor. Sea) CM 1999/Y 15.

Müller-Navarra, D., Brett, M.T., Liston, A.M., and Goldman, C.R. 2000. A highly unsaturated fatty acid predicts carbon transfer between primary producers and consumers. Nature (London), **403**: 74–77.

Nissling, A., Larsson, R., Vallin, L., and Frohlund, K. 1998. Assessment of egg and larval viability in cod, *Gadus morhua*: methods and results from an experimental study. Fish. Res. (Amst.), **38**: 169–186.

Ottersen, G., and Sundby, S. 1995. Effects of temperature, wind and spawning stock biomass on recruitment of Arcto-Norwegian cod. Fish. Oceanogr. **4**: 278–292.

Peters, R.H. 1991. A critique for ecology. Cambridge University Press, Cambridge, U.K.

Ponomarenko, I.Ya., and Yaragina, N.A. 1978. Year-to-year and seasonal fluctuations in the feeding of the Barents Sea cod on capelin in 1947–1976. ICES (Int. Counc. Explor. Sea) CM 1978/G 24.

Ponomarenko, I.Ya., and Yaragina, N.A. 1984. Seasonal, local and year-to-year variations in the feeding of Barents Sea cod on shrimp. ICES (Int. Counc. Explor. Sea) CM 1984/G 7.

SAS Institute Inc. 1989. SAS/STAT user's guide, version 6. 4th ed. SAS Institute Inc., Cary, N.C.

Scott, B., Marteinsdottir, G., and Wright, P. 1999. Potential effects of maternal factors on spawning stock – recruitment relationships under varying fishing pressure. Can. J. Fish. Aquat. Sci. **56**: 1882–1890.

Shepherd, J.G. 1997. Prediction of year-class strength by calibration regression analysis of multiple recruit index series. ICES (Int. Counc. Explor. Sea) J. Mar. Sci. **54**: 741–752.

Shulman, G.E., and Love, R.M. 1999. The biochemical ecology of marine fishes. Academic Press, London, U.K.

Solemdal, P. 1997. Maternal effects—a link between the past and the future. J. Sea Res. **37**: 213–227.

Solemdal, P., Bergh, Ø., Dahle, G., Falk-Petersen, I.B., Fyhn, H.J., Grahl-Nielsen, O., Haaland, J.M., Kjesbu, O.S., Kjørsvik, E., Løken, S., Opstad, I., Pedersen, T., Skiftesvik, A.B., and Thorsen, A. 1993. Size of spawning Arcto-Norwegian cod (*Gadus morhua* L.) and the effects on their eggs and early larvae. ICES (Int. Counc. Explor. Sea) CM 1993/G 41.

Solemdal, P., Kjesbu, O.S., and Fonn, M. 1995. Egg mortality in recruit- and repeat-spawning cod—an experimental study. ICES (Int. Counc. Explor. Sea) CM 1995/G 35.

Tereshchenko, V.V. 1996. Seasonal and year-to-year variations of temperature and salinity along the Kola meridian transect. ICES (Int. Counc. Explor. Sea) CM 1996/C 11.

Tomkiewicz, J., Eriksson, M., Baranova, T., Feldman, V., and Müller, H. 1997. Maturity ogives and sex ratios for Baltic cod: establishment of a database and time series. ICES (Int. Counc. Explor. Sea) CM 1997/CC 20.

Trippel, E.A., Kjesbu, O.S., and Solemdal, P. 1997. Effects of adult age and size structure on reproductive output in marine fishes. *In* Early life history and recruitment in fish populations. *Edited by* R.C. Chambers and E.A. Trippel. Chapman and Hall, London. pp. 31–62.

Yaragina, N.A., and Marshall, C.T. 2000. Trophic influences on interannual and seasonal variation in the liver condition index of Northeast Arctic cod (*Gadus morhua*). ICES (Int. Counc. Explor. Sea) J. Mar. Sci. **56**: 42–55.

Ådlandsvik, B., and Hansen, R. 1998. Numerical simulation of the circulation in the Svalbardbanken area in the Barents Sea. Continental Shelf Res. **18**: 341–355.

Spatial and temporal stability of commercial groundfish assemblages off Oregon and Washington as inferred from Oregon trawl logbooks

Yong-Woo Lee and David B. Sampson

Abstract: Spatial and temporal characteristics of species compositions for 15 major commercial groundfish species off Oregon and Washington (U.S.A.) were studied using Oregon bottom trawl logbook data from 1987 to 1993. Screening procedures to remove questionable data from the original logbook files resulted in the exclusion of information from 46% of the total available tows. Two multivariate methods, detrended correspondence analysis and Ward's hierarchical cluster analysis, were used to derive species ordinations and groupings. A general linear model developed for the primary detrended correspondence analysis axis scores showed that the species compositions were strongly correlated with depth and minimally correlated with the other environmental variables examined (latitude, month, and year). However, there were distinct seasonal changes in species composition at the shallower depths, consistent with the movement of deepwater species onto the shelf during summer. Annual trends in the species compositions were not evident even though the study region is very dynamic oceanographically and was heavily fished during the study period.

Résumé : L'étude de données tirées de journaux de pêche de chalutiers de fond en Oregon de 1987 à 1993 a permis de décrire les caractéristiques spatiales et temporelles des associations d'espèces chez 15 poissons benthiques de grande importance économique sur la côte de l'Oregon et du Washington (É.-U.). Le tri préliminaire visant à retirer les données douteuses des fichiers originaux a conduit à l'exclusion d'informations dans 46% des séries disponibles. Deux méthodes multidimensionnelles, l'analyse des correspondances redressée et l'analyse de groupement hiérarchique de Ward, ont servi à établir des ordinations et des regroupements d'espèces. Un modèle linéaire général basé sur les positions sur le premier axe de l'analyse des correspondances redressée a révélé que la composition des espèces était fortement reliée à la profondeur, mais peu associée aux autres variables de l'environnement examinées (latitude, mois et année). Il y avait des changements saisonniers distincts dans la composition spécifique aux profondeurs les moins grandes, ce qui correspond à la remontée des poissons d'eau profonde sur le plateau continental en été. Nous n'avons observé aucune tendance annuelle marquée, bien que la région d'étude soit océanographiquement très dynamique et que la pêche y ait été intensive au cours de l'étude.

[Traduit par la Rédaction]

Introduction

Because different demersal fish species often occur together and trawl gear is relatively nonselective, fisheries that use bottom trawls almost invariably are multispecies fisheries. Management of such fisheries, however, is usually based on single-species stock assessments that do not account for the complex multispecies characteristics of demersal fish communities (Gabriel 1982; Pimm and Hyman 1987). When productive stocks mix on the fishing grounds with stocks that are much less productive, the weak stocks can easily become overfished (Ricker 1958; Paulik et al. 1967). Arguably, the goal for fishery management should be to maintain harvests of commercially targeted species while also maintaining the general health of the surrounding environment, including the noncommercial species. To achieve this goal, it is important to identify species assemblages and their spatial and temporal characteristics and to understand the conditions, if any, under which fish species are consistently caught together.

Data from standardized bottom trawl surveys along the continental shelf and upper slope off California, Oregon, and Washington (U.S.A.) have been used to define demersal fish assemblages in the region (Gabriel and Tyler 1980; Weinberg 1994; Jay 1996). Although these data are collected randomly using a consistent gear type, vessel size, and sampling protocol, the survey, which is conducted by the National Marine Fisheries Service, occurs only on a triennial basis and only during the summer months. Seasonal variation in the spatial pattern of species compositions thus cannot be investigated. Furthermore, because the trawl survey samples a much more limited depth range (55–366 m) than the commercial fishery, the survey data do not accurately

Received February 25, 2000. Accepted October 18, 2000. Published on the NRC Research Press web site on December 20, 2000. J15631

Y.-W. Lee and D.B. Sampson.[1] Coastal Oregon Marine Experiment Station and Department of Fisheries and Wildlife, Hatfield Marine Science Center, Oregon State University, Newport, OR 97365, U.S.A.

[1] Corresponding author (e-mail: david.sampson@hmsc.orst.edu).

reflect all components of the fish communities that are fished and subject to disturbance.

Logbook data from commercial trawlers operating along the U.S. west coast potentially offer some major benefits relative to the trawl survey data. Fox and Starr (1996) compared catch rates of five commercial species derived from Oregon trawl logbook data and the National Marine Fisheries Service survey data and found that both data sets produced similar spatial patterns. Because the logbook data are available for many years and all months are well represented, seasonal variation and interannual changes in seasonality can be investigated. Also, from a statistical viewpoint, the logbook data should provide less variable results than the trawl survey data because of the much larger sample sizes. For example, during the six triennial trawl surveys spanning 1977–1992, data were collected from 2565 trawl survey hauls coastwide (Jay 1996), but the 1991 logbook data set for Oregon alone records information from more than 30 000 tows off Oregon and Washington.

Trawl logbook data are not without problems, however. These data do not represent random sampling in space and time, and the total weight and species composition of the catches are estimated and therefore may not be accurate or consistent. The trawl fishery uses numerous fishing strategies and gear types that may differ among trips and tows (Sampson et al. 1997). Trawlers do not conduct tows of uniform duration or maintain consistent tow speeds. Long tows, lasting more than 12 h and covering a path of 40–60 km, can result in the integration of species from several assemblages. Thus, trawl logbook data may be too crude to evaluate fine-scale biological or physical processes. Finally, the logbooks have limited species resolution. Fish representing 53 families and 180 species, including more than 33 rockfish species (*Sebastes* spp.), were caught within the study area during the bottom trawl surveys (Jay 1996), but only about 30 species or species groups are routinely recorded in the Oregon logbooks.

In this study, we used trawl logbooks to investigate spatial and temporal variability in species compositions for 15 major species and species groups harvested in the waters off Washington and Oregon (42–48°N latitude) over depths ranging from a few metres to over 1000 m (Fig. 1).

Fig. 1. Map of the study area with starting tow locations from a 10% sample of the logbook records for 1991 used in the multivariate analyses.

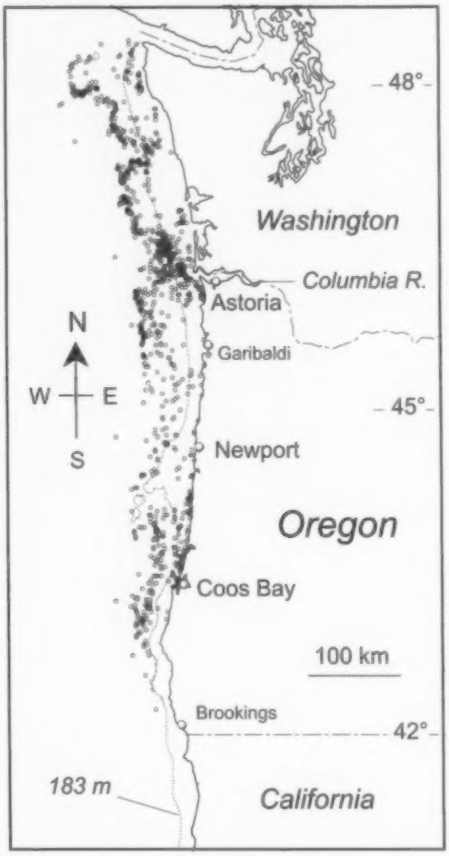

Materials and methods

Logbook and fish ticket data

Data from seven years of trawl logbooks (1987–1993) and corresponding landing receipts (fish tickets) were obtained from the Oregon Department of Fish and Wildlife. Logbooks contain fishers' estimates of retained catch (hails) of each species or species group from each tow. Fish tickets contain the official measured weights of the landings of each species or species group from each trip. One trip usually consists of several tows.

Fifteen commercial species or species groups were selected from the available logbook data based on their commercial importance and the completeness of the logbook information: Pacific cod (*Gadus macrocephalus*), lingcod (*Ophiodon elongatus*), sablefish (*Anoplopoma fimbria*), English sole (*Pleuronectes vetulus*), petrale sole (*Eopsetta jordani*), Dover sole (*Microstomus pacificus*), rex sole (*Errex zachirus*), sanddab (*Citharichthys* spp.), arrowtooth flounder (*Atheresthes stomias*), Pacific ocean perch (*Sebastes alutus*), widow rockfish (*Sebastes entomelas*), yellowtail rockfish (*Sebastes flavidus*), thornyhead (*Sebastolobus* spp.), small rockfish (*Sebastes* spp., with *S. reedi*, *S. crameri*, *S. proriger*, *S. zacentrus*, and *S. elongatus* being the top five species by weight (Crone 1995)), and miscellaneous rockfish (*Sebastes* spp., with *S. pinniger*, *S. paucispinis*, *S. crameri*, *S. borealis*, and *S. reedi* being the top five species by weight (Crone 1995)).

Data screening

The logbook and fish ticket data were processed and screened as follows. (*i*) For each species and fishing trip, hails from the logbooks were matched on the basis of boat and landing date with the landing weights from the fish tickets; then, the ratio of the total hailed weight over the landed weight was calculated for each trip. Logbook data for a given species in a trip were excluded from analyses if the ratio fell outside the acceptable range of 0.6–1.1. (*ii*) For each species and trip, landing weights were compared with any regulatory trip limits that were in effect; data for a given species in a trip were excluded from analyses if the landings were more than 90% of the trip limits. Also, data from November–December 1987 were excluded because the fishery for sablefish was closed on 22 October, thus precluding the occurrence of sablefish in any tows during that time period. Other closures during the study period occurred in late November or December (e.g., widow rockfish on 25 November 1987 and Pacific ocean perch on 13 December 1989) so that valid data were available for at least part of each time period. (*iii*) Logbook data for all species from a given tow were excluded from analyses if the tow was more than 8 h in duration or not made using a sole trawl. (*iv*) Logbook data for a given boat and year were excluded from analyses if the boat during the year made less than 20 tows or only had unacceptable hails for one or more of the 15 species included in the study.

The Pacific Fishery Management Council (PFMC) uses trip limits to regulate the fishery for groundfish along the U.S. west coast and prevent the overfishing of individual species while maintaining year-round harvests (PFMC 1994). When fishers catch more than allowed by the trip limits, they discard the excess catch at sea (Pikitch et al. 1988; Sampson 1994). The logbooks, however, do not report the discarded fish and thus distort the species compositions. For example, if a fisher had already caught his or her limit for a given species, subsequent catches of the species would be discarded and recorded in the logbook as zeroes. During the study period, not all the species reported in the logbooks were regulated by trip limits. In 1987, there were five species or species groups regulated by trip limits: widow rockfish, yellowtail rockfish, Pacific ocean perch, sablefish, and the *Sebastes* complex (all rockfish except widow and Pacific ocean perch). The deepwater species complex (Dover sole, sablefish, and thornyhead during 1989–1993 plus arrowtooth flounder during 1989–1990), *S. paucispinis*, and thornyhead (separately from the deepwater complex) were added in later years. Full details of the trip limit regulations in effect during the study period are given in PFMC (1994).

We limited our analyses to logbook data associated with the sole trawl because the greatest number of tows was made with this gear type (51–75% of the annual reported number of tows) and because this gear is effective at catching flatfish. Four types of trawl gear are recorded in the Oregon logbooks: generic bottom trawl, bottom trawl with rollers, sole trawl, and midwater trawl. Within each type, there undoubtedly are differences in net construction and material that affect fishing performance, but the logbooks do not record such details.

We excluded from the analyses tows more than 8 h in duration because their geographic coverage was too broad. Cumulative distributions of trawl duration by year showed that at least 85% of tows by sole trawls were less than 8 h in duration. These tows sample strips of bottom that are less than about 45 km (24 nautical miles). Tow speed, although not recorded in the logbooks, is also likely to vary among vessels and tows. Because of variable tow duration and speed, we assigned individual tows to geographic areas (described below) rather than treating each tow as a sampling unit.

Data matrices

The screened logbook data were converted to frequencies of occurrence based on sampling areas, defined as classes of starting latitude and starting depth. The relative frequency of occurrence of each species within a class was calculated as the number of nonzero tows divided by the total number of tows. Tows were assigned to classes of 73.2-m (40-fathom) increments of depth (0–40 fathoms, 40–80 fathoms, etc.), 1-degree increments of latitude (41–42°, 42–43°, etc.), and 2-month increments of time (January–February, March–April, etc.). Because the data from any given trip were acceptable for some species but unacceptable (and screened out) for others, the total number of tows at a given sampling area varied from species to species.

Two types of data matrices containing species relative frequencies were prepared: annual areas-by-species matrices (aggregated across boats) for measuring the species compositions and their temporal stability and a boats-by-species matrix (aggregated across months and years) for examining possible boat effects. We created a separate matrix for each year and an additional matrix that combined all years. Areas were excluded from analyses if they had less than 20 valid tows or less than five valid tows for any given species. Valid tows were ones that were not excluded by the data screening processes.

The spatial and temporal scales for the cells were selected on an arbitrary basis, but several other scales were also attempted. The scale must reflect both the density of sampling and the patch size of the organisms. Reasonable numbers of tows were needed at each area to measure the relative frequencies of occurrence for the 15 species, but long tow times, which presumably covered long distances, were incompatible with small spatial scales. Based on observations of fishing operations and conversations with fishers, we assumed that most tows were conducted along depth contours. Given a maximum tow speed of about 5.6 km·h^{-1} (3 kn), tows that were 8 h in duration or less would have covered less than one third of a degree of latitude.

The areas-by-species matrices contained data from tows made by 121 different boats, with some appearing in the logbook files for only one or two years and others appearing for all seven years. The species compositions for a given time period might depend on which boats happened to be operating. Furthermore, individual boats did not operate evenly over the entire study area because different fishers had different fishing strategies and preferences for target species. We created the boats-by-species matrix using only data from six boats that operated extensively in more than 25 latitude–depth classes across all seasons and years.

Data analyses

No single multivariate technique is likely to provide perfectly correct representations of species distribution and co-occurrence in any given community (Jongman et al. 1987). Thus, we employed two different types of multivariate techniques to analyze the areas-by-species data matrices, detrended correspondence analysis (DCA) (Hill and Gauch 1980; Gauch 1982) to develop ordinations (ranked orderings) and cluster analysis to develop classifications. The analyses were made using PC-ORD, a multivariate statistical software package (McCune and Mefford 1995).

Prior to running the multivariate analyses, the relative frequency of occurrence estimates (f) in the individual data matrices were transformed using the angular transformation

$$\frac{2}{\pi}\arcsin(\sqrt{f})$$

which is often considered to be appropriate for proportions or percentage data (Sokal and Rohlf 1981). Such transformations can improve the validity of assumptions of normality, linearity, and homogeneity of variance as well as reduce the effects of having very common or very rare species in species composition data (Noy-Meir et al. 1975; Jensen 1978).

Ordination using DCA

We used DCA to derive measures of species composition in a low-dimensional ordination space that could be interpreted in terms of the extrinsic factors Depth, Latitude, Month, and Year. To measure the relative importance of these factors, the DCA scores were plotted against the factors to explore for nonlinear relationships, and Pearson's correlation coefficients were calculated to relate each factor with the scores for the first two DCA axes. To construct a statistical model relating the external factors with species composition, the general linear model (GLM) procedure (SAS 1988) was applied to the first DCA axis scores obtained from the analysis of the areas-by-species matrix with data from all years. GLM was also applied to the first DCA axis scores from the boats-by-species data matrix to test the significance of possible boat effects. In the GLM analyses, the external variables were treated as discrete class variables. In the correlation analysis, they were treated as continuous variables and the Month values were assigned to mimic a seasonal cycle (January–February and

Table 1. Number of sampling cells and maximum number of tows per cell in the data matrices.

Data matrix	No. of sole trawl tows in logbooks	No. of cells in matrix[a]	Max. total no. of tows[b]	Percentage of possible tows
Areas-by-species				
1987	12 147	90	7 091	58
1988	12 949	123	8 295	64
1989	16 918	171	11 697	69
1990	12 002	135	7 623	64
1991	16 756	161	10 794	64
1992	13 104	134	6 961	53
1993	15 102	140	9 012	60
All years	98 978	956	61 583	62
Boats-by-species	17 945	171	11 165	62

[a] Cells were defined by latitude and depth classes and bimonthly time period for the areas-by-species matrices and by latitude and depth classes and boat identifier for the boats-by-species matrix.

[b] Because of differences among species in hail-to-landing ratios and the influence of trip limits, the number of valid tows at any given cell usually varied among the species.

November–December equal to 1, May–June and July–August equal to 3, March–April and September–October equal to 2).

Classification using cluster analysis

As a complement to DCA, we applied a numerical classification method (hierarchical agglomerative cluster analysis with Ward's minimum variance fusion strategy and the Euclidean distance measure) to define groupings of similar species occurrences (Ward 1963; Gauch and Whittaker 1981) based on the same data matrices that we used with DCA. Cluster analysis produces a treelike hierarchical structure (a dendogram) of similarity that allows groups of similar species occurrences to be objectively delineated.

Ward's method of cluster analysis performs well with respect to the so-called chaining problem, in which there is successive merging of single entities with previously formed clusters. Chaining can severely distort the results of a cluster analysis and make it difficult to identify separate groups of clusters, and the groups may not effectively represent the hierarchical characteristics of a community (Romesburg 1984; Sneath and Sokal 1973).

Potential outliers

Outliers can strongly influence the results of multivariate analyses (Tabachnick and Fidell 1996). To reduce the effect of possible outliers, data from sampling cells containing fewer than three nonzero species values were excluded from the data matrices prior to running the multivariate analyses. Then, we used a two-step process to detect potential outliers. First, we identified data from cells having relatively high standard deviations (>2.0, measured in terms of Euclidean distance; McCune and Mefford 1995). Next, we examined scatterplots of the first and second DCA scores to identify cells with scores that were relatively far from the main cluster of scores. If both methods identified particular cells as being potential outliers, we repeated the DCA without the potential outliers to determine whether they had a substantial influence on the ordination results. If they appeared to have a major influence, they were removed from the data matrix. To maintain consistency between the DCA and cluster analyses, if outliers were removed from a DCA, they were also removed from the corresponding cluster analysis.

Results

Data screening

Almost all 20 000 trips reported in the logbook files for the study period had corresponding fish tickets, but logbooks were unavailable for about 21% of the fish tickets. Distributions of hail-to-landing ratios showed a reasonably consistent pattern from species to species and from year to year, with the fishers tending to slightly underestimate their retained catches. Also, there were numerous trips for which there were landings data for a given species but no corresponding hails (about 20%) and hails without landings (about 2%). On average, about 54% of the trips each year with nonzero catch records had hail-to-landing ratios that fell within the acceptable range. The percentage of trips that were uninfluenced by trip limits varied from year to year and from species to species (widow rockfish, 50–84%; yellowtail rockfish, 46–76%; Pacific ocean perch, 60–79%; *Sebastes* complex, 89–99%; deepwater complex, 83–100%; sablefish, 68–93%; thornyhead, 82–100%).

The initial outlier screening removed cells with fewer than three nonzero species, two cells in 1988 and two in 1993. The additional outlier screening process removed two more cells from the areas-by-species matrix for 1993, which were not regarded as outliers in the analysis with all years combined, and one cell from the boats-by-species matrix. The number of cells and number of tows that were ultimately included in the areas-by-species matrices varied from year to year (Table 1). The entire screening process resulted in matrices that included data from 62% (61 583 tows) of the total reported tows made with sole trawls during the study period.

The information in the data matrices is unevenly spread across the possible categories of Latitude, Depth, and Month in the areas-by-species matrices (Fig. 2) and the categories of Latitude, Depth, and Boat in the boat-by-species matrix. Also, the matrices were unbalanced, with a strong seasonal pattern to the locations (Fig. 3). Trawlers tended to operate in deeper water during winter (November–April) and moved into shallower water during summer (May–October).

Ordinations with DCA

Both the ordination and classification analyses revealed strikingly similar environmental correlations and species patterns among the individual years and in the analysis with all years. For all the data matrices, there was a strong relationship between Depth and the scores for DCA axis 1 and a slightly weaker relationship between Latitude and the scores for axis 2. The linear correlation coefficients between Depth and axis 1 ranged from –0.947 to –0.874 (Table 2), with the

Fig. 2. Nonempty cells by (*a*) Latitude, (*b*) Depth, and (*c*) Month in the areas-by-species data matrix for all years combined.

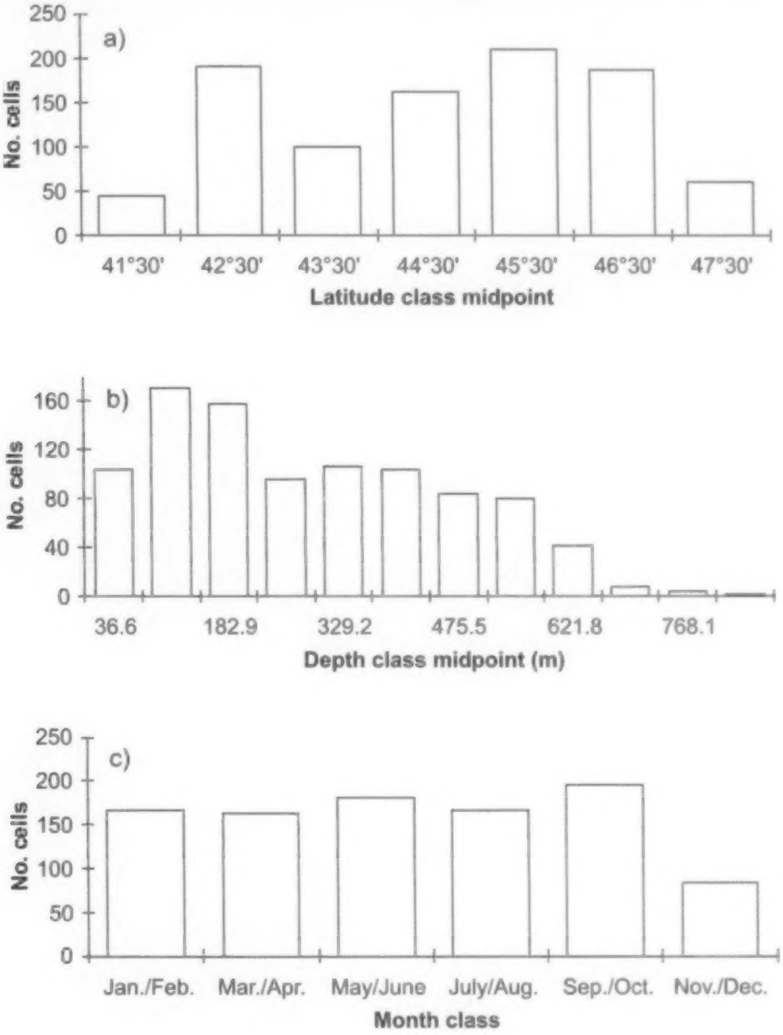

negative coefficients indicating that the depth component in axis 1 was oriented with shallower depths in the positive direction. The other environmental variables (Latitude and Month for each annual matrix and Latitude, Month, and Year for the combined matrix) were only weakly correlated ($r^2 < 0.15$) with axis 1. Latitude was strongly correlated ($r^2 > 0.4$) with the axis 2 scores for all the data matrices except the 1987 matrix ($r^2 = 0.172$) and the boats-by-species matrix ($r^2 = 0.031$). For all the data matrices, there were only weak correlations ($r^2 < 0.1$) between axis 2 and the other environmental variables.

When comparing results for the different data matrices, the relationship between the DCA axes and environmental variables should be interpreted cautiously because from one matrix to the next, each axis has a different ability to account for the variability in the original data. The degree of explanatory power can be gauged by the coefficient of determination (r^2). We used the Euclidean distance measure for calculating the value of r^2 to evaluate how well distances in ordination space represented distances in the original high-dimensional space. Values of r^2 for the first two DCA axes (Table 3) demonstrated that about 70% of the total variance in the species composition data was explained by axis 1, whereas only about 5% was explained by axis 2. Even though the DCA procedure derives more than two ordination axes, the third axis and subsequent axes were not used to examine the species patterns because those axes had very minimal explanatory power. In general, the DCA results indicated that species compositions were associated primarily with Depth and secondarily with Latitude.

Plots of the DCA species scores showed remarkable similarity among all the data matrices. Just as the DCA area scores were related to the environmental variables, so the species scores also were related to the environmental variables.

Fig. 3. Distribution of tows by (*a*) Depth and (*b*) Month in the areas-by-species data matrix for all years combined.

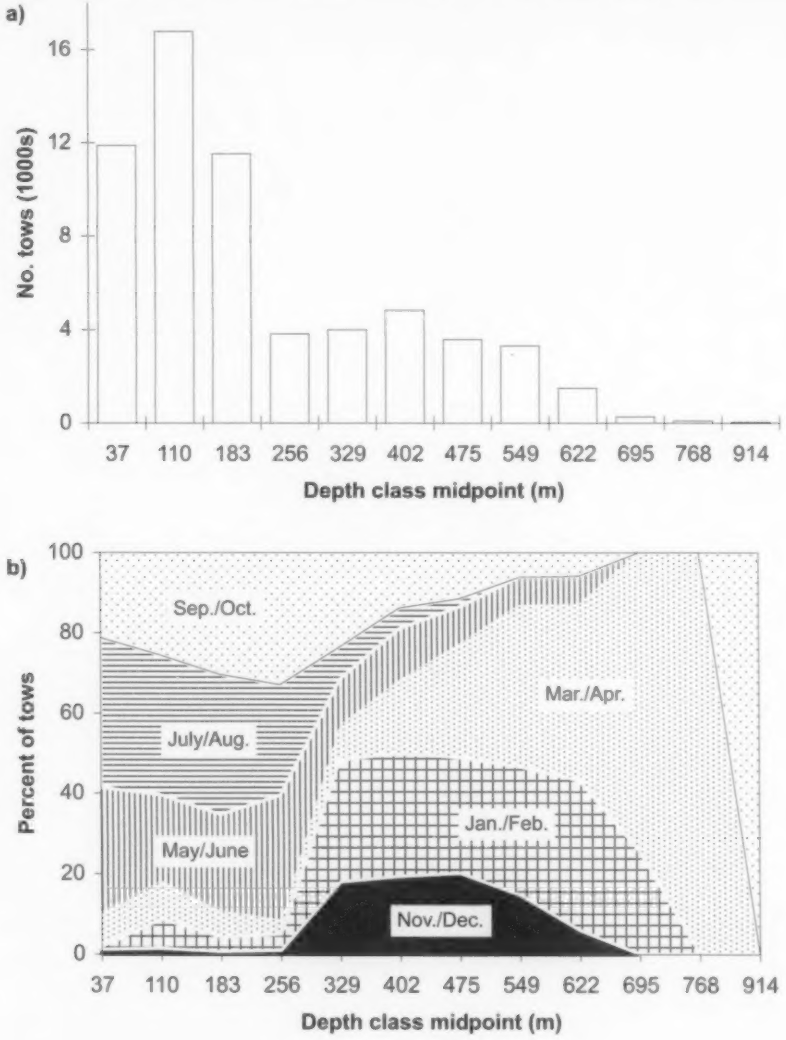

DCA axis 1 was linearly correlated with Depth ($r^2 > 0.764$) for all of the data matrices, and DCA axis 2 was linearly correlated with Latitude ($r^2 > 0.448$) for seven of nine matrices. Thus, the relative locations of the species scores along DCA axis 1 reflected the relative placement of the species with regard to depth, and the species scores for axis 2 reflected the relative placement with regard to latitude (e.g., Fig. 4*a*). In general, the DCA scores for thornyhead, sablefish, and Dover sole were lined up in the middle left portion of each DCA plot, indicating that these species are centered latitudinally within the study area but tend to occur in deeper waters, with Dover sole at shallower depths, thornyhead at deeper depths, and sablefish in between. Pacific ocean perch and small rockfish were consistently at opposite ends of axis 2, which is associated with Latitude. For some species, such as widow rockfish, yellowtail rockfish, and Pacific cod, the relative positions along DCA axis 2 varied from year to year, but the configurations of species scores generally were very consistent from year to year.

The configuration of species scores in the DCA species plot for the data matrix with all years combined (Fig. 4*a*) was very similar to the plots for individual years, with axis 1 scores significantly correlated ($P < 0.001$) with the scores from the individual years (r values ranging from 0.968 to 0.995) and axis 2 scores significantly correlated for all years ($|r|$ values ranging from 0.904 to 0.984) except 1987 ($r = 0.056$). The DCA species plot from the boats-by-species matrix (Fig. 4*b*) had a similar pattern with respect to axis 1, even though the plots from the other data matrices were derived from data collected from more than 100 boats. The boats-by-species scores for axis 1 were significantly correlated ($P < 0.001$) with the scores from the individual years (r values ranging from 0.759 to 0.862), whereas the scores for axis 2 were not significantly correlated ($P > 0.1$). In the

Table 2. Correlations between the DCA scores and environmental variables.

Data matrix	DCA axis 1	DCA axis 2
1987 areas-by-species		
Depth	–0.925	0.116
Latitude	–0.368	0.415
Month	0.371	–0.316
1988 areas-by-species		
Depth	–0.916	–0.129
Latitude	0.038	0.787
Month	0.316	0.051
1989 areas-by-species		
Depth	–0.909	0.195
Latitude	–0.069	0.669
Month	0.153	0.159
1990 areas-by-species		
Depth	–0.882	0.211
Latitude	–0.205	0.689
Month	0.262	–0.010
1991 areas-by-species		
Depth	–0.874	0.040
Latitude	–0.199	0.755
Month	0.170	0.103
1992 areas-by-species		
Depth	–0.884	0.183
Latitude	–0.273	–0.671
Month	0.269	–0.288
1993 areas-by-species		
Depth	–0.895	0.044
Latitude	–0.187	0.782
Month	0.117	0.161
All years areas-by-species		
Depth	–0.894	–0.099
Latitude	–0.138	0.698
Year	–0.025	0.064
Month	0.212	0.190
Boats-by-species		
Depth	–0.947	0.074
Latitude	0.168	–0.177
Boat	–0.051	0.009

Table 3. Explanatory power (r^2) of first and second DCA axes.

	Explanatory power (%)	
Data matrix	Axis 1	Axis 2
Areas-by-species		
1987	70.0	4.3
1988	67.0	4.7
1989	76.0	3.1
1990	78.0	3.6
1991	74.0	5.8
1992	64.0	9.0
1993	71.0	4.8
All years	70.0	5.0
Boats-by-species	72.0	5.2

plot from the boats-by-species matrix, the vertical positions of sanddab, yellowtail rockfish, widow rockfish, and Pacific ocean perch were unusual relative to the other plots. Axis 2 in the boats-by-species analysis should be interpreted cautiously because it was only weakly correlated ($r^2 < 0.031$) with the environmental factors. Relative to the other data matrices, in the boats-by-species analysis, the correlation between DCA axis 1 and Depth was the strongest ($r^2 = 0.897$) and the correlation between DCA axis 2 and Latitude was the weakest ($r^2 = 0.031$). This is probably an artifact of the sampling coverage because in the boats-by-species matrix, there were few samples in the southern part of study area (42–44°N), whereas samples for depths were well represented.

Classifications with cluster analysis

The cluster analysis results were somewhat variable among all the matrices (Table 4), with the species clustered into four groups that retained about 65% or more of the information in the original data (e.g., Fig. 5). Except for the deeper water species, thornyhead, sablefish, and Dover sole, which were grouped together in eight of the nine analyses, the constituent species in a given group varied from matrix to matrix. At about the 45% information level, these deep-water species were clustered into one distinct group and the rest into another. None of the analyses were badly affected by the chaining problem (less than 20%).

Results from the cluster analyses and DCA ordinations were similar in terms of separating deeper water species from the shallower dwelling species, but there generally was less consistency among the individual cluster analyses than there was among the individual DCA ordinations. For example, the cluster analyses did not always differentiate between Pacific ocean perch and small rockfish, whereas these species tended to be at opposite ends of DCA axis 2. Also, the two methods diverged in their placement of sanddab, one of the shallowest occurring species. The clustering process tended to fuse sanddab into a group with widow and yellowtail rockfish; the DCA placed sanddab near English sole and petrale sole.

The groupings of species in the cluster analysis of the boats-by-species matrix were similar to the groupings among the other data matrices (Table 4) with regard to the deeper water species (thornyhead, sablefish, and Dover sole) but not with regard to the other species.

GLM analysis of the DCA scores

Although there were no strong linear correlations between species compositions and the temporal variables Month and Year, the correlations did not measure possible nonlinear effects. Also, the weak correlations could have been artifacts of the unbalanced sampling coverage over time. We applied GLM analysis techniques to the DCA axis 1 scores obtained from the areas-by-species data matrix with all years combined. This allowed us to examine relationships between the species compositions and environmental factors, including possible interactions, while accounting for the effect of the unbalanced data. We constructed a statistical model by starting with all main environmental factors (Depth, Latitude, Month, and Year) and all possible two-way interactions of the main effects and then sequentially removed insignificant terms until only significant ones remained ($P < 0.05$). The

Fig. 4. DCA species scores from the (*a*) areas-by-species matrix for all years combined and (*b*) boats-by-species matrix. Both graphs have the same horizontal scaling, but Fig. 4*b* has extended vertical scaling. The areas-by-species matrices for the individual years produced species plots that were very similar to Fig. 4*a*. See Table 4 for species codes.

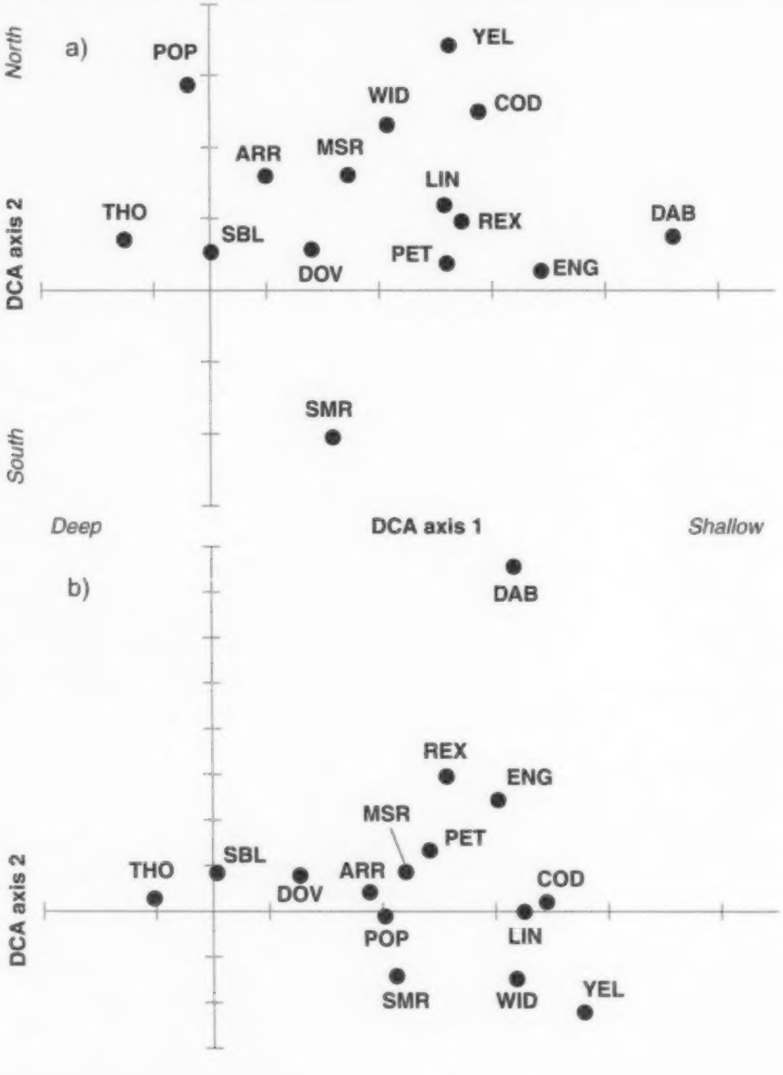

resulting model, which explains most of the variability in the species compositions (DCA axis 1), can be represented as

$$\begin{aligned}\text{DCA } 1 = &\ \text{Depth} + \text{Latitude} + \text{Bimonth} + \text{Year}\\ &+ \text{Depth} \times \text{Latitude} + \text{Depth} \times \text{Bimonth}\\ &+ \text{Depth} \times \text{Year} + \text{Latitude} \times \text{Bimonth}.\end{aligned}$$

The model was highly significant ($F_{198,\ 955} = 109.8$, $P < 0.001$, adjusted $r^2 = 0.958$) and accounted for 96.6% of the variation in species composition expressed by DCA axis 1. In the process of building the model, two interaction terms (Latitude × Year and Month × Year) were removed.

The scatterplot of residuals versus predicted values suggested that the model assumptions were met. We also tested for possible three-way interactions by sequentially adding to the model three-way combinations of the two-way interactions. The Depth × Latitude × Month and Depth × Latitude × Year interactions were statistically significant, but the model with those terms was much more complex (model df = 524) and produced only a modest improvement in the adjusted r^2 (to 0.967). Thus, it was more parsimonious to fit the simpler model that had only two-way interactions.

Even though all terms in the model were significant, the different factors did not have equivalent predictive power. As measured by the mean squares (ms), Depth was the most influential main effect (ms = 88788.3, df = 11) and Month was the second most influential (ms = 2792.6, df = 5). Year was the weakest of the main effects (ms = 476.1, df = 6) and

Table 4. Species groupings derived from hierarchical cluster analyses.

		Data matrix species group								
Species	Code	1987	1988	1989	1990	1991	1992	1993	All years	Boats
English sole	ENG	1	1	1	1	1	1	1	1	1
Petrale sole	PET	1	2	1	1	1	1	1	1	2
Pacific cod	COD	1	1	1	2	1	2	2	1	2
Lingcod	LIN	1	1	1	2	1	2	2	1	2
Rex sole	REX	2	3	1	1	1	2	2	1	1
Small rockfish	SMR	2	3	2	2	1	2	2	3	1
Sanddab	DAB	3	3	2	2	2	2	3	2	1
Widow rockfish	WID	3	3	2	2	2	2	3	2	1
Yellowtail rockfish	YEL	3	3	2	2	2	2	3	2	1
Miscellaneous rockfish	MSR	1	2	3	3	3	3	2	3	3
Arrowtooth flounder	ARR	2	3	2	3	3	3	2	3	3
Pacific ocean perch	POP	3	3	2	3	3	3	2	3	3
Thornyhead	THO	2	4	4	4	4	4	4	4	4
Dover sole	DOV	4	4	4	4	4	4	4	4	4
Sablefish	SBL	4	4	4	4	4	4	4	4	4
Chaining (%)		15	10	7	15	3	18	17	10	5

Fig. 5. Dendograms from the cluster analyses of the data matrices for (*a*) 1988 and (*b*) 1993. The matrices for the other five years in the series produced similar dendograms. See Table 4 for species codes.

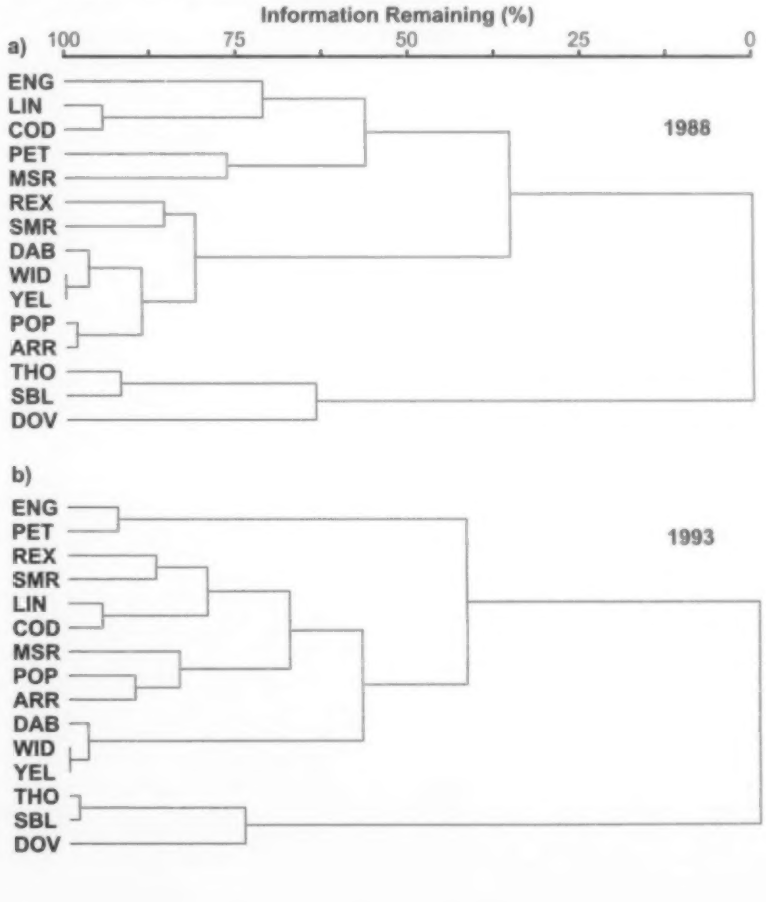

Fig. 6. Predicted values by depth strata from a GLM fit to the DCA axis 1 scores from the areas-by-species matrix for all years combined. Thin solid line, 73.2–146.3 m; broken line, 146.3–219.5 m; solid line with solid circles, 219.5–292.5 m; broken line with open circles, 292.5–365.8 m; solid line with solid squares, 365.8–438.9 m; thick solid line, 438.9–512.1 m.

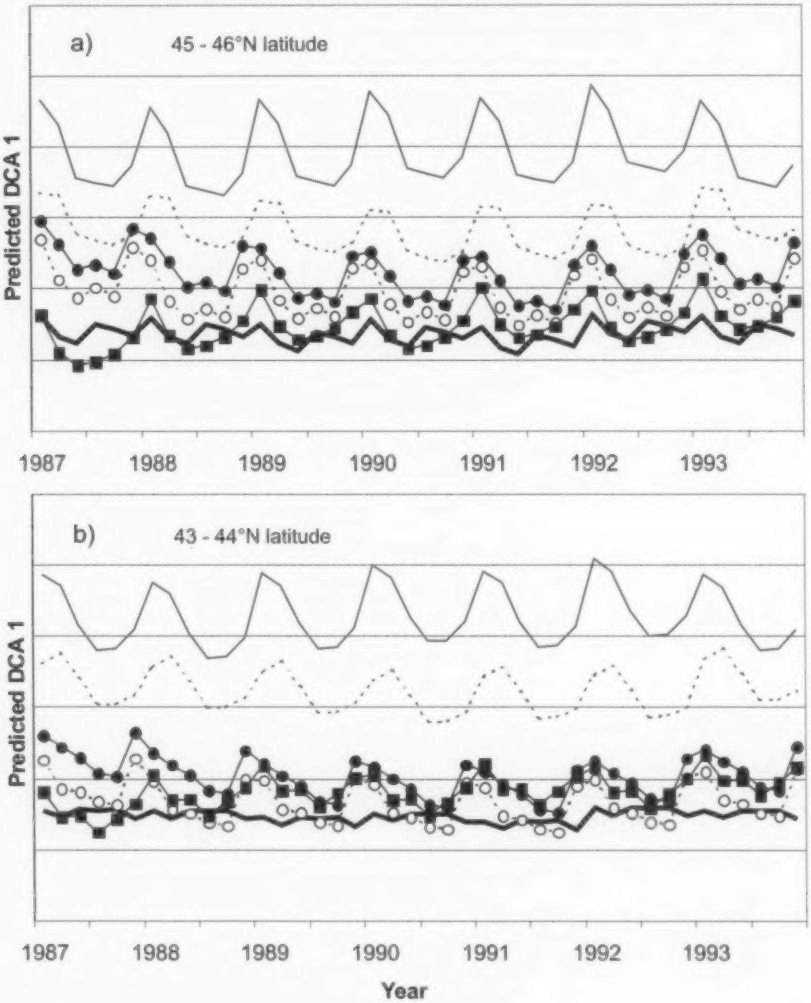

contributed less than the interaction terms Depth × Latitude (ms = 1479.0, df = 48), Depth × Month (ms = 1060.9, df = 38), and Latitude × Month (ms = 560.4, df = 29).

The GLM was used to predict values for the DCA 1 scores and thereby summarize the spatial and temporal variations in the species composition of the bottom trawl landings (e.g., Fig. 6). Larger scores were associated with shallower depths and there was a regular seasonal cycle with higher scores in winter than in summer and decreasing amplitude in the cycles with increasing depth. There was essentially no seasonal pattern in the scores for depths greater than about 439 m (240 fathoms). These seasonal patterns are consistent with the movement of deepwater species onto the shelf in the summer and back to deep water during the winter. Examination of the relative frequency of occurrence data indicated marked increases in the percent occurrence of Dover sole in the shallow depth strata during the summer months. For example, in the 73.2–146.3 m depth stratum, the percent occurrence of Dover sole was about 10% on average during January–February but rose to 60% in May–June and 70% in July–October. There were similar but less pronounced increases in the percent occurrence of sablefish and thornyhead in the shallow depth strata. There were some relatively small differences with latitude in the seasonal patterns of species composition by depth. There was no evidence of annual trends in the species composition.

Discussion

The ordination and cluster analyses in this study indicated that variability in the species compositions was associated primarily with depth and there was a very consistent pattern in the species compositions among all the years. The lack of interannual variation in species compositions was somewhat surprising given that surface and bottom temperature, salinity, upwelling, coastal sea level, and wind stress all show interannual variation over the continental shelf off Oregon (Huyer 1977). Also, one might expect removals by the fisheries to have caused changes in species compositions as more productive species supplanted less productive ones. However, the 7-year time series may be too short to show the effects of fishing. Some might argue that the data used in this study were too crude to measure subtle changes. For example, if we had used data with more complete sets of species, we would have obtained a better representation of the ecological interactions among the species in the study area. Also, if, instead of using relative frequency of species occurrence, we had used catch rates or relative biomass to measure species abundance, as is commonly done in assemblage studies based on survey data, the results might have revealed different temporal characteristics of the assemblages. However, several studies of demersal fish communities that used biomass or relative biomass data from trawl surveys, rather than relative frequency of species occurrence, also report persistent species assemblages over time (e.g., Overholtz and Tyler 1985; Mahon and Smith; 1989 Wright 1989).

One major concern in using logbook data is that there might be distortions of the species compositions because the data were collected by hundreds of different vessels. The comparisons between the DCA results for the areas-by-species data for individual years and the boats-by-species matrix constructed for six selected boats indicated no serious boat effect in the species composition patterns derived from individual years. Also, if there had been a large boat effect, it seems very unlikely that the DCA species plots would have been so consistent from year to year. This lack of a boat effect contradicts the results of Sampson (1997), which analyzed the same logbook data that were used in this study, and found that the factor Boat was the first or second most influential factor for 12 of 15 species in logistic regression models for presence–absence. Sampson (1997) constructed models for individual species whereas the current study accounted for all the species simultaneously in the species composition data matrices. In effect, we treated species occurrence as a repeated measure collected by numerous different samplers. In large-scale lichen studies, McCune et al. (1997) experimented with the effect of having different levels of sampling expertise (such as novice and expert); they concluded that community composition was effectively identified even when the data on species richness contain substantial observer error. This result may also apply to the current study and account for the absence of a boat effect.

The screening criteria that we used to exclude questionable data were chosen subjectively. To develop a more objective basis for screening logbook data, it would be instructive to repeat the study with data matrices that were screened using a series of different criteria.

Rogers and Pikitch (1992) identified six major assemblages of groundfish species off Washington and Oregon using commercial fishery data obtained from observer programs spanning 1985–1987. The main difference from our study was their finding of a shrimp assemblage and a midwater assemblage dominated by widow rockfish. These assemblages were associated with boats that fished with shrimp and midwater trawls, gear types that were not included in our study. The other four assemblages were similar to the assemblages identified in our study. Rogers and Pikitch (1992) could not directly investigate seasonality in the assemblages because of the relatively short study period each year.

Based on National Marine Fisheries Service bottom trawl survey data, Jay (1996) identified 23 species assemblages by using the 33 dominant species from the six surveys combined (1977–1992), and Gabriel (1982) identified 32 assemblages from the 1977 survey. Both studies showed that depth and latitude account for the variability in species assemblages, but neither study was able to examine seasonal variability in species assemblages because the survey occurs only during summer.

One of the drawbacks of using logbook data in a community study is the low level of species resolution and identification. Because logbooks contain only retained catches, it is inevitable that accurate catch information is only available for the valuable commercial species. For example, Pacific hake (*Merluccius productus*) is one species that was not included in our study even though it is a major commercial species (PFMC 1994) and is widely distributed in the study area (Jay 1996). This species is normally targeted by midwater trawlers during summer and forms a large catch in that fishery. In the bottom trawl fishery, Pacific hake are considered a trash fish and are discarded at sea because of poor flesh quality. Many of the groundfish assemblages in Jay (1996) were dominated by Pacific hake, and Jay (1996) concluded that Pacific hake are a major player in the dynamics of groundfish communities off the U.S. west coast. Our results indicate little interannual variation in the composition of the groundfish community exclusive of Pacific hake, even though the biomass of Pacific hake during the study period declined dramatically from a high of 5.7×10^6 t in 1987 to 2.7×10^6 t in 1993 (Dorn et al. 1999).

Other noncommercial species such as skate, spiny dogfish (*Squalus acanthias*), and squid were also not included in our study. As there is no or small market demand for these species, it is unlikely that fishers retain them or keep accurate records of their catches. Also, in the logbooks and fish tickets, the diverse rockfish species were only categorized into two groups, the small rockfish group and the miscellaneous rockfish group. Thus, it was impossible to study interactions of the individual rockfish species and their role in defining assemblages.

In spite of their limitations, logbooks are a very cost-effective way of obtaining information about fish populations that have been disturbed by human exploitation. Analyses based on U.S. west coast trawl logbooks could be greatly improved if the logbooks were enhanced to collect data about discarded as well as retained catches. Also, more detailed information about tow locations (e.g., ending position and depth) would allow researchers to investigate fish communities on a finer geographical scale.

Acknowledgements

We are grateful to the Oregon Department of Fish and Wildlife for providing us access to their logbook and fish ticket data files. We also thank Prof. Bruce McCune (Department of Botany and Plant Pathology, Oregon State University) and Dr. Gary Allison (Department of Zoology, Oregon State University) for instructing us in the art of multivariate analysis of community structure. Funding for this project was provided in part by the Northwest Fisheries Science Center of the National Marine Fisheries Service.

References

Crone, P.R. 1995. Sampling design and statistical considerations for the commercial groundfish fishery of Oregon. Can. J. Fish. Aquat. Sci. **52**: 716–732.

Dorn, M.W., Saunders, M.W., Wilson, C.D., Guttormsen, M.A., Cooke, K., Kieser, R., and Wilkins, M.E. 1999. Status of the coastal Pacific hake/whiting stock in U.S. and Canada in 1998. *In* Status of the Pacific coast groundfish fishery through 1999 and recommended biological catches for 2000: stock assessment and fishery evaluation. Pacific Fishery Management Council, Portland, Oreg.

Fox, D.S., and Starr, R.M. 1996. Comparison of commercial fishery and research catch data. Can. J. Fish. Aquat. Sci. **53**: 2681–2694.

Gabriel, W.L. 1982. Structure and dynamics of northeastern Pacific demersal fish assemblages. Ph.D. dissertation, Oregon State University, Corvallis, Oreg.

Gabriel, W.L., and Tyler, A.V. 1980. Preliminary analysis of Pacific coast demersal fish assemblages. Mar. Fish. Rev. **42**: 83–88.

Gauch, H.G., Jr. 1982. Multivariate analysis in community ecology. Cambridge University Press, Cambridge, U.K.

Gauch, H.G., Jr., and Whittaker, R.H. 1981. Hierarchical classification of community data. J. Ecol. **69**: 537–557.

Hill, M.O., and Gauch, H.G. 1980. Detrended correspondence analysis: an improved ordination technique. Vegitatio, **42**: 47–58.

Huyer, A. 1977. Seasonal variation in temperature, salinity, and density over the continental shelf off Oregon. Limnol. Oceanogr. **22**: 442–453.

Jay, C.V. 1996. Distribution of bottom-trawl fish assemblages over the continental shelf and upper slope of the U.S. west coast, 1977–1992. Can. J. Fish. Aquat. Sci. **53**: 1203–1225.

Jensen, S. 1978. Influence of transformation of cover-abundance values on classification and ordination of lake vegetation. Vegetatio, **48**: 47–59.

Jongman, R.H.J., TerBraak, C.J.F., and Vantongeren, O.F.R. 1987. Data analysis in community and landscape ecology. Pudoc, Wageningen, the Netherlands.

Mahon, R., and Smith, R. 1989. Demersal fish assemblages on the Scotian shelf, Northwest Atlantic: spatial distribution and persistence. Can. J. Fish. Aquat. Sci. **46**: 134–152.

McCune, B., and Mefford, M.J. 1995. PC-ORD. Multivariate analysis of ecological data. MjM Software, Gleneden, Oreg.

McCune, B., Dey, J.P., Peck, J.E., Cassell, D., Heimen, K., Will-Wolf, S., and Neitlich, P.N. 1997. Repeatability of community data: species richness versus gradient scores in large-scale lichen studies. Bryologist, **100**: 40–46.

Noy-Meir, I., Walker, D., and Williams, W.T. 1975. Data transformations in ecological ordination. II. On the meaning of data standardization. J. Ecol. **63**: 779–800.

Overholtz, W.J., and Tyler, A.V. 1985. Long-term responses of the demersal fish assemblages of Georges Bank. Fish. Bull. U.S. **83**: 507–520.

Pacific Fishery Management Council. 1994. Status of the Pacific coast groundfish fishery through 1994 and recommended acceptable biological catches for 1995: stock assessment and fishery evaluation. Pacific Fishery Management Council, Portland, Oreg.

Paulik, G.J., Hourston, A.S., and Larkin, P.A. 1967. Exploitation of multiple stocks by a common fishery. J. Fish. Res. Board Can. **24**: 2527–2537.

Pikitch, E.K., Erickson, D.L., and Wallace, J.R. 1988. An evaluation of the effectiveness of trip limits as a management tool. U.S. Dep. Commer. Natl. Mar. Fish. Serv. NWAFC Proc. Rep. 88-27.

Pimm, S.L., and Hyman, J.B. 1987. Ecological stability in the context of multispecies fisheries. Can. J. Fish. Aquat. Sci. **44**: 84–94.

Ricker, W.E. 1958. Maximum sustained yields from fluctuating environments and mixed stocks. J. Fish. Res. Board Can. **15**: 991–1006.

Rogers, J.B., and Pikitch, E.K. 1992. Numerical definition of groundfish assemblages caught off the coasts of Oregon and Washington using commercial fishing strategies. Can. J. Fish. Aquat. Sci. **49**: 2648–2656.

Romesburg, H.C. 1984. Cluster analysis for researchers. Lifetime Learning Publications, Belmont, Calif.

Sampson, D.B. 1994. Fishing tactics in a two species fisheries model: the bioeconomics of bycatch and discarding. Can. J. Fish. Aquat. Sci. **51**: 2688–2694.

Sampson, D.B. 1997. Effective fishing effort in the Oregon groundfish trawl fishery. Final report to the Oregon Trawl Commission. (Available from D.B. Sampson, Department of Fisheries and Wildlife, Hatfield Marine Science Center, Oregon State University, Newport, OR 97365, U.S.A.)

Sampson, D.B., Crone, P.R., and Saelens, M.R. 1997. Groundfish data collection in Oregon. *In* Commercial fisheries data collection procedures for the U.S. Pacific coast groundfish. *Edited by* D.B. Sampson and P.R. Crone. NOAA Tech. Memo. NMFS-NWFSC-31. pp. 51–100.

SAS Institute Inc. 1988. SAS/STAT user's guide, release 6.03 edition. SAS Institute Inc., Cary, N.C.

Sneath, P.H.A., and Sokal, R.R. 1973. Numerical taxonomy: the principles and practice of numerical classification. W.H. Freeman, San Francisco, Calif.

Sokal, R.R., and Rohlf, F.J. 1981. Biometry. Freeman, New York.

Tabachnick, B.G., and Fidell, L.S. 1996. Using multivariate statistics. 3rd ed. Harper and Row, New York.

Ward, J.H. 1963. Hierachical grouping to optimize an objective function. J. Am. Stat. Assoc. **58**: 236–244.

Weinberg, K.L. 1994. Rockfish assemblages of the middle shelf and upper slope off Oregon and Washington. Fish. Bull. U.S. **92**: 620–632.

Wright, J.M. 1989. Diel variation and seasonal consistency in the fish assemblage of the non-estuarine Sulaibikhat Bay, Kuwait. Mar. Biol. **102**: 135–142.

Predation risk on larval gadids by pelagic fish in the Georges Bank ecosystem. I. Spatial overlap associated with hydrographic features

Lance P. Garrison, William Michaels, Jason S. Link, and Michael J. Fogarty

Abstract: We investigated the relationship between hydrographic variables on Georges Bank and the spatial distribution of larval Atlantic cod (*Gadus morhua*), larval haddock (*Melanogrammus aeglefinus*), and two planktivorous fish, Atlantic herring (*Clupea harengus*) and Atlantic mackerel (*Scomber scombrus*). We conducted cruises during April–May of 1990, 1994, and 1995 to document spatial distributions and employed logistic regression and a spatial-overlap index to assess relationships between hydrographic variables, spatial distributions and spatial overlap between gadid larvae and planktivorous fish. Cod larvae were more abundant in shallow well-mixed areas, while both haddock larvae and herring were more abundant in stratified areas. Atlantic mackerel occurred in deeper water and had little spatial overlap with the other species. In 1995, the presence of Scotian Shelf water and an intrusion of continental slope water altered temperature and salinity distributions and increased spatial overlap between cod larvae and herring. The stratified areas offer a higher concentration of prey for larval haddock, however there is increased exposure to planktivorous fish predators, creating a potential trade-off between predation and starvation. Due to the high abundance of planktivorous fish and high spatial and temporal overlap, predation is likely an important factor influencing survival of gadid larvae on Georges Bank.

Résumé : Nous avons étudié la relation entre les variables hydrographiques sur le banc Georges et la répartition spatiale des larves de la Morue franche de l'Atlantique (*Gadus morhua*), des larves de l'Aiglefin (*Melanogrammus aeglefinus*) et de deux poissons planctonophages, le Hareng atlantique (*Clupea harengus*) et le Maquereau bleu (*Scomber scombrus*). Des croisières en avril–mai en 1990, 1994 et 1995 ont permis d'accumuler des informations sur les distributions spatiales; il a ensuite été possible à l'aide de la régression logistique et d'un indice de chevauchement spatial d'établir les relations entre les variables hydrographiques, les distributions spatiales et le recoupement spatial des larves de gadidés et des poissons planctonophages. Les larves de morue étaient plus abondantes dans les eaux peu profondes et bien brassées, alors que les larves d'aiglefin et les harengs étaient plus nombreux dans les zones stratifiés. Le Maquereau rouge se retrouvait dans les eaux plus profondes et sa répartition recoupait peu celle des autres espèces. En 1995, la présence d'eau provenant de la plate-forme néo-écossaise et une intrusion d'eau provenant du talus continental ont modifié les répartitions de température et de salinité et augmenté le recoupement spatial des larves de morue et des harengs. Les zones stratifiées offrent une plus forte concentration de proies pour les larves d'aiglefin, mais aussi une plus grande exposition aux prédateurs des poissons planctonophages; il se crée donc potentiellement un compromis entre la prédation et la famine. À cause de la forte densité de poissons planctonophages et des forts recoupements spatiaux et temporels, la prédation est vraisemblablement un facteur important dans la survivance des larves de gadidés sur le banc Georges.

[Traduit par la Rédaction]

Introduction

Demersal gadid fish, particularly Atlantic cod (*Gadus morhua*) and haddock (*Melanogrammus aeglefinus*), have experienced intense overfishing on Georges Bank during the last three decades resulting in population declines (Fogarty and Murawski 1998). Fishery exploitation has been reduced in recent years in an effort to rebuild stocks to sustainable levels (Northeast Fisheries Science Center 1998). However, stock recovery is determined in large part by successful recruitment. The strength of an incoming year-class is generally determined during the first year, and the survival of the larval stage is an important component of recruitment success (Hjort 1914; Houde 1987).

Hjort's (1914) critical-period hypothesis proposed that survival of larval fish was limited primarily by nutritional stress during the first feeding period and (or) unfavorable physical transport away from nursery habitats. These two factors have been the particular focus of research on Georges Bank since 1992 (US-GLOBEC 1992). Both field (Buckley and Lough 1987; Lough et al. 1996) and modeling (Werner et al. 1996; Leising and Franks 1999) studies indicate that larval cod and haddock growth can be limited by food

Received June 23, 2000. Accepted October 31, 2000. Published on the NRC Research Press web site on December 20, 2000. J15833

L.P. Garrison,[1] W. Michaels, J.S. Link, and M.J. Fogarty. National Marine Fisheries Service, Northeast Fisheries Science Center, 166 Water Street, Woods Hole, MA 02543, U.S.A.

[1] Corresponding author.

Fig. 1. The southern flank of Georges Bank off the northeastern United States. Typical locations of the tidal-mixing and shelf-slope fronts are outlined in gray. Mean anticyclonic circulation along the southern flank is depicted by the large arrow. Sampling areas for cruises conducted in 1990, 1994, and 1995 are outlined by solid and broken lines.

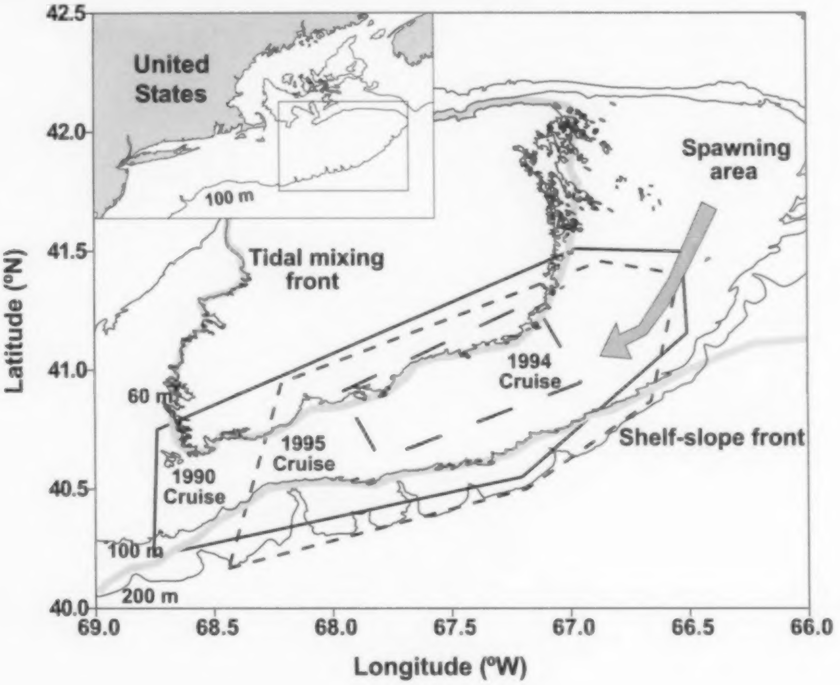

availability under ambient prey concentrations. Physical processes that concentrate larvae and their prey can enhance feeding rates sufficiently to support growth (Lough and Potter 1993; Lough et al. 1996; Leising and Franks 1999).

Larval-cod and -haddock abundances peak over the southern flank from March to May. Haddock spawn primarily over the Northeast Peak from February to June with peak spawning in April and May (Colton and Temple 1961). Cod have a more protracted spawning period throughout the year, and their peak spawning occurs earlier from January to April (Colton and Temple 1961). The larvae of both species are advected in anticyclonic residual currents around the southern flank (Fig. 1; Werner et al. 1993), and juveniles settle over the shallow central portion of the bank and in the Great South Channel during late spring and early summer (Lough and Bolz 1989). A combination of physical and behavioral processes tend to retain larvae on Georges Bank, however episodic events may result in significant advective losses (Werner et al. 1993, 1996).

Vernal warming of surface water drives vertical density stratification and intensifies the anticyclonic currents around the bank. However, the shallow (<60 m) central region remains vertically homogeneous due to strong tidal mixing. During late April, a tidal-mixing front develops that generally coincides with the 60-m isobath (Fig. 1; Townsend and Pettigrew 1996). The southern flank is bounded by warm high-salinity slope waters that can intrude onto the bank above the 100-m isobath (Flagg 1987). In addition, there is intermittent intrusion of cold fresh water from the Scotian Shelf across the Northeast Peak and along the southern flank which can introduce considerable interannual variability into mean hydrographic characteristics (Bisagni et al. 1996).

The primary biotic mechanism thought to regulate recruitment success is starvation mediated by variable physical regimes and metabolic demands (Werner et al. 1996; Leising and Franks 1999). However, predation can also strongly impact larval-fish survival (Bailey and Houde 1989) and has so far received little attention in the study of larval-gadid survival on Georges Bank (Werner et al. 1996). Forthcoming studies have focused exclusively on invertebrate planktonic predators, such as amphipods, euphausiids, decapod shrimp, gelatinous zooplankton, and predatory hydroids (Madin et al. 1996; Madin and Horgan 1997). The current study was implemented to assess the impact of predation by planktivorous fish on the survival of larval and juvenile gadids on Georges Bank.

Atlantic herring (*Clupea harengus*) and Atlantic mackerel (*Scomber scombrus*) may impact larval-gadid survival on the southern flank of Georges Bank. Both species move through this region during the March–May period when larval-gadid abundance is high (Anthony and Waring 1980; Grosslein 1987), and both are planktivores that readily consume larval fish (Øiestad 1985; Pepin et al. 1987; Michaels 1991). Both herring and mackerel stocks were severely reduced by fishing during the late 1960s and early 1970s and remained at low levels until 1990. In the last decade, their spawning-stock sizes have increased by nearly an order of magnitude

Fig. 2. Bottom-temperature and salinity maps for four replicate grids in 1990. (*a* and *b*) Grid 1, 24–28 April: (*a*) temperature; (*b*) salinity. (*c* and *d*) Grid 2, 29 April – 3 May: (*c*) temperature; (*d*) salinity. (*e* and *f*) Grid 3, 8–12 May: (*e*) temperature; (*f*) salinity. (*g* and *h*) Grid 4, 13–17 May: (*g*) temperature; (*h*) salinity.

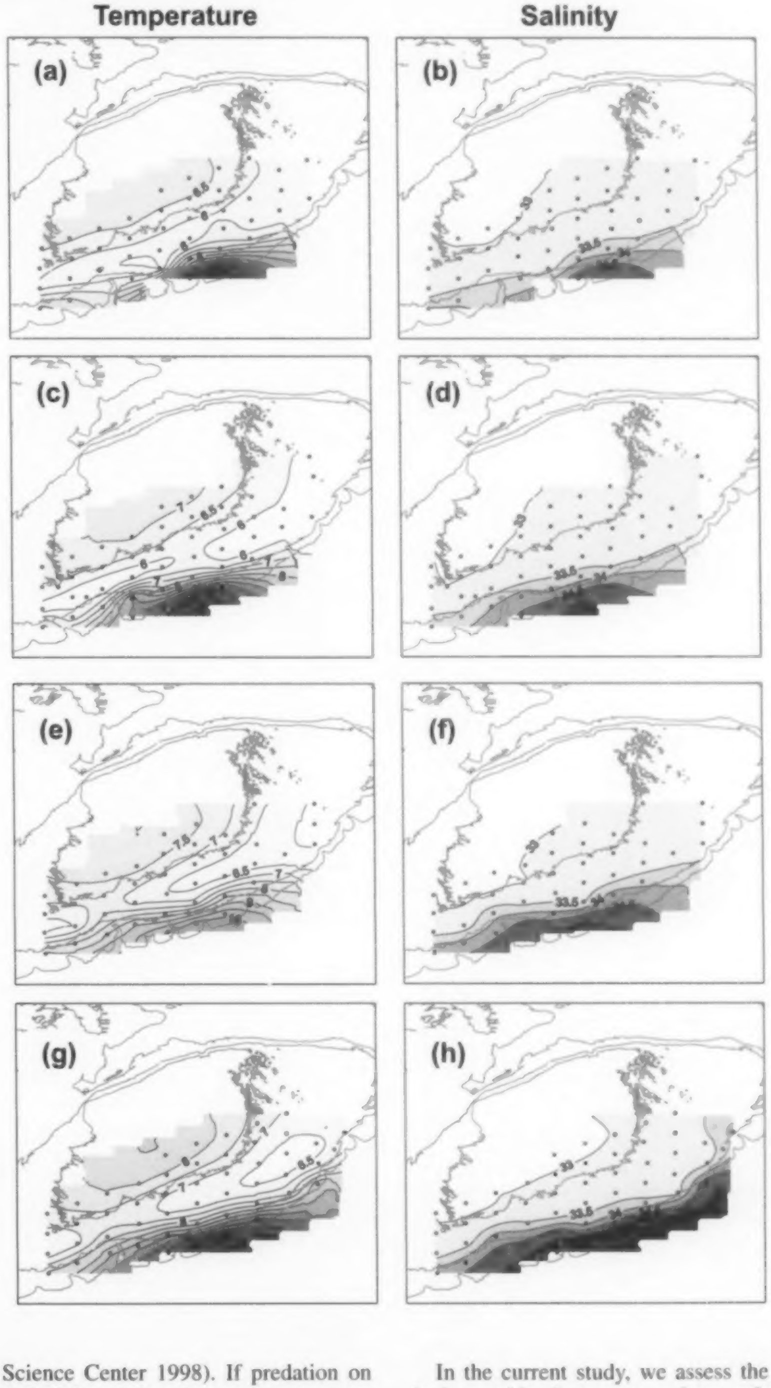
Temperature
Salinity
(a)
6.5
6
8
(b)
33
33.5
34
(c)
7
6.5
6
7
8
(d)
33
33.5
34
(e)
7.5
7
6.5
7
6
8
(f)
33
33.5
34
(g)
6
7
6.5
7
8
(h)
33
33.5
34

(Northeast Fisheries Science Center 1998). If predation on larval gadids by these planktivores is a frequent occurrence, then their high biomass may be an important factor limiting the recovery of gadid stocks.

In the current study, we assess the relationships between hydrographic features on the southern flank of Georges Bank and the spatial overlap of larval cod, larval haddock, and two potential predators, Atlantic herring and Atlantic

Fig. 3. Stratification index ($\Delta - \sigma_t$) maps for replicate grids in 1990. (*a*) Grid 1. (*b*) Grid 2. (*c*) Grid 3. (*d*) Grid 4.

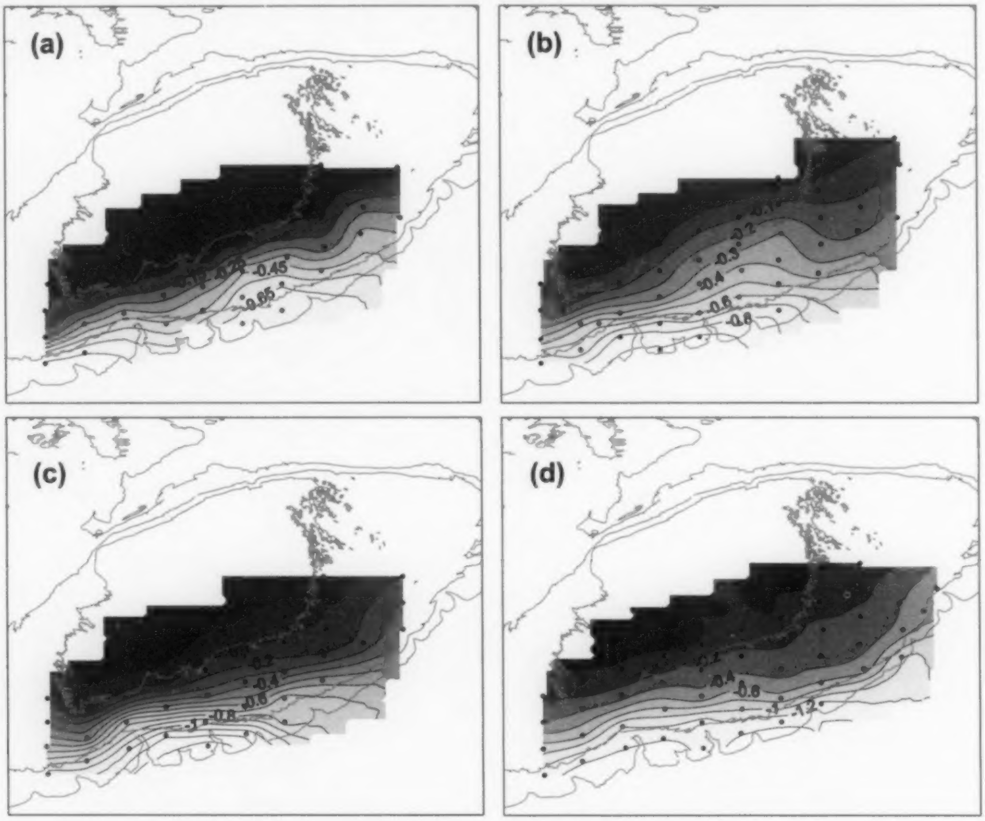

mackerel. We present results from studies conducted during April and May of 1990, 1994, and 1995 that quantify larval densities, planktivorous-fish abundance, and physical features under a range of hydrographic conditions.

Materials and methods

Sampling design and protocols

We present the results from three surveys executed during late April–May of 1990, 1994, and 1995 on the southern flank of Georges Bank (Fig. 1). In each year, three (four in 1990) replicate systematic grid surveys were conducted, generally incorporating the 60- to 200-m depth range. The survey in 1994 incorporated a smaller area than those in the other 2 years (Fig. 1). Each replicate grid proceeded from east to west (west to east in 1994) across the survey area over a period of <1 week. Station locations were separated by distances of 5–15 km depending upon the survey year.

At each station, a twin 61 cm bongo sampler fitted with 333 μm and 505 μm mesh nets and flow meters was deployed to collect larval fish. A Seabird model 19 CTD profiler was also attached, and the array was fished double obliquely from the surface to near bottom and back at 2.8–3.7 km·h^{-1}. All fish larvae from both nets were preserved in 4% formalin and identified in the laboratory. Data from the 333 μm mesh net is unavailable for the 1990 cruise. Based upon larval counts, volume filtered, and water-column depth, the density (number·m^{-2}) of cod and haddock larvae was calculated for each station. There was no significant difference (t test, $p > 0.5$) in catch or size frequency of larvae between the 333 μm and 505 μm mesh nets and, therefore, for 1994 and 1995, we present the average of the two.

Following the ichthyoplankton sampling, herring, mackerel, and other fish were sampled using either a 36 Yankee bottom trawl (1990 and 1994) or a Shuman midwater trawl (1995). The Yankee trawl (mouth opening 3.2 × 10.4 m) was fished at 6.5 km·h^{-1} for 30 min. During the 1995 cruise, a Shuman midwater trawl was fished at 8.3 km·h^{-1} for 30 min. The midwater trawl was set near the bottom but sampled approximately 30 m of the water column. The midwater trawl is much more effective gear for sampling pelagic fish. In the current analysis, we have not corrected for the different fishing powers of the gear and do not attempt to estimate or compare abundance across years. We present the number of fish captured per standard tow as a measure of relative abundance at each station.

Description of hydrographic features

Maps of surface and bottom temperature, salinity, and density (σ_t) were prepared based upon hydrographic profiles at each station. Contour maps for each replicate grid for each cruise were prepared using point krigging based upon fitted variograms that accounted for anisotropy in spatial patterns (Isaaks and Srivastava 1989). In addition to these variables, a proxy for the degree of water-column stratification, $\Delta - \sigma_t$, was calculated as the difference between surface and bottom values of σ_t.

There are two frontal boundaries that are important hydrographic features of the southern flank of Georges Bank. The first is the tidal-mixing front in the vicinity of the 60 m isobath.

Fig. 4. Larval and pelagic fish abundance data for replicate grids in 1990. Densities (number·m^{-2}) are shown for larval cod and haddock, while catches (number·tow^{-1}) are shown for Atlantic herring and mackerel. (*a* and *b*) Grid 1: (*a*) larval gadids; (*b*) pelagic fish. (*c* and *d*) Grid 2: (*c*) larval gadids; (*d*) pelagic fish. (*e* and *f*) Grid 3: (*e*) larval gadids; (*f*) pelagic fish. (*g* and *h*) Grid 4: (*g*) larval gadids; (*h*) pelagic fish. Approximate locations of the tidal-mixing front (broken line) and the shelf-slope front (solid line) are indicated.

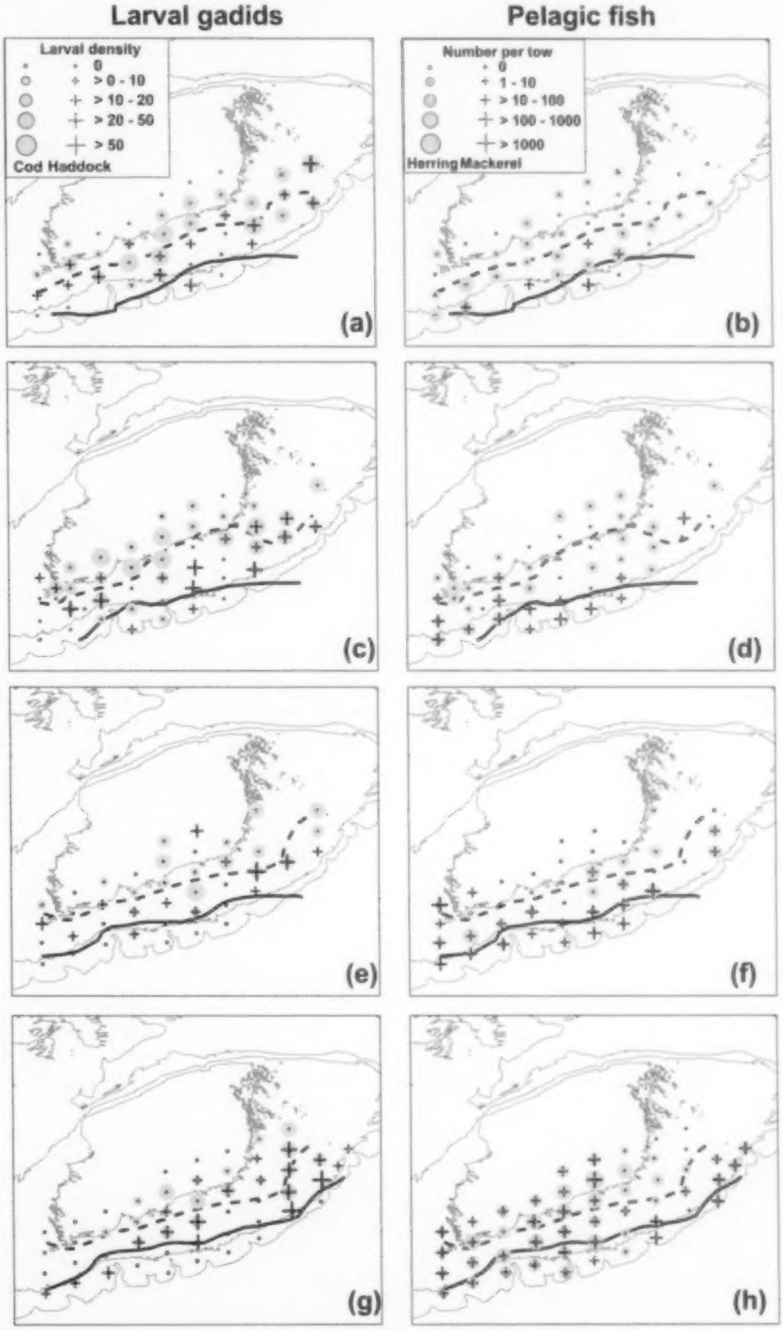
Larval gadids
Pelagic fish
Larval density
0
> 0 - 10
> 10 - 20
> 20 - 50
> 50
Cod Haddock
Number per tow
0
1 - 10
> 10 - 100
> 100 - 1000
> 1000
Herring Mackerel
(a)
(b)
(c)
(d)
(e)
(f)
(g)
(h)

The $\Delta - \sigma_t$ contour corresponding to a σ_t difference of –0.2 was used to identify the approximate location of this front and is roughly consistent with previous studies (Flagg 1987; Townsend and Pettigrew 1996). Second, the shelf-slope front is generally deeper than the 100-m isobath, however it occasionally intrudes up onto the bank (Flagg 1987). The slope water was identified by

Table 1. Logistic regression results.

	Bottom temperature	Bottom salinity	$\Delta - \sigma_t$
1990 cruise			
Larval cod	0.650*	—	7.931***
Larval haddock	0.343***	6.314**	—
Herring	0.635**	—	0.229**
Mackerel	1.564*	—	0.022***
1994 cruise			
Larval cod	—	0.197***	—
Larval haddock	0.557**	—	0.074**
Herring	0.522**	—	0.102*
Mackerel	—	—	—
1995 cruise			
Larval cod	0.785**	—	22.86***
Larval haddock	—	0.393***	0.091**
Herring	0.663***	—	—
Mackerel	—	—	—

Note: Values are odds ratios for significant factors in stepwise logistic regressions for each cruise. All models were highly significant (−2 log likelihood χ^2 $p < 0.001$) and closely fit the data (goodness of fit test, $p > 0.25$). *P* values for individual odds ratios: ***, $p < 0.001$; **, $p < 0.01$; *, $p < 0.05$.

salinity >33.5 psu (practical salinity units) (Flagg 1987), and we have used this contour in surface-salinity plots to delineate the boundary of the shelf-slope front. These frontal boundaries are somewhat arbitrary and are used only for visual reference when discussing larval and fish distributions.

Mean-temperature and salinity values

We calculated the weighted mean temperature and salinity of occurrence for both larvae and planktivorous fish. The weighted mean and 95% confidence intervals (CIs) for each year were calculated for each species. The abundance data were characterized by large numbers of zero values, and positive values were lognormally distributed. Stations with zero abundance do not affect the weighted mean, and the mean salinity and temperature for each species were weighted by log-transformed abundance.

Logistic-regression analysis

The assumptions of parametric analyses (e.g., linear-regression models) are severely violated by the distribution of the abundance data (ter Braak and Looman 1995). Additionally, we must consider spatial autocorrelation, which confounds most statistical tests by violating the assumption of independence of samples (Legendre 1993). We addressed this issue by examining spatial autocorrelation in species distributions for each grid for each cruise. We constructed directional correlograms, using Moran's I as the autocorrelation coefficient, and tested for statistical significance by employing randomization tests (Legendre and Fortin 1989; Manly 1997). There was no significant spatial autocorrelation in these data, and the assumption of spatial independence is therefore not violated.

We addressed the problem of zero values by transforming the observed species abundances into presence–absence data and evaluating the relationship between environmental parameters and species presence within a logistic regression (ter Braak and Looman 1995). The logistic model identifies the environmental variables that limit spatial distribution in these species.

We performed a step-wise logistic regression (Hosmer and Lemeshow 1989) that modeled the probability of occurrence for larval cod, larval haddock, herring, and mackerel for each cruise. Three environmental parameters were entered into the selection procedure: bottom temperature, bottom salinity, and $\Delta - \sigma_t$ (described above). These variables were selected because they best describe the hydrographic features of the bank and the relative positions of the frontal zones of interest. Overall model significance was assessed using the −2 log likelihood χ^2, and adequate model fit was indicated by a nonsignificant goodness of fit test (Hosmer and Lemeshow 1989).

Williamson spatial-overlap index

When both predator and prey distributions are patchy in space, high spatial overlap significantly increases the overall predation risk (Williamson 1993). The Williamson spatial-overlap index characterizes the extent to which the correlation between predator and prey deviates from a random expectation under uniform spatial distributions. The index, O_{ij}, is calculated as:

$$(1) \qquad O_{ij} = \frac{\sum_{z} (N_{iz} N_{jz}) m}{\sum_{z} (N_{iz}) \cdot \sum_{z} (N_{jz})}$$

where z is a sample location, m is the total number of samples, N_i is the abundance of species i, and N_j is the abundance of species j. If the index is equal to 1, then the degree of overlap is not different from the expectation where the species are uniformly distributed. A value <1 indicates less than expected overlap, while a value >1 indicates a greater than expected overlap, with the upper bound determined by the number of locations sampled (Williamson 1993).

There is no statistical test to evaluate the deviation of observed overlap from random expectation. To assess the significance of the Williamson spatial-overlap index, we employed a randomization test appropriate for correlation coefficients with a similar form (Manly 1997). We tested the observed value against a null hypothesis of no spatial relationship by generating a random distribution of overlap values. For each species pair for each cruise, we randomly (with replacement) selected values for species j to pair with the abundance of species i at each site and calculated the randomized O_{ij}. The randomization was completed 4999 times, with the actual observed value being the 5000th instance. The significance level is the proportion of observations from the randomized distribution with deviations from 1 larger than or equal to the observed value. Statistical significance was assessed at the $\alpha = 0.05$ level.

Results

Cod larvae were more abundant than haddock larvae in the bongo samples. Larval densities for cod averaged 11.7, 35.2, and 6.6 larvae·m^{-2} in 1990, 1994, and 1995, respectively. Average larval-haddock densities were 5.0, 21.4, and 2.1 larvae·m^{-2} in 1990, 1994, and 1995, respectively. Larval cod were also larger, on average, than larval haddock. Average lengths for larval cod were 11.2 mm (95% CI = ±0.6), 7.9 mm (±0.2), and 11.1 mm (±0.8) in 1990, 1994, and 1995, respectively. The modal size for cod larvae was 8 mm in all 3 years. Mean lengths of haddock larvae were 6.8 mm (95% CI = ±0.6), 6.2 mm (±0.2), and 6.6 mm (±0.9) in 1990, 1994, and 1995, respectively, with a modal size of 6 mm in all 3 years.

Atlantic herring were more abundant and occurred more frequently than Atlantic mackerel. Herring abundance averaged 49.1, 9.7, and 790.6 fish per tow in 1990, 1994, and 1995, respectively. Herring occurred in 62.6, 63.7, and 55.4% of the trawl tows in 1990, 1994, and 1995, respectively. Atlantic mackerel abundance averaged 11.0, 3.1, and 11.7

Fig. 5. Bottom-temperature and salinity maps for three replicate grids in 1994. (*a* and *b*) Grid 1, 3–7 May: (*a*) temperature; (*b*) salinity. (*c* and *d*) Grid 2, 10–12 May: (*c*) temperature; (*d*) salinity. (*e* and *f*) Grid 3, 17–20 May: (*e*) temperature; (*f*) salinity.

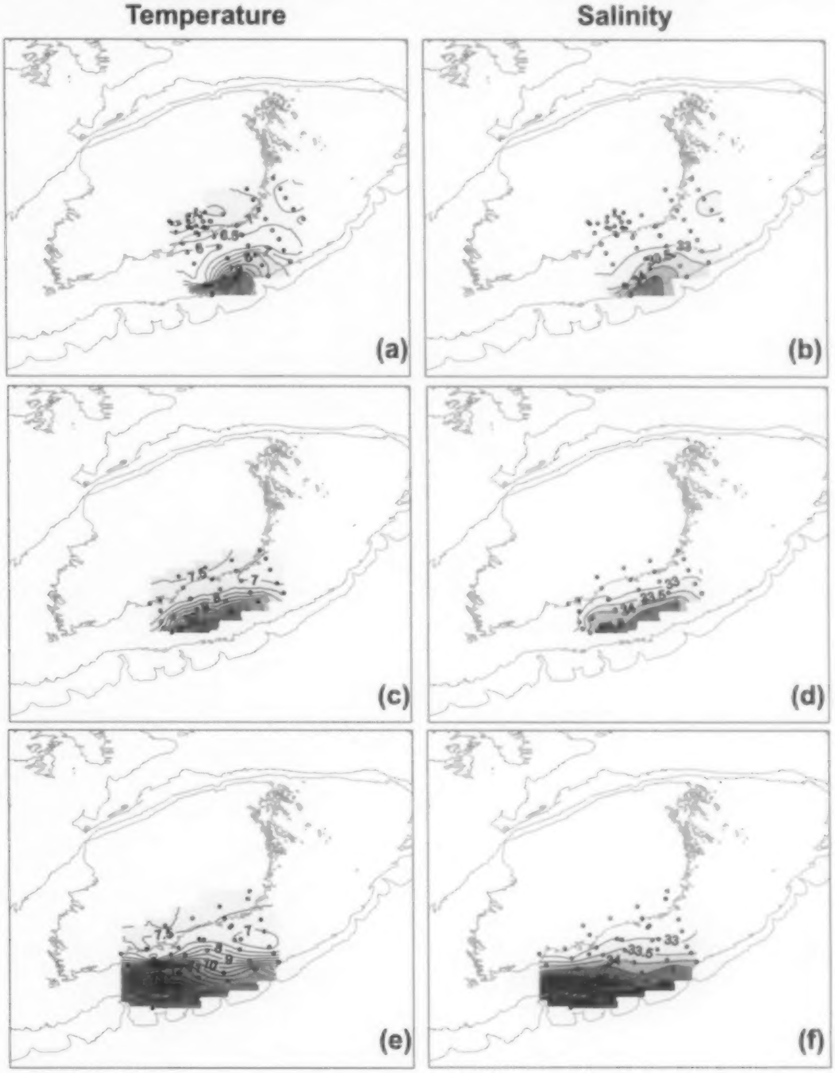

fish per tow and occurred in 43.4, 39.8, and 25.6% of the tows in 1990, 1994, and 1995, respectively.

1990 cruise

Bottom temperatures on the southern flank during 1990 reflected both the developing seasonal stratification and the offshore presence of slope water. A pool of cold water (6–7°C) occurred between the 60- and 80-m isobaths (Fig. 2), while inside the 60-m isobath bottom temperatures were warmer and were similar to surface temperatures (Fig. 2). Bottom temperatures between the 60- and 80-m isobaths were generally 1–1.5°C colder than surface-water temperatures. The presence of warm water >10°C was evident around the 100-m isobath, where bottom salinities were also high (>34 psu) for all four grids (Fig. 2). The stratification patterns reflect these gradients. The water column was well mixed within the 60-m isobath (Fig. 3), and the presence of cold bottom water and the intrusion of warm slope water resulted in a cross-isobath stratification gradient (Fig. 3).

Cod larvae were more abundant within shallow well-mixed waters (Fig. 4). The logistic regression indicated a strong positive association (odds ratio >> 1) with $\Delta - \sigma_t$ indicating a much higher probability of occurrence in less stratified waters (Table 1). There was a negative relationship (odds ratio < 1) with bottom temperatures, indicating that cod larvae occurred more frequently in areas with colder bottom water (Table 1). They were largely absent from deeper waters and very rarely occurred in the region of the shelf-slope frontal boundary (Fig. 4). In contrast, larval haddock were generally more abundant between the 60- and 100-m isobaths in stratified water (Fig. 4). They were also negatively associated with warm bottom water but had a

Fig. 6. Stratification index ($\Delta - \sigma_t$) maps for three replicate grids in 1994. (*a*) Grid 1. (*b*) Grid 2. (*c*) Grid 3.

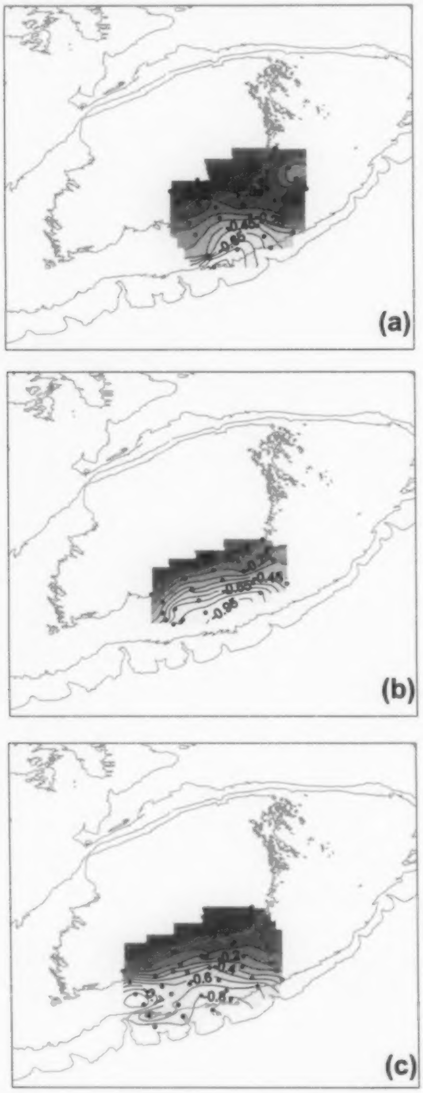

strong positive relationship with bottom salinity (Table 1). Haddock larvae occurred primarily in the stratified region where bottom temperatures were coldest and bottom salinity was relatively high compared with unstratified areas (Figs. 2 and 4). However, haddock larvae were also largely absent from the slope water (Figs. 2 and 4).

Atlantic herring were less likely to occur in warm bottom water and had a negative association with $\Delta - \sigma_t$, indicating that they were more likely to occur in stratified areas (Table 1). They were most abundant between the 60- and 100-m isobaths in grids 1–3, and they rarely occurred deeper than the shelf-slope front (Figs. 4*b*, 4*d*, and 4*f*). Atlantic mackerel occurred in relatively low abundance in grids 1–3, and occurred more frequently in warmer water and in areas >100 m in depth (Table 1; Figs. 4*a*, 4*b*, and 4*f*). In grid 4, both herring and mackerel abundances were much higher, and they were more evenly distributed across the sampling area (Fig. 4*h*).

1994 cruise

As in the 1990 cruise, bottom temperatures were cold (6.5–7°C) in areas between the 60- and 80-m isobaths, and surface temperatures were generally uniform across this region at approximately 8°C (Fig. 5). The intrusion of slope water well up onto the bank was apparent in grids 2 and 3, and temperatures >10°C and salinities >34 psu occurred as shallow as the 80-m isobath (Fig. 5). Very warm bottom water with salinities as high as 35 psu intruded well up onto the bank in grid 3 (Figs. 5*e* and 5*f*). In grid 1, the majority of the sampled area was well-mixed out to an approximate depth of 80 m (Fig. 6*a*). However, as slope water intruded up onto the bank, the cross-isobath stratification gradient intensified, and for these periods, the boundary of well-mixed water was closer to the 60-m isobath (Figs. 6*b* and 6*c*).

Cod larvae were broadly distributed in grids 1 and 2 in 1994 (Figs. 7*a* and 7*b*). Larval cod were much less likely to occur in areas with high bottom salinity, and they rarely occurred in areas with bottom salinity >33 psu (Table 1; Fig. 7). Larval-cod densities were very low in grid 3, and they were never present in the intruding slope water (Fig. 7*d*). Haddock larvae were more frequent in areas deeper than 60 m (Figs. 7*a*, 7*b*, and 7*d*). Larval haddock were less likely to occur in warm bottom water and were negatively associated with $\Delta - \sigma_t$ (Table 1); they were largely absent from the intruding slope water in grid 3 (Fig. 7*d*).

Abundance data for herring and mackerel were not collected for grid 1. Herring were abundant in grids 2 and 3 and were broadly distributed across the sampling area; however, they were generally absent from areas deeper than the shelf-slope front (Figs. 7*c* and 7*e*). Herring were negatively associated with bottom temperature and $\Delta - \sigma_t$ (Table 1) and were more abundant in stratified water between the 60- and 100-m isobaths in grid 3 (Fig. 7*e*). Mackerel were present in lower abundances in grid 2 but were more abundant in grid 3 (Figs. 7*c* and 7*e*); they were present across the sampling area and showed no significant association with any physical variable (Table 1).

1995 cruise

There were several unique hydrographic features evident during the 1995 cruise. In grid 1, there was intrusion of cold (5–6°C) low salinity (<32 psu) water from the Scotian Shelf in the northeast corner of the grid between the 60- and 100-m isobaths (Figs. 8*a* and 8*b*). The intrusion of this cold water was evident in both surface and bottom waters. Following this intrusion, there was a cross-isobath gradient in both salinity and temperature in grid 2 (Figs. 8*c* and 8*d*). Warm (>9°C) high salinity (>34 psu) water also intruded well above the 100-m isobath (Figs. 8*c* and 8*d*). Bottom temperatures ranged between 8 and 14°C between the 60- and 100-m isobaths, and bottom salinities were >34 psu. In grid 3, temperatures >8°C were present above the 60-m isobath, and high-salinity water intruded to the 80-m isobath (Figs. 8*e* and 8*f*). Stratification was weak inside the 60-m isobath in grid 1 and, as the slope water intruded, the well-mixed water also moved shoalward (Figs. 9*a*–9*c*). The degree of stratification was

Fig. 7. Larval and pelagic fish abundance data for replicate grids in 1994. Densities (number·m^{-2}) are shown for larval cod and haddock, while catches (number·tow^{-1}) are shown for Atlantic herring and mackerel. No pelagic fish were collected for grid 1. (*a*) Grid 1: larval gadids. (*b* and *c*) Grid 2: (*b*) larval gadids; (*c*) pelagic fish. (*d* and *e*) Grid 3: (*d*) larval gadids; (*e*) pelagic fish. Approximate locations of the tidal-mixing front (broken line) and the shelf-slope front (solid line) are indicated.

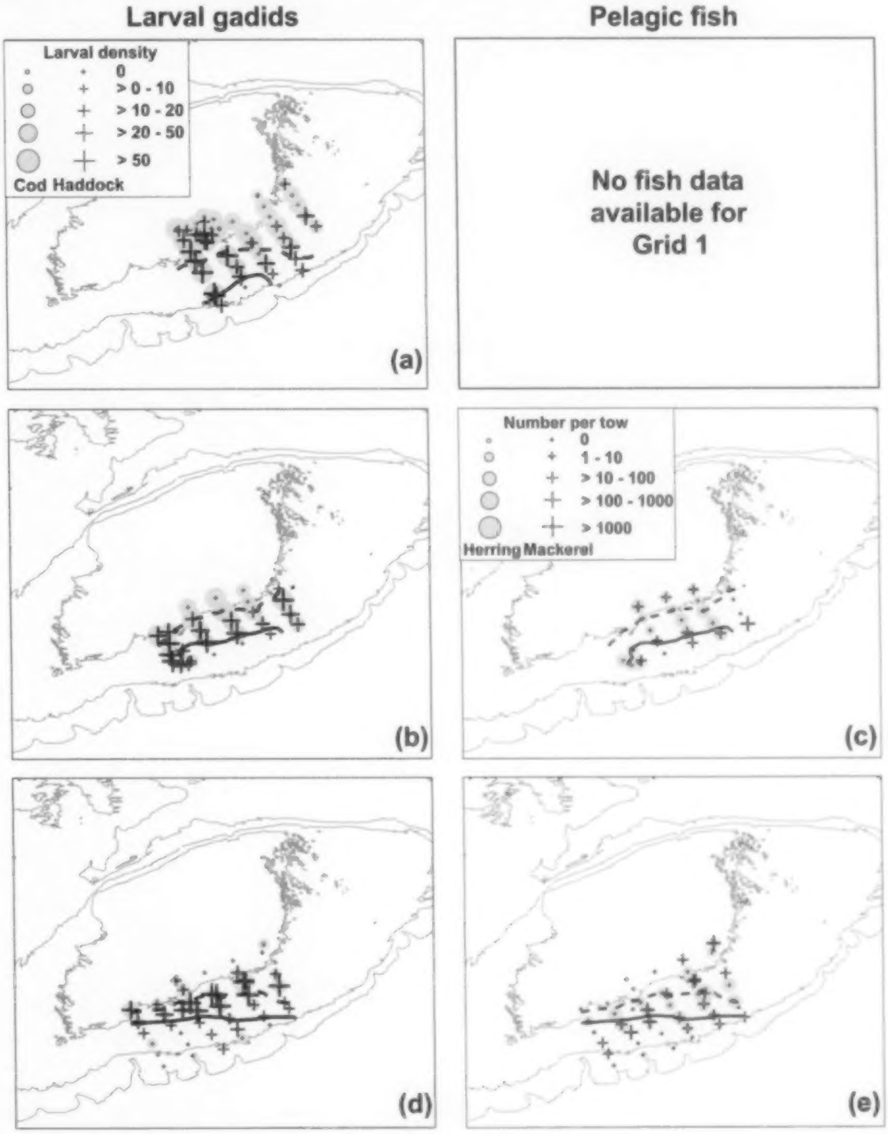

highest between the 60- and 100-m isobaths in grid 2 (Fig. 9*b*) but showed a cross-bathymetry gradient in grid 3 (Fig. 9*c*). Well-mixed water was associated with only a narrow area of temperatures <8°C in grid 3 (Figs. 8*e* and 9*c*).

Larval cod were abundant in grids 1 and 2 inside the region of well-mixed water shallower than 60-m (Figs. 10*a* and 10*c*). The odds ratio with $\Delta - \sigma_t$ was very large, indicating a strong association with well-mixed water (Table 1). Larval cod were also negatively associated with bottom temperature and were more likely to occur in colder water (Table 1). Their abundance was lower in grid 3, and they were mostly present in the well-mixed water on the eastern end of the survey area (Fig. 10*e*). Larval haddock were only sparsely present during this cruise and were generally distributed between the 60- and 100-m isobaths. They were negatively associated with $\Delta - \sigma_t$ (Table 1) and were primarily abundant in the stratified areas between the 60- and 80-m isobaths (Fig. 10). Haddock larvae were also negatively associated with bottom salinity and were absent from intruding slope water (Fig. 10).

Atlantic herring were associated with cold bottom water (Table 1). In grid 1, herring were broadly distributed, but in

Fig. 8. Bottom-temperature and salinity maps for three replicate grids in 1995. (*a* and *b*) Grid 1, 30 April – 3 May: (*a*) temperature; (*b*) salinity. (*c* and *d*) Grid 2, 10–17 May: (*c*) temperature; (*d*) salinity. (*e* and *f*) Grid 3, 20–28 May: (*e*) temperature; (*f*) salinity.

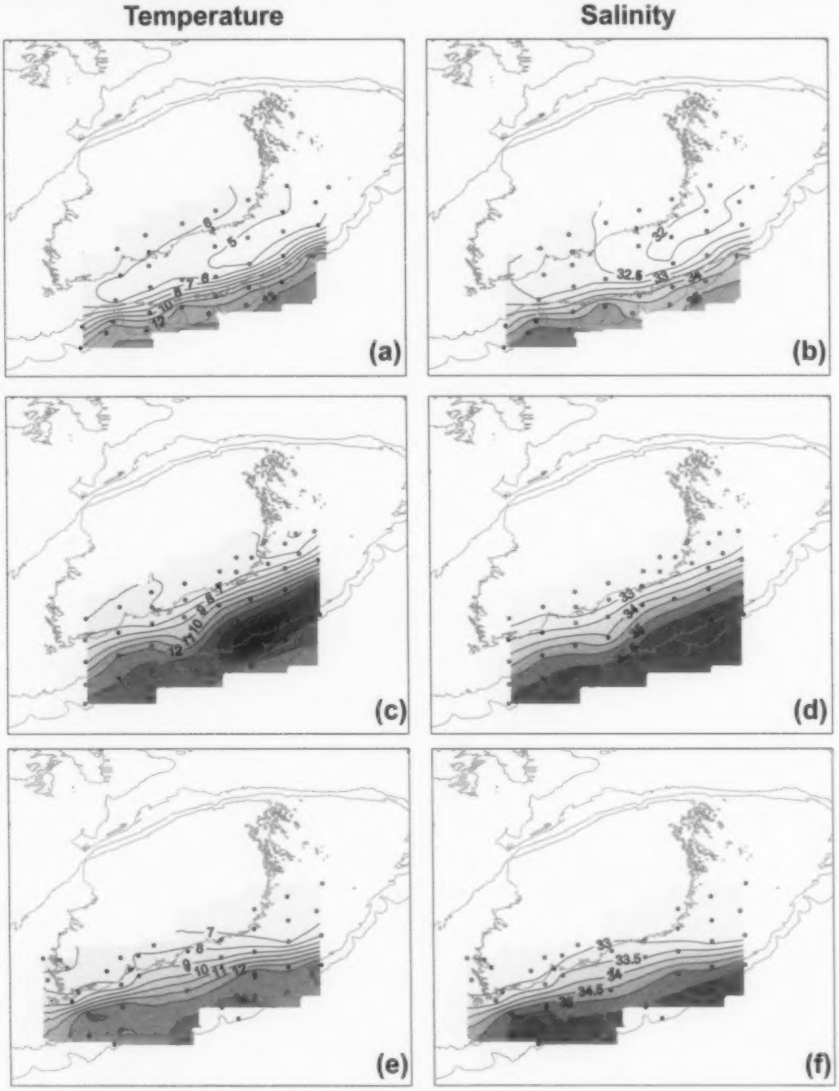

grids 2 and 3, they were more concentrated in areas around the 60-m isobath (Fig. 10) and very rarely occurred in warm slope waters. Atlantic mackerel were only abundant in grid 2 and occurred in deeper water than herring (Fig. 10). Mackerel had no significant association with the physical variables (Table 1).

Mean environmental parameters and spatial overlap

The average-temperature range for cod larvae was consistently lower than that for the other species in all three cruises (Fig. 11). The average temperature value for cod larvae was typically <7°C for both surface and bottom water, with the exception of the warm surface temperatures in 1994. Haddock and herring had consistently similar temperature and salinity ranges (Fig. 11). However, in the 1995 cruise, the mean surface and bottom temperatures and salinities were very similar for larval cod and Atlantic herring (Fig. 11). Mean temperatures and salinities were both higher for mackerel than for the other species (Fig. 11).

The spatial overlap reflects these environmental patterns. For the 1990 and 1994 cruises, the spatial overlap between cod and herring was not significantly different from the random expectation. However, for the 1995 cruise, their overlap was very high, indicating significant spatial association (Table 2). The spatial overlap between haddock and herring was positive in all 3 years (Table 2), reflecting the similar environmental preferences of these species. The spatial overlap between mackerel and both larval species was generally near

1, and the spatial overlap between mackerel and cod was significantly less than 1 in 1990 (Table 2).

Discussion

Despite the variable hydrographic conditions we observed, cod larvae were consistently more abundant in the shallow well-mixed region of Georges Bank than in the stratified areas. In contrast, both haddock larvae and Atlantic herring were more abundant in the stratified areas of the southern flank. Haddock and herring spatial overlap was positive in all 3 years, and they had very similar distributions with respect to bottom temperature and the stratification index. Atlantic mackerel were consistently more abundant in warmer and higher-salinity water than the other species and generally occurred in low abundance at this time of year. All four species showed a negative response to the intrusion of warm high-salinity water from the continental slope, which typically resulted in reduced abundance below the 100-m isobath. In general, the degree of spatial overlap, and thus the risk of predation, is stronger between herring and larval haddock than between herring and cod. The interaction between mackerel and the two larval gadids is likely weak due to low spatial overlap.

An exception occurred in 1995 when two anomalous hydrographic conditions existed. First, cold low-salinity Scotian Shelf water (SSW) occurred on the southern flank. Second, the shelf-slope front intruded onto the bank. Herring were more likely to occur in cold water in all years, and their abundance was very high within the cold SSW in 1995. Likewise, cod larvae occurred in colder water than the other species, and their frequency of occurrence was much higher within the SSW inside the tidal-mixing front. Finally, the intrusion of the shelf-slope front resulted in the shoaling of cod, haddock, and herring (and to some extent mackerel), further concentrating these species within a relatively small region of the southern flank. As a result of these conditions, the spatial overlap between herring and cod larvae was very high in 1995. Interannual variation in hydrographic conditions, particularly the intrusion of SSW, can influence the likelihood of predator–prey interactions between herring and cod larvae.

The larval distributions we observed are consistent with other studies on the southern flank of Georges Bank (Lough and Bolz 1989; Lough et al. 1996; Townsend and Pettigrew 1996). The timing, location, and depth of spawning plays a large role in determining both the rate of transport and the distribution of gadid larvae. The higher abundance of cod in the well-mixed area is associated with their earlier and more protracted spawning period and broader spawning distribution (Werner et al. 1993) and the resulting differences in advective transport during the larval period (Bolz and Lough 1983; Lough and Bolz 1989). The earlier larval release by cod also increases the likelihood that they will be entrained in SSW that occasionally intrudes onto the bank during March and April (Bisagni et al. 1996). This occurred both during the 1995 survey in the current study and during a SSW intrusion in April 1992 (Manning 1995; Townsend and Pettigrew 1996).

Fig. 9. Stratification index ($\Delta - \sigma_t$) maps for three replicate grids in 1995. (*a*) Grid 1. (*b*) Grid 2. (*c*) Grid 3.

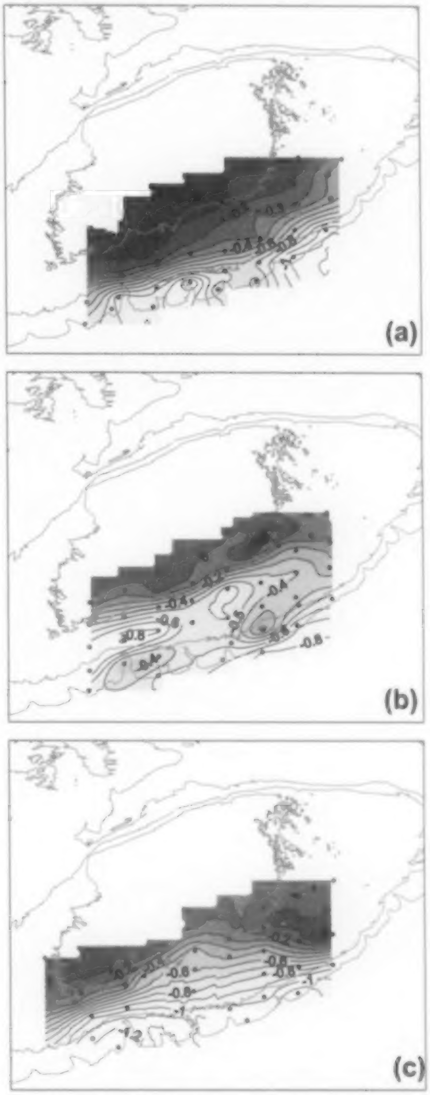

Both field and modeling studies indicate that cod larvae are better adapted to the lower food availability in well-mixed regions of Georges Bank. Trophodynamic models based upon temperature variation, feeding behaviors, and ambient prey concentrations indicate that both larval cod and larval haddock will starve in the absence of physical mechanisms that increase contact rates with prey (Werner et al. 1996; Leising and Franks 1999). Both species experience nutritional stress, but cod larvae were in consistently better condition than haddock larvae at well-mixed sites (Buckley and Lough 1987; Lough et al. 1996). In stratified regions, both larval gadids (Lough and Potter 1993) and their zooplankton prey (Buckley and Lough 1987) were concentrated around the pycnocline. Larval haddock required the high concentration of prey within the pycnocline to support growth and survival (Werner et al. 1996; Leising and Franks

Fig. 10. Larval and pelagic fish abundance data for replicate grids in 1995. Densities (number·m^{-2}) are shown for larval cod and haddock, while catches (number·tow^{-1}) are shown for Atlantic herring and mackerel. (*a* and *b*) Grid 1: (*a*) larval gadids; (*b*) pelagic fish. (*c* and *d*) Grid 2: (*c*) larval gadids; (*d*) pelagic fish. (*e* and *f*) Grid 3: (*e*) larval gadids; (*f*) pelagic fish. Approximate locations of the tidal-mixing front (broken line) and the shelf-slope front (solid line) are indicated.

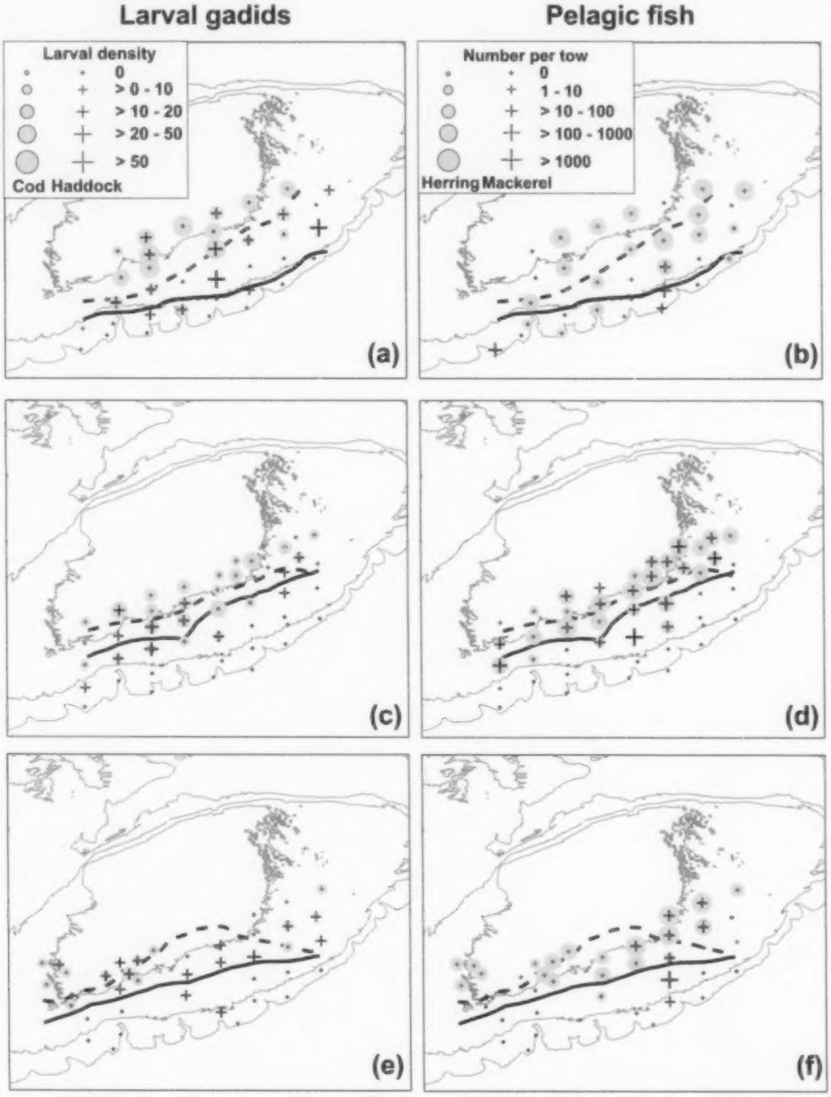

1999). In contrast, larval cod appear to be better adapted to grow in colder well-mixed waters (Buckley and Lough 1987). Moderate turbulence increases the contact rate between larvae and their prey, particularly in the case of pause–search predators like larval cod (Leising and Franks 1999). Turbulent mixing is higher in well-mixed areas, increasing larval-cod feeding rates and mitigating the effects of both lower temperatures and lower prey availability (Leising and Franks 1999). When including the effects of turbulence in trophodynamic models, all surviving cod larvae straddled the 60-m isobath (Werner et al. 1996), which is consistent with the distribution of larvae observed in this and other studies.

While the stratified area between the 60- and 100-m isobaths is a better nutritional environment for larval haddock, it is also the region of highest exposure to planktivorous fish. Atlantic herring were more abundant between the 60- and 100-m isobaths. There was consistent and positive spatial overlap between herring and larval haddock and, therefore, an increased risk of predation. There are also spatial differences in the abundance of invertebrate predators between the well-mixed and stratified areas. Predatory

Fig. 11. Weighted mean surface (*a*) and bottom (*b*) temperature and salinity values for larval cod, larval haddock, Atlantic herring, and Atlantic mackerel during the years of the study: ◆, 1990; ■, 1994; and ▲, 1995. Error bars indicate 95% confidence intervals.

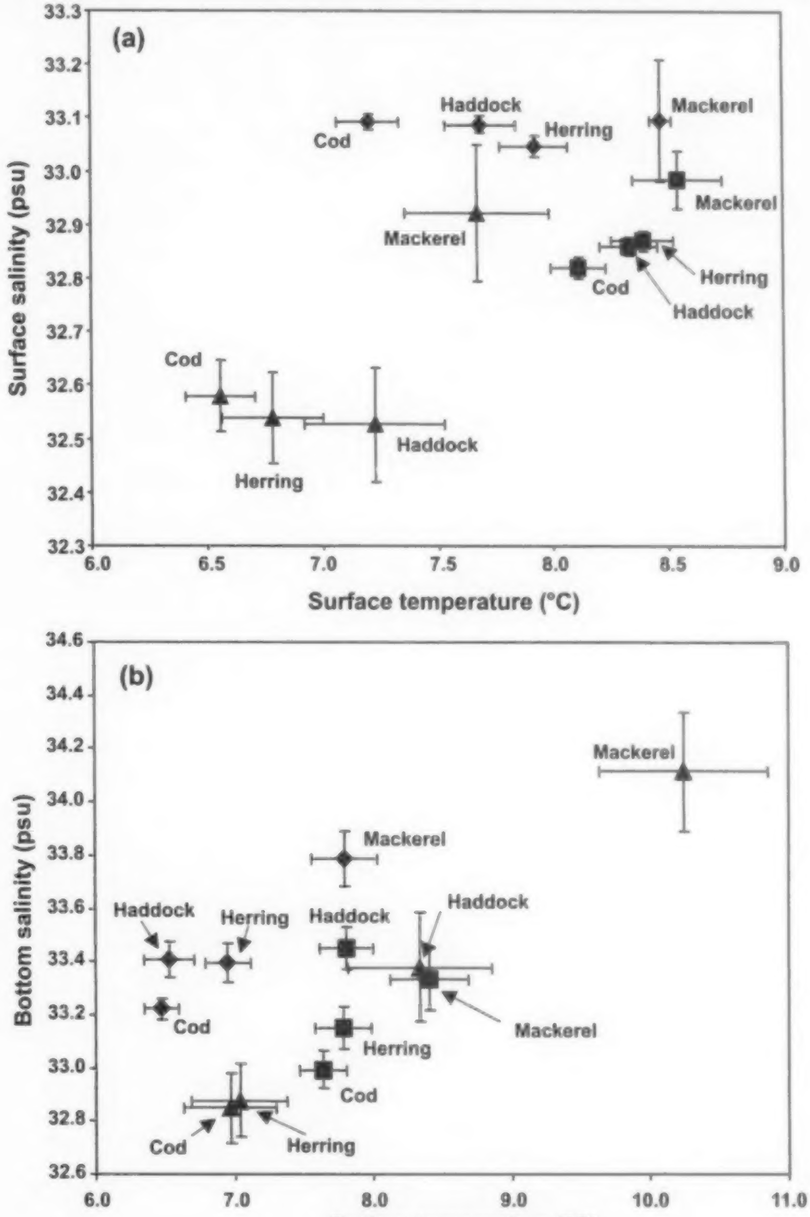

hydroids were extremely abundant in the mixed region and were much less abundant in stratified areas (Madin et al. 1996). However, chaetognaths, amphipods, euphausiids, and decapod shrimps were more abundant in deeper water on the southern flank (Madin and Horgan 1997). Depending upon the ability of these various predators to consume fish larvae, there may be extreme differences in the exposure to predation in these regions. The concentration of larvae and small zooplankton along frontal convergence zones and in the pycnocline will tend to concentrate their predators as well. There is a strong relationship between larval-fish density and predation rate by both invertebrate and fish predators (Bailey and Houde 1989). It is therefore likely that predation, including that by Atlantic herring, will be higher and a more consistent source of mortality for haddock larvae than for cod larvae as a result of spatial differences in the

Table 2. Matrix of Williamson's spatial-overlap index.

	Larval cod	Larval haddock	Atlantic herring
1990 cruise			
Larval haddock	1.294**		
Atlantic herring	0.971	1.165†	
Atlantic mackerel	0.545***	1.028	1.343**
1994 cruise			
Larval haddock	1.091*		
Atlantic herring	1.085†	1.144**	
Atlantic mackerel	1.038	1.050	1.157
1995 cruise			
Larval haddock	1.095		
Atlantic herring	1.636***	1.232*	
Atlantic mackerel	0.789	1.044	1.135

Note: The p value is the proportion of randomized overlap values for each pair that has a greater deviation from 1 than the observed value; ***, $p < 0.001$; **, $p < 0.01$; *, $p < 0.05$; †, $0.05 < p < 0.10$.

predator fields on Georges Bank. Lough and Potter (1993) noted that larval haddock exhibit earlier development of both dorsal and pectoral fins than do cod larvae. They proposed that the improved maneuverability and thrust may allow haddock larvae to more actively seek high concentrations of prey. Improved swimming ability would also improve their escape response from predators, thereby reducing their vulnerability (Bailey and Houde 1989).

The timing of spawning for haddock also creates greater temporal overlap with Atlantic herring than does the timing for cod. Herring spawn on Georges Bank during September–October and then migrate south to the New York bight to overwinter. The spring migration back to Georges Bank occurs in April and mid-May (Anthony and Waring 1980; Grosslein 1987). The herring migration coincides with peak larval-haddock abundance on the southern flank, but it occurs well after the peak in cod larvae during February–March. Atlantic mackerel generally migrate through this region during late May and June (Sette 1950) and, therefore, do not have strong temporal overlap with the peak abundance of either larval gadid.

Both Atlantic herring and Atlantic mackerel have demonstrated the ability to feed upon fish larvae. In large-mesocosm studies, juvenile Atlantic herring caused high mortality in larval fish, including larval cod (Øiestad 1985). Atlantic mackerel also fed upon a variety of larval fish species, ranging in size from 5 to 10 mm, in the presence of natural zooplankton as alternative prey (Pepin et al. 1987). Planktivorous fish have been hypothesized to be the dominant predators of fish larvae (Hunter 1981; Bailey and Houde 1989). Larval fish are highly vulnerable to predation by both invertebrate and fish predators as a result of high encounter rates due to their patchy distribution in space and slow swimming speeds, increased predator detection due to their relatively large size, and limited ability to avoid capture due to undeveloped sensory organs and musculature (reviewed in Bailey and Houde 1989). Intermediate-sized larvae tend to be most vulnerable to fish predators because they have a high probability of detection by the predator but a relatively low probability of escape (Bailey and Houde 1989).

The importance of nutritional stress as a source of larval mortality has clearly been demonstrated on Georges Bank. However, owing to the high abundance of planktivorous fish and invertebrate predators and the high vulnerability of fish larvae, it is clear that the predator–prey interaction is an important component of the ecology, life-history strategies, and recruitment variability of larval fish on Georges Bank. There is an potential trade-off in the recruitment strategies of larval haddock between starvation and predation as sources of mortality. There are nutritional advantages to concentrating in the stratified areas where food availability is high. However, this results in increased exposure to both fish and invertebrate predators. In contrast, larval cod appear to be adapted to relatively poor nutritional environments, where they may avoid high exposure to predators. The relative magnitude of predation versus starvation mortality remains unclear, and future efforts will directly investigate this important trade-off. We demonstrate in the current study that spatial overlap with highly abundant planktivorous fish is a consistent pattern under variable hydrographic conditions and likely imposes a consistent source of mortality on larval gadids. Forthcoming studies will estimate the magnitude of predation mortality due to planktivorous fish, examine the relative impacts of starvation and predation mortality, and investigate the role of pelagic predators in limiting the recruitment and stock recovery of Atlantic cod and haddock on Georges Bank.

Acknowledgements

We recognize the work of many researchers who participated in these cruises and acknowledge members of the Food Web Dynamics program, including Frank Almeida, Karen Bolles, Brian Kamminer, Nancy Mchugh, Cheryl Milliken, and Rodney Rountree. Richard Yetter provided invaluable assistance by identifying and measuring over 15 000 larval fish. Reviews were provided by S. Whipple, J. Boreman, and two anonymous reviewers. This work was supported by the National Oceanic and Atmospheric Administration Coastal Ocean Program Georges Bank Predation Study.

References

Anthony, V.C., and Waring, G. 1980. The assessment and management of the Georges Bank herring fishery. Rapp. P.-V. Reun. Cons. Int. Explor. Mer. No. 177. pp. 72–111.

Bailey, K.M., and Houde, E.D. 1989. Predation on eggs and larvae of marine fishes and the recruitment problem. Adv. Mar. Biol. **25**: 1–83.

Bisagni, J.J., Beardsley, R.C., Rusham, C.M., Manning, J.P., and Williams, W.J. 1996. Historical and recent evidence of Scotian Shelf Water on southern Georges Bank. Deep-Sea Res. Part II Top. Stud. Oceanogr. **43**: 1439–1471.

Bolz, G.R., and Lough, R.G. 1983. Growth of larval Atlantic cod, *Gadus morhua*, and haddock, *Melanogrammus aeglefinus*, on Georges Bank, spring 1981. Fish. Bull. **81**: 827–836.

Buckley, L.J., and Lough, R.G. 1987. Recent growth, biochemical composition, and prey field of larval haddock (*Melanogrammus aeglefinus*) and Atlantic cod (*Gadus morhua*) on Georges Bank. Can. J. Fish. Aquat. Sci. **44**: 14–25.

Colton, J.B., and Temple, R.F. 1961. The enigma of Georges Bank spawning. Limnol. Oceanogr. **6**: 280–291.

Flagg, C.N. 1987. Hydrographic structure and variability. *In* Georges Bank. *Edited by* R.H. Backus. MIT Press, Cambridge, Mass. pp. 108–124.

Fogarty, M.J., and Murawski, S.A. 1998. Large-scale disturbance and the structure of marine systems: fishery impacts on Georges Bank. Ecol. Appl. **8**: S6–S22.

Grosslein, M.D. 1987. Synopsis of knowledge of the recruitment process for Atlantic herring (*Clupea harengus*), with special reference to Georges Bank. Northwest Atl. Fish. Organ. Sci. Counc. Stud. **11**: 91–108.

Hjort, J. 1914. Fluctuations in the great fisheries of Northern Europe. Rapp. P.-V. Reun. Cons. Int. Explor. Mer, No. 20. pp. 1–13.

Hosmer, D.W., and Lemeshow, S. 1989. Applied logistic regression. John Wiley & Sons Inc., New York.

Houde, E.D. 1987. Fish early life history and recruitment variability. Am. Fish. Soc. Symp. **2**: 17–29.

Hunter, J.R. 1981. Feeding ecology and predation of marine fish larvae. *In* Marine fish larvae: morphology, ecology, and relation to fisheries. *Edited by* R. Lasker. University of Washington Press, Seattle. pp. 33–77.

Isaaks, E.H., and Srivastava, R.M. 1989. An introduction to applied geostatistics. Oxford University Press, New York.

Legendre, P. 1993. Spatial autocorrelation: trouble or new paradigm? Ecology, **74**: 1659–1673.

Legendre, P., and Fortin, M.J. 1989. Spatial pattern and ecological analysis. Vegetatio, **80**: 107–138.

Leising, A.W., and Franks, P.J.S. 1999. Larval Atlantic cod (*Gadus morhua*) and haddock (*Melanogrammus aeglefinus*) growth on Georges Bank: a model with temperature, prey size, and turbulence forcing. Can. J. Fish. Aquat. Sci. **56**: 25–36.

Lough, R.G., and Bolz, G.R. 1989. The movement of cod and haddock larvae onto the shoals of Georges Bank. J. Fish Biol. **35**(Suppl. A): 71–79.

Lough, R.G., and Potter, D.C. 1993. Vertical distribution patterns and diel migrations of larval and juvenile haddock *Melanogrammus aeglefinus* and Atlantic cod *Gadus morhua* on Georges Bank. Fish. Bull. **91**: 281–303.

Lough, R.G., Caldarone, E.M., Rotunno, T.K., Broughton, E.A., Burns, B.R., and Buckley, L.J. 1996. Vertical distribution of cod and haddock eggs and larvae, feeding and condition in stratified and mixed waters on southern Georges Bank, May 1992. Deep-Sea Res. Part II Top. Stud. Oceanogr. **43**: 1875–1904.

Madin, L.P., and Horgan, E.F. 1997. Estimating the impact of invertebrate predation on target species of copepods on Georges Bank. ICES (Int. Counc. Explor. Sea) CM 1997/T:16.

Madin, L.P., Bollens, S.M., Horgan, E., Butler, M., Runge, J., Sullivan, B.K., Klein-MacPhee, G., Durbin, E., Durbin, A., Bucklin, A., and Clarke, M.E. 1996. Voracious planktonic hydroids: unexpected predatory impact on a coastal marine ecosystem. Deep Sea Res. Part II Top. Stud. Oceanogr. **43**: 1823–1829.

Manly, B.F.J. 1997. Randomization, bootstrap, and Monte Carlo methods in biology. Chapman & Hall, London.

Manning, J. 1995. Oceanographic conditions of Georges Bank spawning grounds: 1992–1994. Northwest Atl. Fish. Organ. Sci. Counc. Stud. **24**: 125–141.

Michaels, W.M. 1991. The impact of mackerel predation on the survival of pealgic age-0 sand lance, cod, and haddock on Georges Bank during the spring of 1986. M.S. thesis, Southeastern Massachusettes University, North Dartmouth.

Northeast Fisheries Science Center (NEFSC). 1998. Status of the fishery resources off the Northeastern United States for 1998. NOAA Tech. Mem. NMFS-NE-115.

Øiestad, V. 1985. Predation on fish larvae as a regulatory force, illustrated in mesocasm studies with large groups of larvae. Northwest Atl. Fish. Organ. Sci. Counc. Stud. **8**: 25–32.

Pepin, P., Pearre, S., Jr., and Koslow, J.A. 1987. Predation on larval fish by Atlantic mackerel, *Scomber scomburs*, with a comparison of predation by zooplankton. Can. J. Fish. Aquat. Sci. **44**: 2012–2017.

Sette, O.E. 1950. Biology of Atlantic mackerel: migrations and habits. Fish. Bull. **49**: 251–358.

ter Braak, C.J.F., and Looman, C.W.N. 1995. Regression. *In* Data analysis in community and landscape ecology. *Edited by* R.G.H. Jongman, C.J.F. ter Braak, and O.F.R. Van Tongerman. Cambridge University Press, New York. pp. 29–72.

Townsend, D.W., and Pettigrew, N.R. 1996. The role of frontal currents in larval fish transport on Georges Bank. Deep-Sea Res. Part II Top. Stud. Oceanogr. **43**: 1773–1792.

US-GLOBEC. 1992. Global Ocean Ecosystems Dynamics, Northwest Atlantic Implementation Plan, Rep. No. 6, June 1992. Joint Oceanographic Institutions Inc., Washington, D.C.

Werner, F.E., Page, F.H., Lynch, D.R., Loder, J.W., Lough, G.R., Perry, I.R., Greenberg, D.A., and Sinclair, M.M. 1993. Influences of mean advection and simple behavior on the distribution of cod and haddock early life stages on Georges Bank. Fish. Oceanogr. **2**: 43–64.

Werner, F.E., Perry, R.I., Lough, R.G., and Naimie, C.E. 1996. Trophodynamics and advective influences on Georges Bank larval cod and haddock. Deep-Sea Res. Part II Top. Stud. Oceanogr. **43**: 1793–1822.

Williamson, C.E. 1993. Linking predation risk models with behavioral mechanisms: identifying population bottlenecks. Ecology, **74**: 320–331.

Optimal swimming speeds and forward-assisted propulsion: energy-conserving behaviours of upriver-migrating adult salmon

Scott G. Hinch and Peter S. Rand

Abstract: Anadromous salmon migrations are energetically expensive. Long-distance migrants should be efficient in their use of energy and minimize swimming costs wherever possible. We explore swimming strategies and energy-saving tactics employed by three long-distance-migrating sockeye salmon (*Oncorhynchus nerka*) stocks in the Fraser River watershed, British Columbia. We used stereovideography and bank-side observations to estimate swimming speeds (from tailbeat frequency) and ground speeds (using distance traveled and duration) for individuals at several sites. Salmon were highly efficient at migration (i.e., ground speeds equaled or exceeded swimming speeds) through reaches with relatively low encountered currents (<0.25 m·s^{-1}). We speculate that salmon exploit small reverse-flow vortices to achieve this feat. With low encountered currents, most salmon migrated according to an optimal swimming speed model: migrants minimized transport costs per unit distance traveled. Generally, salmon were less efficient at migration with fast currents, although the Chilko stock were superoptimal migrants, possibly owing to unique morphology and (or) behaviours. The risk of significant delays is enhanced when fast currents are encountered. Under these conditions, relatively fast swimming speeds could minimize travel time, despite high costs. Migrants may be balancing energetic costs of migration against the fitness costs of spawning delays.

Résumé : Les migrations anadromes des saumons coûtent cher en énergie. Les poissons qui migrent sur de longues distances doivent faire une utilisation efficace de l'énergie et minimiser chaque fois que c'est possible le coût de la nage. Nous avons examiné les stratégies de nage et les tactiques de conservation d'énergie chez trois populations de saumons rouges (*Oncorhynchus nerka*) qui migrent sur de longues distances dans le bassin du fleuve Fraser en Colombie-Britannique. À l'aide de vidéographie stéréoscopique et d'observations depuis la rive, il a été possible d'estimer la vitesse de nage (à partir de la fréquence de battement de la queue) et la vitesse au sol (au moyen de la distance parcourue et de la durée du trajet) pour des individus à plusieurs sites. Les saumons sont très efficaces dans leur migration (i.e., la vitesse au sol équivaut à la vitesse de nage ou la surpasse) dans les zones où les courants sont relativement faibles ($<0,25$ m·s^{-1}). Nous pensons que les saumons utilisent des petits remous en contre-courant pour réaliser cet exploit. Dans les courants faibles, la migration de la majorité des saumons correspond à un modèle de vitesse de nage optimale : les poissons migrateurs minimisent leur coût de déplacement par unité de distance parcourue. En général, les saumons sont moins efficaces dans les courants rapides, bien que la population de Chilko se soit révélée être composée de migrateurs sur-optimaux, probablement à cause de sa morphologie et (ou) de son comportement particuliers. Le risque de délais importants est accru par la traversée de zones à courant rapide; dans ces situations, une vitesse de nage relativement rapide peut réduire la durée du trajet, malgré son coût élevé. Les saumons migrateurs doivent probablement faire un compromis entre les coûts énergétiques de la migration et les pertes de fitness dues aux délais de la fraye.

[Traduit par la Rédaction]

Introduction

Many stocks of Pacific salmon travel long distances upriver to spawning areas. These migrations are energetically expensive and must be completed solely on energy reserves, as no feeding takes place en route. Anadromous migrants should be naturally selected to be efficient in their use of energy and may attempt to minimize energetic costs of swimming wherever possible. Transport costs could be reduced through several different tactics including swimming in low-speed or reverse-flow current paths (Hinch and Rand 1998), swimming in a burst-then-coast fashion (Weihs 1974), and (or) swimming steadily at hydrodynamic or metabolic optimal speeds (Weihs 1973; Ware 1975). This last tactic, defined as the cruising speed that minimizes the total energy expended in moving unit mass through unit distance,

Received February 25, 2000. Accepted October 31, 2000. Published on the NRC Research Press web site on December 20, 2000. J15632

S.G. Hinch.[1] Department of Forest Sciences and Westwater Research Unit in the Institute for Resources and Environment, 2424 Main Mall, University of British Columbia, Vancouver, BC V6T 1Z4, Canada.
P.S. Rand. Department of Zoology, 1 Clark Labs, North Carolina State University, Raleigh, NC 27695-7617, U.S.A.

[1] Corresponding author (e-mail: shinch@unixg.ubc.ca (alternate e-mail: scott.g.hinch@ubc.ca)).

Can. J. Fish. Aquat. Sci. **57**: 2470–2478 (2000)

has received attention theoretically and empirically for fish swimming in still-water environments (Brett 1995; Webb 1995 and references therein). Most researchers have ignored or greatly simplified the influence of currents on energy-saving swimming behaviours.

Bernatchez and Dodson (1987) compared energetic costs of migration for short- and long-distance upriver-migrating anadromous fishes and concluded that only the long-distance migrants (particularly some stocks of Pacific salmon) swam at optimal speeds. Their approach involved estimating swimming speeds in the field from laboratory respirometry trials based on total energy expenditure, migration duration, and mean river current speeds. Key assumptions in their analysis were that fish experienced the mean (in a river cross-sectional sense) river current speeds, swam at steady speeds, and incurred no additional costs from anaerobic metabolism (i.e., no burst swimming). However, it is widely known that anadromous fishes do not encounter the "mean" river current speeds; in fact, mean speeds of many large rivers exceed maximum sustained swimming speeds of Pacific salmon (Osborne 1961; Brett 1965). By assuming that fish experience mean river currents, Bernatchez and Dodson (1987) likely overestimated costs. There is also considerable evidence that fish swim under nonsteady-state conditions during migrations (Rand and Hinch 1998; Hinch and Bratty 2000). Applying this steady-state swimming assumption over the whole migration, in addition to ignoring burst swimming, could lead to underestimates of true costs (Rand and Hinch 1998). It is not clear how these different biases would have influenced the conclusions of Bernatchez and Dodson (1987). This argues for a closer examination of how riverine-migrating salmon may behave when they encounter variability in encountered current speeds.

This paper explores several issues regarding the swimming strategies and potential energy-saving tactics used by long-distance anadromous migrating salmon to reduce transport costs. Our main objective was to determine if migrants minimize transport costs by swimming at metabolically optimal speeds, and if so, did this depend on flow conditions? We addressed these questions through the use of stereo-videography and bank-side visual observations to measure swimming and ground speeds at sites representing a range of encountered current speeds for three different long-distance-migrating stocks of Fraser River sockeye salmon (*Oncorhynchus nerka*).

Methods

Site description and selection

We studied three stocks of adult Fraser River sockeye salmon, each of which migrates relatively long distances from the Pacific Ocean (Fig. 1). The Early Stuart stock travels upriver 1100 km and gains 700 m of elevation, the Chilko stock travels 660 km and gains 1160 m of elevation, and the Horsefly stock travels 850 km and gains 760 m of elevation (Gilhousen 1980). These stocks migrate up different Fraser River tributaries en route to their specific spawning grounds (Fig. 1). These migratory tributaries are relatively large with widths at their mouths ranging from approximately 50 to 150 m, depending on the river system. In August 1997, we made observations on fish in these tributaries. We were not able to observe fish in the Fraser River mainstem due to high turbidity, which prevented the use of video; also, stock identification is more certain after fish have left the mainstem. In these large tributaries, sockeye often travel in narrow bands, parallel to and near the shore, and are usually highly visible from the banks. This type of migration behaviour, termed "line swimming," is a common phenomenon in large river systems and has been previously documented in the Fraser River and its main tributaries (Ellis 1966*a*). Line swimming is less common in slow-moving small rivers and creeks (Ellis 1966*a*); however, the majority of the migratory routes of our study stocks are in relatively large river systems. We are uncertain whether line swimming would be prevalent in large river systems that have "unnatural" flow patterns (i.e., are influenced by impoundments).

Sites were chosen for observations based on accessibility, presence of clearly visible migrating sockeye, and their surface water speeds. We attempted to choose sites that, when taken together, reflected the natural and commonly occurring range in surface current speeds where sockeye were migrating. In other words, the sites were selected to be representative of typical migration sites. Speeds of surface currents in close proximity to migrating sockeye were assessed by averaging speeds of five small wooden floats (5 cm^3) that were deployed immediately upstream of a study site. This information was only used to help select sites and was not used in any analyses. Although sockeye may not encounter water speeds that exist on the surface of a river, these values should be a useful surrogate to represent among-site variability in currents that they may encounter. Previous studies in noncanyon reaches of the Fraser River mainstem and some of its large tributaries have found that surface currents, which were in close proximity to migrating sockeye salmon, ranged up to 2 $m \cdot s^{-1}$ but generally were less than 1.5 $m \cdot s^{-1}$ (Ellis 1966*a*; Hinch and Rand 1998). For several reasons, we did not study sites with surface currents in excess of 2 $m \cdot s^{-1}$. First, these sites occur relatively rarely along the tributary migratory routes of Fraser River sockeye. Second, anaerobiosis (burst swimming) is often invoked during passage through these types of extremely fast water sites (Rand and Hinch 1998), so one would not expect optimal swimming speeds to be elicited. Third, these sites are usually associated with river constrictions that create rapids and multidirectional flows (Rand and Hinch 1998); thus, the presence of whitewater would have reduced water clarity and prevented us from obtaining behavioural information using bank-side observational approaches. We selected 13 sites for observations (Fig. 1) but only used 11 in analyses owing to low fish sample sizes at two sites (Table 1).

Underwater video system description and deployment

We deployed two black and white Charged Couple Device (CCD) cameras (Panasonic WV-BP312; 570 lines of horizontal resolution) fitted with aspherical high-speed aperture lens (Panasonic WV-LA408C3; 4.5-mm focal length) oriented in parallel (optical axis separation of 10 cm) and fixed to a stand located 1–2 m away from the band of fish. Each camera was enclosed in a cylindrical anodized aluminum housing fitted with a flat Plexiglas port. Video signals were sent to a multiplexer-quad unit (Panasonic WJ-420) and then to a VHS time-lapse recorder (Panasonic AG-6124) where images from both cameras were recorded simultaneously on the same video frame at 60 $frames \cdot s^{-1}$. Thus, the left camera image filled the left side of our monitor and the right camera image filled the right side. A black and white video monitor (Panasonic WV-5470; 850 lines of horizontal resolution, 41-cm diagonal size) was used to assist in focus, calibration, camera orientation, and determination of water and fish speeds. All components of the system were powered by a single 12-V battery.

Cameras were deployed perpendicular to river flow, wherever possible underwater, with the optical axis parallel to the river surface. In cases where line-swimming fish were within 1 m from shore, we deployed the cameras out of water with the optical axis incident to the river surface. The approximate volume of habitat

Fig. 1. Map of the Fraser River watershed, British Columbia, Canada. Asterisks show the location of the study sites. Numbers indicate sampling order and correspond to the stock-specific information in Table 1. Sites 6 and 7 had low sample sizes and were not used in analyses. Adults from all stocks share a common lower Fraser River migration route. The Chilko stock heads westward at the Chilcotin River towards spawning areas near Chilko Lake. The Horsefly stock heads eastward at the Quesnel River towards spawning areas near Quesnel Lake and the Horsefly River. The Early Stuart stock heads northwestward at the Nechako River towards spawning areas near the Middle River and Takla Lake.

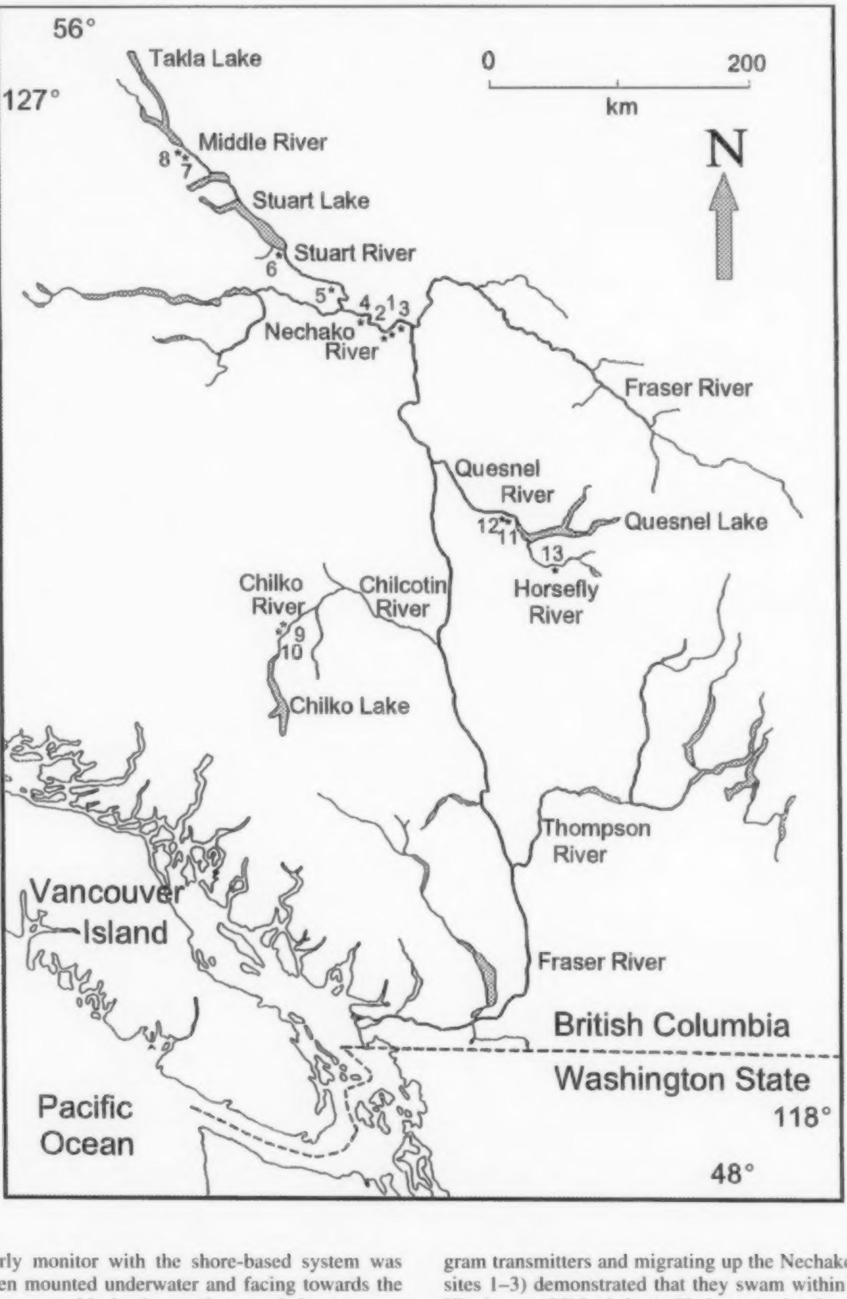
56°
127°
Takla Lake
0
200
km
N
Middle River
8
7
Stuart Lake
Stuart River
6
5
4
2
1
3
Nechako River
Fraser River
Quesnel River
12
11
Quesnel Lake
13
Horsefly River
Chilko River
Chilcotin River
9
10
Chilko Lake
Thompson River
Vancouver Island
Fraser River
British Columbia
Washington State
Pacific Ocean
118°
48°

that we could clearly monitor with the shore-based system was 1 m^3; however, when mounted underwater and facing towards the middle of the river, we could clearly monitor much larger water volumes out to a distance of 5 m depending on water clarity. Were we monitoring "typical" migrants with our system? Previous observations of Early Stuart sockeye that were carrying electromyogram transmitters and migrating up the Nechako River (our present sites 1–3) demonstrated that they swam within 3 m of shore (S.G. Hinch, unpublished data). Hydroacoustic observations of sockeye passage in the Fraser River mainstem near Yale, B.C., revealed that the overwhelming majority of migrants swam within 1 m of the shore-mounted fish detection weir (Macdonald et al. 2000). We

Table 1. Surface current speeds, water temperature, and sample size of fish (*n*) by stock at each study site.

Stock	Site	Date	Surface current ($m \cdot s^{-1}$)	Temperature (°C)	Observation type	*n*
Early Stuart	1	7 Aug.	–0.10	18	Video	270
Early Stuart	2	7 Aug.	1.43	18	Video	29
Early Stuart	3	8 Aug.	1.10	18	Video	28
Early Stuart	4	8 Aug.	1.00	17	Video	26
Early Stuart	5	9 Aug.	0.15	18	Visual	13
Early Stuart	8	11 Aug.	0.13	19	Video	23
Chilko	9	18 Aug.	1.40	10	Video	27
Chilko	10	19 Aug.	1.80	12	Video	20
Horsefly	11	22 Aug.	0.60	18	Video	20
Horsefly	12	22 Aug.	1.40	18	Video	25
Horsefly	13	23 Aug.	0.20	16	Visual	20

Note: Site numbers correspond to those in Fig. 1. Negative current speed implies upstream movement of water.

are therefore comfortable that our system was able to monitor most of the migrants that passed our observation sites on our side of the river and thus were monitoring typical individuals.

Calibration and data acquisition

We followed the approach first described by Klimley and Brown (1983) and elaborated on in Boisclair (1992). For calibration purposes, we deployed a 1-m-long fibreglass rod marked into 10-cm segments at 25-cm distances along the optical axis away from the cameras out to a maximum distance of 2.5 m. The rod was placed in the field of view of the cameras through the use of a telescoping aluminum pole. We recorded images of the calibration rod at each distance interval by extending the pole along the optical axis out to the point where the pole bisected the typical trajectory of fish observed from shore. In the laboratory, these images were replayed on the monitor's screen upon which a coordinate system was overlain. Measurements of the calibration rod were made manually off the monitor with a ruler by one technician. The same technician also transcribed all of the fish coordinates described below. These two-dimensional coordinates were converted to three-dimensional coordinates using methods outlined in Boisclair (1992). Calibration error was determined at each distance by comparison of actual rod dimensions with estimated dimensions at successive distance intervals. This information was used to correct for any biases caused by optical distortions resulting from different camera deployments.

Fish were selected from the video images only if they were clearly visible (i.e., not obstructed by conspecifics or out of our viewing area) and observed along our calibration plane. We observed and recorded information on fish that migrated as isolated individuals and as members of groups; generally, only fish that migrated on the edge of groups could be clearly observed. We recorded images for 0.5–6 h depending on fish abundance. Our goal was to record 20–30 fish per site and have an equal representation of fish that migrated as individuals and as members of groups. For fish that met the above criteria, we recorded *x* and *y* coordinates of the head and tail at the point of entry and exit of the observation site in both the left and right camera images. We also recorded elapsed time by counting frames. Following the calibration methods in Boisclair (1992), we converted the three-dimensional screen coordinates to real-world dimensions. This allowed us to estimate distance traveled and ground speed of fish migrating through each site. We also counted the number of tailbeats performed by each fish through the site. These data were used to estimate swimming speed using the tailbeat – swimming speed relationship reported in Hinch and Rand (1998) for adult sockeye. We computed a swim efficiency index (SEI) by dividing each individual's ground speed by its swimming speed. This permits an evaluation of an individual's energy utilization strategies and provides insights into migration behaviour. For instance, values below 1 indicate that individuals are working relatively hard to achieve forward progress, values equal to 1 imply relatively easy forward progress (analogous to moving through still water), and values greater than 1 indicate that fish are receiving some type of forward assist. It was not possible to determine an individual's sex from video records. The amplitude for a given tailbeat could also not be assessed from the video images, a limitation of the side-viewing video system. Generally, tailbeat amplitude decreases with increasing beating frequency until the fish starts burst swimming, at which point the amplitude stabilizes (S.G. Hinch, unpublished laboratory flume data). Thus, at nonburst speeds, variation in beating frequency will explain much of the variation in amplitude. Yet it is possible that subtle individual- or stock-specific differences in amplitude may affect swimming speeds and we are unable to account for this in our analyses.

The video approach was used at all sites except two (sites 5 and 13, Table 1). Here, fish were 2–3 m from shore, but due to poor water clarity, we were not able to use video cameras. However, we wanted to increase our number of sample sites and we lacked sites, within stocks, that had these particular surface water speeds. At both sites, surface currents were relatively slow and nonturbulent, and fish were swimming at steady paces within 10 cm of the water surface. In each case, one observer was positioned overtop of the migrating salmon on bridge abutments and another was on shore. The set of observers visually estimated the time to migrate a set distance and counted the number of tailbeats. These data allowed us to calculate ground and swimming speeds. Preliminary observations of tailbeat counts at these sites revealed that beating frequency was relatively low (rarely exceeding $2 \cdot s^{-1}$) and all beats were visible and could be tallied.

At the video sites, we imposed a hypothetical three-dimensional cube comprising 18 cells ($3 \times 3 \times 2$ arrangement) in the viewing area. We used a CMC-2 current meter (Hydrological Services Ltd.) to measure current speed at the centre of each of these cells. By videotaping the location of the current meter's propeller, we were able to determine the real-world coordinates of each cell. With this information, we determined the trajectory of each fish and its encountered current speeds through the cells. The encountered current values for each fish were averaged, and then these values were averaged among fish at each site to characterize encountered river current speeds for each site. We approximated encountered current speeds at sites 5 and 13 using wooden blocks (10 cm^3) that floated just below the water surface. At these sites, migrants were line swimming just below the water surface at the same depths as the blocks.

Statistical analyses and optimality modeling

For each stock, we used analysis of variance and the least-squared means a posteriori test to compare swimming speed, ground speed, and SEI among sites. To control for type II errors,

Fig. 2. Energy costs per distance traveled for a 2.5-kg sockeye salmon at 19°C across a range of ground speeds in the (A) still-water model (0 $m \cdot s^{-1}$ encountered current speed) and (B) moving-water model (0.6 $m \cdot s^{-1}$ encountered current speed). Energy costs are calculated for standard metabolism (dotted line), activity (i.e., swimming) metabolism (dashed line), and their sum, total metabolism (solid line). Arrowheads indicate where total metabolic costs are at a minimum. Ground speed is equivalent to swimming speed minus encountered current speed. In the still-water model, ground speeds and swimming speeds are the same values.

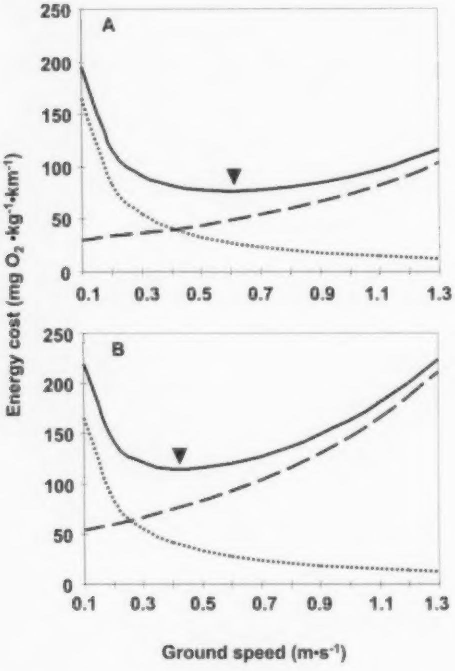

Fig. 3. General energy expenditure model for a 2.5-kg sockeye salmon migrating at 19°C. Total metabolic costs are calculated for encountered current speeds of 0.6 $m \cdot s^{-1}$ (thin line), 0.2 $m \cdot s^{-1}$ (medium line), and 0 $m \cdot s^{-1}$ (thick line) across a range of ground speeds. Arrows indicate the ground speed for each encountered current speed where total metabolic costs are at a minimum. The swimming speeds required to produce the minimum metabolic costs (i.e., the optimal swimming speeds) are (*a*) 1.05 $m \cdot s^{-1}$, (*b*) 0.75 $m \cdot s^{-1}$, and (*c*) 0.6 $m \cdot s^{-1}$.

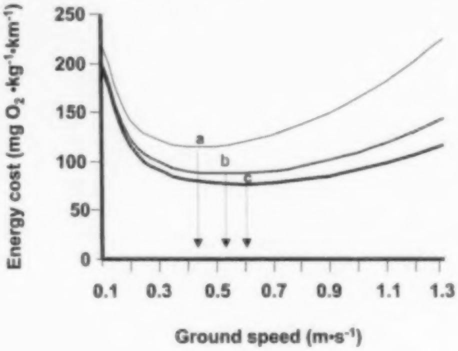

Bonferroni's correction was used to lower the level of significance for the within-stock among-site multiple contrasts. The Early Stuart analyses involved eight sites resulting in 15 contrasts, so the significance level was set to 0.003 (which is 0.05/15). Significance levels for the Chilko and Horsefly analyses were set to 0.05 (0.05/1) and 0.017 (0.05/3), respectively. We also examined Pearson correlations between encountered water speed and our three main fish variables (SEI, ground speed, and swimming speed) using data from all stocks and sites to see if general relationships exist between swimming behaviours and flow conditions.

Using salmon respirometry data collected by Roly Brett and colleagues, Webb (1995) constructed a conceptual model that predicted the speeds that sockeye should swim at to minimize energetic costs of transport per unit body mass per unit distance traveled in still water. Webb (1995) reported a hyperbolic function that integrated the negative exponential decline of costs per kilometre traveled from standard metabolism, with the positive exponential increase in swimming activity metabolism per kilometre traveled, over a range of ground speeds (still-water model, Fig. 2A). Standard metabolism per kilometre decreases with increasing swimming activity because less time would be spent in any given kilometre of water. In this model, because fish do not encounter any currents, swimming speeds and ground speeds are the same values. This model allowed for the computation of a swimming speed that minimized cost of transport in still water. Although Webb (1995) did not provide equations for his model, we were able to identically recreate his conceptual figure using a bioenergetic model for sockeye provided in Beauchamp et al. (1989). Beauchamp et al. (1989) used the same original respirometry data as Webb (1995) but provided equations and parameters that we used to calculate weight- and temperature-specific standard and activity metabolic costs for sockeye salmon moving in still water. We extended the model to moving-water environments by including the cost of making forward progress through any encountered current speed. This was accomplished by summing swimming speed with encountered current speed, thus generating the fish's ground speed (moving-water model, Fig. 2B). For instance, to achieve a ground speed of 0.4 $m \cdot s^{-1}$ while encountering a current speed of 0.6 $m \cdot s^{-1}$, a fish would have to swim at 1.00 $m \cdot s^{-1}$. Therefore, the activity costs in the still-water model (Fig. 2A) for swimming at 1.00 $m \cdot s^{-1}$ against a current of 0.6 $m \cdot s^{-1}$ are the same as swimming at 0.4 $m \cdot s^{-1}$ in the moving-water model (Fig. 2B). A fish swimming at 1.00 $m \cdot s^{-1}$ in still water would use the same amount of energy per unit time but would travel a greater distance than the same fish in moving water. With this approach, we could predict costs of swimming over a range of ground speeds. The resulting model allowed us to generate separate hyperbolic curves for given encountered current speeds. As examples, we show predictions of energy expenditures for encountered current speeds of 0, 0.2, and 0.6 $m \cdot s^{-1}$ (Fig. 3). For the model runs presented in Figs. 2 and 3, average wet weight and water temperature were assumed to be 2.5 kg and 19°C, respectively.

We applied the model to predict minimum cost of transport based on observed water speeds encountered at each of our sites. We assumed a 2.5-kg wet weight (a typical mature adult weight) for all calculations and used temperatures specific to each site (Table 1) in our calculations of standard and activity metabolism. We then calculated observed cost of transport by applying the model to our estimated mean swimming speed at each site. We computed an optimal migration index (OMI) at each site by dividing the theoretical minimum energy expenditure (for that site's encountered water speed) by our observed estimate of energy expenditure. Therefore, an index value of 1 represents an optimal migrator. Values lower than 1 represent suboptimal, or inefficient, swimming behaviours.

Conversely, values exceeding 1 represent superoptimal, or highly efficient, swimming behaviours. The among-site relationship between the OMI and encountered current speed will provide insights into how flow conditions may cause departures from optimal migration behaviour.

Results

Statistical analyses

For Early Stuart sockeye salmon, swimming speeds at sites 2 and 3 (both approximately 1.8 $m \cdot s^{-1}$) were significantly different, about two times faster, than at the other four sites (all $P < 0.001$) (Fig. 4A). Sites 2 and 3 did not differ from each other in swimming speeds, and sites 1, 4, 5, and 8 did not differ from each other in swimming speeds (all $P > 0.003$). Ground speeds at sites 1 and 8 (both approximately 1.0 $m \cdot s^{-1}$) were faster than at sites 2, 3, and 5 (all $P < 0.001$). Ground speeds at site 3 were faster than those at sites 2 and 4 (both $P < 0.001$). In terms of ground speeds, sites 1 and 8 did not differ, sites 2 and 4 did not differ, and sites 3 and 5 did not differ (all $P > 0.003$). SEI, which ranged among sites from 2.2 to 0.3, was higher at site 1 than at sites 2, 3, and 4 (all $P < 0.003$); sites 5 and 8 were intermediate in SEI but did not differ from the other sites (all $P > 0.003$).

For Chilko sockeye, there were no differences between sites 9 and 10 in ground speeds (both approximately 0.42 $m \cdot s^{-1}$; $P = 0.367$) (Fig. 4B), but swimming speeds were greater at site 10 ($P = 0.05$). SEI was correspondingly lower at site 10 but did not differ from that at site 9 ($P = 0.078$). For Horsefly sockeye, ground speeds differed among all three sites, being highest at site 12, intermediate at site 11, and lowest at site 13 ($P < 0.016$ for each contrast) (Fig. 4B). SEI was highest at site 11 and lowest at site 12 ($P < 0.016$ for each contrast). Swimming speed was 2.5–3 times faster at site 12 compared with sites 11 and 13. In general, across all stocks, relatively low SEI values (e.g., sites 2, 3, and 12) appeared to be associated with high average swimming speeds, whereas high SEI values (e.g., sites 1, 8, 9, and 10) tended to occur at sites where average swimming and ground speeds were similar (Fig. 4).

Pooling together all stocks and sites, we found a significant positive correlation between average swimming speed and encountered current speed ($r = 0.617$, df = 9, $P = 0.04$) (Fig. 5A). The correlation based just on data for the Early Stuart stock was particularly strong ($r = 0.947$, df = 4, $P = 0.005$). We were not able to examine similar types of correlations for the Chilko and Horsefly stocks individually because the number of sites was limited (two and three, respectively). However, both stocks appeared to show the same positive association between swimming speed and current speed (Fig. 5A). There was no general correlation between average ground speed and encountered current speed ($r = -0.255$, df = 9, $P = 0.55$) and, individually, the stocks seemed to show very different relationships (e.g., positive association for Horsefly, no association for Chilko, and negative association for Early Stuart) (Fig. 5B). Although there was no general correlation between average SEI and encountered water speed ($r = -0.378$, df = 9, $P = 0.25$), individually, all stocks demonstrated a negative association (Fig. 5C). Further, if the two Chilko sites were removed from this analysis, a very strong correlation emerged ($r = -0.851$, df = 7, $P = 0.004$).

Fig. 4. Histograms representing mean (plus 1 SE) ground speeds (solid bars), swimming speeds (open bars), and encountered current speeds (stippled bars) for each study site along the migration of (A) Early Stuart sockeye (sites 1–8) and (B) Chilko sockeye (sites 9 and 10) and Horsefly sockeye salmon (sites 11–13). Negative current speeds reflect currents flowing in an upstream direction. Diamonds represent mean SEIs (plus 2 SE) for each study site. In many instances, the standard error is very small and is obscured by other symbols on the figure. Sites are ordered, within stock, from lowest to highest encountered currents.

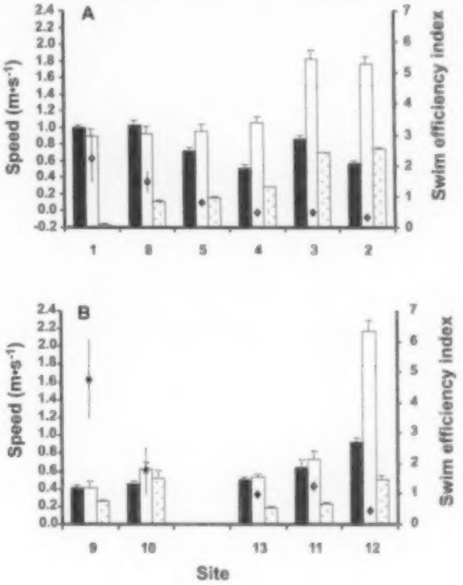

Optimal migration analyses

Standard metabolic costs do not change for a given ground speed in either of the two models (Fig. 2); thus, differences in model predictions of optimal swimming speeds are solely due to changes in activity costs. When current speed was zero (see Fig. 3), total metabolic costs per distance traveled for a 2.5-kg fish in 19°C water were minimized when swimming at 0.6 $m \cdot s^{-1}$ (the optimal swimming speed). In order for fish to make forward progress, swimming speeds must increase as encountered current speed increases. However, our model predicts that optimal swimming speeds would not increase at the same rate as does the increase in encountered current speeds. Specifically, the ratio of optimal swimming speed increase to current speed increase was 0.75. In our examples, when encountered currents were 0.2 and 0.6 $m \cdot s^{-1}$, transport costs were minimized when swimming speeds were 0.75 and 1.05 $m \cdot s^{-1}$, respectively (Fig. 3). The resultant ground speeds were 0.55 and 0.45 $m \cdot s^{-1}$, respectively (Fig. 3).

OMI values computed on all stocks and sites ranged from 0.35 to 1.08 for Horsefly fish, from 1.1 to 1.20 for Chilko fish, and from 0.60 to 0.98 for Early Stuart fish (Fig. 6). Migrants that encountered water speeds in excess of 0.25 $m \cdot s^{-1}$

Fig. 5. Plots of (A) mean swimming speed, (B) mean ground speed, and (C) mean SEIs versus mean encountered current speed for Early Stuart sockeye (solid squares), Chilko sockeye (open squares), and Horsefly sockeye salmon (stippled squares). All means are bounded by ±1 SE. Negative current speeds reflect currents flowing in an upstream direction.

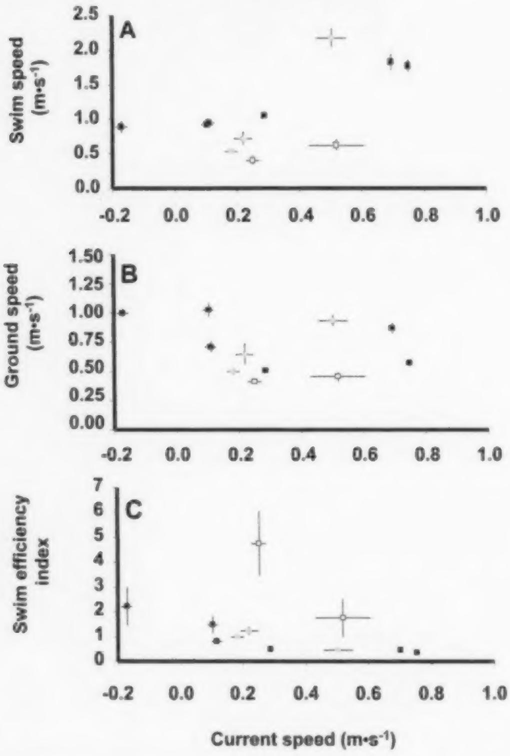

had OMI values that deviated from 1 (their 95% confidence intervals did not overlap unity). These included both Chilko sites (9 and 10), one Horsefly site (12), and half of the Early Stuart sites (2, 3, and 4) (Fig. 6). OMI from the remaining five sites, where encountered water speeds were less than 0.25 m·s^{-1}, did not deviate from unity.

Discussion

Our test to evaluate if long-distance migrants minimize transport costs per unit distance traveled yielded mixed results. We found that at encountered currents up to about 0.25 m·s^{-1}, sockeye salmon migrated according to the optimal swimming speed model. Although there were no sites for Chilko sockeye that were slower than 0.25 m·s^{-1}, both the Early Stuart and Horsefly stocks followed this pattern. We used our model to reexamine data previously collected by others to assess the generality of this phenomenon. In a relatively slow-flowing, small coastal river in British Columbia, Ellis (1966*b*) used underwater visual methods to estimate migration and swimming speeds of Sproat River sockeye, a relatively short-distance migrator. We calculated that OMI for these fish ranged from 0.96 to 1.00, conforming closely to the theoretical optimal swimming speed. Quinn (1988) and Madison et al. (1972) used telemetry to calculate swimming and migration speeds for adult salmon migrating along the coast of British Columbia and Washington State. We estimate that OMI averaged 0.99 for each study. Taken together, these results suggest that migrating sockeye, whether in the ocean or freshwater, swim at speeds that minimize energy costs per distance traveled when swimming in slow-current environments. Because these studies were conducted on much broader time and space scales than ours, this suggests that optimization principles of locomotion may operate across broad temporal and spatial scales for this species, and perhaps other Pacific salmon. Furthermore, the reevaluation of Ellis' (1966*b*) work reveals that this phenomenon may not be restricted solely to long-distance migrants as Bernatchez and Dodson (1987) first hypothesized.

Fig. 6. Plot of mean OMIs (±1 confidence interval) versus mean encountered current speed for Early Stuart sockeye (solid squares), Chilko sockeye (open squares), and Horsefly sockeye salmon (stippled squares). Negative current speeds reflect currents flowing in an upstream direction. Numbers reflect study location and correspond to those in Table 1.

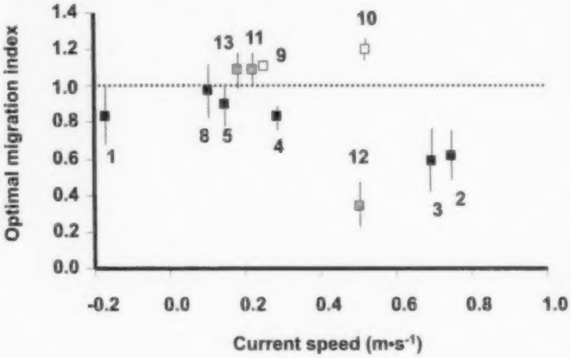

It is possible that many more species and stocks of anadromous fish than was first suggested by Bernatchez and Dodson (1987) migrate according to optimization principles. Key assumptions used in their modeling efforts were that fish experienced mean river current speeds and that fish swam under steady-state conditions for their entire migration. The former would lead to overestimation of transport costs whereas the latter may cause underestimation of costs. By measuring encountered currents and observing time steps of only a few seconds each, our approach should be expected to provide a more realistic assessment of swimming energetics. Despite this, additional videographic fieldwork is needed to examine short-distance migrants as well as other anadromous species in order to test the generality of migration optimization theory. Additionally, the role of non-steady-state swimming needs to be incorporated into these types of studies.

How do salmon achieve optimal speeds in flowing slow-water environments? One way may be to take advantage of certain types of flow features. We found that SEI values equaled or exceeded unity at all sites where encountered currents speeds were under 0.25 m·s^{-1}. This means that fish were able to propel themselves through currents at these sites as though they were moving through still water. We speculate that adult salmon can locate and exploit very small reverse-flow vortices, created by rough substrates or banks (Vogel 1994), which could reduce drag, making it easier for upstream passage. This phenomenon may even help propel migrants upstream. At several sites, migration speeds of some individuals exceeded their swimming speeds, suggesting that they were being "carried" upstream (many individuals had SEI values that far exceeded unity at these sites). Not surprising, this was evident at site 1 where the average migrant was encountering currents that were flowing upstream. However, this was also evident at sites 8–10 where encountered currents were in the downstream direction. Although mean SEI did not differ from 1 at these sites, SEI values for some individuals were far above 1 and the video images for these particular individuals clearly show them being propelled upstream. Site characteristics such as cobble size or bank configuration may determine the presence or magnitude of flow features that are responsible for these migration assists. Regardless, these flow features (e.g., vortices) may be only a few centimetres in diameter and very dynamic in structure and location and thus could be difficult to identify or measure (Vogel 1994). Studies that use more sophisticated means of measuring microsite currents than our approach may be needed for a better understanding of this energy-saving migration phenomenon.

Salmon that must travel long distances to the interior of British Columbia are under strong selection to complete spawning early enough in the summer to ensure sufficient degree-days for egg and alevin development and thus reduce chances of overwinter mortality caused by spawning ground freezeup (Macdonald and Williams 1998). The sockeye stocks that we studied are thus faced with an energetic dilemma. They need to conserve energy during their migration to ensure that they can reach spawning grounds and still have enough energy to mature their gonads and successfully spawn. However, they have a limited amount of time available to reach spawning areas; any migration delays could have a negative impact on fitness. Under these conditions, it is perhaps not surprising that different migration tactics are used when faced with different flow conditions. When currents were slow, energy-conserving behaviours like swimming at optimal speeds and forward-assisted propulsion were adopted. Under high-flow conditions, the risk of experiencing significant delays is quite large; moreover, it is probably difficult to locate and utilize microsite flow patterns. Thus, migrants may be exhibiting extremely fast (i.e., suboptimal) swimming speeds in order to minimize time of travel rather than swimming at speeds that minimize energy use. This could explain why both Early Stuart and Horsefly sockeye, when encountered with fast currents ($>0.25\ \mathrm{m\cdot s^{-1}}$), had low OMI values, indicating faster than optimal swimming speeds.

Chilko sockeye, like the other two stocks, showed a negative relationship between SEI and encountered current speeds, but the absolute values of the SEI and OMI suggested that this stock is unique. Chilko sockeye appear to be superoptimal migrators, i.e., they exhibit greater stride lengths (i.e., high ground speed achieved at a given tailbeat frequency, indicated by a high SEI value) and were capable of traversing the study sites using less energy than would be predicted if they adopted optimal swimming behaviours based on the predictions of our theoretical model (indicated by a high OMI value). There are two possible explanations for these results. The least likely explanation is that we did not adequately characterize the small-scale flow field dynamics over the substrates at our Chilko River sites. This error would lead to an overestimation of the true current speeds encountered by these fish, and this would inflate our estimates of OMI for this stock. However, this possible error would not change the absolute values that we observed for SEI (encountered flow fields are not used to compute this parameter), which seem to be unique from those of the other stocks. The most likely explanation is that this stock has a unique propulsive mechanism. The high SEI values suggest that these fish achieve greater forward progress per tailbeat, irrespective of encountered current fields. This greater stride length could be caused by a greater amplitude of the tailbeat, which could result in greater propulsion per tailbeat; however, we were not able to quantify this parameter from our side-viewing video observations. It is also possible that greater stride lengths were a result of Chilko fish having different morphologies than the other stocks. Recent morphometric work has revealed that adult migrating Chilko sockeye are relatively rounder in girth and shorter in length than Horsefly or Early Stuart sockeye (G. Crossin, Forest Sciences Department, University of British Columbia, Vancouver, B.C., unpublished data). This "torpedo" shape of Chilko fish would enhance water flow over the body surface, potentially decreasing drag and leading to an increase in stride length. The Chilko sockeye migration is one of the most demanding as a result of a grade that is nearly twice as steep as that of any of the other Fraser River stocks (Gilhousen 1980). This fact should place a premium on tactics and body shapes that reduce costs of migration. Proximate analyses of body constituents were conducted in 1999 on sockeye from our three stocks sampled at the Fraser River mouth and again upon arrival at their respective spawning grounds. Chilko sockeye used the least amount of somatic energy during their river migration and clearly were the most efficient migrators in terms of energy used per metre of elevation gained (G. Crossin, Forest Sciences Department, University of British Columbia, Vancouver, B.C., unpublished data). In summary, these preliminary whole-body energy and morphometric results, conducted on a large geographic scale, support the notion that Chilko fish have a unique and highly efficient propulsion mechanism — a hypothesis that we identified with underwater video observations obtained from very small spatial scales.

There are many different swimming tactics that migrating salmon may employ to help maximize their reproductive fitness (Webb 1995). Swimming at speeds that minimize costs per distance traveled could be important, but how strong might the selection pressure be for migrants to adopt this tactic? Our optimal swimming speed model predicted that migrants need to be able to adjust their swimming speeds based on encountered current speeds. Migrants that lack the ability to adjust their swimming speeds accordingly may put themselves at higher risk of migration mortality resulting from a premature depletion of energy reserves (Rand and Hinch 1998) and elevated stress levels (Black 1958). There are very few data available to test this hypothesis. Hinch and Bratty (2000) used electromyogram telemetry to estimate swimming speeds of sockeye salmon that were migrating through Hells Gate in the Fraser River, British Columbia. This 150-m reach is the most energetically costly one for sockeye migration in the Fraser because of its fast and turbulent currents (Hinch and Rand 1998). Migrants that successfully ascended this reach swam at average speeds of 1.0–1.5 $m \cdot s^{-1}$ whereas speeds of those that failed averaged 2.0–3.0 $m \cdot s^{-1}$ (Hinch and Bratty 2000). (Prior to reaching Hells Gate, all of the transmitter-carrying migrants successfully ascended the 35-km Fraser Canyon.) Based on observed differences between ground speeds and swimming speeds, it is reasonable to assume that these migrants encountered water speeds of about 0.8–1.0 $m \cdot s^{-1}$. Swimming speeds of the successful group are within the range of optimal speeds whereas those of the unsuccessful ones clearly are not. All of the unsuccessful migrants descended downstream, never passing Hells Gate, and died prior to spawning. Although the sample sizes were small and the mechanisms of the mortality not fully understood, these results suggest that the ability to swim at or near optimal speeds may be under strong natural selection.

Acknowledgements

We thank Jody Frolek for transcribing the video data and Matt Bone from All-Sea Enterprises Ltd. for designing and constructing the underwater camera housings and cables. We appreciate the logistic support provided by the Canadian Department of Fisheries and Oceans at Chilko Lake and Takla Lake. Comments on earlier drafts by Dave Geist, Martyn Lucas, and an anonymous reviewer were very helpful. Funding was provided from the Fraser River Action Plan through Canada's Green Plan and a Natural Sciences and Engineering Research Council of Canada research grant to S.G. Hinch.

References

Beauchamp, D.A., Stewart, D.J., and Thomas, G.L. 1989. Corroboration of a bioenergetics model for sockeye salmon. Trans. Am. Fish. Soc. **118**: 597–607.

Bernatchez, L., and Dodson, J.J. 1987. Relationship between bioenergetics and behaviour in anadromous fish migrations. Can. J. Fish. Aquat. Sci. **44**: 399–407.

Black, E.C. 1958. Hyperactivity as a lethal factor in fish. J. Fish. Res. Board Can. **15**: 573–586.

Boisclair, D. 1992. An evaluation of the stereocinematographic method to estimate fish swimming speed. Can. J. Fish. Aquat. Sci. **49**: 523–531.

Brett, J.R. 1965. The relation of size to rate of oxygen consumption and sustained swimming speed of sockeye salmon (*Oncorhynchus nerka*). J. Fish. Res. Board Can. **22**: 1491–1501.

Brett, J.R. 1995. Energetics. *In* Physiological ecology of Pacific salmon. *Edited by* C. Groot, L. Margolis, and W.C. Clarke. University of British Columbia Press, Vancouver, B.C. pp. 3–68.

Ellis, D.V. 1966*a*. A survey of the behaviour of salmon on spawning migration through a large river system. Fish. Res. Board Can. Manuscr. Rep. No. 876.

Ellis, D.V. 1966*b*. Swimming speeds of sockeye and coho salmon on spawning migration. J. Fish. Res. Board Can. **23**: 181–187.

Gilhousen, P. 1980. Energy sources and expenditures in Fraser River sockeye salmon during their spawning migration. Int. Pac. Salmon Fish. Comm. Bull. No. 22.

Hinch, S.G., and Bratty, J. 2000. Effects of swim speed and activity pattern on success of adult sockeye salmon migration through an area of difficult passage. N. Am. J. Fish. Manage. **129**: 604–612.

Hinch, S.G., and Rand, P.S. 1998. Swim speeds and energy use of upriver-migrating sockeye salmon (*Oncorhynchus nerka*): role of local environment and fish characteristics. Can. J. Fish. Aquat. Sci. **55**: 1821–1831.

Klimley, A.P., and Brown, S.T. 1983. Stereophotography for the field biologist: measurement of lengths and three-dimensional positions of free-swimming sharks. Mar. Biol. **74**: 175–185.

Macdonald, J.S., and Williams, I.V. 1998. Effects of environmental conditions on salmon stocks: the 1997 run of early Stuart sockeye salmon. *In* Speaking for Salmon Workshop Proceedings. *Edited by* P. Gallaugher and L. Wood. Institute of Fisheries Analysis, Simon Fraser University, Burnaby, B.C. pp. 46–51.

Macdonald, J.S., Foreman, M.G.G., Farrell, T., Williams, I.V., Grout, J., Cass, A., Woodey, J.C., Enzenhofer, H., Clarke, W.C., Houtman, R., Donaldson, E.M., and Barnes, D. 2000. The influence of extreme water temperatures on migrating Fraser River sockeye salmon (*Oncorhynchus nerka*) during the 1998 spawning season. Can. Tech. Rep. Fish. Aquat. Sci. No. 2326.

Madison, D.M., Horrall, R.M., Stasko, A.B., and Hasler, A.D. 1972. Migratory movements of adult sockeye salmon (*Oncorhynchus nerka*) in coastal British Columbia as revealed by ultrasonic tracking. J. Fish. Res. Board Can. **29**: 1025–1033.

Osborne, M.F.M. 1961. The hydrodynamical performance of migratory salmon. J. Exp. Biol. **38**: 365–390.

Quinn, T.P. 1988. Estimated swimming speeds of migrating adult sockeye salmon. Can. J. Zool. **66**: 2160–2163.

Rand, P.S., and Hinch, S.G. 1998. Swim speeds and energy use of upriver-migrating sockeye salmon (*Oncorhynchus nerka*): simulating metabolic power and assessing risk of energy depletion. Can. J. Fish. Aquat. Sci. **55**: 1832–1841.

Vogel, S. 1994. Life in moving fluids. The physical biology of flow. Second Edition. Princeton University Press.

Ware, D.M. 1975. Growth, metabolism, and optimal swimming speed of pelagic fish. J. Fish. Res. Board Can. **32**: 33–41.

Webb, P.W. 1995. Locomotion. *In* Physiological ecology of Pacific salmon. *Edited by* C. Groot, L. Margolis, and W.C. Clarke. University of British Columbia Press, Vancouver, B.C. pp. 71–99.

Weihs. D. 1973. Optimal fish cruising speed. Nature 245: 48–50.

Weihs, D. 1974. Energetic advantages of burst swimming of fish. J. Theor. Biol. 48: 215–229.

Predicting the recruitment strength of an annual squid stock: *Loligo gahi* around the Falkland Islands

David J. Agnew, Simeon Hill, and John R. Beddington

Abstract: Two cohorts of *Loligo gahi* recruit to the fishery around the Falkland Islands, the first in summer and the second in autumn–winter. We investigated factors affecting recruitment to these cohorts using 13 years of data (1987–1999). The first evidence for density-dependent effects on recruitment in a squid population is reported, with very high spawning stock biomass leading to a reduction in recruitment in both cohorts. October sea surface temperature was negatively correlated with recruitment to the second cohort 6 months later, and a linear model explained 66% of the variance in recruitment strength. A model combining sea surface temperature and spawning stock size explained 77% of the variance. Thus, low October temperatures and moderate stock sizes lead to higher recruitment the following year than high October temperatures and high stock sizes. A strong negative relationship was also found between sea surface temperature in May and the timing of recruitment to the first cohort the following January–February, suggesting that higher temperatures lead to faster development of embryos or paralarvae and earlier recruitment to the fishery. A predictive model of recruitment size and timing should enable better management of *L. gahi*.

Résumé : Deux cohortes contribuent au recrutement de la population exploitée de *Loligo gahi* dans la région des îles Falkland, l'une en été et la seconde en automne–hiver. Des données récoltées sur une période de 13 ans (1987–1999) ont permis d'étudier les facteurs qui affectent le recrutement de ces cohortes. C'est la première fois que l'on rapporte des effets de densité-dépendance sur le recrutement d'un calmar; en effet, une biomasse des stocks de reproducteurs très élevée entraîne une réduction du recrutement des deux cohortes. La température de l'eau de surface de la mer en octobre est en relation inverse avec le recrutement de la seconde cohorte 6 mois plus tard; un modèle linéaire explique 66% de la variance dans l'importance du recrutement. Un modèle qui relie la température de surface de la mer à la taille des stocks des reproducteurs explique 77% de la variance. Ainsi, des températures basses en octobre et des stocks moyens entraînent un recrutement plus important l'année suivante que des températures d'octobre et densités de stocks élevées. Il existe aussi une forte corrélation négative entre la température de surface de la mer en mai et la date de déclenchement de la reproduction dans la première cohorte en janvier–février, ce qui laisse croire que les températures plus chaudes accélèrent le développement des embryons ou des paralarves et amènent un recrutement plus hâtif. Un modèle prédictif de l'importance et de la phénologie du recrutement devrait permettre un meilleur aménagement de la population de *L. gahi*.

[Traduit par la Rédaction]

Introduction

Squid fisheries pose particular problems for management because these species often live for only 1 year and have a single-cohort population structure. Management is often dependent on estimates of the size of the incoming recruitment or on in-season assessments. While methods for in-season assessments exist (Agnew et al. 1998), they only provide estimates of stock size after peak recruitment (which is also usually the time of peak catch rates). Our experience from the Falkland Islands is that, for both the Patagonian longfin squid *Loligo gahi* and the shortfin squid *Illex argentinus*, assessments based on DeLury depletion analyses are often not possible or not completely reliable until the end of the fishing season (Basson et al. 1996; Agnew et al. 1998).

Trawl fisheries in the Southwest Atlantic started catching *L. gahi* in the early 1980s, but fishing was not managed until the Falkland Islands Interim Conservation Zone was set up in 1987 (Hatfield and des Clers 1998). Since then, there have been two fishing seasons each year, from February to May and from August to October. These target two distinct cohorts (i.e., groups of animals of similar age). The first is spawned in April–May (George and Hatfield 1995), hatches between June and October (Hatfield 1991), recruits to the fishery between October and January, and forms the bulk of catches in the first season (from February to April). The second cohort is spawned in October–November, hatches between October and January, recruits from April–May to July, and is caught primarily in the second season (from August to October) but also at the end of the first season, usually in May. The two cohorts have distinct life histories and peaks

Received June 29, 2000. Accepted October 25, 2000. Published on the NRC Research Press web site on December 20, 2000 J15843

D.J. Agnew,[1] S. Hill, and J.R. Beddington. Renewable Resources Assessment Group, Imperial College, Royal School of Mines, Prince Consort Road, London SW7 2BP, U.K.

[1]Corresponding author (e-mail: d.agnew@ic.ac.uk).

Table 1. Critical parameters (with SE in parentheses) from assessments of the *L. gahi* cohorts fished in 1987–1999.

	Number of recruits (millions)	Biomass of recruits (kt)	Spawning stock biomass (kt)	Average weight at recruitment (g)	Week of peak CPUE
First cohort					
1987	2471 (38)	101 (1.6)		41	11
1988	2802 (283)	115 (11.6)	3.5 (0.1)	41	6
1989	6837 (241)	165 (5.8)	24.1 (2.4)	24	10
1990	5566 (671)	206 (24.8)	35.3 (1.2)	37	7
1991	1392 (136)	53 (5.2)	50.0 (6.0)	38	6
1992	3233 (324)	97 (9.7)	7.7 (0.8)	30	8
1993	1163 (72)	47 (2.9)	15.7 (1.6)	40	14
1994	1702 (201)	55 (6.5)	8.9 (0.6)	32	7
1995	4534 (631)	195 (27.1)	3.7 (0.4)	43	11
1996*	2280 (35)	98 (1.5)	50.7 (7.1)	43	7
1997	975 (172)	40 (7.1)	35.4 (0.5)	41	10
1998	1991 (40)	60 (1.2)	10.2 (1.8)	30	9
1999	1556 (258)	45 (7.5)	21.1 (0.4)	29	6
Second cohort					
1987	4745 (1337)	202 (56.9)		43	
1988	777 (82)	39 (4.1)	41.7 (11.8)	50	
1989	1062 (115)	46 (5.0)	2.6 (0.3)	43	
1990*	3407 (116)	104 (3.5)	4.3 (0.5)	31	
1991	3811 (745)	146 (28.5)	17.3 (0.6)	38	
1992	7336 (1900)	264 (68.4)	11.4 (2.2)	36	
1993*	1682 (37)	90 (2.0)	47.7 (12.4)	54	
1994	2377 (111)	116 (5.4)	6.8 (0.2)	49	
1995	2422 (222)	141 (12.9)	4.4 (0.2)	58	
1996	1950 (123)	130 (8.2)	11.5 (1.1)	67	
1997	2124 (201)	82 (7.8)	9.4 (0.6)	39	
1998	2170 (139)	82 (5.3)	11.5 (1.1)	38	
1999	1213 (51)	54 (2.3)	8.0 (0.5)	45	

Note: DeLury assessments were not successful in years marked with an asterisk, and the DeLury extension method (Agnew et al. 1998) was used instead.

of hatching (Hatfield 2000) and are assumed to be two discrete stocks. Occasionally, a third period of recruitment is seen, at the end of October (Hatfield 1996; Agnew et al. 1998, 1999). This is usually very brief and is more likely to be an early recruitment to the first cohort than a separate stock. It is therefore not considered further in the present paper.

A characteristic of many squid fisheries is very high interannual variability in fishable biomass (Boyle and Boletzky 1996), which arises from recruitment variability (Hatfield and des Clers 1998). For instance, the coefficient of variance of recruitment in numbers for *L. gahi* around the Falkland Islands is 64% for the first cohort and 66% for the second (data in Table 1). Although the pattern of recruitment to the *L. gahi* fishery around the Falkland Islands is now well known, the causes of interannual variability in cohort size and the timing of recruitment to the fishery are not. Work on other squid species has suggested that short-term fluctuations in environmental factors may often have an important influence on the abundance and distribution of squid stocks (*Lologo vulgaris reynaudii*, Roberts and Sauer 1994; Northeast Atlantic *Loligo* species, Pierce et al. 1998; *Illex illecebrosus*, Dawe et al. 2001). In the Southwest Atlantic, Waluda et al. (1999) have suggested a negative correlation between sea surface temperature (SST) at spawning grounds on the Northern Patagonian shelf and recruitment to the *I. argentinus* population that feeds to the north of the Falkland Islands in the austral autumn. No previous studies have considered the causes of variation in the recruitment of *L. gahi*.

The rate of embryonic development (Sakurai et al. 1996) and the rate of growth in the 2–4 months after the animal has hatched (Forsythe and van Heukelem 1987; Forsythe 1993) are both influenced by temperature in cephalopods. We might therefore expect a relationship between temperature during the early life stages, indicated by SST, and the development rate and timing of recruitment of *L. gahi*.

Any information about the possible size and timing of a recruiting cohort would be particularly welcome to management. This paper examines the influence that two factors, environment (indicated by SST) and stock size, have on the strength and the timing of recruitment to *L. gahi* stocks around the Falkland Islands.

Materials and methods

Throughout the Materials and methods and Results sections, reference is made to weeks. Weeks are 7-day sequential periods starting on 1 January. The fishery is open in the first season from February to May inclusive (weeks 5–22) and in the second season from August to October inclusive (weeks 31–44).

Fig. 1. Positions from which SST data were extracted. Each position is the centre of a 1° latitude × 1° longitude square. The location of the ACCLAIM tide gauge at Stanley is indicated by a star. The *Loligo* fishing area is indicated by a dotted line, and the concentric circles around the Falkland Islands are the Falkland Islands Interim Conservation Zone (FICZ) and Outer Conservation Zone (FOCZ). The two main islands are East Falkland Island and West Falkland Island.

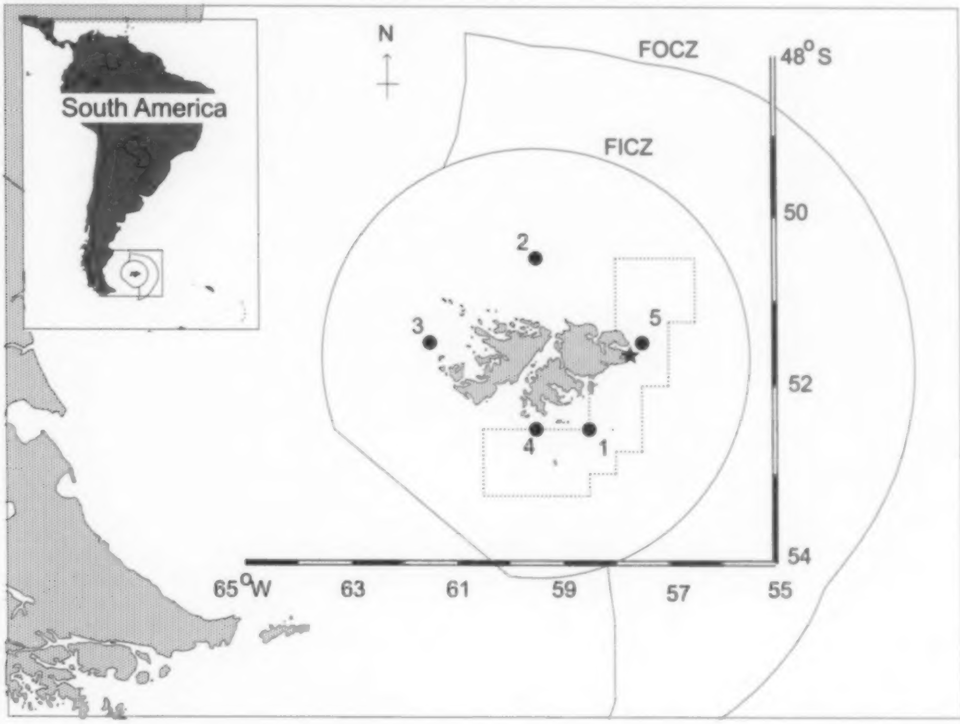

Assessments of Falkland Islands *L. gahi* were performed using either the Lesley–DeLury method or the DeLury extension method (Agnew et al. 1998). The assessments presented in Agnew et al. (1998) were extended to cover 13 years (1987–1999). As noted in the Introduction, the first season's fishery encounters both the first cohort (from February to April) and the second cohort (in May). The changeover between these two cohorts is characterised in the first season by an increase in the proportion of small immature animals being caught. The first cohort was assessed using the depletion before this changeover point, and a single cohort was assumed to be present during this period. The second cohort was assessed using the depletion in the second season, also when there was a single cohort present.

Because the timing of recruitment events varies between years, the assessments produce estimates of recruitment and spawning stock size for different dates each year. Furthermore, in years where the fishery has been closed early, the assessment produces an estimate of spawning stock for an earlier end-of-season time than in normal years. To eliminate this problem, spawning stock size estimates were standardised to the end of week 20 (for the first cohort) or week 44 (for the second cohort) using the equation

$$N_s = N_f \mathrm{e}^{-M(s-f)}$$

where N_s is the number of individuals in the population at week s, the week to which spawning numbers are standardised, f is the week of the final point estimate from the assessment, and M is natural mortality (assumed to be 0.06 per week following Agnew et al. 1998). Recruitment numbers were standardised to week 1 (for the first cohort) and the changeover week (for the second cohort).

Biological data are collected as part of the Falkland Islands Government Fisheries Department observer programme. Spawning stock biomass was calculated by multiplying spawning stock numbers by the maximum weekly mean weight observed for the cohort. Recruitment biomass was calculated by multiplying recruitment numbers by mean weight at recruitment. Finally, the week of peak catch per unit effort (CPUE, in tonnes of *L. gahi* per hour), the week in which the maximum average CPUE occurred, was recorded for the first cohort. CPUE is an index of abundance, and the week of peak CPUE is assumed to be the time at which the cohort is fully recruited to the fishery. Peak recruitment to the second cohort appears to occur in June or July, before the fishery opens and when no data are available. It was therefore not possible to test hypotheses concerning the time of peak recruitment to the second cohort.

SST data are available from the National Center for Atmospheric Research (U.S.A.) and were acquired at a spatial resolution of 1° latitude × 1° longitude and a temporal resolution of 1 month. Previous work by Waluda et al. (1999) has confirmed that these SSTs, measured using satellites, are well correlated with in situ measurements of sea temperature in the Southwest Atlantic. We augmented this validation by comparing SST data with sea temperature data collected between November 1992 and October 1998 by a thermometer attached to a tide gauge positioned at a depth of approximately 1.9 m below midtide, on a fixed mooring, at the eastern end of Port Stanley Harbour. Port Stanley is situated in a shallow-water inlet at the northeast of East Falkland Island (Fig. 1). The data were collected during phase 2 of the Antarctic Circumpolar Current Levels by Altimetry and Island Measurements (ACCLAIM) programme run by Proudman Oceanographic

Laboratory and were used with permission. Average monthly temperatures from the ACCLAIM tide gauge were very close to (with differences of, on average, 0.56°C) and highly correlated with ($r >$ 0.6) satellite-derived SSTs for all positions in winter and spring. The correlation broke down in summer, when warming of the enclosed body of water off Port Stanley led to December temperatures that were an average of 3.52°C higher than satellite-derived SSTs for the open ocean. We concluded that satellite-derived SSTs were reliably indicating open-ocean surface water temperatures.

While it has been suggested that *L. gahi* in the Falkland Islands fisheries recruit from waters on the continental coast, as far north as 42°S (Wysokinski 1996), there is more evidence that these squid spawn locally (George and Hatfield 1995; A. Arkhipkin, Falkland Islands Fisheries Department, Stanley, Falkland Islands, personal communication). In fact, paralarvae have been found all around the islands (Hatfield and Rodhouse 1994). Five positions for satellite-derived SST measurements were chosen around the islands (Fig. 1) representing the range of oceanographic regimes that might affect *L. gahi* in their inshore spawning grounds and paralarval nursery areas. Hatching probably extends over several months in this species. However, we retained temporal resolution of temperature by using monthly SST data.

Preliminary investigation demonstrated that SST at each of the positions around the islands (Fig. 1, positions 1–5) was highly correlated with the SST at the other positions in the same month ($r =$ 0.67 or greater for all positions). Although found all around the Falkland Islands, juveniles are particularly abundant to the southeast of the islands (Hatfield and Rodhouse 1994). Spawning is also known from the south coast (A. Arkhipkin and D. Middleton, Falkland Islands Fisheries Department, Stanley, Falkland Islands, personal communication), and the fishery often concentrates to the south of East Falkland Island. Consequently, the SST at 52.5°S, 58.5°W (i.e., position 1) was chosen as most representative of the area occupied by paralarval and recruiting *L. gahi*. Each of the parameters of size and timing of recruitment were compared with mean SST at this position for the 13 months up to and including the month of recruitment.

Results

Stock–recruitment relationships

The results of assessments of stock size and recruitment for the years 1987–1999 are shown in Table 1. The stock and recruitment plots suggest cyclical behaviour in both cohorts (Fig. 2). This behaviour is only apparent in the early years of the second cohort (Fig. 2*b*), but it seems to be repeated in the first cohort (Fig. 2*a*). With the exception of the first cohort of 1990, the highest recruitments were seen following intermediate to low spawning stock sizes, and the highest stock sizes led to low or average recruitment.

A Ricker function was fitted to these stock–recruit plots as $R_{y+1} = aS_y e^{-bS_y}$ (Hilborn and Walters 1992) where R_{y+1} is the number of recruits in year $y + 1$, S_y is spawning stock biomass giving rise to those recruits, and a and b are constants. Ricker functions explain only a small part of the variance in both the first cohort ($a = 470.162 \pm 210.133$ SE, $b = 0.048 \pm 2.844$ SE; $R^2 = 0.16$, $n = 12$) and second cohort ($a = 630.595 \pm 202.763$ SE, $b = 0.068 \pm 0.023$ SE; $R^2 = 0.23$, $n = 12$). In neither case did the Ricker model provide a significant improvement over a model based on mean recruitment alone (analysis of variance, $P > 0.05$). We concluded that the best description of the relationship between stock and recruitment for both cohorts is that recruitment is variable throughout most of the range of stock sizes but there is a reduction in recruitment at very high stock sizes.

Fig. 2. Stock–recruit relationships for the (*a*) first and (*b*) second cohorts of *L. gahi* with fitted Ricker functions. Points are labelled by the year of recruitment.

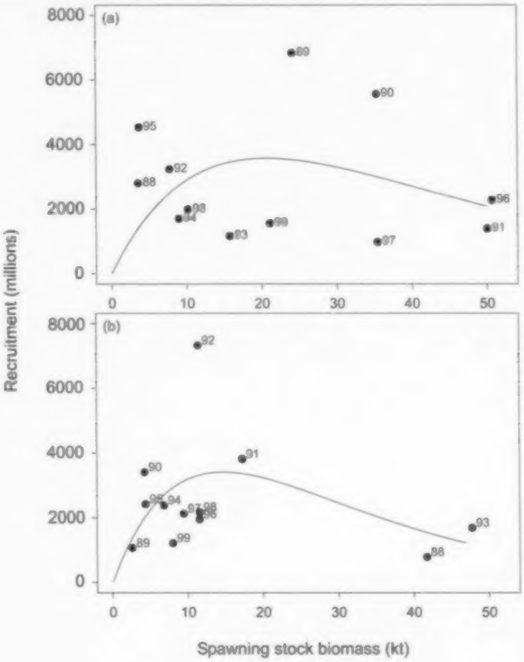

Relationships between sea temperature around the Falkland Islands and *L. gahi* recruitment

There was a strong negative relationship between recruitment to the second cohort and SST at position 1 (Fig. 3), and the relationship held true for several adjacent months (Table 2). Linear regressions of recruitment on October SST at position 1 were significant (t test, $P = 0.012$ and $P <$ 0.001 for recruitment numbers (N_0) and biomass (B_0), respectively):

$$N_0 \text{ (millions)} = 16\,397\ (\pm 4596\text{ SE}) - \text{SST} \times 2394\ (\pm 954\text{ SE});\ R^2 = 0.45$$

$$B_0 \text{ (kt)} = 707.7\ (\pm 128.6\text{ SE}) - \text{SST} \times 103.6\ (\pm 22.4\text{ SE});\ R^2 = 0.66.$$

In addition to the relationship with October temperature, there were also significant negative correlations between temperature in March and April and recruitment size (Table 2). However, the regression models (above) were not significantly improved by the addition of March–April temperatures.

There was no significant relationship between SST and the number of recruits to the first cohort. Although the relationship between SST at position 1 in February and recruitment biomass of the first cohort in the same year was significant at $P < 0.05$, it was dependent on a single year (1990) and did not hold for SST from adjacent months (Table 3).

We examined whether the relationship between SST and second-cohort recruitment held true for other SST positions around the islands. There was a similar correlation between recruitment and SST in October of the previous year at positions 3, 4, and 5 (Fig. 1), i.e., to the south, east, and west of the islands. Again, the relationship was stronger for biomass (correlation coefficients less than –0.64) than for numbers (correlation coefficients less than –0.53) and in each case was significant for biomass (t test, $P < 0.05$, df = 11). However, there was no significant correlation between number or biomass of recruits and October SST at position 2 to the north of the islands. SST at position 1 was used in all subsequent analyses.

A combined model for second-cohort recruitment size

The above results suggest both a density-dependent relationship between spawning stock size and recruitment to the second cohort and a negative correlation between SST around the Falkland Islands and recruitment. Figure 3 shows that the years of density-dependent reduction in recruitment (1988 and 1993) are outside the lower 95% confidence intervals of the regression of recruitment on SST. We therefore investigated the combined effects of SST and the stock size on recruitment.

Taking the above interpretation of the stock–recruit relationship ("recruitment is variable throughout most of the range of stock sizes but there is a reduction in recruitment at very high stock sizes"), we assumed a step function, where recruitment is affected only when spawning stock biomass is above a threshold. The value of this threshold is not known, although available data suggest that it lies between 17 and 42 kt for the second cohort. Stepwise regression was used to produce the following model of the combined effects of SST and spawning stock biomass on recruitment for the years 1988–1999:

$$B_0 = 711\ (\pm 110\ \mathrm{SE}) - \mathrm{SST} \times 103\ (\pm 19\ \mathrm{SE}) - f(\mathrm{SSB}) \times 60\ (\pm 26\ \mathrm{SE});\ R^2 = 0.77$$

where

$$f(SSB) = \begin{cases} 1\ for\ SSB > 30\,000\ \mathrm{t} \\ 0\ for\ SSB \leq 30\,000\ \mathrm{t} \end{cases}$$

and B_0 is recruitment biomass (kilotonnes), SSB is spawning stock biomass, and SST is sea surface temperature (degrees Celsius) in the October before recruitment ($n = 12$). The addition of the spawning stock biomass term improves the fit over the simple linear model of SST on recruitment (explained variance increases from 66 to 77%), and analysis of variance demonstrates that this is close to being significant at the 5% level (SS = 5481, df = 1, $P = 0.0506$).

Estimates of recruitment are associated with varying degrees of uncertainty. To account for this uncertainty, a revised model was constructed using recruitment biomass weighted by inverse standard error. This resulted in a model that was similar to the unweighted model given above but was largely unaffected by years of the high spawning stock biomass and high variance (1987 and 1992). Consequently, the slope was less steep than that of the unweighted model. The weighted model also had a lower R^2 value of 0.64. Weighting by uncertainty in the biomass estimate supports the general form of the unweighted model but inevitably fails to explain years in which biomass was estimated with high uncertainty.

Fig. 3. Recruitment biomass of the second *L. gahi* cohort versus SST from position 1 on Fig. 1 in October of the previous year. Points are labelled by the year of recruitment. The linear fit with 95% confidence intervals is shown (see text). Note that the years 1988 and 1993 (the two high biomass – low recruitment years in Fig. 2*b*) are just outside the 5% confidence limit for the regression.

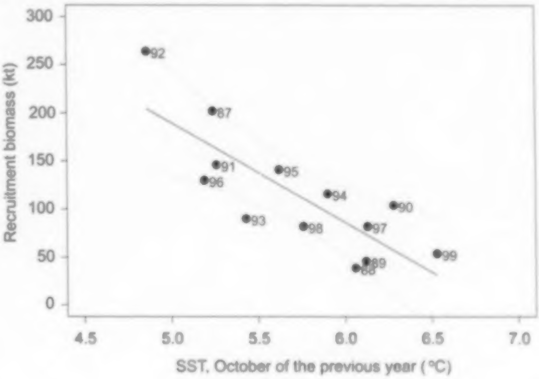

Relationships between sea temperature around the Falkland Islands and the timing of *L. gahi* recruitment

Correlations of SST with other recruitment parameters are shown in Table 3. There was no relationship between SST and weight at recruitment for either cohort. However, the time of peak CPUE in the first cohort was negatively correlated with SST in the early part of the year before recruitment, particularly May and June, the period in which spawning occurs and hatching begins (Fig. 4; also see Table 2). This relationship suggests that higher autumn temperatures lead to earlier recruitment of the first cohort in the following year.

Discussion

There was a strong relationship between SST and recruitment strength of second-cohort *L. gahi* around the Falkland Islands in the years 1987–1999. There was also an apparent negative density-dependent effect in the stock–recruit relationship for both cohorts, with high spawning stock sizes leading to below-average recruitment. A model combining these two effects explained 77% of recruitment variability in the second cohort. Given the few years in the study, it is noteworthy that the combined model was very close to explaining significantly more of the variance than the model with SST alone. However, there were only two years of high stock size – low recruitment for each cohort, and more data for years with high spawning stocks will be required to test this relationship.

Table 2. Pearson correlation coefficients between recruitment parameters and SST at position 1 (Fig. 1) in the 13 months before recruitment.

	Biomass of recruits (second cohort)	Number of recruits (second cohort)	Week of peak CPUE (first cohort)
February (–1)			–0.61*
March (–1)			–0.66*
April (–1)	0.06	0.15	–0.54
May (–1)	–0.26	–0.15	–0.71**
June (–1)	–0.30	–0.19	–0.71**
July (–1)	–0.22	–0.10	–0.49
August (–1)	–0.38	–0.27	–0.40
September (–1)	–0.62*	–0.44	–0.35
October (–1)	–0.81**	–0.67*	–0.23
November (–1)	–0.58*	–0.49	–0.29
December (–1)	–0.45	–0.40	0.21
January	–0.52	–0.37	0.32
February	–0.31	–0.18	0.12
March	–0.71**	–0.60*	
April	–0.57*	–0.42	

Note: *Significantly different from zero correlation at $P < 0.05$ (*t* test); **significant at $P < 0.01$ (*t* test).

Influence of temperature on recruitment strength

Cool sea surface conditions in the austral spring, especially October, and March were associated with greater recruitment to the second cohort. This relationship suggests that second-cohort *L. gahi* are more likely to survive through their early life stages when SSTs are low. In a study of *I. argentinus* in the Southwest Atlantic, Waluda et al. (1999) also suggested that environmental variability, indicated by SSTs, has the most important influence on squid recruitment when it affects the early life stages.

SSTs in squid nursery areas may simply be an indication of the availability of favourable water masses and current structures. For instance, temperature around the islands might indicate the strength of the Falkland Current and its incursion onto the Patagonian shelf. Paralarval and juvenile *L. gahi* probably stay in shallow-water nursery grounds until they recruit to the adult populations on the fishing grounds (Hatfield and Rodhouse 1994). The survival of juveniles may therefore depend on nearshore productivity in the critical exponential phase of their growth (Forsythe and van Heukelem 1987; Forsythe 1993), which in turn may be linked to the strength of the Falkland Current, associated upwelling, and SSTs in spring. Interestingly, the only position on Fig. 1 for which SST was not correlated with recruitment strength was position 2. This area is in an eddy to the north of the islands (Glorioso and Flather 1995), which may not be typical of Falkland Current waters.

In addition to indirect effects, temperature might act directly on survival. For instance, both squid and fish are known to have optimal temperatures for development and survival in their egg stages. Further, the communal spawning behaviour and fixed placement of egg masses in loliginids should result in localised areas with a high density of paralarvae at the time of hatching. Although passive dispersal of paralarvae may quickly spread them over a larger area, reducing density, it is likely that competition for food among *Loligo* paralarvae is most intense in the few days after hatching, which will be greater at elevated temperatures when metabolism and therefore food requirement is higher. For instance, higher temperatures have been found to result in faster yolk absorption and lower conversion efficiency of yolk to tissues, causing reduced survival in laboratory-reared chinook salmon (*Oncorhynchus tshawytscha*) (Heming 1982). High temperatures should also lead to a shorter incubation period that, if it led to lower variability in hatching times, could also create increased competition between paralarvae. Finally, higher water temperatures might be associated with oxygen reduction, which is known to severely restrict the distribution of *L. vulgaris reynaudii* on the west coast of South Africa (Augustyn 1991). The waters around the islands are, however, generally very well mixed.

The strongest correlation between SST and recruitment to the second cohort was in October, a time that is either before or very early in the hatching period for this cohort (Hatfield 2000). If there is a direct influence of temperature, therefore, it is likely to act at this very early life stage and is possibly mediated through competition for food immediately after hatching.

The most striking difference between the first and second cohorts is the absence of any relationship between SST and recruitment to the first cohort. We do not currently understand the reason for this, but it does suggest that an indirect effect of temperature, acting as a proxy for favourable environmental conditions, is more likely to be important than a direct effect of temperature acting to increase competition for food in young paralarvae. It appears that SST is not a good indicator of (i.e., proxy for) favourable environmental conditions for early life stages of the first cohort. In other respects (such as the apparent density-dependent stock–recruit relationship), the two cohorts may be similar.

Influence of temperature on timing of recruitment

Increasing temperature accelerates the rate of embryonic development and both paralarval and juvenile growth in squid (*Loligo forbesi*, Forsythe and Hanlon 1989; *Todarodes pacificus*, Sakurai et al. 1996; *Lolliguncula brevis*, Jackson et al. 1997). Hatfield (2000) has shown that Falkland Islands *L. gahi* hatched in the summer months are significantly larger than squid of the same age hatched in the winter months. Temperature seems to have more influence on the growth of paralarval squid than on that of later life stages (Forsythe 1993; Grist and des Clers 1998).

Temperature might be expected to affect the date of peak recruitment, as well as growth rate, if animals recruit to the fishery at a threshold size or developmental stage. In warmer years, therefore, animals should grow and develop faster and recruit to the fishery earlier. Our results support this. Furthermore, the strongest relationship between the timing of first-season peak CPUE (the time when the first cohort is fully recruited) and temperature was for May of the previous year. This is at the beginning of the first-cohort hatching period but 2 or 3 months before the majority of the brood will hatch (Hatfield 1991, 2000). It therefore seems likely that the dominant effect of sea temperature on the time of recruitment is through increased embryonic development rates

Table 3. Strongest correlations (r) between SST to the southeast of the Falkland Islands (Fig. 1, position 1) and recruitment parameters, obtained using monthly SST for the 13 months before recruitment (February for the first cohort and August for the second cohort).

Cohort	Dependent factor	df	Maximum $\lvert r\rvert$	Probability (unadjusted)	Month of strongest correlation	Number of months with significant correlation
1	Number of recruits	11	0.50	0.082	February	0
1	Biomass of recruits	11	0.57	0.042	February	1
1	Weight at recruitment	11	–0.48	0.097	April (–1)	0
1	Week of peak CPUE	11	–0.71	0.007	May (–1)	4
2	Number of recruits	11	–0.67	0.012	October (–1)	2
2	Biomass of recruits	11	–0.81	0.001	October (–1)	5
2	Weight at recruitment	11	–0.35	0.241	July (–1)	0

Fig. 4. Week, from 1 January, of peak CPUE (W_{peak}) in the first *L. gahi* cohort versus mean SST during May in the year before recruitment. Points are labelled by the year of recruitment. The linear fit with 95% confidence intervals is also shown: W_{peak} = 43.71 (±10.41 SE) – SST × 4.93 (±1.46 SE); R^2 = 50.8%.

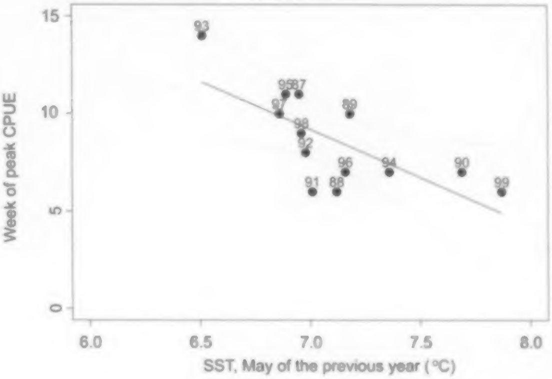

of most of the population and paralarval growth of animals that hatch early.

We did not find any relationship between the SST and the size of squid. However, if (as noted above) squid recruit when they reach a threshold size or developmental stage, the size of squid in the fishery should be largely independent of interannual variability in environmental conditions during the early life stages. Unfortunately, the peak of the second-cohort recruitment could not be identified, so a relationship between temperature and time of recruitment could not be determined for the second cohort. However, future close monitoring of the fishery, and routine age determination for squid from the fishery, should allow further investigation of the relationship between temperature and time of recruitment.

Density-dependent effects

As far as we are aware, this is the first suggestion of a density-dependent response of recruitment to stock size in a squid population. There are very few examples of loliginid assessments in the literature, and most do not provide both stock and recruitment estimates for long enough time series to investigate the relationship between the two (e.g., Augustyn et al. 1993; Brodziak and Rosenberg 1993). However, Rosenberg et al. (1996) reported recruitment and stock biomass indices for *Loligo pealei* resulting from autumn research surveys from 1967 to 1992. Their data suggested a weak Ricker-type density-dependent effect at higher stock sizes, although a Beverton–Holt function could probably be fitted equally well to the data. Unfortunately, interpretation of these data is problematic, since the authors reported the presence of two distinct spawning groups (winter and spring), which they did not attempt to separate. In other squid taxa, data are similarly lacking and what studies are available usually suggest no relationship between stock and recruitment, with the assumption that environmental effects are of paramount importance (Basson et al. 1996; Rodhouse et al. 1998).

Density-dependent reduction in recruitment at high stock sizes is usually attributed to increased disease transmission, cannibalism of juveniles by adults, damage by adults of one another's spawning sites, or density-dependent predation (Hilborn and Walters 1992). We do not know whether these mechanisms might act on *L. gahi* at the adult spawning stages (reducing the number of eggs laid, for instance) or at the egg or juvenile stages. Our current knowledge suggests that disruption of spawning or increased predation at spawning sites is unlikely to be a mechanism, since no very large spawning sites have yet been found for *L. gahi* (A. Arkhipkin, Falkland Islands Fisheries Department, Stanley, Falkland Islands, personal communication). Evidence from other species is mixed. Sauer and Smale (1991) reported low rates of predation on the South African chokka squid *L. vulgaris reynaudii*, which form dense spawning aggregations. On the other hand, Vaughan and Recksiek (1978) reported that spawning Californian market squid (*Loligo opalescens*) do attract seabirds and marine mammals.

Although cannibalism is well known in cephalopods (Boyle 1983) intercohort cannibalism (which is often suggested as a cause of density-dependent recruitment in fish populations) cannot operate in squid populations where only one cohort is present at a time. Hatfield and Rodhouse (1994) have demonstrated that the life history stages of *L. gahi*, which might overlap in time (for instance, paralarvae or juveniles of one cohort and adults of another), are in any case separate in space, occupying different areas and depths. However, intracohort cannibalism, which could cause the effects seen in this study, is known to occur in squid. There is even some evidence that cannibalism in adult *L. gahi* is higher when population density is high than when it is low (M. Rasero and J. Portela, Instituto Espanol de Oceanographia, P.O. Box 1552, 36200 Vigo, Spain, personal communication). If this is true, early life history stages might be similarly affected.

There is a further possible mechanism for density-dependent reduction in recruitment, similar to the arguments developed above about increased competition for food at higher temperatures. Augustyn et al. (1992, 1994) suggested that there is a critical phase, of about 4 days after hatching, when *L. vulgaris reynaudii* must find food in order to survive. Very high hatch volumes, arising following years of very high biomass, might therefore result in increased death through starvation before paralarvae disperse to areas of lower competition.

Implications for management

Although the management strategy adopted by the Falkland Islands Government has so far been successful in maintaining the sustainability of the fishery, there have been two early closures of the second season (which fishes the second cohort) to preserve spawning stock size. This is disruptive to the fishers and makes retrospective analysis and comparison with other years difficult. In-season assessments using DeLury methodology (Agnew et al. 1998) are generally successful but are difficult to apply during the early weeks of any fishing season.

The relationships described in this paper could be used to modify the management approach. For instance, temperatures in the previous autumn may allow prediction of the timing of recruitment to the first cohort. With a fixed season, early recruitment and departure of the first cohort would mean that more of the fishing pressure of the first season (February to May) would fall on the second cohort. This could be avoided by altering the timing of fishing in the first season. Although not demonstrated in this study, one might expect that spring temperatures would similarly affect the timing of recruitment to the second cohort so that colder temperatures lead to a later recruitment.

The combined model of spring SST and spawning stock size should allow prediction of the population size of the second cohort that will recruit the following autumn, taking into account the error likely in such a prediction through, for instance, the construction of Bayesian priors. Fishing effort on this cohort could be adjusted to match the expected size of recruitment and to minimise the risk that a season would have to close early. A similar environmental predictor might yet be found for the first cohort. Recent work on other squid species provides evidence that environmental conditions at early life stages may have an important influence on subsequent recruitment of squid to other commercial fisheries (*L. vulgaris* and *L. forbesi*, Robin and Denis 1999; *I. argentinus*, Waluda et al. 1999). The relationships demonstrated in this paper for *L. gahi* may therefore have wider application in the management of squid stocks.

Acknowledgements

Mr. John Barton, Director of the Falkland Islands Fisheries Department, provided access to the fisheries data used in this study. The work was undertaken under contract to the Falkland Islands Government. The work of Falkland Islands Fisheries Department observers in collecting data from the *L. gahi* fishery over the course of the fishery is gratefully acknowledged. Mr. Thomas Marlow and Mr. Philip Axe helped with the environmental data. Dr. Alexander Arkhipkin and the anonymous referees provided helpful comments on the draft, for which we are very grateful.

References

Agnew, D.J., Baranowski, R., Beddington, J.R., des Clers, S., and Nolan, C.P. 1998. Approaches to assessing stocks of *Loligo gahi* around the Falkland Islands. Fish. Res. **35**: 155–169.

Agnew, D.J., Nolan, C.P., and des Clers, S. 1999. On the problem of identifying and assessing populations of Falkland Island squid *Loligo gahi*. *In* Cephalopod biodiversity, ecology and evolution. *Edited by* A.I.L. Payne, M.R. Lipinski, M.R. Clarke, and M.A.C. Roeleveld. S. Afr. J. Mar. Sci. **20**: 59–66.

Augustyn, C.J. 1991. The biomass and ecology of chokka squid *Loligo vulgaris reynaudii* off the west coast of South Africa. S. Afr. J. Zool. **26**: 164–181.

Augustyn, C.J., Lipinski, M.R., and Sauer, W.H.H. 1992. Can the *Loligo* squid fishery be managed effectively? A synthesis of research on *Loligo vulgaris reynaudii*. S. Afr. J. Mar. Sci. **12**: 903–918.

Augustyn, C.J., Roel, B.A., and Cochrane, K.L. 1993. Stock assessment of the Chokka squid *Loligo vulgaris reynaudii* fishery off the coast of South Africa. *In* Recent advances in fisheries biology. *Edited by* T. Okutani, R.K. O'Dor, and T. Kubdera. Tokai University Press, Tokyo. pp. 3–14.

Augustyn, C.J., Lipinski, M.R., Roberts, M.J., and Mitchell-Innes, B.A. 1994. Chokka squid on the Agulhas Bank: life history and ecology. S. Afr. J. Sci. **90**:143–154.

Basson, M., Beddington, J.R., Crombie, J.A., Holden, S.J., and Purchase, L.V. 1996. Assessment and management techniques for migratory annual squid stocks: the *Illex argentinus* fishery in the Southwest Atlantic as an example. Fish. Res. **28**: 3–27.

Boyle, P.R. 1983. (*Editor*). Cephalopod life cycles. Vol. I. Species accounts. Academic Press, London, U.K.

Boyle, P.R., and Boletzky, S. von 1996. Cephalopod populations: definitions and dynamics. *In* The role of cephalopods in the world's oceans. *Edited by* M.R. Clarke. Philos. Trans. R. Soc. Lond. B, Biol. Sci. **351**: 985–1002.

Brodziak, J.K.T., and Rosenberg, A.A. 1993. A method to assess squid fisheries in the Northwest Atlantic. ICES J. Mar. Sci. **50**:187–194.

Dawe, E.G., Colbourne, E.B., and Drinkwater, K.F. 2001. Environmental effects on recruitment of short-finned squid (*Illex illecebrosus*). ICES J. Mar. Sci. **58**. In press.

Forsythe, J.W. 1993. A working hypothesis of how seasonal temperature change may impact the field growth of young cephalopods. *In* Recent advances in fisheries biology. *Edited by* T. Okutani, R.K. O'Dor, and T. Kubdera. Tokai University Press, Tokyo. pp. 133–143.

Forsythe, J.W., and Hanlon, R.T. 1989. Growth of the Eastern Atlantic squid, *Loligo forbesi* Steenstrup (Mollusca: Cephalopoda). Aquacult. Fish. Manage. **20**: 1–4.

Forsythe, J.W., and van Heukelem,W.F. 1987. Growth. *In* Cephalopod life cycles. Vol. II. Comparative reviews. *Edited by* P.R. Boyle. Academic Press, London, U.K. pp. 135–156.

George, M.J.A., and Hatfield, E.M.C. 1995. First records of mated female *Loligo gahi* (Cephalopoda: Loliginidae) in the Falkland Islands. J. Mar. Biol. Assoc. U.K. **75**: 743–745.

Glorioso, P.D., and Flather, R.A. 1995. A barotropic model of the current off SE South America. J. Geophysl. Res. **100**: 13 427 – 13 440.

Grist, E.P.M., and des Clers, S. 1998. Modelling the growth and maturation of annual squid species. IMA J. Math. Appl. Med. Biol. **15**: 187–209.

Hatfield, E.M.C. 1991. Post-recruit growth of the Patagonian squid *Loligo gahi* (D'Orbigny). Bull. Mar. Sci. **49**: 349–361.

Hatfield, E.M.C. 1996. Towards resolving multiple recruitment into loliginid fisheries: *Loligo gahi* in the Falkland Islands fishery. ICES J. Mar. Sci. **53**: 565–575.

Hatfield, E.M.C. 2000. Do some like it hot? Temperature as a possible determinant of variability in the growth of the Patagonian squid, *Loligo gahi* (Cephalopoda: Loliginidae). Fish. Res. **47**: 27–40.

Hatfield, E.M.C., and des Clers, S. 1998. Fisheries management and research for *Loligo gahi* in the Falkland Islands. Calif. Coop. Oceanic Fish. Invest. Rep. **39**: 81–91.

Hatfield, E.M.C., and Rodhouse, P.G. 1994. Migration as a source of bias in the measurement of cephalopod growth. Antarct. Sci. **6**: 179–184.

Heming, T.A. 1982. Effects of temperature on utilisation of yolk by chinook salmon (*Oncorhynchus tshawytscha*) eggs and alevins. Can. J. Fish. Aquat. Sci. **39**: 184–190.

Hilborn, R., and Walters, C.J. 1992. Quantitative fisheries stock assessment. Chapman and Hall, New York.

Jackson, G.D., Forsythe, J.W., Hixon, R.F., and Hanlon, R.T. 1997. Age, growth, and maturation of *Lolliguncula brevis* (Cephalopoda: Loliginidae) in the northwestern Gulf of Mexico with a comparison of length–frequency versus statolith age analysis. Can. J. Fish. Aquat. Sci. **54**: 2907–2919.

Pierce, G.J., Bailey, N., Stratoudakis, Y., and Newton, A. 1998. Distribution and abundance of the fished population of *Loligo forbesi* in Scottish waters: analysis of research cruise data. ICES J. Mar. Sci. **55**: 14–33.

Roberts, M.J., and Sauer, W.H.H. 1994. Environment: the key to understanding the South African chokka squid (*Loligo vulgaris reynaudii*) life cycle and fishery? Antarct. Sci. **6**: 249–258.

Robin, J.P., and Denis, V. 1999. Squid stock fluctuations and water temperature: temporal analysis of English Channel Loliginidae. J. Appl. Ecol. **36**: 101–110.

Rodhouse, P.G., Dawe, E.G., and O'Dor, R.K. (*Editors*). 1998. Squid recruitment dynamics. The genus *Illex* as a model, the commercial *Illex* species and influences on variability. FAO Fish. Tech. Pap. 376.

Rosenberg, A., Mace, P., Thompson, G., Darcy, G., Clark, W., Collie, J., Gabriel, W., MacCall, A., Methot, R.J., Powers, J., Restrepo, V., Wainwright, T., Botsford, L., Hoenig, J., and Stokes, K. 1996. Scientific review of definitions of overfishing in U.S. fishery management plans. NOAA Tech. Memo. NMFS-F/SPO-17.

Sakurai,Y., Bower, J.R., Nakamura, Y., Yamamoto, S., and Watanabe, K. 1996. Effect of temperature on development and survival of *Todarodes pacificus* embryos and paralarvae. Am. Malacol. Bull. **13**: 89–95.

Sauer, W.H.H., and Smale, M.J. 1991. Predation patterns on the inshore spawning grounds of the squid *Loligo vulgaris reynaudii* (Cephalopoda: Loliginidae) off the Eastern cape, South Africa. S. Afr. J. Mar. Sci. **11**: 513–523.

Vaughan, D.L., and Recksiek, C.W. 1978. An acoustic investigation of market squid, *Loligo opalescens*. Fish. Bull. U.S. **169**: 135–147.

Waluda, C.M., Trathan, P.N., and Rodhouse, P.G. 1999. Influence of oceanographic variability on recruitment in the *Illex argentinus* (Cephalopoda: Ommastrephidae) fishery in the South Atlantic. Mar. Ecol. Prog. Ser. **183**: 159–167.

Wysokinski, A. 1996. Biology and catches of the squid *Loligo gahi* in the Falkland region — Polish research results, 1988–1994 (Biologia i polowy kalamara patagonskiego *Loligo gahi* — wyniki polskich badan w rejonie Falklandow, 1988–1994). Studia i Materialy seria B 68, Morski Instytut Rybacki, Gdynia.

Drift pathways on the western Scotian Shelf and its environs

Jennifer A. Shore, Charles G. Hannah, and John W. Loder

Abstract: Particle tracking and velocity streamlines in three-dimensional seasonal mean current and tidal-current fields are used to develop a Lagrangian view of circulation in the western Scotian Shelf region. The flow fields, taken from a finite element prognostic model, have pronounced spatial structure associated with topography and inflows, and this structure is explored with emphasis on implications for biological populations. The velocity streamlines show the seasonal variations in the locations of throughflows, closed (recirculation) areas, and associated saddle points. Particle tracking from the Browns Bank gadoid nursery provides a spring mean drift pattern and retention times similar to those observed. On-shelf drift pathways through Northeast Channel (with peak summer inflow) and the Scotian Gulf are identified and provide a mechanism for supplying slope water, nutrients, and organisms to shelf basins with significant vertical structure. The Nova Scotian Current provides a near-surface drift pathway from zooplankton overwintering sites in Emerald and Lahave basins to the Browns Bank region in spring and winter. A direct near-surface pathway from outer Browns Bank to outer Georges Bank across Northeast Channel provides the potential for farther downstream drift. Sensitivities to additional flow components are identified.

Résume : Nous nous sommes servis du pistage des particules et des lignes de courant de la vitesse dans les champs tridimensionnels de la moyenne saisonnière des courants et des courants de marées pour construire une image lagrangienne de la circulation dans la région occidentale de la plate-forme Néo-Écossaise. Les champs d'écoulement, établis à partir d'un modèle pronostique aux éléments finis, présentent une structure spatiale marquée associée à la topographie et aux apports, et nous examinons cette structure en nous attardant sur ses incidences pour les populations vivantes. Les lignes de courant de la vitesse montrent les variations saisonnières de l'emplacement des apports transversaux, la présence de zones fermées (recirculation) et l'existence de points-selles associés. Le pistage des particules provenant de la nourricerie de gadidés du banc Browns fait ressortir un patron de dérive (moyenne printanière) et des durées de rétention semblables à ceux qui ont été observés. Nous avons identifié les trajectoires de dérive sur la plate-forme par le chenal Nord-Est (avec un pic d'apport en été) et le golfe Scotian, qui constituent un mécanisme apportant l'eau de pente, les nutriants et les organismes aux bassins de la plate-forme, avec une structure verticale marquée. Le courant de Nouvelle-Écosse constitue une trajectoire de dérive proche de la surface qui va des zones d'hivernage du zooplancton situé dans les bassins Émeraude et Lahave jusqu'à la région du banc Browns au printemps et en hiver. Une trajectoire directe proche de la surface, qui va de l'extérieur du banc Browns à l'extérieur du banc George en passant par le chenal Nord-Est, présente un potentiel complémentaire de dérive vers l'aval. Nous définissons les sensibilités aux composantes supplémentaires de l'écoulement.

[Traduit par la Rédaction]

Introduction

The western Scotian Shelf and adjacent areas in the Gulf of Maine form a complex hydrodynamic region, involving a variable-width (150–400 km) shelf with many banks and basins and multiple forcings (Fig. 1*a*). Two of the banks, Georges and Browns, have been widely studied (see Naimie et al. (1994) and Hannah et al. (2001) for reviews of recent regional physical oceanographic studies) and are intrinsic to the life cycles of commercially important fish species such as cod, haddock, lobster, and scallops (e.g., O'Boyle et al. 1984). There are two cross-shelf channels, Northeast Channel, between Georges and Browns banks, and the Scotian Gulf, between Lahave and Emerald banks, that connect inner-shelf basins, like Georges and Emerald, to the deep ocean and that are important both to the replenishment of deep shelf waters (e.g., Brown and Beardsley 1978) and to the life cycles of species such as *Calanus finmarchicus* (e.g., Head et al. 1999).

There have been numerous field studies in the region that have focussed on localized areas (e.g., Bumpus 1976; Flagg et al. 1982; Smith 1989), including a recent intensive study on Georges Bank that was part of the U.S. GLOBEC (Global Ocean Ecosystems Dynamics) program (e.g., Wiebe and Beardsley 1996). These studies provide a detailed description of the regional physical oceanography and, together with modelling studies, an increasing understanding of the underlying hydrodynamics. However, with the exception of near-surface drifters on Georges Bank (e.g., Naimie

Received January 20, 2000. Accepted June 30, 2000. Published on the NRC Research Press web site on December 20, 2000. J15549

J.A. Shore,[1,2] **C.G. Hannah, and J.W. Loder.** Bedford Institute of Oceanography, Fisheries and Oceans Canada, P.O. Box 1006, Dartmouth, NS B2Y 4A2, Canada.

[1] Corresponding author.
[2] Present address: Ohio State University, 108 Scott Hall, 1090 Carmack Rd., Columbus, OH 43210-1002, U.S.A. (e-mail: shore.13@osu.edu).

Fig. 1. (*a*) Map of the Scotian Shelf and adjacent regions, with major features and selected isobaths (100, 200, 1000 m). The prognostic circulation model's cross-shelf boundaries are indicated by thick lines. (*b*, *c*) Seasonal mean velocities at 30 m for winter (January–February) (*b*) and spring (April–May) (*c*) linearly interpolated onto a 10-km uniform grid. Binned, moored current meter observations that fall between 20 and 50 m in the water column are shown as thick lines (with solid dots at the mooring sites).

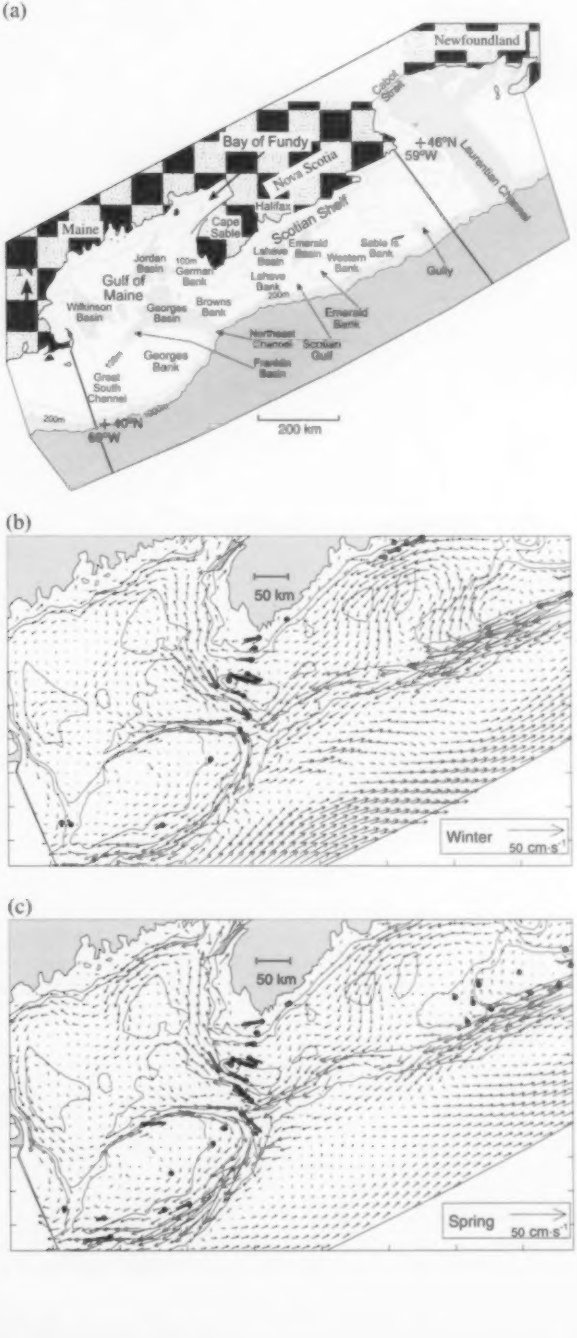
(a)
Newfoundland
Cabot Strait
Bay of Fundy
Nova Scotia
+46°N
59°W
Laurentian Channel
Halifax
Maine
Cape Sable
Scotian Shelf
Emerald Basin
Lahave Basin
Sable Is.
Sable Bank
Western Bank
Jordan Basin
100m
German Bank
Lahave Bank
200m
Gully
N
Gulf of Maine
Wilkinson Basin
Georges Basin
Browns Bank
Emerald Bank
Northeast Channel
Scotian Gulf
Georges Bank
Franklin Basin
Great South Channel
200m
1000m
+40°N
66°W
200 km
(b)
50 km
Winter
50 cm·s⁻¹
(c)
50 km
Spring
50 cm·s⁻¹

et al. 2000), the observations generally lack the spatial and temporal coverage required for evaluations of drift pathways and rates.

Various studies have shown that tidal rectification, density gradients associated with upstream and offshore water masses, tidal fronts, local runoff, wind stress, and Gulf Stream rings contribute to circulation variability in the region (e.g., Butman and Beardsley 1987; Naimie et al. 1994; Hannah et al. 2001). Owing to the region's location at the entrance to the energetic Bay of Fundy – Gulf of Maine system, the M_2 tide is the predominant current component. The tides, together with the upstream inflow of subpolar water, produce a strong and generally persistent seasonal flow pattern, with equatorward throughflows on the shelf edge and inner shelf, and clockwise and counterclockwise circulation tendencies around banks and basins, respectively (Hannah et al. 2001). Important aspects of the seasonal circulation from the perspective of drift pathways are the pronounced spatial structure, associated primarily with topography, tides, wind, and stratification, and competing forcings, such as tidal rectification and baroclinic flow on the northern flank of Browns Bank.

In this study, we used realistic 3-dimensional (3-D) seasonal- and tidal-flow fields from Hannah et al. (2001) to explore drift pathways on the western Scotian Shelf and adjoining areas. Our focus, motivated by biological questions in the GLOBEC Canada and U.S. GLOBEC programs, is on drift pathways in the Browns Bank gadoid spawning area, in the major cross-shelf channels, and from the *C. finmarchicus* overwintering areas in Emerald and Lahave basins. We complement this with a broader-scale evaluation of seasonal flow patterns and potential retention areas, using streamlines for selected vertical intervals. In view of the basic nonlinearity of the Euler–Lagrange transformation in a spatially and temporally variable flow field, and the neglect of a detailed representation of some important flow components (e.g., storm band), this exploration is an intermediate step towards the longer-term goal of simulating full temporal variability in the drift of organisms. Our focus on the western Scotian Shelf is complementary to other recent model-based evaluations of larval fish and zooplankton drift in the Georges Bank region (e.g., Werner et al. 1993; Hannah et al. 1998; Lynch et al. 1998).

Methods

Particles were tracked numerically in 3-D seasonal- and tidal-flow fields for a domain extending from Cape Cod to Cape Breton Island, with realistic bathymetry down to 1000 m (Fig. 1*a*). The flow fields, computed using a nonlinear prognostic model and observationally based forcing by density, tides, and wind stress, are fully described in Hannah et al. (2001).

Seasonal mean and M_2 tidal velocity fields for 4 bimonthly (January–February, April–May, July–August, October–November) periods were computed using a 3-D prognostic advanced-turbulence model (Lynch et al. 1996; Naimie 1996; Hannah et al. 2001).

Seasonal mean initial density fields were obtained using optimal linear interpolation and a historical data base of temperature and salinity observations archived at the Bedford Institute of Oceanography (Loder et al. 1997). Boundary conditions included tidal and seasonal mean (basically steric) elevations at the open and Bay of Fundy boundaries, and seasonal mean (spatially uniform) wind

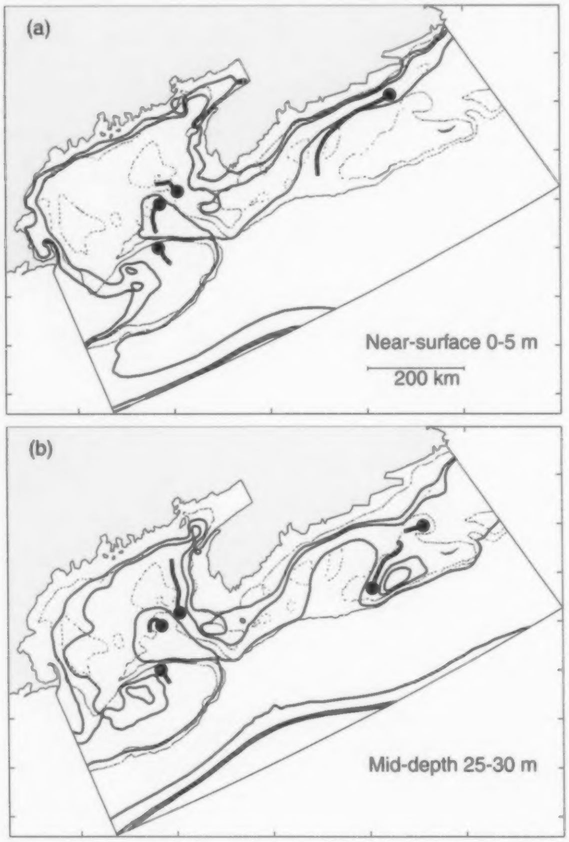

Fig. 2. Velocity streamlines (thin lines) for 5-m vertically averaged near-surface (*a*) and mid-depth (*b*) seasonal mean winter flow fields. Dotted lines show the 100- and 200-m isobaths. Thick lines show 15-day fixed-depth particle trajectories in the vertically averaged winter seasonal mean and tidal flow fields (solid dots are initial positions) for each layer.

stress and a temperature-restoring term at the surface. There were no normal flux conditions at land boundaries for velocity, temperature, and salinity, or at the surface for salinity and turbulence. At the open boundaries, temperature and salinity were fixed. Initial-velocity fields were estimated using nonlinear harmonic diagnostic solutions on a larger domain under density, tidal, and wind forcing.

The flow fields incorporate tidal, seasonal mean wind, and baroclinic-density forcings, together with turbulent mixing. The accuracy of the solutions was checked against independent moored current meter observations, and showed good agreement with observed seasonal mean currents in the southwest Nova Scotia and inner-shelf regions but poorer agreement with those in the Sable Island Bank and shelf-edge regions, where density observations are sparser and tidal influences weaker.

The model and observed seasonal mean flow fields in the central–western Scotian Shelf and Georges Bank regions at 30 m, which reflect the shelf- and bank-scale circulation patterns at mid-depths, are shown in Figs. 1*b* and 1*c* for winter and spring, respectively. A key feature of the regional circulation is the southwestward shelf-edge flow derived from the Labrador Current and the Gulf of St. Lawrence outflow. Observed and modelled along-shelf currents in winter and spring range from 40–50 $\mathrm{cm \cdot s^{-1}}$ along the shelf edge off Halifax to 10–20 $\mathrm{cm \cdot s^{-1}}$ around Browns Bank. Southwest of Sable Island, part of the shelf-edge flow crosses Western Bank onto the Scotian Shelf, forced by baroclinic density gradients along the shelf break. The meander joins with the Nova Scotian Current on the inner shelf to sweep southwestward along the Scotian Shelf, before splitting into flows to the north and south of Browns Bank. The southern branch of this flow also splits into two flows, with one branch flowing into the Gulf through the Northeast Channel and one continuing along the shelf edge. The Gulf of Maine waters primarily exit around Georges Bank, with smaller outflows across Georges Bank and through Great South Channel.

Particles were tracked in the seasonal mean and tidal (M_2) velocity fields by solving $\delta \mathbf{X}(\mathbf{A},t)/\delta t = \mathbf{v}(\mathbf{X},t)$, where the particle position $\mathbf{X}$ is a function of its initial position $\mathbf{A} \equiv (X_0, Y_0, Z_0)$ and time t, through integrating the 3-D velocity field v over time along the trajectory. The methodology is described in Werner et al. (1993) and Blanton (1995). Particles tracked in the full 3-D flow field so that they respond to vertical as well as horizontal flow velocities are called "passive particles," otherwise they are called "fixed-depth particles" for a given depth. Additional random horizontal displacements were included to estimate the influence of unmodelled processes (such as storm events, which fall outside the seasonal- and tidal-frequency bands), following Hannah et al. (1998). These displacements (δx, δy) were taken as

$$(1) \qquad \delta x = \zeta\sqrt{2K\Delta t}, \;\; \delta y = \zeta\sqrt{2K\Delta t}$$

where ξ is a random deviate from a Gaussian distribution of zero mean and unit variance, K is a specified horizontal eddy diffusivity, and Δt is the time step. The particle-tracking scheme uses a fourth-order Runge–Kutta method, with constant Δt = 358 s. The root mean squared displacements after 1 week resulting from eq. 1 for K = 10, 25, and 50 $\mathrm{m^2 \cdot s^{-1}}$ were 5, 8, and 11 km, respectively.

Results

Lagrangian-circulation characterization

A 2-D steady- or periodic-flow field can be characterized through the identification of "closed" recirculation areas (in which particles are trapped) and saddle points connecting particle trajectories that delineate the closed areas (Ridderinkhof and Loder 1994). The stream function ψ for the seasonal mean velocity in a selected vertical interval provides an approximate but succinct method for illustrating the flow pathways and identifying potential closed areas in the model solutions. For each season, the 3-D seasonal mean velocity field was vertically averaged over two 5-m ranges (0–5 and 25–30 m) chosen to represent the near-surface and mid-depth flow regimes. For each regime, the averaged horizontal velocity field (u, v) was assumed to be nondivergent, thereby allowing a solution to $\nabla^2\psi = \nabla \times (u, v)$, which, assuming no flow through the coast and the Bay of Fundy boundary, yields a velocity stream function, ψ, characterizing the flow field. The estimated streamlines are only approximations to particle trajectories, owing to the neglect of tidal (and other time-dependent) motions, possible divergences in the 2-D flow fields, and vertical motions of passive particles. Computations showed only a few small regions with significant divergence in the vertically averaged fields and, overall, the seasonal mean flow features are well represented by the streamlines. However, in local areas with strong tidal currents or divergences, there can be significant differences (see below).

Fig. 3. Velocity streamlines (solid lines) for 25- to 30-m vertically averaged seasonal mean spring (*a*), summer (*b*), and fall (*c*) flow fields. Dotted lines show the 100- and 200-m isobaths. In the summer and fall fields, the closed streamline that covers the largest area on Georges Bank is shown, since the location of the Great South Channel saddle point (not shown) is influenced by its proximity to the downstream boundary.

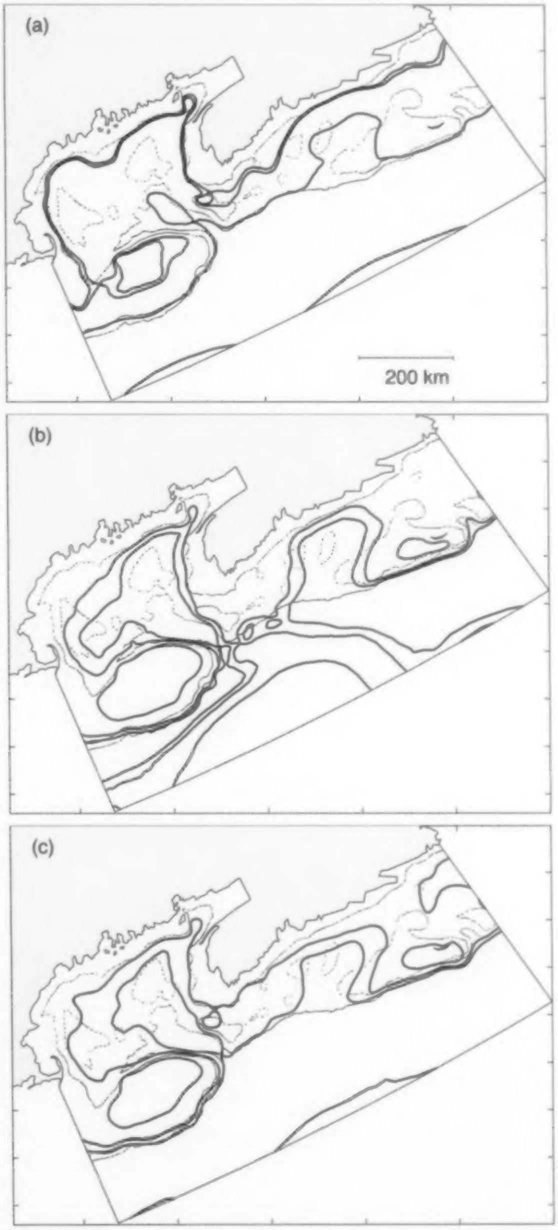

Figure 2 shows velocity streamlines for the winter near-surface and mid-depth layers and Fig. 3 shows mid-depth streamlines for the other seasons. The streamlines provide a shelf-scale pictorial representation of prominent features in the drift patterns, such as the seasonal and vertical changes in closed areas and throughflows. The seasonal mean winds are strongest in winter, enhancing vertical structure in the flow fields that is reflected in differences in the near-surface and mid-depth streamlines. Smaller vertical differences are generally found in other seasons, owing to the weaker seasonal mean stress, although increased summer stratification (and associated fronts) can partly offset this. The overall structure of local closed areas embedded in a southwestward flow following shelf bathymetry can be seen, including the Nova Scotian Current, which extends from surface to bottom on the inner shelf off Halifax (see Hannah et al. (2001) for detailed discussion of the flow fields). The streamlines were chosen to show closed areas of particular interest and are not constant increments of ψ; thus, one should not estimate the gradient of ψ (and therefore velocity magnitude) from these figures.

The closed areas are regions in which the seasonal mean circulation contributes to gyrelike recirculation and, possibly (depending on other flow components), to enhanced retention of particles. We focus on three such areas: the well-known clockwise gyres on central Georges Bank and the cap of Browns Bank (e.g., Naimie et al. 1994; Ridderinkhof and Loder 1994; Hannah et al. 2001) and a counterclockwise gyre in Georges Basin (e.g., Lynch et al. 1996). There are other closed areas in the flow fields that are not discussed or shown in Figs. 2 and 3 (e.g., around Sable Island Bank and Emerald Basin).

Each closed area has an associated saddle point: for central Georges Bank, the saddle point is in Great South Channel; for Georges Basin it is in Northeast Channel; and for Browns Bank it is in the Northern Channel along the bank's northern edge. Particle trajectories are sensitive to the details of the flow field near saddle points, and small perturbations in particle position can lead to large changes in trajectories. The location of saddle points depends on the larger-scale geometry and flow field, as well as on local physical forcing. For example, the saddle point in Great South Channel is required by the combination of a closed area on central Georges Bank (with northward flow on the channel's eastern side) and the coastal current leaving the Gulf of Maine on the channel's western side (see Ridderinkhof and Loder (1994) for further discussion of the saddle point in this region). The exact location of each saddle point depends on the details of the topography and the local flow pattern (in particular, the exact location of the Great South Channel saddle point in these solutions is unreliable, because of proximity to the model's downstream boundary).

In a similar fashion, the Northeast Channel saddle point is required by the combination of a closed area over Georges Basin and the shelf-edge current that crosses the mouth of the channel and flows into (out of) the Gulf on the channel's eastern (western) side. The Georges Basin closed area is a function of this saddle point, the counterclockwise circulation around the Gulf of Maine, and the clockwise circulation around Georges Bank. Likewise, the Browns Bank saddle point is a function of the closed area on Browns Bank and the eastward flow through the Northern Channel and around Cape Sable.

On the central Scotian Shelf, the mid-depth streamlines show an on-shelf meander of the shelf-edge flow across Western and Emerald banks, and a subsequent counterclockwise circulation tendency around Emerald and Lahave basins. The on-shelf meander persists throughout the year and, except in winter when the surface Ekman transport increases offshore drift, is also present in the near-surface layer. As a result, subsurface (fixed-depth) particles released on the eastern end of the Scotian Shelf in winter are more likely to reach the Gulf of Maine than those in the near-surface layer.

The summer field has the weakest throughflow of all four seasons, resulting in a weak shelf-edge flow south of Browns Bank that tends to turn off shelf. Consequently, there are small-scale features of uncertain reliability in the velocity streamlines upstream of the mouth of the Northeast Channel (Hannah et al. 2001). Over Georges Bank, the mid-depth velocity streamlines show the known seasonal variations in the extent and intensity of the gyre, with the flow out of the Gulf of Maine across the eastern end of the bank replaced by an expanded gyre in summer and fall (e.g., Naimie 1996; Hannah et al. 1998) (note, however, the boundary influences on the circulation in western Great South Channel).

These streamlines have been compared with drifter trajectories in the combined seasonal- and tidal-flow fields. Trajectories of four fixed-depth particles released in the near-surface winter-flow fields and tracked for 15 days are shown in Fig. 2*a*, and five particles similarly tracked in the mid-depth circulation fields are included in Fig. 2*b*. In general, such trajectories move parallel to and closely follow the streamlines, but there are some discrepancies. The near-surface trajectory on the inner Scotian Shelf crosses a streamline in the direction of surface Ekman transport, probably owing to the coastal divergence in Ekman transport not being adequately represented by the streamline estimates. Also, the near-surface drifter in Georges Basin eventually crosses a streamline on the northern edge of Georges Bank, associated with a combination of near-surface divergence and strong tidal currents. The winter wind-forced near-surface offshore drift affects a two-layer flow structure in the Gulf of Maine with enhanced onshore mid-depth flow. On Georges Bank, the Ekman layer is deeper; hence, the flows are weaker and particle drift shows less vertical structure.

Drifter observations on Browns Bank

Ocean drifters provide direct fixed-depth Lagrangian flow measurements and, thus, a means for validating model flow fields. We compare the spring model field in the Browns Bank region (Hannah et al. 2001) with the circulation pattern estimated from 10-m drifters described in Smith (1989). Naimie et al. (2000) showed that similar model fields in the Georges Bank region are in good agreement with the seasonal current pattern inferred from a large near-surface drifter data set obtained from the U.S. GLOBEC program.

Browns Bank is an elongated dog-legged bank with an effective overall width of 40 km and a shallow (40 m) western cap with a radius of 14 km (Fig. 1*a*). In April and May of 1983–1984, 10 drifters were released over a number of deployments on the bank as part of a multifaceted study including moored current meter measurements (e.g., Smith 1989). From the drifter observations, Smith (1989) concluded that, at 10 m, water is more likely to leave the cap of Browns Bank along its northern flank, most likely at the northwest corner. However, moored current meters (see Fig. 1) showed little to no off-bank flow on the northern flank (perhaps owing to their location), while providing evidence for a clockwise gyre on the cap.

For the present model–observation comparison, Lagrangian velocities were computed from Smith's (1989) drifter data. The drifter positions (typically at 1- to 3-h intervals) were fitted to cubic splines that were subsampled to time series with a 6.21-h sampling interval (half an M_2 tidal period) to suppress the tides. Weighted means for each position were computed from a surrounding 24- to 48-h period. After this low-pass filtering, a pattern of irregular boxes was judiciously fitted over the paths, so that each box had a number of daily drifter observations with similar behaviour.

Figure 4*a* presents the filtered drifter paths overlying 15 boxes. The drifters showed two primary pathways for exiting Browns Bank. Drifters released on the southeastern part of the bank in spring 1984 travelled clockwise, exited the northeastern edge of the cap, and continued northeastward. Those released in spring 1983 near the northern flank did not travel clockwise around the cap, exited the northern flank, and continued westward. The observations indicate that different flow regimes existed in spring in 1983 and 1984.

The number of days of data per box is shown in Fig. 4*b*. For example, in the northwesternmost box, the number of days of drifter data is 40 (Fig. 4*b*) but the data and, hence, the average velocity estimate, come from a single drifter (Fig. 4*a*). Around Browns Bank, about 4–5 drifters fall within each box that has about 20 observation days.

Average velocities and standard deviations computed from the filtered positions are shown in Fig. 5*a*. The average pattern is consistent with a partial gyre embedded in a throughflow, but the standard deviations and trajectories (Fig. 4*a*) indicate significant temporal variability. North of Browns Bank, the standard deviations are generally larger than the average velocities, while south of the bank, the persistent inflow into the Gulf of Maine along the 200-m isobath results in reduced variability.

The average velocities from the drifter observations are compared with model Lagrangian velocities on a uniform horizontal grid (Fig. 5*b*). The latter are estimated by tracking fixed-depth particles at 10 m in the seasonal mean and tidal flows over two M_2 tidal cycles and computing their average velocity. The partial gyre over the cap of Browns Bank is in evidence, as are the inflows to the Gulf of Maine off Cape Sable and on the eastern side of Northeast Channel. The model flow along the southern flank of Browns Bank is similar in direction to that inferred from the drifters. The model also shows the tendency for flow to be off-bank on the northern flank, with a similar average speed to that inferred from the observed drifters, but the drifters show stronger recirculation behaviour (i.e., a stronger ($10\ \mathrm{cm \cdot s^{-1}}$) eastward flow). From comparison with moored current meter observations, Hannah et al. (2001) concluded that the tidally rectified eastward flow on the northern flank is likely underestimated, owing to smoothing of the model bathymetry.

There are also differences between the model and drifter observations in the Northern Channel between Browns Bank

Fig. 4. (*a*) Filtered drifter trajectories from Smith's (1989) observations (thick solid lines; filled dots are initial positions) shown within 15 nonregular boxes (thin solid lines). Selected isobaths (100, 200 m) are shown but not labeled (dotted lines). (*b*) Number of days of drifter data in each box.

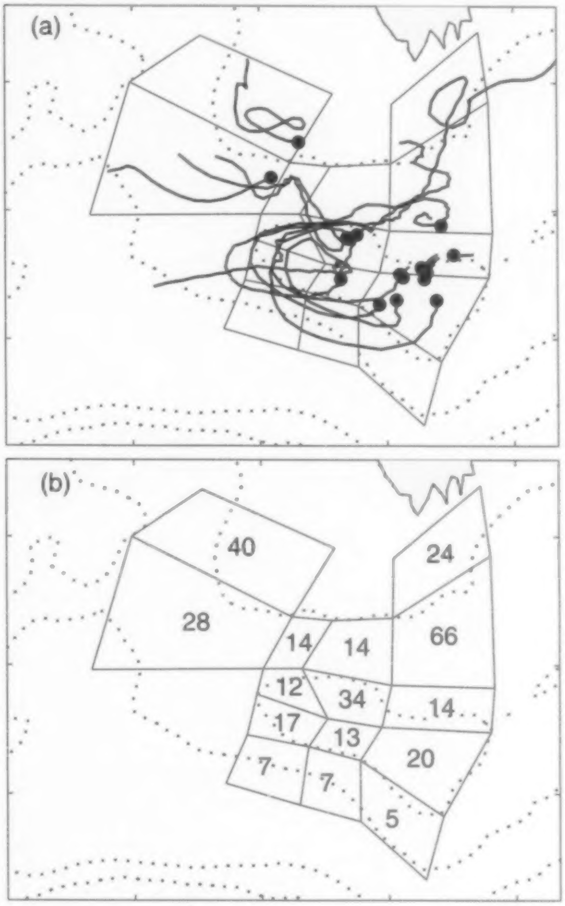

Fig. 5. (*a*) Computed observational drifter velocities (arrows) for 15 nonregular boxes (see Fig. 4*a*), and the magnitude and direction of their associated minimum and maximum standard deviations (bars). Dotted lines show the 100- and 200-m isobaths. (*b*) Computed observational drifter velocities (thick lines and solid dots at the middle of the nonregular boxes) overlying Lagrangian velocities (arrows) computed from the spring seasonal mean and tidal flow field.

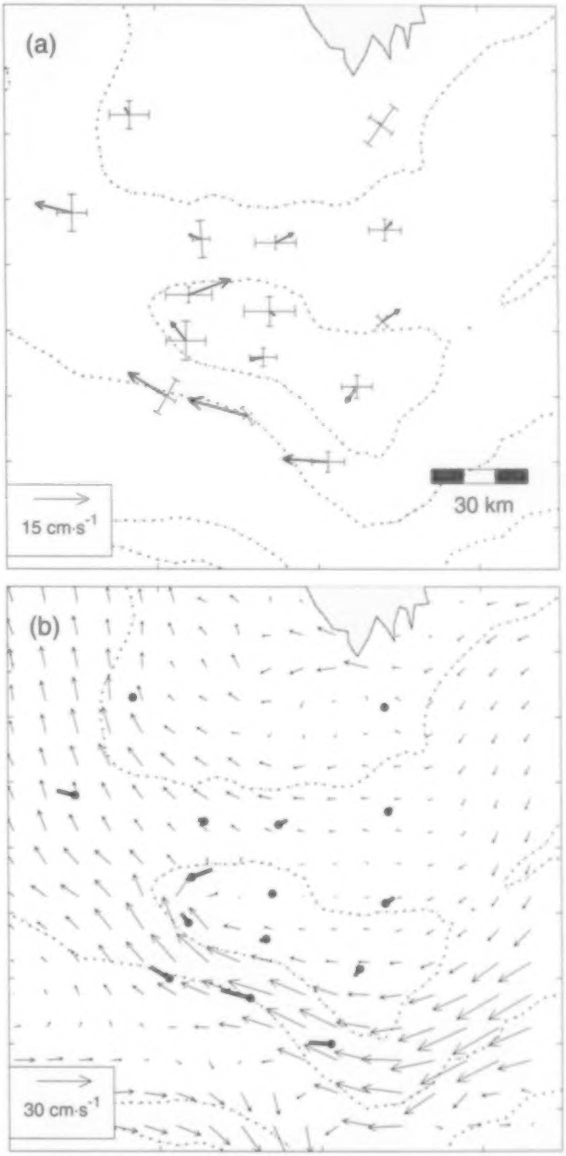

and Cape Sable. Some of these differences may be related to the spring wind directions in 1983 (westward) and 1984 (southwestward) being different from the model climatology (eastward), but it appears that there are significant contributions from interannual variability in other flow components (e.g., different baroclinic circulation) as well. Nevertheless, the drifter-data comparison supports the finding of Hannah et al. (2001) that the model seasonal flow fields are generally in good agreement with observed currents on Browns Bank, with the exception of underestimation of eastward flow on the northern flank.

Drift from the Browns Bank haddock-spawning area

Browns Bank is one of the primary spawning areas for commercial fish species in the region (Hurley and Campana 1989). It was the target area of the 1983–1985 Fisheries Ecology Program, which was designed to explore links between biological production and physical processes, and involved larval surveys (e.g., Campana et al. 1989) and current measurements (Smith 1989). These and more recent studies (Frank 1992; Shackell et al. 2000) have provided strong evidence that variable drift is an important influence on distributions of various cod and haddock life stages and have also raised questions regarding implications for growth and survival. In particular, Shackell et al. (2000) showed that some

Fig. 6. Weekly (0-, 7-, 14-, and 21-day) snapshots of passive particles released from Browns Bank under two different mixing conditions in the spring seasonal mean and tidal flow field : weak mixing, $K = 10$ m^2·s^{-1} (*a*, *c*, *e*, and *g*); strong mixing, $K = 50$ m^2·s^{-1} (*b*, *d*, *f*, and *h*). For clarity, only a twentieth (fifth) of the 491 modelled drifters released are shown in *a* and *b* (*c* and *d*). Solid lines show the 100- and 200-m isobaths.

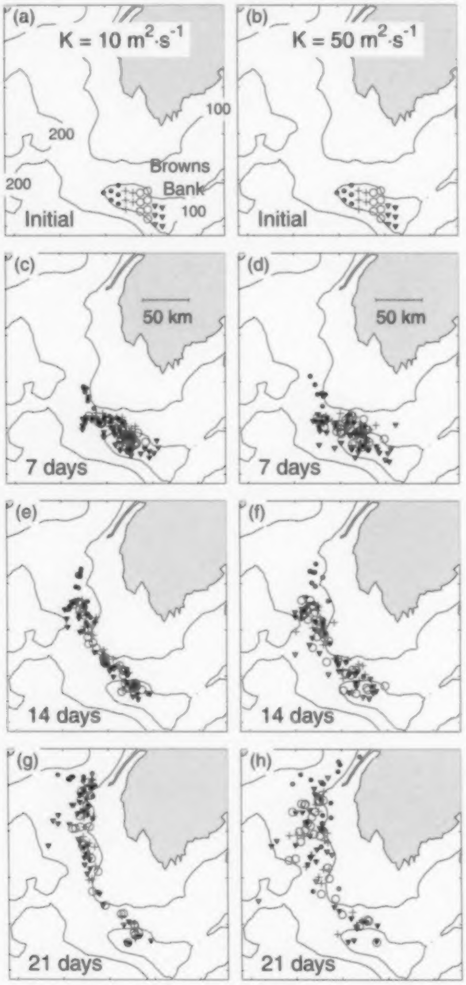

Fig. 7. Snapshots of passive-particle positions at 30 days in the winter (*a*) and spring (*b*) seasonal mean and tidal flow fields with additional horizontal mixing ($K = 50$ m^2·s^{-1}). Initial particle positions are 10 m below the surface at the same horizontal positions as the releases shown in Fig. 6. Solid lines show the 70-, 100-, and 200-m isobaths.

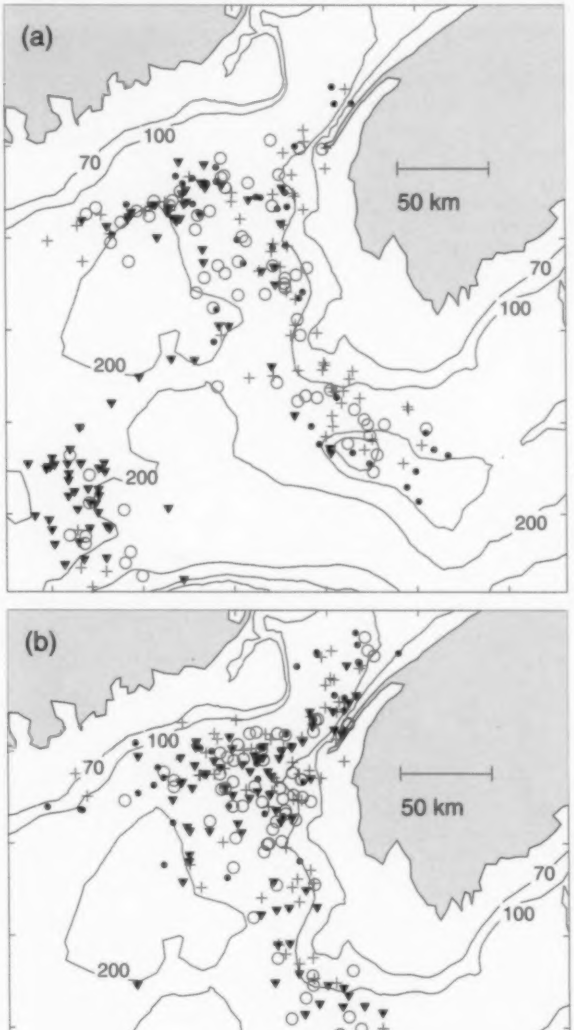

year-classes of age 2 haddock displayed bimodal length–frequency distributions, suggesting separation at an earlier stage due to variable drift, followed by growth at different rates. Correlation analyses indicate that increased survival to age 1 is associated with reduced wind stress (possibly increased retention) and lower growth rate (mechanism unclear), leaving unresolved questions about the importance of various physical and biological processes in the survival of haddock early life stages.

To explore the model drift pathways from Browns Bank during the winter–spring spawning period for cod and haddock, particles were released in the model with a grid covering the core of the spawning area. Figure 6 shows weekly snapshots of the positions of passive particles released at 10 m in the spring seasonal mean and tidal flow field, at the same stage of the tide but for two different horizontal eddy diffusivities ($K = 10$ or 50 m^2·s^{-1} in eq. 1). These K values bracket the range estimated by Smith (1989) from drifter studies for patch scales of about 10–50 km (but note that the effective dispersion in combination with tidal and mean shears

Fig. 8. Percentage of particles remaining within initial-release region (see Fig. 6) for passive particles initially at 10 m (*a–d*) or 30 m (*e–h*) in the winter (*a* and *e*), spring (*b* and *f*), summer (*c* and *g*), and fall (*d* and *h*) seasonal mean and tidal flow fields. Results are shown for cases with $K = 0\ \mathrm{m^2 \cdot s^{-1}}$ (solid line) and $50\ \mathrm{m^2 \cdot s^{-1}}$ (broken line) (eq. 1).

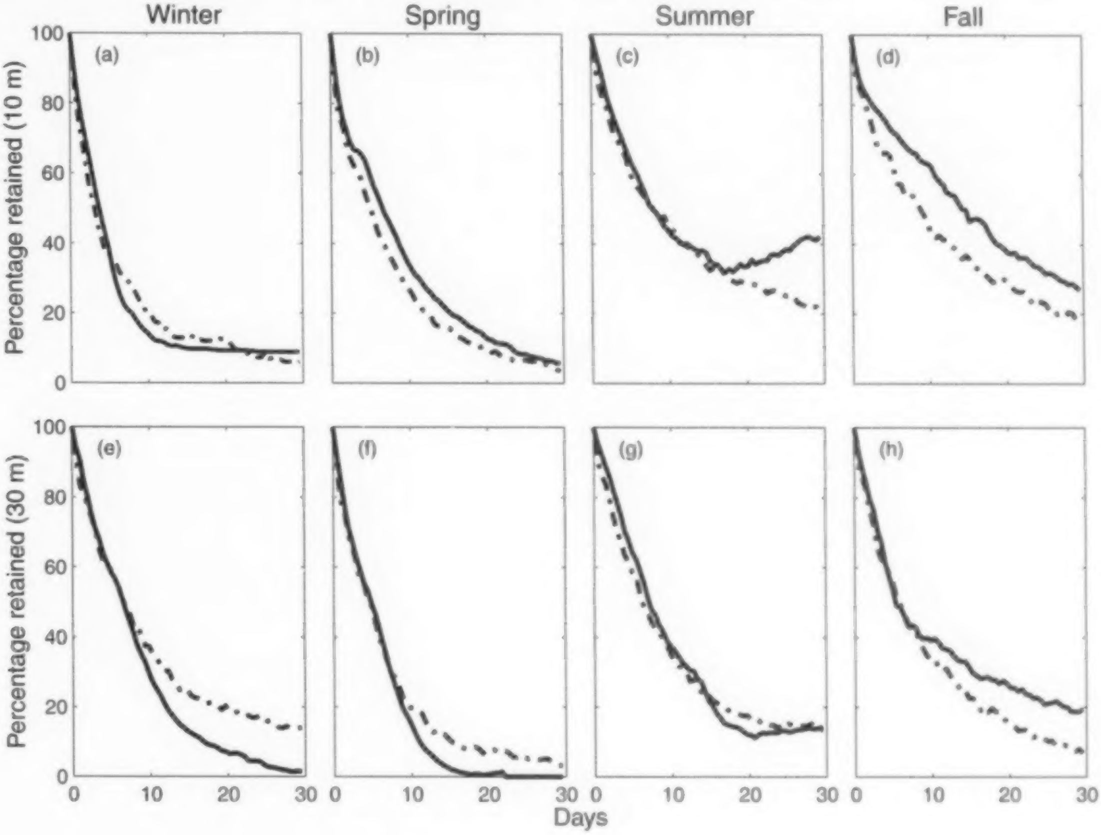

in the model can be larger). The additional component of random horizontal motion is intended to represent, to some degree, motions such as storm events and eddies, which fall outside the seasonal- and tidal-frequency bands and therefore do not appear in the model flow fields. The particle distributions show that the drift is primarily northwestward towards the Bay of Fundy, via an exit pathway on the northern flank of the cap; however, even after 21 days and with high horizontal diffusivity, some (5–10%) of the particles remain over Browns Bank. This behaviour is similar to that observed by Smith (1989) for ocean drifters drogued at 10 m in April of 1983 (Fig. 4). The primary effect of the increased diffusivity in this case is a small amount of spreading normal to the overall drift direction.

The sequential distributions of particles released from an area in winter (not shown) are similar to those of particles released in the same area in spring, except that, in winter, most particles leave Browns Bank from its western end (instead of across the northern flank of the cap) and do not leave as quickly. Figure 7 shows snapshots, after 30 days, of the winter and spring particle distributions for $K = 50\ \mathrm{m^2 \cdot s^{-1}}$ (only half of the 491 released particles are shown). The 30-day positions stretch from the spawning region north to the Bay of Fundy approaches and west to Jordan Basin. There is a bifurcation in the flow off German Bank, with pathways along the eastern and southern sides of Jordan Basin. In winter, the particles are roughly evenly divided between these pathways; in spring, they largely continue north towards the Bay of Fundy. There is a second bifurcation near the mouth of the Bay of Fundy, with some particles moving into the Bay (particularly in spring) but with more moving westward along the northern side of Jordan Basin. The distributions for particles released at 30 m are similar, but suggest that the flow pathway on the southern side of Jordan Basin is much weaker in winter.

A measure of retention on Browns Bank can be obtained by computing the percentage of particles remaining in the release area over time. Figure 8 shows the percentage of passive particles released at 10 and 30 m that remain in the release area by season, for cases with and without random horizontal motions. In all seasons, about 50% of the particles leave the bank within 5–15 days and about 70% within 5–25 days. These results are consistent with Smith's (1989) average residence time of 14 days (range of 5–25 days) for 10 drifters on the bank's cap in the summer of 1983 and Loder et al.'s (1988) estimate of 12 days (with a standard

Fig. 9. Geographical domain of the Northeast Channel. Ramp et al. (1985) sites are marked (solid triangles). Two lines from which particles are released are shown (lines *A* and *C*). A line showing the position of the sill is also drawn.

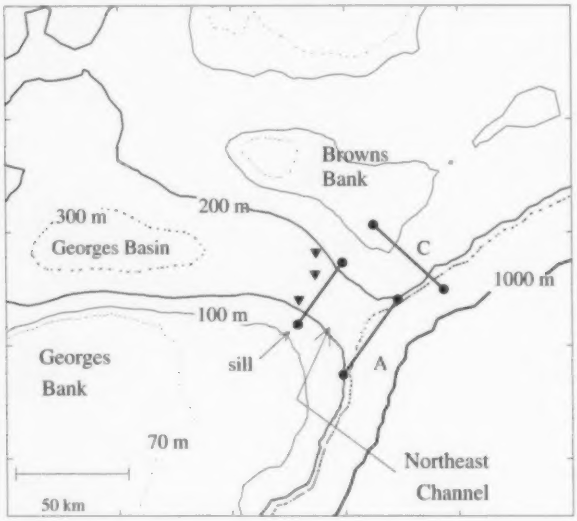

deviation of 9 days) for Smith's larger data set of 23 drifters during April–November 1983–1985. The results, without additional mixing, indicate that particles either at 10 m during the summer and fall or at 30 m during the winter have the best chance of remaining on Browns Bank (30–40% remain after 30 days). Winter and spring show the lowest retention on Browns Bank, with less than 10% remaining after 30 days. The inclusion of additional random motions does not show a consistent effect throughout the seasons or water column. In spring at 30 m, the addition of horizontal mixing results in fewer particles leaving the spawning area, indicating that the exit pathway from the Bank is narrow during that time and that there can be increased retention at depth.

Cross-shelf exchange in Northeast Channel

Northeast Channel, situated between Browns and Georges banks, is the primary conduit for exchange between the Gulf of Maine and the deep ocean (Fig. 9). It is relatively straight, about 20 km wide, and has a sill that rises to a depth of approximately 220 m. It connects with Georges Basin, in which depths are greater than 300 m, and which in turn connects to the north and west with Jordan and Wilkinson basins. Physical oceanographic studies (e.g., Ramp et al. 1985; Smith et al. 2000) have indicated that there is a persistent inflow of slope water through the channel. This flow is supported by persistent (tidal rectification, local density gradient) and time-varying (wind, seasonal upstream throughflow) forcing. Schlitz and Cohen (1984) found that this inflow provided the primary external source of nitrogen to the Gulf of Maine – Georges Bank system, and Head et al. (1999) have suggested that channel inflows, such as those in the Northeast Channel and the Scotian Gulf (see below), may be important in seeding shelf populations of *C. finmarchicus* from the offshore slope region. In this section, we examine the structure of the Lagrangian flow into the Gulf of Maine through Northeast Channel, with an eye towards implications for *C. finmarchicus* populations and nutrient supply.

The model fields show a persistent on-shelf flow on the eastern side of Northeast Channel and an off-shelf flow on the western side (e.g., Fig. 1). In 1976–1978, Ramp et al. (1985) measured currents at three sites just north of the sill in the Northeast Channel (Fig. 9). Figures 10*a* and 10*b* show normal velocities from the summer model field across transect A at the channel's mouth and a line through the Ramp et al. (1985) sites (Fig. 9) with the observed currents superimposed. Figures 10*c* and 10*d* compare the summer model density fields on the same transects. On the western side of the channel, the model and observed velocities are similar. Ramp et al. (1985) noted that, on this side, deep flow is directed on-shelf, but the model velocities suggest that this occurs only on the inside of the sill (since flow is off-shelf at the channel's mouth). On the channel's eastern side, the model velocities match the observations less well but are of the same magnitude and direction. Other observed velocities in the channel show 50-m summer inflows on the eastern side of about 13 $cm \cdot s^{-1}$ and outflows on the western side of about 3 $cm \cdot s^{-1}$ (Flagg et al. 1982), which are of the same magnitude as those predicted by the model. Comparison of the vertical density structure at the mouth and sill indicates that the seasonal mean circulation has only limited penetration of heavier near-bottom waters ($>27.5\ \sigma_t$) from the mouth to the sill. Ramp et al. (1985) described bursts, at time scales of 4–11 days, of flow into and out of the Gulf of Maine in winter and spring, which may provide a mechanism for the on-shelf supply of the heavier water. There are similarities in the velocity structure in other seasons compared with the Ramp et al. (1985) data, but there are differences in the magnitudes of the same order as in summer.

To explore on-shelf drift pathways in Northeast Channel, passive particles were released at 12-m increments on a vertical cross section extending from surface to bottom at the channel's mouth (transect A, Fig. 9) and tracked for 60 days in the seasonal mean and tidal flows (without additional random motions). Panels in the left column in Fig. 11 show, for all seasons, the trajectories of particles that subsequently entered the Gulf of Maine, taken to be those that crossed and spent 30 days inshore of the sill. The right column shows the initial vertical positions of these particles overlying the normal seasonal mean velocities on transect A.

In winter, drifters enter the Gulf on the eastern side of the mouth, if they are in the lower half to two-thirds of the water column (Fig. 11*b*). The winter trajectories indicate that, over 2 months, some particles travel as far north as Jordan Basin, while others begin to curl (counterclockwise) around Georges Basin. Drifters at initial depths above 150 m in winter move closest to the Bay of Fundy. These results are similar to the observed movement into the Gulf of cold Labrador slope water in the winter of 1998 (K.F. Drinkwater, D.B. Mountain, and A. Herman, Bedford Institute of Oceanography, Fisheries and Oceans Canada, unpublished data). Cold slope water observed at the mouth of the Northeast Channel in January penetrated into the Gulf and occupied most of Georges Basin by April (4 months later).

In spring (Figs. 11*c* and 11*d*), there is an approximately 100 m deep window at the channel's mouth on the eastern side (two-thirds the height of the winter window, but narrower)

Fig. 10. Normal flow (U_n (cm·s^{-1}); positive to the northwest) and density (σ_t) through line A (*a* and *c*) and a line through the Ramp et al. (1985) sites (*b* and *d*) taken from the summer seasonal mean field.

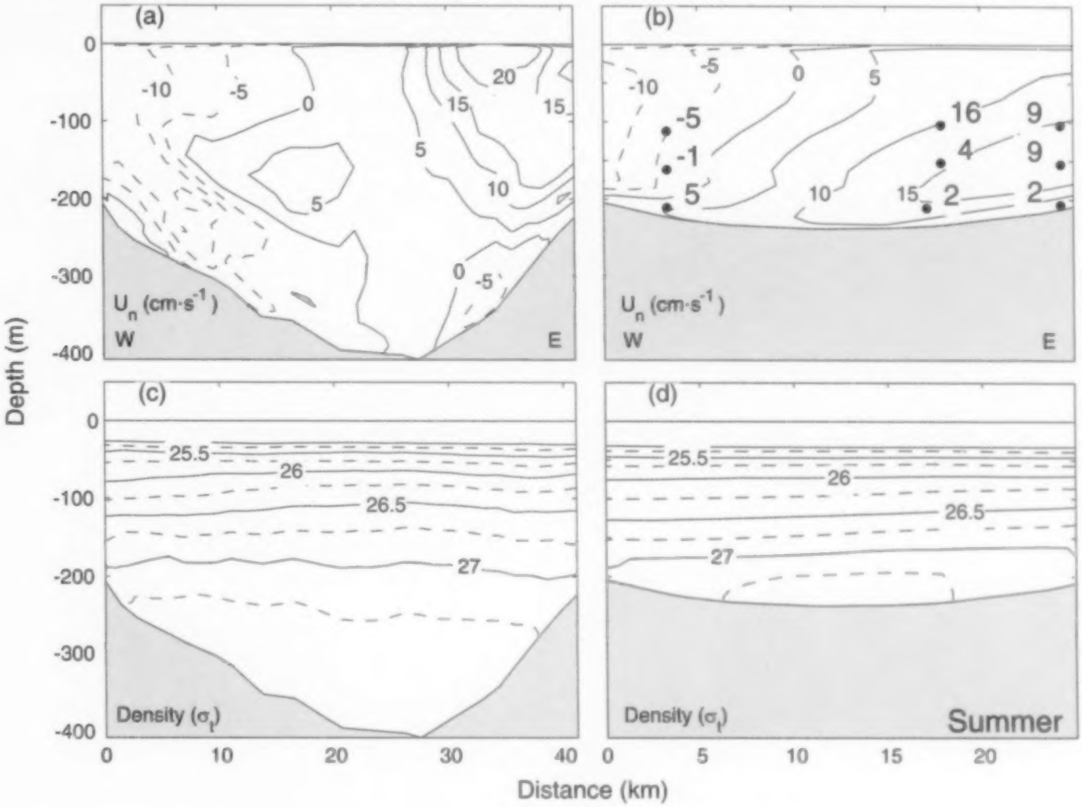

between 75 and 175 m, through which drifters enter the Gulf of Maine. Flow in the Gulf is generally weakest in the spring, and most trajectories only extend to the outer part of Georges Basin. This behaviour is consistent with that inferred from the (fixed-depth) streamline analysis for mid-depths (Fig. 3) and contrasts with the seasonal variation for particles released inside the 100-m isobath on Browns Bank, where passive drifters travel farther towards the Bay of Fundy in spring than in winter (Fig. 7).

The summer source window (Fig. 11*f*) covers the eastern two-thirds of the mouth over most of the water column. A large group of particles (from the upper 150 m of the eastern third of the release transect (shown as triangles in Fig. 11*f*)) moves north around Jordan Basin. A second group circulates around Georges Basin and a third, smaller group moves west into Franklin Basin north of Georges Bank. Fall (Figs. 11*g* and 11*h*) shows an intermediate state between summer and winter, with penetration to Franklin Basin being similar to summer and penetration to Jordan Basin being similar to winter. Over all seasons, particles reaching Jordan Basin tend to originate in the upper eastern part of the mouth, and particles circulating in Georges or Franklin basins tend to originate from parts that are deeper and farther west.

Summer (Figs. 11*e* and 11*f*) has the highest number of particles crossing and remaining north of the sill, while spring has the least; this is consistent with the seasonal cycle in transport at the mouth of the channel. The transports in Table 1 were computed across the sides of a box defined by the sill, transect A, and the lines joining their endpoints (the west (east) transect represents the western (eastern) side of the box; see Fig. 9). Transport across the sill out of the Northeast Channel peaks in summer and is weakest in winter. The strong transport across the sill in summer is concurrent with a shutdown of transport through the west transect (the west side of the box). This decrease in westward transport is associated with the peak summer maximum strength and easterly extent of the Georges Bank gyre. In other seasons,

Table 1. Transport through a box defined by the four corners of two lines: the sill and transect A.

	Transport (Sv)			
Transect	Winter	Spring	Summer	Fall
Transect A	0.16	0.06	0.25	0.20
Sill	0.04	0.05	0.18	0.12
East	0.19	0.29	–0.06	0.13
West	0.31	0.30	0.0	0.21
Transect A + east	0.34	0.35	0.18	0.33

Note: Positive values for the sill and transect A are shoalward (northeastward). Positive values for the west and east lines indicate southwestward transport.

Fig. 11. Two-month-long trajectories (*a*, *c*, *e*, and *g*) for passive particles released from line A (see Fig. 9) in the seasonal mean and tidal flow fields. Only trajectories that cross and remain north of a line crossing Browns Bank, the sill, and Georges Bank (see Fig. 9) for 30 days are shown (for clarity, only half the trajectories are shown). The 100- and 200-m isobaths are also shown. Initial vertical positions (*b*, *d*, *f*, and *h*; *y*-axis is depth (m)) for these same particles are shown overlying the normal seasonal mean velocities (cm·s^{-1}; positive to the northwest) through line A (triangles indicate those reaching Jordan Basin and circles otherwise).

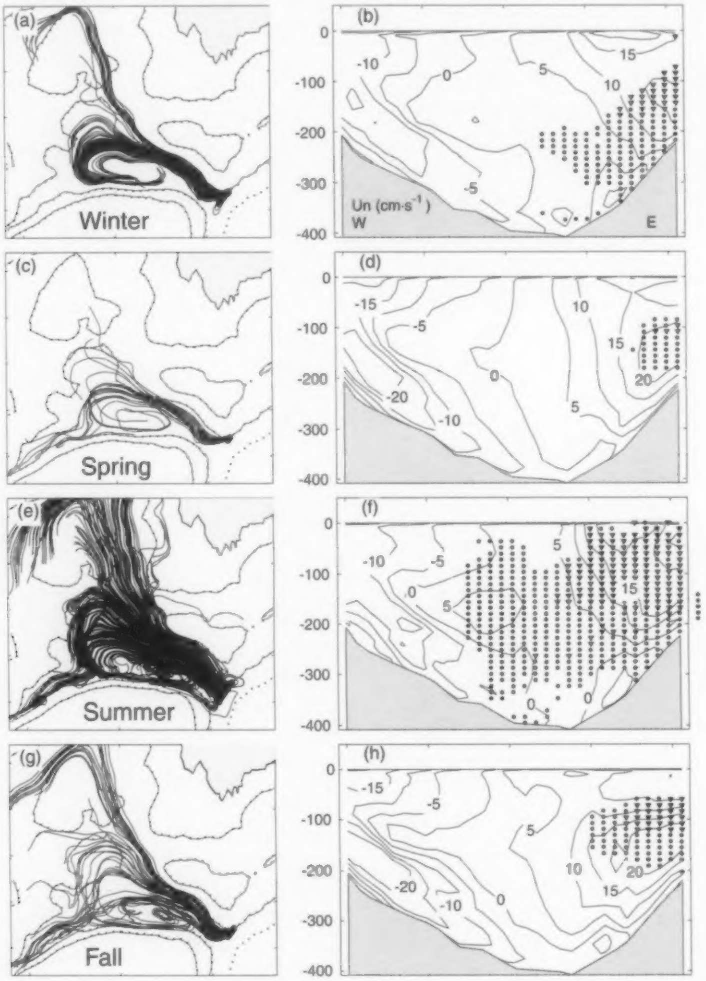

transport through this section is upwards of 0.2 Sv. These results are consistent with previous inferences (based on a box model tuned to seasonal observations) of low westward transport across the channel in summer (Flagg et al. 1982). The total transport into the box (transect A + east) throughout the year is fairly constant (about 0.34 Sv), with the exception of summer, owing to weaker upstream baroclinic forcing. The on-shelf velocities through transect A are similar in fall and summer; however, in the fall, flow in the channel exits to the west, resulting in comparatively fewer particles crossing the sill (see also Figs. 11*f* and 11*g*).

Crossovers from Browns Bank to Georges Bank

One of the emerging results from the U.S. GLOBEC program is the importance of direct crossovers of Scotian Shelf water from Browns Bank to Georges Bank, which provide a "short circuit" for the supply of upstream water properties and organisms to Georges Bank (Bisagni et al. 1996; Meise and O'Reilly 1996; Smith et al. 2000). The model circulation fields indicate a potential climatological pathway for crossover flow from outer Browns Bank to Georges Bank across the Northeast Channel (e.g., Figs. 1 and 3).

In winter, a substantial fraction of the particles released at 0- and 12-m depths along a line across the shelf edge on southern Browns Bank (transect C in Fig. 9) crossed the Northeast Channel and reached the eastern edge of Georges Bank over a 2-month period (Fig. 12*a*). In Fig. 12*b*, the initial positions of these particles are shown superimposed on the normal velocities through this transect. It is evident that the two dominant outcomes for the near-surface particles in winter are either flow along the eastern side of the Northeast Channel into the Gulf of Maine (and subsequent movement

Fig. 12. Two-month-long trajectories (*a*, *c*, *e*, and *g*) for fixed-depth particle releases from line C (see Fig. 9) for particles at 0 and 12 m in the winter seasonal mean and tidal flow field (*a*), particles at 72 m in the winter seasonal mean and tidal flow field (*c*), particles that reach the 200-m isobath around Georges Bank within 2 months in the winter seasonal mean and tidal flow field (*e*), and particles that reach the Georges Bank 200-m isobath within 2 months in the spring seasonal mean and tidal flow field (*g*). The associated initial positions for these cases are shown overlying the normal seasonal mean velocities (cm·s^{-1}; positive to the southwest; *y*-axis is depth (m)) through line C in *b*, *d*, *f*, and *h*.

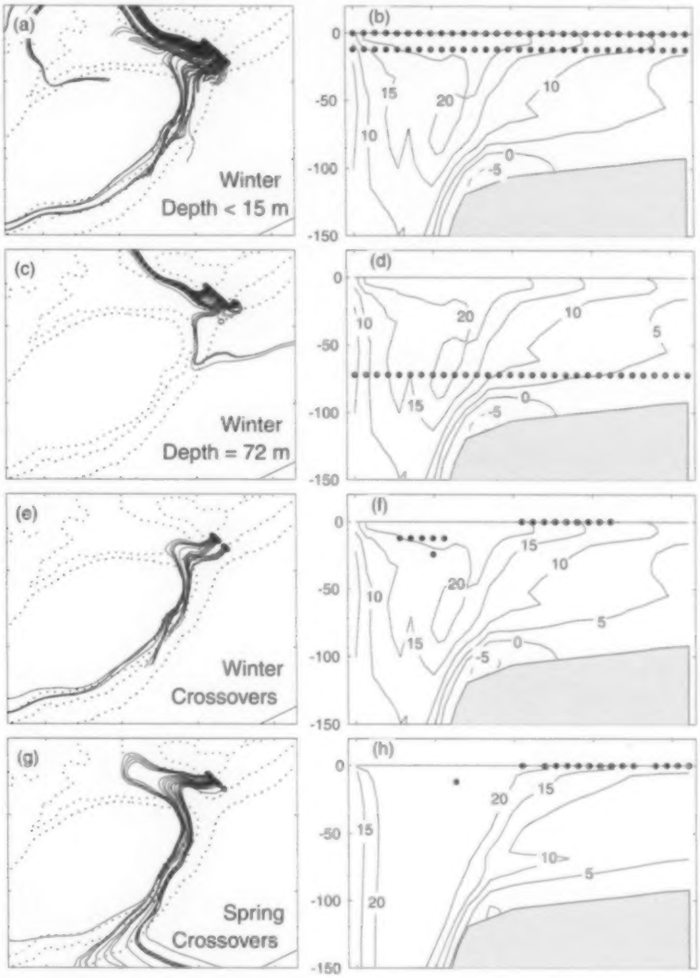

around the northern side of Jordan Basin (not shown)) or flow across the channel to the outer edge of Georges Bank. Figure 12*c* shows the trajectories for fixed-depth particles released at 72 m on the same line in the winter flow field. For the most part, the subsurface particles stay on the eastern side of the channel and move into the Gulf. A few that start near the 200-m isobath do cross the channel, but they do not penetrate onto Georges Bank beyond the 200-m isobath.

To further explore the vertical extent of the potential crossovers, fixed-depth particles were released in the winter and spring circulation fields along transect C at 12-m vertical increments from surface to bottom and tracked for 2 months. The trajectories of winter particles that crossed the 200-m isobath on Georges Bank are shown in Fig. 12*e* and their initial vertical positions overlying the normal velocities are shown in Fig. 12*f*. Results for spring are shown similarly in Figs. 12*g* and 12*h*. In both seasons, only particles above 25 m cross to Georges Bank. Since the spring flow field over Georges Basin is weak, additional particles may reach Georges Bank after 2 months, via the cyclonic circulation in Georges Basin. Summer results (not shown) indicate that no particles cross to Georges Bank.

The above results are consistent with the seasonal variation in the circulation described by Hannah et al. (2001). The primary influence is the shelf-edge throughflow associated with the shelf-scale baroclinic circulation, which is strongest in winter and spring and weakest in summer and fall. The seasonal variation in wind stress also contributes to the seasonal changes in near-surface crossovers. In particular,

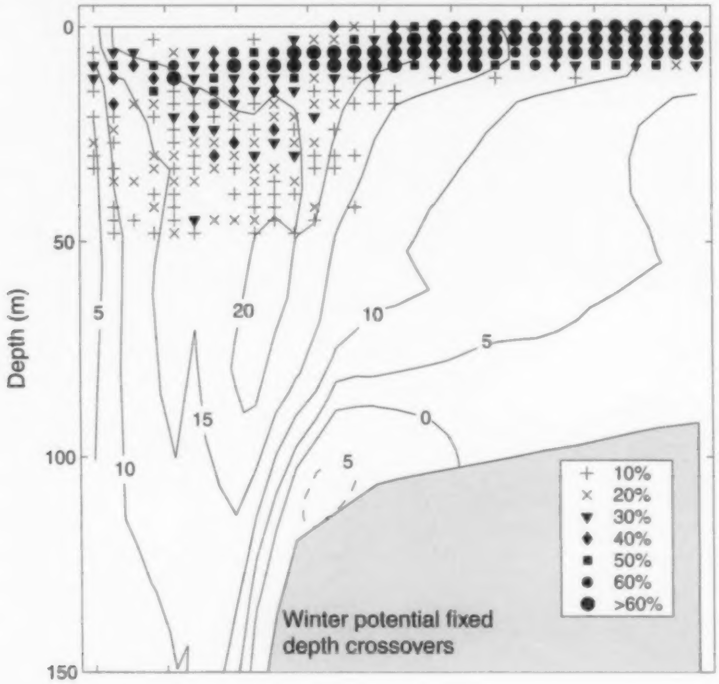

Fig. 13. Probabilities for initial positions reaching the Georges Bank 200-m isobath within a 2-month period from line C (see Fig. 9) in the winter seasonal mean and tidal flow field. Probabilities for each position (represented by symbols) are shown overlying the normal ($cm \cdot s^{-1}$; positive to the southwest) winter seasonal mean flow through this transect.

the winter wind stress (to the east-southeast) supports a south-southwestward near-surface transport, in contrast with the northeastward summer wind stress. The seasonal changes in the crossover pathways are also interrelated with the variations in the Georges Bank and Georges Basin gyres. In summer, the Georges Bank gyre reaches its maximum strength and extent, enhancing the cyclonic gyre in Georges Basin. Associated with the weakened summer shelf-edge flow, the Georges Basin gyre has its maximum southerly extent, shutting down crossovers from Browns Bank to Georges Bank (Fig. 3). The strong shelf-edge flows in winter and spring, together with the smaller Georges Basin gyre, allow crossovers in these seasons.

It is interesting to examine how higher-frequency motions affect the winter results. Statistics for crossovers from Browns Bank to Georges Bank were computed from repeated releases on line C (Fig. 9), using different seeding for the random deviate in the additional horizontal mixing terms (eq. 1) and a K value of 50 $m^2 \cdot s^{-1}$. Vertical release positions were between the surface and 50 m in 3-m increments, and probabilities for each release position were computed as the ratio of the number of crossovers (reaching the 200-m isobath of Georges Bank) to the total number of releases (10). These probabilities are shown overlying the winter (seasonal mean) normal velocities in Fig. 13.

In general, particles initially between 20 and 50 m and over the shelf edge have a small (typically 20%) chance of reaching Georges Bank, while releases below 20 m inside the 100-m isobath on Browns Bank have little chance of reaching Georges Bank (in the modelled climatology). Particles released between 9 and 20 m on outer Browns Bank (near the shelf edge) have a moderate (about 20–50%) chance of reaching Georges Bank, while those released above 9 m on Browns Bank have a fair chance (above 50%) of crossing Northeast Channel. The depth of this "fair probability" zone is related to the surface Ekman and mixed-layer depths on Browns Bank in the model (about 10 m). These results suggest that the climatological circulation can contribute to crossovers of Scotian Shelf water, in addition to intermittent "events" suggested in other studies (e.g., Bisagni and Smith 1998).

Near-surface drift from Emerald and Lahave basins

Emerald and Lahave basins, situated on the inner Scotian Shelf off Halifax, are important overwintering sites for large populations of *C. finmarchicus* (Sameoto and Herman 1990) and potential source regions for the seeding of downstream populations of *C. finmarchicus* in the Gulf of Maine (e.g., Meise and O'Reilly 1996). The overwintering populations are also a potential source of (*C. finmarchicus* eggs and nauplii) for the Browns Bank – southwest Nova Scotia gadoid nursery area (Suthers et al. 1989). Each basin covers about 2500 km^2 (defined by the 200-m isobath) and has depths greater than 250 m. The model solutions indicate that, in all seasons, the Nova Scotian Current sweeps across the northern part of Emerald Basin and then Lahave Basin (Figs. 1, 2, and 3). Hydrographic analyses indicate that the deep waters in these basins are replenished by slope water

Fig. 14. Positions at 30 days for particles released from Lahave and Emerald basins in the winter (*a*, *c*, and *e*) and spring (*b*, *d*, and *f*) seasonal mean and tidal flow fields under weak ($K = 10\ \mathrm{m^2 \cdot s^{-1}}$; *c* and *d*) and strong ($K = 50\ \mathrm{m^2 \cdot s^{-1}}$; *e* and *f*) mixing conditions. Solid lines show the 70-, 100-, 200-, and 1000-m isobaths.

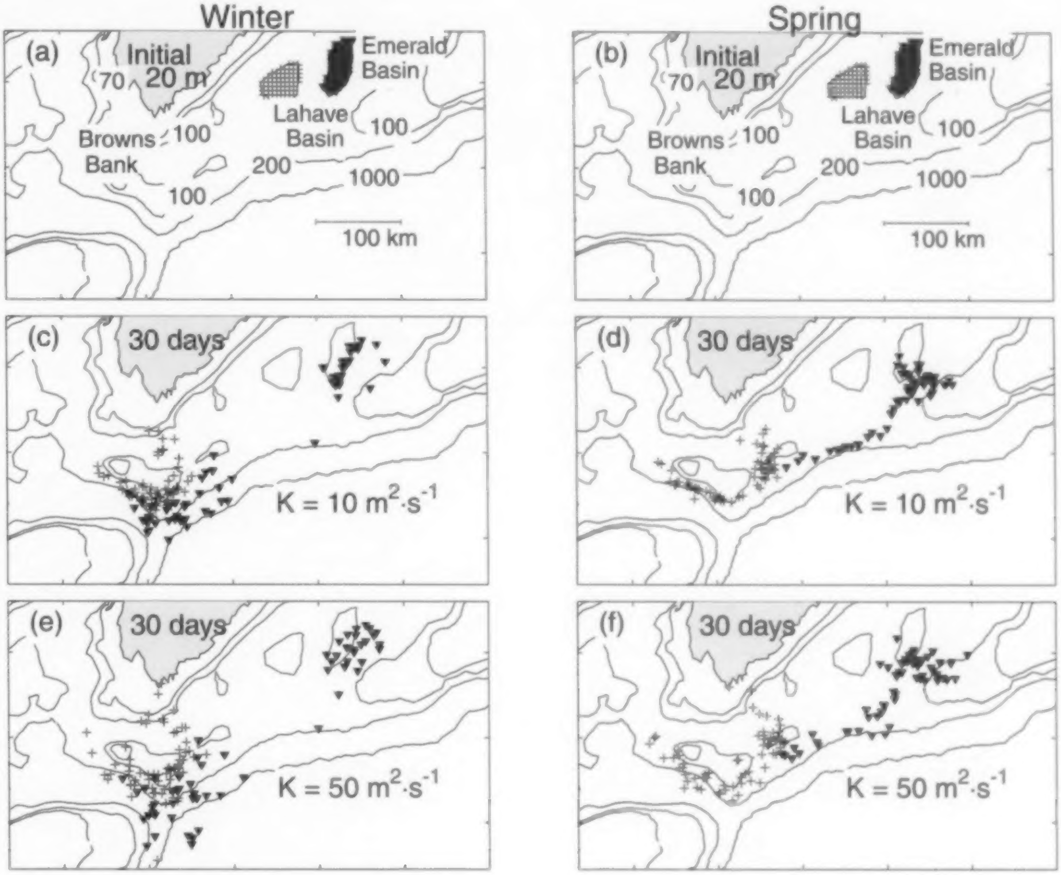

intrusions through the Scotian Gulf (e.g., Petrie and Drinkwater 1993; Loder et al. 1997; K.F. Drinkwater, D.B. Mountain, and A. Herman, Bedford Institute of Oceanography, Fisheries and Oceans Canada, unpublished data.

Particles were released over Emerald and Lahave basins (inside the 200-m isobaths) and tracked in the winter and spring seasonal mean and tidal circulation fields, to explore potential pathways for the supply of *C. finmarchicus* to the gadoid nursery off southwest Nova Scotia. The particles were fixed at a depth of 20 m, based on observations of peak April concentrations at this depth (Sameoto and Herman 1990). Figure 14 shows their positions after 30 days under two different random horizontal motion conditions ($K = 10$ and $50\ \mathrm{m^2 \cdot s^{-1}}$). With weaker random motions, particles tend to reach the Browns Bank region along the outer shelf in both seasons, but there is limited drift onto the bank's plateau (inside the 100-m isobath) and to the inner shelf off Cape Sable. Stronger random motions result in more particles moving onto the bank and to the inner shelf. These results suggest that the strong wind-driven currents (a significant portion of the subtidal current variance) and large horizontal diffusivities ($50 \le K_H \le 100\ \mathrm{m^2 \cdot s^{-1}}$) found by Smith (1989) for the Browns Bank region could work in concert with the seasonal mean circulation to enhance prey supply to larval gadoid populations.

There are notable differences in the pathways from the two release basins (Fig. 14). Most of the particles from Lahave Basin remain on the shelf and are in the Browns Bank – southwest Nova Scotia region after 30 days, with many moving into the Gulf of Maine. In contrast, many particles from Emerald Basin remain near the release area after 30 days. Some particles from Emerald Basin move to or towards the outer Browns Bank region in both seasons and, particularly in winter, move off the shelf. The multiple pathways from Emerald Basin are related to its location near the edge of the Nova Scotian Current and to the overlying counterclockwise partial gyre that provides a tendency to move particles onto the northern edge of Emerald Bank (Fig. 1).

The 60-day trajectories (not shown) for the Emerald–Lahave basin releases show that particles reach the eastern side of Jordan Basin in both seasons primarily by way of outer Browns Bank, supporting potential *C. finmarchicus* supply from the Scotian Shelf basins (or shelf edge) to Georges and Jordan basins. Results (for both *K* values in winter and

Fig. 15. Trajectories originating in the Scotian Gulf (along a line connecting Lahave and Emerald banks) for passive particles tracked (over 2 months) in the winter (*a*, *c*, *e*, and *g*) and spring (*b*, *d*, *f*, and *h*) seasonal mean and tidal flow fields. Particles initially between 50 and 100 m for these releases are shown in *a* and *b* (only half the trajectories are shown for clarity). Particles trajectories that initially move northward and originating between 0 and 100 m (*c* and *d*) or below 100 m (*e* and *f*) are shown for both seasonal circulation fields. Initial positions for trajectories that initially move northward are shown overlying the normal seasonal mean velocities ($cm{\cdot}s^{-1}$; positive northward) through this transect (*g* and *h*).

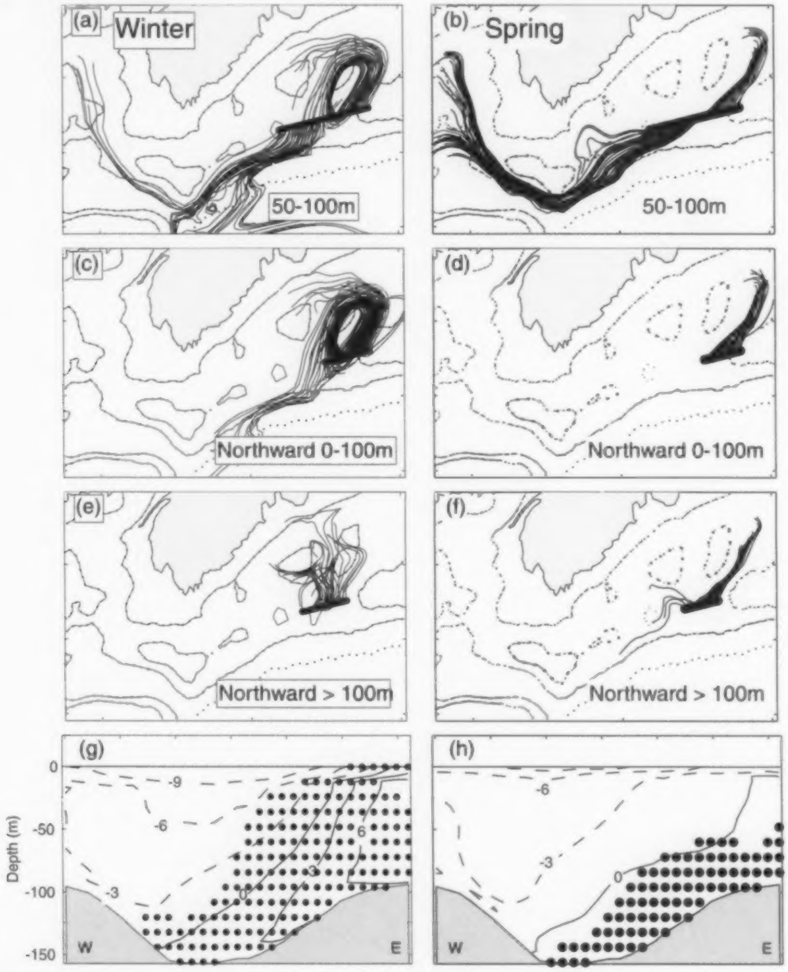

for $K = 50\ m^2{\cdot}s^{-1}$ in spring) also show particles from Emerald and Lahave basins drifting southwestward along the southern edge of Georges Bank, indicating a possible contribution from Scotian Shelf *C. finmarchicus* populations to those on Georges Bank.

Cross-shelf exchange in the Scotian Gulf

The Scotian Gulf cuts across the outer shelf between the Emerald and Lahave banks and has been recognized as the predominant pathway for the movement of slope water onto the Scotian Shelf, particularly at depths associated with wind- and eddy-forced current fluctuations (Smith and Petrie 1982; Petrie 1983). However, the cross-shelf meanders of the Nova Scotian and shelf-edge currents in the model solutions provide a potentially important contribution to cross-shelf exchange from the climatological seasonal circulation as well (Hannah et al. 2001). Similar to the Northeast Channel's role in the Gulf of Maine, cross-shelf exchange in the Scotian Gulf has important implications for both nutrient supply to the Scotian Shelf and possible seeding of shelf *C. finmarchicus* populations from the slope (Head et al. 1999).

To explore the Scotian Gulf exchange pathways in winter and spring, passive particles were released in the model along a line between the Lahave and Emerald banks and tracked for 2 months in the seasonal mean and tidal circulation fields. Figures 15*a* and 15*b* show trajectories for particles released between 50 and 100 m (12-m vertical increments) that reflect the main cross-shelf flow structure. Particles released on the Emerald Bank side drift northward (into and around Emerald Basin in the winter), while those released in the middle of the Gulf and on the Lahave Bank side move offshore and southwestward along the shelf edge.

Focussing on the on-shelf drift, Figs. 15*c*–15*f* show trajectories that initially proceed northward away from the release line (for passive particles initially between 0 and100 m or below 100 m). In Figs. 15*g*–15*h*, these initial positions are superimposed on the normal velocities across this transect. The vertical structure of the initial positions closely resembles the normal velocity distribution, contrasting with the results for the Northeast Channel (Fig. 11), in which not all particles with an initial on-shelf velocity moved through the channel and the release line was off-shelf from the sill.

Discussion

Velocity streamline estimates and numerical particle tracking have been used to describe drift pathways and identify potential retention areas in the western Scotian Shelf region. The investigation is based on a set of recently developed numerical model fields of climatological seasonal mean and M_2 tidal currents in the region (Hannah et al. 2001). These model fields, and similar fields developed by others (e.g., Naimie 1996), show good overall agreement with established flow features and moored current meter measurements. Comparison of the spring drift pattern around Browns Bank with observations (Smith 1989) showed that the model also reproduces the major Lagrangian drift features—flow into the Gulf of Maine on the bank's southern side and recirculation around its cap. Likewise, the modelled drift patterns on Georges Bank are similar to those derived from observed near-surface drifters (Naimie et al. 2000), providing further confidence in the model fields. However, there are some inadequacies in the seasonal-mean fields (e.g., underestimation of flow on northern Browns Bank), and the effects of random horizontal motions in the particle-tracking experiments suggest that current fluctuations outside the seasonal and tidal bands can have important influences on the drift patterns. Thus, the present results should be regarded as indicative of gross features rather than as definitive drift pathways.

The predominant features of the drift patterns in the western Scotian Shelf region are an equatorward topographically steered throughflow, and partial gyres around banks and basins that result in potential closed (recirculation) areas. Discussion here focussed on closed areas over Browns and Georges banks and Georges Basin and their associated saddle points. Such closed areas are expected to be areas of enhanced retention and to be of potential importance to biological communities such as the early life stages of fish on Browns and Georges banks. The streamline estimates provide indications of important seasonality and vertical structure in the closed areas, such as a reduced near-surface extent of the Georges Bank area in winter. Estimates of the horizontal scale of each area in relation to particle excursions associated with current fluctuations provides a means of assessing potential retentiveness, but drifter tracking (observed or modelled) is required to determine the detailed drift patterns (e.g., flushing times and exit pathways). Additional important closed areas over Sable Island Bank and Emerald Basin were also noted.

Overall, the model fields indicate considerable interseasonal persistency and vertical coherence in the drift pathways from Browns Bank. Particle releases from the Browns Bank haddock-spawning area provided retention-time estimates similar to those observed for 10-m drifters by Smith (1989) and Loder et al. (1988). About 50% of the particles left the bank (over all seasons and mixing conditions) within 5–15 days, and 70% left within 5–25 days. The results support biological inferences of both larval retention on Browns Bank and larval drift towards the Bay of Fundy (Campana et al. 1989; Shackell et al. 2000). It is interesting to note that, while spring is the peak spawning period for haddock, particle retention in spring is low (less than 10% left on the bank after 30 days) and drift to the high-growth Bay of Fundy is greater in spring than in winter. If spring is the season with the greatest probability of drift to the high-growth Bay of Fundy region, and retention on Browns Bank favours larval survival (as indicated by the analysis of Shackell et al. 2000), then the timing of haddock spawning favours growth over survival. However, current fluctuations outside the seasonal and tidal frequency bands may enhance retention during peak spawning, since the exit pathway from the cap is narrow (Fig. 6) and additional horizontal dispersion enhanced retention in the area at depth. Various physical and biological influences on larval drift and survival in this region are being investigated in follow-up studies using the model flow fields (D. Brickman, N. Shackell, and K. Frank, Bedford Institute of Oceanography, Fisheries and Oceans Canada, unpublished data; Hannah et al. 2001).

The drift pathways in Northeast Channel, illustrated together with the velocity streamlines and particle trajectories, provide further evidence for the channel's importance in supplying slope water, nutrients, and organisms to the Gulf of Maine. The persistent but vertically structured pathways into the gulf suggest that there is the potential for seeding of *C. finmarchicus* populations in Gulf of Maine basins by shelf-edge populations, but the extent of this seeding will depend on their vertical distribution, as well as on important current fluctuations that are not represented in the present model solutions (Ramp et al. 1985; Greenberg et al. 1997). The seasonal variation of peak penetration in summer supports a baroclinic circulation origin (e.g., Mountain and Jessen 1987). The spatial structure of the flow in the channel implies that small changes in position can be important to trajectories and, therefore, the seasonal mean and tidal flows are only part of the climatological drift patterns.

Similar to the Northeast Channel region, the seasonal circulation in the Scotian Gulf region provides an avenue through which slope and shelf-edge waters penetrate onto the Scotian Shelf, although the vertical structure of the on-shelf pathways differs with a broader zone of on-shelf flow at depth in the Scotian Gulf. The drift pathways in both winter and spring show a similar vertical structure, with the on-shelf drift zone extending from Emerald Bank westward past the middle of the Scotian Gulf at depth (>100 m) and the off-shelf drift zone extending increasingly eastward from Lahave Bank to the Emerald Bank side for shallower depths.

The on-shelf near-bottom drift in the Scotian Gulf points to a barotropic component of the on-shelf flow attributed to interactions of baroclinic flow with shelf-edge topography (Hannah et al. 2001). This near-bottom drift should be particularly effective in providing an on-shelf supply route for nutrients, the concentrations of which generally increase with depth. The on-shelf flow in the Scotian Gulf, together with previous findings of wind- and eddy-driven inflows (Smith and Petrie 1982; Petrie 1983), provide the potential for shelf-edge seeding of *C. finmarchicus* populations in Emerald and Lahave basins (Head et al. 1999).

The overall throughflow on the Scotian Shelf, clearly manifested in the distribution of hydrographic properties (e.g., Loder et al. 1997), provides the potential for the alongshelf supply of organisms to downstream regions. The streamline results and the central Scotian Shelf particle releases indicated that, in winter and spring, there are drift pathways from Lahave and Emerald basins to the Browns Bank gadoid nursery area, providing a potential supply route for various stages of *C. finmarchicus* as gadoid prey. The near-surface drift pathways from Lahave and Emerald basins, together with the crossover pathways from outer Browns Bank to outer Georges Bank, provide support for a supply route from these basins to Georges Bank in winter and spring (also see Lynch et al. 1998). However, the limited number of particles reaching Georges Bank in the present simulations suggests that either additional flow components or longer drift periods would be required for a major fraction of the *C. finmarchicus* populations of the Lahave and Emerald banks to move to Georges Bank. The different pathways from these basins suggest that Lahave Basin is more likely to contribute to the Browns Bank region, and Emerald Basin to contribute to Georges Bank, but this result is sensitive to uncertain details of the cyclonic gyre and associated saddle point in Emerald Basin. Further, at times, the basins could be overwintering sites for *C. finmarchicus*, whereas at other times, off-shelf sites would be more favourable (Sameoto and Herman 1990; Head et al. 1999).

The streamlines and particle releases point to an upper-ocean crossover pathway (across the mouth of Northeast Channel) from outer Browns Bank to outer Georges Bank in the winter and spring flow fields. The pathway does not exist in summer, largely owing to the reduced shelf-edge throughflow and the increased southerly extent of the Georges Basin gyre. The winter and spring pathway provides a persistent seasonal mechanism for the short-circuit supply of relatively cold and fresh Scotian Shelf water, and of associated organisms (e.g., *C. finmarchicus* populations originating in Emerald Basin; gadoid larvae from Browns Bank), to outer Georges Bank. However, the importance of this mechanism to Georges Bank as a whole may be limited by its narrow (cross-shelf) extent and offshore location, as well as by strong flow perturbations by Gulf Stream rings that can entrain shelf water (e.g., Butman and Beardsley 1987) and potentially disrupt crossovers. While it is possible that there are inadequacies in the model's representation of the extent and location of the crossovers (e.g., Bisagni et al. (1996) describe observed crossovers that are farther on-bank), it seems likely that other time-varying currents (interannual, winds, eddies) are also of major importance to intrusions of Scotian Shelf water onto Georges Bank (e.g., Bisagni and Smith 1998).

Acknowledgements

We are grateful to our colleagues in the GLOBEC programs who contributed to model development, observational data analysis, and discussions. We thank Brian Blanton, Dan Lynch, Chris Naimie, and Cisco Werner for providing model algorithms; Shawn Oakey for assisting with the computations and figures; Liam Petrie for assisting with the figures; and Peter Smith for access to drifter data. We are also grateful to Peter Smith, Ken Drinkwater, and two anonymous reviewers for their constructive comments. This is a contribution to the GLOBEC Canada program, jointly funded by Fisheries and Oceans Canada and the Natural Sciences and Engineering Research Council, and contribution No. 159 of the U.S. GLOBEC program, jointly funded by National Oceanic and Atmospheric Administration and the National Science Foundation. We also acknowledge support for the model applications from the (Canadian) Federal Panel of Energy, Research and Development.

References

Bisagni, J., and Smith, P.C. 1998. Eddy-induced flow of Scotian Shelf water across Northeast Channel, Gulf of Maine. Continental Shelf Res. **18**: 515–539.

Bisagni, J., Beardsley, R., Ruhsam, C., Manning, J., and Williams, W. 1996. Historical and recent evidence of Scotian Shelf water on southern Georges Bank. Deep-Sea Res. Part II Top. Stud. Oceanogr. **43**: 1439–1472.

Blanton, B. 1995. DROG3D: user's manual for 3-dimensional drogue tracking on a finite element grid with linear finite elements. Program in Marine Sciences, University of North Carolina, Chapel Hill.

Brown, W.S., and Beardsley, R.C. 1978. Winter cooling in the western Gulf of Maine: part 1. Cooling and water mass formation. J. Phys. Oceanogr. **8**: 265–277.

Bumpus, D.F. 1976. A review of the physical oceanography of Georges Bank. Int. Comm. Northwest Atl. Fish. Res. Bull. **12**: 119–134.

Butman, B., and Beardsley, R.C. 1987. Long-term observations on the southern flank of Georges Bank, I: a description of the seasonal cycle of currents, temperature, stratification and wind stress. J. Phys. Oceanogr. **17**: 367–383.

Campana, S.E., Smith, S.J., and Hurley, P.C.F. 1989. Drift—retention dichotomy for larval haddock (*Melanogrammus aeglefinus*) spawned on Browns Bank. Can. J. Fish. Aquat. Sci. **46**: 93–102.

Flagg, C.N., Magnell, B.A., Frye, D., Cura, J.J., McDowell, S.E., and Scarlet, R.I. 1982. Interpretation of the physical oceanography of Georges Bank. Vol. 1 of the Final Rep. from E.G.&G. Enviromental Consultants, 300 Bear Hill Road, Waltham, MA 02254, U.S.A.

Frank, K.T. 1992. Demographic consequences of age-specific dispersal in marine fish populations. Can. J. Fish Aquat. Sci. **49**: 2222–2231.

Greenberg, D.A., Loder, J.W., Shen, Y., Lynch, D.R., and Naimie, C.E. 1997. Spatial and temporal structure of the barotropic response of the Scotian Shelf and Gulf of Maine to surface wind stress. J. Geophys. Res. C, Oceans, **102**: 20 897 – 20 915.

Hannah, C.G., Naimie, C.E., Loder, J.W., and Werner, F.E. 1998. Upper-ocean transport mechanisms from the Gulf of Maine to Georges Bank, with implications for *Calanus* supply. Continental Shelf Res. **17**: 1887–1911.

Hannah, C.G., Shore, J.A., and Loder, J.W. 2001. The drift–retention dichotomy on Browns Bank: a model study of interannual variability. Can. J. Fish. Aquat. Sci. **57**: 2506–2518.

Hannah, C.G., Shore, J.A., Loder, J.W., and Naimie, C.E. 2001. Seasonal circulation on the western and central Scotian Shelf. J. Phys. Oceanogr. In press.

Head, E.J.H., Harris, L.R., and Petrie, B. 1999. Distribution of *Calanus* spp. on and around the Nova Scotia Shelf in April—evidence for an offshore source of *Calanus finmarchicus* to the mid- and western regions. Can. J. Fish Aquat. Sci. **56**: 2463–2476.

Hurley, P.C.F., and Campana, S.E. 1989. Distribution and abundance of haddock (*Melanogrammus aeglefinus*) and Atlantic cod (*Gadus morhua*) eggs and larvae in the waters off southwest Nova Scotia. Can. J. Fish Aquat. Sci. **46**: 103–112.

Loder, J.W., Ross, C.K., and Smith, P.C. 1988. A space- and time-scale characterization of circulation and mixing over submarine banks, with application to the Northwestern Atlantic Continental Shelf. Can. J. Fish Aquat. Sci. **45**: 1860–1885.

Loder, J.W., Han, G., Hannah, C.G., Greenberg, D.A., and Smith, P.C. 1997. Hydrography and baroclinic circulation in the Scotian Shelf region: winter versus summer. Can. J. Fish. Aquat. Sci. **54**(Suppl. 1): 40–56.

Lynch, D.R., Ip, J., Naimie, C., and Werner, F.E. 1996. Comprehensive coastal circulation model with application to the Gulf of Maine. Continental Shelf Res. **16**: 875–906.

Lynch, D.R., Gentleman, W.C., McGillicuddy, D., and Davis, C.S. 1998. Biological/physical simulations of *Calanus finmarchicus* population dynamics in the Gulf of Maine. Mar. Ecol. Prog. Ser. **169**: 189–210.

Meise, C.J., and O'Reilly, J.E. 1996. Spatial and seasonal patterns in abundance and age-composition of *Calanus finmarchicus* in the Gulf of Maine and on Georges Bank: 1977–1987. Deep-Sea Res. Part II Top. Stud. Oceanogr. **43**: 1473–1501.

Mountain, D.G., and Jessen, P.F. 1987. Bottom waters of the Gulf of Maine. J. Mar. Res. **45**: 310–345.

Naimie, C.E. 1996. Georges Bank residual circulation during weak and strong stratification periods—prognostic numerical model results. J. Geophys. Res. C, Oceans, **101**: 6469–6486.

Naimie, C.E., Loder, J.W., and Lynch, D.R. 1994. Seasonal variation of the three-dimensional residual circulation on Georges Bank. J. Geophys. Res. C, Oceans, **99**: 15 967 – 15 989.

Naimie, C.E., Limeburner, R., Hannah, C.G., and Beardsley, R.C. 2000. On the geostrophic and seasonal patterns of the near-surface circulation on Georges Bank—from real and simulated drifters. Deep-Sea Res. Part II Top. Stud. Oceanogr. In press.

O'Boyle, R.N., Sinclair, M., Conover, R.J., Mann, K.H., and Kohler, A.C. 1984. Temporal and spatial distribution of ichthyoplankton communities of the Scotian Shelf in relation to biological, hydrological, and physiological features. Rapp. P.-V. Reun. Cons. Int. Explor. Mer, No. 183. pp. 27–40.

Petrie, B., and Drinkwater, K. 1993. Temperature and salinity variability on the Scotian Shelf and in the Gulf of Maine 1945–1990. J. Geophys. Res. C, Oceans, **98**: 20 079 – 20 089.

Petrie, B.D. 1983. Current response at the shelf break due to transient wind forcing. J. Geophys. Res. **88**: 9567–9578.

Ramp, S., Schlitz, R.J., and Wright, W.R. 1985. The deep flow through the Northeast Channel, Gulf of Maine. J. Phys. Oceanogr. **15**: 1790–1808.

Ridderinkhof, H., and Loder, J.W. 1994. Lagrangian characterization of circulation over submarine banks with application to the outer Gulf of Maine. J. Phys. Oceanogr. **24**: 1184–1200.

Sameoto, D.D., and Herman, A.W. 1990. Life cycle and distribution of *Calanus finmarchicus* in deep basins on the Nova Scotia shelf and seasonal changes in *Calanus* spp. Mar. Ecol. Prog. Ser. **66**: 225–237.

Schlitz, R.J., and Cohen, E.B. 1984. A nitrogen budget for the Gulf of Maine and Georges Bank. Biol. Oceanogr. **3**: 203–222.

Shackell, N.L., Frank, K.T., Petrie, B., Brickman, D., and Shore, J.A. 2000. Dispersal of haddock (*Melanogrammus aeglefinus*) during early life history inferred from the spatial distribution and variability in length-at-age of juveniles. Can. J. Fish. Aquat. Sci. **56**: 2350–2361.

Smith, P.C. 1989. Circulation and dispersion on Browns Bank. Can. J. Fish. Aquat. Sci. **46**: 539–559.

Smith, P.C., and Petrie, B.D. 1982. Low-frequency circulation on the edge of the Scotian Shelf. J. Phys. Oceanogr. **12**: 28–46.

Smith, P.C., Houghton, R.W., Fairbanks, R.G., and Mountain, D.G. 2000. Interannual variability of boundary fluxes and water mass properties in the Gulf of Maine and on Georges Bank: 1993–97. Deep-Sea Res. Part II Top. Stud. Oceanogr. In press.

Suthers, I.M., Frank, K.T., and Campana, S.E. 1989. Spatial comparison of recent growth in postlarval Atlantic Cod (*Gadus morhua*) off southwestern Nova Scotia: inferior growth in a presumed nursery area. Can. J. Fish. Aquat. Sci. **46**: 113–124.

Werner, F.E., Page, F.H., Lynch, D.R., Loder, J.W., Lough, R.G., Perry, R.I., Greenberg, D.G., and Sinclair, M.M. 1993. Influence of mean advection and simple behavior on the distribution of cod and haddock early life stages on Georges Bank. Fish. Oceanogr. **2**: 43–64.

Wiebe, P., and Beardsley, R.C. 1996. Physical-biological interaction on Georges Banks and its environs. Deep-Sea Res. Part II Top. Stud. Oceanogr. **43**: 1437–1438.

The drift–retention dichotomy on Browns Bank: a model study of interannual variability

Charles G. Hannah, Jennifer A. Shore, and John W. Loder

Abstract: Interannual variability in drift and retention in the Browns Bank region in spring was investigated by tracking particles in numerical-model estimates of the seasonal mean circulation and monthly mean flow anomalies computed using wind and sea-level data. The circulation changes associated with the variable forcing tend to reinforce either drift to the Bay of Fundy or retention in the vicinity of Browns Bank. Regular spring spawning can lead to widely different distributions of 1-month-old larvae, supporting the concept of a drift–retention dichotomy for Atlantic cod (*Gadus morhua*) and haddock (*Melanogrammus aeglefinus*) larvae in the region. Analysis of interannual variability indicates that retention has bounded properties that must be accounted for when relating retention variability to forcing indices. As well, the nonlinearities associated with calculating particle trajectories from velocity fields contribute about 10% of the variance in retention indices. Comparison with biologically based indices of haddock survival indicates that circulation variability alone is not the dominant influence on survival to ages 1 and 2 years. However, it can be expected to have a significant influence in conjunction with biological factors such as the location and timing of peak spawning and the variable vertical position of eggs and larvae.

Résumé : Nous avons étudié la variabilité inter-annuelle de la dérive et de la rétention au printemps dans la région du banc Browns, en faisant le suivi de particules à l'aide d'estimations des anomalies dans la circulation saisonnière moyenne et le flux mensuel moyen provenant d'un modèle numérique basé sur les données de vent et de niveau de la mer. Les changements de circulation associés au forçage des variables tendaient à accentuer soit la dérive vers la baie de Fundy, soit la rétention dans les environs du banc. La fraye régulière du printemps peut donc résulter en des distributions très divergentes des larves de 1 mois, ce qui s'accorde avec la dichotomie entre la dérive des larves de morue (*Gadus morhua*) et la rétention des larves d'aiglefin (*Melanogrammus aeglefinus*) dans la région. L'analyse de la variabilité inter-annuelle montre que la rétention possède des propriétés bornées dont il faut tenir compte lorsqu'on relie la variabilité de la rétention aux indices de forçage. De plus, l'absence de linéarité dans le calcul des trajectoires des particules à partir des champs de vitesse explique environ 10% de la variance des indices de rétention. Une comparaison avec des indices biologiques de la survie chez l'aiglefin montre que la variabilité de la circulation seule n'est pas le facteur le plus important pour la survie aux âges d'un et 2 ans. Toutefois, cette variabilité peut vraisemblablement avoir un effet significatif si elle est associée à des facteurs biologiques, tels que le site et la date de la fraye maximale, ainsi que la position verticale variable des oeufs et des larves.

[Traduit par la Rédaction]

Introduction

Physical drift and retention are important factors in various theories of marine population regulation, such as the member–vagrant and migration-triangle hypotheses (Sinclair 1988; Harden-Jones 1968; Sinclair and Page 1995). Potential consequences of variability in drift and retention include differences in food availability, ocean temperature, exposure to predators, and probability of recruitment to resident populations. However, the pronounced spatial and temporal variability in the physical and biological environment around many spawning areas complicates the effects of drift and retention and confounds their explanation.

Browns Bank on the southwestern Scotian shelf (Fig. 1) is an important spawning area for Atlantic cod (*Gadus morhua*) and haddock (*Melanogrammus aeglefinus*) populations (Hurley and Campana 1989; Brander and Hurley 1992) that were the subject of the 1983–1985 Fisheries Ecology Program (FEP), an intensive field investigation of physics–plankton–fish dynamics. Results of the study included the identification of both partial retention on Browns Bank and a preferred drift pathway towards the Bay of Fundy (Smith 1989), spatial structure in prey fields and larval growth rates (Suthers et al. 1989), and evidence in fish-larva distributions of both retention and drift influences, with differences between cod and haddock (Campana et al. 1989*a*,1989*b*). In particular, Campana et al. (1989*b*) proposed a "drift–retention dichotomy" for cod and haddock larvae involving drift and retention processes acting in concert to split the larval populations into varying portions retained in the Browns Bank spawning area or transported towards the Bay of Fundy. Further, Page and Smith (1989) pointed out the importance of

Received January 20, 2000. Accepted October 27, 2000. Published on the NRC Research Press web site on December 20, 2000. J15548

C.G. Hannah,[1] J.A. Shore, and J.W. Loder. Fisheries and Oceans Canada, Bedford Institute of Oceanography, Box 1006, Dartmouth, NS B2Y 4A2, Canada.

[1] Corresponding author (e-mail: hannahC@mar.dfo-mpo.gc.ca).

Fig. 1. Map showing location and topography of the Scotian Shelf off Atlantic Canada, with the mean circulation shown schematically. The thick line on the eastern Scotian Shelf is the model boundary; the hatched portion of the line shows the active portion of the boundary for the boundary-forced anomalies.

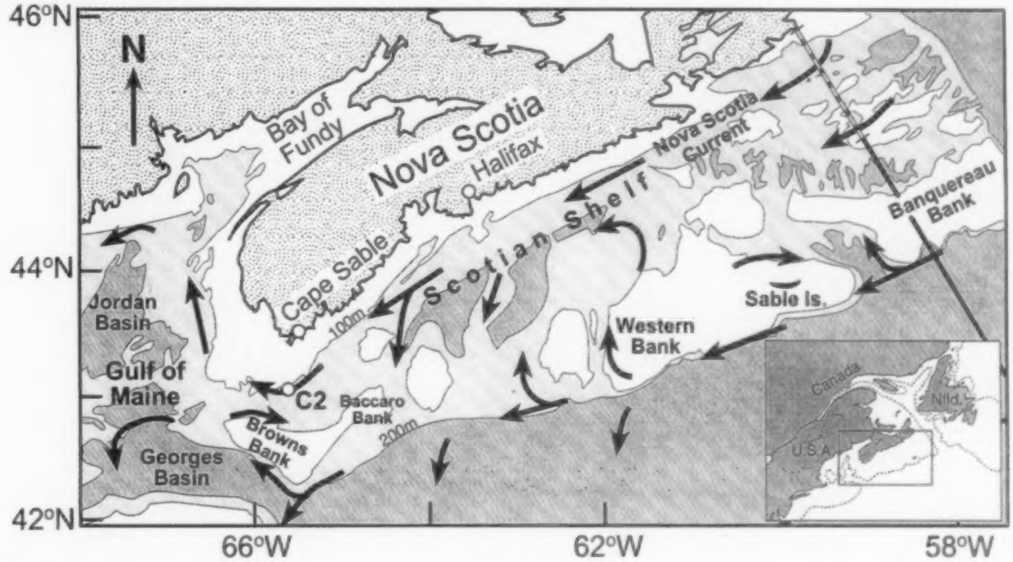

tidally rectified and wind-driven flows to variable drift in the region. However, many issues regarding the origin, variability, and implications of the partitioning in larval distributions have not been resolved.

One of the goals of the Global Ocean Ecosystem Dynamics (GLOBEC) Canada Program has been to examine further the roles of physical and biological factors in the survival and growth of gadoid early life stages on Browns Bank. Model fields for the seasonal mean circulation (Hannah et al. 2001; Shore et al. 2000) show good agreement with observations, providing a base-line representation of the Bank's partial gyre and the major drift pathway along its southwestern flank towards the Bay of Fundy. Model fields for wind-driven flow provide 3-dimensional (3D) representations of the combined effects of local forcing (surface Ekman layer) and larger scale pressure-field variations (Greenberg et al. 1997). Together with the FEP findings, the new model results indicate that the Browns Bank retention area is leaky because of its location in the equatorward throughflow on the Scotian Shelf and its small size relative to low-frequency and tidal water-parcel excursions.

A complementary component of the GLOBEC Canada program has been the development (Shackell et al. 2000) of a biologically based retention–survival index for early life stages of haddock on Browns Bank, based on length-at-age 2 (years) frequency distributions for each year class from 1968 to 1993. In some years, length-at-age values show a distinct bimodal distribution that was interpreted as representing a mixture of haddock which were retained on Browns Bank and grew slowly during early life, and others which were advected to the Bay of Fundy and grew more rapidly. This interpretation is based on the observations that there is little haddock spawning in the Bay of Fundy, and that juvenile haddock sampled there in July are generally larger than those found on the southwestern Scotian Shelf because of higher growth rates (Hurley et al. 1997). Two intriguing suggestions from Shackell et al.'s (2000) analysis are that (1) while haddock in the Bay of Fundy have higher growth rates, survival to age 1 is greater in years when there is increased retention on the offshore shelf; and (2) retention of early life stages in the lower growth offshore region is the most common condition, whereas the climatological circulation indicates a greater tendency for drift away from Browns Bank than for retention (Shore et al. 2000). These apparent discrepancies point to the need for further investigations of drift and retention in the region, and their implications for fish survival and recruitment.

We investigate interannual variability in drift and retention on the southwestern Scotian Shelf, using particle tracking in composite model flow fields that capture the salient features of spatial structure and temporal variability in the regional circulation. Our goals are to provide estimates of interannual variability in retention and drift in the region, explore their relation to biologically based retention and survival indices, and illustrate aspects of the complexity of the retention concept from a physical perspective. We examine interannual variability in wind-driven flow and throughflow using observational data from 1975–1990 and the extent to which variability in drift and retention indices in a simplified (but nonlinear) physical system can be predicted from forcing indices and velocity observations. This provides background to more realistic model evaluations of the evolution of early life stages of haddock on Browns Bank that involve both biological and physical factors (Brickman and Frank 2000; Brickman et al. 2000).

Methods

Circulation and drift were simulated for the individual months April and May from 1975 to 1990. These months were chosen

Fig. 2. The particle-release areas on Browns Bank east (E) and west (W) and the particle-counting zones on the Scotian Shelf (SS) and Bay of Fundy (BoF). The Browns Bank particle-counting zone is the union of the east and west release areas.

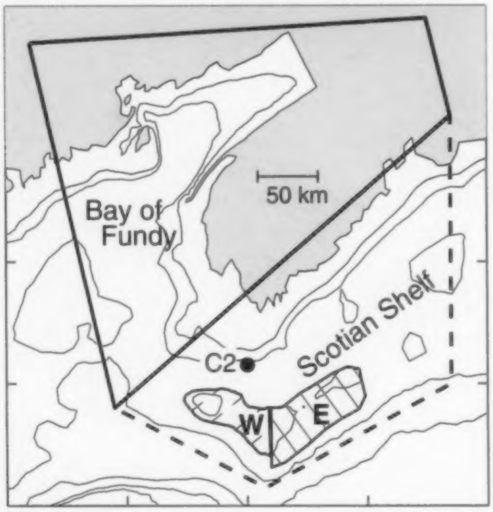

Fig. 3. (*a*) The empirical vertical viscosity profile for the surface Ekman layer, based on Madsen (1977) and others. (*b*) The velocity profile for a 0.1-Pa wind stress towards the north (the solid line shows eastward velocity and the broken line shows northward velocity).

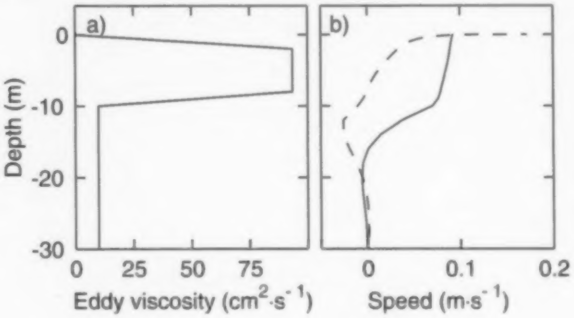

because peak haddock spawning occurs in spring (Hurley and Campana 1989) and the general decline in wind strength from April to May provides a contrast in forcing. During each month, particles were tracked in velocity fields representing flow in the surface Ekman layer (the vertical average of the upper 5 m; "U5" or "near-surface") and the velocity field at 20 m representing the flow below the Ekman layer. These vertical levels approximate the basic modes in Frank et al.'s (1989) observations in which early egg stages were concentrated in the near-surface layer and later egg stages and larvae were concentrated below it. Two adjoining release areas were used (Fig. 2), one covering the western portion of Browns Bank ("west"), which is believed to be the primary haddock spawning area (Shackell et al. 2000), and the other covering the outer-shelf portions of Browns and Baccaro banks ("east"), where important spawning also occurs (Hurley and Campana 1989).

Flow fields

The estimated mean flow field ($\mathbf{v}_T$) for a given month (e.g., April 1982) comprises a linear combination of 4 components: the seasonal mean circulation ($\mathbf{v}_m$) and the responses to the along-shelf (τ_A) and cross-shelf (τ_C) monthly wind-stress anomalies and to anomalous monthly forcing at the upstream boundary (ς_B). This can be written as

$$(1) \qquad \mathbf{v}_T = \mathbf{v}_m + \mathbf{v}_a \, \tau_A/\tau_a + \mathbf{v}_c \, \tau_C/\tau_c + \mathbf{v}_b \, \varsigma_B/\varsigma_b$$

where $\mathbf{v}_a$ is the velocity response to a reference along-shelf wind stress (τ_a), $\mathbf{v}_c$ is the response to a reference cross-shelf wind stress (τ_c), $\mathbf{v}_b$ is the response to a reference upstream boundary forcing with coastal amplitude, ς_b. These flow components were computed on a model domain extending from the eastern Scotian Shelf (Fig. 1) to the western Gulf of Maine and offshore into the slope region.

The seasonal mean component, the spring field described in Hannah et al. (2001) and Shore et al. (2000), is constant across months and years. It was computed with a 3D prognostic advanced-turbulence model (Lynch et al. 1996), initialized, and forced with observational data on M_2 tides, and on seasonal mean density gradients and wind stress. The flow field is in good quantitative agreement with the seasonal mean currents from moored measurements at 46 (3D) positions on the southwestern Scotian Shelf, the kinetic energy of the difference field being only 37% of that of the observed currents. The field at 10 m is also in approximate agreement with the spring velocity pattern on Browns Bank estimated from a small drifter data set (Smith 1989), but there are differences along the northern edge and north of the Bank (Shore et al. 2000).

The year-to-year variability comes from the wind- and boundary-forced components. The wind-forced component is based on monthly anomalies of Sable Island wind stress, computed by subtracting the long-term April–May mean stress (0.0194 Pa at 100°T (degrees True), which was included in the seasonal mean forcing) from each monthly mean. The responses to the along- and cross-shelf anomalies were calculated using a linear 3D barotropic model (Lynch et al. 1992; Greenberg et al. 1997) with specified vertical eddy viscosities and bottom friction coefficients. The latter were taken as the time-averaged coefficients from the seasonal mean solution plus the additional bottom friction due to $0.1 \ \mathrm{m \cdot s^{-1}}$ of unmodelled flow.

The specified vertical eddy viscosities were a combination of those derived from the seasonal mean solution and an empirical upper-ocean profile. The empirical eddy–viscosity profile (Fig. 3*a*), which is based on the work of Madsen (1977), Csanady (1984), and Craig et al. (1993), provides a high (vertical) resolution representation of some of the effects of processes such as storm-band mixed-layer dynamics and surface waves that are not present in the seasonal mean solution. In the upper 2 m, the viscosity is defined as $\nu = -\kappa u_* z$, where the friction velocity, $u_* = 0.012 \ \mathrm{m \cdot s^{-1}}$, is computed using the rms (root mean squared) wind stress for April and May (0.14 Pa; from hourly estimates), $\kappa = 0.4$ is the von Karman constant, and z is the vertical coordinate, positive upwards with origin at the sea surface. The viscosity is taken to be constant at $\nu = 0.0094 \ \mathrm{m^2 \cdot s^{-1}}$ for $z = -2$ to -8 m (approximating the results in Csanady 1976) and to decrease linearly to a background value of $\nu = 0.001 \ \mathrm{m^2 \cdot s^{-1}}$ at $z = -10$ m.

To resolve the near-surface velocity structure, additional vertical nodes were added to the linear model (yielding 6 in the upper 1 m and 5 in the next 5 m). The wind-driven velocity profile (Ekman-layer response) derived from the empirical profile is shown in Fig. 3*b*. Flow is largely at a 90° angle to the right of the wind stress in the upper 10 m, with enhanced downwind drift in the upper 1 m and Ekman spiral effects penetrating to 30 m, providing a reasonable representation of near-surface wind-forced current structure under typical conditions. In locations where the seasonal mean

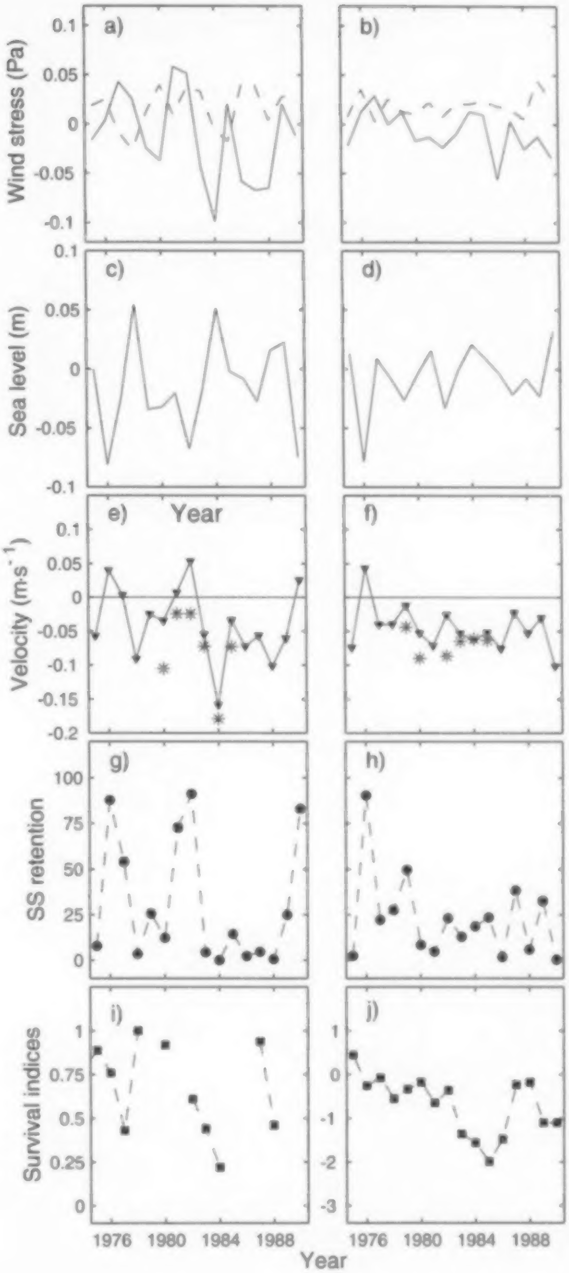

Fig. 4. (*a* and *b*) Monthly wind-stress anomalies for April and May, respectively; the solid lines are the along-shelf anomalies (positive northeastward) and the broken lines are the cross-shelf anomalies (positive northwestward). (*c* and *d*) Monthly boundary-forcing anomaly for April and May, respectively. The wind-stress anomalies are with respect to the April–May mean of 0.0194 Pa at 100°T. The boundary anomalies are with respect to the monthly means for the period 1970–1993. (*e* and *f*) Monthly mean eastward component of the near-surface currents at C2 for April and May, respectively. The observed currents (*) are between 15 and 30 m below the surface and the modelled currents (solid line with solid triangles) are 20 m below the surface. (*g*–*j*) Retention indices for Browns Bank; *g* and *h* are the Scotian Shelf (SS) retention indices for the west release for April and May, respectively, computed as the average of the near-surface and 20 m depth results; *i* and *j* are the retention–survival and survival indices, respectively, from Shackell et al. (2000).

solution gives viscosities greater than the empirical profile, the latter is used for $z \geq -1$ m and the profile makes a smooth transition to the eddy viscosities from the seasonal mean solution (with a minimum value of $\nu = 0.001\ \mathrm{m^2 \cdot s^{-1}}$ imposed for $z \leq -1$ m).

For calculating the wind-forced anomaly, the reference along-shelf and cross-shelf wind stress in (1) was 0.1 Pa at 56°T and 0.1 Pa at 326°T, respectively. The elevations were clamped at zero along the upstream and offshore boundary; thus, any non-zero interior elevations are due to the wind forcing over the model domain. The response patterns are similar to those described in Greenberg et al. (1997).

The boundary-forced component is based on the monthly mean adjusted sea level (ASL) at Halifax. An anomaly time series for April was computed by subtracting the average April ASL for 1970–1993 from the April time series. Then for each April, the component (ζ_{Hw}) of ASL due to the anomalous wind stress over the model domain was computed from

$$(2) \qquad \zeta_{Hw} = \zeta_{Ha}\ \tau_A\ /\ \tau_a + \zeta_{Hc}\ \tau_C\ /\ \tau_c$$

where ζ_{Ha} and ζ_{Hc} are the model elevation responses at Halifax due to the reference along-shelf and cross-shelf wind stresses, respectively; ζ_{Hw} was then subtracted from the Halifax ASL anomaly to yield the de-winded ASL anomaly (that component due to forcing from outside the model domain). A similar calculation was done for May. This approach assumes that the Halifax elevation associated with the seasonal mean circulation field is a good approximation of the long-term average ASL for April and May.

The velocity response to boundary forcing was calculated using the same linear model, bottom friction coefficients, and vertical eddy viscosities used for the wind response. The upstream boundary forcing was specified as a linear decrease in elevation from the coast to midshelf (Fig. 1), with the rest of the upstream and offshore boundary clamped to zero. The boundary-forcing anomaly ζ_B was chosen to give an elevation magnitude at Halifax that matched the de-winded ASL anomaly.

The time series of anomalous wind stress (τ_A, τ_C) and boundary (ζ_B) forcing are shown in Fig. 4. Both the stress and boundary anomalies are generally largest in April, with peak stress anomalies that are an order of magnitude larger than the long-term seasonal average, and ASL anomalies that are of comparable magnitude to the seasonal range.

In addition to the monthly mean flow fields, the M_2 tidal currents (the most energetic current component in the region) from the prognostic model (Hannah et al. 2001) were included in the simulations. The Stokes drift (the difference between mean velocity measured at a point and mean velocity of a drifter) associated with large spatial variations in the tidal currents across the edges of banks can make important contributions to residual drift (e.g., Loder 1980; Page and Smith 1989; Ridderinkhof and Loder 1994).

Particle tracking

Particles were tracked in the monthly mean ($\mathbf{v}_T$) and tidal (M_2) velocity fields using a fourth-order Runge–Kutta method (Werner et al. 1993) and a time step $\Delta t = 357.7$ s. Additional random horizontal kicks were added that correspond to a horizontal eddy diffusivity of 50 $\mathrm{m^2 \cdot s^{-1}}$, comparable to that estimated by Smith

(1989) from drifter measurements. These random kicks approximate the effects of unmodelled motions such as eddies and storm-driven currents. Nevertheless, the flow fields and particle trajectories are only an approximation of reality because the spatial and temporal structures of such motions and their influence on vertical mixing are not fully represented.

In total, 128 different particle-tracking experiments of 30 days' duration were conducted: 16 years, 2 months per year, two vertical levels per month, and two release areas per level. The west and east release areas (Fig. 2) had 2737 and 4501 particles, respectively, spaced at 850-m intervals. To describe the overall spatial pattern of particle dispersal, the particles were counted at the end of each simulation using a regular 50 × 50 km grid covering the entire domain. Interannual variability in retention and drift was quantified using retention and drift indices computed as the percentage of total particles in specified zones after 30 days in each simulation. Particles were fixed at one of the vertical levels to examine sensitivity extremes in physical retention and drift.

Results

Circulation variability

The basic flow fields used to construct the monthly mean circulation fields are shown in Fig. 5. The forcing magnitudes of the wind- and boundary-forced components were chosen to represent very large positive anomalies (Fig. 4) in order to illustrate the spatial structure. Note that negative anomalies simply reverse the directions of the flows, owing to linearity.

The primary features in the seasonal mean fields (Figs. 5*a*, 5*e*) are strong northwestward and northward velocities along the southwestern side of Browns Bank and extending northwards to the mouth of the Bay of Fundy; a southwestward flow on the western Scotian Shelf with a small nearshore branch following the 100-m isobath around Cape Sable and a large branch going to the shelf break and then along the southwestern side of Browns Bank; some eastward flow on the northern flank of Browns; and only small differences between the near-surface and 20-m levels. The circulation associated with upstream inflow (positive ASL anomaly; Fig. 5*d*) shows similarity to the seasonal mean in having a southwestward flow on the inner and outer Scotian Shelf, a northward flow towards the Bay of Fundy, and little vertical structure. However, it differs from the seasonal mean in being weak along the western side of Browns Bank, with the flow towards the Bay of Fundy primarily supplied from the inner Scotian Shelf.

The wind-forced components (Figs. 5*b*, 5*c*, 5*f*) differ from the others in that they introduce substantial vertical structure associated with the surface Ekman layer. Northeastward along-shelf wind stress gives rise to a generally southeastward near-surface flow (i.e., 90° to the right of the stress direction), modified in some areas by the associated barotropic pressure-field response. At 20 m, the pressure-field contribution dominates the wind-forced component, and primarily involves flow on the inner shelf around Cape Sable (and on-shelf flow in the Northeast Channel) supplying the Ekman divergence on the Scotian Shelf. Similarly, northwestward cross-shelf wind stress gives rise to a generally northeastward near-surface flow, but in this case there is only a weak pressure-field response.

Fig. 5. The current components used to construct the monthly mean flow fields: the near-surface currents (upper 5 m) off southwestern Nova Scotia for the seasonal mean solution (*a*); the along-shelf wind solution for $\tau_A = 0.1$ Pa (*b*); the cross-shelf wind solution for $\tau_C = 0.1$ Pa (*c*); and the boundary-forced solution for $\zeta_B = 0.1$ m (*d*). (*e* and *f*) The 20-m currents for the seasonal mean solution and the along-shelf wind solution for $\tau_A = 0.1$ Pa, respectively. The cross-shelf wind solution at 20 m (not shown) is small, and the boundary-forced solution is very similar to the near-surface solution (*d*).

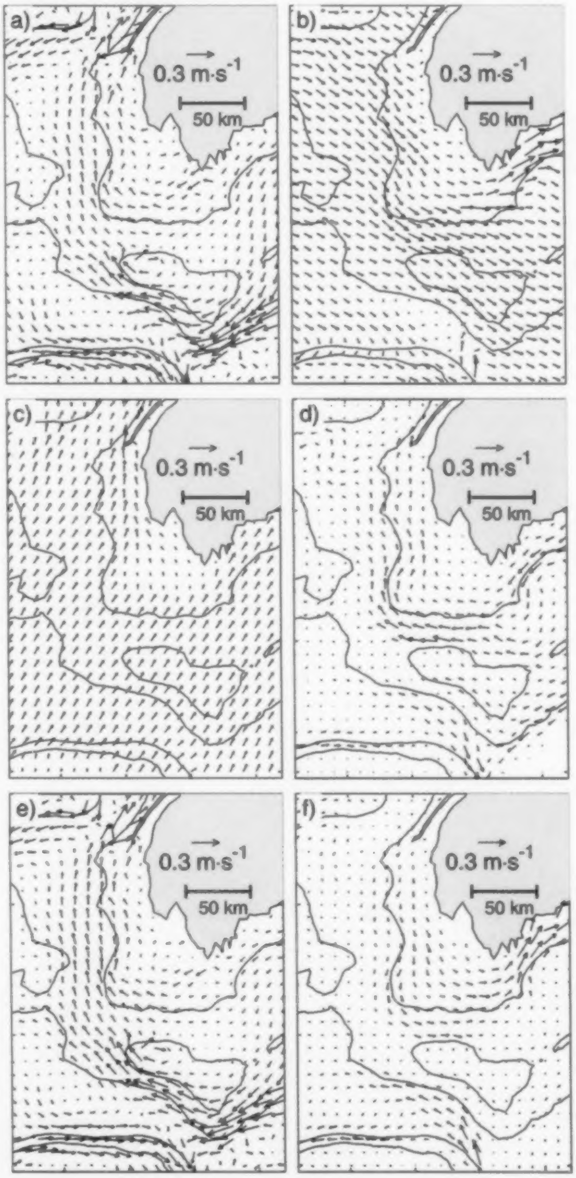

At both levels, along-shelf stress and boundary-forcing anomalies provide the potential to either offset or reinforce key pathways in the seasonal mean flow, particularly the

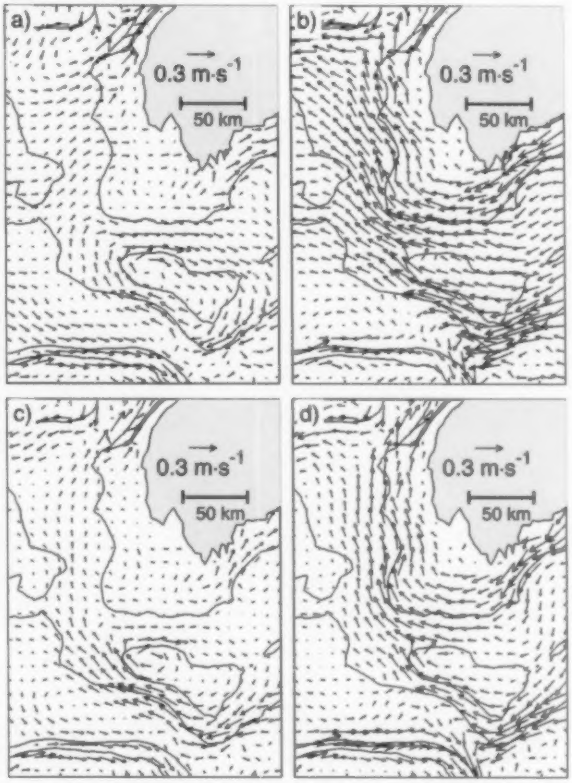

Fig. 6. Near-surface (*a* and *b*) and 20-m (*c* and *d*) currents off southwestern Nova Scotia for April 1982 (*a* and *c*) and April 1984 (*b* and *d*).

westward drift on the inner shelf off Cape Sable and the northward drift towards the Bay of Fundy. The effect should be largest in the near-surface layer, where the Ekman transport and pressure-field contributions can be reinforcing, but could also be important below the Ekman layer, especially when along-shelf stress and boundary-forcing anomalies have opposite signs.

The most extreme events in the anomaly forcing occur in April 1982, when the along-shelf stress anomaly is strongly positive (northeastward) and the boundary-forcing anomaly is strongly negative (coastal set-down), and in April 1984, when the opposite occurs. In April 1982, the wind- and boundary-forcing components dramatically change the circulation pattern at both depths (Figs. 6*a*, 6*c*). The northward flow off western Nova Scotia has been eliminated in the near-surface and substantially reduced at 20 m, and there is a broad gyre around Browns Bank. This expanded gyre, with contributions from tidal rectification, density gradients, and wind and boundary forcing, contrasts with the small topographic-scale gyre due to tidal and density forcing in the seasonal-mean flow. In April 1984, the anomalous forcings largely reinforce the seasonal mean, and there is enhanced throughflow in the region, with only a small recirculation area on the cap of Browns Bank (Figs. 6*b*, 6*d*).

Examples of the 30-day particle distributions that result from the different circulation fields are shown in Fig. 7. For the near-surface seasonal-mean flow (Figs. 7*a*, 7*b*), the west-release particles are spread out between Browns Bank and the Bay of Fundy, with some turning west around Georges Basin and some remaining on Browns Bank. The case of the east release is similar, but there are almost no particles remaining near Browns Bank because the release grid lies on the main artery of the seasonal mean flow, which sweeps the particles around Browns Bank into the Gulf of Maine. These particles tend to move into the Gulf in deeper water than those from the west release, but many eventually move towards the Bay of Fundy.

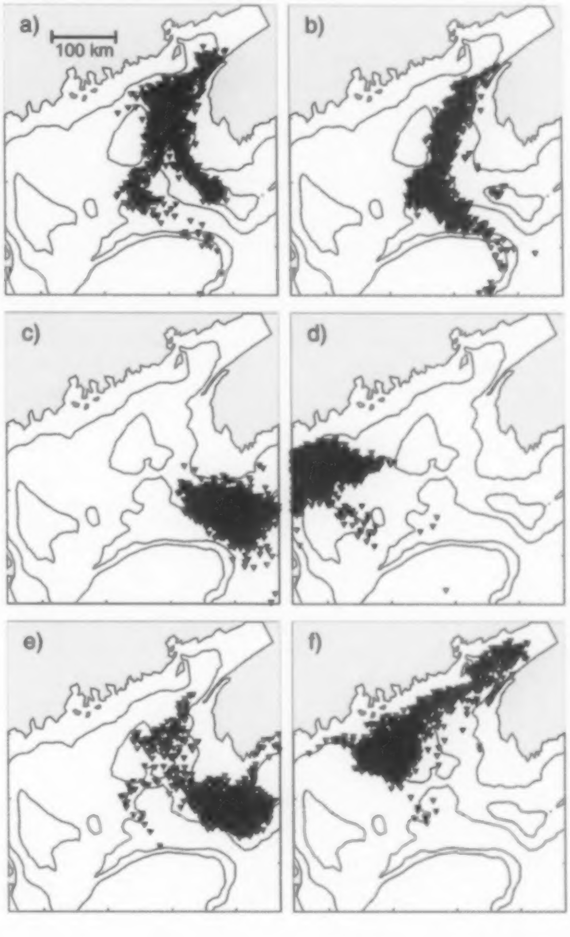

Fig. 7. Particle distributions after 30 days for the west release with the near-surface seasonal mean currents (*a*), the east release with the near-surface seasonal mean currents (*b*), the west release with the April 1982 near-surface currents (*c*), the west release with the April 1984 near-surface currents (*d*), the west release with the April 1982 20-m currents (*e*), and the west release with the April 1984 20-m currents (*f*). For clarity, only 50% of particles are shown.

Figures 7*c* and 7*d* show the dramatic difference in particle distributions for the near-surface flows in April of 1982 and 1984. In April 1982 most particles are retained near Browns Bank in the expanded gyre, while in April 1984 all particles are swept to the western Gulf of Maine. The effects of the extreme wind events are not as great at 20 m (Figs. 7*e*, 7*f*), and the particle distributions are generally intermediate between the individual year and seasonal mean distributions for the near-surface cases.

Validation of interannual variability in the modelled circulation is difficult because of the paucity of multiyear current-meter observations. We focus on site C2 (Smith 1989) on the 110-m isobath south of Cape Sable (Fig. 1), where 6 years of data are available for each of April and May. The modelled and observed monthly mean currents at 20 m at site C2 are compared in Figs. 4*e* and 4*f*. Both the model and observations show much more year-to-year variability in April than in May, which is consistent with the larger forcing anomalies. The time series shows very good agreement for 1983–1985 but poorer agreement for 1979–1982. In particular, the largest westward current anomaly was observed in April 1984, with magnitude in agreement with the model prediction, while April 1982 was one of two months with the largest eastward anomaly, although it was smaller than predicted. It is not clear whether the discrepancies in 1979–1982 reflect a spatial shift in the currents or a broader scale deficiency in the model fields associated with interannual variability in baroclinic circulation or with the estimation of the forcing anomalies.

Composite particle distributions

Composite monthly particle distributions were created by combining individual-month results over all years for each of the two release grids (Fig. 8). Overall, most of the particles end up in the northeastern Gulf of Maine (approaching the mouth of the Bay of Fundy) after 30 days. This is similar to the distributions computed using only the seasonal mean circulation (Figs. 7*a*, 7*b*), although there is broad scatter and sensitivity to depth, month, and release location. The April and near-surface composites show the most scatter, which reflects the importance of temporal variability in the circulation to overall larval dispersal. There is also increased overall retention on Browns Bank (especially for the near-surface west releases) associated with the expanded gyre in some years.

Most of the near-surface particles for the April east release (Fig. 8*e*) are found in the northeastern Gulf, but some have drifted off-shelf south of Georges Bank. Near-surface particles from the west release have spread over a large area of the Gulf, with maximum concentrations on the cap of Browns Bank and in the Gulf's northern coastal region (Figs. 8*a*, 8*b*). The reduced year-to-year variability in the May currents (compared with April) results in tighter distributions with larger peaks. For example, the near-surface April west release shows two peaks surrounded by a large region of low particle concentration, whereas the May release shows the same peak on Browns Bank but tighter clustering of particles in the northeastern Gulf (Figs. 8*a*, 8*b*).

The 20-m east releases (April and May) show most of the particles clustered together between western Nova Scotia and Jordan Basin, with relatively few in the Browns Bank region. On the other hand, the 20-m April west release shows that upwards of 15% remain on the Bank after 30 days. For the 20-m May west release, upwards of 25% remain on Browns Bank, while the rest have spread into the

Fig. 8. Particle-concentration maps for the composite of the simulations over the period 1975–1990. The symbols represent the percentages of the total number released that were in each 50 × 50 km cell: ◆, >15%; ▼, 10–15%; ●, 5–10%; •, 1–5%. (*a*) April west 0–5 m. (*b*) May west 0–5 m. (*c*) April west 20 m. (*d*) May west 20 m. (*e*) April east 0–5 m. (*f*) May east 0–5 m. (*g*) April east 20 m. (*h*) May east 20 m.

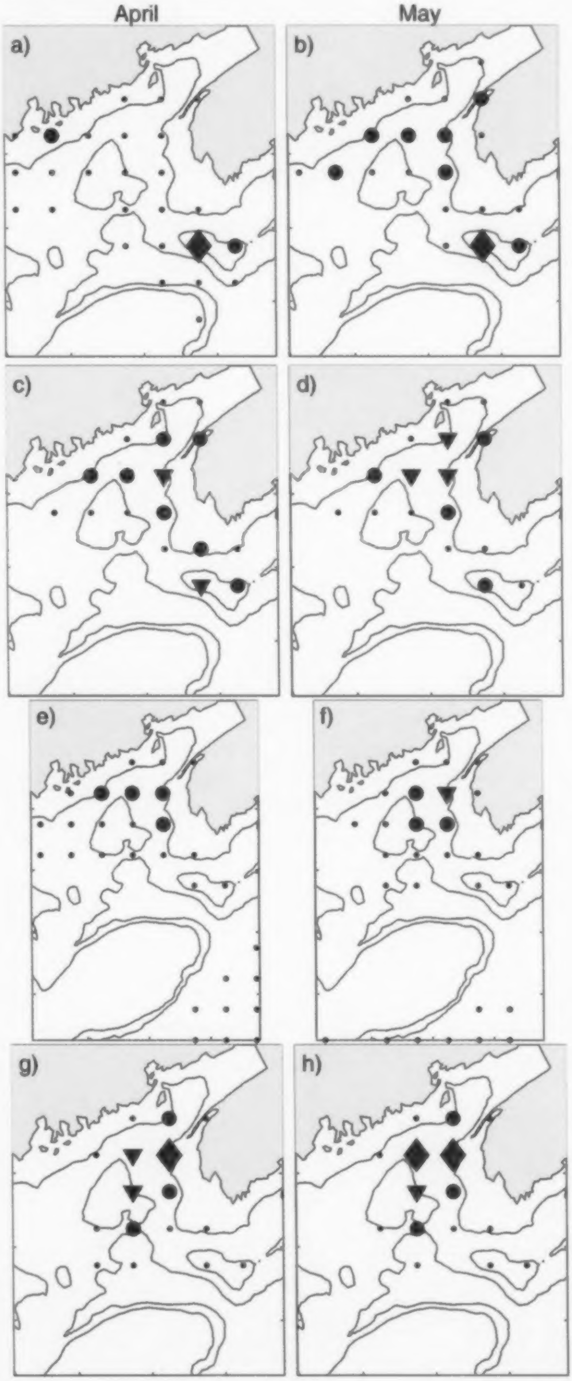

Fig. 9. Interannual variability in particle retention in the Scotian Shelf zone (solid bars) and drift into the Bay of Fundy zone (open bars). (*a*) April west 0–5 m. (*b*) May west 0–5 m. (*c*) April west 20 m. (*d*) May west 20 m. (*e*) April east 0–5 m. (*f*) May east 0–5 m. (*g*) April east 20 m. (*h*) May east 20 m.

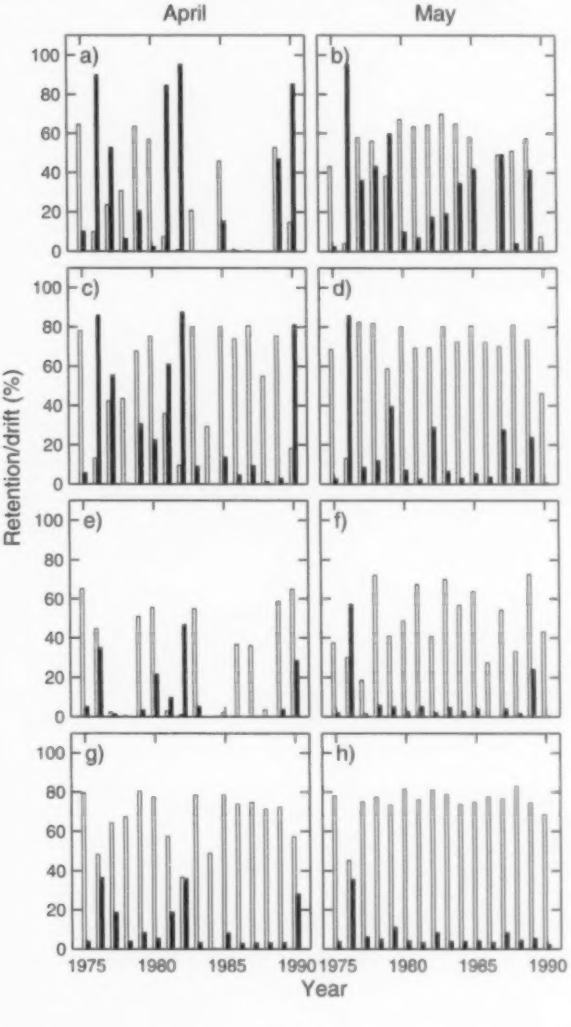

northeastern Gulf of Maine or have crossed the Northeast Channel heading southwestward out of the domain. For both release grids the April and May 20-m distributions are similar, the east release resulting in a large concentration near the mouth of the Bay of Fundy and the west release showing two peaks in concentration (near the mouth of the Bay of Fundy and on Browns Bank). However, the east-release distributions are shifted into deeper water in the northeastern Gulf.

The west-release results reflect known drift behaviour around Browns Bank. Smith (1989) and Loder et al. (1988) computed average residence times of 14 days (± 9 days (SD)) for drifters drogued at 10 m and released on the Bank's cap during May–October (1983–1985), and 5 (± 4) days for releases in April and November. Model experiments in the seasonal mean circulation indicate that about 70% of the particles released at 10 m on the west grid leave within 5–25 days depending on season and background diffusivity, which is consistent with the observational estimates (Shore et al. 2000). Some near-surface particles from the west grid cross the Northeast Channel to the eastern flank of Georges Bank, which is consistent with the pathways identified in the seasonal mean circulation by Shore et al. (2000).

Retention and drift indices

To quantify interannual variability in drift and retention, we computed the percentage of particles in three zones after 30 days (Fig. 2). Two of the zones, the Scotian Shelf polygon (SS) and the Browns Bank polygon (BB), include the release grids, so percentages can be interpreted as retention indices. BB corresponds to the primary haddock spawning area (the union of the west and east release areas) and SS corresponds to the broader offshore shelf region (groundfish survey strata), for which Shackell et al. (2000) infer that higher retention leads to higher survival. The Bay of Fundy (BoF) zone corresponds to the region (survey strata) with higher growth rates for juvenile, and possibly larval, haddock. It is located away from the release areas, so we refer to its particle percentages as drift indices.

The retention indices (Fig. 9) show large year-to-year variability for SS, with greater retention for the west releases than for the east releases (cf. Fig. 8). The April near-surface releases show large variability in the number of particles delivered to BoF but the other releases show much weaker variability. The May releases at 20 m show almost constant delivery of particles to BoF, which is consistent with the 20-m composite particle-concentration maps (Fig. 8), which show a narrow distribution of particles between Browns Bank and the Bay of Fundy. In many of the near-surface cases the sum of particle concentrations for SS and BoF is less than 100%, since some particles go elsewhere (e.g., 1984). In the composite distributions, this shows up in the broad distribution of the low percentages. Retention in BB is generally less than in SS but has the same overall features.

The circulation fields suggest that retention of particles in the vicinity of Browns Bank should be increased for both positive τ_A anomalies and negative ζ_B anomalies because they both induce circulation that reduces the (northward) seasonal mean flow from Browns Bank to the Bay of Fundy. Table 1 shows the linear correlations between various measures of retention in the vicinity of Browns Bank and the forcing functions. In each case the retention values for April and May have been grouped together in order to look for a general relationship between retention measures and forcing indices. The results generally show highly significant ($p < 0.05$) correlations between retention values and both τ_A and ζ_B (with opposite signs, as expected) and poor correlations with τ_C. Of the forcing functions, ζ_B is the best overall predictor of retention. The correlations for BB, the smaller retention zone, are generally weaker than for SS, but not dramatically so. This indicates that for this system, the 30-day retention variability in the vicinity of Browns Bank is not a strong function of retention-zone size.

Table 1 also shows that the retention indices for SS and BB are significantly correlated with the eastward currents at C2 (C2U) in the model ($r \geq 0.67$, $p < 0.05$). This is due to

Table 1. Linear correlations (r) between retention measures and other indices, with April and May grouped together.

	τ_A	τ_C	ζ_B	C2U
SS west U5	0.69*	0.22	–0.67*	0.87*
SS west 20 m	0.48*	0.22	–0.86*	0.90*
SS east U5	0.31†	0.49*	–0.76*	0.67*
SS east 20 m	0.50*	0.19	–0.81*	0.87*
BB west U5	0.69*	0.15	–0.63*	0.83*
BB west 20 m	0.40*	0.29	–0.87*	0.87*
BB east U5	0.35†	0.41*	–0.74*	0.68*
BB east 20 m	0.43*	0.23	–0.82*	0.84*

Note: The name of each retention measure contains the retention zone (Scotian Shelf, SS) or Browns Bank (BB)), the release grid (east or west), and the flow field (near-surface (U5) or 20 m). The forcing indices are the along- and cross-shelf wind-stress anomalies (τ_A and τ_C), the boundary-forcing anomaly (ζ_B), and the model eastward velocity at mooring location C2 (C2U). *, correlation is significant at the 0.05 level (two-tailed); †, correlation is significant at the 0.1 level (two-tailed); df = 30.

Fig. 10. Particle retention in the Scotian Shelf zone (zone SS) for the near-surface west release as a function of eastward model currents at C2. April (×) and May (○) are indicated but the solid line is the best fit ($r^2 = 0.77$) for the two months together. The broken line is the best fit ($r^2 = 0.84$) through the data points in the linear regime described in the text.

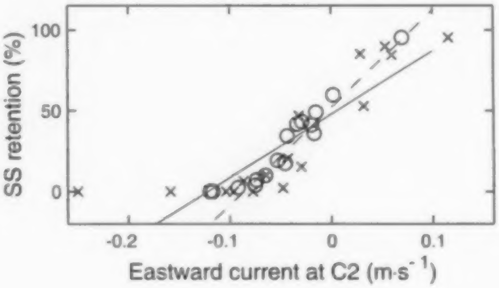

C2's location on the main artery of the flows induced by τ_A and ζ_B. Large retention values generally correspond to eastward (positive) or slightly westward currents at C2, and zero retention often corresponds to large westward (negative) currents (Fig. 10). Figure 10 shows that the linear relationship between retention (SS west U5) and C2U is good but breaks down for strong westward currents. This breakdown is an example of the nonlinearity associated with retention being a bounded function; extremes in forcing cannot reduce retention below 0% or increase it above 100%. In Fig. 10, the linear region is roughly $-0.1 < \mathrm{C2U} < 0.1\ \mathrm{m \cdot s^{-1}}$.

To determine how much of the variability in retention in this system can be predicted by linear functions of the forcing anomalies, we conducted a multiple (linear) regression analysis (Table 2). To account for the boundedness of retention, C2U was used to determine the linear regime for each retention time series. Mean retention was computed for $0.02\ \mathrm{m \cdot s^{-1}}$ bins of C2U and the data points were retained for analysis if they fell in a bin with mean retention in the range 1–95% (the retention thresholds). The number of samples removed in each case was small, between 1 and 8. For example, in Fig. 10 (SS west U5) the five points with C2U < $-0.1\ \mathrm{m \cdot s^{-1}}$ were removed, as were the two points with C2U $\geq 0.07\ \mathrm{m \cdot s^{-1}}$. Removing these seven points increases the r^2 value of the correlation with C2U from 0.77 to 0.84.

Table 2 shows that when all the data are used, 60–84% of the variance in retention is linearly related to the forcing anomalies. When the analysis is repeated for the linear regime, the explained variance (r^2) increases to 78–97%. The bounded properties of retention account for 5–27% of the variance, which is generally more than 50% of the unexplained variance in the "all data" regression model. The r^2 value for each case of BB retention is less than for the respective SS case, and the effects of zone size are largest for the near-surface cases using the linear regime.

Cross-shelf wind stress (τ_C) is poorly correlated with retention (Table 1), and its contribution to the regression models is limited to the two cases with a significant linear correlation (SS/BB east U5). The generally good correlations with τ_A imply dependence on wind-stress direction, which results in weak correlations between retention and the magnitude of the wind-stress anomaly ($|\tau|$), generally with $|r| < 0.2$ and $p > 0.1$. There is one marginally significant correlation between BB west U5 retention and $|\tau|$ ($r = -0.29$, $p = 0.1$), which is consistent with Shackell et al.'s (2000) finding that survival and wind-stress magnitude are negatively correlated. However, this correlation disappears when the analysis is restricted to the linear regime. There is also a negative correlation ($r = -0.46$, $p < 0.05$) between wind-stress magnitude and the residuals from the multiple regression for BB west U5 retention (linear regime), indicating that wind-stress magnitude can account for about 5% of the retention variance for this case.

Relation to biological indices

Retention–survival indices and a survival (to age 1 year) index described by Shackell et al. (2000) are shown in Figs. 4*i* and 4*j*. For comparison, the SS retention for the west releases is shown in Figs. 4*g* and 4*h*. The correlation between the biological indices and the various model-based retention indices is very weak in all cases ($|r| < 0.28$, $p > 0.1$, $n = 16$). The survival index is dominated by the steady decrease from 1975 to 1985, which is not present in our indices. There is also no relationship between the observed currents at C2 and the biological indices.

Discussion

Circulation and retention variability

The spatial structures of the seasonal mean and anomaly currents provide basic explanations for most of the features of the retention time series shown in Fig. 9. Consider the east release at 20 m, which exhibits almost constant delivery of particles to BoF. The drift pathway in the seasonal-mean flow follows the core of strong currents between the 100- and 200-m isobaths from the release site to the entrance to the Bay of Fundy and is only weakly influenced by the anomaly currents at that depth. In contrast, there is enormous variability in the transport of particles to BoF for the west near-surface releases because all the anomaly components have an influence on the primary drift pathway to the northwest of Browns Bank.

Comparison of the average retention indices with their values in the seasonal mean flow confirm that the inclusion of wind- and boundary-forced flow anomalies can result in increased overall retention in SS, in spite of broader overall scatter. Average values of retention (over all years) for the near-surface and 20-m levels increase to 20 and 15% from 10 and 6%, respectively, in the seasonal mean circulation. This reflects the significant occurrence of wind and sea-level anomalies that act in concert with the seasonal mean flow to enhance retention, such as through the expanded Browns Bank gyre. Retention percentages should not be interpreted as percentages of larvae retained, since the larger influences of predation and mortality are not included here.

The close correlation between SS retention and both the τ_A and ζ_B anomalies is due to the spatial relationship between the induced flows and the seasonal mean flow. Alongshelf wind stress towards the northeast (positive τ_A) reduces the northward mean flow from Browns Bank to the Bay of the Fundy (through an ocean pressure-field response) and reduces the westward flow off Cape Sable (through both Ekman transport and a pressure-field response). A negative sea-level anomaly has a similar effect. Extreme combinations of positive τ_A and negative ζ_B have the potential to create an expanded gyre in the Browns Bank region (e.g., April 1982). In less extreme years the combination reduces the magnitude of the currents that carry particles away from Browns Bank. For the most part, the currents that determine the magnitude of retention in SS are not the currents on Browns Bank but those in the deep water around the edges of the Bank and along the pathways from the Bank to the Bay of Fundy. For example, the circulation associated with ζ_B has no signature inside the 100-m isobath on Browns Bank but has the greatest impact on retention variability.

The currents at each point are completely determined as linear functions of the forcing terms (in the present approach), thus any unexplained variance in the linear-regression analysis of retention variability must arise from either the process of computing particle trajectories from velocity fields or the process of computing retention from particle positions. The regression analysis showed that the bounded properties of retention are important when relating retention variability to the forcing anomalies. When the bounded properties are accounted for, the unexplained variance substantially decreases: to 3 and 5% for SS and BB west 20-m cases, respectively, and to the 10–22% range for the other cases. The linear-regime analysis is crude and it is likely that some of the unexplained variance is still due to the boundedness of retention. For example, the retention thresholds could be set on a case-by-case basis.

There are also nonlinearities associated with calculating particle trajectories (or displacements) from velocity fields, the Eulerian-to-Lagrangian transformation, which is nonlinear (even for steady flows) when there is spatial structure in the velocity fields. This is why it is important to have a good representation of the spatial structure of all the flow components. There are further nonlinearities in the Eulerian-to-Lagrangian transformation associated with the interaction between spatial structure and the temporal variability provided by the tidal currents and unmodelled flows such as those associated with storm-band wind forcing. These are expected to become important as the size of the retention zone is reduced to the order of the excursion scale of the temporal perturbations (e.g., the tidal excursion). We note that the width of the western portion of BB is about 20 km, roughly two M_2 tidal excursions. The strong influence of the spatial structure in the flow components on the particle trajectories, and the greater unexplained variability in BB cases than in SS cases, suggest that the nonlinearities of the Eulerian-to-Lagrangian transformation are an important source of unexplained variance. For the present set of simulations, the maximum contribution of these nonlinearities to the retention variance is of the order of 5–20%, which places an upper bound (80–95%) on the predictability of retention based on linear functions of the forcing anomalies or velocity fields. Furthermore, Ridderinkhof and Loder (1994) showed that storm-intensity wind stress can cause chaotic motion in the Browns Bank region, which would further reduce the predictability of drift and retention from the forcing anomalies.

Table 2. Results of the multiple linear regression analysis between the retention indices and forcing anomalies.

	n	R_0	R_3	r^2
All data				
SS east U5	32	14	8.5	0.63
SS east 20 m	32	10	4.8	0.78
SS west U5	32	31	15	0.76
SS west 20 m	32	28	11	0.84
BB east U5	32	5.5	3.5	0.60
BB east 20 m	32	4.0	2.1	0.73
BB west U5	32	17	9.1	0.70
BB west 20 m	32	14	6.4	0.80
Linear regime				
SS east U5	24	15	5.5	0.87
SS east 20 m	31	10	4.2	0.83
SS west U5	25	27	8.6	0.90
SS west 20 m	28	28	5.2	0.97
BB east U5	24	6.0	2.7	0.80
BB east 20 m	31	4.0	1.9	0.78
BB west U5	27	16	7.5	0.79
BB west 20 m	28	15	3.4	0.95

Note: For each retention measure, R_0 is the rms value of the retention time series with the mean removed (%), R_3 is the rms values of the residual (%) after the contribution of three forcing anomalies (τ_A, τ_C, ζ_B) is removed, and $r^2 = 1 - (R_3/R_0)^2$ is the variance explained. The results shown under "all data" use all the data and the results under "linear regime" use the data in the linear regime as described in the text. The name of each retention measure contains the retention zone (Scotian Shelf (SS) or Browns Bank (BB)), the release grid (east or west), and the flow field (near-surface (U5) or 20 m). All regressions are significant at the 0.05 level (two-tailed).

For each release scenario the retention statistics for SS and BB have a very similar relationship with the forcing anomalies, although the smaller BB has lower overall retention. Thus, we conclude that the results (for the present flow fields) are robust to the details of the retention zone; in particular, retention in SS is not dominated by particles leaving BB but not quite leaving SS in 30 days. However, for retention zones on Browns Bank smaller than BB, the results would be expected to become sensitive to the details of the retention calculation, as well as to increased resolution of small-scale flow features. For example, a more sophisticated definition of retention would be required to account for particles repeatedly moving into and out of the retention zone because of the tidal currents.

The strong correlations between retention in both SS and BB and the eastward currents at C2 are due to C2's location on one of the main flow arteries for both τ_A and ζ_B and the spatial coherence of the model responses to sea-level and (spatially uniform) wind-stress anomalies. For each flow component the spatial structure is fixed and its magnitude at any location reflects the value of the forcing anomaly. However, Smith et al. (2001) show that the monthly anomalies in volume transport in the upper ocean (<75 m) over the 200-m isobath on the western flank of Browns Bank are poorly correlated with the monthly transport anomalies at C2. Therefore, while the currents at C2 are likely a good measure of the currents along the 100-m isobath west of Cape Sable, they are probably not a good measure of the currents in the deeper water to the west and north of Browns Bank. This spatial incoherence, which is probably associated with baroclinic flow variability not addressed here, places an important limitation on the use of C2 as a measure of circulation for the purpose of estimating retention.

The circulation due to boundary forcing is a crucial part of drift and retention dynamics, but there are a number of approximations in the transformation of Halifax sea-level data into boundary forcing. One issue is the averaging period used to provide the mean wind stress and mean Halifax sea level used in calculating ζ_B. We estimate that the choice of averaging period introduces uncertainty of the order of 1–2 $cm \cdot s^{-1}$ into the mean value of the modelled currents at C2, the present value probably having an eastward bias. For comparison the rms difference between the observed and modelled currents is 5 and 3 $cm \cdot s^{-1}$ for April and May, respectively. A second issue is the distribution of elevations across the upstream boundary. While the flow patterns around Browns Bank are quite robust to changes in the details of the upstream boundary, there is some sensitivity to whether the flow is concentrated over the inner shelf or the shelf break. There are also issues regarding mean and trend removal in the Halifax ASL and the relative contributions of barotropic and baroclinic flows to the ASL anomalies (we have assumed that the anomalies are 100% barotropic). All of these issues can affect the magnitude of ζ_B and its importance relative to the wind-stress anomalies and the seasonal mean circulation.

Relation to biological indices

The comparison of the circulation-based retention indices with the biological indices indicates that circulation variability alone is not the predominant influence on regulation of the Browns Bank haddock population. This is not unexpected for a nonlinear ecosystem comprising many interacting biological components with their own spatial and temporal variability. Whereas Shackell et al. (2000) found a negative correlation between survival and wind-stress magnitude, the one marginally significant correlation between retention and wind-stress magnitude in our results (near-surface BB west) disappears when the analysis is restricted to the estimated linear regime. However, the negative correlation between wind-stress magnitude and the regression residuals for this case indicates that wind-stress magnitude can account for about 5% of the retention variance. The variance explained (25%) by Shackell et al.'s result is at the level of the uncertainty in our calculations, so a relationship between retention and wind-stress magnitude cannot be ruled out. In particular, if life-history processes favour survival of larvae retained on Browns Bank (perhaps in a region even smaller than our BB), then the influence of wind-stress magnitude could be magnified.

The spatial structures in the flow fields and the weak correlation between the forcing anomalies in April and May of a given year mean that the timing and location of spawning are likely very important to the drift/retention fate of the larvae. This raises two important points with respect to retrospective studies of early life stages: (1) since the timing and location of peak spawning are poorly known, they will be significant sources of uncertainty and possible tuning parameters; and (2) the circulation may have to be resolved on time scales of less than 1 month in order to match the peak spawning period. In addition, the dominant drift pathways are narrow relative to the station spacing in typical ichthyoplankton surveys (e.g., FEP), and the exit pathways for drifters from Browns Bank are not stationary (Shore et al. 2000; Smith 1989). Thus, it is likely that the spatial structure of fish-larva distributions are not fully resolved in existing data sets for the region. These points are consistent with the findings on Western Bank (Scotian Shelf), where the spatial distributions of a wide variety of fish larvae and other planktonic species are consistent with the circulation only when both the circulation and the plankton distributions are sampled in order to resolve the relevant spatial and temporal scales (Reiss et al. 2000).

Brickman et al. (2000) and Brickman and Frank (2000) have developed an early life history model for Browns Bank haddock that uses the flow fields described here and includes an egg-production model, vertical motions, and temperature-dependent growth and survival rates. They found that combining biological and circulation variability provides a better model-based estimate of retention–survival indices than that provided by the drift indices given herein. Their model, together with our findings, provides a potential basis for determining the relative contribution of the different physical and biological processes to the overall survival of early life stages.

In conclusion, the model evaluations of circulation and drift variability support the concept of a drift–retention dichotomy (Campana et al. 1989*b*) for cod and haddock larvae in the Browns Bank region; there is both retention on the Bank and drift away from it. They also point to aspects of circulation variability that can amplify, as well as complicate, the roles of drift and retention in larval survival rates and in marine population regulation in the region. The spatially structured circulation, with persistent retention features and drift pathways, provides the potential for current fluctuations to have important influences on population dynamics and recruitment variability. The present results show that the circulation changes associated with variable wind stress and upstream inflows tend to reinforce either drift to the high-growth Bay of Fundy region or retention in the high-survival offshore shelf region, but they can also introduce additional loss pathways from the overall region. The computed indices indicate that the reinforcing tendencies are not infrequent, supporting a potentially important role in population dynamics.

The results also show how spatial and temporal structure in the circulation can contribute to complexity in population regulation, both through direct drift or retention effects and through effects in combination with biological factors. Haddock spawning in the Browns Bank region has been distributed in time across a period with a seasonal change in the intensity of circulation anomalies (e.g., the contrasts in estimated retention indices between April and May), and in space across an area with different retention–drift responses to circulation anomalies (e.g., the limited correlation between the west and east retention indices). Further, the dependence of drift and retention on depth introduced by the Ekman-layer component of the response to wind forcing results in well-known sensitivities to the timing of wind influences in relation to egg and larval development. With such spatial and temporal structure in the circulation on biologically important scales, the effects of circulation variability on population regulation can be expected to be complicated.

It should be emphasized that the circulation variability provided by the model solutions used here is simplified and approximate. The use of monthly mean fields for wind and boundary influences illustrates potential effects but does not fully represent associated circulation variability. As well, baroclinic flow variations associated with density-gradient fluctuations are not represented and may contribute to the discrepancies with observed currents, add additional complexity, or modify the effects in the present simulations.

The combination of multiple forcings and associated spatial and temporal complexity in an apparently simple and persistent circulation system like that in the Browns Bank region may help explain the difficulty in unravelling the environmental influences on recruitment variability in many marine populations.

Acknowledgements

We thank Dan Lynch, Chris Naimie, and Cisco Werner for providing the circulation and particle-tracking models, Brian Petrie for assistance with the sea-level and wind-stress data, Nancy Shackell for providing the biological indices and for discussions, Dave Brickman and Peter Smith for discussions and internal reviews, and two anonymous reviewers for constructive comments. This is a contribution of the GLOBEC Canada Program, jointly funded by Fisheries and Oceans Canada and the Natural Sciences and Engineering Research Council of Canada.

References

Brander, K., and Hurley, P.C.F. 1992. Distribution of early-stage Atlantic cod (*Gadus morhua*), haddock (*Melanogrammus aeglefinus*), and witch flounder (*Glyptocephalus cynoglossus*) eggs on the Scotian Shelf: a reappraisal of evidence on the coupling of cod spawning and plankton production. Can. J. Fish. Aquat. Sci. **49**: 238–251.

Brickman, D., and Frank, K.T. 2000. Modelling the dispersal and mortality of Browns Bank egg and larval haddock (*Melanogrammus aeglefinus*). Can. J. Fish. Aquat. Sci. **57**: 2519–2535.

Brickman, D., Shackell, N.L., and Frank, K.T. 2000. Modelling the retention and survival of Browns Bank haddock using an early life stage model. Fish. Oceanogr. In press.

Campana, S.E., Frank, K.T., Hurley, P.C.F., Koeller, P.A., Page, F.H., and Smith, P.C. 1989*a*. Survival and abundance of young Atlantic cod (*Gadus morhua*) and haddock (*Mellanogrammus aeglefinus*) as indicators of year-class strength. Can. J. Fish. Aquat. Sci. **46**: 171–182.

Campana, S.E., Smith, S.J., and Hurley, P.C.F. 1989*b*. Drift–retention dichotomy for larval haddock (*Melanogrammus aeglefinus*) spawned on Browns Bank. Can. J. Fish. Aquat. Sci. **46**: 93–102.

Craig, P., Hunter, J., and Johnston, B. 1993. The implications of linearly varying eddy viscosity for wind-driven current profiles. Cont. Shelf Res. **13**: 1–24.

Csanady, G.T. 1976. Mean circulation in shallow seas. J. Geophys. Res. **81**: 5389–5399.

Csanady, G.T. 1984. The free surface turbulent shear layer. J. Phys. Oceanogr. **14**: 402–411.

Frank, K.T., Page, F.H., and McRuer, J.K. 1989. Hydrographic effects on the vertical distribution of haddock (*Melanogrammus aeglefinus*) eggs and larvae on the southwestern Scotian Shelf. Can. J. Fish Aquat. Sci. **46**: 82–92.

Greenberg, D.A., Loder, J.W., Shen, Y., Lynch, D.R., and Naimie, C.E. 1997. Spatial and temporal structure of the barotropic response of the Scotian Shelf and Gulf of Maine to surface wind stress: a model based study. J. Geophys. Res. **102**: 20 897–20 915.

Hannah, C.G., Shore, J.A., Loder, J.W., and Naimie, C.E. 2001. Seasonal circulation on the western and central Scotian Shelf. J. Phys. Oceanogr. In press.

Harden-Jones, F.R. 1968. Fish migration. Edward Arnold Ltd., London.

Hurley, P., Black, G., Mohn, R., and Comeau, P. 1997. Assessment of 4X Haddock in 1996 and the first half of 1997. Canadian Stock Assessment Secretariat Research Document 97/108. Fisheries and Oceans Canada, Ottawa. <http://www.dfo-mpo.gc.ca/CSAS/ CSAS/English/Publications/Research_Doc_e.htm>

Hurley, P.C.F., and Campana, S.E. 1989. Distribution and abundance of haddock (*Melanogrammus aeglefinus*) and Atlantic cod (*Gadus morhua*) eggs and larvae in the waters off southwest Nova Scotia. Can. J. Fish Aquat. Sci. **46**: 103–112.

Loder, J.W. 1980. Topographic rectification of tidal currents on the sides of Georges Bank. J. Phys. Oceanogr. **10**: 1399–1416.

Loder, J.W., Ross, C.K., and Smith, P.C. 1988. A space- and time-scale characterization of circulation and mixing over submarine banks, with application to the northwestern Atlantic shelf. Can. J. Fish Aquat. Sci. **45**: 1860–1885.

Lynch, D.R., Ip, J., Naimie, C., and Werner, F.E. 1996. Comprehensive coastal circulation model with application to the Gulf of Maine. Cont. Shelf Res. **16**: 875–906.

Lynch, D.R., Werner, F.E., Greenberg, D.A., and Loder, J.W. 1992. Diagnostic model for baroclinic, wind-driven and tidal circulation in shallow seas. Cont. Shelf Res. **12**: 37–64.

Madsen, O.S. 1977. A realistic model of the wind-induced Ekman boundary layer. J. Phys. Oceanogr. **7**: 248–255.

Page, F.H., and Smith, P.C. 1989. Particle drift in the surface layer off southwest Nova Scotia: description and evaluation of a model. Can. J. Fish. Aquat. Sci. **46**: 21–43.

Reiss, C., Panteleev, G., Taggart, C., Sheng, J., and deYoung, B. 2000. Observations on larval fish transport and retention on the Scotian Shelf in relation to geostrophic circulation. Fish. Oceanogr. **9**: 195–213.

Ridderinkhof, H., and Loder, J.W. 1994. Lagrangian characterization of circulation over submarine banks with application to the outer Gulf of Maine. J. Phys. Oceangr. **24**: 1184–1200.

Shackell, N.., Frank, K.T., Petrie, B., Brickman, D., and Shore, J.A. 2000. Dispersal of haddock (*Melanogrammus aeglefinus*) during early life history inferred from the spatial distribution and variability in length-at-age of juveniles. Can. J. Fish. Aquat. Sci. **56**: 2350–2361.

Shore, J.A., Hannah, C.G., and Loder, J.W. 2000. Drift pathways on the western Scotian Shelf and its environs. Can. J. Fish. Aquat. Sci. **57**: 2488–2505.

Sinclair, M. 1988. Marine populations: an essay on population regulation and speciation. University of Washington Press, Seattle.

Sinclair, M., and Page, F. 1995. Cod fishery collapses and North Atlantic GLOBEC. U.S. GLOBEC NEWS No. 8. U.S. GLOBEC Scientific Steering Coordinating Office, University of Berkeley, CA 94730–3140.

Smith, P.C. 1989. Circulation and dispersion on Browns Bank. Can. J. Fish. Aquat. Sci. **46**: 539–559.

Smith, P.C., Houghton, R.W., Fairbanks, R.G., and Mountain, D.G. 2001. Interannual variability of boundary fluxes and water mass properties in the Gulf of Maine and on Georges Bank: 1993–1997. Deep-Sea Res. II, **48**: 37–70.

Suthers, I.M., Frank, K.T., and Campana, S.E. 1989. Spatial comparison of recent growth in postlarval Atlantic cod (*Gadus morhua*) off southwestern Nova Scotia: inferior growth in a presumed nursery area. Can. J. Fish. Aquat. Sci. **46**: 113–124.

Werner, F., Page, F., Lynch, D., Loder, J., Lough, R., Perry, R., Greenberg, D., and Sinclair, M. 1993. Influence of mean advection and simple behavior on the distribution of cod and haddock early life stages on Georges Bank. Fish. Oceanogr. **2**: 43–64.

Modelling the dispersal and mortality of Browns Bank egg and larval haddock (*Melanogrammus aeglefinus*)

David Brickman and Kenneth T. Frank

Abstract: An early life stage model is described with constant mortality for egg and larval stages. The model is used to simulate the stage 4 egg and larval data for haddock (*Melanogrammus aeglefinus*) in southwest Nova Scotia for the years 1983–1985. The model is initialized using published abundance and mortality estimates for these years, and its output is compared with field data. We find that the model does a systematically poor job of reproducing both the spatial–temporal and area-integrated versions of the data. To understand the discrepancy, we derive an integrated version of the model (integral model) and analyze its properties. This leads to a general method for determining whether sequential stage abundance data is consistent with a stage-dependent constant-mortality model. We use this method to show that a constant-mortality early life stage model is not consistent with the data. The integral model allows for year-day dependent mortality functions, which results in almost perfect fits to the abundance data. These functions can be transferred to the early life stage model with significantly improved model performance, although spatial differences remain. The implications of the integral-model analysis for sequential stage mortality estimation are discussed.

Résumé : On trouvera ici une modélisation de la première partie du cycle biologique qui suppose une mortalité constante des oeufs et des larves. Le modèle a été appliqué à des données sur des oeufs de stade 4 et des larves de l'Aiglefin (*Melanogrammus aeglefinus*) du sud-ouest de la Nouvelle-Écosse de 1983–1985. Le modèle est initialisé à l'aide d'estimations publiées de la densité et de la mortalité pour ces années et les résultats sont comparés aux données de terrain. Le modèle s'avère constamment inefficace à générer les versions spatio-temporelles ou spatiales intégrées des données. Pour comprendre cet écart, nous avons élaboré une version intégrée du modèle (modèle intégral) et analysé ses propriétés. Il en résulte une méthode générale pour déterminer si les données d'abondance des stades consécutifs sont compatibles avec un modèle de mortalité constante dépendant des stades. Il appert que le modèle à mortalité constante pour les premiers stades ne se conforme pas aux données. Le modèle intégral permet d'élaborer des fonctions journalières et annuelles de mortalité qui s'ajustent presque parfaitement aux données d'abondance. Ces fonctions peuvent être incorporées au modèle des premiers stades et en augmenter significativement la performance, bien qu'il reste des différences spatiales. Les conséquences de l'utilisation du modèle intégral pour estimer la mortalité de stades consécutifs font l'objet d'une discussion.

[Traduit par la Rédaction]

Introduction

There are many examples of fisheries that have become, owing to excessive depletion of the mature stock, heavily dependent on recruitment to sustain the commercial catch. For many fish stocks, there is no apparent stock–recruitment relationship. That is, the spawning stock biomass (a measure of the number of spawned eggs) does not strongly correlate with the number of fish surviving to reproductive age. Because mortality in the early life stages is so high, the understanding of egg and larval development is considered key to being able to predict interannual variation in recruitment. As a result, biophysical, or "trophodynamic," modelling of the early life stages of fish eggs and larvae has become an area of active research.

A coupled biophysical early life stage (ELS) model has two main components: (1) a physical model of the flow field in which the eggs–larvae are transported and (2) a biological model of the growth and survival of eggs and larvae that is solved along the flow-field trajectory. Recent development of accurate high-resolution coastal circulation models (Hermann and Stabeno 1996; Lynch et al. 1996; Hannah et al. 2000*b*) has provided significantly improved flow fields for describing the dispersion of the (semi) passive eggs and (or) larvae. This dispersion is usually modelled on an individual basis, using Lagrangian particle tracking (Werner et al. 1996), but advection–diffusion equation models are also used (Lynch et al. 1998).

Biological models fall into two basic categories. One, the larval trophodynamic models, is based on the growth and mortality equations for individual larvae developed by Laurence (1985). While these food-based equations are rather complex, they lack any representation of predation mortality, and the requirement to know the prey field is often

Received January 20, 2000. Accepted October 15, 2000. Published on the NRC Research Press web site on December 20, 2000. J15547

D. Brickman[1] and K.T. Frank. Department of Fisheries and Oceans, P.O. Box 1006, Dartmouth, NS B2Y 4A2, Canada.

[1] Corresponding author (e-mail: brickmand@mar.dfo-mpo.gc.ca).

a prohibitive one. The other (see, for example, Heath and Gallego 1997, 1998) uses an age–temperature relationship, to model the growth of larvae, and a size-based mortality equation, representing an increased ability to avoid predators as size increases. While considered to be a realistic representation, the temperature-based equations lack the ability to model growth when food supply is a limiting factor. Regardless of which larval-evolution equations an ELS model may use, the important egg stage tends to be modelled using a constant-mortality assumption. Because mortality is typically higher for the egg than for any other life stage, and the number of eggs spawned is enormous, understanding the factors that control egg mortality is one of the most important challenges in early life stage and recruitment modelling.

The southwest Nova Scotia – Bay of Fundy (SWN–BoF) ecosystem provides an interesting testing ground for biophysical modelling of the early life stages of haddock (*Melanogrammus aeglefinus*). Browns Bank, off the southwest tip of Nova Scotia, is the principal spawning ground for haddock, with a peak spawning period between mid-April and mid-May (Page and Frank 1989). Currents in the region are characterized by a partial gyre on the Bank and a downstream drift toward the mouth of the BoF. Numerous field programs, with various temporal and spatial resolutions, have collected ichthyoplankton data in the area. Notable are the larval herring program (LHP; 1975–1995), the Scotian Shelf Ichthyoplankton Program (SSIP; 1977–1982), and the Fisheries Ecology Program (FEP; 1983–1985), which last had the most complete egg- and larval-sampling program and was the subject of a special issue of the *Canadian Journal of Fisheries and Aquatic Sciences* (Vol. **46**(Suppl. 1), 1989).

This paper presents the results from a retrospective ELS model simulation of Browns Bank haddock eggs and larvae for the FEP years 1983–1985. Using a constant egg and larval mortality model and the parameters from the Campana et al. (1989) survival–abundance analysis, we attempt to model the exact distributions of eggs and larvae as reported in Hurley and Campana (1989). This represents one of the first attempts at using a ELS model in a realistic modelling exercise (see also Heath and Gallego 1998). The next section describes the components of the ELS model, and the one following the data used for model comparison. We show, in ELS model results, that the model does a systematically poor job of simulating the data. To help understand the behavior of the ELS model, the model is first slightly simplified and then an integral version of it is derived. We analyze the properties of the ELS integral model (ELSIM) and derive a general method for determining whether field data are consistent with a constant-mortality model. This is described in The early life stage integral model. In ELSIM results, this technique is used to assess the applicability of using a constant-mortality model on the FEP data. The integral model can be generalized, to allow egg and larval mortality that is a function of year-day. We show that doing so significantly improves the model–data fit, and that these changes can be incorporated into the more complicated ELS model. In the section following this, we then discuss the implications of the ELSIM results in determining abundance and mortality from survey data and, lastly, summarize the findings.

ELS model

The components of the biophysical model, shown schematically in Fig. 1, are (*i*) an egg-production model, describing the spatial and temporal history of the release (spawning) of haddock eggs; (*ii*) a circulation model, which provides the flow fields in which the eggs and larvae evolve; (*iii*) a conceptual life-stage model, which describes the interaction of the eggs and larvae with the physical flow field; and (*iv*) the growth–survival model, which describes the evolution of eggs and larvae as they move through the fluid.

Egg-production model

The distribution of spawned eggs in space and time determines their future evolution in the flow field, and makes the egg-production model one of the key elements of a realistic ELS model. Haddock spawn once a year in a well-defined period in midspring (Page and Frank 1989; Waiwood and Buzeta 1989). Similar to the work of Heath and Gallego (1998) on North Sea haddock, we assume that the spawning distribution is Gaussian in time, characterized by a peak spawning time t_p, a spread σ_s, and a total number of eggs N_T (see Table A1 for a list of the repeated-use symbols).

The spatial distribution of recently spawned haddock eggs is difficult to determine. Typically, it is assumed that the majority of eggs are spawned on Browns Bank. This fact is inferred from field measurements of cod–haddock–witch (CHW) eggs, which also occasionally show significant egg concentrations upstream of the Bank. The most direct evidence for the spawning pattern comes from the distribution of the spawners themselves. The majority of ripe and spawning haddock occupy the sand and gravel (central and southeast) portion of Browns Bank, with lesser but significant numbers of spawners on the upstream Baccaro and Lahave banks (Waiwood and Buzeta 1989). We therefore divide the spawning region into four areas (R1–R4)—central Browns, southeast Browns, Baccaro, and Lahave—and infer, from the work of Waiwood and Buzeta (1989), a canonical regional-spawning proportion of R1 = 0.20, R2 = 0.50, R3 = 0.20, and R4 = 0.10.

Circulation model

The circulation model used was the three-dimensional (3-D) prognostic finite element model, QUODDY4 (Lynch et al. 1996). This model has demonstrated significant skill at reproducing the features of the seasonal climatological circulation on the Scotian Shelf (Han et al. 1999; Hannah et al. 2000*b*). Particles are tracked in the M2 tidal and residual flow fields. The tidally averaged horizontal diffusivity, calculated from the model, is used in a random displacement model of horizontal-turbulence dispersion (Rodean 1996). No vertical turbulence scheme is used. Roughly 10 000 particles are tracked in the 3-D flow field, with each particle representing a "cluster" of eggs or larvae. The particles are initally distributed among the four regions described above, with uniform seeding in each of the regions. The initial weight (number of eggs) for each particle is determined by dividing the total number of eggs spawned in the region during a particular time period by the number of particles seeded in that region. Each cluster of eggs is considered to

Fig. 1. Schematic of the early life stage model.

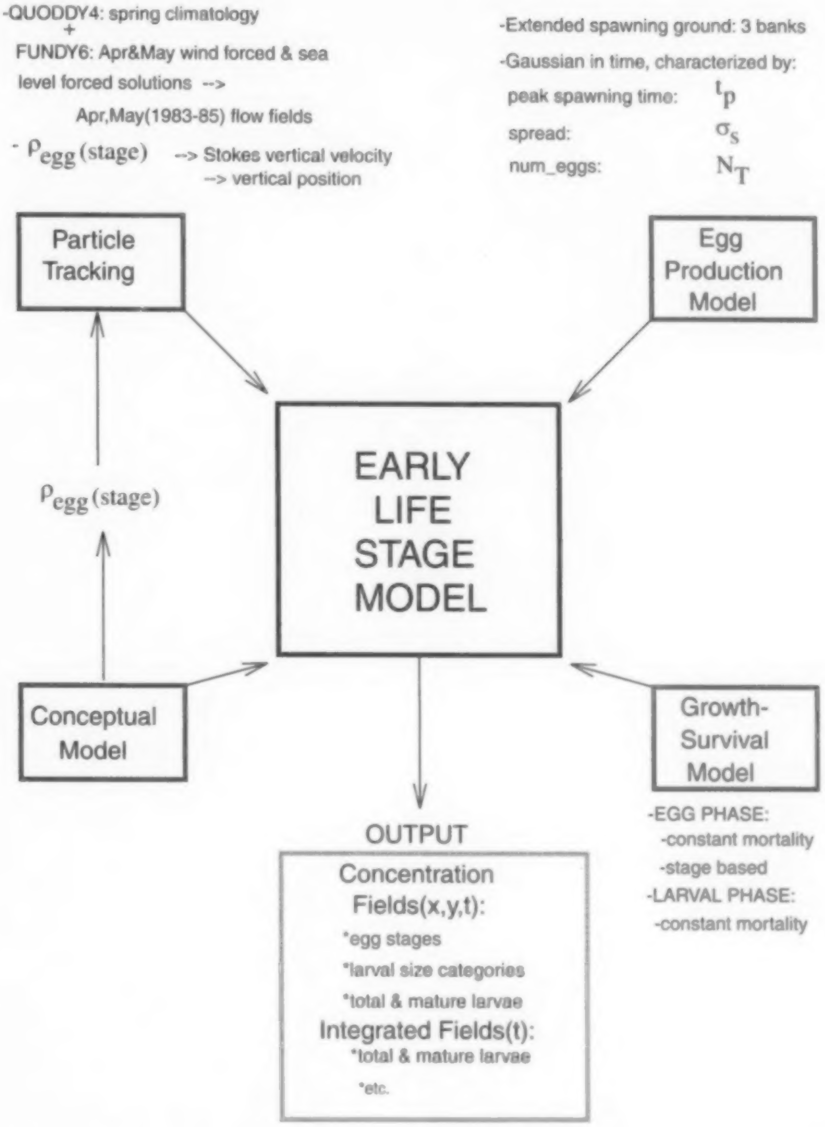
-QUODDY4: spring climatology
+
FUNDY6: Apr&May wind forced & sea
level forced solutions -->
Apr,May(1983-85) flow fields
- ρ_{egg} (stage) --> Stokes vertical velocity
--> vertical position
-Extended spawning ground: 3 banks
-Gaussian in time, characterized by:
peak spawning time: t_p
spread: σ_s
num_eggs: N_T
Particle Tracking
Egg Production Model
EARLY LIFE STAGE MODEL
ρ_{egg} (stage)
Conceptual Model
Growth-Survival Model
-EGG PHASE:
-constant mortality
-stage based
-LARVAL PHASE:
-constant mortality
OUTPUT
Concentration Fields(x,y,t):
*egg stages
*larval size categories
*total & mature larvae
Integrated Fields(t):
*total & mature larvae
*etc.

evolve uniformly, that is, we do not try to model variability within an egg–larval mass.

The FEP data cover the spring–summer periods of 1983–1985 and, thus, flow fields are needed for each of these years. Predominant causes for interannual current variability in SWN are variability in wind forcing and the strength of the Nova Scotian current (Smith 1983, 1989). Monthly flow fields were created by assuming that the variability in forcing can be linearly added to a climatological spring Quoddy run. This was done in the following way (see Hannah et al. (2000*a*) in this issue for a more complete explanation). First the climatological spring flow field was determined from a Quoddy run using the climatological temperature, salinity, wind, and M2 tidal fields. The wind-forced addition was determined using a linear 3-D barotropic model (Lynch et al. 1992), forced by the average monthly Sable Island wind stress anomaly for each April and May from 1983 to 1985. Then, the sea-level setup at Halifax from the wind-forced solution was subtracted from the monthly mean detrended Halifax sea level, leaving a component of setup at Halifax considered to be due to variability in the strength of the Nova Scotian current. This setup increment was used as a boundary condition for another barotropic-model run. The result was monthly mean April and May sea level and wind stress forced flow fields, which were added to the climatological flow field to produce the required annually and seasonally varying flow fields.

The egg-production model releases eggs over an extended time period and, in principle, each egg release should experience a different flow field. As just described, only average

Fig. 2. Conceptual life-stage model. The typical progression from eggs to juveniles is shown in the top panel. The model of egg and larval development is shown below. Because larval swimming ability increases with time, passive-particle tracking ends at 60 days.

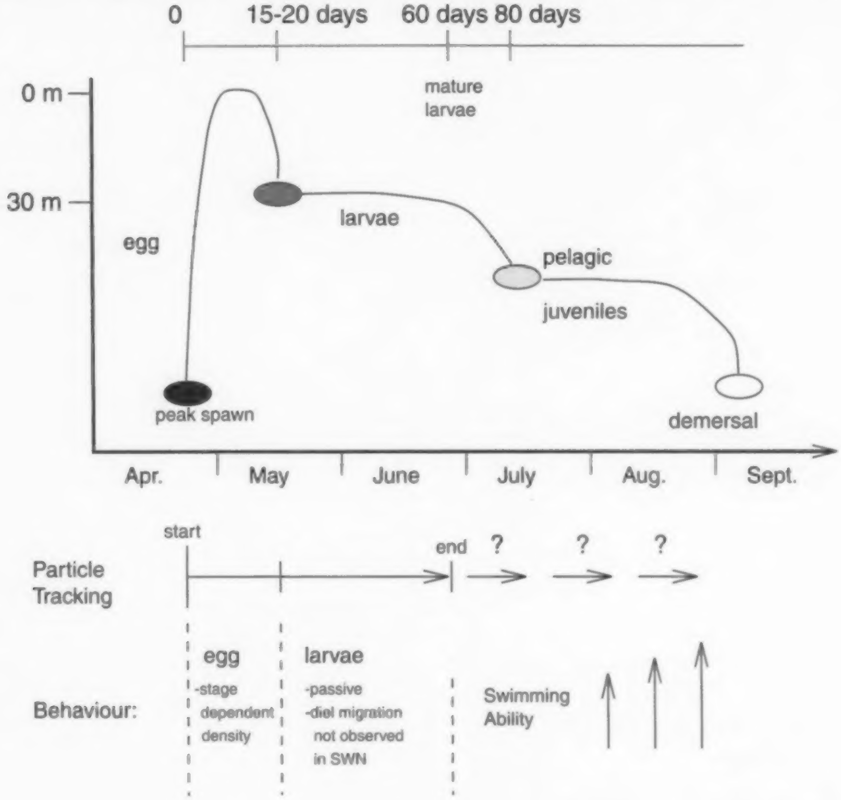

April and May flow fields were available. To simulate time-varying flow fields, particle tracking was done using varying amounts of the April and May flow fields. For example, eggs released during the first 10 days of April would evolve in a 60-day flow field made up of 30 days of April and 30 days of May (30d April – 30d May). Five April–May flow fields were created covering 0d April – 60d May to 40d April – 20d May. While not perfect, this was considered to be a reasonable method for approximating the different flow fields applicable to different release periods. Because no March or June flow fields existed, March was represented by the April field, and the May field was taken to represent June. This approximation is justifiable, because forcing is similar (and weak) in May and June and, while March and April are not necessarily similar, few eggs are spawned in March, so that possible errors should not be significant.

Conceptual life-stage model

An ELS model requires a conceptual model for how the eggs and larvae develop and interact with the flow field and other variables. For example, the larvae of many species are observed to exhibit a diurnal vertical migration, and this behavior would have to be coded into the growth, survival, and particle-tracking routines. As well, larval swimming ability increases with age, and this affects the length of time and degree to which they can be considered to be passive particles.

Figure 2 is a schematic of the conceptual life-stage model used in this paper. Haddock eggs exhibit four stages. They are spawned near the bottom, and are initially positively buoyant and rise to the surface. Their density increases with time and, by stage 4, they occupy a mid-depth position where they hatch after 15–20 days (Page and Frank 1989). In the SWN region, there is no evidence for vertical migration of larvae (Frank et al. 1989). Because larval swimming ability increases with age, the total runtime for a particle was chosen to be 60 days, resulting in a 40- to 45-day larval period. After about 60 days of life, larvae migrate toward the bottom and begin to adopt a more demersal lifestyle, becoming settled juveniles after about 90 larval days.

The stage-dependent egg density is modelled using the temperature-dependent stage-duration relationship of Page and Frank (1989) combined with an analysis of the FEP larval vertical distribution data (Frank et al. 1989). The resultant equation is (see also Anderson and deYoung 1995)

$$\rho_e(t) = \rho_{ei} + (\rho_{ef} - \rho_{ei})\Delta t / t_h \quad (1)$$

where $t_h = a(T(t) + 2)^b$ is the Page–Frank hatch time ($a = 10^{1.88}$, $b = -0.85$, and $T(t)$ is the water temperature experienced by the advected egg (T is a time-dependent Lagrangian variable)); $\rho_{ei} = 1025.0\ \mathrm{kg \cdot m^{-3}}$ and $\rho_{ef} = 1025.70\ \mathrm{kg \cdot m^{-3}}$ are the initial and final egg densities, respectively; and Δt is the age of the egg. This equation provides the egg density used by the particle-tracking routine in a Stoke's equation for the egg-settling velocity w_e:

$$w_e = \frac{gd^2(\rho - \rho_e)}{18\nu}$$

where g is gravity, d = 1.5 mm is the egg diameter, and ν and ρ are the viscosity and density of water, respectively. Equation 1 is tuned to give a final egg density of, roughly, the average water density corresponding to the observed vertical position of early-stage larvae. The initial egg density is chosen to be less than the average surface density in the circulation-model domain.

Growth–survival model

The growth–survival model is the set of equations describing the growth and mortality of egg–larvae clusters as they move through the flow field. The particle-tracking routine outputs the position and average temperature of particles at daily intervals, and the growth–survival model is run as a post-processing routine using this data. This allows for multiple ELS model runs based on one run of the particle-tracking routine—a sensible approach, given that the latter takes at least 50 times as much computer time.

Egg mortality is modelled using an exponential mortality function:

$$E(t) = E_0 e^{-M_E \Delta t}$$

where M_E is the (constant) egg mortality rate (fraction·day^{-1}), t is the time increment in days, and E_0 is the initial number of eggs. An equation of this form is solved at each time step (with Δt and E_0 adjusted accordingly) and, in keeping with the Campana et al. (1989) analysis, mortality for egg stages 1–3 (E13) and egg stage 4 (E4) was modelled using the Page–Frank stage-duration equation to determine developmental stage.

The model is coded to use the same larval growth and survival equations as the Heath and Gallego (1998) model. These are the Campana and Hurley (1989) age–temperature equation for larval length ($l(t)$) and a (modified) larval-mortality equation based on Houde (1997).

$$(2) \qquad M_L(t) = f_1 \frac{1.5}{\sqrt{W(t)}} + f_2$$

where $W(t) = 0.495l\,(t)^{3.029}$ is the larval weight, and f_1 and f_2 are parameters allowing for a scaling of M_L ($f_2 = 0$) or constant M_L ($f_1 = 0$). The formulation with $f_2 = 0$ is thought to be realistic, because the decreasing mortality with time (i.e., $W(l(t))$) is consistent with observations of larval behavior (Houde 1997). Motivated by the Campana et al. (1989) analysis, the model was run in constant-mortality mode. Note that, in a constant-mortality model, larval length is not important to survival, so that temperature effects on growth are not relevant.

Data

The data used for model comparison are presented in Hurley and Campana (1989) and Campana et al. (1989) (hereinafter H89 and C89, respectively). Field surveys were done on a monthly basis from February to June 1983–1985. In this paper, the haddock-egg and -larval data for April–June was used. H89 Figs. 2, 3, and 5 show expanding dot plots of stage-1 CHW eggs, stage-4 haddock eggs, and total haddock larvae. For comparison purposes, the stage-4 egg and larval data were interpolated onto the same 10 × 10 km grid that was chosen for output of the ELS model.

Table 1. Table of model parameters.

Year	M_{E13}	M_{E4}	M_L	t_p	σ_s	N_T
1983	0.20	0.37	0.08	105	20	3.0×10^{13}
1984	0.15	0.20	0.25	125	40	2.0×10^{13}
1985	0.07	0.21	0.50	110	25	2.0×10^{13}

Note: M_{E13}, M_{E4}, and M_L are the mortality rates (fraction·day^{-1}) of egg stages 1–3, egg stage 4, and larvae, respectively; t_p is the peak in spawning distribution (year-day); σ_s is the spread in the Gaussian distribution (days); and N_T is the total number of spawned eggs.

The C89 paper used research vessel survey data and the FEP data to estimate the abundance and mortality of the sequential life stages from egg to adult. Figure 2 in C89 shows the stage 1 egg abundance curve for 1983–1985 from which we estimate t_p and σ_s for the egg-production model. From Fig. 3 in C89, we obtain N_T and, from Fig. 4 in C89, we obtain mortality estimates for E13, E4, and larvae (M_{E13}, M_{E4}, M_L).

The area-integrated (i.e., abundance) data are used in ELS model results. Because we did not have the haddock stage 1 egg data, these data were taken from Fig. 2 in C89. The gridded FEP larval and stage 4 egg data and equivalent ELS model data were integrated over the same region used by C89, to allow direct comparison. (Owing to differences in the averaging procedure, we get slightly different values from theirs; however, our method is internally consistent.) Table 1 shows the parameter values used in the ELS-model runs.

ELS model results

Contour plots of FEP and modelled larval concentrations for the years 1983–1985 are shown in Figs. 3–5. The spawning banks and FEP sampling grid are shown in the d100 (i.e., year-day 100 or April) panel of Fig. 3. Figure 6 shows the E4 and larval data integrated over the FEP grid. (The E4 model – data contour plots lead to the same conclusions as the larval plots and, thus, are not shown. Also, eggs and larvae found on Georges Bank are considered external to the study area.)

The year 1983 was considered to be somewhat extraordinary, because, while the CHW-egg field seemed ordinary, there were virtually no haddock stage 4 eggs or larvae found in SWN. Nevertheless, the ELS model predicted significant larval concentrations in all 3 months, with a peak in mid-May. This is confirmed in the integrated-data plot for that year (Fig. 6), which also shows a peak in E4 in mid-May versus a near zero value from the field data.

In 1984, there was a peak in modelled larval concentration in mid-May, while the data peaked in mid-June. This is apparent in Fig. 6 for both E4 and larvae. Note that the April-model result would indicate significant numbers of larvae outside the FEP grid. We return to this point below.

The 1985 result is similar to that for 1984, inasmuch as the model predicted a peak in larvae in mid-May, about

Fig. 3. FEP data – model comparison: 1983, larvae. The FEP d100 (year-day 100) panel shows the data-sampling grid and the spawning banks: Browns (R1 and R2), Baccaro (R3), and Lahave (R4). The contour and shading interval is 2.0·m^{-2} for concentrations greater than 2.0 (solid lines). For concentrations less than 2.0, the contour interval is 0.3 (broken lines).

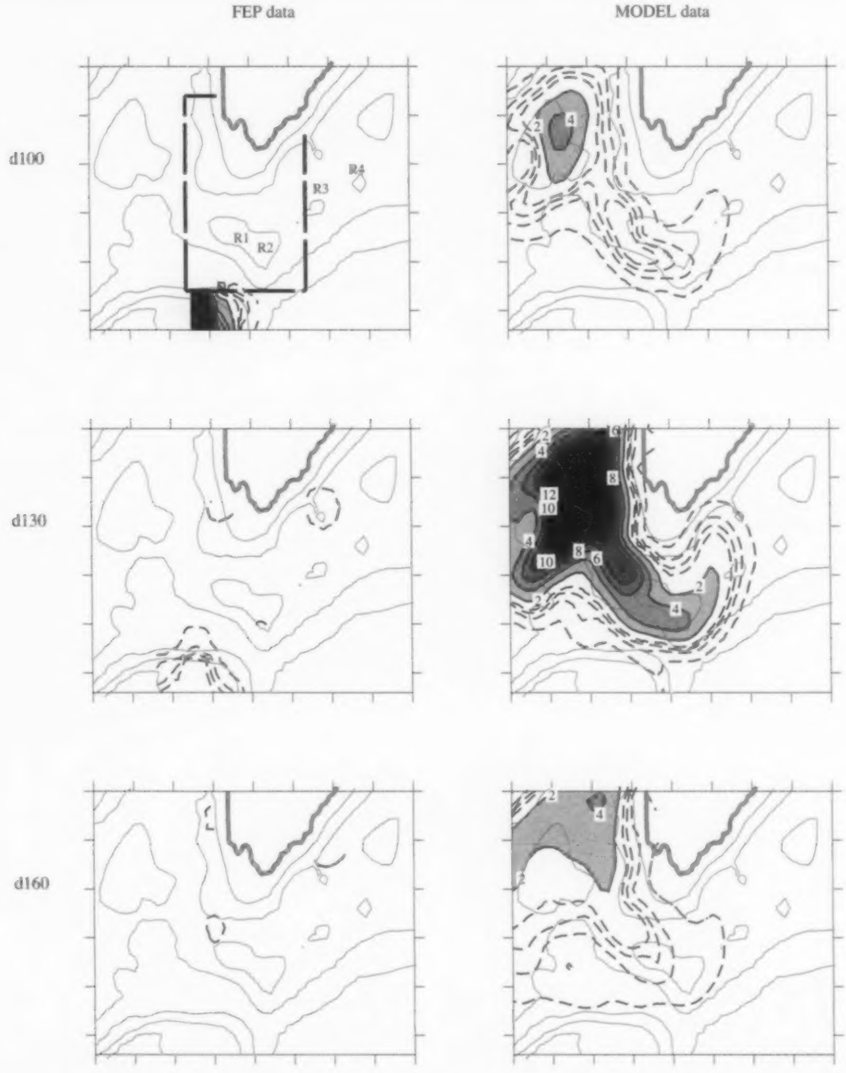

1 month earlier than indicated by the data. The E4 result overestimates the data, but more closely approximates the location of the peak.

Note that, in several instances (in 1983 in all months and in 1984 in April), the ELS model suggests that the FEP grid missed significant larval concentrations. However, the poor performance of the model makes it difficult to defend this observation. Some support for this claim comes from the result of particle tracking alone (see Hannah et al. 2000*a*, this issue), which suggests that April 1984 was an anomalous month with enhanced flow toward the BoF. Therefore, it is likely that the FEP grid was deficient in this month.

Note, as well, that the model tends to systematically predict higher concentrations of larvae downstream toward the BoF, an effect that is accentuated for times later than year-day 160. Although limited in spatial coverage, historical data do not seem to support this prediction. As well, the analysis of Shackell et al. (1999) indicates that the majority of surviving larvae seem to be retained near or on Browns Bank. Shackell et al. (1999) used this information to infer a differential mortality between the BoF and SWN. Our model results would improve if this feature was included.

We next explore the possible reasons why the ELS-model results agree poorly with the FEP data.

The early life stage integral model (ELSIM)

In this section, we derive a simpler model that describes the area-integrated properties of the ELS model. Analyzing

Fig. 4. FEP data – model comparison: 1984, larvae. The contour and shading interval is 2.0·m^{-2} for concentrations greater than 2.0 (solid lines). For concentrations less than 2.0, the contour interval is 0.3 (broken lines).

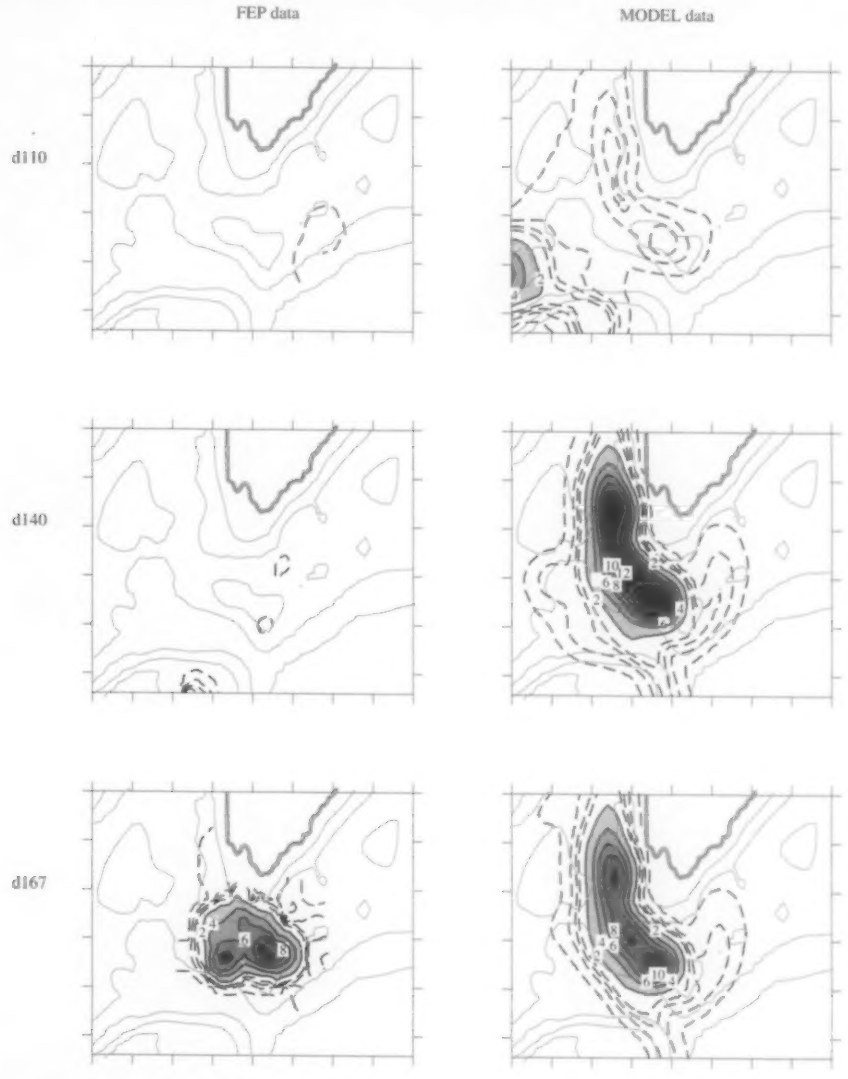

the properties of this model will lead to an explanation of the discrepancy between model and data.

Consider a Gaussian spawning duration curve:

$$G(t) = \frac{N_T}{\sqrt{2\pi\sigma_s^2}} \exp\left(-\frac{(t - t_p)^2}{2\sigma_s^2}\right)$$

We seek to derive expressions for the total number of eggs and larvae in the water column as a function of time. For comparison with the C89 data, we assume that the eggs have two stages—E13 and E4—and that the stage durations ts_{13} and ts_4 (where $ts_{13} + ts_4 = t_h$), hatch time (t_h), and mortalities (M_{E13}, M_{E4}) are constant. Similarly, let the larvae be characterized by constant mortality M_L and a time in which to become juveniles t_j.

Consider the number of eggs g_i, spawned during an interval dt centered at t_i ($g_i(t_i) = \int_{t_i-dt/2}^{t_i+dt/2} G(t'')dt''$). The contribution from this spawning interval to the total number of larvae found at time t is

$$(3)\qquad L_i(t) = \{g_i\, e^{-M_{E13}ts_{13}} \times e^{-M_{E4}ts_4}\}\{e^{-M_L(t-t')}\}$$

$$\equiv \{E_i(t')\}\{e^{-M_L(t-t')}\}$$

where $t' = t_i + t_h$. This is shown schematically in Fig. 7*a*. The first term on the right hand side, $E_i(t')$, represents the number of larvae resulting from the original g_i eggs after suffering ts_{13} days of mortality at rate M_{E13} followed by ts_4 days at M_{E4}. That is, $E_i(t') = \{k_{13} \times k_4\}g_i = Kg_i$, where K is the total egg mortality and $k_{13} \times k_4 = e^{-M_{E13}ts_{13}} \times e^{-M_{E4}ts_4}$. The second term in eq. 3 is $E_i(t')$, reduced owing to the $t - t'$ days

Fig. 5. FEP data – model comparison: 1985, larvae. The contour and shading interval is $2.0 \cdot m^{-2}$ for concentrations greater than 2.0 (solid lines). For concentrations less than 2.0, the contour interval is 0.3 (broken lines).

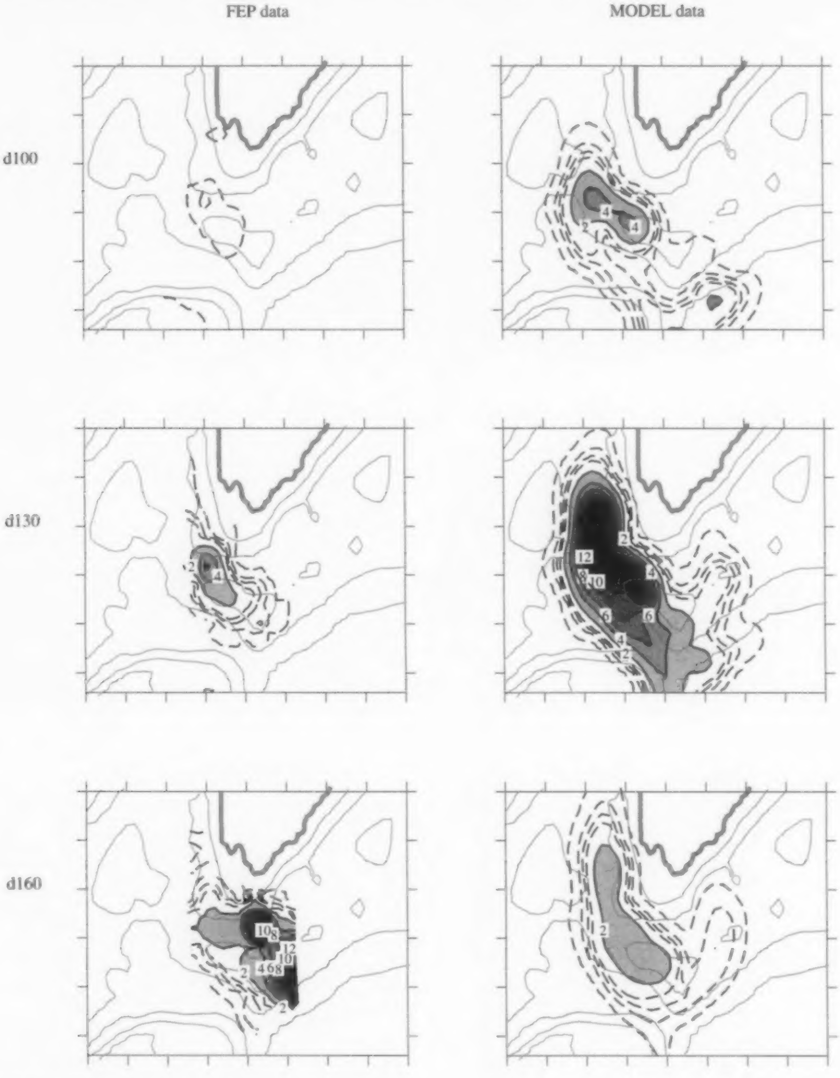

of exponential mortality at the larval mortality rate M_L. The total number of larvae at t is the convolution integral

$$L(t) = \int_{t-t_j}^{t} \{K\, G(t' - t_h)\}\, e^{-M_L(t-t')} dt' \qquad (4)$$

The integral starts at $t - t_j$, because before this time, all surviving eggs would have become juveniles and thus should not be included in the larval total.

Note that the constant-mortality assumption is chosen to be consistent with the C89 analysis. If mortality is a function of time, then replace $e^{-M_L(t-t')}$ with $e^{-\int_{t'}^{t} M_L(t'')dt''}$ in the above, with similar expressions for egg mortalities k_{13} and k_4.

In a similar fashion, we can derive the equation for the total number of stage-4 eggs E4(t)

$$E4(t) = \int_{t-ts_4}^{t} \{k_{13}\, G(t' - ts_{13})\}\, e^{-M_{E4}(t-t')} dt'$$

where the integral starts at $t - ts_4$ and ends at t, because this is the interval in which stage-4 eggs exist. The only difference between this model and the ELS model with constant mortality integrated over all space is the assumption of constant stage durations.

Various properties can be derived from the integral model (see Fig. 7b) but, for our present purposes, we need only two.

1. The peak L_p in larval distribution $L(t)$ occurs at $t_p + t_h + t_j/2.0$ for $M_L = 0$ and tends to $t_p + t_h + 1/M_L$ for $M_L \geq \sim 0.1$ (Fig. 8a). This result is insensitive to the value of σ_s.

Fig. 6. Model – FEP data comparison for integrated E4 and larval data: 1983 (*a*, *b*), 1984 (*c*, *d*), and 1985 (*e*, *f*). The crosses are the field data and the solid circles represent the model output.

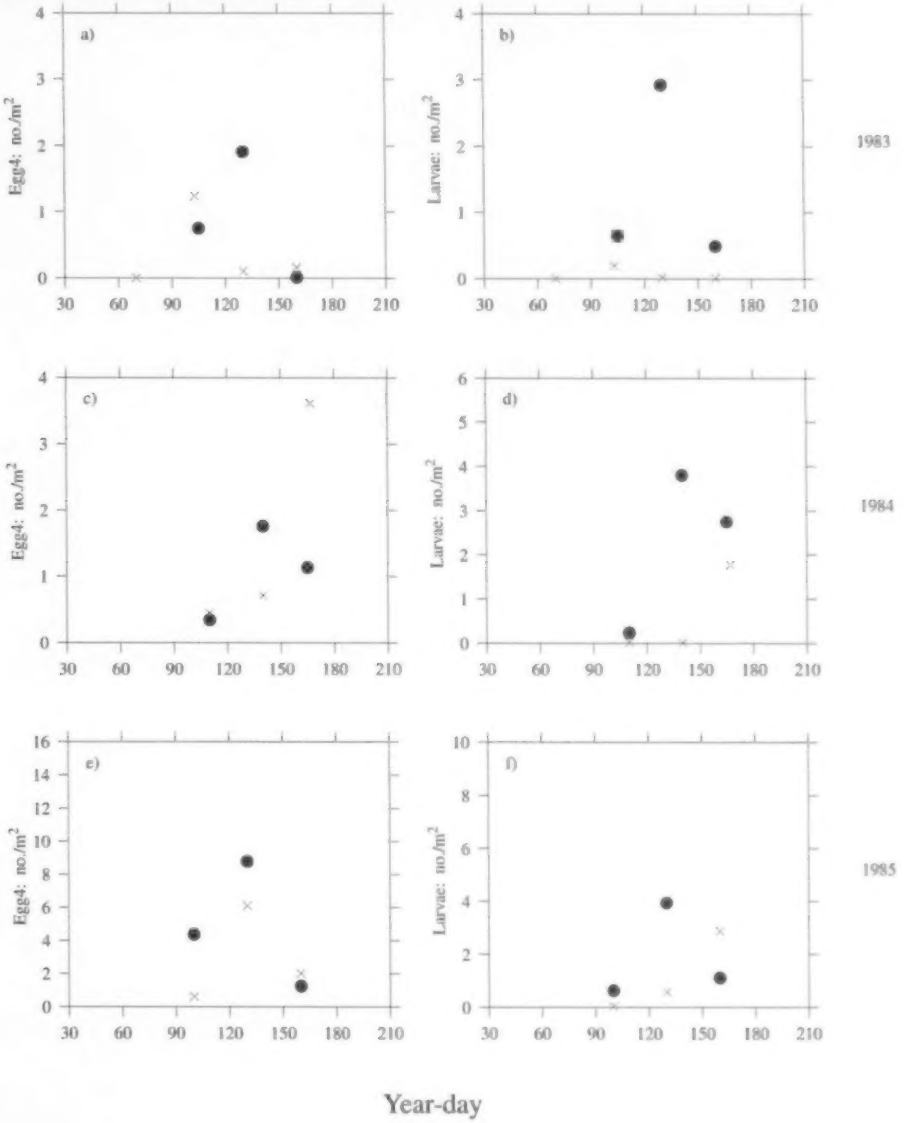

In general, for any life stage characterized by a stage duration ts, mortality M_S, and preceded by other stages of duration ts_p, the peak in the "stage" curve S_p is bounded by $t_p + ts_p$ and $t_p + ts_p + ts/2$ and varies like $1/M_S$ in between, *provided* that $1/M_S << ts/2$. Thus, for the peak in the E4 distribution ($E4_p$), we have

$$(t_p + ts_{13}) \le E4_p \le (t_p + ts_{13}) + ts_4/2$$

Using typical values for SWN, $t_h \sim 15$ days, $ts_{13} \sim 10$ days, $ts_4 \sim 5$ days, $t_j \sim 45$ days (the latter appropriate to the ELS model), the expectation for the offset in the larval and E4 peaks is (roughly) in days

$$15 \le L_p \le 40$$

$$10 \le E4_p \le 13$$

Note that, with respect to the general stage curve S, the effect of the total preceeding mortality over the preceeding stage length ts_p (e.g., the factor $\{KG(t' - t_h)\}$ in eq. 4) is that of a shrink and shift operator, *shifting* the time from which S receives a maximum contribution from t_p to $t_p + ts_p$.

2. For a given variance σ_s^2 in the spawning duration curve, subsequent stages will have a variance $\ge \sigma_s^2$. That is, mortality tends to increase the initial spread in the spawning-duration curve. The effect is small (typically

Fig. 7. Schematic of the ELSIM and its properties. (*a*) The spawning curve, showing how an increment g_i of spawned eggs contributes to the number of surviving larvae at time t. Note: $t_h = ts_{13} + ts_4$; t_j = larval-stage duration. (*b*) Some properties of the ELSIM: σ_s is the spread in the spawning curve centred at t_p; σ_L is the spread in the larval distribution centred at L_p later; L_{area} is the area under the larval-distribution curve.

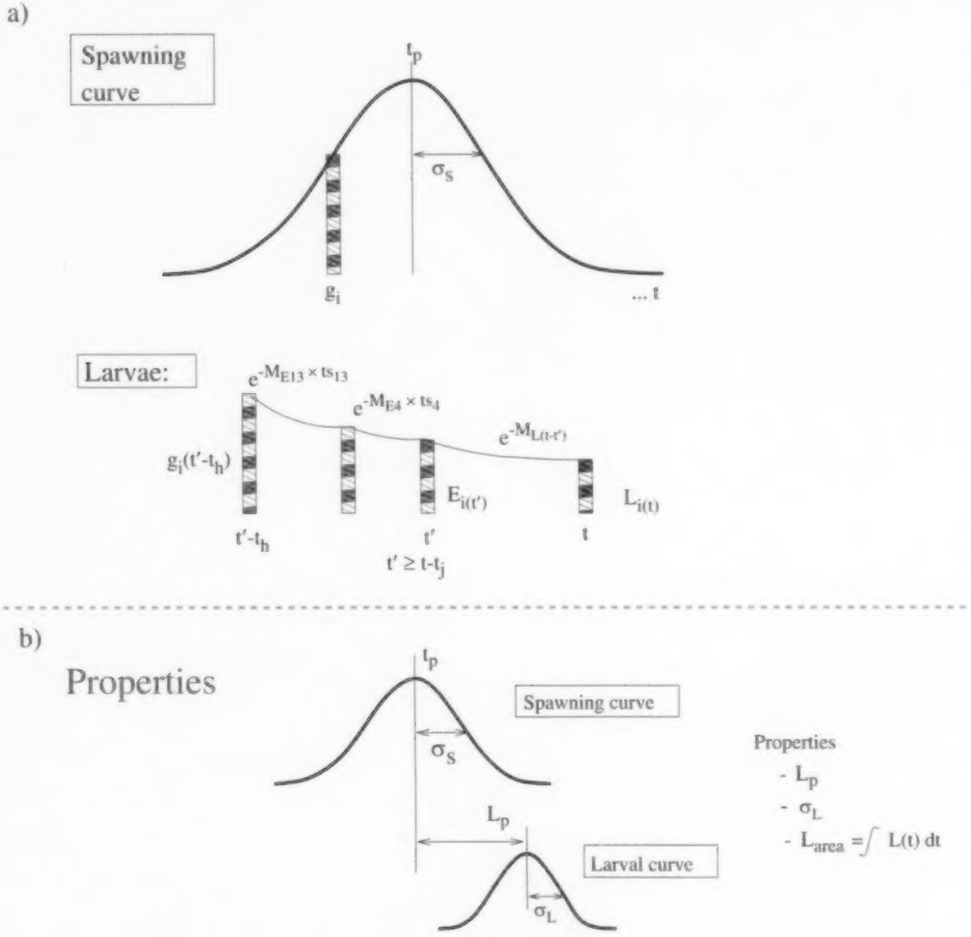

<10% for $M \geq 0.1$) but increases with decreasing M_L. Figure 8*c* is a plot of σ_L/σ_s versus M_L for various σ_s, where σ_L^2 is the variance in $L(t)$.

Property 1 is the most important one and we explain it in the following way. Consider the equation for $L(t)$. The factor $e^{-M_L(t-t')}$ weights the contribution from the spawning duration curve at time t' and has an influence scale ~$1/M_L$. Therefore, L_p should be found, roughly, $1/M_L$ from where the greatest contribution of $G(t' - t_h)$ comes from, i.e., $t' = t_p + t_h$. In the limit $M_L \rightarrow \infty$, eggs are hatched and die "instantaneously," so L_p coincides with $t_p + t_h$. If $M_L = 0$, L_p occurs at $t_p + t_h + t_j/2$, because the interval $(t_p + t_h) - t_j/2 \leq t' \leq (t_p + t_h) + t_j/2$ captures the largest values of G. Therefore, L_p is bounded by $t_p + t_h$ and $(t_p + t_h) + t_j/2$ and varies like $1/M_L$, provided $1/M_L << t_j/2$. This is shown by the curve fit in Fig. 8*a*. If $1/M_s$ is not << ts /2, as is the case for E4, then a linear fit is more appropriate (Fig. 8*b*). Again note that this explanation can be generalized to where we would expect to find the peak in any general stage, assuming that all stage mortalities are constant.

In the next section, we use these results to interpret the C89 integrated data for each of the FEP years.

ELSIM results

In this section, we use the properties of the ELSIM to assess whether a constant-mortality model is consistent with the FEP data. It will be shown that, in 1983, 1984, and (likely) 1985, this was not the case. As mentioned in the previous section, the ELSIM is not restricted to a constant-mortality assumption. We run the model using year-day dependent mortality functions and show that the data can be matched almost perfectly. These functions can be transferred to the ELS model, and doing so improves the model–data fit.

Fig. 8. Derived quantities from the ELSIM versus mortality. (*a*) The offset of the peak in the larval distribution L_p (solid line). The broken line is a $1/M_L$ curve fit. (*b*) The peak in the E4 distribution. (*c*) The ratio of the spread in the larval distribution to the spread in the spawning curve. (*d*) Scaled area under the larval distribution. The broken line is a $1/M_L$ curve fit.

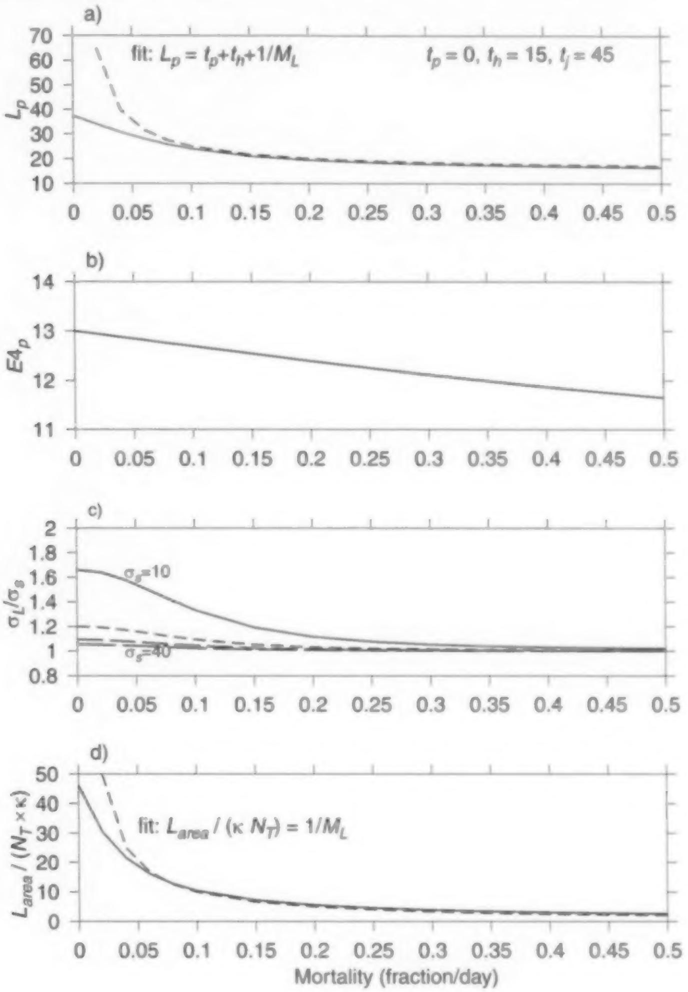

Resolving the model discrepancies: 1983

Figures 9*a*–9*c* show the 1983 (integrated) FEP data for egg stages 1 (E1) and 4 and larvae, and possible Gaussian fits to the data. The Gaussian fits are intended to define the locations of peaks in the data. From the discussion above, we would expect the peak in E1 to occur, at most, $ts_1/2$ days from the (unknown) peak spawning time. Since $ts_1 \sim 2$–4 days for haddock eggs in this region (Page and Frank 1989), the peak in E1 should closely follow t_p. The fit to the E1 data is how t_p and σ_s were calculated as inputs to the ELS model (see Table 1).

What is remarkable about the E1, E4, and larval data is that they all seem to have a peak at about year-day 105 and, although significant quantities of stage-4 eggs were found, almost no larvae were found. The ELS model result (Fig. 3) would indicate that the lack of larvae (and eggs) was not a result of the FEP sampling grid missing the bulk of the data. Therefore, we consider the data to be essentially correct.

From property 1, $E4_p$ should occur 10–13 days after t_p (Fig. 8*b*), and L_p (from Fig. 8*a*) should be about 20–25 days after t_p. These deductions do not seem to be supported by the data. Thus we conclude that, for 1983, the field data are not consistent with a constant-mortality model.

Resolving the model discrepancies: 1984

The year 1984 is problematic, because as Fig. 4 suggests, there is a distinct possibility that the sampling grid missed significant larval concentrations in April. This is also evident in the E4 model–data contour plots (not shown). This leads to two related problems. First, the C89 mortality calculations require no losses from the sampling domain. This point is discussed in the next section. Second, there is the possibility

Fig. 9. FEP integrated data (solid circles) and possible Gaussian fits (broken lines): 1983 (*a, b, c*), 1984 (*d, e, f*), and 1985 (*g, h, i*). The solid lines in (*h*) and (*i*) are optimal fits from the ELSIM.

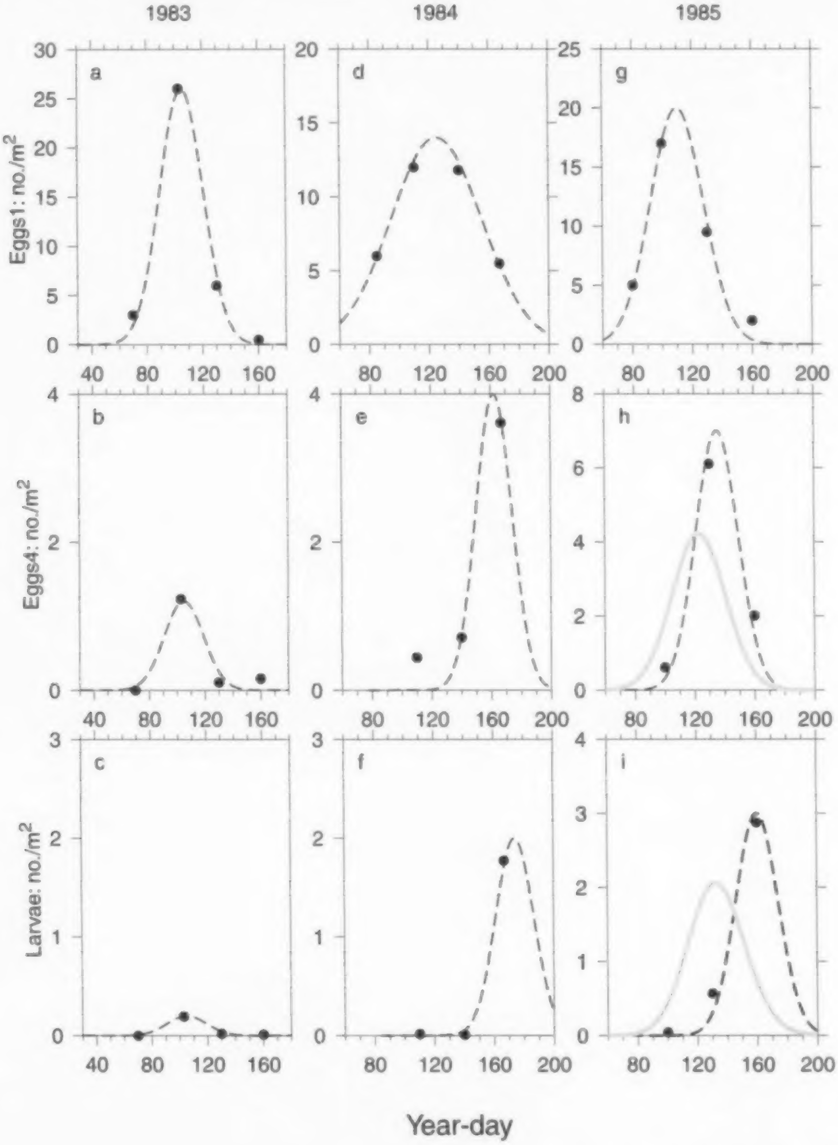

that the abundance data are underestimated for April, which affects interpretations based on the ELSIM analysis.

Figures 9*d*–9*f* show the 1984 FEP E1, E4, and larval data and possible Gaussian fits. Regardless of the uncertainty in the year-day 110 data, the data suggest the following. The spawning-duration curve peaked around year-day 120–130, with the E4 and larval peaks between year-days 160 and 180. There is a suggestion of a reduction in the spread of the latter two curves, in violation of property 2. The offset in $E4_p$ (30–40 days), from property 1, is not consistent with the peak in spawning. Similarly, the observed L_p would imply an extremely low mortality. Note that the C89 estimate $M_L = 0.25$ would imply a roughly 20-day offset in L_p, which is consistent with the 1984-model output but not with the data. These deductions lead us to conclude that a constant-mortality model is not consistent with the 1984 FEP data.

Resolving the model discrepancies: 1985

The 1985 FEP data are shown in Figs. 9*g*–9*i*. Peak spawning is suggested to have occurred at about year-day 110, with the E4 curve peaking around year-day 130 and the larval distribution 20–30 days later. While the delay in the E4 peak is somewhat long based on property 1 of the ELSIM, it is within the uncertainty in the estimation of these parameters.

Fig. 10. Results from the integral model with year-day dependent mortality (solid lines) compared with the FEP data (solid circles) for E4 and larvae (*L*). The mortality parameters are indicated in the figure.

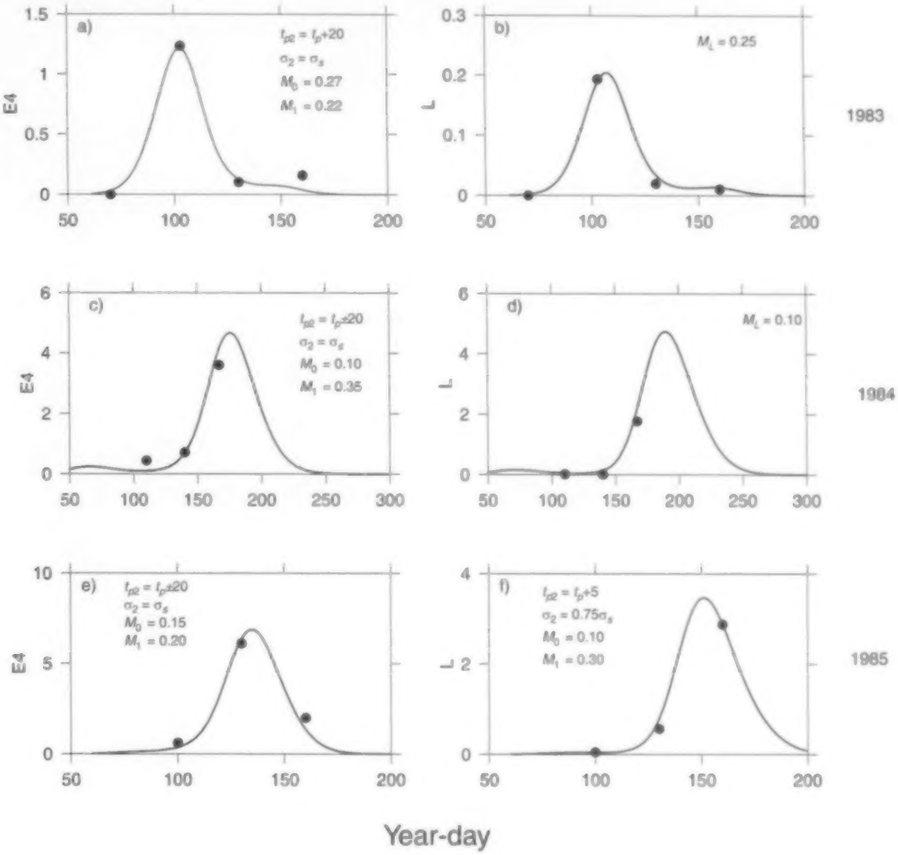

The peak in the larval data, however, is not consistent with the high (0.5·day^{-1}) mortality estimate in C89. From Fig. 8*a*, a larval mortality of 0.5 results in an offset in L_p of about 20 days relative to t_p, much shorter than the 40- to 50-day delay suggested by the data, which implies that a much lower mortality is required.

To see how well these data could be simulated by the ELSIM, the model was run in an optimization mode that searched for a minimum least squared model–data error with N_T, M_{E13}, M_{E4}, M_L, t_p, and σ_s as tunable parameters (t_p and σ_s were strongly constrained by the data). The result, shown as the thick curves in Figs. 9*h* and 9*i*, is rather unsatisfactory. The problem stems from the fact that the low larval mortality required to offset L_p relative to t_p would result in far too many larvae. The model best fit is a compromise that misses the E4 and larval points roughly equally. We conclude that a constant-mortality model cannot reproduce these data.

Year-day dependent mortality

The ELSIM with constant-stage mortality can be replaced with one in which mortality is time dependent. While this, in general, does not result in a unique solution, it is interesting to see if better fits to the data can be made using a simple model in which mortality is a function of year-day.

Our conceptual model is the following. We consider that the primary causes of mortality are variable egg quality, predation, and larval food supply. Of these, only predation is common to both stages and we assume that it would affect eggs and young larvae equally. In other words, the "average" predator consumes both eggs and larvae—an assumption consistent with Table 1 of Bailey and Houde (1989). We use a canonical year-day dependent mortality ($M(t)$) function of the form:

$$M(t) = M_0 + M_1 \exp\left(-\frac{(t - t_{p2})^2}{2\sigma_2^2}\right) \qquad (5)$$

where M_1, t_{p2}, and σ_2 are the amplitude, peak time, and spread for the year-day dependent part of the mortality function, and M_0 represents a baseline mortality. This mortality function could apply to eggs and larvae separately (different parameters) or simultaneously. If the latter pertains, then predation mortality is implicated, otherwise egg viability or larval food supply is suggested. We stress that we are only offering *possible* interpretations consistent with the required mortality—the interpretations, like the functions themselves, are not unique. As well, spatially dependent predation, not possible in the ELSIM, could explain apparent time-dependent effects, if, for example, eggs and larvae drifted into different regions at different times and encountered predators.

We deduce the various parameters from inspection of the data. For example, in 1983, the fact that the E4 curve is not offset relative to the spawning curve suggests that egg mortality increased somewhere near the spawning peak. In Fig. 10*a*, we show the result of applying eq. 5 to the egg stage (with $t_{p2} = t_p + 20$, $\sigma_2 = \sigma_s$, $M_0 = 0.27$, and $M_1 = 0.22$), with larval mortality constant ($M_L = 0.25$). The fact that egg mortality is a function of year-day while larval mortality is constant suggests that egg viability rather than predation was relevant. If egg predation was important, then we would expect that this would affect larvae as well, because the peak in $M(t)$ occurs when there would be young larvae in the water column.

In 1984, the delayed E4 peak with respect to spawning suggests that eggs spawned early experienced increased mortality. We ran the ELSIM with year-day dependent egg mortality ($t_{p2} = t_p - 20$, $\sigma_2 = \sigma_s$, $M_0 = 0.10$, and $M_1 = 0.35$) and larval mortality constant ($M_L = 0.10$). The result (Fig. 10*b*) again shows the ability to match the data with a year-day dependent mortality model, and suggests the same conclusion as for 1983, i.e., that differences in spawned egg viability can account for the shapes in the egg and larval distributions.

As shown previously, the 1985 data were impossible to fit using a constant-mortality model, even when optimally determined. To match the data using the year-day dependent mortality ELSIM required separate mortalities for both egg and larval stages. The egg-stage values were $t_{p2} = t_p - 20$, $\sigma_2 = \sigma_s$, $M_0 = 0.15$, and $M_1 = 0.20$, while those for the larval stage were $t_{p2} = t_p + 5$, $\sigma_2 = 0.75\ \sigma_s$, $M_0 = 0.10$, and $M_1 = 0.30$.

The result is shown in Figs. 10*e* and 10*f*. The interpretation of the mortality functions is more difficult in this case. Under the assumption that predation would affect eggs and small larvae equally, the fact that the year-day mortality functions are different would reject this possibility. Given this, the larval function, with its peak at $t_{p2} = t_p + 5$, suggests a starvation effect for larvae hatched near t_{p2}, with an egg viability deficiency explaining the egg mortality.

The year-day dependent mortality functions can be transferred to the ELS model as well. However, because the hatch times and stage durations in the ELS model are not constant, and the two models are not *numerically* equivalent, the transfer is not seamless. In practice, starting from the ELSIM parameters, the ELS model needed a few iterations to obtain correct integral values. The ELSIM serves as a useful front end for the ELS model because it integrates quickly and allows the testing of various mortality possibilities.

Figure 11 shows model versus data contour plots of the larval distributions for 1984 and 1985 for the months where larvae were found in the data. These can be compared with Figs. 4 and 5. Because no larvae were found in 1983, the E4 comparison is shown. The results are far superior to the constant-mortality runs, but indicate that, although the model integrated values are correct, significant discrepancies still exist in the spatial distributions.

Determining abundance and mortality from survey data

We have seen that the constant-mortality ELS model run with the C89 mortality estimates gives a rather poor fit to the spatial–temporal FEP data. The analysis of the ELSIM has shown that improvements can be made to the mortality estimates, but that a constant-mortality model is not supported by the data. We ask whether there is an inconsistency here.

The C89 mortality estimates were based on sequential stage equations of the form

$$(6)\qquad N_1 = N_0 e^{-M_{01} ts_{01}}$$

where N_0 and N_1 are the total number in the sequential stages 0 and 1, respectively; M_{01} is the mortality; and ts_{01} is the (average) duration between stages. By estimating N_0 and N_1 from data and knowing ts_{01}, M_{01} can be determined. Although this is not discussed in C89 in detail, there is nothing in the above equation that requires the actual mortality to be constant. The equation is simply the statement that, if the total abundances are known, then they can be equated via an exponential-mortality assumption. If mortality is constant, then eq. 6 is exact. If mortality is a function of time, then the consistency requirement is that $M_{01} ts_{01} = M(t)dt$, i.e., that the average mortality over the average stage duration is equal to the time integral of the actual mortality.

The problem lies in determining total stage abundances from data such as that shown in Fig. 9 to estimate mortality. The C89 expression for total abundance is found by integrating the abundance data, i.e.,

$$N_1 = \frac{\int N_1(t)dt}{ts_1}$$

where ts_1 is the stage duration, and $N_1(t)$ is time-dependent field data. It can be shown (for any $N_1(t)$) that this expression is exact only if mortality is zero (i.e., $N_1(t)dt = ts_1 N_1$), otherwise it underestimates N_1. As an illustration, suppose we want to determine the total number of larvae

$$\boldsymbol{L} = \frac{\int L(t)dt}{t_j}$$

using the ELSIM, to estimate the effective egg mortality from

$$(7)\qquad \boldsymbol{L} = \boldsymbol{E}\, e^{-M_E \Delta t}$$

where $\boldsymbol{E} = \int E(t)\, dt / t_h$ is the total number of eggs and Δt is the duration between stages. The bottom panel of Fig. 8 is a plot of the area under the larval curve:

$$L_{area} = \int L(t)dt = \int_{-\infty}^{\infty} \left\{ \int_{t-t_j}^{t} g(t' - t_h) e^{-M_L(t-t')} dt' \right\} dt$$

normalized by $N_T \times K$, versus M_L for $t_j = 45$ days. (Recall that K is the total egg mortality.) The quantity $N_T \times K$ is the total number of eggs surviving to become larvae (the value of $\boldsymbol{L}$ that we desire). The curve has an intercept at t_j and varies like $1/M_L$ for $M_L \geq 0.05$. Because $L_{area}/(K \times N_T) \leq t_j$, $\boldsymbol{L}$ underestimates the total larval abundance for $M_L \neq 0$. Note

Fig. 11. ELS model run with year-day dependent mortalities versus FEP data for 1983–1985. Solid lines connect panels for direct comparison. See text for details.

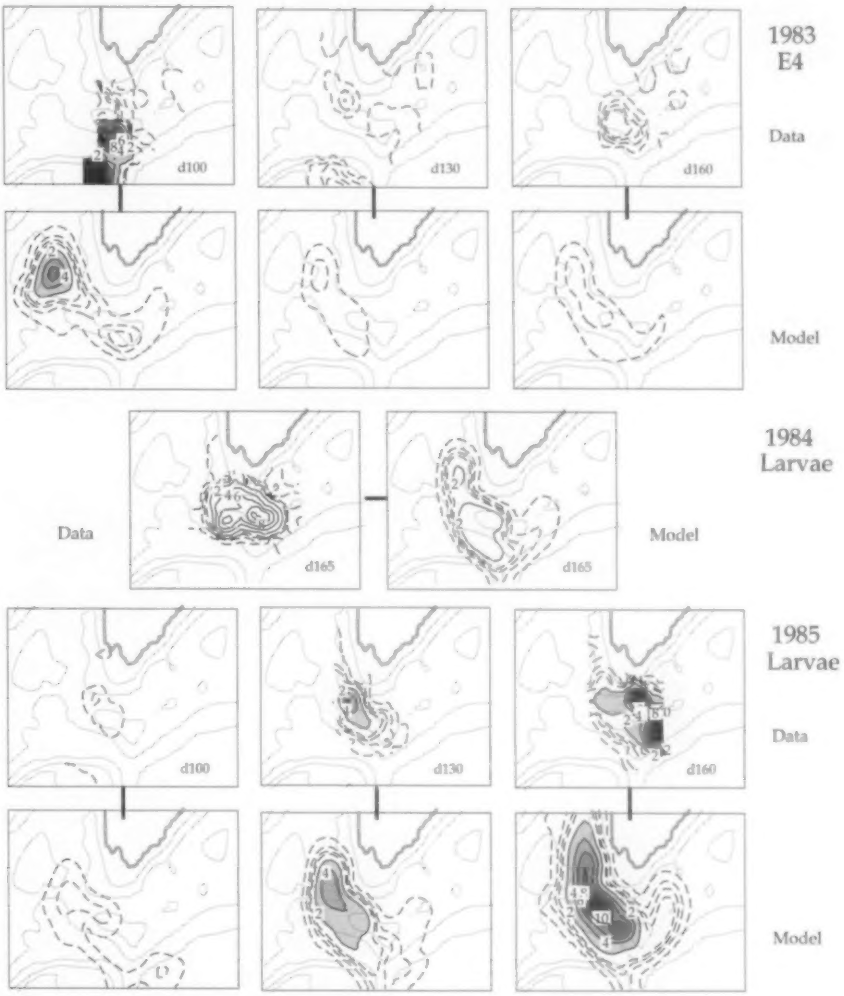

that both ***L*** and ***E*** will be underestimated, so that eq. 7 could still yield a reasonable estimate of M_E.

The reason $L_{area}/t_j \leq K \times N_T$ is because the larval distribution is the result of the production (hatching) and decay (mortality) of larvae, and both these terms are strongly time dependent over the larval time scale. In other words, there is significant death of larvae before the juvenile stage begins, so it is impossible, without a model such as the ELSIM, to recover the total number of larvae by integrating under the larval-distribution curve.

How do we estimate effective mortality from this kind of field data? The properties of the ELSIM give us two possible methods. The simplest (method 1) is to fit a Gaussian curve to the data and determine where the peak lies relative to peak spawning. Curves such as the one in Fig. 8*a* allow estimation of mortality. Similarly, by curve-fitting and integrating under the curve (method 2), if N_T and the total previous-stage mortality are known, then the mortality can be read from curves such as the one in Fig. 8*d*. (We assume that N_T is known from stock-assessment and fecundity estimates—itself a key assumption.) Note that, if mortality is truly constant, then the two methods would give the same answer. If the answers are different, then this discrepancy indicates that the data are not consistent with a constant-mortality model. This explains the problem in fitting the 1985 data using the ELSIM: the low larval mortality demanded by property 1 is contrary to the higher mortality required to fit the total number of larvae. This ability to discern the appropriateness of a constant-mortality model is one of the most useful results of the analysis of the integrated model.

Which of these methods is superior? First of all, note that, aside from the problem of fitting curves to a limited number of data points, both methods suffer from a high sensitivity, owing to the slope of the curves at high mortalities. If there were enough data points so that there was high confidence in the curve fit, then this inherent sensitivity problem would be reduced. A downside of the second method is the necessity to know the total mortality up to the stage in question, for example, K in $L_{\mathrm{area}}/(K \times N_{\mathrm{T}})$. This means that this method would have to be applied successively, starting from a stage that has no previous mortality. Using the example from the ELS model, we have

$$\frac{\mathrm{E13}_{\mathrm{area}}}{N_{\mathrm{T}}} = f_1(M_{\mathrm{E13}})$$

where E13 represents egg stages 1–3. This gives us M_{E13}.

$$\frac{\mathrm{E4}_{\mathrm{area}}}{N_{\mathrm{T}}\, k_{13}} = f_2(M_{\mathrm{E4}})$$

where $k_{13} = \mathrm{e}^{-M_{\mathrm{E13}}\mathrm{ts}_{13}}$, which yields M_{E4}, and

$$\frac{L_{\mathrm{area}}}{N_{\mathrm{T}}\, K} = f_3(M_{\mathrm{L}})$$

where $K = k_{13}\,\mathrm{e}^{-M_{\mathrm{E4}}\mathrm{ts}_{4}}$, which yields M_{L}. Note that we require a curve for E13 that is not available for this data set. Therefore, a possible advantage of method 2—the ability to derive bulk estimates of mortality where method 1 would fail (e.g., 1983, where the abundance peaks seem to coincide)—may not always be realizable.

An implicit assumption in calculating abundance mortalities is that there are no losses from the sampling grid. We have seen that this is likely to have been the case in April 1984, with hints that the FEP grid missed eggs and larvae in other months as well. Although there is no systematic way to adjust for this, method 1 could still give a correct answer, because it depends on estimating the time of the peak in the distribution and, if the sampling grid is representative of the total domain, this peak will be unaffected. On the other hand, an integral method will yield an incorrect answer, if there are losses from the sampling domain.

Summary

We have described an early life stage model applied to the evolution of haddock eggs and larvae in SWN. Motivated by the C89 abundance–survival calculations, the model was run in constant-mortality mode, and its output compared with the 1983–1985 FEP data. The model did a systematically poor job of simulating the data. To investigate this problem, an integral version of the ELS model was derived.

Analysis of the early life stage integral model led to a method for determining whether sequential-stage field data are consistent with a stage-dependent constant-mortality model, and showed that the FEP data could not be modelled using a constant-mortality model. Because the ELSIM integrates quickly, it serves as a useful tool for exploring possible time-dependent-mortality models. We have shown that the FEP abundance data can be matched by using simple year-day dependent egg and (or) larval mortality functions, and discussed what these may mean in terms of likely causes of egg and larval mortality.

The ELS model reported here does not explicitly make use of the Campana–Hurley age–temperature relationship to predict larval length and the length based mortality model, eq. 2. This sort of model has shown some skill in simulating environmental data (Brickman et al. 2001; Heath and Gallego 1998). However, for the FEP egg and larval data, runs with this version of the model were not significantly better than with the constant-mortality model, especially when compared with the time dependent mortality model results derived from the ELSIM analysis.

This illustrates how important mortality is in determining egg and larval distributions and how the temperature-based growth and mortality relations, which can be thought of as representing behaviour in average conditions, may not be good enough in specific instances. As a corollary, if the egg viability relations and predator–prey fields are required to be known in detail to satisfactorily simulate the evolution of the early life stages—a fact that is not surprising—then the demands on modelling and data streams are much greater. Future work in biophysical modelling and data comparison will help determine the necessary degree of complexity required to answer specific questions.

Acknowledgements

We thank Charles Hannah and Jennifer Shore for making the circulation fields available; Charles Hannah for the method of adapting them for individual months; and John Loder and Nancy Shackell for comments and internal review. This is a contribution of the GLOBEC Canada Program, jointly funded by the Department of Fisheries and Oceans and the Natural Sciences and Engineering Research Council of Canada.

References

Anderson, J.T., and deYoung, B. 1995. Application of a one-dimensional model to vertical distributions of cod eggs on the northeastern Newfoundland shelf. Can. J. Fish. Aquat. Sci. **52**: 1978–1989.

Bailey, K.M., and Houde, E.D. 1989. Predation on eggs and larvae of marine fishes and the recruitment problem. Adv. Mar. Biol. **25**: 1–83.

Brickman, D., Shackell, N.L., and Frank, K.T. 2001. Modelling the retention and survival of Browns Bank haddock larvae using an early life stage model. Fish. Oceanogr. In press.

Campana, S.E., and Hurley, P.C.F. 1989. An age- and temperature-mediated growth model for cod (*Gadus morhua*) and haddock (*Melanogrammus aeglefinus*) larvae in the Gulf of Maine. Can. J. Fish. Aquat. Sci. **46**(Suppl. 1): 603–613.

Campana, S.E., Frank, K.T., and Hurley, P.C.F. 1989. Survival and abundance of young Atlantic cod (*Gadus morhua*) and haddock (*Melanogrammus aeglefinus*) as indicators of year-class strength. Can. J. Fish. Aquat. Sci. **46**(Suppl. 1): 171–182.

Frank, K.T., Page, F.H., and McRuer, J.K. 1989. Hydrographic effects on the vertical distribution of haddock (*Melanogramus aeglefinus*) eggs and larvae on the Southwestern Scotian shelf. Can. J. Fish. Aquat. Sci. **46**(Suppl. 1): 82–92.

Han, G., Loder, J.W., and Smith, P.C. 1999. Seasonal-mean hydrography and circulation in the Gulf of St. Lawrence and on the eastern Scotian and southern Newfoundland shelves. J. Phys. Oceanogr. **29**: 1279–1301.

Hannah, C.G., Shore, J.A., and Loder, J.W. 2000*a*. The drift–retention dichotomy on Browns Bank: a model study of interannual variability. Can. J. Fish. Aquat. Sci. **57**: 2506–2518.

Hannah, C.G., Shore, J.A., Loder, J.W., and Naimie, C.E. 2000*b*. Seasonal circulation on the central and western Scotian Shelf. J. Phys. Oceanogr. In press.

Heath, M., and Gallego, A. 1997. From the biology of the individual to the dynamics of the population: bridging the gap in fish early life studies. J. Fish Biol. **51**(Suppl. A): 1–29.

Heath, M., and Gallego, A. 1998. Bio-physical modelling of the early life stages of haddock, *Melanogrammus aeglefinus*, in the North Sea. Fish. Oceanogr. **7**: 110–125.

Hermann, A., and Stabeno, P. 1996. An eddy resolving model of circulation on the western Gulf of Alaska shelf. I. Model development and sensitivity analysis. J. Geophys. Res. **101**: 1129–1149.

Houde, E.D. 1997. Patterns and trends in larval-stage growth and mortality of teleost fish. J. Fish Biol. **51**(Suppl. A): 52–83.

Hurley, P.C.F., and Campana, S.E. 1989. Distribution and abundance of haddock (*Melanogrammus aeglefinus*) and Atlantic cod (*Gadus morhua*) eggs and larvae in the waters off southwest Nova Scotia. Can. J. Fish. Aquat. Sci. **46**(Suppl. 1): 103–112.

Laurence, G.C. 1985. A report on the development of stochastic models of food limited growth and survival of cod and haddock larvae on Georges Bank. NOAA (Natl. Ocean. Atmos. Adm.) Tech. Mem. NMFS-F/NEC-36.

Lynch, D., Ip, J., Naimie, C., and Werner, F. 1996. Comprehensive coastal circulation model with application to the Gulf of Maine. Continental Shelf Res. **6**: 875–906.

Lynch, D.R., Werner, F.E., Greenberg, D.A., and Loder, J.W. 1992. Diagnostic model for barloclinic, wind-driven and tidal circulation in shallow seas. Continental Shelf Res. **12**: 37–64.

Lynch, D.R., Gentleman, W.C., McGillicuddy, D.J., and Davis, C.S. 1998. Biological/physical simulations of *Calanus finmarchicus* population dynamics in the Gulf of Maine. Mar. Ecol. Prog. Ser. **169**: 189–210.

Page, F.H., and Frank, K.T. 1989. Spawning time and egg stage duration in Northwest Atlantic haddock (*Melanogrammus aeglefinus*) stocks with emphasis on Georges and Browns Bank. Can. J. Fish. Aquat. Sci. **46**(Suppl. 1): 68–81.

Rodean, H.C. 1996. Stochastic Lagrangian models of turbulent diffusion. American Meteorological Society, 45 Beacon St., Boston, MA 02108.

Shackell, N.L., Frank, K.T., Petrie, B., Brickman, D., and Shore, J. 1999. Dispersal of early life stage haddock (*Melanogrammus aeglefinus*) as inferred from the spatial distribution and variability in length-at-age of juveniles. Can. J. Fish. Aquat. Sci. **56**: 2350–2361.

Smith, P.C. 1983. The mean and seasonal circulation off southwest Nova Scotia. J. Phys. Oceanogr. **46**: 539–559.

Smith, P.C. 1989. Seasonal and interannual variability of current, temperature and salinity off southwest Nova Scotia. Can. J. Fish. Aquat. Sci. **46**(Suppl. 1): 4–20.

Waiwood, K.G., and Buzeta, M.I. 1989. Reproductive biology of southwest Scotian shelf haddock (*Melanogrammus aeglefinus*). Can. J. Fish. Aquat. Sci. **46**(Suppl. 1): 153–170.

Werner, F.E., Perry, R.I., Lough, R.G., and Naimie, C.E. 1996. Trophodynamic and advective influences on Georges Bank larval cod and haddock. Deep-Sea Res. **43**: 1793–1822.

Appendix. Repeated-use symbols.

Symbol	Definition
ELS model	
t_p	Peak in spawning distribution
σ_s	Spread in Gaussian distribution
N_T	Total number of spawned eggs
t_h	Hatch time
M_X	Exponential mortality rate for stage X (fraction·day^{-1})
E13	Egg stages 1–3
E4	Egg stage 4
ELSIM	
t	Time
$G(t)$	Gaussian spawning duration curve
$L(t)$	Larval distribution
t_j	Duration of larval stage
ts_{13}	Duration of E13
ts_4	Duration of E4
k_{13}	Total mortality of E13
k_4	Total mortality of E4
K	Total mortality of egg stage
E4(t)	E4 distribution
L_p	Peak in larval distribution (year-day)
$\mathrm{E4}_p$	Peak in E4 distribution (year-day)
σ_L	Spread in larval distribution (days)
M_0	Baseline mortality rate for year-day dependent mortality model
M_1	Amplitude of year-day dependent mortality
t_{p2}	Peak (year-day) of year-day dependent mortality model
σ_2	Spread (days) of year-day dependent mortality model
Determining abundance and mortality from survey data	
N_0	Total number in sequential stage 0
N_1	Total number in sequential stage 1
M_{01}	Mortality rate between stages 0 and 1
ts_{01}	Duration between stages 0 and 1
$N_1(t)$	Time distribution of stage 1
L	Total number of larvae
E	Total number of eggs
L_{area}	Area under larval-distribution curve
$\mathrm{E13}_{\mathrm{area}}$	Area under E13-distribution curve
$\mathrm{E4}_{\mathrm{area}}$	Area under E4-distribution curve

Annual and interannual variability of nutrients and their estimated fluxes in the Scotian Shelf – Gulf of Maine region

Brian Petrie and Philip Yeats

Abstract: Nitrate, silicate, and phosphate observations are used to determine their annual cycles for the Scotian Shelf and the Gulf of Maine. Concentrations increase from fall through winter, decrease rapidly at shallow depths in late winter, and remain at low levels through spring and summer. Deep layers exhibit a weak annual cycle with highest concentrations in summer. Winter nitrate concentrations (depth ≤50 m) are highest on the eastern Scotian Shelf, decreasing southwestwards into the Gulf of Maine. The Gulf of St. Lawrence is the primary source of nitrate (9300 mol·s^{-1}) and silicate (7680 mol·s^{-1}) during winter for the Scotian Shelf; in spring and summer, vertical diffusive fluxes, 1500–1000 mol·s^{-1} for the central Scotian Shelf, are as large as the horizontal advective ones and can provide the entire nitrate requirement. The 50-m vertical diffusive fluxes of nitrate and silicate vary by a factor of 4 in the Scotian Shelf – Gulf of Maine region. The interannual variability of nitrate and dissolved oxygen on the Scotian Shelf are coupled to water mass changes, with low (high) nitrate and high (low) dissolved oxygen concentrations corresponding to the dominance of Labrador (Warm) Slope water.

Résumé : À partir d'observations portant sur le nitrate, le silicate et le phosphate, nous avons déterminé les cycles annuels de ces composés pour la plate-forme Néo-Écossaise et le golfe du Maine. Les concentrations augmentent pendant l'automne et l'hiver, baissent rapidement à faible profondeur à la fin de l'hiver, et restent à un bas niveau pendant le printemps et l'été. Dans les couches profondes, on observe un cycle annuel peu marqué, avec les plus fortes concentrations en été. Les concentrations hivernales de nitrate (profondeur ≤ 50 m) sont les plus élevées sur l'est de la plate-forme Néo-Écossaise, et diminuent en direction sud-ouest vers le golfe du Maine. Le golfe du Saint-Laurent est la première source de nitrate (9300 mol·s^{-1}) et de silicate (7680 mol·s^{-1}) pour la plate-forme Néo-Écossaise; au printemps et en été, les flux diffusifs verticaux, de 1500 à 1000 mol·s^{-1} pour le centre de la plate-forme Néo-Écossaise, sont aussi grands que les flux advectifs horizontaux, et peuvent fournir l'ensemble de l'apport en nitrate. Les flux diffusifs verticaux de nitrate et de silicate dans la couche de 50 m varient d'un facteur de 4 dans l'ensemble de la région (plate-forme Néo-Écossaise – golfe du Maine). La variabilité interannuelle du nitrate et de l'oxygène dissous sur la plate-forme Néo-Écossaise est couplée à des changements dans les masses d'eau, car on observe, selon la masse d'eau dominante, eau de pente du Labrador (eau de pente chaude), des concentrations faibles (fortes) de nitrate et fortes (faibles) d'oxygène dissous.

[Traduit par la Rédaction]

Introduction

Although a considerable amount of nutrient data have been collected in the Scotian Shelf – Gulf of Maine region, the annual cycle of nutrients has only been examined in a few cases and then for individual years. Fournier et al. (1977) showed, from four cruises, one in each season over a 16-month period, nitrate and phosphate distributions across the Scotian Shelf on a line running south-southeast from Halifax to the 2500-m isobath on the continental slope (see the Halifax section, Fig. 1). In the upper 50 m across the shelf and over the continental slope, the maximum observed nitrate concentrations of 5–10 µM occurred in March. By May, this layer was largely depleted of nitrate, remaining that way through August and November. Throughout the year, nitrate in the deep inner basins of the shelf remained fairly constant with values of about 20 µM. Surface phosphate concentrations were also highest in March (0.5–0.9 µM, 0–50 m) but decreased more slowly than nitrate through the seasons. Deep basin concentrations were fairly steady at about 1.5 µM. Platt et al. (1972) sampled more frequently over a year in St. Margarets Bay a 60-m-deep inlet just to the west of Halifax. Maximum nitrate concentrations of 5 µM in the 0–20 m layer occurred in mid-March and declined precipitously to about 0.5 µM in mid- to late April. Concentrations remained low until mid- to late November

Received March 22, 2000. Accepted August 17, 2000. Published on the NRC Research Press web site on December 20, 2000. J15673

B. Petrie.[1] Fisheries and Oceans Canada, Ocean Sciences Division, Bedford Institute of Oceanography, P.O. Box 1006, Dartmouth, NS B2Y 4A2, Canada.
P. Yeats. Fisheries and Oceans Canada, Marine Environmental Sciences Division, Bedford Institute of Oceanography, P.O. Box 1006, Dartmouth, NS B2Y 4A2, Canada.

[1] Corresponding author (e-mail: petrieb@mar.dfo-mpo.gc.ca).

Fig. 1. Study region showing the location of areas (Cabot Strait (CS), Sydney Bight (SB), eastern (ESS), central (CSS), and western Scotian Shelf (WSS), Bay of Fundy (BF), and eastern (EGM), central (CGM), and western Gulf of Maine (WGM)) used to compute monthly mean nutrient concentrations and lines (Cabot Strait, Gully (1), Western Bank (2), Halifax section (A), Scotian Gulf (4), and Cape Sable (5)) for nutrient flux estimates. Place-names mentioned in the text include Emerald Basin (3), Browns Bank (6), Northeast Channel (7), and Georges Bank (8).

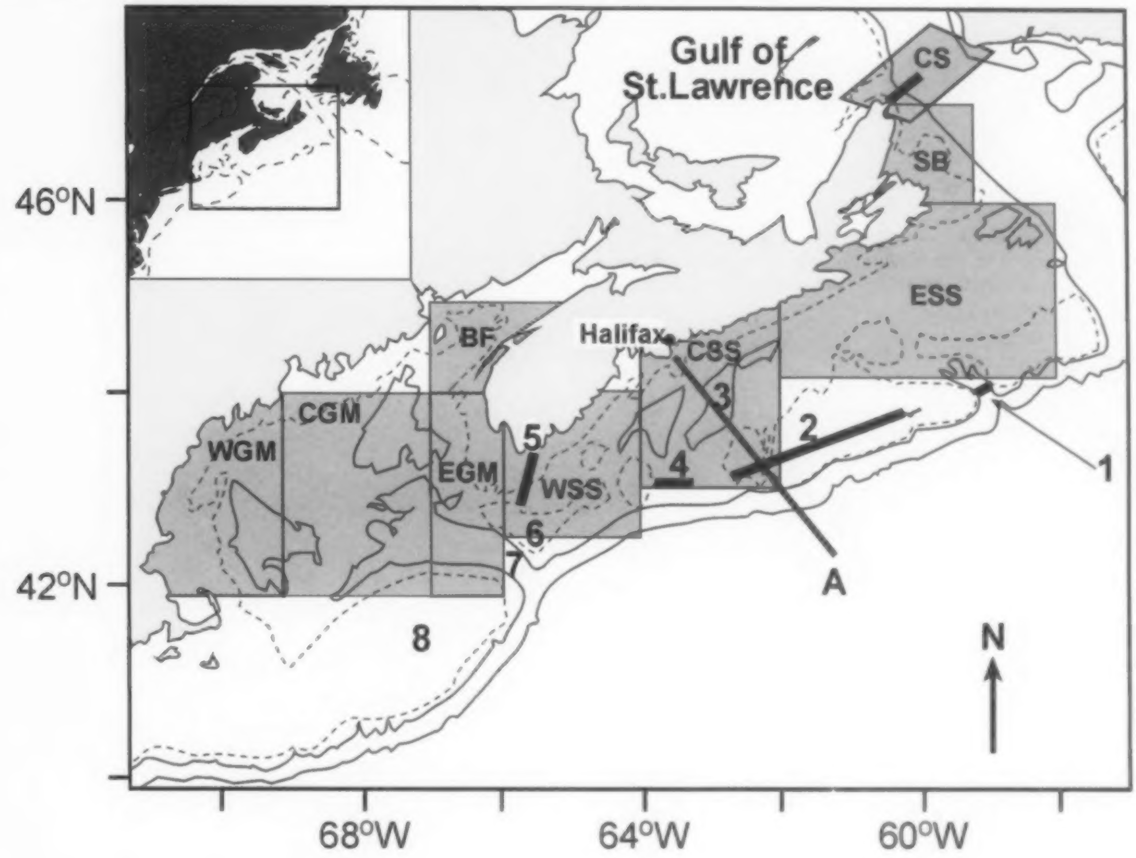

when they began to increase. For depths >20 m, the spring decline was more gradual, occurring over 2–3 months and decreasing from about 6 to 2 μM.

Schlitz and Cohen (1984) considered the nitrogen budget for the Gulf of Maine and Georges Bank. They did not present the annual cycle of nutrients but rather considered the supply from a number of mechanisms including advection. The two major advective sources of nitrate into the gulf were through the Northeast Channel (annual average transport was 5800 mol·s^{-1}) and from the inner shelf off southwest Nova Scotia (1 100 mol·s^{-1}). The total advective flux was about the same magnitude as the largest biological flux term (from macrozoplankton) and almost half the total flux from all biological components. On the northern flank of Georges Bank, nitrate in the 0–65 m layer shows an annual cycle with maximum mean concentrations in February of nearly 7 μM, falling to <1 μM by late May (Pastuzak et al. 1982). Concentrations in the layer with depths of 120 m to the bottom reach a peak of about 20 μM in December and fall to <10 μM in May. Samples were collected over a 13-month period on eight cruises with about 10–40 samples in each layer. The deeper layers showed more variability within a single cruise than the shallower layers. Similar variations were found in waters to the southwest of Georges Bank (Ketchum et al. 1958).

Since the early 1990s, the Marine Environmental Science Division (MESD) at the Bedford Institute of Oceanography (BIO) has been compiling a nutrient database that also includes a number of other chemical, biological, and physical variables. The data include not only those collected by MESD and other BIO divisions but also those archived by the Marine Environmental Data Service (MEDS) in Ottawa and the National Oceanographic Center (NODC) in Washington. In addition, considerable effort has been made to recover data from sources including government agencies, universities, and consulting firms, which may not have sent their observations to a national agency. Of the 16 variables in the database, by far the most extensive holdings are for nitrate, phosphate, silicate, temperature, salinity, and dissolved oxygen (for a description of the database holdings, see Petrie et al. 1999). The area of interest, 35–90°N and 40–90°W, encompasses the Atlantic coast of Canada, including the Gulf of St. Lawrence and the eastern Arctic Archipelago. For the Canadian Atlantic coast, the Scotian Shelf and the Gulf of Maine have the most extensive data set.

In this paper, we present the annual cycle in the form of monthly means of nitrate, silicate, and phosphate concentrations for the waters of the Scotian Shelf and the Gulf of Maine (Fig. 1). Examination of the data indicated that extensive editing was required before credible statistics could be derived. We used temperature, salinity, and dissolved oxygen observations to assist in editing the data and characterize water masses by their hydrographic and nutrient properties. We consider the spatial and temporal distribution of available data for the Scotian Shelf and the Gulf of Maine, the interannual variability of nutrients, and the vertical and horizontal fluxes of nitrate. The results will be used in a companion paper (B. Petrie et al., unpublished data) that considers the relationships between these distributions and fluxes and primary productivity.

Fig. 2. Annual cycle of the long-term monthly means (μM) of (*a*) nitrate, (*b*) silicate, and (*c*) phosphate concentrations for the central Scotian Shelf.

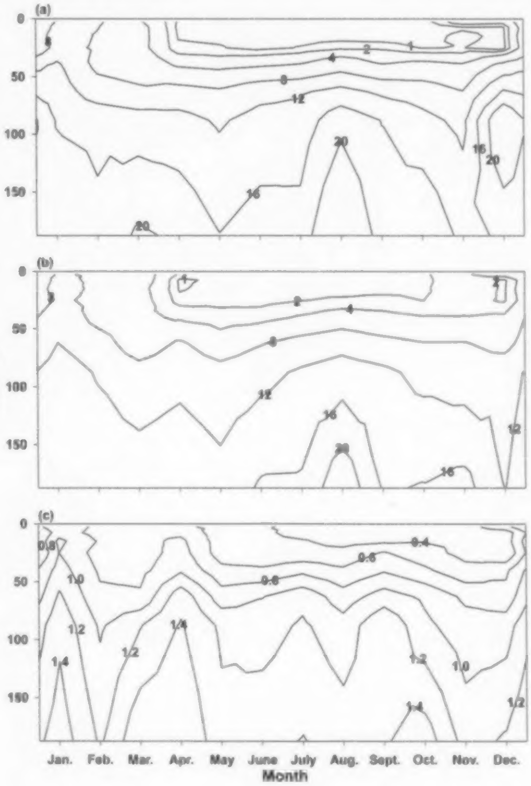

Methods

The seasonal and spatial distributions of nutrient observations used in this paper are given in Petrie et al. (1999). The density of data is greatest for the western half of the Scotian Shelf and the Gulf of Maine. The total number of observations is approximately equal for nitrate, silicate, and phosphate, with about 4000, 9500, 10 000, and 6000 measurements for each nutrient in winter, spring, summer, and fall. The eastern half of the Scotian Shelf, the upper Bay of Fundy, western Georges Bank, and the continental slope region are the least sampled areas. The data density generally decreases with depth, particularly for the fall and winter.

To describe the annual nutrient cycles, the Scotian Shelf was divided into five areas consisting of Cabot Strait, Sydney Bight, and eastern, central, and western Scotian Shelf (Fig. 1). The Gulf of Maine was divided into four areas consisting of the Bay of Fundy and eastern, central, and western Gulf of Maine. The sizes of the areas and the depth intervals (0–5, 5–10, 10–20, 20–30, 30–50, 50–75, 75–100, and 100–275 m) were chosen to assure that, for the most part, there were sufficient data to calculate meaningful monthly statistics. The Cabot Strait, Sydney Bight, and Bay of Fundy regions had the fewest data and the most months with fewer than 10 observations. The monthly mean concentrations and statistics for all areas are presented in Petrie et al. (1999).

Optimal estimation was used to convert randomly distributed values of a chosen variable to a grid fixed in space and time (Bretherton et al. 1976). The technique, as applied here to the nutrients, requires a four-dimensional (x, y, z, and t corresponding to the east, north, depth, and time coordinates) correlation function to be specified, where the correlation decreases with a specified decay scale. We chose the function covariance = $e^{-s}(1 + s + s^2/3)$ used by Petrie et al. (1996) for the temperature, salinity, and density fields, with (x, y, z, t) scales of (40 km, 40 km, 15 m, 45 days) for January–March for 0–30 m and (30 km, 30 km, 15 m, 30 days) for the other months (below 30 m, the z scale was 25 m for all months). The variable s is the nondimensional pseudo-distance from the fixed grid points to each data point and is defined as the square root of the sum of the squares of the three spatial distances and the time difference divided by their respective scales. We included time in the interpolation scheme because of data sparseness, particularly in late fall and winter when nutrient concentrations can change rapidly. Additional details of the technique and the choice of scales are given in Petrie and Dean-Moore (1996). The input data consist of the observations in our database after quality control and removal of data from inlets. Uncertainties increase as distance from the observation sites to the point of estimation in space or time. The technique uses a fixed number of points nearest (in the nondimensional sense) to the grid point where an estimate is to be made. Fifteen and 50 nearest neighbours gave nearly the same results in test runs. We settled on the former to economize on computation times. We used a grid with 12 × 12′ resolution in latitude and longitude, levels at 0, 30, 50, 100, and 150 m, where the depth permitted, and the bottom depth (or 1000 m, whichever was shallower). Estimates were made for the 15th of February, May, August, and November, the midpoints of the seasons. A complete set of nutrient distributions is given in Petrie et al. (1999). In this paper, we shall concentrate on the nitrate distributions.

Results and discussion

Annual cycle of nitrate, silicate, and phosphate

The annual cycles of nitrate, silicate, and phosphate are shown for the central Scotian Shelf in Fig. 2. This region had an average of 31 observations in each depth range for all months except December, which had about three samples per interval below the 0–5 m layer. Nitrate and silicate at shallow depths reach their highest values of about 10 μM in the winter, after which there is a rapid decrease in the late winter and the early spring. Concentrations remain low throughout the summer before starting to increase in the late fall. This general pattern is followed in the other regions as well; however, the absolute concentrations and the rate of

Fig. 3. Long-term monthly 0–50 m average (*a*) nitrate, (*b*) silicate, and (*c*) phosphate concentrations for the eastern (circles), central (squares), and western (triangles) Scotian Shelf (solid symbols) and the Gulf of Maine (open symbols). The solid line is used for the central Scotian Shelf to provide a reference for comparison among regions.

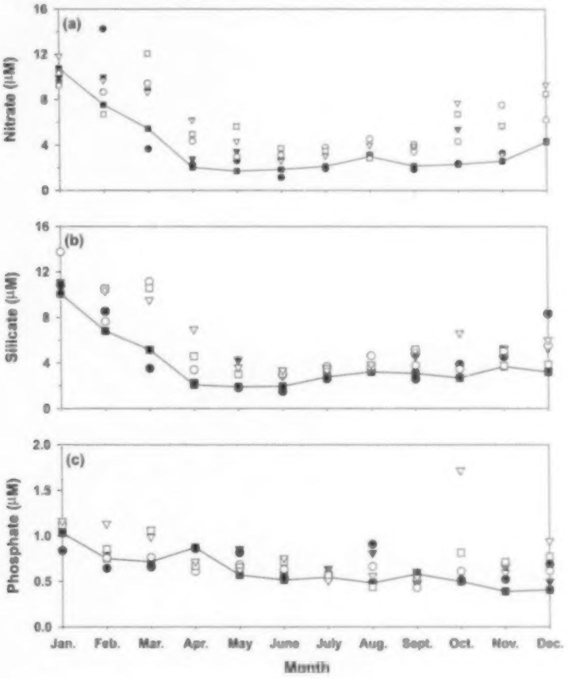

decrease differ (Petrie et al. 1999). This is illustrated in Fig. 3 where the monthly averaged nutrient concentrations in the 0–50 m depth range for six regions are shown. A representative standard deviation for nitrate and silicate is about 1 µM, and that for phosphate is about 0.1 µM. Maximum concentrations in the central Gulf of Maine occur later than on the Scotian Shelf; moreover, the decrease of nitrate is more rapid. It also appears that nutrient levels in the central and eastern Scotian Shelf are generally lower than in the other four regions.

Nitrate and silicate levels increase from February to August by about 40% in the 75–135 m layer in the central Scotian Shelf region (where the average bottom depth is 135 m) (Fig. 2). These increases may partially reflect the sinking and decomposition of the spring bloom. There is no evidence of an annual cycle of the temperature and salinity in this layer that varies systematically with the nutrients; thus, the annual cycle of nutrients does not appear to be simply related to water mass variations. Again, this general pattern holds in the other regions but can occur with different timing and magnitude. For example, in the 50–100 m range for the western Scotian Shelf, which is generally shallower than the other regions, nitrate increases by 25% from April to June, while silicate increases by about 20%. Concentrations then remain reasonably constant through to November. Additional increases are indicated in December, although we have less confidence in the result because of fewer observations.

Near-surface phosphate concentrations do not show the dramatic decrease that nitrate and silicate do in the late winter and early spring (Figs. 2 and 3). The concentrations decrease gradually, reaching minimum values in midsummer that are relatively high compared with those of nitrate. Rapid recycling of phosphate in surface water by the planktonic ecosystem could account for these observations (Harrison 1983). Problems associated with editing the phosphate data are illustrated by the high October concentration for the western Gulf of Maine (Fig. 3). There was an average of 43 observations for each depth interval; at each depth, the data were spread continuously from their minimum to maximum values, i.e., there were not any obvious outliers.

The variability of concentrations is dependent on nutrient, depth, and month. However, a representative standard deviation for nitrate and silicate for depths >50 m and for all months is 3.5 µM. For individual depths in the range 0–50 m, a representative standard deviation is about 2 µM. For phosphate, the values for concentration and standard deviation are about one tenth of those for nitrate and silicate.

Seasonal, optimally estimated nutrient distributions

The seasonal, optimally estimated nitrate fields at 0 m shown in Fig. 4 complement the depth–time contours of Fig. 2 and show a number of interesting features: (*i*) the strong, wintertime along-shelf gradient on the Scotian Shelf, (*ii*) the rapid depletion of nitrate from winter to spring but with some relatively high concentrations remaining in the Gulf of Maine, (*iii*) the increase from summer to fall with the exception of the eastern Scotian Shelf, and (*iv*) the minimum in nitrate concentration in the middle Scotian Shelf, particularly in winter.

Nitrate levels are highest during winter on the eastern end of the Scotian Shelf and generally decrease southwestwards into the Gulf of Maine. The high values at the eastern end of the region could be attributed to several factors including (*i*) delayed onset of primary production relative to the rest of the shelf, (*ii*) an enhanced vertical supply of nutrients through mixing or upwelling processes, (*iii*) inadequate sampling during winter, and (*iv*) export of nitrate from the Gulf of St. Lawrence. There is evidence in the data that the nitrate levels in the eastern Scotian Shelf in the upper 50 m reach a well-defined maximum in February (Fig. 3), whereas nitrate decreases in the central Scotian Shelf and in the Gulf of Maine from January to February by 16–38%. Enhanced vertical supply through mixing or upwelling will be dealt with in more detail later when we estimate nitrate fluxes. The observations from this area in winter, January–March, are from only three years and thus could bias the optimally estimated field. There are even fewer data from the eastern Gulf of St. Lawrence at this time of year. As more winter data are collected, we shall be able to determine if the apparent alongshore gradient of nitrate in the near-surface waters is a real feature.

By spring, nitrate levels have decreased substantially throughout the region. However, concentrations are higher off southwest Nova Scotia, at the mouth of the Bay of Fundy, part way along the Maine coast, and over Georges Bank. Circulation models and limited in situ observations

Fig. 4. Optimally estimated surface nitrate concentrations (µM) for (*a*) midwinter, (*b*) midspring, (*c*) midsummer, and (*d*) midfall.

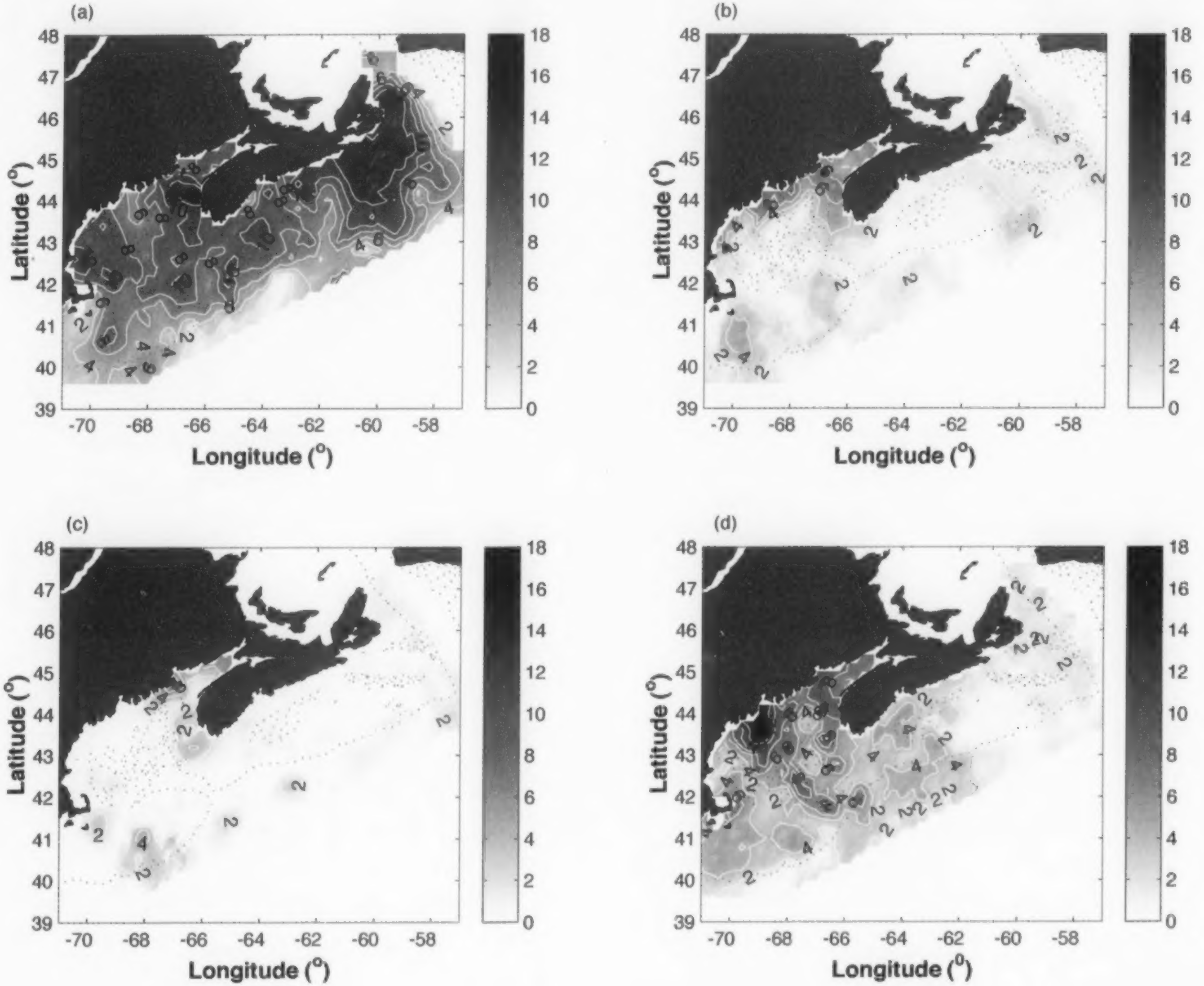
(a)
(b)
(c)
(d)
Latitude (°)
Longitude (°)
48
47
46
45
44
43
42
41
40
39
-70
-68
-66
-64
-62
-60
-58
18
16
14
12
10
8
6
4
2
0

Table 1. Nutrient fluxes on the Scotian Shelf (on-shelf positive) for the sections shown in Fig. 1.

	Nitrate flux (mol·s^{-1})		Silicate flux (mol·s^{-1})	
Area	December–February	June–August	December–February	June–August
Cabot Strait	9300	2290	7680	2180
Gully	450	700	290	500
Western Bank	1100	1850	770	1370
Western Scotian Gulf	–2450	–750	–1680	–1050
Cape Sable outflow	–2510	–320	–2730	–1040
Browns Bank gyre	1350	540	1500	810

Note: The fluxes were determined by combining long-term means for the nutrients with flows from archived current meter data.

have indicated that these are areas where vertical diffusivity is high, caused by strong tidal flows (Garrett et al. 1978; Gregory and Bussard 1996; Hannah et al. 2001); therefore, nutrient levels could remain elevated even in the presence of high primary productivity. Throughout the summer, concentrations are generally low, with an indication of higher values off southwest Nova Scotia, the Bay of Fundy, and Georges Bank. By fall, the nitrate levels have increased to the west of the Halifax section but remain low to the east. This pattern is followed at 30 m and less strongly at 50 m.

There is a minimum in the surface nitrate concentrations, particularly in winter, that extends south-southeast from Halifax in the central shelf and that widens towards the shelf edge. It is possible that this feature, which is also seen at 30 and 50 m, arises from the greater density of observations on the Halifax section that has been run intermittently along this track since 1950. On the other hand, both Han et al. (1997) and Sheng and Thompson (1996) showed on-shelf flow in this area between 61 and 62°W that may transport waters with lower nitrate concentrations onto the shelf.

Silicate does not show the marked along-shelf gradient in winter; the surface concentrations are more uniform throughout the region and generally range between 6 and 10 μM (Petrie et al. 1999). There is a large decrease in spring, with continuing low surface concentrations (1–2 μM) during summer. By fall, silicate levels increase quite uniformly over the entire region. A trough in the silicate concentrations is also evident in the middle of the Scotian Shelf as it was for nitrate.

Phosphate concentrations do not show the strong temporal or spatial gradients shown for silicate and nitrate. Winter surface concentrations have a range of 0.6–1.0 μM, with a tendency for higher values in the Gulf of Maine. Concentrations decrease about 0.2 μM by spring, a further 0.2 μM in summer, and then persist into the fall (Petrie et al. 1999).

Nutrient fluxes on the Scotian Shelf

We have combined current observations from moored instruments with long-term measurements of nitrate and silicate to determine the nutrient fluxes at a number of key areas on the Scotian Shelf for periods of high and low near-surface concentrations (Table 1). The areas include Cabot Strait, where the outflow from the Gulf of St. Lawrence is found, the Gully, Western Bank, and the Scotian Gulf, regions of cross-shelf flow, and southwest Nova Scotia, a site of outflow from the Scotian Shelf to the Gulf of Maine (see Han et al. (1997, 1999) and Hannah et al. (2001) for the general circulation of the region derived from diagnostic numerical modelling). Currents were obtained from the BIO database that contains monthly mean flows and statistics based on individual instrument records (http://www.mar.dfo-mpo.gc.ca/science/ocean/database/data_query.html). Nutrient profiles were from Petrie et al. (1999) or from additional queries of the MESD database. The section widths and maximum depths were 50 km and 150 m for Cabot Strait, 10 km and 150 m for the Gully, 210 km and 100 m for Western Bank, 50 km and 150 m for the western Scotian Gulf, 49 km and 100 m for the Cape Sable outflow, and 10 km and 100 m for the Browns Bank gyre (Fig. 1).

On-shelf transports of nitrate and silicate are dominated by the Cabot Strait outflow from the Gulf of St. Lawrence during the December–February period when near-surface concentrations are high. Off-shelf transports from the western Scotian Gulf and the Cape Sable outflow are about 50–60% of the inflow at Cabot Strait. For the June–August period when near-surface concentrations are low, there are comparable on-shelf transports of nitrate and silicate at Cabot Strait and Western Bank; off-shelf fluxes again occur in the western Scotian Gulf and Cape Sable. There is a significant component of on-shelf transport associated with the Browns Bank gyre, which may largely move off the shelf on the southeast corner of the bank as part of its nearly closed circulation.

Uncertainties associated with the flux calculations are difficult to estimate, since the current meter records and the nutrient observations are not made at the same time or generally at the same locations. In addition, the former are usually made at fixed sites for extended time periods; for example, the Cape Sable – Browns Bank data span a number of years, whereas the latter are from bottle casts made from a ship. As a guide, we shall take a typical standard deviation for current on the Scotian Shelf of 0.1 m·s^{-1} (Gregory and Bussard 1996; Petrie et al. 1998), and a standard deviation of 2 μM for nitrate and silicate. Then, for a typical depth of 100 m and a width of 10 km, we have an uncertainty of 200 mol·s^{-1} (2 μM × 0.1 m·s^{-1} × 10^2 m × 10^4 m).

Vertical fluxes of nutrients can be calculated from the nutrient profiles if estimates of the vertical eddy diffusivity (K_v) and the vertical velocity are available. Umoh (1992) and Umoh and Thompson (1994) used a one-dimensional vertical diffusion equation modified to include the effect of horizontal advection to model the seasonal and interannual variability of temperature on the central Scotian Shelf. They estimated K_v at discrete depths in the model by minimizing the error in the annual cycle of temperature expressed as monthly mean values. They also estimated the vertical

Fig. 5. (*a*) Vertical eddy diffusivity (K_v) at 50 m from Umoh (1992) (solid circles) and derived from the annual temperature harmonic (open circles) based on the model of Petrie et al. (1991). (*b*) Vertical diffusive (solid symbols) and advective (open symbols) fluxes of nitrate (circles, solid line) and silicate (squares, broken line) for the central Scotian Shelf.

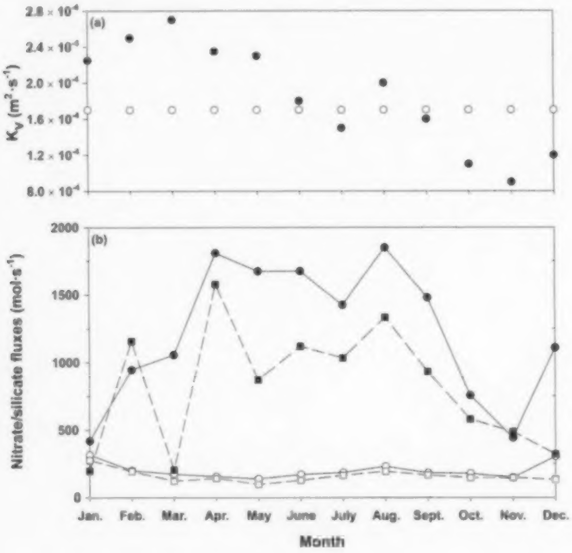

Fig. 6. (*a*) Nitrate and (*b*) silicate vertical gradients at 50 m for the eastern (circles), central (squares), and western (triangles) Scotian Shelf (solid symbols) and the Gulf of Maine (open symbols). The central Scotian Shelf is plotted with a line to serve as a reference for the other regions.

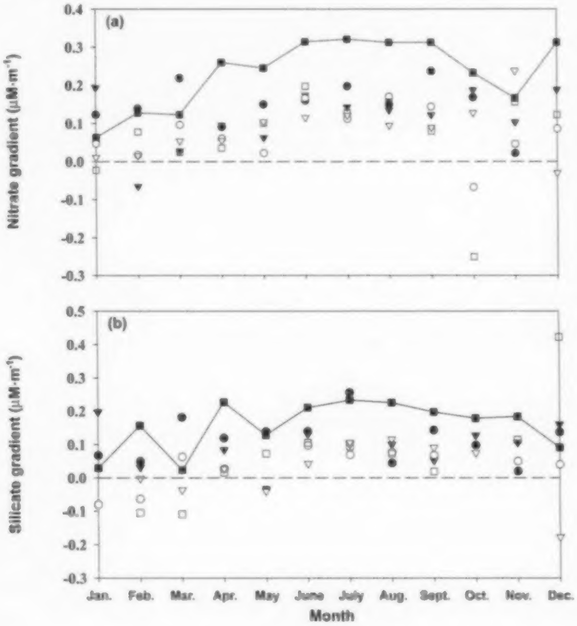

upwelling velocity from calculations of the curl of the windstress. The K_v at 50 m (calculated by taking the simple average of their 40- and 62.5-m values from the model grid) shows an annual cycle with the highest values in the late winter, the lowest in the fall, and an annual mean of 1.85×10^{-4} $m^2 \cdot s^{-1}$ (Fig. 5*a*). The vertical velocity (not shown, upwelling in all months) is quite noisy with a peak of 1.3×10^{-6} $m \cdot s^{-1}$ in May, a minimum of 0.3×10^{-6} $m \cdot s^{-1}$ in September, and an annual mean of 0.8×10^{-6} $m \cdot s^{-1}$. Because of the large scatter and low magnitudes of Umoh's (1992) computed vertical flow, we have used the annual mean upwelling velocity to estimate the advective flux in the calculations discussed below. The annual mean eddy diffusivity would correspond to a vertical mixing scale of about 4 m in a day, whereas the annual mean vertical velocity would cause upwelling of about 0.07 $m \cdot day^{-1}$. We anticipate that vertical diffusion will make a greater contribution to nutrient fluxes than the vertical velocity, provided the vertical nutrient gradients are not too weak.

The vertical diffusive fluxes of nitrate and silicate on average exceed the advective values by a factor of 6 and 5 (Fig. 5*b*). The diffusive fluxes for the central Scotian Shelf box are particularly strong during the spring and summer, about 1500 and 1000 $mol \cdot s^{-1}$ for nitrate and silicate, and are nearly as large as the largest horizontal fluxes for the months of June–August (Table 1). The implications of these fluxes for primary productivity are explored in a companion paper (B. Petrie et al., unpublished data); however, we note that Fournier et al. (1977) indicated that during the April–September period, a minimal nitrate requirement to support primary production was 7.6 g $N \cdot m^{-2}$; 80% of this they assumed came from recycling within the euphotic zone. Our estimate of vertical diffusion for the central Scotian Shelf would supply about 11 g $N \cdot m^{-2}$, approximately the entire amount needed by Fournier et al. (1977).

The differences between the nitrate and silicate diffusive fluxes (Fig. 5*b*) depend solely on the vertical gradients because the eddy diffusivities in both calculations are the same. The low silicate flux in March is caused by a weak gradient; the rather high nitrate flux in December is not considered reliable because of a lack of data (only three observations at depths below the surface layer).

To extend our results for the diffusive fluxes to other parts of the region requires an estimate of the K_vs and vertical gradients. The latter can be derived from the data (Petrie et al. 1999) and are shown in Fig. 6. With the data that are available, 136 gradients at 50 m can be calculated from differences between the average concentrations at 40 and 62.5 m. Of these, 14 were negative; for these 14 cases, 10 had <10 observations for at least one of the depth levels used in the gradient estimation. This indicates that the lack of data may be a problem in the determination of some gradients. The gradients for the central Scotian Shelf are generally larger than for all other regions. On average, the [nitrate, silicate gradient] ratios for the central Scotian Shelf compared with the other areas are [1.5, 1.4] and [2, 1.6] for the eastern and western Scotian Shelf and [3.1, 4.5], [3.5, 2.2], and [2.8, 7.8] for the eastern, central, and western Gulf of Maine. If K_v is relatively constant throughout the region, then the vertical nutrient flux in the central Scotian Shelf would be the largest,

Fig. 7. Observed (solid symbols) and modelled (open symbols) annual temperature harmonics for the central Scotian Shelf (circles) and Gulf of Maine (triangles) from 0 to 100 m. The surface values have the largest amplitudes and the earliest phases. The phase multiplied by 365/360 corresponds to the day of the year when the largest amplitude occurs on average.

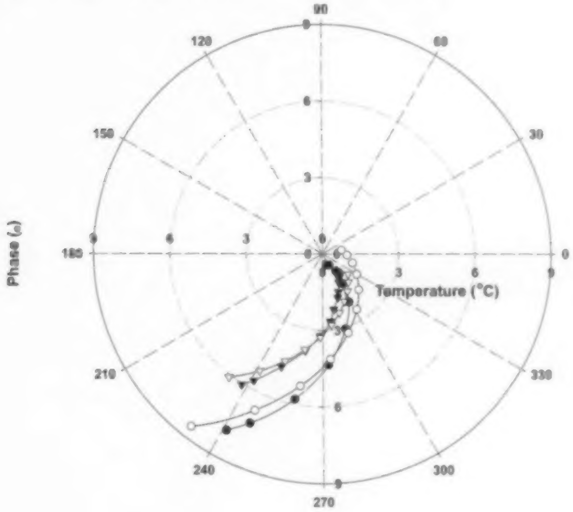

since this is the area with the largest gradients. On the other hand, there is good reason to believe that K_v may vary in the region, e.g., the strong tidal flows in the Gulf of Maine lead to greater vertical mixing.

Hannah et al. (2001) used a Mellor–Yamada turbulence model to estimate the vertical eddy diffusion throughout the Scotian Shelf and Gulf of Maine. However, except for the southwest Scotian Shelf, the mouth of the Bay of Fundy and a region extending westward, part way along the Maine coast, and Georges Bank, their model defaults to a minimum value of 10^{-4} $m^2 \cdot s^{-1}$. Petrie et al. (1991) derived a solution for the one-dimensional vertical eddy diffusion equation with a constant K_v, i.e., similar to the modelling of Umoh (1992) but without accounting for horizontal advection. They used the annual and semiannual harmonics for temperature and salinity at 10-m depth intervals to derive best-fit eddy diffusivities. The resulting K_v represented an annual average value from 0 to 100 m. They were most confident with the results from the annual harmonics derived from temperature, since they were based on the most data and had the greatest range relative to error estimates of the observations. We have applied their technique to the six regions of the Scotian Shelf and the Gulf of Maine.

The observed and modelled harmonics for the central Scotian Shelf and central Gulf of Maine are shown in Fig. 7. Each point represents the amplitude and phase of the harmonics at 10-m intervals for the depth range 0–100 m. The central Scotian Shelf has a larger amplitude and phase variation with depth compared with the central Gulf of Maine. Greater uniformity of temperature amplitude and phase with depth indicates enhanced vertical mixing. This implies that the value of K_v should be larger for the central Gulf of Maine, since the surface heat flux should be nearly the same over the small distance separating the two regions. The model indicates that K_v is about two times larger in the central Gulf of Maine. Table 2 summarizes the model results for the other areas. The highest eddy diffusivity is found in the eastern Gulf of Maine; this is not surprising, since it is a region of strong tidal currents and consequently enhanced vertical mixing. The lowest values are found for the eastern and central Scotian Shelf. The errors in Table 2 represent the average root mean square temperature error of the model for a single depth. These errors are smaller than the 3°C root mean square error (constant K_v) and comparable with the 1°C error ($K_v = f(z,t)$) of Umoh and Thompson (1994). Umoh and Thompson (1994) fitted their models to the monthly mean temperatures from 0 to 100 m and thus considered variability in addition to the annual harmonic. The annual harmonic, however, accounts for most of the temperature variance in this depth range. Nevertheless, their results indicate that the vertical flux estimates for nutrients could be improved with a model that allowed K_v to vary with depth and time. In Fig. 5*a*, we show the K_v value for the central Scotian Shelf based on the model fit to the 0–100 m observations compared with Umoh's (1992) calculation interpolated to 50 m. We underestimate the eddy diffusion during winter and spring and overestimate its value in fall. Our value of 1.7×10^{-4} $m^2 \cdot s^{-1}$ compares well with Umoh's (1992) annual mean of 1.85×10^{-4} $m^2 \cdot s^{-1}$.

Table 2. Vertical eddy diffusivities (K_v) calculated from the 0–100 m annual temperature harmonics and the model of Petrie et al. (1991) and the temperature error representing the root mean square difference between the observed and modelled annual cycle.

Area	K_v ($m^2 \cdot s^{-1}$)	Error (°C)
Eastern Scotian Shelf	1.7×10^{-4}	0.96
Central Scotian Shelf	1.7×10^{-4}	0.64
Western Scotian Shelf	3.4×10^{-4}	0.56
Eastern Gulf of Maine	12.3×10^{-4}	0.35
Central Gulf of Maine	4.1×10^{-4}	0.29
Western Gulf of Maine	3.0×10^{-4}	0.33

It is the combination of the nutrient gradient and the K_v that gives the flux into the upper 50-m layer. Keeping only the positive gradients for all sites, we find that the annual average vertical fluxes per unit area are highest for the eastern Gulf of Maine, about three times greater than the central Scotian Shelf, and lowest for the eastern Scotian Shelf, about two thirds of the flux for the central Scotian Shelf. For nitrate, the average annual fluxes for the eastern, central, and western Scotian Shelf and eastern, central, and western Gulf of Maine are 2.5×10^{-8}, 4.0×10^{-8}, 4.4×10^{-8}, 10.8×10^{-8}, 4.4×10^{-8}, and 2.8×10^{-8} $mol \cdot s^{-1} \cdot m^{-2}$, respectively, and for silicate are 1.9×10^{-8}, 2.7×10^{-8}, 3.7×10^{-8}, 7.6×10^{-8}, 4.7×10^{-8}, and 2.3×10^{-8} $mol \cdot s^{-1} \cdot m^{-2}$, respectively. The vertical fluxes for the western Scotian Shelf and the central Gulf of Maine are slightly greater than for the central Scotian Shelf, whereas the fluxes for the western Gulf of Maine are slightly smaller. Combining the differing areas, vertical gradients, and eddy diffusivities for the eastern, central, and western Gulf of Maine, we find average vertical fluxes of 4400 and 3800 $mol \cdot s^{-1}$ for nitrate and silicate. The vertical nitrate flux of 4400 $mol \cdot s^{-1}$ is comparable with the horizontal advective

Fig. 8. Time series of the annual (*a*) temperature and (*b*) salinity anomalies (100–200 m) and (*c*) nitrate, (*d*) dissolved oxygen, (*e*) silicate, and (*f*) phosphate anomalies (depth 150 m) for the central Scotian Shelf and (*g*) nitrate, (*h*) dissolved oxygen, (*i*) silicate, and (*j*) phosphate anomalies (depth 150 m) for the Gulf of Maine. Nitrate values represented by a triangle in Fig. 8*c* have been computed from a regression with dissolved oxygen. In order to reduce the effects of a yearly cycle in any of the time series, the annual anomalies are the averages of monthly anomalies. Representative standard deviations of the monthly anomalies are 0.9°C (temperature), 0.2 (salinity), 1.9 µM (nitrate), 24 µM (oxygen), 2.4 µM (silicate), and 0.13 µM (phosphate).

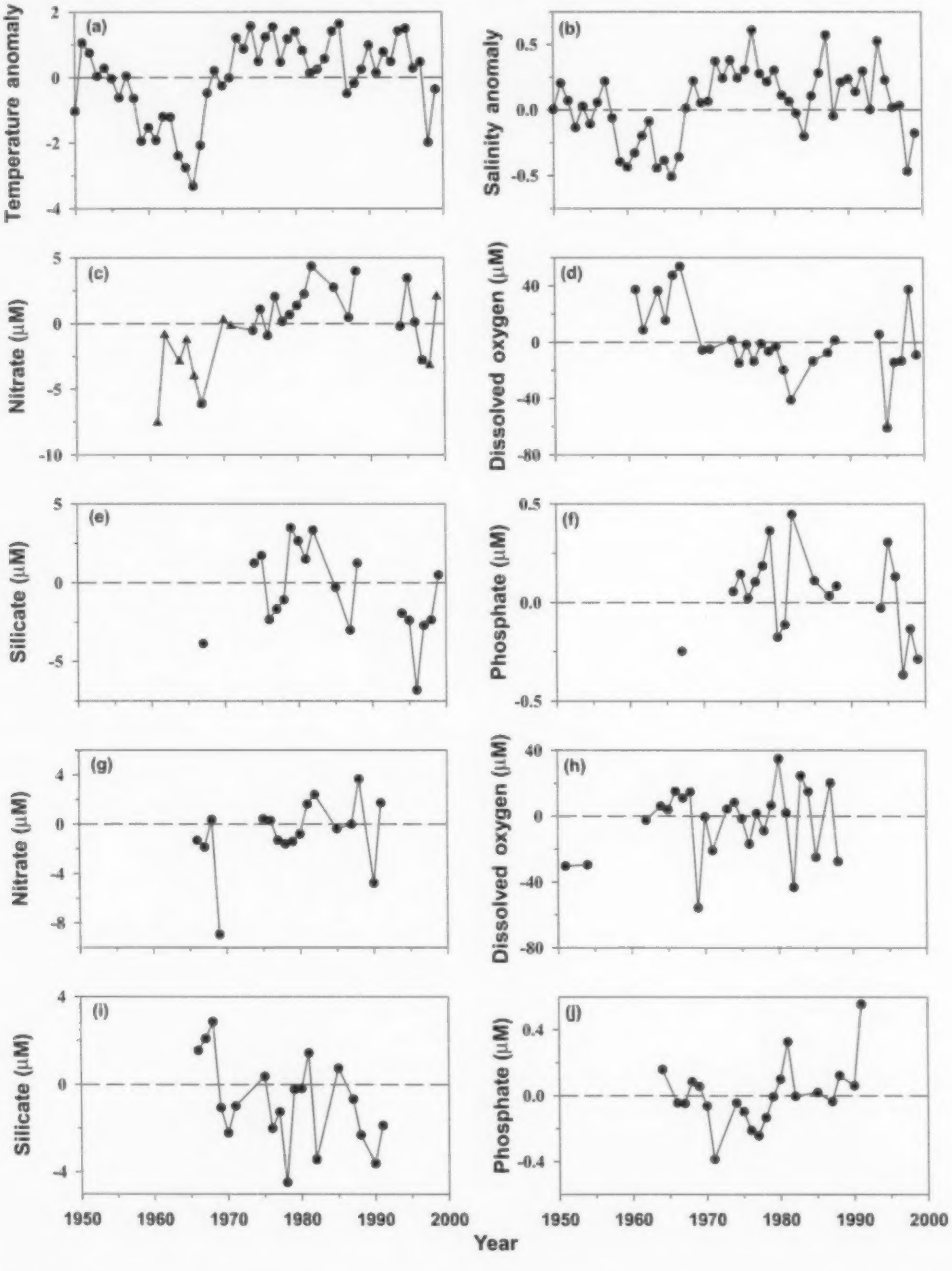

flux of 5800 mol·s^{-1} through the Northeast Channel estimated by Schlitz and Cohen (1984). Moreover, if we scale our vertical flux by the ratio of the area that we considered (79 400 km^2) to theirs (103 000 km^2), our flux is equivalent to 5700 mol·s^{-1}. Unfortunately, Schlitz and Cohen (1984) did not present the vertical distribution of their nitrate transport, but it is reasonable to conclude that most of the flux through the Northeast Channel would be deeper than 50 m. Thus, vertical diffusion may be the mechanism for transporting their horizontal advective flux, which would be mostly at depth, into the shallower layers.

We have used a simple model that gives depth- and annually averaged K_v; we have calculated monthly, vertical nutrient gradients that often have few observations (the average number of observations for months with data in the depth intervals bracketing 50 m is 28 (nitrate, SD = 32) and 27 (silicate, SD = 29)). These results should be viewed as indicative of how the fluxes vary from region to region. Other data sets, such as primary productivity, could provide support for the flux estimates.

Interannual variability of nutrients

Petrie and Drinkwater (1993) found that temperature and salinity in the Scotian Shelf and Gulf of Maine region had similar low-frequency interannual variations; amplitudes of about 4°C and 0.6 were found in the deeper waters of Emerald Basin (also see Figs. 8*a* and 8*b*). They attributed these changes to the variations of the water mass structure on the upper continental slope with subsequent on-shelf flow. Periods of relatively cold, fresh water, the mid-1960s and most recently in 1998, were associated with the dominance of Labrador Slope water, while warm, salty periods were related to the presence of Warm Slope water. Nutrient and dissolved oxygen anomalies should exhibit similar low-frequency variability if they are related to the water mass structure.

The annual temperature and salinity anomalies of the 100–200 m layer in the central Scotian Shelf decreased from the early 1950s, reached a minimum in the mid-1960s, and a rapid transition to above-normal values followed (Figs. 8*a* and 8*b*). Temperature and salinity generally remained above normal for about 25 years. In October 1997, Labrador Slope water again dominated on the upper Scotian Slope with penetration onto the shelf early in the winter of 1998 and continuing throughout the year (K. Drinkwater, Department of Fisheries and Oceans, Bedford Institute of Oceanography, P.O. Box 1006, Dartmouth, NS B2Y 4A2, Canada, personal communication). Recent sampling of the central Scotian Shelf indicates a return to warm, salty conditions characteristic of Warm Slope water.

Nutrient and oxygen data, although less plentiful, generally correspond to the gross changes in temperature and salinity (Figs. 8*c* and 8*d*). Dissolved oxygen anomalies were generally high in the 1960s with peak values in the mid-1960s corresponding to the Labrador Slope water period. A period of lowered values followed when Warm Slope water dominated. In 1998, an influx of Labrador Slope water raised dissolved oxygen to its highest values since the 1960s but not to the maximum anomalies of the mid-1960s. Nitrate, and to a certain extent silicate and phosphate (Figs. 8*e* and 8*f*), showed opposing tendencies, i.e., negative anomalies in the 1960s and 1998 with generally higher values in between. (Note that nitrate and dissolved oxygen are strongly correlated (r^2 = 0.64) for depths ≥150 m; for 1961, 1962, 1964–1966, 1970, and 1971, years without nitrate data, nitrate concentrations were derived from a regression with dissolved oxygen for all years and are plotted with a different symbol in Fig. 8*c*.) However, the nitrate anomaly is also low in 1997, as is silicate in 1994–1998 and phosphate from 1997 to 1999. We have investigated the depth dependence of the nutrients and dissolved oxygen to determine if sampling biases, e.g., most samples in one year come from 150 m and in another from 250 m and deeper, could have affected the anomalies. We found only a weak correlation of concentrations with depth and no qualitative difference between depth-corrected anomalies and those shown in Fig. 8.

The long-term correlations of the annual anomalies of temperature and salinity with the nutrients are all positive, with the highest values for nitrate (r = 0.71 with temperature and r = 0.61 with salinity). For silicate and phosphate, only the correlation between silicate and temperature (r = 0.40) is significant at the 95% confidence level. Dissolved oxygen is negatively correlated with temperature and salinity (r = –0.77 and r = –0.68, respectively). In all cases, the best correlations are with temperature. The correlations with temperature and salinity together are only slightly better than for temperature alone. This is not surprising, since temperature and salinity are highly correlated (r = 0.84); thus, the addition of the extra variable adds little to the correlation.

Even though we consolidated the eastern, central, and western regions of the Gulf of Maine, we had barely enough nutrient and dissolved oxygen observations for depths ≥150 m to determine if the long-term variability seen on the central Scotian Shelf occurred in the gulf (Figs. 8*g* and 8*h*). Overall, there appears to be little correspondence. Nitrate shows similar behaviour with low values in the mid-1960s and higher values at other times (correlation of 0.66 with central Scotian Shelf values). However, the minimum in the 1960s was not as low as seen for the Scotian Shelf. Dissolved oxygen anomalies in the 1960s were slightly above average, i.e., qualitatively similar to the Scotian Shelf, but not significantly higher than normal. Phosphate anomalies in the 1960s were essentially equal to the mean, whereas silicate, with above-normal concentrations, showed the opposite tendencies to those on the Scotian Shelf (Figs. 8*i* and 8*j*).

In conclusion, there is a strong annual cycle of nitrate and silicate in the upper 50 m in all regions that features a rapid decrease in concentrations beginning in late winter. Concentrations remain low in the summer, followed by a buildup during fall and winter. For depths >75 m, there is an indication of a general increase of nitrate and silicate from spring to summer. Phosphate does not show as pronounced an annual cycle as do nitrate and silicate but rather decreases slowly over approximately a 6-month period in the upper 50 m.

The annual cycle of nitrate in particular exhibits spatial variability, with higher winter near-surface concentrations over the eastern Scotian Shelf and decreasing values southwestward into the Gulf of Maine. In spring and summer, relatively higher concentrations are found in areas such as the eastern Gulf of Maine, the mouth of the Bay of Fundy, and Georges Bank where there is enhanced vertical mixing. Nitrate and silicate concentrations increase earlier in the fall in the region west of the central Scotian Shelf.

The major advective source of nitrate and silicate for the Scotian Shelf is the Gulf of St. Lawrence outflow during winter. However, during summer, the on-shelf transport at Western Bank is almost as strong. Vertical fluxes of nitrate and silicate were calculated by combining an estimate of K_v, derived from the vertical variation of the annual cycle of temperature and an idealized model, and the vertical nutrient gradient. The vertical eddy flux for the central Scotian Shelf was significant and comparable with the horizontal fluxes, particularly during summer. The K_vs varied by a factor of 7 throughout the region, with the largest values in the eastern Gulf of Maine. However, large eddy diffusivities tend to reduce vertical gradients so that the fluxes varied by a factor of 4. The vertical diffusive flux in the central Scotian Shelf region was sufficient to supply the entire nitrogen requirement for primary production estimated by Fournier et al. (1977) for the April–September period. The nitrate vertical flux calculated for the Gulf of Maine nearly balances the horizontal advective flux through the Northeast Channel estimated by Schlitz and Cohen (1984). Thus, vertical diffusion appears to play a strong role in determining the primary production in the Gulf of Maine.

Nutrients and dissolved oxygen showed significant interannual variability that appears to be related to water mass structure based on data from the central Scotian Shelf. Periods of Labrador (Warm) Shelf water dominance were generally associated with high (low) oxygen and low (high) nutrient concentrations. However, while the variation of nitrate and dissolved oxygen in the Gulf of Maine is qualitatively similar, particularly for the former, silicate and phosphate changes differ from those on the Scotian Shelf. Part of the difference could be related to the paucity of observations, especially for the 1960s. However, the differences could also reflect regional changes in supply and consumption of nutrients.

Acknowledgements

We thank Fasil WoldeGeorgis and Elizabeth Gonzalez for technical support preparing this manuscript. A number of individuals provided nutrient data that allowed for the expansion of the database; in particular, we thank Brian Irwin and Glen Harrison. We thank GLOBEC Canada for providing some financial assistance for this project. Ken Drinkwater, Glen Harrison, and two referees provided useful reviews.

References

Bretherton, F., Davis, R., and Fandry, C. 1976. A technique for objective analysis and design of oceanographic experiments applied to MODE-73. Deep-Sea Res. **27**: 559–582.

Fournier, R., Marra, J., Bohrer, R., and van Det, M. 1977. Plankton dynamics and nutrient enrichment of the Scotian Shelf. J. Fish. Res. Board Can. **34**: 1004–1018.

Garrett, C., Keeley, R., and Greenberg, D. 1978. Tidal mixing versus thermal stratification in the Bay of Fundy and the Gulf of Maine. Atmos.–Ocean, **16**: 403–423.

Gregory, D., and Bussard, C. 1996. Current statistics for the Scotian Shelf and Slope. Can. Data Rep. Hydrogr. Ocean Sci. No. 144.

Han, G., Hannah, C., Loder, J., and Smith, P. 1997. Seasonal variation of the three-dimensional mean circulation over the Scotian Shelf. J. Geophys. Res. **102**: 1011–1025.

Han, G., Loder, J., and Smith, P. 1999. Seasonal-mean hydrography and circulation in the Gulf of St. Lawrence and on the eastern Scotian and southern Newfoundland shelves. J. Phys. Oceanogr. **29**: 1279–1301.

Hannah, C., Shore, J., Loder, J., and Naimie, C. 2001. Seasonal circulation on the western and central Scotian Shelf. J. Phys. Oceanogr. In press.

Harrison, W.G. 1983. Uptake and recycling of soluble reactive phosphate by marine microplankton. Mar. Ecol. Prog. Ser. **10**: 127–135.

Ketchum, B., Vaccaro, R., and Corwin, N. 1958. The annual cycle of phosphorus and nitrogen in New England coastal waters. J. Mar. Res. **17**: 282–301.

Pastuzak, M., Wright, R., and Patanjo, D. 1982. One year of nutrient distribution in the Georges Bank region in relation to hydrography, 1975–1976. J. Mar. Res. **40**(Suppl.): 525–542.

Petrie, B., and Dean-Moore, J. 1996. Temporal and spatial scales of variability of temperature and salinity on the Scotian Shelf. Can. Tech. Rep. Hydrogr. Ocean Sci. No. 177.

Petrie, B., and Drinkwater, K. 1993. Temperature and salinity variability on the Scotian Shelf and in the Gulf of Maine 1945–1990. J. Geophys. Res. **98**: 20 079 – 20 089.

Petrie, B., Loder, J., Akenhead, S., and Lazier, J. 1991. Temperature and salinity variability on the eastern Newfoundland Shelf: the annual harmonic. Atmos.–Ocean, **29**: 14–36.

Petrie, B., Drinkwater, K., Gregory, D., Pettipas, R., and Sandström, A. 1996. Temperature and salinity atlas for the Scotian Shelf and the Gulf of Maine. Can. Tech. Rep. Hydrogr. Ocean Sci. No. 171.

Petrie, B., Shore, J., Hannah, C., and Loder, J. 1998. Physical oceanography. *In* The Gully: a scientific review of its environment and ecosystem. *Edited by* G. Harrison and D. Fenton. Can. Stock Assess. Secretariat Res. Doc. 98/83.

Petrie, B., Yeats, P., and Strain, P. 1999. Nitrate, silicate and phosphate atlas for the Scotian Shelf and the Gulf of Maine. Can. Tech. Rep. Hydrogr. Ocean Sci. No. 203.

Platt, T., Prakash, A., and Irwin, B. 1972. Phytoplankton, nutrients and flushing of inlets on the coast of Nova Scotia. Nat. Can. **99**: 253–261.

Schlitz, R., and Cohen, E. 1984. A nitrogen budget for the Gulf of Maine and Georges Bank. Biol. Oceanogr. **3**: 203–222.

Sheng, J., and Thompson, K. 1996. A robust method for diagnosing regional shelf circulation from scattered density profiles. J. Geophys. Res. **101**: 25 647 – 25 659.

Umoh, J. 1992. Seasonal and interannual variability of sea temperature and surface heat fluxes in the Northwest Atlantic. Ph.D. thesis, Dalhousie University, Halifax, N.S.

Umoh, J., and Thompson, K. 1994. Surface heat flux, horizontal advection, and the seasonal evolution of water temperature on the Scotian Shelf. J. Geophys. Res. **99**: 20 403 – 20 416.

Comparison between consumption rates of yellow perch (*Perca flavescens*) estimated with a digestive tract model and with a radioisotope approach

Jérôme Gingras and Daniel Boisclair

Abstract: We compared consumption rates of yellow perch (*Perca flavescens*) obtained from surveys of complete digestive tract contents (CDTC) with two radioisotope approaches using ^{137}Cs as a biological tracer. We sampled fish of age 1+, 2+, and 3+ from three lakes for a total of six lake – age-class combinations. The two radioisotope methods provided very similar estimates of consumption rates. The relative differences between the CDTC approach and the radioisotope approaches ranged from 67 to 128% when the sampling interval length was 28–35 days. At the time scale of 70 days, the relative differences between the approaches ranged from 15 to 20%. We propose that the ratio of the sampling interval length to the biological half-life of the contaminant determines the discrepancy between consumption estimates obtained using CDTC and radioisotopic approaches. Our analyses suggest that, under the specific conditions encountered in our study, a minimum value for this ratio to obtain adequate consumption rates may be 45%. Although our work represents a corroboration of the radioisotope approach in systems where ^{137}Cs is present at trace levels, it also suggests that consumption rates obtained for time periods shorter than 70 days should be interpreted with caution.

Résumé : Nous avons comparé des taux de consommation de la perchaude (*Perca flavescens*) estimés à partir du taux de remplacement du contenu du tractus digestif complet (CTDC) du poisson à deux approches radio-isotopiques utilisant le ^{137}Cs comme traceur biologique. Nous avons échantillonné des poissons d'âge 1+, 2+ et 3+ provenant de trois différents lacs, pour un total de six combinaisons de lac – classes d'âge. Les deux méthodes radio-isotopiques ont donné des estimés très similaires de taux de consommation. La différence relative entre les taux de consommation estimés par l'approche du taux de remplacement du CTDC et par les approches radio-isotopiques a varié de 67 à 128% pour un intervalle d'échantillonnage de 28–35 jours. À l'échelle temporelle de 70 jours, la différence relative entre les deux approches a été de 15 à 20%. Nous proposons que le ratio entre l'intervalle de temps entre les deux échantillonnages et la demi-vie biologique du contaminant détermine la difference entre les taux de consommation obtenus par les approches basées sur les CTDC et sur les radio-isotopes. Nos analyses suggèrent que, sous les conditions rencontrées lors de nos travaux, la valeur minimale de ce ratio pour obtenir des taux de consommation adéquats peut être de 45%. Bien que nos travaux représentent une corroboration de l'approche radio-isotopique dans des systèmes où le ^{137}Cs est présent à l'état de traces, ils suggèrent aussi que des taux de consommations estimés sur des périodes de temps plus courtes que 70 jours devraient être interprétés avec prudence.

Introduction

Estimates of fish consumption rates are useful for quantifying trophic interactions between fish and their prey (Thomann 1981; Schindler and Eby 1997). Field surveys of fish digestive tract contents have been used to estimate in situ consumption rates (Eggers 1977; Elliott and Persson 1978; Boisclair and Leggett 1988). However, these methods require an intense sampling effort. Davis and Foster (1958) suggested that fish consumption rates could be more easily obtained by evaluating the turnover rate of a radioactive contaminant within organisms. For instance, radiocesium-137, or cesium-137 (^{137}Cs; half-life of 30.2 years), is ubiquitous in the environment and is found at relatively high concentrations in regions affected by nuclear reactor incidents (e.g., Chernobyl; see Ugedal et al. 1997; Jonsson et al. 1999) and at trace level in areas that have received fallout from nuclear weapon tests (Rowan and Rasmussen 1994).

Modeling of the dynamics of ^{137}Cs requires information on the assimilation efficiency and the elimination rate of this contaminant by fish (Hakonson et al. 1975; Forseth et al. 1999; Tucker and Rasmussen 1999). Elimination rate of ^{137}Cs is expected to be a function of fish weight and water temperature (Gallegos and Whicker 1971). Ugedal et al. (1992) developed the first functional model of elimination rate for ^{137}Cs using 13 experiments performed on brown trout (*Salmo trutta*). Using this model, Forseth et al. (1992, 1994) corroborated a radioisotope approach to estimate the consumption rate of brown trout and Arctic char (*Salvelinus alpinus*) by comparing their results with those obtained using surveys of digestive tract contents. That corroboration provides the only evidence that radioisotope methods may

Received July 24, 2000. Accepted October 12, 2000. Published on the NRC Research Press web site on December 20, 2000.
J15885

J. Gingras and D. Boisclair.[1] Département de sciences biologiques, Université de Montréal, C.P. 6128, Succursale Centre-ville, Montréal, QC H3C 3J7, Canada.

[1] Corresponding author (e-mail: daniel.boisclair@umontreal.ca).

be used to estimate fish consumption rates and that elimination rates and assimilation efficiency of ^{137}Cs obtained for one fish species may be applicable to another (Forseth et al. 1994). It must be recognized that this corroboration involved two relatively similar fish species (brown trout and Arctic char). Rowan and Rasmussen (1995) combined the data of Ugedal et al. (1992) for brown trout with seven additional published estimates of ^{137}Cs elimination rates for bluegill (*Lepomis macrochirus*) and summer flounder (*Paralichthys dentatus*) to develop an empirical model considered applicable to many fish species. However, Forseth et al. (1998) found that for 50% of the 12 elimination experiments that they performed on bream (*Abramis brama*), Atlantic salmon (*Salmo salar*), Arctic char, and whitefish (*Coregonus lavaretus*), the elimination rates of ^{137}Cs predicted by the model of Rowan and Rasmussen (1995) were statistically different from experimental values (difference from −85 to +63%). While sensitivity analyses suggest that ±10% perturbations of radioisotope elimination rate may be attenuated to ±5% changes in consumption rate estimates (Rowan and Rasmussen 1996), such analyses do not allow us to assess the accuracy of elimination rates predicted by the model of Rowan and Rasmussen (1995). Hence, the accuracy of the ^{137}Cs elimination model of Rowan and Rasmussen (1995) remains in question. Rowan and Rasmussen (1996) also proposed a new radioisotope model to estimate fish consumption rates. One assumption of this model specifies that fish growth can be adequately described by an exponential model. The model of Rowan and Rasmussen (1996) has been criticized on many aspects, namely, that an exponential model may not be appropriate to describe fish growth on a yearly basis (He and Stewart 1997). In a reply to these criticisms, Rowan and Rasmussen (1997) suggested using their radioisotope consumption model on a time scale smaller than a year (week to month). The sufficiency of working at a shorter temporal scale to allow adequate estimation of consumption rates using the model of Rowan and Rasmussen (1996) has not been evaluated. Regardless of the nature and the number of assumptions involved in radioisotope methods, the main impediment to the routine use of this approach appears to be the lack of studies that corroborate the use of ^{137}Cs to estimate fish consumption rates.

The objective of our work was to compare consumption rates determined using the radioisotope approach (models of Forseth et al. (1992) and Rowan and Rasmussen (1996)) with consumption estimates obtained with an approach based on surveys of fish digestive tract contents (Eggers 1977). Since both radioisotopic consumption models employed were implemented with ^{137}Cs elimination rates obtained using the model of Rowan and Rasmussen (1995), our study also constitutes a test of the accuracy of this model.

Materials and methods

Species and lakes studied

Yellow perch (*Perca flavescens*) was studied because this species is not comprised in the original data set used by Rowan and Rasmussen (1995) to develop their empirical model for radiocesium elimination rate. A study on perch therefore tests the robustness of that general elimination model. Sampling was performed in three lakes of the Laurentian region of Québec: Lakes Masson (45°58′N, 74°01′W), Raymond (46°01′N, 76°09′W), and Beaulac (46°01′N, 73°53′W). These lakes were chosen because they contained perch densities (more than one perch of a given age-class per 100 m^2) that can support the sampling effort required by our work, at least for some age-classes. In Lake Masson, we studied fish from three age-classes (1+, 2+, and 3+), while in Lake Raymond, our work focussed on 2+ and 3+ fish. Only one age-class (1+) was sampled in Lake Beaulac.

Sampling

Fieldwork involved two (Lake Raymond: June, July; Lake Beaulac: July, August) to three (Lake Masson: June, July, August) sampling sessions of 48 h in each lake during the summer of 1998. Lakes visited during two sampling sessions allowed the calculation of average consumption rates over periods ranging from 28 days (one in Lake Beaulac) to 35 days (two in Lake Raymond). These average consumption rates were calculated by each method (digestive tract surveys and radioisotope models) and are further referred to as monthly consumption rates. In Lake Masson, the three sampling sessions permitted the calculation of average consumption rates on a monthly (June–July, July–August) and seasonal basis (June–August). Although the period of June–August does not cover the complete growing season of perch, the term "seasonal consumption rates" is used here solely to simplify the presentation of our results. On each sampling session, data were collected to estimate, for each perch age-class studied, daily consumption rates based on a survey of fish digestive tract contents according to the Eggers (1977) model. Samples were simultaneously collected to estimate, for each perch age-class, the concentration of ^{137}Cs in fish and in their prey and hence to estimate consumption rates using two radioisotope models: the model proposed by Forseth et al. (1992) and that developed by Rowan and Rasmussen (1996).

Estimation of daily consumption rates using the model of Eggers (1977) required us to survey variations of fish digestive tract contents and to quantify evacuation rates of the digestive tract during that day. Variations of fish digestive tract contents were estimated by studying 5–10 perch of each age-class at 4- to 5-h intervals over 48 h using a beach seine (50 × 3 m, mesh size 0.5 cm). Fish were killed by cervical dislocation, weighed (±0.01 g wet), and measured (±0.1 cm total length) immediately after capture. Each fish sampled was aged using the opercular bone (LeCren 1947). The complete digestive tract contents (CDTC) of each fish collected were removed by dissection within 2 h of capture. Stomach and intestinal contents were preserved separately in a desiccator for analysis of diet composition and of ^{137}Cs concentration (see Sample processing section). Fish were kept on ice prior to deep-freezing within 2 days of capture. Digestive tract contents were dried (60°C for 48 h) and weighed (±0.0001 g dry). Evacuation rates were estimated independently for each age-class studied and for each sampling session. This strategy presumes that evacuation rate of a given perch age-class within a specific lake is similar over 2 consecutive days. Evacuation rates of the complete digestive tract were obtained by confining 25 fish in a food-free basin set on the shore of the lakes studied. A pump continually supplied the basin with filtered lake water (Nytex, 125 μm) such that water temperature inside the basin would be kept within 1°C of mean epilimnetic temperature (surface to a depth of 5 m). Lake water temperature was noted at every 0.5 m from surface to 5 m depth using an YSI oxymeter–thermometer. It was assumed that this adequately represented the preferential habitat of the perch that we studied (Boisclair and Leggett 1988). Five fish were killed at 4- to 6-h intervals during a 24-h period and the CDTC were collected, weighed, and dried individually.

Sample processing

Fish were thawed, dried (60°C for 48 h), and weighed (±0.01 g dry) in the laboratory. Fish diet for each combination of lake, age-class, and sampling session was estimated by analyzing stomach contents under a microscope and by expressing diet composition as a volumetric percentage of fish, zooplankton, mollusks, surface insects, chironomid zoobenthos, and other zoobenthos taxonomic groups (this functional classification was proposed by Forseth et al. (1992)). Fish from a given combination of lake, age-class, and sampling session were pooled and homogenized. Pooling of stomach contents across perch age-classes for a given lake and sampling session was performed when these had identical diet composition. Radioactivity of fish and stomach contents was measured by gamma spectrometry in a well-type or a coaxial germanium detector. Radioactivity measurements were realized on dried or hashed material (1–10 g), and replicates periodically obtained assessed of the quality of the protocol.

Computations

Consumption rates according to surveys of fish digestive tract contents

Daily consumption rates (D_E, grams dry per gram wet per day) based on surveys of fish digestive tract contents were estimated following the model of Eggers (1977) (see Boisclair and Leggett (1988) for a complete description of computations). Evacuation rates were estimated by linear regression of the natural logarithm of relative CDTC over time during the evacuation rate experiment. During this procedure, we used a special case of linear regression described by Sokal and Rohlf (1995) where we observed many y values for each x value with unequal sample size. This procedure properly estimates the standard error associated with evacuation rates.

Average daily consumption rate of perch for a given combination of lake and age-class was estimated as the area under the curve describing the daily ration as a function of time (following appropriate normalization of the relative CDTC) estimated for that combination (from four to six daily ration values). Confidence intervals around our estimates of daily consumption rates and average consumption rates were determined using Monte Carlo simulations based on the combination of standard errors of digestive tract contents and evacuation rates (see Trudel and Boisclair (1993) for a complete description of the simulation procedure). Hence, our sampling strategy allowed us to obtain nine estimates of monthly consumption rates (from subsequent months) and three estimates of seasonal consumption rates using digestive tract surveys (six daily rations on a 3-month period).

Consumption rates according to the radioisotope approach of Forseth et al. (1992)

Estimation of consumption rates by the approach proposed by Forseth et al. (1992) (referred to by the authors as the short-term method) requires calculations performed by increments of 1 day. Daily consumption rate for a specific day (D_j, grams dry per gram wet per day) was estimated as

$$(1) \qquad D_j = \frac{I_j}{A_j W_j}$$

where I_j is the daily ^{137}Cs intake (becquerels), A_j is the ^{137}Cs concentration (becquerels per gram dry) absorbed by the fish from its prey, and W_j is the average weight (grams wet) of fish on day j. The I_j was estimated as

$$(2) \qquad I_j = \frac{(Q_{j+1} - Q_j\,\mathrm{e}^{-E_j})E_j}{1 - \mathrm{e}^{-E_j}}$$

where Q_j and Q_{j+1} are ^{137}Cs body burden (becquerels) of fish at 2 consecutive days and E_j is the ^{137}Cs elimination rate (becquerels per becquerel per day) at day j. Values of Q_j were estimated by linear interpolation of body burden values that we obtained at successive sampling sessions. In our study, E_j was estimated using the model of Rowan and Rasmussen (1995):

$$(3) \qquad \ln E_j = -6.853 - 0.111 \ln W_j + 0.093\,T_j + 0.326\,\mathrm{SS}$$

where T_j is the water temperature (degrees Celsius) on that day and SS is a dummy variable describing whether or not fish were expected to be under steady-state (SS = 0) or unsteady-state (SS = 1) conditions. Equation 3 explained 97% of the variations in E_j values used by Rowan and Rasmussen (1995) to develop their model. The steady-state condition refers to a situation where contaminant concentrations in a fish and its environment are in a dynamic equilibrium (Rowan and Rasmussen 1995, 1997). Unsteady-state conditions are found during periods ranging from 1 to 3 years following important contaminant pulses (e.g., nuclear incident). During this interval, fish are expected to eliminate the contaminant at a faster rate. An alternative approach for modeling the unsteady-state conditions consists of adding two-component elimination curves (Kolehmainen 1974; Forseth et al. 1999). Since the fish that we studied were in environments that have not been subjected to a recent significant pulse of ^{137}Cs, we believe that our assumption regarding their steady-state conditions is valid. Average fish weight and water temperature on any given day were estimated by linear interpolation of our data of fish weight and water temperature during successive sampling sessions. The A_j was estimated as

$$(4) \qquad A_j = [^{137}\mathrm{Cs}]_d\,\alpha_j$$

where $[^{137}\mathrm{Cs}]_d$ is the concentration of ^{137}Cs (becquerels per gram dry) in the prey and α_j is the assimilation efficiency of ^{137}Cs by fish. Estimates of α_j were obtained as

$$(5) \qquad \alpha_j = \sum_{i=1}^{n} \mathrm{vp}_{ij}\,\alpha_i$$

where vp_{ij} is the volumetric percentage of each prey type i noted during the description of perch diet for day j (obtained by linear interpolation between the two samplings), α_i are the values of assimilation for prey type i published by Forseth et al. (1992) for brown trout, and n is the number of prey type present in the diet at day j. These values are 0.816 for zooplankton, 0.759 for freshwater snails, 0.659 for brown trout muscle, 0.548 for Chironomidae larvae, 0.480 for *Gammarus lacustris*, and 0.234 for Ephemeroptera larvae. In our study, the value for Ephemeroptera larvae was assumed to be representative of surface insects and the value for freshwater snails appropriate for mollusks. The α_i value for detritus was fixed at 3% (Kolehmainen 1974).

Average consumption rates following the approach proposed by Forseth et al. (1992) (D_F, grams dry per gram wet per day) were estimated as the area under the trajectory of D_j versus time (days) divided by the number of days within periods modeled. Monthly consumption rates were estimated for nine combinations of lakes, age-classes, and months. Seasonal consumption rates in Lake Masson were estimated using two approaches. First, we calculated three seasonal consumption rates (one for each age-class sampled in this lake) using data collected during June, July, and August. Second, we calculated three additional seasonal consumption rates based only on data collected during the surveys of June and August. This allowed us to obtain six estimates of seasonal consumption rates with radiocesium models and hence to test the effect of sampling regime (two versus three sampling sessions) on estimates of seasonal consumption rates obtained using the radioisotope model of Forseth et al. (1992).

Confidence intervals were calculated using Monte Carlo simulation (10 000 runs) and the standard error associated with each parameter (Trudel and Boisclair 1993). The number of fish used for our calculations ranged from 26 to 74 (median value of 41). The lack of knowledge of the error associated with the volumetric percentage of prey in the diet suggested that the standard error associated with the assimilation efficiency could not be included in the calculation of our confidence intervals (Forseth et al. 1992).

Consumption rates according to the radioisotope approach of Rowan and Rasmussen (1996)

The model proposed by Rowan and Rasmussen (1996) allows estimates of average consumption rates (D_R, grams dry per gram wet per day) during a time interval of variable length as

$$(6)\qquad D_R = \frac{(Q_t - Q_0\,e^{-(E+k)t} + Q_g)(G + E + k)}{\alpha[^{137}\mathrm{Cs}]_d W_0(e^{Gt} - e^{-(E+k)t})}$$

where Q_0 and Q_t are, respectively, fish ^{137}Cs burden (becquerels) at the beginning and at the end of the time interval defined by two successive sampling sessions, Q_g is the gonadal ^{137}Cs burden released at spawning, G is the specific growth rate (ln(grams wet per gram wet per day)) from an exponential growth model, E is the average ^{137}Cs elimination rate (becquerels per becquerel per day), k is the ^{137}Cs physical decay (6.28×10^{-5} Bq·Bq^{-1}·day^{-1}), $[^{137}\mathrm{Cs}]_d$ is the average concentration of ^{137}Cs (becquerels per kilogram) in the diet, α is the average assimilation efficiency (fraction) of ^{137}Cs, and W_0 is the average fish weight (kilograms) at the beginning of the time interval. In our study, Q_g was set to zero because no spawning occurred during the summer. Average assimilation efficiency and concentration of ^{137}Cs in the diet for the period of the modeling were estimated as the mean values obtained at each sampling period. The elimination rate of ^{137}Cs was estimated with eq. 3 using the average fish weight and water temperature between two sampling periods as inputs.

Average consumption rates were obtained using the model of Rowan and Rasmussen (1996) on a monthly (nine monthly estimates) and seasonal (six seasonal estimates) basis using the strategy used with the model of Forseth et al. (1992). Confidence intervals were calculated using an approach identical to that used for the model of Forseth et al. (1992).

Results

Consumption rates according to surveys of fish digestive tract contents

Analysis of variance (five-way ANOVA; SAS Institute Inc. 1989) indicated that fish digestive tract content (F_j) varied significantly among lakes ($F_{2,1457} = 7.65$, $p < 0.001$), age-classes ($F_{2,1457} = 3.16$, $p < 0.05$), months ($F_{2,1457} = 69.72$, $p < 0.001$), and hours ($F_{4,1457} = 7.64$, $p < 0.001$). No significant difference was found between the F_j value of the first and second day of each sampling session of 48 h ($F_{1,1457} = 0.63$, $p > 0.05$). Daily feeding cycles were similar among lakes, age-classes, months, and days, with highest F_j values at 20:00 and lowest F_j values at 04:00–08:00. The only exception to this pattern was found for 1+ fish from Lake Masson for which no feeding cycle could be observed in August.

Evacuation rates ranged from $3.5 \times 10^{-2} \cdot \mathrm{h}^{-1}$ (Lake Masson 3+, June) to $2.0 \times 10^{-1} \cdot \mathrm{h}^{-1}$ (Lake Masson 3+, August). A test of equality of slopes (Sokal and Rohlf 1995) revealed that the evacuation rates were not estimated from populations of equal slopes ($F_{14,293} = 10.64$, $p < 0.001$). Our in situ estimates of evacuation rates were not related to water temperature ($r^2 = 0.13$, $p > 0.05$), fish age ($r^2 = 0.01$, $p < 0.05$), or fish weight ($r^2 = 0.02$, $p > 0.05$).

Daily consumption rates ranged from 0.05 g dry·100 g wet^{-1}·day^{-1} (Lake Masson 3+, July, first day) to 1.09 g dry·100 g wet^{-1}·day^{-1} (Lake Masson 1+, June, second day). Daily consumption rates varied significantly (four-way ANOVA) among age-classes ($F_{2,1485} = 7.03$, $p < 0.001$) and months ($F_{2,1485} = 5.64$, $p < 0.01$) but not among lakes ($F_{2,1485} = 1.47$, $p > 0.05$) or consecutive days ($F_{1,1485} = 1.33$, $p > 0.05$).

Monthly consumption rates ranged from 0.16 g dry·100 g wet^{-1}·day^{-1} (Lake Masson 3+, June–July) to 0.70 g dry·100 g wet^{-1}·day^{-1} (Lake Masson 1+, July–August). The 95% confidence intervals of these estimates (Fig. 1) suggest the presence of three distinct levels of monthly consumption rates (0.10–0.25, 0.35–0.52, and 0.60–0.81 g dry·100 g wet^{-1}·day^{-1}). Seasonal consumption rates (calculated only for Lake Masson) ranged from 0.27 to 0.66 g dry·100 g wet^{-1}·day^{-1} (Fig. 2) and, based on 95% confidence intervals, appeared to form two different levels (from 0.21 to 0.36, age 1+; from 0.42 to 0.77, age 2+ and 3+).

Radioisotope model input parameters

Water temperature ranged from 17.1°C (Lake Masson, June) to 23.1°C (Lake Beaulac, August). Water temperature varied significantly among months (two-way ANOVA, $F_{2,8} = 16.93$, $p < 0.01$) but not among lakes ($F_{2,8} = 0.24$, $p > 0.05$). Water temperature averaged 16.8, 22.0, and 21.8°C in June, July, and August, respectively (Table 1).

Mean fish weight during any given sampling session ranged from 6.39 g wet (Lake Raymond 1+) to 34.3 g wet (Lake Masson 3+) (Table 1). Three-way ANOVA revealed significant differences among lakes ($F_{2,637} = 87.28$, $p < 0.001$), age-classes ($F_{2,657} = 830.57$, $p < 0.001$), and months ($F_{2,657} = 54.36$). The interactions between month and age ($F_{4,657} = 3.01$, $p < 0.05$) and between month, age, and lake ($F_{1,657} = 8.15$, $p < 0.01$) suggested that fish weight trajectories for each age-class differed among populations. The three samplings of Lake Masson allowed characterization of the growth curves (Fig. 3). Age-class 1+ presented an exponential growth curve (r^2 of linear model versus data = 0.985, r^2 of exponential model versus data = 0.999), while the growth curves of age-classes 2+ and 3+ tended to depart from the exponential growth model (r^2 of linear model versus data = 0.755–0.951, r^2 of exponential model versus data = 0.724–0.940).

Water temperature and fish weight values were within the range of the variables used by Rowan and Rasmussen (1995) to develop their radiocesium elimination model. Elimination rates estimated using this model on a daily basis ranged from 4.7×10^{-3} Bq·Bq^{-1}·day^{-1} (Lake Masson 3+, June) to 9.3×10^{-3} Bq·Bq^{-1}·day^{-1} (Lake Masson 1+, July). Our estimates of the ^{137}Cs assimilation efficiency ranged from 53.1 to 81.3% with a median value of 70.2% (Table 1).

The diet of fish from Lake Raymond (Table 2) mainly consisted of surface insects (30–35%) and forage fish (0–65%). In this lake, a small proportion of zooplankton was present in the diet of the month of June (10–30%). In contrast, the diet of fish from Lake Beaulac was dominated by zooplankton (30–40%) and surface insects (25–30%). Yellow perch from Lake Masson feed mostly on zooplankton (40–100%) and mollusks (0–40%). Overall, the presence of detritus in the diet was small for all age-classes (0–10%), and no major diet shift was observed.

Fig. 1. Monthly consumption rates estimated by the Eggers (1977) (squares), Forseth et al. (1992) (circles), and Rowan and Rasmussen (1996) (crosses) methods for each age-class and modeling period. The 95% confidence intervals are represented by the vertical lines.

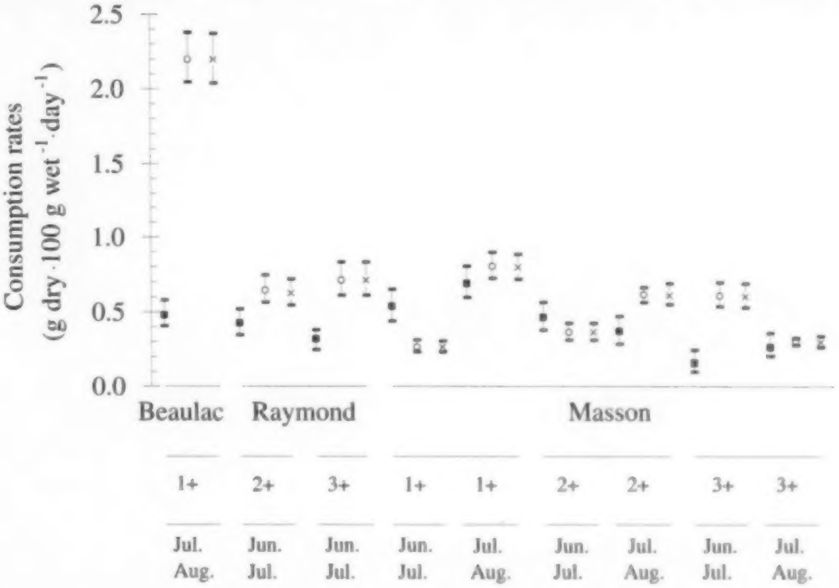

Fig. 2. Seasonal consumption rates estimated by the Eggers (1977) (squares), Forseth et al. (1992) (circles), and Rowan and Rasmussen (1996) (crosses) methods. The number below indicates the number of sampling sessions involved (2, June and August; 3, June, July, and August). The 95% confidence intervals associated with these values are represented by the vertical lines.

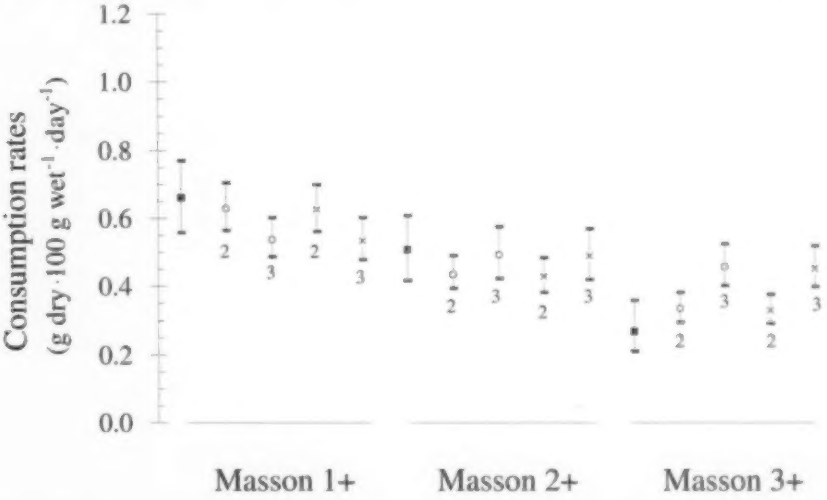

From diet data, we estimated that food consumed by perch had ^{137}Cs concentrations of 7.5 Bq·kg dry^{-1} (Lake Raymond 2+, June) to 24.2 Bq·kg dry^{-1} (Lake Beaulac 1+, July) with a median value of 14.6 Bq·kg dry^{-1} (Table 1). Concentration of ^{137}Cs in fish tissues ranged from 4.8 to 12.0 Bq·kg dry^{-1} with a median value of 7.4 Bq·kg wet^{-1} (Table 1).

Consumption rates according to the radioisotope approach

Monthly and seasonal consumption rates evaluated with the method proposed by Forseth et al. (1992) and Rowan and Rasmussen (1996) gave very similar results (Figs. 1 and 2). Relative differences between the two methods ranged from 0 to 3%. This situation was further confirmed by the correlation that we found between consumption estimates obtained using both radioisotopic methods ($r^2 = 1$, $p < 0.001$, $n = 15$). Inclusion of our 15 estimates of consumption rates in the correlation analysis indicated that both methods provide very similar estimates regardless of the age-class, lake, length of modeling interval, and number of sampling sessions.

Mean daily consumption rates estimated over monthly periods by either radioisotope methods ranged from 0.27 g dry·100 g wet^{-1}·day^{-1} (Lake Masson 1+, June–July) to

Table 1. Descriptive statistics of the input parameters used for the radioisotope approach modeling.

Input parameter	Minimum	Maximum	Median
Water temperature (°C)	16.0	23.1	20.8
Fish weight (g)	6.4	34.3	18.6
Assimilation efficiency (%)	53.1	81.6	70.2
Fish tissue ^{137}Cs concentration (Bq·kg wet^{-1})	4.8	12.0	7.4
Fish diet ^{137}Cs concentration (Bq·kg dry^{-1})	7.5	24.2	14.6

2.19 g dry·100 g wet^{-1}·day^{-1} (Lake Beaulac 1+). Mean daily consumption rates over seasonal periods (which could only be calculated for Lake Masson) using the radioisotope approach involving two samplings were, respectively, 0.63, 0.44, and 0.34 g dry·100 g wet^{-1}·day^{-1} for age-classes 1+, 2+, and 3+. The estimates based on three samplings were, respectively, 0.54, 0.44, and 0.34 g dry·100 g wet^{-1}·day^{-1} for age-classes 1+, 2+, and 3+.

Comparison between digestive tract contents and radioisotope approaches

Average consumption rates estimated with the Eggers (1977) model and the radioisotope approach were compared using our nine monthly estimates. No statistically significant relationship was found between the two approaches ($F_{1,7}$ = 0.29, $p > 0.05$, $r^2 = 0.03$). For two of the nine cases studied, estimates from both approaches differed by less than 20%.

Seasonal consumption rates of age-classes 1+, 2+, and 3+ presented relative differences between approaches of –5, –15, and 20% when only two samplings were involved (June and August) and of –20, –3, and 52% when three samplings were included in the calculations (June, July, and August). Five of the six estimates presenting relative difference to the mean of 20% or less were obtained on a seasonal basis. This suggested that the agreement between both approaches increased as the time interval over which consumption is estimated increased. Our data suggested that a third sampling over a 2-month period might not be necessary.

The comparison between the degree of correspondence between the Eggers and radioisotope approaches on a monthly (–67 to 128% difference) and seasonal (two samplings, –15 to 20% difference) basis indicated that the major determinant of the difference between estimates using these two methods might be the length of the sampling interval. However, it is important to note that all our seasonal estimates were obtained for one specific lake. It is therefore possible that the relatively good agreement between the Eggers and radioisotope approaches occurred strictly because the assumptions that we used for digestive tract or isotopic models were applicable only to Lake Masson. We assessed this possibility by calculating the percent difference between consumption estimates obtained using the Eggers and radioisotope approaches for all our fish groups and temporal scales using only two samplings (Fig. 4). As expected, the percent differences between monthly estimates derived using the Eggers and isotopic approaches for Lakes Beaulac and Raymond were generally large (128, 41, and 77%). These calculations indicated that the correspondence between monthly estimates obtained for Lake Masson using the Eggers and isotopic approaches was relatively poor (–67 to 118% difference) despite a good correspondence on a seasonal basis (≤20% difference in five of six of our comparisons). Our calculations support our interpretation that the length of the sampling interval, and not the particular conditions encountered in Lake Masson, was responsible for the similarity of the consumption estimates obtained using the Eggers and radioisotope models on a seasonal basis.

Fig. 3. Average fish weight for given sampling periods. The 95% confidence intervals associated with these values are represented by the vertical lines. Solid squares, Lake Raymond 2+; solid diamonds, Lake Raymond 3+; circles, Lake Masson 1+; open squares, Lake Masson 2+; open diamonds, Lake Masson 3+; crosses, Lake Beaulac 1+.

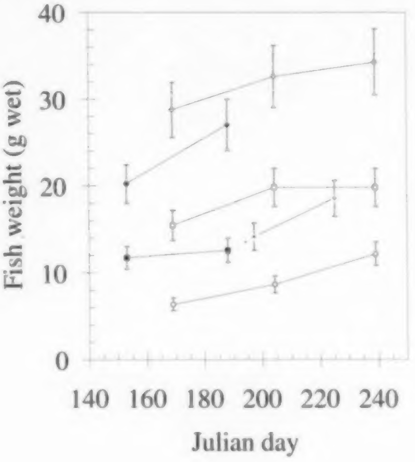

Discussion

We compared estimates of average consumption rate of yellow perch in situ obtained using three methods: one method based on surveys of fish digestive tract contents (Eggers 1977) and two radioisotope methods (Forseth et al. 1992; Rowan and Rasmussen 1996). We found that the two radioisotope methods are equivalent for the time scale that we used, the range of input parameters covered by our study, and the consumption rate levels that we observed. Convergence between consumption values obtained with the radioisotope approach using ^{137}Cs as a tracer and those based on surveys of fish CDTC was observed for feeding rates estimated over time periods of approximately 70 days. However, we found no relationship between consumption estimates obtained using the isotopic approach and the method based on surveys of CDTC over time periods of approximately 30 days.

The major difference between the short-term method of Forseth et al. (1992) and the method of Rowan and Rasmussen (1996) is that for each day modeled with the method of Forseth et al. (1992), fish weight is estimated using a linear interpolation between values at the beginning and the end of the period modeled. The equation of Rowan and Rasmussen (1996) assumes that fish display an exponential growth

Table 2. Volumetric percentage of prey items in the diet of fish.

			Prey type						Assimilation efficiency
Lake	Age-class	Month	Zooplankton	Mollusks	Fish tissues	*G. lacustris*	Surface insects	Detritus	(α_j, fraction)
Raymond	2+	June	30	30	—	—	35	5	0.55
		July	—	5	65	—	30	—	0.54
	3+	June	10	30	30	—	30	—	0.57
		July	—	5	65	—	30	—	0.54
Beaulac	1+	July	40	20	—	10	30	—	0.60
		August	30	15	10	10	25	10	0.53
Masson	1+	June	100	—	—	—	—	—	0.82
		July	65	35	—	—	—	—	0.80
		August	60	15	15	—	—	10	0.70
	2+	June	85	10	5	—	—	—	0.80
		July	60	15	25	—	—	—	0.77
		August	60	15	15	—	—	10	0.70
	3+	June	40	25	5	—	30	—	0.62
		July	60	40	—	—	—	—	0.75
		August	60	40	—	—	—	—	0.75

trajectory. This assumption has been criticized by He and Stewart (1997), who argued that forcing an exponential growth model on an annual basis may affect the validity of the consumption rates predicted by the model of Rowan and Rasmussen (1996). Our study suggests that these differences have no measurable impact on monthly or seasonal consumption rates predicted by these two isotopic models. To further test the effect of the mathematical formulation of the models to estimate consumption rates using the isotopic approach, we developed a model that incorporates a linear growth trajectory (see the Appendix for the mathematical demonstration):

$$(7) \qquad D_{\mathrm{L}} = \frac{(Q_t - Q_0\,\mathrm{e}^{-Et})E^2}{\alpha[^{137}\mathrm{Cs}]_{\mathrm{d}}(E G_{\mathrm{l}} t + (E w_0 - G_{\mathrm{l}})(1 - e^{-Et}))}.$$

The parameters of this equation are identical to those of eq. 6 except for G_{l}, which is a linear growth rate (grams wet per day) between two sampling periods. It is important to note that eq. 7 is not valid if spawning occurs during the modeling period. We used this model and the data of our study to estimate consumption rates of perch on a monthly or seasonal basis. The values provided by the model incorporating a linear growth model never differed by more than 4% from estimates obtained using the model of Rowan and Rasmussen (1996), thereby confirming that, for a time scale of 30–70 days, assumptions adopted for the growth trajectory may have negligible effects on the predictions made by the isotopic approach.

The lack of correspondence between consumption estimates obtained monthly using surveys of CDTC and ^{137}Cs may be attributed to errors associated with either approach. Estimates of daily consumption rates using surveys of CDTC depend on two variables: the variations in quantity of food in the digestive tract of fish in nature and the evacuation rate of fish (Eggers 1977; Elliott and Persson 1978). Adequate description of daily variations of fish digestive tract content is believed to be potentially affected by the number of hours between consecutive samplings within a day. In our study, fish were sampled at 4- to 5-h intervals, although sampling intervals ranging from 4 to 12 h have been shown to cause a <20% change in daily consumption rate obtained using the Eggers model (Boisclair and Leggett 1988; Boisclair and Marchand 1993). Evacuation rates are expected to be affected by fish weight, water temperature, and diet composition (Persson 1979). Because of this situation, we estimated evacuation rates independently for each population, age-class, and sampling session. Hence, evacuation rates were estimated with fish that had the same size and diet as the fish targeted by our study. Furthermore, since filtered water was continuously pumped from the lake to the holding tanks used to perform evacuation rate experiments, these fish are expected to have experienced water temperatures similar to those of the fish living at that time in the littoral of the lakes studied. Regurgitation of food by fish during their capture is an additional potential problem that may affect the two variables used to estimate daily consumption rates using surveys of CDTC. Indeed, regurgitation may provoke an underestimation of the digestive tract contents and of the evacuation rate of fish. Although it is impossible to perfectly assess the impact of this potential bias in our study, one key piece of information may be that the evacuation rates that we obtained (0.035–$0.20 \cdot \mathrm{h}^{-1}$) at water temperatures ranging from 17 to 23°C are very similar to those reported for perch maintained at water temperatures ranging from 15 to 21°C (0.038–$0.14 \cdot \mathrm{h}^{-1}$) and under laboratory conditions where regurgitation could be controlled (Boisclair and Leggett 1988). The difference between these values does not suggest that we underestimated evacuation rates. Unless consumption rate is estimated every day, estimation of fish consumption rates for a period of time longer than a day requires the assumption that daily consumption rates do not vary significantly among days. The validity of this assumption ensures that interpolation of daily consumption rates between consecutive sampling days does not seriously affect consumption estimates over longer time periods. To our knowledge, the only study that has assessed the potential impact of day-to-day variation in daily consumption

Fig. 4. Relative difference to the mean between the radioisotope approach using ^{137}Cs as a tracer and the Eggers (1977) method in relation to the sampling interval length between the two sampling sessions. Dotted horizontal lines indicate the ±20% relative difference to the mean. Cross, Lake Beaulac; squares, Lake Raymond; diamonds, Lake Masson.

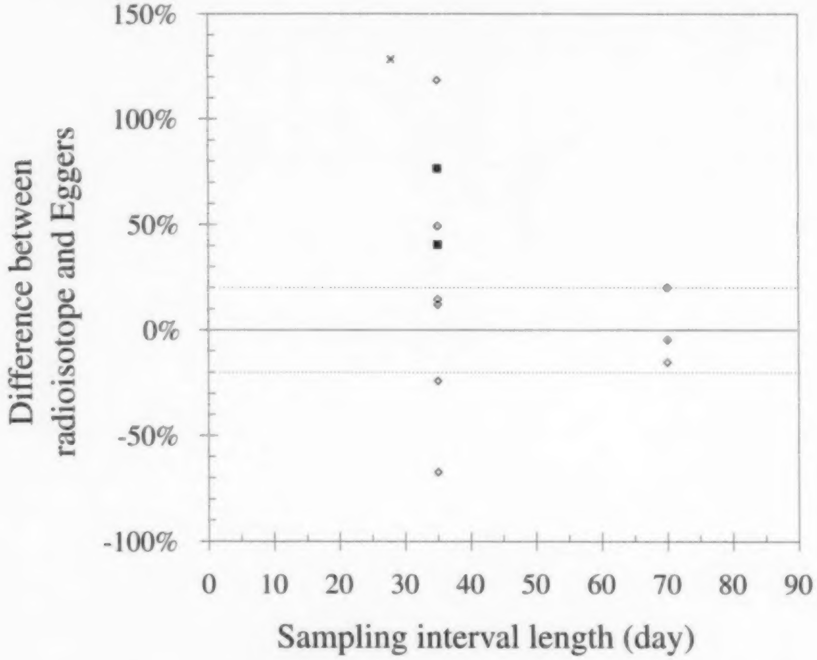

Fig. 5. Absolute value of the relative difference between the radioisotope approach and the Eggers (1977) method in relation to the ratio of the sampling interval length to the biological half-life. The lines correspond to the fitted regression model ($y = 0.0155e^{1.1442/x}$; $r^2 = 0.54$, $p < 0.01$, $n = 12$) and its 95% confidence intervals.

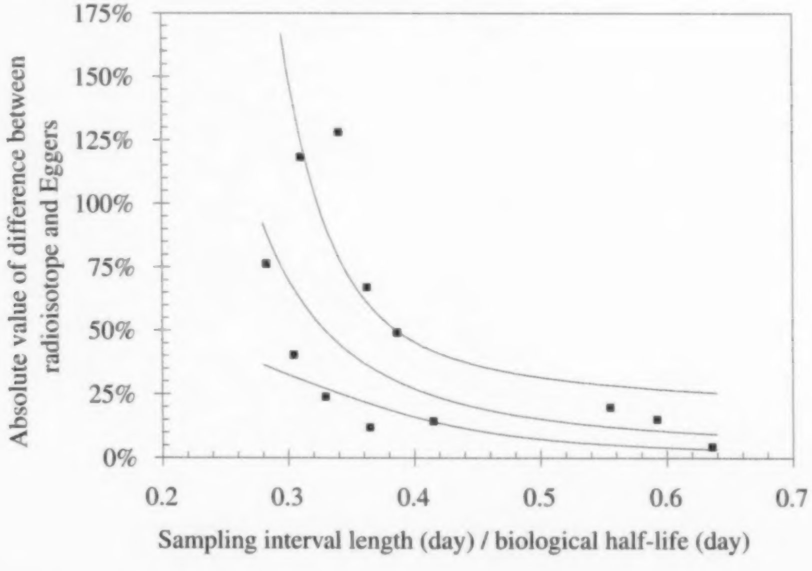

rates on seasonal consumption values showed that estimation of one fish daily consumption rate at intervals ranging from 1 to 30 days could be expected to cause a <20% variation in estimates of seasonal consumption rates. In our study, we estimated two consecutive daily consumption rates per month. Since the discrepancies between results obtained with surveys of CDTC and isotopic approaches ranged from 5 to 125%, we believe that this assumption may not be sufficient to explain the differences between these approaches. Furthermore, since the probability of events that would violate assumptions allowing the interpolation of daily consumption rate estimates (changes in prey abundance or fish diet) decreases as the time interval decreases, it is expected that monthly consumption rates obtained using digestive tract contents are more trustworthy than seasonal values.

Isotopic approaches assume that the time interval used to estimate consumption rates does not have to be sufficiently long to allow the kinetics of the contaminant to be biologically perceptible. We tested this assumption by evaluating the existence of a relationship between the absolute value of the percent difference between consumption rates from the isotopic approach and from surveys of digestive tract contents (y, percent), and the ratio (x) of the length of the sampling interval (days) to the estimated biological half-live of ^{137}Cs in fish ($t_{1/2}$, 75–147 days in our study). The difference between the isotopic and digestive tract content methods tended to decrease as the sampling interval, expressed as a fraction of the biological half-life of ^{137}Cs, increased ($y = 0.0155e^{1.1442/x}$; $r^2 = 0.54$, $p < 0.01$, $n = 12$) (Fig. 5). This relationship suggests that, with the isotopic approach, consumption rates within 20% ($y = 0.2$) of values determined with surveys of CDTC can be obtained with sampling intervals that correspond to at least 45% of the biological half-life of the contaminant ($x = 0.45$). Since the biological half-life of a contaminant is related to its elimination rate E (per day) by $t_{1/2} = \ln 2/E$, the length of the sampling interval (SIL, days) used in isotopic studies to obtain consumption rates within 20% of values obtained by surveys of digestive tract contents could be represented by $\mathrm{SIL} \geq 0.45t_{1/2}$ (or $\mathrm{SIL} \geq 0.312/E$). The expression $1 - e^{-\mathrm{SIL} \times E}$ is an estimation of the contaminant burden eliminated (percent) and it suggests that at least 27% of the contaminant burden should be eliminated to obtain reliable estimates of elimination rates using the empirical model of Rowan and Rasmussen (1995). It is important to note that the interpretation of the interaction described by Fig. 5 between the percent difference between consumption rates estimated using both approaches, the length of the sampling interval, and the biological half-life of a contaminant may be appropriate only for contaminants having a biological half-life similar to that of ^{137}Cs and for sampling intervals ranging from few weeks to months. Furthermore, the applicability of our model of sampling interval length to other fish species, environments, or contaminant concentration is not known but, if confirmed, could facilitate the definition of sampling strategies for isotopic studies designed to estimate fish consumption rates. The influence of the time interval on the difference between consumption estimates obtained using CDTC and isotopic models could be hypothesized to be related to other factors such as the importance of the increase of body burden, fish weight, or fish growth. We tested these hypotheses by evaluating the effect of these variables on the percent difference between consumption rates obtained with the Eggers and the isotopic models. We found no relationship between percent difference between consumption rates obtained with the Eggers and the isotopic models and any of these variables.

Isotopic modeling has been shown to be very sensitive to estimates of assimilation efficiency of ^{137}Cs (Rowan and Rasmussen 1996; Ugedal et al. 1997; Tucker and Rasmussen 1999). A better understanding of the factors that affect assimilation efficiency of ^{137}Cs may hence contribute to the improvement of isotopic models. Kevern (1966) noted that the assimilation efficiency of radiocesium by carp (*Cyprinus* sp.) fed on algae and kept at two different water temperatures was relatively constant despite different evacuation rates (retention time of food in the digestive tract was 37 h at 12.5°C and 22 h at 20°C). This suggested that assimilation efficiency of ^{137}Cs is a property of the food itself and not of the time spent by food in the digestive tract or of water temperature (also see Kolehmainen 1974; Forseth et al. 1992). In our study, we found a statistically significant correlation between evacuation rate and assimilation efficiency of ^{137}Cs ($r^2 = 0.29$). Evacuation rates, like assimilation efficiency, were not affected by water temperature or fish weight but were significantly influenced by prey type. In particular, the percent contribution to perch diet of prey difficult to digest (surface insects) had a significant negative effect on evacuation rates ($r^2 = 0.29$). According to Forseth et al. (1992), these prey are also associated with the lowest ^{137}Cs assimilation efficiencies. Hence, our study complements that of Kevern (1966) by suggesting that tissues difficult to process and digest may promote low evacuation rates and low assimilation efficiencies of ^{137}Cs. By extension, our work corroborates the use of the Forseth et al. (1992) method to estimate the assimilation efficiency of ^{137}Cs by brown trout for perch with a similar diet.

The convergence of consumption estimates supports the use of the model of Rowan and Rasmussen (1995) to estimate the elimination rate of ^{137}Cs by perch at a temporal scale of 70 days, although this species was not part of the data set used to develop their model. Our analyses also support the suggestion that interspecific variation of the elimination rate may be small (less than ±10%). Hence, our study strengthens an approach that has the potential to greatly reduce the sampling effort required to obtain fish consumption rates in the field. Although our work represents a corroboration of an attempt to estimate average consumption rates of specific age-classes at a temporal scale of a few weeks to a season, it also suggests that consumption rates obtained for time periods shorter than 70 days should be interpreted with caution. In light of the potential problems discussed above, before generalizing our results, we can only recommend the study of additional fish species, the use of multiple approaches, and the combination of laboratory and field experiments to further quantify the dynamics of contaminants.

Acknowledgements

We thank Hugo Asselin, Chantal Vis, Marie-Noëlle Chouinard, Mélanie Duquette, Marie-Hélène Forget, Nathalie Gaudreau, André-Hugues Gingras, Guillaume Rivest, and Marc Trudel for their help in the field and in the laboratory and for reviewing the manuscript. The quality of the manuscript was greatly enhanced by two anonymous referees. Funding for this research was provided by NSERC, FCAR-Nouveau chercheur, and FCAR-Équipe grants to D. Boisclair. J. Gingras was supported by postgraduate scholarships from FCAR and La Fondation J.A. Paulhus.

References

Boisclair, D., and Leggett, W.C. 1988. An in situ experimental evaluation of the Elliott and Persson and the Eggers models for estimating fish daily ration. Can. J. Fish. Aquat. Sci. **45**: 138–145.

Boisclair, D., and Marchand, F. 1993. The guts to estimate fish daily ration. Can. J. Fish. Aquat. Sci. **50**: 1969–1975.

Davis, J.J., and Foster, R.F. 1958. Bioaccumulation of radioisotopes through aquatic food chains. Ecology, **39**: 530–535.

Eggers, D.M. 1977. Factors in interpreting data obtained by diel sampling of fish stomachs. J. Fish. Res. Board Can. **34**: 290–294.

Elliott, J.M., and Persson, L. 1978. The estimation of daily rates of food consumption for fish. J. Anim. Ecol. **47**: 977–990.

Forseth, T., Jonsson, B., Naeumann, R., and Ugedal, O. 1992. Radioisotope method for estimating food consumption by brown trout (*Salmo trutta*). Can. J. Fish. Aquat. Sci. **49**: 1328–1335.

Forseth, T., Ugedal, O., and Jonsson, B. 1994. The energy budget, niche shift, reproduction and growth in a population of arctic charr, *Salvelinus alpinus*. J. Anim. Ecol. **63**: 116–126.

Forseth, T., Ugedal, O., and Jonsson, B. 1998. Radiocaesium elimination in fish: variation among and within species. J. Appl. Ecol. **35**: 847–856.

Forseth, T., Næsje, T., Jonsson, B., and Hârsaker, K. 1999. Juvenile migration in brown trout: a consequence of energetic state. J. Anim. Ecol. **68**: 787–793.

Gallegos, A.F., and Whicker, F.W. 1971. Radiocesium retention by rainbow trout as affected by temperature and weight. *In* Radionuclides in ecosystems. *Edited by* D.J. Nelson. U.S. AEC Rep. CONF-710501-P1. U.S. AEC, Washington, D.C. pp. 361–371.

Hakonson, T.E., Gallegos, A.F., and Whicker, F.W. 1975. Cesium kinetics data for estimating food consumption rates of trout. Health Phys. **29**: 301–306.

He, J., and Stewart, D.J. 1997. Comment — Measuring the bioenergetic cost of fish activity in situ using a globally dispersed radiotracer (^{137}Cs). Can. J. Fish. Aquat. Sci. **54**: 1953–1954.

Jonsson, B., Forseth, T., and Ugedal, O. 1999. Chernobyl radioactivity persists in fish. Nature (Lond.), **400**: 417.

Kevern, N.R. 1966. Feeding rate of carp estimated by radioisotopic method. Trans. Am. Fish. Soc. **95**: 363–371.

Kolehmainen, S.E. 1974. Daily feeding rates of bluegill (*Lepomis macrochirus*) determined by a rafined radioisotope method. J. Fish. Res. Board Can. **31**: 67–74.

LeCren, E. 1947. The determination of the age and growth of the perch (*Perca fluviatilis* L.) from the opercular bone. J. Anim. Ecol. **16**: 188–204.

Persson, L. 1979. The effects of temperature and different food organisms on the rate of gastric evacuation in perch (*Perca fluviatilis*). Freshwater Biol. **9**: 99–104.

Rowan, D.J., and Rasmussen, J.B. 1994. Bioaccumulation of radiocesium by fish: influence of physico-chemical factors and trophic structure. Can. J. Fish. Aquat. Sci. **51**: 2388–2410.

Rowan, D.J., and Rasmussen, J.B. 1995. The elimination of radiocesium from fish. J. Appl. Ecol. **32**: 739–744.

Rowan, D.J., and Rasmussen, J.B. 1996. Measuring the bioenergetic cost of fish activity in situ using a globally dispersed radiotracer (^{137}Cs). Can. J. Fish. Aquat. Sci. **53**: 734–745.

Rowan, D.J., and Rasmussen, J.B. 1997. Reply — Measuring the bioenergetic cost of fish activity in situ using a globally dispersed radiotracer (^{137}Cs). Can. J. Fish. Aquat. Sci. **54**: 1955–1956.

SAS Institute Inc. 1989. SAS/OR user's guide, version 6, first edition. SAS Institute Inc., Cary, N.C.

Schindler, D.E., and Eby, A.E. 1997. Stoichiometry of fishes and their prey: implications for nutrient recycling. Ecology, **78**: 1816–1831.

Sokal, R.R., and Rohlf, F.J. 1995. Biometry: the principles and practice of statistics in biological research. 3rd ed. W.H. Freeman and Company, New York.

Thomann, R.V. 1981. Equilibrium model of fate of mirocontaminants in diverse aquatic food chains. Can. J. Fish. Aquat. Sci. **38**: 280–296.

Trudel, M., and Boisclair, D. 1993. An in situ evaluation of the day-to-day variation in the quantity of food consumed by fish. Can. J. Fish. Aquat. Sci. **50**: 2157–2165.

Tucker, S., and Rasmussen, J.B. 1999. Using ^{137}Cs to measure and compare bioenergetic budgets of juvenile Atlantic salmon (*Salmo salar*) and brook trout (*Salvelinus fontinalis*) in the field. Can. J. Fish. Aquat. Sci. **56**: 875–887.

Ugedal, O., Forseth, T., and Jonsson, B. 1992. Effects of temperature and body size on radiocesium retention in brown trout, *Salmo trutta*. Freshwater Biol. **28**: 165–171.

Ugedal, O., Forseth, T., and Jonsson, B. 1997. A functional model of radiocesium turnover in brown trout. Ecol. Monogr. **7**: 1002–1016.

Appendix

The ^{137}Cs mass balance described by Rowan and Rasmussen (1996, formula 3; considering the physical decay (k) negligible compared with the elimination rate (E)) is

$$\text{(A1)} \quad \frac{\mathrm{d}Q}{\mathrm{d}t} = \alpha[^{137}\mathrm{Cs}]_{\mathrm{d}}\, C\, w - EQ$$

where Q is the fish ^{137}Cs body burden (becquerels), α is the assimilation efficiency (fraction), $[^{137}\mathrm{Cs}]_{\mathrm{d}}$ is the diet ^{137}Cs concentration (becquerels per gram dry), C is the relative consumption rate (grams dry per gram wet per day), w is the fish weight (grams wet), and E is the ^{137}Cs elimination rate (becquerels per becquerel per day). Assuming a linear trajectory of the fish weight in time:

$$\text{(A2)} \quad w = G_1 t + w_0$$

where G_1 is the growth rate (grams wet per day) and w_0 is the initial fish weight (grams wet). After proper rearrangement of eqs. A1, A2, and A3, we have

$$\text{(A3)} \quad \frac{\mathrm{d}Q}{\mathrm{d}t} + EQ = \alpha[^{137}\mathrm{Cs}]_{\mathrm{d}} C\,(G_1 t + w_0)\cdot$$

The solution of this differential equation is (Derrick and Grossman 1987)

$$\text{(A4)} \quad Q_t = \frac{(\alpha[^{137}\mathrm{Cs}]_{\mathrm{d}}C)}{\mathrm{E}^2} \times (E(G_1 t + w_0) - G) + \frac{Q_0 - \alpha[^{137}\mathrm{Cs}]_{\mathrm{d}}C)}{E^2} \times (Ew_0 - G_1))\mathrm{e}^{-Et}$$

Rearranging, we obtain

$$\text{(A5)} \quad C = \frac{(Q_t - Q_0\,\mathrm{e}^{-Et})E^2}{\alpha[^{137}\mathrm{Cs}]_d(EG_1t + (Ew_0 - G_1)(1 - \mathrm{e}^{-Et}))}.$$

Appendix references

Derrick, W.R., and Grossman, S.I. 1987. A first course in differential equations with applications. 3rd ed. West Publishing Company, St. Paul, Minn.

Rowan, D.J., and Rasmussen, J.B. 1996. Measuring the bioenergetic cost of fish activity in situ using a globally dispersed radiotracer (^{137}Cs). Can. J. Fish. Aquat. Sci. **53**: 734–745.

Canadian Journal of Fisheries and Aquatic Sciences

Author Index
Volume 57, 2000

Journal canadien des sciences halieutiques et aquatiques

Index des auteurs
Volume 57, 2000

Aarestrup, K., 2086
Aas, P., 755
Acou, A., 1627
Adams, S., 1448
Addison, R.F., 405
Adlerstein, S.A., 2363
Agnew, D.J., 429, 2479
Agustí, S., 25
Ahlgren, G., 2267
Ainaire, T., 755
Albessard, E., S3-91, S3-104
Allan, D.J., 192
Allen, S.E., 1919
Alpers, C.N., 380
Amiard, J.C., 34
Amiard-Triquet, C., 34
Amyot, M., S1-155
Andrew, N.L., 2293
Arbuckle, C.J., 1380
Archambault, J.-F., S1-164
Arendt, J.D., 351
Arrhenius, F., 2402
Atkinson, A., S3-31
Auclair, J.-C., 86, 870
Auer, M.T., 1033
Avois, C., 1940
Babcock, E.A., 357
Bachmann, R.W., 1574
Baglinière, J.-L., 497
Bandekar, R.R., 775
Banks, M.A., 915
Baranowski, R., 429
Bardonnet, A., 497
Barillé, L., 837
Barnard, E., S1-86
Barrowman, N.J., 665
Barry, K.L., 2032
Basu, B.K., S1-7
Bath, G.E., 2122
Bauer-Nemeschkal, E., 789
Baxter, C.V., 1470
Beacham, T.D., 1985
Beamish, F.W.H., 2345
Beaulieu, S.E., 1434
Beckvar, N., 1103
Beddington, J.R., 429, 2479
Bednarek, A.T., 530
Bedo, A., S3-38
Béland, P., S1-101
Benoit, H.P., 856
Berejikian, B.A., 628, 1911
Berglund, O., 1160
Bernatchez, L., 1, 797
Bert, D.G., 570
Bertilsson, S., 875
Bérubé, P., 1562
Biberhofer, J., S1-52
Biggs, B.J.F., 1380
Bilby, R.E., 699
Bilos, C., 1139
Bird, D.F., 600, 1284
Bishop, K., 1888
Bjerkely, F., 1423
Bjerselius, R., 557
Bjorkstedt, E.P., 459
Björnsson, B.T., 1969
Bloom, N.S., 1092
Blum, J.D., 2280
Boberg, M., 2267
Bodini, A., 1999
Boisclair, D., 581, 1482, 2065, 2547
Botsford, L.W., 616, 980
Boutoute, M., S3-91
Bouza, C., 2130
Bowen, M., 755
Bowen, W.D., 898
Bradbury, I.R., 1761
Bradford, M.J., 13, 677
Brady, V.J., 1243
Branch, G.M., 2175
Brant, H.A., 171
Brauner, C.J., 2054
Brawley, S.H., 66
Brazner, J.C., 1243
Breault, R.F., 1073, 1080
Breen, P.A., 2293
Brickman, D., 513, 2519
Bridgeman, T.B., 1539
Brierley, A.S., S3-24
Brochu, C., 1139
Brodeur, J., 441
Bromhead, D., 732
Brooks, C.M., 1033
Brown, C.D., 1574
Brown, J.A., 856, 2223
Bryan, A.L., Jr., 171
Bryden, C.A., 2186
Buchholz, F., S3-38, S3-115
Buckley, L.J., 1957
Bulger, A.J., 1515
Burger, C.V., 2096
Burger, J., 171
Burgetz, I., 2248
Burke, J.S., 1870
Burnham, K.P., 886
Burrows, M., S3-38
Bush, B., S1-86
Buso, D.C., S2-19
Butler, M.G., 76
Buttle, J.M., S2-5
Buzby, K.M., 1773
Cain, D.J., 380
Calavetta, M.J., 915
Campbell, L.M., 1258
Campbell, M.M., 1151
Campbell, P.G.C., 1330, 1692, S1-126, S1-164
Campbell, R.W., 518
Campton, D.E., 2096
Canfield, D.E., Jr., 1574
Cardinale, M., 2402
Carignan, R., S1-63, S2-1, S2-105, S2-118, S2-129, S2-136, S2-155
Carpenter, S.R., 1524, 1617, S2-50
Carter, J.L., 380
Casey, A., S1-86
Casillas, E., 1911
Cass, A., 962
Chalanchuk, S.M., 192
Chambers, P.A., 125, 1342
Charlton, M.N., 86, 371, 870
Chen, D.G., 1878

Note: Page numbers preceded by S1, S2, and S3 represent articles published in Supplements 1, 2 and 3, respectively.

Nota : Les numéros précédés de S1, S2 et S3 désignent les articles publiés dans les suppléments 1, 2 et 3, respectivement.

Chen, Y., 2293
Chesson, P.L., 1190
Chiarenzelli, J., S1-86
Chick, J.H., 106, 872
Cho, Y.-C., S1-95
Clarke, A., S3-178
Clarke, C., 1668
Clason, B., 1410
Cognie, B., 837
Colautti, D., 1139
Cole, J.J., 487, 1524
Collier, D.C., 231
Collier, T.K., 1911
Colman, J.A., 1073, 1080
Colombo, J.C., 1139
Cope, W.G., 1092
Cosby, B.J., 1515
Cossa, D., S1-78, S1-138
Couillard, Y., 1692, S1-126
Cowan, J.H., Jr., 478
Cowell, L.G., 2010
Coyle, K.O., 2112, 2306
Crayton, M., 231
Creed, I.F., 1977
Cripps, G.C., S3-31
Crowder, D.W., 1497
Crowder, L.B., 2010
Culp, J.M., 125
Cunjak, R.A., 1326
Cuzin-Roudy, J., S3-6
D'Arcy, P., S2-105, S2-118
Dauble, D.D., 1636
Davies, C.R., 1448
Dean, C.A., 915
de Lafontaine, Y., 1843, S1-174
DeLury, N., 1668
Desrosiers, M., S2-136
Désy, J.C., S1-164
Devito, K.J., 1977, S2-60
Devlin, R.H., 939
deYoung, B., 644
Diamond, S.L., 2010
Dillon, A.K., 1701
Dinsmore, W.P., S2-73
Diplas, P., 1497
Dixon, D.G., 1489
Doerr, S.M., 1033
Dolgov, A.V., 2433
Donald, D.B., 1258
Douglas, M.S.V., 2163
Downing, J.A., 1482
Doyon, M.-R., S1-155
Driscoll, C.T., 1033
Driscoll, S., 1120
Duarte, C.M., 25
Duchesne, P., 1
Dugoua, J.J., 2211
Dulvy, N.K., 116
Dumont, P., S1-174
Dutil, J.-D., 815, 826
Eadie, J.M., 1843
Eaton, B., 1120
Edlund, M.B., 610
Effler, S.W., 1033
Eggleston, D.B., 1870
Elliott, J.K., 1537
Elliott, N.G., S3-51
Enache, M., S2-146
Engstrom, D.R., 1062
Erm, V., 451
Essington, T.E., 205, 548
Evans, J.E., S2-60
Ewald, G., 1160
Ewert, V.E., 205
Fabrizio, M.C., 775
Fahnenstiel, G.L., 1901
Falk-Petersen, S., S3-178
Farrell, A.P., 1668
Feder, J.L., 637
Fend, S.V., 380
Ferguson, M., 805
Ferraris, J., 51
Feunteun, E., 1627
Field, J.G., 2044
Filion, A., S1-113
Findlay, C.S., 570
Findlay, R.H., 1113
Finkelstein, K., 1103
Finstad, A.G., 1718
Fischer, J.M., 538
Fischer, P., 2336
Flagg, T.A., 628
Flessas, C., S1-126
Fletcher, G.L., 644
Flore, L., 342
Fogarty, M.J., 2455
Folt, C.L., 2280
Forney, J.L., 742
Francoeur, S.N., 1380
Frank, K.T., 513, 1747, 2393, 2519
Franks, P.J.S., 1961
Fraser, S., 1761
Frazier, B.E., 1062
French, B.L., 1911
Friedland, K.D., 1181
Frischer, M.E., 591
Fu, C., 2420
Fuller, S.D., 2357
Furgal, J.A., 371
Gagnon, P., S1-31, S1-174
Gallaugher, P., 1668
Garcia, E., S2-129
Garcí-Marín, J.L., 2201
Garrison, L.P., 1679, 2455
Gaudreau, N., 581
Geffard, A., 34
Geist, D.R., 1636, 1647
Giannico, G.R., 1804
Gibson, J.J., S2-73
Gilligan, E., S1-86
Gingras, J., 2547
Glickman, B., 405
Gobeil, C., S1-138
Goddard, S.V., 644
Goedkoop, W., 2267
Goetze, E., 1434
Goldstein, R.M., 307
Gordon, R., 405
Goshorn, C.J., 886
Granéli, H.W., 875
Grant, G.C., 557
Greenberg, B.M., 371
Groulx, S-R., S2-136
Grout, J.A., 181, 2032
Guay, J.C., 2065
Gunn, J.M., S2-97
Hadderingh, R.H., 708
Hagen, W., S3-178
Hall, R.I., 333
Ham, K.D., 17
Hamner, P.P., S3-192
Hamner, W.M., S3-192
Hampton, J., 1002
Hannah, C.G., 2488, 2506
Hansen, M.M., 2130
Hanson, M.A., 76
Hardy, F.J., 231
Hare, L., 327
Hargreaves, N.B., 1878
Harmelin-Vivien, M., 1291
Haro, A., 1326
Harvey, C.J., 1395
Hattala, K.A., 886
Hauer, F.R., 1470
Haure, J., 837
Hayward, R.S., 1131
He, P., 1200
He, X., 886
Head, E.J.H., 518
Healey, M.C., 2248
Heath, D.D., 2186
Hebert, P.D.N., 687
Hedgecock, D., 915, 2368
Hedrick, P.W., 2368
Heintz, R.A., 2076
Hellebust, J.A., 2163
Helu, S.L., 1784
Henderson, M.A., 2248
Heppell, S.A., 148
Herzka, S.Z., 137
Hesslein, R., 1489
Heyes, A., 2211
Hickie, B.E., S1-101
Hill, J.A., 939
Hill, S., 2479
Hill, W.R., 530
Hinch, S.G., 2470
Hodgson, J.R., 548
Hodson, P.V., S1-101
Hogg, I.D., 1843

Holland, D.S., 1307
Holst, R., 1551
Holt, G.J., 137
Hontela, A., 441, 1692
Hornbeck, J.W., S2-19
Hoshino, N., 1300
Houser, J.N., 1524
Hoyer, M.V., 1574
Hrudey, S.E., 1584
Hubert, J., S1-164
Hubert, W.A., 468
Hudon, C., S1-16, S1-31
Hunt, C., 1220
Hunt, G.W., 1545
Huryn, A.D., 1380
Hutchings, J.A., 805
Hutchings, L., 2044
Incze, L.S., 755
Irvine, J.R., 13, 677
Isaak, D.J., 468
Jacoby, J.M., 231
Jagoe, C.H., 171
Jansen, P.A., 1718
Jarman, S.N., S3-51
Jeffrey, J.A., 1728
Jeffries, D.S., S2-40
Jenner, H.A., 708
Jennings, S., 116
Jensen, F.B., 2054
Johannsson, O., 1489
Johnsen, P.B., 557
Johnson, G., S1-86
Johnson, L.E., 993
Johnson, S.L., 906, S2-30
Jones, C.M., 2122
Jones, J.A., 1636, S2-30
Jugdaohsingh, R., 1151
Kahn, D.M., 886
Kahnle, A.W., 886
Kalff, J., 25, S1-7
Kalish, J., 732
Kamler, E., 789
Kapuscinski, A.R., 391
Kattner, G., S3-178
Kauppila, P., 844
Keckeis, H., 342, 789
Kehler, D.G., 2357
Keller, A.A., 2382
Kellison, G.T., 1870
Kennedy, B.P., 2280
Kerans, B.L., 1190
Kern, J.W., 2112
Khlobystov, V.V., 1932
Kidd, K.A., 1258
Kiessling, A., 939
Kim, J., S1-95
Kimmerer, W.J., 478
Kimura, D.K., 160
Kingsley, M.C.S., S1-101
Kitchell, J.F., 548, 1395
Kjellman, J., 451
Klein-MacPhee, G., 2382
Klug, J.L., 538
Knudsen, E.E., 2319
Kotak, B.G., 1584, S2-60
Kraft, C.E., 993
Kreiberg, H., 1668
Kulka, D.W., 644
Kummerow, E., 628
Kuns, M.M., 2240
Kushneriuk, R.S., S2-82
Kuznetsov, Y.A., 1208
Lachance, S., 1562
Laffaille, P., 1627
Laflamme, J.-S., 1692
Lalonde, S., S1-31
Lam, A.K.-Y., 1584
Lam, D.C.L., S2-40
Lambert, Y., 815, 826
Lamberti, G.A., 637
Lamontagne, S., S2-105, S2-118
Landoni, P., 1139
Langeland, A., 1718
Langness, O.P., 1742
Lantry, B.F., 1594
Lapointe, M., 1120, 2065
Lappalainen, J., 451
LaRae, A.L., 628
Larsen, I.L., 530
Larsson, P., 1160
Lasker, J.M., 1434
Lathrop, R.C., 1617
Latulippe, C., 1120
Laudon, H., 1888
Lavoie, D., 1853
Lawson, G.L., 1011
Le, K.D., 1985
Lean, D.R.S., S1-1, S1-43, S1-155
Leavitt, P.R., S2-50
LeBreton, G.T.O., 2345
Leclerc, M., 2065
Lee, D.C., 1834
Lee, Y.-W., 2443
Legault, A., 1627
Legendre, P., 1940, 2065
Leggett, M.F., 1489
Leggett, W.C., 1537
Lehtonen, H., 451
Leising, A.W., 1961
Lemieux, M., 1562
Lenicov, M.R., 1139
Lepage, S., S1-52
Leroy, A., 837
Lester, N.P., 725
Levings, C.D., 2032
Lewis, K.M., 637
Li, W., 557
Likens, G.E., S2-19
Lilly, G.R., 1355, 2230
Lindell, M.J., 875
Link, J.S., 2455
Little, J.L., 333
Liu, Y., 1878
Loder, J.W., 2488, 2506
Lohrenz, S.E., 1901
Lonzarich, D.G., 1508
Lonzarich, M.R., 1508
Lorenzen, K., 2374
Lorrain, S., S1-52, S1-63
Lough, R.G., 1957
Luoma, S.N., 380
MacIsaac, E., 96
Mackay, D., S1-101
Madenjian, C.P., 1025
Madsen, S.S., 2054, 2086
Maes, J., 1404
Magnan, P., S2-165
Magnuson, J.J., 1042
Magnusson, K., 2319
Mahnken, C.V.W., 628
Mailhot, Y., S1-174
Mangel, M., S3-1
Maniak, P.J., 557
Manske, M., 241
Mapstone, B.D., 1448
Marshall, C.T., 2433
Martens, D., 405
Martin, C.W., S2-19
Martineau, D., S1-174
Marwood, C.A., 371
Maselko, J.M., 2076
Masson, S., 1940
Mather, M.E., 1607
Matthews, J., S3-38
Mayer, C.M., 742
Mayfield, S., 2175
Mayzaud, P., S3-38, S3-91, S3-104
McConnaughey, R.A., 2410
McCormick, M.J., 1901
McCormick, S.D., 1969
McCrohan, C.R., 1151
McEachern, P., S2-73
McIntosh, A.R., 2140
McMenemy, J.R., 1607
McMinn, A., S3-51
Meekan, M.G., 1291
Meeuwig, J.J., 844
Ménard, C., 1482, S1-174
Mensberg, K.-L.D., 2130
Menshutkin, V.V., 789
Merritt, M.F., 1459
Messick, G., 1539
Metcalfe, N.B., 719
Metcalfe, R.A., S2-5
Meyer, R., 43
Michaels, W., 2455
Mikaelian, I., S1-174
Millar, R.B., 43, 507
Millar, R.G., 928
Miller, K.M., 1985

Miller, L.W., 478
Mills, E.L., 742
Mills, K.H., 192
Milner, A.M., 2319
Minns, C.K., 1657
Mitro, M.G., 951
Moore, T.R., 2211
Moran, M.D., S2-40
Morbey, Y., 1252
Morgan, L.E., 980
Morin, A., S1-113
Morita, K., 1300
Mouneyrac, C., 34
Mueter, F.J., 1169
Muir, D.C.G., 1258, S1-101
Mulholland, P.J., 66
Mullin, M.M., 1434
Munger, C., 327
Murray, C.J., 1636
Myers, R.A., 665, 677, 2357
Naiman, R.J., 699
Naimo, T.J., 1092
Nelson, R.J., 1985
Nemeschkal, H.L., 789
Newman, R.M., 307
Nichols, P., S3-104
Nickelson, T.E., 906
Nicol, S., S3-1, S3-51, S3-168
Nidle, B.H., 2032
Nielsen, E.E., 2130
Nielsen, J.R., 1551
Nielson, C., 2086
Nierzwicki-Bauer, S.A., 591
Nislow, K.H., 2280
Nolan, C.P., 429
Nolan, D.T., 708
Norcross, B.L., 1169
Nortrup, D.A., 1025
O'Connor, D.V., 1025
O'Driscoll, R.L., 1355
O'Keefe, P., S1-86
Okla, L., 1160
Olding, D.D., 2163
Ollevier, F., 1404
Pace, M.L., 487
Padilla, D.K., 1617
Pakhomov, E.A., S3-68
Paquet, S., S2-136
Paré, D., S2-118
Parkhouse, W., 1668
Parkinson, E., 766
Parrish, D.L., 1607
Parsons, R.H., 591
Patarnello, T., S3-16
Patoine, A., S2-155
Patterson, A.K., 1701
Paul, A.J., 1220
Paulsen, C.M., 616
Pavlov, D.F., 1932
Pearsons, T.N., 17
Peck, M.A., 1957
Pelletier, D., 51
Pelletier, L., S1-174
Penn, M.R., 1033
Pepin, P., 856
Perry, S.A., 1773
Peterman, R.M., 181
Petrie, B., 2536
Petrosky, C.E., 1742
Pham, T.-T., S1-78
Phillips, I.T., 2319
Pick, F.R., S1-148
Piercey, G.E., 2032
Pikitch, E.K., 357
Pinel-Alloul, B., 1940, S1-7, S1-126, S1-164, S2-155
Pitkänen, H., 844
Pla, C., 2201
Plagányi, É.E., 2044
Planas, D., S2-136
Poissant, L., S1-155
Poléo, A.B.S., 1423
Polkinghorne, C.N., 557
Porter, M., 766
Post, J.R., 1220
Poulsen, S., 1551
Powell, J.J., 1151
Prairie, Y.T., 600, 1284, S2-118, S2-146,
Prepas, E.E., 125, 1584, 1977, S2-60, S2-73, S2-155
Proulx, S., S1-78
Purchase, C.F., 2223
Pyper, B.J., 181
Quinlan, R., 333
Quinn, T.J., II, 1459, 2420
Quinn, T.P., 205, 1911
Rada, R.G., 1062
Rand, P.S., 2470
Randall, R.G., 1657
Rashbrook, V.K., 915, 2368
Rasmussen, J.B., 414, 441, 725, 871
Raz, J., 775
Reckendorfer, W., 342
Reddin, D.G., 1181
Reed-Andersen, T., 1617
Reeves, G.H., 2152
Rennie, C.D., 928
Reynolds, J.D., 116
Rhee, G-Y., S1-95
Ricciardi-Rigault, M., 1284
Rice, S.D., 2076
Richard, Y., S1-174
Richards, L.J., 962
Rickman, S.J., 116
Rinaldi, S., 1208
Rioux, D., 2065
Ritz, D.A., S3-59
Robarts, R.D., 1932
Robertson, A.L., 2319
Rodgers, J.D., 906
Roff, J.C., 1965
Rondeau, B., S1-78
Rose, G.A., 644, 1011, 1355
Rose, K.A., 478
Rosemond, A.D., 66
Rosenfeld, J., 766, 1369
Rot, B.W., 699
Rothwell, R.L., 1977
Roussel, J.-M., 1326
Routledge, R., 1668
Rowan, D.J., 441
Rudd, J.W.M., 2211
Rudstam, L.G., 742
Russ, G.R., 1448
Ruzzante, D.E., 2130
Sabik, H., S1-78
Saborowski, R., S3-38, S3-115
Salazar, M., 1103
Salazar, S., 1103
Sampson, D.B., 1784, 2443
Sand-Jensen, K., 2022
Sanz, N., 2201
Sargent, J., S3-178
Sastri, A.R., 1965
Saucier, F.J., 1853
Schaller, H.A., 1742
Scheffer, M., 1208
Schell, D., 2319
Schelske, C.L., 610, 1901
Schetagne, R., 414, 871
Schick, R.S., 2193
Schindler, D.W., 1258
Schneider, D.C., 1355
Schnute, J.T., 962
Scholz, N.L., 1911
Schwarz, C.J., 241, 247
Scribner, K.T., 2096
Scrimgeour, G.J., 125, 1342
Scully, N.M., S1-43, S2-50
Seelye, J.G., 557
Seidelin, M., 2054
Sein, R., S2-97
Senanan, W., 391
Servos, M.R., 1489
Shackell, N.L., 1747
Shelton, P.A., 2230
Sherwood, G.D., 441
Shields, P.J., 1053
Shore, J.A., 2488, 2506
Shrimpton, J.M., 1969
Shuter, B.J., 725
Shuttleworth, S., 1232
Siegel, V., S3-130, S3-151
Sigler, M.F., 1270
Simard, Y., 1853
Sinclair, A.F., 1321
Skúlason, S., 719
Smith, B., S1-86
Smith, B.D., 255, 271, 285, 980
Smith, D.R., 886

Smith, K.R., 2410
Smith, R.E.H., 317, 371
Smol, J.P., 333
Smoot, J.C., 1113
Snelgrove, P.V.R., 1761
Snodgrass, J.W., 171
Soiseth, C., 2319
Sokol, R.C., S1-95
Solazzi, M.F., 906
Solomon, K.R., 371
Sonesten, L., 2267
Sorensen, P.W., 557
Spanings, F.A.T., 708
Spearman, W.J., 2096
Sprules, W.G., 2240
Stanley, E.H., 1545
Stauffer, J.C., 307
St-Cyr, L., 1330, S1-126
Steedman, R.J., S2-1, S2-82, S2-92
Stein, R.A., 1190
Stepien, C.A., 1701
Sterling, G.L., 1220
Stewart, D.J., 1594
Stobo, W.T., 247
Stoermer, E.F., 610
Stone, R.A., 1901
St-Onge, I., S2-165
Stæhr, K.-J., 1551
Sullivan, C.V., 148
Suthers, I., 1534
Swain, D.P., 1321, 2393
Swanton, C.O., 2096
Taggart, C.T., 1728
Takahashi, H., 1814
Takata, K., 1814
Tanasichuk, R.W., 2258
Tang, M., 1482
Tanner, D.K., 1243
Tarling, G., S3-38
Taylor, C.M., 610
Taylor, H.E., 380
Taylor, W.D., 1489
Teeter, J.H., 557
Tessier, N., 797
Tezak, E.P., 628
Thedinga, J.F., 2076
Thompson, W.L., 1834
Thompson-Roberts, E.S., S1-148
Thomson, R.E., 1919
Thorrold, S.R., 1232, 2122
Townsend, C.R., 1380
Tremblay, A., 414, 871
Trudel, M., 414, 871
Truelove, N.K., 1911
Twiss, M.R., 86, 870
Urban, D.L., 2193
Valdimarsson, S.K., 719
Van Den Avyle, M.J., 106, 872
van der Meeren, G.I., 1794
Vanderploeg, H.A., 1539
Vander Zanden, M.J., 725
VanDeValk, A.J., 742
Vathanodorn, K., 591
Vestergaard, O., 2022
Vigliola, L., 1291
Vincent, W.F., S1-43
Virtue, P., S3-91, S3-104
Waitkus, K.R., 591
Waldron, M.C., 1080
Walker, T.I., 214
Walsh, S.J., 1200
Ward, B.R., 255, 271, 298
Ware, D.M., 1878
Waring, P., 732
Warren, M.L., Jr., 1508
Watkins, J.L., S3-24
Webb, J.R., 1515
Weisse, T., 96
Welch, D.W., 225
Welch, E.B., 231
Welleman, H.C., 2363
Wells, B.K., 2122
Wendelaar Bonga, S.E., 708
Werner, F.E., 1957
Wertheimer, A.C., 2076
Westling, O., 1888
Whalen, K.G., 1607
White, K.N., 1151
Whitehead, H., 223
Whitledge, G.W., 1131
Wiener, J.G., 1053, 1062, 1092
Wilhelm, S.W., 317
Williams, J.G., 1739
Willis, T.V., 1042
Wilson, D.S., 351
Wilson, J.Y., 405
Wing, S.R., 980
Winger, P.D., 1200
Withler, R.E., 1985
Witt, J.D.S., 687
Wong, I., S2-40
Xenopoulos, M.A., 600
Xiao, Y., 214
Yamamoto, S., 1300
Yaragina, N.A., 2433
Yeats, P.A., 2536
Yee, K.A., 125
Yin, Y., 1784
Young, R., 1380
Zabel, R.W., 1739
Zale, A.V., 951
Zane, L., S3-16
Zauke, G.-P., 1410
Zheng, L., 570
Zhulidov, A.V., 1932
Zimmer, K.D., 76
Zimmerman, C.E., 2152
Ådlandsvik, B., 2433

The index and/or table of contents has been removed and photographed separately within this volume year.

For roll film users, this information for the current volume year is at the beginning of the microfilm. For a prior year volume, this information is at the end of the microfilm.

For microfiche users, the index and/or contents is contained on a separate fiche.

National Research Council Canada | Conseil national de recherches Canada | Copyright Transfer

ASSIGNMENT OF COPYRIGHT

Ms. No. ____________

To: NATIONAL RESEARCH COUNCIL OF CANADA ("NRC") Research Press

From: ____
____
____
____
(name and address of author signing this form)

This refers to the manuscript entitled: ____
____

written by myself and the following additional author(s): ______________________________
____

for publication in: ____

1. I declare that the list of authors fairly conforms to academic conventions about who should be listed. I declare that the manuscript, or its equivalent, has not been submitted for publication elsewhere. If it is accepted for publication by the National Research Council of Canada, I will ensure that it, or its equivalent, is not submitted for publication elsewhere.

2. I declare that I am (check ONE):

☐ (a) the sole owner of the copyright relating to the manuscript, and → I **assign** to NRC the entire copyright.

☐ (b) a part owner of the copyright, in conjunction with interests held by co-authors or their employers, and → I **assign** to NRC my entire interest in the copyright, and I expect the co-authors to also sign a form like this one.

☐ (c) an agent of my employer with authority to assign the copyright owned by the employer, who is: ______________________, and → I **assign** to NRC, on behalf of my employer, my employer's entire interest in the copyright relating to the manuscript, and I expect the co-authors to also sign a form like this one.

☐ (d) a public servant in Canada (federal, provincial or territorial) or the United Kingdom, so that the copyright is owned by Her Majesty, and → I have obtained the approval of my employer, according to the terms of my employment, to grant NRC **non-exclusive permission** to publish the manuscript and administer the copyright.

☐ (e) a public servant of the United States of America, and subject to the law that creates no U.S. copyright for the manuscript, and → I **assign** to NRC, on behalf of my employer, my employer's entire interest in any copyright that may exist outside the U.S., and I expect the co-authors to sign a form like this one.

3. I understand that my submission of this document does not guarantee publication, and that publication will not occur until **all authors** have provided a copyright transfer. If the manuscript is not published within 2 years after I sign this, the assignment is revoked.

Signed at ______________________________________ on ______________________
(City and Province/State) (Date)

____
(Signature)

[Standard NRC form; alterations not acceptable.]

Comments on Copyright Transfer
(with extracts from the *Copyright Act*, Revised Statutes of Canada 1985, chapter C-42, as amended)

The publisher is not permitted to publish the manuscript without permission or an assignment of ownership of copyright. For greatest flexibility, and to be prepared to deal with future uses of the published material, the publisher requires ownership.

The owner may assign the right, but that assignment must be in writing:

13.(4) The owner of the copyright in any work may assign the right, either wholly or partially, and either generally or subject to territorial limitations, and either for the whole term of the copyright or for any other part thereof, and may grant any interest in the right by licence, but no assignment or grant is valid unless it is in writing signed by the owner of the right in respect of which the assignment or grant is made, or by his duly authorized agent.

The owner may be the author, but in many cases, the owner is the author's employer:

13.(3) Where the author of a work was in the employment of some other person under a contract of service or apprenticeship and the work was made in the course of his employment by that person, the person by whom the author was employed shall, in the absence of any agreement to the contrary, be the first owner of the copyright, but where the work is an article or other contribution to a newspaper, magazine or similar periodical, there shall, in the absence of any agreement to the contrary, be deemed to be reserved to the author a right to restrain the publication of the work, otherwise than as part of a newspaper, magazine or similar periodical.

The only exception to taking ownership arises when the manuscript is covered by Crown copyright owned by a Canadian government.

12. Without prejudice to any rights or privileges of the Crown, where any work is, or has been, prepared or published by or under the direction or control of Her Majesty or any government department, the copyright in the work shall, subject to any agreement with the author, belong to Her Majesty and in that case shall continue for the remainder of the calendar year of the first publication of the work and for a period of fifty years following the end of that calendar year.

Governments, and in particular the federal government, do not have a simple mechanism for assigning ownership of this particular type of Crown asset. Therefore, when an author is a public servant so that there is Crown copyright in the manuscript, a simple permission to use is acceptable to the publisher, if it is granted by a person with appropriate authority.

Conseil national de recherches
Canada

National Research Council
Canada

Cession du droit d'auteur

CESSION DU DROIT D'AUTEUR

Document n° ________

Au : CONSEIL NATIONAL DE RECHERCHES DU CANADA («CNRC») - Presses scientifiques

De : ____________________________________

____

____

____

(nom et adresse de l'auteur qui signe le présent formulaire)

La présente cession porte sur le document intitulé : ____________________________________

____

rédigé par moi, en collaboration avec l'auteur/les auteurs suivant(s) : ____________________

____

aux fins de publication dans : ____________________________________

1. Je déclare que la liste des auteurs ci-dessus respecte les pratiques usuelles de rédaction savante quant aux personnes dont le nom doit être cité. Je déclare que le document ou son équivalent n'a pas été soumis à quelque autre organisme aux fins de publication. Si le CNRC accepte de publier le document, je m'assurerai que celui-ci ou son équivalent n'est soumis à aucun autre organisme aux fins de publication sans en obtenir la permission préalable du CNRC.

2. Je déclare être (UN SEUL choix) :

☐	(a)	le seul titulaire de droit d'auteur afférent au document,	et →	je **cède** le droit d'auteur intégral au CNRC.
☐	(b)	un titulaire partite du droit d'auteur, de concert avec des coauteurs ou leurs employeurs,	et →	je **cède** ma part du droit d'auteur au CNRC et m'attends à ce que les coauteurs signent une entente comparable.
☐	(c)	un agent de mon employeur ayant l'autorité de céder le droit d'auteur appartenant à l'employeur, nommément : ____________________,	et →	je **cède** au CNRC, au nom de mon employeur, la part entière du droit d'auteur afférent au document appartenant à mon employeur, et m'attends à ce que les coauteurs signent une entente comparable.
☐	(d)	un fonctionnaire du Canada (fédéral, provincial ou territorial) ou du Royaume-Uni, donc le droit d'auteur appartient à Sa Majesté,	et →	j'ai obtenu de mon employeur, en vertu de mes conditions d'emploi, l'autorisation d'accorder au CNRC la **permission non exclusive** de publier le document et de gérer le droit d'auteur.
☐	(e)	un fonctionnaire des États-Unis d'Amérique, donc sujet à la loi qui n'associe aucun droit d'auteur américain au document,	et →	je **cède** au CNRC, au nom de mon employeur, la part entière de quelque droit d'auteur en vigueur ailleurs qu'aux É.-U. appartenant à mon employeur, et m'attends à ce que les coauteurs signent une entente comparable.

3. Je comprends que la soumission du document ne garantit aucunement sa publication et que la publication ne pourra être réalisée tant que **tous les auteurs** n'auront pas signé une cession du droit d'auteur. Si le document n'est pas publié dans les deux années suivant ma signature des présentes, la cession sera automatiquement révoquée.

Signé à ____________________________________, le ____________________

(ville et province/état) (date)

____

(signature)

[Formulaire normalisé du CNRC; aucune modification permise.]

Commentaires sur la cession du droit d'auteur
(accompagnés d'extraits de la *Loi sur le droit d'auteur*, Lois révisées du Canada 1985, chapitre C-42 modifié)

L'éditeur ne peut publier un document sans la permission ou une cession du droit d'auteur. Pour des raisons de souplesse et en vue de l'utilisation future du document publié, l'éditeur doit devenir titulaire du droit d'auteur.

Le titulaire peut céder le droit, mais cette cession doit être faite par écrit :
13.(4) Le titulaire du droit d'auteur sur une oeuvre peut céder ce droit, en totalité ou en partie, d'une façon générale, ou avec des restrictions territoriales, pour la durée complète ou partielle de la protection; il peut également concéder, par une licence, un intérêt quelconque dans ce droit; mais la cession ou la concession n'est valable que si elle est rédigée par écrit et signée par le titulaire du droit qui en fait l'objet, ou par son agent dûment autorisé.

Le titulaire peut être l'auteur, mais dans plusieurs cas, le titulaire est l'employeur de l'auteur:
13.(3) Lorsque l'auteur est employé par une autre personne en vertu d'un contrat de louage de service ou d'apprentissage, et que l'oeuvre est exécutée dans l'exercice de cet emploi, l'employeur est, à moins de stipulation contraire, le premier titulaire du droit d'auteur; mais lorsque l'oeuvre est un article ou un autre contribution, à un journal, à une revue ou à un périodique du même genre, l'auteur, en l'absence de convention contraire, est réputé posséder le droit d'interdire la publication de cette oeuvre ailleurs que dans un journal, une revue ou un périodique semblable.

La seule exception dans la cession du droit d'auteur est lorsque le document est associé au droit d'auteur de la Couronne, qui appartient au gouvernement du Canada .
12. Sous réserve de tous les droits ou privilèges de la Couronne, le droit d'auteur sur les oeuvres préparées ou publiées par l'entremise, sous la direction ou la surveillance de Sa Majesté ou d'un ministère du gouvernement, appartient, sauf stipulation conclue avec l'auteur, à Sa Majesté et, dans ce cas, il subsiste jusqu'à la fin de la cinquantième année suivant celle de la première publication de l'oeuvre.

Les gouvernements, en particulier le gouvernement fédéral, ne disposent pas d'un mécanisme simple de cession de droit d'auteur pour ce genre de biens de la Couronne. C'est pourquoi lorsqu'un auteur est un fonctionnaire et que, par conséquent, le droit d'auteur appartient à la Couronne, une simple permission d'usage est suffisante pour l'éditeur, pour autant que celle-ci ait été octroyée par une personne jouissant de l'autorité nécessaire pour ce faire.

Contents (concluded) / Table des matières (suite et fin)

Yong-Woo Lee and David B. Sampson 2443–2454 Spatial and temporal stability of commercial groundfish assemblages off Oregon and Washington as inferred from Oregon trawl logbooks

Lance P. Garrison, William Michaels, Jason S. Link, and Michael J. Fogarty 2455–2469 Predation risk on larval gadids by pelagic fish in the Georges Bank ecosystem. I. Spatial overlap associated with hydrographic features

Scott G. Hinch and Peter S. Rand 2470–2478 Optimal swimming speeds and forward-assisted propulsion: energy-conserving behaviours of upriver-migrating adult salmon

David J. Agnew, Simeon Hill, and John R. Beddington 2479–2487 Predicting the recruitment strength of an annual squid stock: *Loligo gahi* around the Falkland Islands

Jennifer A. Shore, Charles G. Hannah, and John W. Loder 2488–2505 Drift pathways on the western Scotian Shelf and its environs

Charles G. Hannah, Jennifer A. Shore, and John W. Loder 2506–2518 The drift–retention dichotomy on Browns Bank: a model study of interannual variability

David Brickman and Kenneth T. Frank 2519–2535 Modelling the dispersal and mortality of Browns Bank egg and larval haddock (*Melanogrammus aeglefinus*)

Brian Petrie and Philip Yeats 2536–2546 Annual and interannual variability of nutrients and their estimated fluxes in the Scotian Shelf – Gulf of Maine region

Jérôme Gingras and Daniel Boisclair 2547–2557 Comparison between consumption rates of yellow perch (*Perca flavescens*) estimated with a digestive tract model and with a radioisotope approach

Author index for Volume 57 / Index des auteurs pour le volume 57 AI-1

Contents index for Volume 57 / Sommaire pour le volume 57 C-1

National Research Council Canada
Ottawa, Canada
K1A 0R6

Conseil national de recherches Canada
Ottawa, Canada
K1A 0R6

Postage paid at Ottawa
Publications mail
Registration No. 1240579

Port payé à Ottawa
Poste-publication
Enregistrement n° 1240579

Canadian Journal of Fisheries and Aquatic Sciences

Volume 57, Number 12, December 2000

Journal canadien des sciences halieutiques et aquatiques

Volume 57, numéro 12, décembre 2000

RAPID COMMUNICATIONS / COMMUNICATIONS RAPIDES

Ransom A. Myers, Susanna D. Fuller, and Daniel G. Kehler 2357–2362 A fisheries management strategy robust to ignorance: rotational harvest in the presence of indirect fishing mortality

Sara A. Adlerstein and Henny C. Welleman 2363–2367 Diel variation of stomach contents of North Sea cod (*Gadus morhua*) during a 24-h fishing survey: an analysis using generalized additive models

ARTICLES / ARTICLES

Philip W. Hedrick, Vanessa K. Rashbrook, and Dennis Hedgecock 2368–2373 Effective population size of winter-run chinook salmon based on microsatellite analysis of returning spawners

Kai Lorenzen 2374–2381 Allometry of natural mortality as a basis for assessing optimal release size in fish-stocking programmes

Aimee A. Keller and Grace Klein-MacPhee 2382–2392 Impact of elevated temperature on the growth, survival, and trophic dynamics of winter flounder larvae: a mesocosm study

D.P. Swain and K.T. Frank 2393–2401 Depth-dependent vertebral number of Atlantic cod (*Gadus morhua*) on the Magdalen Shallows and Scotian Shelf: stock mixing or microgeographic trends within populations?

M. Cardinale and F. Arrhenius 2402–2409 The influence of stock structure and environmental conditions on the recruitment process of Baltic cod estimated using a generalized additive model

Robert A. McConnaughey and Keith R. Smith 2410–2419 Associations between flatfish abundance and surficial sediments in the eastern Bering Sea

Caihong Fu and Terrance J. Quinn II 2420–2432 Estimability of natural mortality and other population parameters in a length-based model: *Pandalus borealis* in Kachemak Bay, Alaska

C. Tara Marshall, Nathalia A. Yaragina, Bjørn Ådlandsvik, and Andrey V. Dolgov 2433–2442 Reconstructing the stock–recruit relationship for Northeast Arctic cod using a bioenergetic index of reproductive potential

Continued on inside back cover / Suite au verso

Canada

Printed in Canada by / Imprimé au Canada par
INTRA MÉDIA INC./datamark systems
Typesetting by / Typographie par
NRC Research Press / Presses scientifiques du CNRC

0706-652X(200012)57:12;1-L